
**Regulation of mitochondrial dynamics and bioenergetics:
implications of circadian clock and neurosteroids
in health and diseases**

Inauguraldissertation

zur

Erlangung der Würde eines Doktors der Philosophie

vorgelegt der

Philosophisch-Naturwissenschaftlichen Fakultät

der Universität Basel

von

Karen Schmitt

aus Colmar, Frankreich

Basel, 2018

Originaldokument gespeichert auf dem Dokumentenserver der Universität Basel
edoc.unibas.ch

Genehmigt von der Philosophisch-Naturwissenschaftlichen Fakultät auf Antrag von:

Fakultätsverantwortlicher: Prof. Dr. Stephan Krähenbühl

Dissertationsleiter: Prof. Dr. Anne Eckert

Korreferent: Prof. Dr. Stephan Frank

Basel, February 23rd, 2016.

(Datum der Genehmigung durch die Fakultät)

Prof. Dr. Stephan Krähenbühl
Fakultätsverantwortlicher

Prof. Dr. Jörg Schibler
Dekan der Philosophisch Naturwissenschaftlichen Fakultät

TABLE OF CONTENTS

FIGURES LIST	I
PREFACE	III
ACKNOWLEDGEMENTS	IV
SUMMARY	1
INTRODUCTION	5
A. The circadian rhythm: the living clock making life tick.	5
1. Clock genes and clock machinery.....	7
2. Organization of the circadian timing system.....	9
2.1. <i>Suprachiasmatic nuclei, the conductor(s) of the circadian orchestra</i>	9
2.2. <i>Peripheral clocks: keeping up with the master clock</i>	11
2.3. <i>How to study circadian timing system: from bench to bedside</i>	12
3. Circadian rhythms and metabolism.....	15
B. Keeping mitochondria in shape: a matter of life and death	17
1. Mitochondria: powerhouses of the cell	18
1.1. <i>Mitochondrial features</i>	18
1.2. <i>Mitochondrial respiratory capacity</i>	20
2. Mitochondria: paradoxical organelles	21
3. From mitochondria to mitochondrial network	23
3.1. <i>Mitochondrial fusion</i>	24
3.2. <i>Mitochondrial fission</i>	27
3.3. <i>Biological functions of mitochondrial dynamics</i>	28
4. Circadian clock regulation of mitochondrial functions	30
C. Mitochondrial dysfunction: Aging, Amyloid β, and tau – a deleterious trio	31
1. Etiological factors and clinical symptoms.....	32
2. Histopathological Alzheimer’s Disease related-features	33
2.1. <i>Cleavage pathway of APP and Aβ deposits</i>	33
2.2. <i>Phosphorylation of tau and development of neurofibrillary lesions</i>	35
3. Age-related A β and tau effects on mitochondria in AD.....	36
3.1. <i>Mitochondrial aging—the beginning of the end in AD?</i>	38
3.2. <i>Separate modes of Aβ and tau toxicity on mitochondria</i>	38
3.3. <i>Synergistic modes of Aβ and tau toxicity on mitochondria</i>	40
3.4. <i>The Alzheimer’s disease mitochondrial cascade hypothesis</i>	41
4. Mitochondria: potential target of neurosteroids.....	42

TABLE OF CONTENTS

5. Circadian disruption in aging and AD	44
REFERENCES	47
MANUSCRIPTS	58
A. Circadian control of Drp1 activity regulates mitochondrial dynamics and bioenergetics	59
B. Improvement of neuronal bioenergetics by neurosteroids: Implications for age-related neurodegenerative disorders	105
C. Amyloid-β-induced imbalance between mitochondrial network and bioenergetics	141
CONCLUSION	168
ABBREVIATIONS	173
CURRICULUM VITAE	Fehler! Textmarke nicht definiert.
PUBLICATIONS	Fehler! Textmarke nicht definiert.
APPENDICES	176

FIGURES LIST

Figure 1: The circadian system model.	5
Figure 2: Parameters of an hypothetical rhythm.....	6
Figure 3: The molecular mechanism of the circadian clock in mammals.	7
Figure 4: Circadian rhythm hierarchy in humans.....	10
Figure 5: Protocol to study circadian rhythms in human skin fibroblasts.....	14
Figure 6: The circadian clock and metabolism converge.....	16
Figure 7: Mitochondrion, unique organelle.....	18
Figure 8: The mammalian oxidative phosphorylation system (OxPhos).....	20
Figure 9: Pathways of reactive oxygen species (ROS) generation and their enzymatic detoxification.	22
Figure 10: Different shapes of the mitochondrial network.....	24
Figure 11: The core machinery of mitochondrial dynamics in mammals.....	26
Figure 12: Biological functions of mitochondrial dynamics.....	28
Figure 13: The pathology of Alzheimer's disease.....	33
Figure 14: APP processing and tau phosphorylation.....	35
Figure 15: Aging, Amyloid-Beta and tau: toxic consequences on mitochondria.....	37
Figure 16: The AD mitochondrial cascade hypothesis.....	42
Figure 17: A β -ABAD interaction and estradiol level in mitochondria.....	44
Figure 18 : A hypothetical sequence of the interplay between mitochondrial functions, the circadian clock and neurosteroids in health, aging and age-related diseases as AD.....	171

A mes parents, Béatrice et Jean-Yves,

A ma sœur, Jennifer,

À mes grands-parents, Betty et René.

PREFACE

This present thesis was performed at the Neurobiology Laboratory for Brain Aging and Mental Health of the Psychiatric University Clinics of Basel (UPK), under the supervision of Prof. Dr. Anne Eckert.

The following dissertation was written by the author. The INTRODUCTION is partly based on an updated version of previous reviews (see Appendices).

The MANUSCRIPTS section of this dissertation consists of one published manuscript and two others that will shortly be submitted for publication. Please refer to the author contributions section of the manuscripts where the contribution of each co-author to this work is listed.

ACKNOWLEDGEMENTS

‘The best scientist is open to experience and begins with romance - the idea that anything is possible.’ - Ray Bradbury

Pursuing a PhD project is a wonderful and often overwhelming experience. You are forced to confront all of your fears, insecurities and doubts you have about yourself and somehow overcome them. It is like finding your way in a labyrinth where the journey through the complex branching puzzle is accompanied with hardships, frustration, encouragement and trust and, particularly, with so many people’s kind help. Thus, I am indebted to many people for making the time working on my PhD an unforgettable experience. I would not be the person I am today without you!

First of all, I am deeply grateful to my supervisor, Prof. Dr. Anne Eckert. You have been a steady influence throughout my PhD journey by providing so much advice and orienting me in the right direction. While you always kept me on track, you also gave me freedom in my work and encouraged me to take initiative and responsibility from the beginning to develop my scientific skills.

I would like to thank Prof. Dr. Steven Brown and Prof. Dr. Stephan Frank, who always kindly answered my questions and contributed with their advices and ideas to improve my Ph.D. work as well as my scientific skills.

My thanks go to Prof. Dr. Stephan Krähenbühl who accepted to be my Faculty representative and Prof. Dr. Stephan Frank who accepted to be the co-referee in my dissertation. I also wish to acknowledge Prof. Dr. Christoph Meier for his participation as Chairman in my dissertation.

My warmest thanks go to Amandine Grimm. In 2010, I met a colleague with the similar working values but more important I gained a very close friend who has been there for me in the good but also in the bad time. I will always cherish our time spend in and out of the lab, during congress around the world (The Mito Twins are in the place!) or during our overnight experiments (2 o’clock in the morning is a perfect time for a pasta dish). Always full of fluffiness and sometimes nonsense! Let’s not forget our common humour which is our best way to move on after a bad day.

Kind thanks to Imane Lejri for being a great colleague in and out of the lab. I enjoyed a lot our diverse conversations: from work to fashion (hello Michael Kors ☺).

My heartfelt thanks go out to Fides Meier and Ginette Baysang who provided support, inspiration and motivation, in jokes and sometimes in waterworks, along the way. I will never

ACKNOWLEDGEMENTS

forget our linguistic misunderstandings and all the scientific and non-scientific discussions we had in and outside the lab.

Thank you to the rest of the fantastic team and collaborators I have been fortunate to work with over the years, including the former members, the master students and the 'Zivi' guys (Stefano, Ricky, David, Fabio, Joel, Jonas and all the others).

A huge thank you to my friends from near and far. I am honored to have an eclectic support network to challenge and check in on me. I am particularly grateful to Virginie Rhein, Laetitia Wioland and Karelle Benardais from the 'neuroiennes' team and Nathanael Sanchez for their support, their advice, their friendship and the priceless time I spend with each of you. Even separate by sea and earth, we always found a way to stay in touch (thank you Skype and others) and to be there for each other.

I would like to thank Virginie Gabel and Julien Delezie (and Amandine) for the good time spend in congress and in Basel, for the scientific and much less scientific conversations (☺). It's always a terrific moment with you guys !

Et le meilleur pour la fin, du fond du cœur, je remercie ma famille :
À Christiane et Eugène pour avoir été présents à chaque étape de ma vie.
À mes grands-parents, Betty et René, toujours dans mon cœur.
À mes parents Béatrice et Jean-Yves, ma (petite) sœur Jennifer et Fabien pour leur indéfectible soutien depuis le début, leur encouragement, leur patience dans les bons comme dans les moins bons moments. Merci de m'avoir transmis la force et les qualités nécessaires pour avancer toujours plus loin sur cette route parfois périlleuse, de m'avoir appris à exploiter ma soif de connaissances et mais surtout de m'avoir appris qu'au final, mon seul job dans la vie, c'est d'être heureuse !

Thanks to all of you from the bottom of my heart,

Karen

SUMMARY

The cellular metabolism is a highly dynamic process where mitochondria network is a prominent actor in regulation of both energy metabolism and apoptotic pathways. To preserve the integrity of a healthy mitochondrial population within the cell but also the integrity of the cell itself, mitochondrial networks come in varied shapes and ultrastructures to ensure the main energy supply, stored in the form of adenosine triphosphate (ATP), by oxidative reactions from nutritional sources. Therefore, alterations in both mitochondrial dynamics and metabolism are often related to each other as early and prominent events in the pathogenesis of several age-related disorders including Alzheimer's disease (AD). Advances in the understanding of the mechanisms underlying the coordination between mitochondrial dynamics and the functional state of mitochondria in health are essential for the characterization of disease-related changes of mitochondria in the course of neurodegenerative disorders.

The purpose of this thesis was therefore to pinpoint the mechanistic processes that are involved in the regulation of mitochondrial bioenergetics and dynamics. To better understand **(I)** the tight equilibrium between mitochondrial morphology and function in physiological state and **(II)** its impact on abnormal mitochondrial, the thesis was divided in two main parts:

I. The first aim of the thesis was to investigate the potential influence of **(A)** the circadian clock and **(B)** neurosteroids on the maintenance of mitochondrial homeostasis.

(A) Since biological clocks are tightly connected to metabolic processes within the cell, we first determined whether mitochondrial dynamics and metabolism are coupled events that are coordinated by the circadian system.

(B) Considering compelling evidence that highlighted neuroprotective effects of steroids in the brain, we examined whether different neurosteroids are able to improve mitochondrial bioenergetics to prevent age-related mitochondrial alterations which eventually lead to neurodegeneration.

II. In the second part **(C)**, we determined whether amyloid-beta ($A\beta$) impacts the integrity of the mitochondrial structure–function relationship since both mitochondrial dynamics and bioenergetics are hallmarks of $A\beta$ -induced neuronal toxicity in AD.

I. (A) The circadian clock is a hierarchical network of oscillators that coordinate a wide variety of daily biological functions, including metabolic functions, to the optimal time of day anticipating the periodical changes of the external environment for all living organisms. Mitochondria are dynamic organelles at the crossroad of the cellular metabolism that fuse

and divide continuously to fulfill their role in the maintenance of the cellular bioenergetic homeostasis. While it is well known that metabolism is a complex biochemical network that is tightly intertwined with the circadian clock through reciprocal regulation from metabolites to transcription factors, the mechanistic connections between the biological clock and the mitochondrial network remain mostly elusive. We therefore addressed the questions whether and how the circadian clock intervenes in the coordination between mitochondrial dynamics and functions and whether the coupled mitochondrial network- metabolism may be able to influence the circadian clock.

We demonstrated *in vitro* and *in vivo* that mitochondrial fission-fusion dynamics were strongly clock-controlled, as well as all other aspects of mitochondrial metabolic flux, including oxidative phosphorylation, generation of ATP and reactive oxygen species (ROS). The changes in cell cycle-based mitochondrial morphology required the circadian phosphorylation of the key protein, dynamin-related protein 1 (DRP1), the major protein involved in mitochondrial fission. Genetic or pharmacological abrogation of DRP1 activity abolished circadian mitochondrial network dynamics and mitochondrial respiratory activity, as well as eliminated circadian ATP production. The disruption of circadian mitochondrial dynamics furthermore feeds back to impair the core circadian clock.

Overall, our findings are consistent with the existence of a crosstalk between the clock and the mitochondrial network that maintains bioenergetic homeostasis in response to circadian metabolic changes.

I. (B) We aimed to investigate the potential role of different neurosteroids on mitochondrial bioenergetics and redox homeostasis in neuronal cells. In contrast to steroid hormones produced by endocrine glands, neurosteroids are synthesized within the nervous system itself and are defined as neuroactive molecules acting on the nervous system in an auto/paracrine manner. Neurosteroids exhibit several biological functions that are essential during brain development as well as in the adult brain. Moreover, progressive depletion in neurosteroid content might contribute to an age-related neuronal decline that eventually leads to the development of neurodegenerative disorders including AD. Although compelling evidence has shown that estradiol interacts with mitochondria to counteract oxidative stress occurring in age-related diseases such as AD, the potential role of other neurosteroids on mitochondria is rather poorly investigated and understood.

To expand our knowledge on the mechanisms behind the neuroprotective action of neurosteroids, a selection of sex-hormone-related neurosteroids, including progesterone, estradiol, estrone, testosterone, 3α -androstenediol, dehydroepiandrosterone (DHEA) as well as allopregnone, were tested on mitochondrial function. Using human SH-SY5Y neuroblastoma cells, we determined which of the neurosteroids exhibited the capacity to enhance mitochondrial metabolism by increasing ATP content along with an augmentation of

mitochondrial membrane potential and mitochondrial respiration. Interestingly, particular bioenergetic profiles were found for each neurosteroid, which might be due to an involvement of different receptors. When the respective steroid receptors were blocked with specific inhibitors, ATP contents were entirely depleted confirming a receptor-specific mode of action of neurosteroids. Concomitantly with the enhanced mitochondrial metabolism, treatment with neurosteroids induced an augmentation of ROS levels in parallel to an up-regulation of antioxidant defenses suggesting a direct or indirect role of neurosteroids on redox homeostasis in neuronal cells.

Collectively, these novel findings demonstrate that neurosteroids are able to differentially improve mitochondrial function as well as to modulate redox homeostasis through distinct receptors. Because of the disparate effects of neurosteroids on mitochondrial metabolism, the underlying mechanisms have to be further elucidated in future studies, particularly the effect of neurosteroids on mitochondrial dynamics, as well as those in models of neurodegenerative diseases, such as AD.

II. (C) The aim of the second part of this thesis was to investigate the impact of $A\beta$ on the balance between mitochondrial structure and function since abnormalities in mitochondrial dynamics and bioenergetics are hallmarks of $A\beta$ -induced neuronal toxicity in AD. For that purpose, we examined mitochondrial architecture and bioenergetics in cell-cycle controlled human primary fibroblast cultures treated with $A\beta_{1-42}$ peptide compared to non-treated cells. We demonstrated that variations in mitochondrial respiration, ATP and ROS content coincided with the oscillations pattern of the mitochondrial network in physiological conditions in control cells confirming the existence of a direct link between the mitochondrial network and the metabolic state of mitochondria. Indeed, in between the switch from tubular to fragmented mitochondrial network, we observed an increase in ATP level which correlated with a higher oxygen consumption rate (OCR) in the basal respiration as well as in ATP turnover and maximal respiration. In contrast, $A\beta_{1-42}$ almost completely dampened the oscillations of mitochondrial dynamics followed by a decline of mitochondrial metabolism including reduced ATP level and OCR. Furthermore, $A\beta$ -induced mitochondrial defects provoked a drastic augmentation in mitochondrial ROS level which might participate, along with an imbalance in the $NAD^+/NADH$ ratio, in the generation of oxidative stress confirming the oxidative stress theory of aging and AD.

Hence, these new insights support the concept that mitochondrial bioenergetics is coordinated by mitochondrial architecture transitions and that $A\beta$ induced a functional imbalance in the mitochondrial structure-function relationship, which might contribute already at an early disease state to AD pathogenesis.

Altogether, in the present thesis, we gained new insights on factors regulating mitochondrial dynamics and metabolism in health and disease states, e.g. AD. We firstly revealed that the circadian clock system, even in nondividing cells and tissues, regulates the phosphorylation of DRP1 resulting in cycles of fission and fusion that are essential for circadian oscillations in ATP production. These findings provide multiple implications into the understanding of metabolic homeostasis in human health as well as in disorders linked to impairments in circadian clock and/ or mitochondrial function. Secondly, we determined that neurosteroids are able to differentially modulate mitochondrial metabolism at the physiological state suggesting that these molecules might be considered as promising candidates in neuroprotective approaches to counterbalance mitochondrial deficiencies. Finally, we contributed to a better understanding of A β -induced neurotoxicity that is mediated by mitochondrial malfunctions further emphasizing the mitochondrial cascade hypothesis of AD.

INTRODUCTION

A. The circadian rhythm: the living clock making life tick.

Circadian rhythm is recognized as an evolutionarily conserved adaptation to periodical changes of the external environment that can be traced back to the earliest life forms [1]. This rhythm is a roughly-24-hour cycle that times/coordinates a wide range of metabolic, physiological and behavioral events of living beings, including plants, animals, fungi and cyanobacteria. These rhythmic processes are governed by an integrated system involving environmental cues, such as fluctuations in light intensity associated with food viability, an internal circadian timing system composed of a central pacemaker in the brain's suprachiasmatic nuclei (SCN) and subsidiary clocks in nearly every body cell, and the interaction between this timekeeping system and environmental signals in order to provide time information required for the control of behavior, physiology, and gene expression (Figure 1).

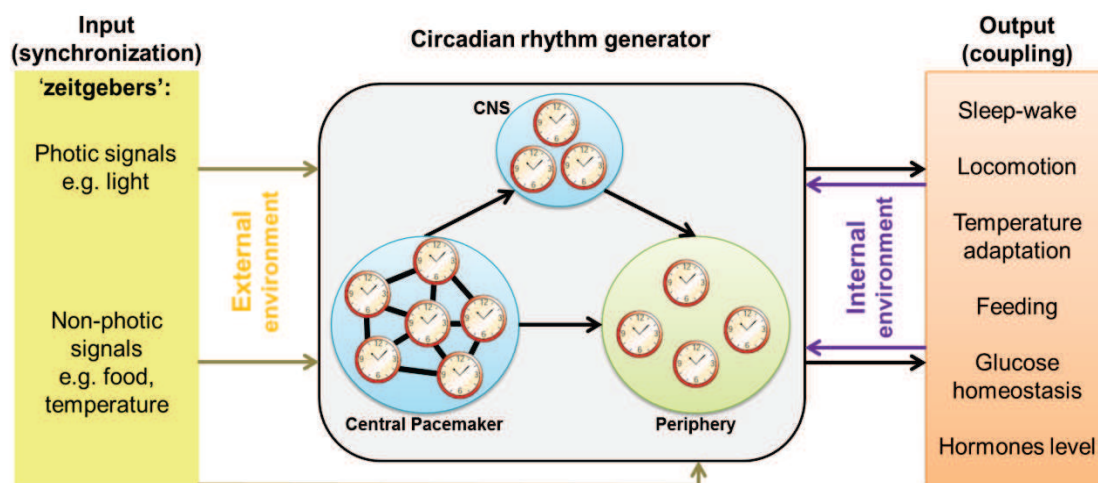


Figure 1: The circadian system model.

In order to maintain and generate a variety rhythmic behavior and functions, the circadian rhythm oscillators resynchronize themselves each day with external stimuli such as the brightness of the ambient light (adapted from [2]).

Briefly, to consider a biological rhythm as circadian, the endogenous rhythm generators have to present the ability to generate and maintain a “free-running” rhythm at periods slightly different than 24 hours. Moreover, circadian rhythms are characterized by two key features: they are self-sustained in absence of environmental cue (‘free-running conditions’) and they can be entrained to daily changes in the environment (entrained conditions). To maintain their accuracy, the circadian rhythm generators are entrained or

synchronized to the environment by input pathways initiated from receptors perceiving and transmitting environmental cues (e.g. the most important being the light/dark cycle), commonly named “zeitgebers”. The output pathways translate then the oscillations into behavioral and physiological rhythms. Another fundamental feature of circadian clocks is the ability to counteract inappropriate signals and to be persistent under stable ambient conditions. The most well-known example is illustrated in the temperature compensation observed in all molecular and behavioral circadian rhythms.

Overall, circadian timekeeping system can be analyzed as an integrated system – beginning with genes related to the molecular clock machinery and leading ultimately to behavioral outputs. Moreover, circadian rhythms share common fundamental properties (Figure 2). The parameters include the free-running, or the length of one oscillation under constant environmental conditions and phase response/entrainment, the ability of the clock to alter its phase in response to external stimuli and the amplitude of the rhythm, that is the force of the oscillations.

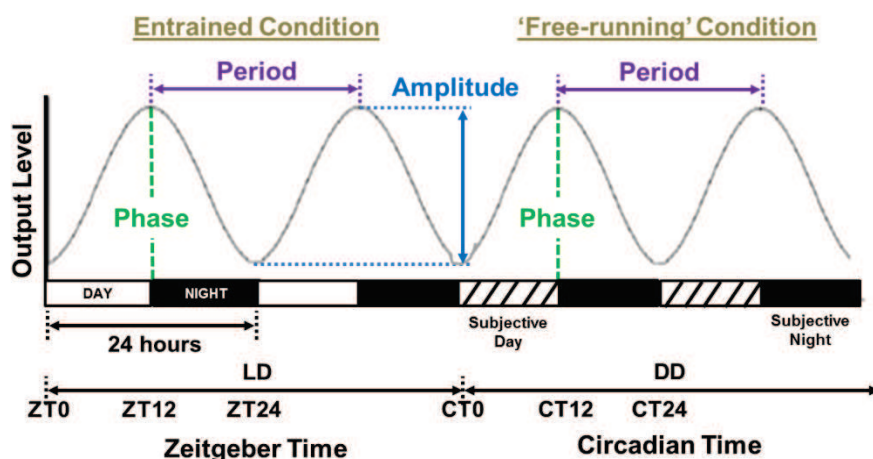


Figure 2: Parameters of an hypothetical rhythm.

Three important parameters of circadian rhythm are indicated: phase, period and amplitude. The amplitude refers to the maximum absolute value of a periodically varying quantity. The period refers to the time spent between two peaks. The phase represents the position of a peak compared to the time unit. Under entrained conditions (standard light-dark cycles), the time of lights on usually defines zeitgeber time zero (ZT 0) for diurnal organisms and the time of lights off defines zeitgeber time twelve (ZT 12) for nocturnal animals. The circadian time refers to a standard of time based on the free-running period of a rhythm. By convention, the onset of activity of diurnal organisms (or subjective day) defines circadian time zero (CT 0) under 'free-running' condition, while the onset of activity of nocturnal organisms (or subjective night) defines circadian time twelve (CT 12). LD, a regular alternation of light and darkness each day; DD, Constant darkness.

1. Clock genes and clock machinery

Generation and maintenance of circadian rhythms rely on complex interlaced feedback loops (positive and negative) based on transcriptional and posttranscriptional events involving clock genes and kinases that mandate fine-tuning of the clock and yet provide for its plasticity by which it can adjust to changes in the environment [3-5] (Figure 3). This mechanism of transcriptional-translational feedback loop (TTFL) that is at the basis of the mammalian circadian machinery is well conserved amongst many other species, such as bacteria (e.g. Cyanobacteria), plants (e.g. *Arabidopsis thaliana*) and animals (e.g. *Drosophila melanogaster*) beings [5, 6].

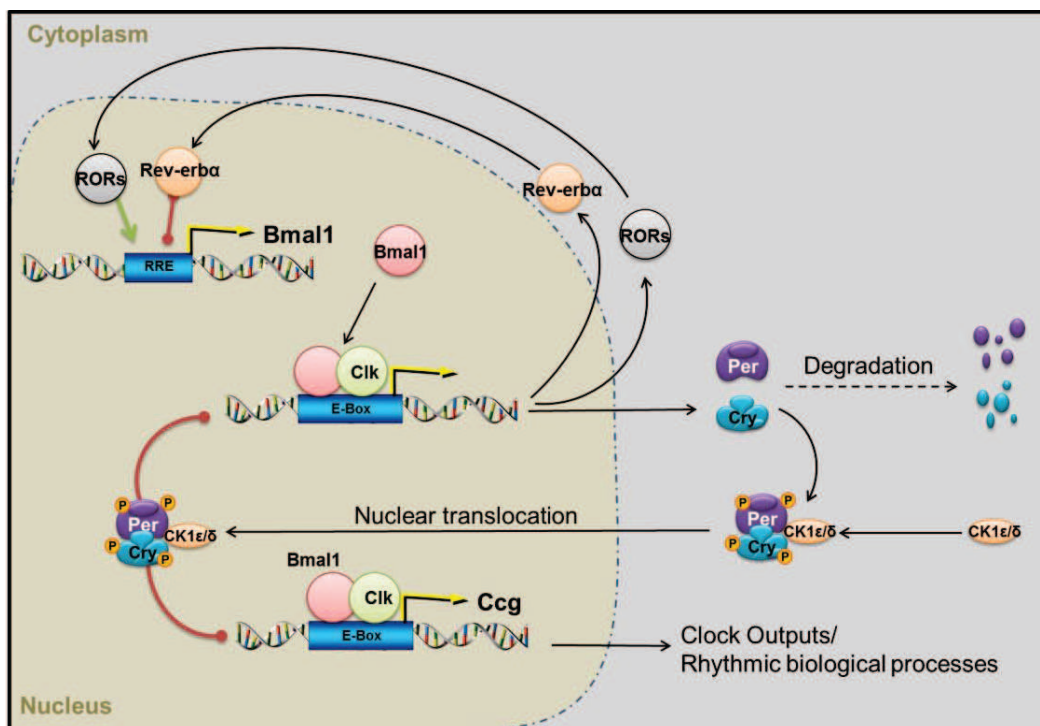


Figure 3: The molecular mechanism of the circadian clock in mammals.

The core circadian clock consists in an autoregulatory transcription-translation feedback loop (TTFL) involving activators CLOCK/NPAS2 (Clk; green circle) and BMAL1 (red circle) which dimerize and bind to specific promoter sequences, E-Box leading to activation of the transcription of the negative elements *Per* (isoforms 1,2) and *Cry* (isoforms 1,2). Moreover, Rev-Erba negatively regulates the expression of BMAL1, whereas RORs positively regulate the expression of BMAL1. As a consequence, also the negative key components CRY and PER and REV-ERBa decrease their own concentration in the cell. CLOCK: BMAL1 also regulates many downstream target genes known as clock-controlled genes (CCG) which provide a circadian output in physiology. P, phosphate; Cry, cryptochrome; Per, Period (adapted from [7]).

In mammals, the primary feedback loop is made up of the positive elements that include members of the basic helix-loop-helix (bHLH)-PAS (Period-Arnt-Single-minded) transcription factor family, CLOCK/NPAS2 (circadian locomotor output cycles kaput/neuronal

PAS domain protein 2) and BMAL1 (brain and muscle ARNT-1) [8, 9]. Both factors form a heterodimer that binds E-Box sequences (CACGTC) present in clock and clock-controlled gene (CCG, or circadian output genes) promoters. This binding initiates the transcription of period (*Per*) and cryptochrome (*Cry*) messenger RNA. *PER* and *CRY* mRNAs are translated into proteins in the cytoplasm. These proteins then form heteropolymeric complexes (PER/CRY and PER/PER) that enter the cell nucleus and interact with the CLOCK/BMAL1 heterodimer inhibiting the transcription process and hence the production of PER and CRY. As a consequence *cry* and *per* mRNAs and proteins decrease in concentration and once the nuclear levels of the CRY–PER complexes are insufficient for auto-repression, a new cycle of *Per* and *Cry* transcription can start.

In addition to this core transcriptional feedback loop, expression of Rev-Erb α and retinoic-related orphan nuclear receptors (RORs), circadian-controlled metabolic transcription factors, is also induced by CLOCK:BMAL1 heterodimers [8, 9]. Contributing to the robustness of this molecular clockwork circuitry, REV-ERB α and ROR α subsequently compete to bind retinoic acid-related orphan receptor response elements (ROREs) present in *Bmal1* promoter. RORs activate transcription of *Bmal1* [10-12], whereas REV-ERBs repress the transcription process [12, 13].

At a posttranslational level, mechanisms such as phosphorylation and ubiquitination significantly contribute to keep the clocks ticking at a normal speed (~24 hours oscillations) by affecting the stability and nuclear translocation of aforementioned core clock proteins [8, 14]. For instance, Casein kinase 1 epsilon and Casein kinase 1 delta (CK1 ϵ and CK1 δ) and AMP kinase (AMPK) are critical factors that regulate the core circadian protein turnover in mammals [8, 15, 16]. The kinases phosphorylate the PER and CRY proteins, respectively, to promote polyubiquitination by their respective ubiquitin ligase complexes, which in turn tag the PER and CRY proteins for degradation by the proteasome complex.

Additional genes with promoters containing E-box, D-box and retinoic acid responsive element (RRE) consensus sequences are also clock regulated and make up a large body of circadian clock–controlled genes (CCG). Genome-wide transcriptome profiling studies revealed that up to 10% of all mammalian genes display oscillations in their expression levels with a period of about 24 hours in the brain as well as in peripheral organs [17, 18]. Among these rhythmic genes, several regulatory genes and transcription factors are involved in metabolic processes such as carbohydrate, lipid, and cholesterol metabolism as well as detoxification mechanisms (for details, see section A.3. Circadian rhythms and Metabolism). In the liver, the transcription factors identified belong to the PAR bZip family such as DBP, TEF, and HLF that bind to D-elements, the PAR bZip-related repressor E4BP4, the Krüppel-

like factors KLF10 and KLF15 , and nuclear receptors (review in [2]). All these transcription factors are known to be linked remotely or closely to the metabolic homeostasis.

Although the TTFL is well recognized as essential for the timekeeping in the SCN and virtually in cells of the body, recent studies may revise the typical view of how the rhythmicity is sustained within the cells. Interestingly, it has been demonstrated that transcription is not required for circadian oscillations in human red blood cells which have no nucleus (or DNA) and, therefore, cannot perform transcription and non-transcriptional events seem to be sufficient to sustain cellular circadian rhythms [19, 20]. Moreover, these rhythms are entrainable (that is, tunable by environmental stimuli) and temperature-compensated, both key features of circadian rhythms. Consequently the idea that oscillations persist in absence of nucleus suggests a more complex view of the circadian timing system where other players act as critical modulators (e.g: metabolites) of the biological timekeeping (see also section A.3. Circadian rhythms and metabolism).

2. Organization of the circadian timing system

A highly refined circadian system is already present in invertebrates such as arthropods and insects, but the most complex organization of the circadian system is found in mammals and humans. The mammalian circadian system is organized in a hierarchical manner that consists of the central circadian rhythm generator, also known as the conductor of the circadian orchestra or the 'master clock', and all the subsidiary clocks in the other parts of the brain as well as in nearly every body cell (Figure 4).

2.1. *Suprachiasmatic nuclei, the conductor(s) of the circadian orchestra*

In mammals, the master circadian clock resides in the suprachiasmatic nuclei (SCN), a pair of distinct and bilateral groups of neurons (~20 000 neurons) located above the optic chiasm at the basis of the hypothalamus. In the 1970's, lesion studies in rodents conducted almost simultaneously by two laboratories identified the exact location of the master clock which was shown to be both necessary and sufficient for the generation of circadian activity rhythms [21, 22]. In a nutshell, lesion of the SCN abolished circadian rhythmicity in entrained condition and resulted in the loss of corticosterone rhythms as well as in the disruption of the locomotor activity. Moreover, the tract tracing experiment revealed a bilateral projection from the retina to the hypothalamus named the retinohypothalamic tract (RHT). Inversely, when SCN-lesioned hamsters were transplanted with fetal SCN tissue into the third ventricle, circadian locomotor activity was restored (review in [23]). Furthermore, rhythms in SCN-lesioned wild-type hamsters were reestablished but with a shortened period length

characteristic of the *Tau* mutant hamsters displaying circadian rhythmicity [24]. Overall, these results converged nicely to support the idea that the SCN as the master circadian clock is synchronized by the environmental light.

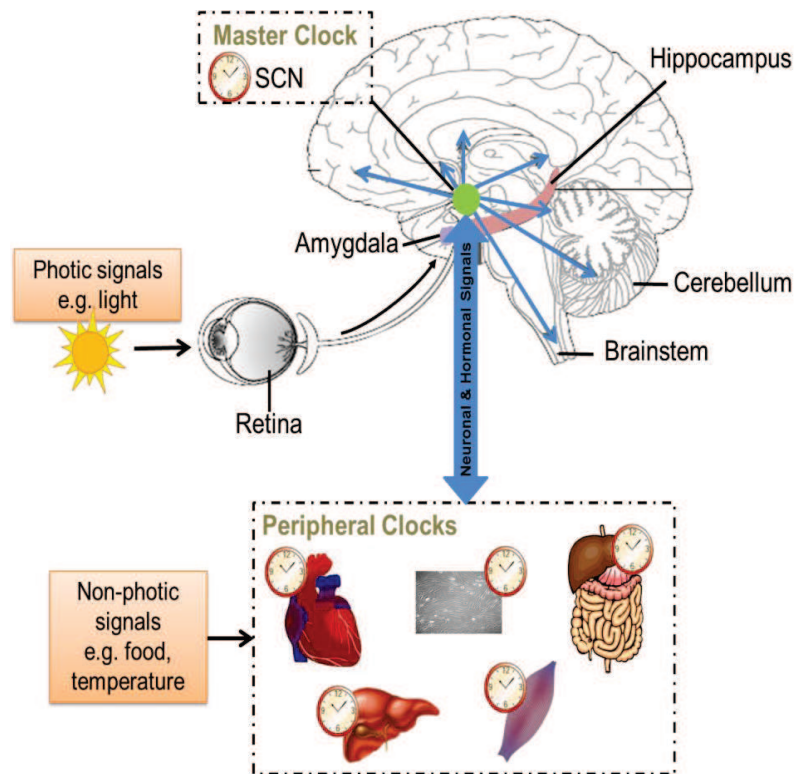


Figure 4: Circadian rhythm hierarchy in humans.

The circadian system is composed of a central circadian rhythm generator and subsidiary clocks. Environmental light is detected by the retina that, through the retina-hypothalamic tract, sends signals to the master clock, the suprachiasmatic nucleus (SCN) of the hypothalamus. SCN elaborates this light information and synchronizes its circadian rhythm with the external light-dark rhythm. Moreover, through neuronal and hormonal output pathways, SCN synchronizes virtually all cells of the body. Like feeding rhythms, body temperature rhythms appear to play an important role in the coordination of peripheral clocks.

To maintain its accuracy, the central biological clock resynchronizes itself each day with external stimuli such as the brightness of the ambient light, by means of the optic nerves, which bring this information to the SCN from ganglion cells in the retina through the RHT. While SCN is structurally and functionally heterogeneous at the single-cell level [7, 25-27], SCN can generate and maintain a basic and independent rhythm as a network in which the SCN cells are mutually coupled and oscillate in a consistent manner, even if the external cues of the cycle of day and night are eliminated [27, 28]. When the SCN were isolated as explant or when single SCN neurons were cultured *in vitro* (review in [23]), electrical activity remained circadian and individual neurons showed circadian firing rhythms, even after three

weeks in culture demonstrating that the robustness of the SCN network oscillatory system is critically dependent of the intracellular coupling of SCN neurons.

To function as a pacemaker and synchronizer for other brain and peripheral clocks, the intrinsic timekeeping signal from the SCN has to be transmitted once the SCN has integrated the time-related information from the environmental inputs. SCN uses both signals and neural efferents to convey timing information (i.e, entrain, synchronize) to other parts of the brain (e.g. hypothalamic nuclei) and the periphery. In fact, SCN get directly involved into the sleep/arousal, reproductive and endocrine systems in part through neuroanatomic connections by which the SCN can synchronize peripheral clocks, e.g. by inducing the release of glucocorticoids [29]. Inversely, activity rhythms as well as circadian outputs from other tissues can feed back on the SCN and on other peripheral oscillators.

2.2. Peripheral clocks: keeping up with the master clock

Although it was initially believed that the SCN is the only mammalian tissue capable of circadian rhythm generation, the identification of core genetic component of the mammalian circadian clock suggested that virtually all cell types can be considered as circadian oscillators by sharing the same molecular mechanism [30]. Therefore, cell autonomous and self-sustained circadian rhythms are found outside the SCN [31] and even outside the brain [32] in many peripheral organs and tissues [33] in the body such as oesophagus, lung, liver, pancreas, spleen, thymus and the skin; the cells constituting these tissues are called peripheral oscillators [34, 35]. First evidence was described by Tosini and Menaker in cultured mammalian retina where melatonin (the so called 'night hormone', mainly produced by pineal gland) was secreted in a circadian fashion [36]. Following studies revealed that all examined peripheral tissues (with the exception of testis) virtually transcribe main clock genes (mBmal1, mNpas2, mReverba, mDbp, mRev-erb β , mPer3, mPer1 and mPer2) in a cyclic fashion, however, with a mRNA peak occurring 4 hours later than those in the central pacemaker, SCN [13, 32, 37, 38].

Many circadian overt output cycles of the circadian timing system involve circadian clocks in peripheral cell types (3-10% of all mRNAs in a given tissue) [7, 30]. However, the expression of these CCG is largely nonoverlapping in each tissue, reflecting the necessity for temporal modulation peculiar to each single cell type. As a result, a large number of key biological processes, including many aspects of metabolism [39], glucose homeostasis [40] and lipogenesis [41] is subject to control of the circadian clock. The liver is the most well-known organs in term of circadian transcription with close to 1000 circadian transcripts identified encoding key enzymes involved in metabolic pathways, energy homeostasis, food processing and detoxification (review in [23]).

Given the hierarchical organization of the circadian system, peripheral circadian clocks, and thus daily physiology and behavior, are coordinated by systemic cues emanating from the SCN, such as neuronal signals and circulating hormones or metabolites, and/or by local peripheral oscillators synchronized by the SCN [2, 7, 23]. Moreover, although the SCN serves as the master synchronizer of the entire system, food intake or body temperature change can uncouple peripheral clocks from control by the SCN [2]. Such a system has the potential benefit of temporary uncoupling between SCN and peripheral clocks. For instance, changes in feeding schedule lead to the alteration in the phase relationship between the central clock in the SCN and the clocks in the liver, suggesting that changes in metabolism caused by alterations in feeding rhythm may affect the circadian system [42]. Understanding the complexity of tissue-specific circadian expression patterns remains a major challenge. Several mechanisms have been proposed to explain the tissue-specific rhythm generation: (1) variations of the core clock across different tissues, (2) tissue-specific rhythmically expressed transcription factors and co-factors, (3) and systemic cues such as hormone secretion, sympathetic innervation, body temperature, and activity rhythms (review in [43]).

Unlike the SCN explants, the peripheral cell or tissue rhythms tend to damp out within a few cycles until restarted by a wide range of resetting stimuli, including serum shock, glucocorticoids, cold pulses, and even medium changes in cell culture models [44-47]. The difference in damping between SCN and other tissues appears to be quantitative rather than qualitative. It has been observed that damping of the circadian rhythms is explained by loss of coupling among cells rather than damping of individual cell rhythms [48-50]. Individual fibroblast cells are capable of functioning as independently phased circadian oscillators that are self-sustained for many days *in vitro*. In fact, their circadian function appears very similar to SCN neurons assayed on multielectrode arrays for rhythms of neuronal firing [27]. It is thus possible to use peripheral oscillator as model to study molecular mechanisms of circadian rhythms.

2.3. *How to study circadian timing system: from bench to bedside*

It is believed that the intrinsic period length of the SCN affect the phase of diurnal behavior. Mammalian circadian system can be investigated at different levels from molecular and cellular processes to behavior in a whole organism.

In rodents, locomotor activity is mostly used to determine the circadian rhythm [51]. In human, many physiological, biochemical and neuroendocrine parameters such as sleep/wake cycle, body temperature, melatonin, cortisol, heart rate, and blood pressure are broadly used as circadian output [52]. The analyses of the circadian rhythms of these markers can give hints about circadian parameters, such as amplitude, phase and period

length (for details, see Figure 2). However, the major concerns in circadian studies are that endogenous circadian clocks are not only determined by the biological clock and the sleep homeostasis but also zeitgebers such as light exposure, temperature, body position and food intake [53]. Therefore, these factors can have direct or indirect effects on many functions, so-called “masking” effects. To overcome these difficulties, it was necessary to develop protocols that control or at least attenuate for masking effects. Principally, the individuals are placed in constant and controlled conditions (e.g. constant darkness, short or long sleep time) in order to elucidate the characteristics of the endogenous circadian pacemaker [54]. Nevertheless, measurement of the circadian period length, normally accomplished by prolonged subject observation, remains difficult and costly in humans.

Since it is believed that SCN and most cells of the body virtually share the same cell-intrinsic mechanism of the biological clock [32, 37], several circadian studies developed ex-vivo protocols using cells - skin, blood, or hair root cells - or explants from animal or human tissue that can be obtained easily. Although the period length of circadian behavior in rodents is straightforwardly determined by analysis of wheel-running behavior in constant darkness [54], success in developing transgenic animals in which the luciferase gene has been fused to a circadian reporter permits to complement wheel-running behavioral analyses by measuring the period length of circadian genes *in vitro* [55, 56]. Furthermore, explants from different tissues as well as cultured mouse fibroblasts from these animals were used to analyze the circadian rhythm by real-time measurement of light output [48, 57]. As anticipated, the circadian oscillators of these cells are self-sustained and cell-autonomous, similar to those operative in SCN neurons.

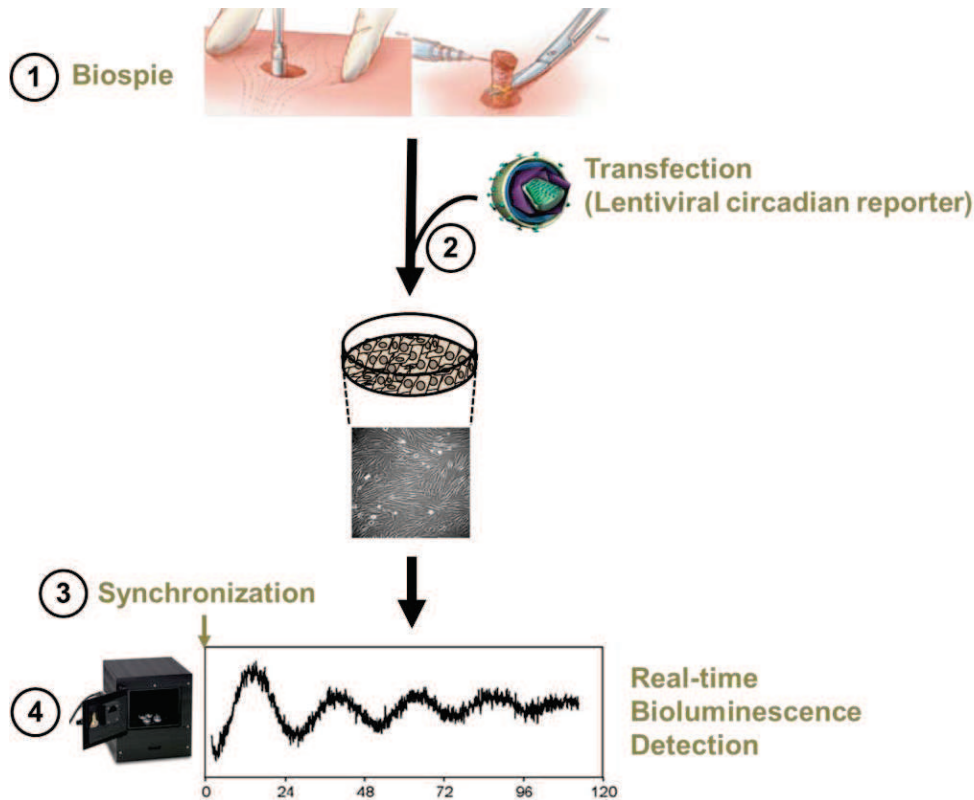


Figure 5: Protocol to study circadian rhythms in human skin fibroblasts.

Punch skin biopsy is (1) harvested and cultivated under sterile conditions. Fibroblasts that grow around the biopsy are isolated, amplified and (2) infected with a circadian reporter coding for firefly luciferase under a clock gene promoter, i.e. *Bmal1*. The infected cells are selected and then, (3) after synchronization of circadian rhythms, (4) the light emitted by the cells is measured in the Lumicycle (Actimetrics) or in a home-made device able to detect and measure bioluminescence.

Likewise, it has been reported that the period of human circadian behavior is mostly driven by cellular clock properties in normal individuals and can be approximated by measurement in peripheral cells such as fibroblasts using lentivirally-delivered circadian reporter vectors (Figure 5) [49, 58]. For example, the cellular clocks of early chronotypes (i.e., “larks”) have shorter circadian periods than those of later chronotypes (“owls”) [59], and circadian period length *in vitro* is proportional to physiological period *in vivo* [58].

Except for the damping tendency of peripheral clocks which can be counteracted with a wide range of resetting stimuli *in vitro* including serum shock, glucocorticoids, cold pulses, and even medium changes in cell culture models [44-47], primary cells are a good model to study circadian aspects for their accuracy in circadian characteristics, such as the period length, even isolating *in vitro* oscillators. Moreover, the ability to transfect peripheral oscillators such as fibroblasts with dominant-negative constructs is another important tool that can be used to investigate particular aspects of circadian rhythm. In this way, it was possible to ensure that circadian genetic differences are reflected in the rhythms of fibroblast gene expression [49]. Overall, *in vitro* studies on isolated peripheral oscillators can be

associated to *in vivo* studies to investigate a circadian question from more points of view, in both physiological and pathological states.

3. Circadian rhythms and metabolism

Circadian rhythms control a wide range of physiological events, including metabolism, in all organisms. Over the last decades, accumulating evidence has revealed that, from metabolites to transcription factors, circadian rhythms and metabolism converge to optimize energy harvesting and utilization across the light/ dark cycle [60, 61]. While the regulation of metabolic pathways is well known to be achieved by the circadian clock, it has also been suggested that various hormones, nutrient sensors, redox sensors and metabolites are not only clock output but can also regulate in turn the biological clock by acting as an input signal [57, 62] (Figure 6). Moreover, as demonstrated by individuals working night or rotating, but also by rodent models of circadian arrhythmia, circadian cycle is strongly associated with metabolic imbalance among the living organisms [63-65]. Understanding more the interplay between these two systems will provide not only needed insights about circadian physiology and metabolic mechanisms but also novel knowledge about the pathophysiologic consequences of disruption of this molecular interplay.

The interplay between circadian and metabolic cycles has been described in recent studies showing that the circadian clock exerts its control over metabolism by (i) controlling the expression of ascertained genes and enzymes involved in metabolic processes, (ii) intertwining nuclear receptors and nutrient sensors (e.g. SIRT1 and CLOCK, AMPK and CRY1) with the clock machinery, and/ or (iii) regulating metabolite levels (e.g. NAD⁺, cAMP) [66, 67]. Of note, various hormones, nutrient sensors, redox sensors and metabolites are not only clock output but can also regulate in turn the biological clock by acting as an input signal.

As mentioned above, in addition of transcription factors known to regulate genes involved in metabolism, a large fraction of rhythmic genes transcripts encode for important metabolic regulators. However, a much larger percent of the proteome oscillates in either expression or activity [60]. This implies that, in order to achieve a well time-coordinated expression, a powerful and cyclic mechanism of chromatin remodeling has to be partly involved in order to response rapidly and adequately to specific cues. This is likely to be obtained through rhythmic alterations in histone modifications such as phosphorylation or acetylation associated directly with circadian clock proteins [68-70]. Interestingly, CLOCK itself contains histone acetyltransferase activity which contributes to the rhythmic acetylation of histone of its binding partner, BMAL1 [71].

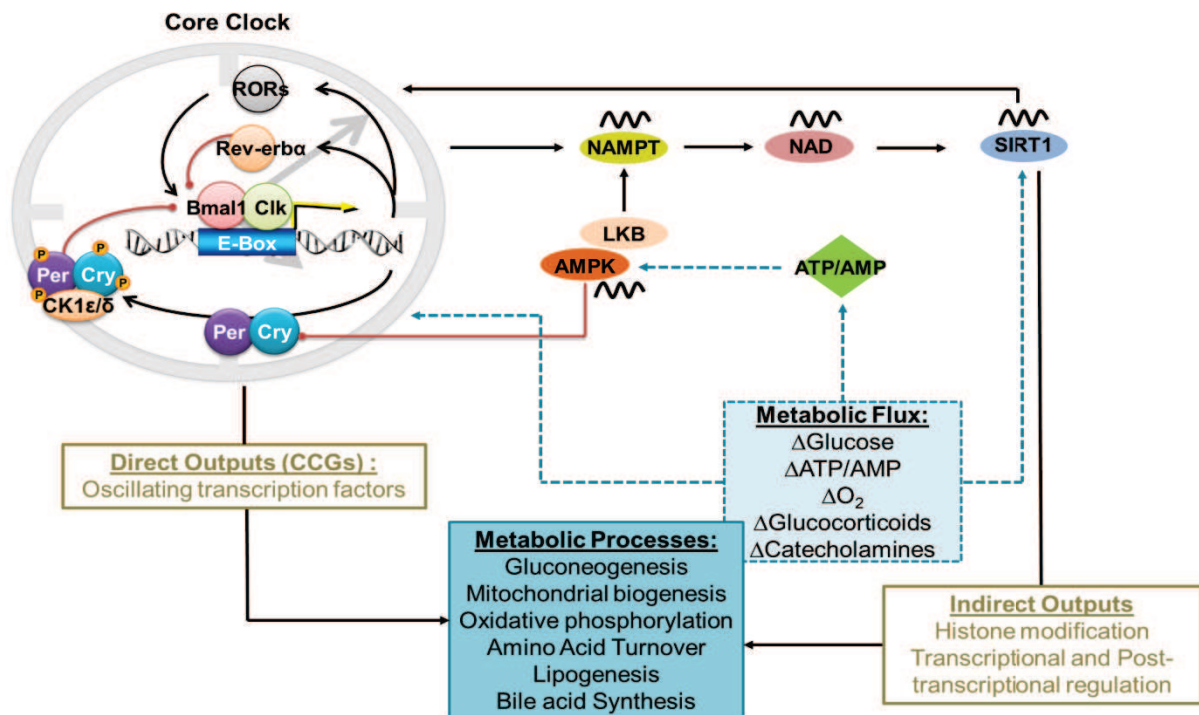


Figure 6: The circadian clock and metabolism converge.

The core clock requires the transcription- translation feedback loop (TTFL) that synchronizes diverse metabolic processes through both direct and indirect outputs, including oxidative metabolism. Reciprocally, inputs from the byproducts of metabolism processes (e.g. NAD^+ , ATP/AMP) are transferred back to the clock through nutrient signaling pathways (including SIRT1 and AMPK) which act as rheostats to couple metabolic flux with daily cycles of sleep/ wakefulness and fasting/ feeding, especially in peripheral tissues. NAMPT, nicotinamide phosphorribosyltransferase; SIRT1, Sirtuin 1; AMPK adenosine monophosphate-dependent protein kinase; LKB, serine–threonine kinase liver kinase (adapted from [61]).

Over the last years, a growing body of evidence highlighted that metabolic byproducts (e.g.: NAD^+ , ATP) display 24 h oscillation and can in turn regulate the clock. Thus it has become clearer that the relationship between the clock machinery and metabolism is not only unilateral but reciprocal. One of the earliest study supporting the concept that metabolism can affect the clock machinery investigated the role of cellular redox translated by the couple $NAD^+/NADH$ and $NADP^+/NADPH$ [72]. When the oxidized forms (NAD^+ and $NADP^+$) are predominant, the DNA binding of the Clock:BMAL1 and NPAS2:BMAL1 heterodimers is strongly diminished whereas the reduced forms enhance. Interestingly, these observations can be nicely correlated with observations made in human red blood cells where transcription is not required for circadian oscillations in, and non-transcriptional events such as redox state changes seem to be sufficient to sustain cellular circadian rhythms [19, 20]. The most known byproduct is nicotinamide adenine dinucleotide (NAD^+) which is, among others, involved in cellular redox reactions as key cofactors. Importantly, recent data reveal that NAD^+ produced

by the salvage pathway oscillates in a circadian manner in peripheral tissues such as liver and adipose tissue, even when animals are maintained in constant darkness [73-75]. The circadian biosynthesis of NAD^+ in mammals relies on the activity of the rate-limiting enzyme nicotinamide phosphoribosyltransferase (NAMPT) whose its expression is controlled by CLOCK–BMAL1 activator complex in conjunction with NAD^+ - activated SIRT1, a histone deacetylase involved to the translation from the cellular energy states to chromatin remodeling.

The activation of AMPK (adenosine monophosphate-dependent protein kinase) by the variation of ratio ATP/AMP, key metabolites, is central for the transmission of nutrient and energy-dependent signals to the molecular clock (review in [16]). It has been reported that when AMP levels are elevated, structural changes in AMPK, a nutrient sensor, enhance phosphorylation by liver kinase B1 (LKB1), resulting in regulation of circadian rhythm, energy metabolism and gene expression in isoform- and tissue-specific manners [76]. Then AMPK can directly modulate the core clock machinery by phosphorylation of the clock repressor proteins CRY and PER, targeting them for proteasomal degradation (for detailed mechanisms see section A.1. Clock genes and clock machinery) [77, 78].

Although extensive evidence shows a tight and mutual connection between the clock and the metabolism, the implication of the mitochondrion which is yet at the crossroad of cellular metabolism is only starting to arise. Reports on circadian oscillations in mitochondrial dynamics started surfacing last year first in macrophages [79] and more recently in liver [80]), but the underlying molecular mechanisms by which these changes occur remain mostly elusive.

B. Keeping mitochondria in shape: a matter of life and death

Present in almost all eukaryotes cells (except in erythrocyte), mitochondria are highly dynamic organelles that participate in energy conversion, metabolism, intracellular signaling, cell migration and synaptic plasticity [81, 82]. To fulfill their multiple tasks, mitochondrial network come in varied morphologies and ultrastructures to ensure the energy supply, stored in the form of adenosine triphosphate (ATP), by oxidative reactions from nutritional sources [83, 84]. While mitochondria are essential for cell survival, the mitochondrial network participates actively to apoptotic signaling pathways through release of a stream of harmful compounds such as reactive oxygen species (ROS) [85].

1. Mitochondria: powerhouses of the cell

Unlike any other organelle, except for chloroplasts, mitochondria are thought to have originated from an endosymbiosis accompanied by gene transfers when a nucleated cell engulfed an aerobic prokaryote about 1.5 billion years ago [86]. Owing to their ability to generate ATP through respiration, they became a driving force in the evolution [87]. Consequently, several characteristics sustain the endosymbiotic theory making mitochondria unique (Figure 7).

1.1. Mitochondrial features

Mitochondria are rod-shaped organelles characterized by a double-membrane organization which divides the mitochondrion in four compartments, distinct in appearance and in composition, thus determining the biochemical function of each compartment (Figure 7). These compartments or regions include the outer membrane (OMM), the intermembrane space (IMS), the inner membrane (IMM), and mitochondrial matrix.

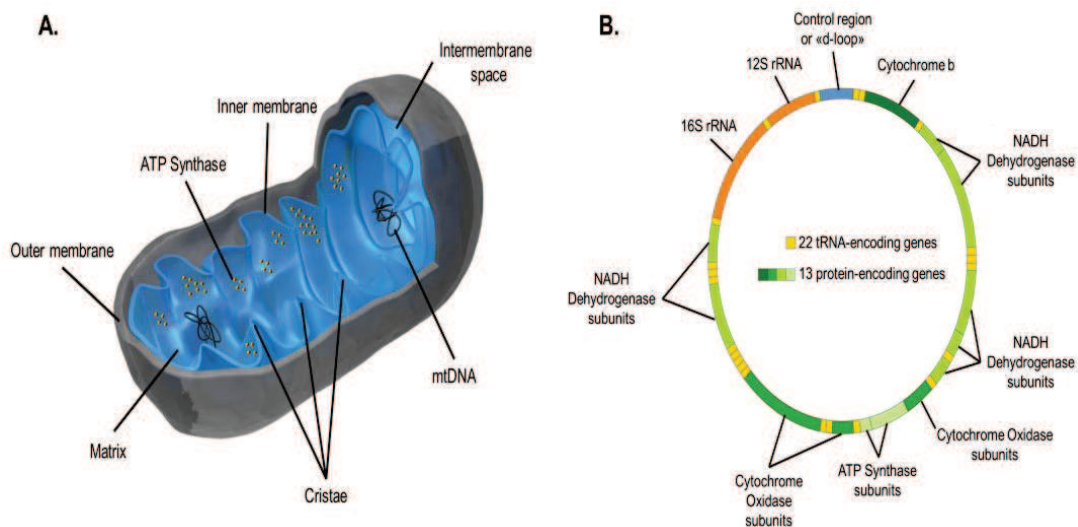


Figure 7: Mitochondrion, unique organelle.

(A) Diagram of mitochondrion showing the inner and outer membranes, the matrix, the circular mitochondrial DNA (mtDNA) and the folded cristae. **(B)** Schematic representation of the mammalian mitochondrial genome (16,569 bp). Mitochondrial DNA encodes 22 tRNA genes (light-orange), two ribosomal RNA genes (dark-orange) and 13 genes encoding polypeptides of complex I (ND1-ND6), complex III (cytB), complex IV (COX1-3) and complex V (ATP6/8) (Courtesy of F. Wanner and adapted from [88])

The porous OMM fully encompasses the IMM, with the IMS in between. The OMM is widely permeable due to the high presence of many protein-based pores that are big enough to allow the passage of ions and molecules as large as a small protein (up to 5000Da) [89]. In opposition to the permeable OMM, the IMM does not contain porin, thus this membrane is

highly impermeable to the stream of small molecules and ions, much like the plasma membrane of the cell [90]. The IMM houses numerous proteins involved in apoptosis such as cytochrome c [91] and apoptosis-inducing factor (AIF) [92], in the electron transport chain and ATP synthesis as well as in mitochondrial fusion and fission [93, 94]. The presence of numerous folds, also called cristae, provides a large amount of surface area of the IMM, enhancing its ability to produce ATP. Finally, the mitochondrial matrix, which is surrounded by the IMM, contains a wide range of enzymes for metabolic pathways including the tricarboxylic acid (TCA) cycle, also known as the Krebs cycle or citric acid cycle and the beta-oxidation of fatty acids which generates acetyl CoA that enters the TCA cycle [95, 96].

Although most of a cell's DNA is contained in the cell nucleus, the mitochondrion has its own independent genome and the machinery to manufacture their own RNAs and proteins in the mitochondrial matrix (Figure 7). Each mitochondrion possesses 2-10 copies of mitochondrial DNA (mtDNA) [97]. The mtDNA copy number as well as the number mitochondria per cells vary depending on the energy requirements: tissues with a high capacity to perform aerobic metabolic functions such as brain or skeletal muscle will have a larger number of mitochondria [98]. The mtDNA is a circular double-stranded DNA inherited solely from the mother in most species, including humans, and is organized into compact particles named nucleoids [99]. The human mtDNA encodes 37 genes including 13 genes which are integrated into the inner mitochondrial membrane, along with proteins encoded by nuclear genes, to achieve the mitochondrial respiratory capacity. It comprises 7 of 46 subunits of complex I (ND1, 2, 3, 4, 4L, 5 and 6), one of 11 subunit of complex III (cytochrome b (Cyt b)), 3 of 13 subunits of complex IV (Cytochrome c oxidase (COX) I, II and III), 2 of 17 subunits of complex V (ATPase 6 and ATPase 8). Subunits of complexes I, III, IV and V are encoded by both mtDNA and nDNA, while subunits of complex II is solely originates from nDNA (nucleoids). In addition, the mitochondrial genome contains the genes encoding for 2 rRNAs (12S and 16S) and 22 tRNAs (one-letter code) required for intramitochondrial protein synthesis [97]. Unlike nDNA, mtDNA lacks histones [100] making it more susceptible to injury, such as oxidative stress [101], and its mutation rate is about 10-fold higher than that of nDNA [102], especially in tissues with a high ATP demand like the brain. Because both nDNA and mtDNA are essential to mitochondrial function, it is not surprising that a disruption of both nuclear and mitochondrial genes may therefore result in (pathological) alterations in mitochondrial function leading to aging and mitochondrial diseases once a certain threshold ("threshold effect") is reached [103].

1.2. Mitochondrial respiratory capacity

Although mitochondria house many biosynthetic and major enzymatic systems, ATP is the major energy currency molecule of the cell. More than 90% of our cellular energy is synthesized within the mitochondria through two metabolic pathways: the Krebs cycle (TCA) and the oxidative phosphorylation system (OxPhos) (Figure 8).

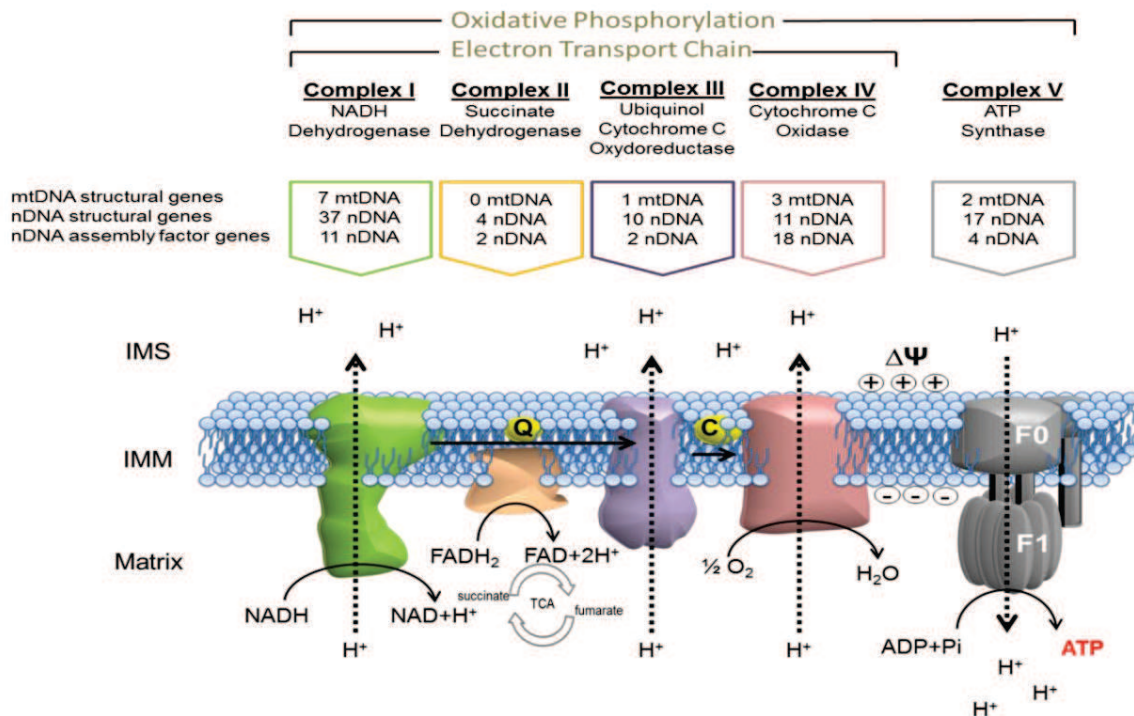


Figure 8: The mammalian oxidative phosphorylation system (OxPhos).

Complexes I (NADH:ubiquinone oxidoreductase) and II (succinate dehydrogenase, belongs to the tricarboxylic acid cycle called TCA) receive electrons from NADH and $FADH_2$ respectively. Electrons are then driven from complexes by the mobile carrier molecules coenzyme Q/ubiquinone (UQ) and cytochrome c (Cyt c) to the final acceptor, molecular oxygen (O_2). Transfer of electrons along ETC maintains the membrane potential via proton pumping into the IMS. The resulting proton gradient is harvested by complex V to generate ATP. The number of protein subunits encoded by mitochondrial (mtDNA) and nuclear (nDNA) genomes are indicated. mtDNA, mitochondrial DNA; nDNA, nuclear DNA; IMS, intermembrane space; IMM, inner mitochondrial membrane. (adapted from [97])

Once the cytosolic glycolytic reactions are completed to break down one molecule of glucose, the two produced pyruvate molecules cross the mitochondrial membrane into the matrix where they can be catabolized to acetyl-CoA which then enters the citric acid cycle (TCA or Krebs cycle), resulting in the generation of two molecules of ATP and the cofactors nicotinamide adenine dinucleotide (NADH) and flavin adenine dinucleotide ($FADH_2$). These two compounds ensure the transport of free energy via electron into the mitochondrial respiratory machinery (OxPhos).

Also known as the mitochondrial respiratory chain, the last step in cellular respiration is composed of the electron transport chain (ETC) consisting of four multisubunit protein complexes (complex I to IV) as well as the F1F0-ATP synthase (complex V) inserted in the IMM with an enrichment in the cristae. It was demonstrated that these complexes can assemble into supramolecular assemblies called “supercomplexes” or respirasomes [104]. The five complexes are functionally connected by mobile electron acceptors and donors: ubiquinone and cytochrome c. The electrons are also transferred along the ETC in a series of oxidation reduction steps via cytochromes, iron-sulfur clusters and copper centres. Briefly, electrons carried away from the TCA by NADH and FADH₂ are used to power complex I (NADH dehydrogenase) and complex II (Succinate dehydrogenase) respectively. These electrons are then passed freely through the IMM by coenzyme Q/ubiquinone (UQ) from both complexes to complexes III (Ubiquinol cytochrome c oxidoreductase). Cytochrome c eventually transports the electrons from complex III to IV (Cytochrome c oxidase) leading to the conversion of oxygen to water. It has been estimated that about 90% of mammalian oxygen consumption is mitochondrial, which primarily serves to synthesize ATP, although in variable levels according to the tissue considered and the organism’s activity status [105]. As electrons are carried along the ETC, protons are translocated from the matrix into the IMS resulting to the generation of a proton electrochemical gradient across the IMM. Two components define the proton electrochemical gradient: a difference in the concentration of protons (ΔpH , alkaline inside) and a difference in the electrical potential (negative inside: $\Delta\psi$: -150 to -180 mV). This redox energy is finally used by the F1F0-ATP synthase. ATP synthase has been first described as rotary molecular motor by John Walker and Paul Boyer, (review in [106]) where F0 is the transmembrane element ferrying the protons from the matrix back to the IMS to power the rotor activity of F1, the catalytic component, where one ATP is synthesized with each turn via the addition of inorganic phosphate (Pi) to ADP. The net gain of OxPhos is typically 32 ATPs from one molecule of glucose.

2. Mitochondria: paradoxical organelles

When mitochondria fulfill their physiological function, it is as if Pandora’s box has been opened, as this vital organelle contains potentially harmful proteins and biochemical reaction centers; mitochondria are the major producers of reactive oxygen species (ROS) at the same time being susceptible targets of ROS toxicity [107] (Figure 9).

Although approximately 90% of O₂ utilized by the cells is reduced to water during ATP generation, O₂ can instead react with a small portion of electrons (up to 2%) escaping the ETC, mostly at complex I and III, and is incompletely reduced to give the superoxide radical (O₂^{•-}) which can be converted into other ROS such as hydrogen peroxide (H₂O₂) and the

highly reactive hydroxyl radical (OH^\cdot) through enzymatic and non-enzymatic reactions [108, 109]. Besides ETC as the major source, ROS can be generated by peroxisomes as well as a variety of cytosolic enzymes systems (e.g. xanthine oxidase, mitochondrial monoamine oxidase (MAOA and MAOB), nitric oxide synthase (NOS), and NADPH oxidase) [110].

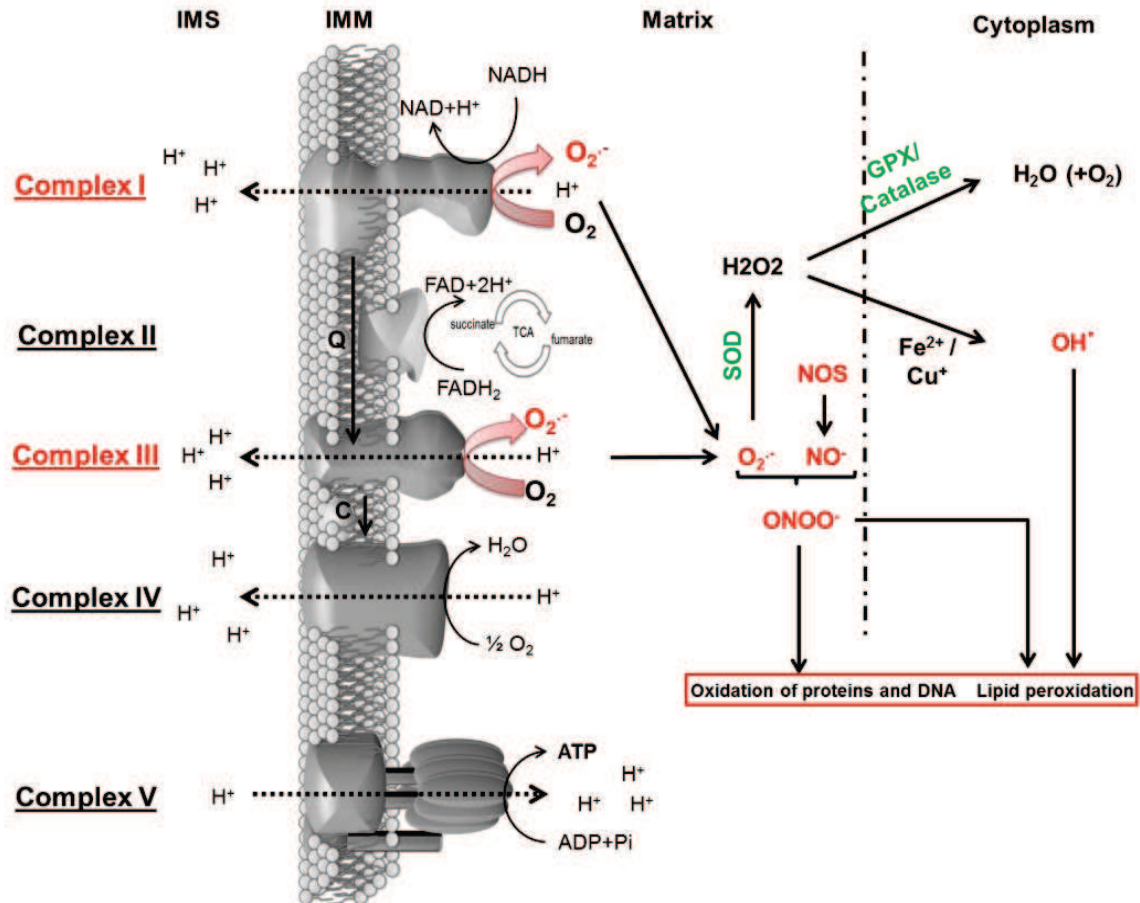


Figure 9: Pathways of reactive oxygen species (ROS) generation and their enzymatic detoxification.

Complexes I and III generate superoxide anion radical ($\text{O}_2^{\cdot-}$) during the electron transfer process. $\text{O}_2^{\cdot-}$ can interact with NO, produced by nitric oxide synthase (NOS), to generate peroxynitrite (ONOO^-). The enzymatic activity of mitochondrial manganese superoxide dismutase (SOD) converts $\text{O}_2^{\cdot-}$ to hydrogen peroxide (H_2O_2), which may then diffuse to the cytoplasmic compartment where glutathione peroxidase (GPX) and catalase convert H_2O_2 to H_2O . H_2O_2 can interact with Fe^{2+} or Cu^+ to generate hydroxyl radical (OH^\cdot), a highly reactive free radical, that can induce as well as ONOO^- , lipid peroxidation and oxidative damage to proteins and DNA. Of note, NO and its derivatives (reactive nitrogen species or RNS) belong also to the group of ROS.

Given the reactivity and toxicity of ROS at high levels, cells are equipped with endogenous antioxidants regulatory strategies to counteract excessive ROS (Figure 9). First, $\text{O}_2^{\cdot-}$ is detoxified to H_2O_2 by manganese superoxide dismutase (MnSOD) or copper/zinc superoxide dismutase (Cu/Zn SOD) and then to water by glutathione peroxidase (GPX) or catalase (CAT) [111]. Interestingly, it has been found that the redox state of the ETC as well

as the proton electrochemical gradient $\Delta\psi$ are major determinant of ROS production [108] For instance, recent data suggest that neuronal UCP proteins by regulating mitochondrial biogenesis, calcium flux, free radical production and local temperature [112], may reduce ROS production.

When the endogenous antioxidant systems are overwhelmed, unstable ROS are capable of damaging many types of mitochondrial components; this includes oxidative deterioration of mtDNA, lipids of the mitochondrial membrane, and mitochondrial proteins, and it is thought that this damage that may accumulate over time from ROS generated from aerobic respiration may play a significant role in aging [113]. Moreover, it was previously demonstrated that nitrosative stress evoked by increased nitric oxide synthesis also leads to protein oxidation as well as mitochondrial and DNA damage, which are common mechanisms occurring in the elderly [107]. All in all, oxidative damages of the mitochondrial compounds lead to a shutdown of energy production [114], which in turn, leads to a depletion of antioxidant defense (e.g. GSH) and the enhancement of ROS triggering the vicious cycle of oxidative stress, mitochondrial dysfunction and apoptosis.

Whereas ROS have been traditionally thought of as toxic metabolic byproducts that cause cellular damage, a constant growing body of evidence highlights the role of ROS in cellular signaling regulating various cellular events such as proliferation, differentiation, metabolic adaptation and the regulation of adaptive and innate immunity [115, 116] (for details see section B.3.3. *Biological functions of mitochondrial dynamics*).

3. From mitochondria to mitochondrial network

Once perceived as solitary structures, mitochondria are now recognized as highly mobile along cytoskeletal tracks and dynamic organelles that continually fuse and divide [117] (Figure 10). Mitochondrial dynamics comprise all processes relating to the biogenesis, subcellular distribution and correct spatial recruitment, as well as the defined morphology of this organelle. The control and maintenance of mitochondrial dynamics requires a tight regulation by three large GTPases and their interacting factors. These mediators constitute the core machinery of mitochondrial dynamics which is well conserved from yeast to mammals (Figure 11).

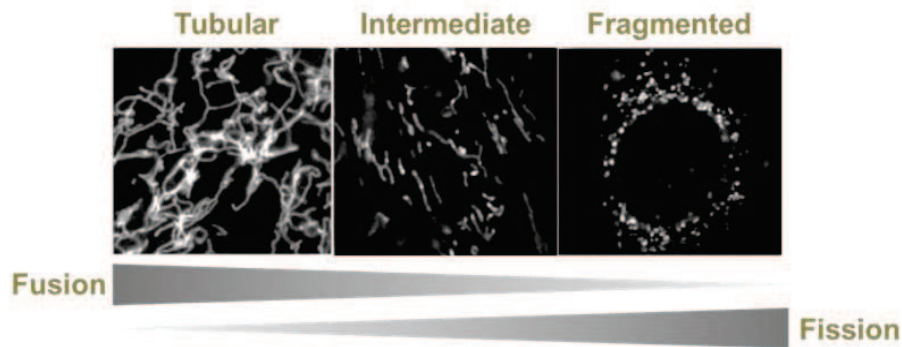


Figure 10: Different shapes of the mitochondrial network.
(adapted from [118])

Moreover, the balance between fission and fusion rates varies in response to metabolic, cellular and environmental changes in order to maintain the bioenergetic homeostasis [118-120]. For instance, a shift towards fusion favours a tubular network which is beneficial in metabolically active cells. In contrast, quiescent cells have numerous small spherical mitochondria which are often referred as fragmented network. At cellular level, mitochondrial dynamics has been connected to several functions including mtDNA stability, respiratory capacity and apoptosis [121, 122]. Because of these functions, mitochondrial dynamics play a central role in the quality control of mitochondria and therefore, even mild defects can lead to disease [123].

3.1. Mitochondrial fusion

In mammals, the core mitochondrial fusion machinery consists of three large GTPases named mitofusins (MFN1/2) and optic atrophy 1 (OPA1) (Figure 11). Mitofusins 1 and 2 are transmembrane GTPase proteins of 741 and 757 residues, respectively [124]. Both mitofusins are characterized by a GTPase domain associated to a coiled-coil domain (also name heptad repeat domain) in the NH₂-terminal part to ensure the GTP binding. A second heptad repeat domain in the COOH-terminal side is required for the first step of the mitochondrial fusion, namely, the tethering of two adjacent mitochondria through a dimeric antiparallel coiled-coil structure. Although MFN1 is exclusively present in the OMM, it has been reported that MFN2 is also located in the endoplasmic reticulum (ER) and controls ER morphology and its tethering with mitochondria [125].

OPA1 is a transmembrane dynamin-related GTPase protein of 960 to 1015 amino acids, located in the mitochondrial intermembrane space in soluble forms or is tightly attached to the IMM [124]. Whereas OPA1 sequence presents similar functional domains as mitofusins, OPA1 contains an NH₁-terminal mitochondrial targeting sequence enriched in

positively charged amino acids which confer the mitochondrial localization of OPA1 and a region that is alternatively spliced (exons 4, 4b and 5b, 149-208 amino acids). Because of differential RNA splicing and protein processing, OPA1 can be processed from 8 distinct splice precursors into a long isoform or a short isoform. Although, under physiological conditions, the membrane fusion requires a combination of both long and short isoforms, the long isoform alone appears to be sufficient to enhance mitochondrial fusion under stress conditions [126].

Since mitochondria have double membranes, mitochondrial fusion is a two-step process, where the outer and inner mitochondrial membranes fuse by sequential events [127]. First, MFN1 and MFN2 on the outer membrane of adjacent mitochondria form complexes *in-trans* that bring the opposing OMM to within approximately 100 Å of each other and tether mitochondria together [128]. This event induces outer-membrane fusion, followed by fusion of the inner membrane mediated by OPA1. Manipulation of mitochondria *in vitro* demonstrated that the fusion events are depending of GTP content and of mitochondrial membrane potential (MMP). Under limiting GTP concentrations, only the fusion of the OMM occurs and dissipation of the MMP disrupts the OMM fusion but not the IMM membrane fusion [129].

Targeted deletion of any of the three fusion genes results in embryonic lethality, a dramatic reduction of mitochondrial fusion activity, impaired mitochondrial functions such as oxidative metabolism and disturbance in mitochondrial axonal transport [124]. Consequently, mutations in MFN2 or OPA1 are responsible for several human diseases such as obesity, Type 2 diabetes, Charcot-Marie-Tooth type 2A and autosomal dominant optic atrophy (review in [124]).

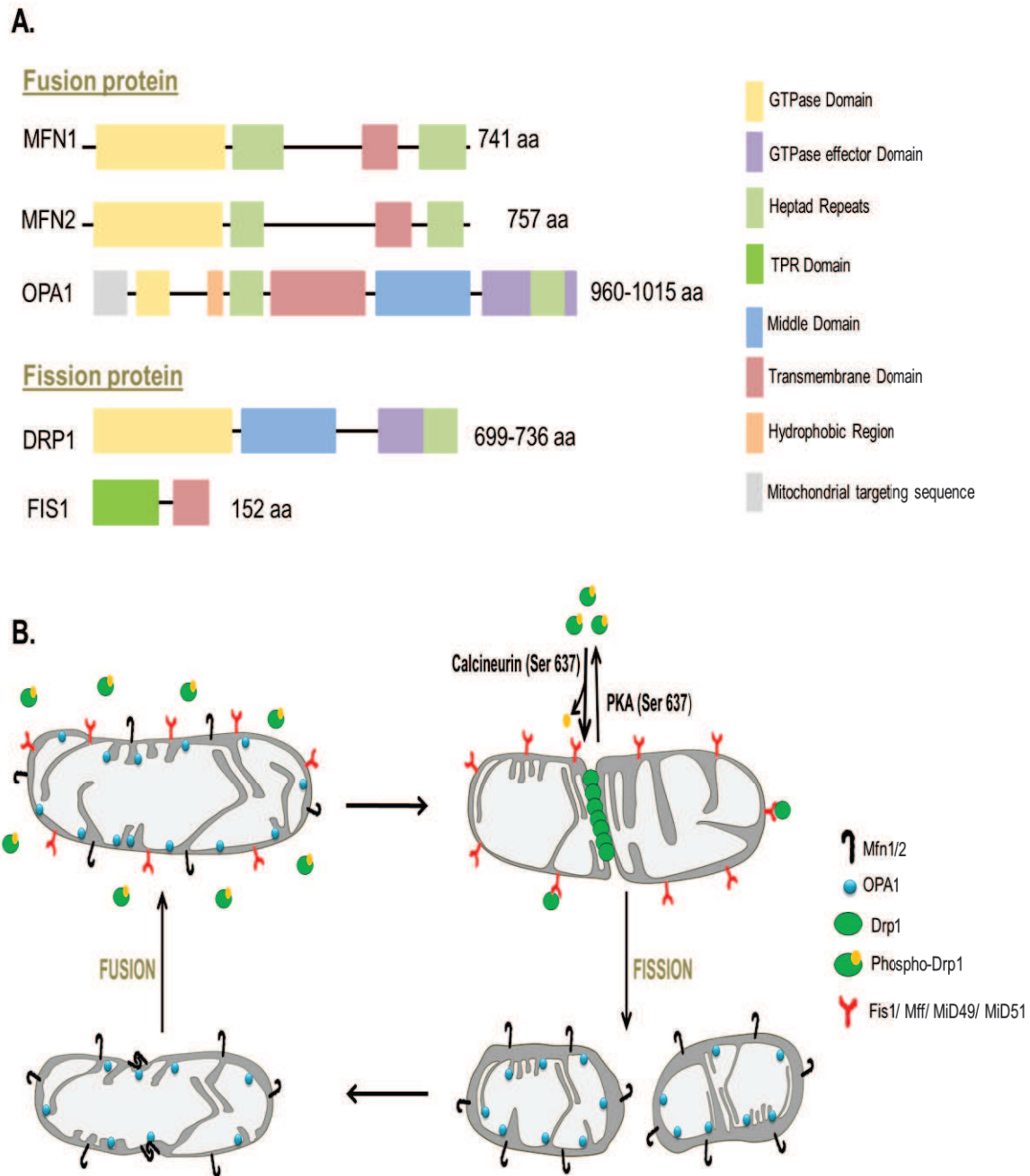


Figure 11: The core machinery of mitochondrial dynamics in mammals.

(A) Schematic of main molecules involved in mitochondrial fusion and fission. The lengths of human proteins (numbers of amino acids) are indicated. Proteins are not drawn to scale. (B) Mitochondrial fusion is a highly regulated process that requires the coordination of both the inner mitochondrial membrane (IMM) and the outer mitochondrial membrane (OMM). The OMM uses proteins such as mitofusin 1 and mitofusin 2 (MFN1/2), which are GTPase proteins, whereas the IMM uses optic atrophy 1 (OPA1) to coordinate the joining of the membrane. Mitochondrial fission factor (Mff) and Fission-1 (FIS1) are anchored to the outer mitochondrial membrane where they recruit cytosolic Drp1, which then oligomerises and forms a ring-like structure around the mitochondria to constrict and divide them into multiple smaller mitochondria. TPR, tetratricopeptide repeat.

3.2. *Mitochondrial fission*

The main factor for controlled noncytokinetic mitochondrial division is a member of the conserved dynamin large GTPase superfamily covering diverse membrane fission functions termed DRP1 in mammals [130] (Figure 11). The typical dynamin domains of mammalian DRP1 (isoform 3, 699 residues) consist of multiple motifs including GTPase, middle and GTPase effector domains that are important for both intramolecular and intermolecular interactions. This isoform is broadly expressed in the organism including skeletal muscle, heart, kidney and liver with high to low levels of expression [124]. Interestingly, the brain is known to express a specific isoform derived from the insert of 37 amino acids by alternative splicing of DRP1 mRNA (isoform 1, 736 residues) [124]. Under normal conditions, the localization of DRP1 is predominantly cytoplasmic, but an extensive pool of this protein is also associated to the OMM into spiral structures ringing the organelle, which, upon GTP hydrolysis, becomes constricted, thereby facilitating mitochondrial scission [130]. DRP1 is recruited to the mitochondrial membrane by receptor-like receptors including FIS1 and mitochondrial fission factor (Mff) on the OMM [131] (Figure 11). Surprisingly, Fis1 inhibition by RNA interference does not disrupt the mitochondrial localization of DRP1 [132], whereas knockdown of Mff reduces the amount of DRP1 that is recruited to mitochondria [133], suggesting that Mff may play a dominant role in mitochondrial fission.

Although the exact mechanism remains mostly unresolved, multiple posttranslational modifications, including phosphorylation, ubiquitination and sumoylation, have been implicated in the regulation of DRP1 function and thereby of various activities during mitochondrial fission [120, 134]. For instance, three distinct phosphorylation sites have been described with contrary effects on fission activity (review in [120]). Cyclin B-dependent kinase promotes mitochondrial fission during mitosis through DRP1 phosphorylation at residue Ser585 whereas DRP1 phosphorylation at residue Ser637 through cAMP-dependent kinase (PKA) is thought to inhibit GTPase activity thereby promoting fusion. Calcineurin is the phosphatase responsible for the dephosphorylation of Ser637. The third site has been only reported in the Drp1 isoform 3 which is phosphorylated at residue Ser600 by the Ca²⁺/calmodulin-dependent protein kinase Ia upon the induction of a calcium influx.

Inhibition of DRP1 function, either by expression of a dominant-negative variant or RNA interference, results in very elongated mitochondria that entangle and collapse [130, 132]. Because DRP1 is essential for embryonic development and synapse formation, targeted deletion of DRP1, as for the three fusion genes, results in embryonic lethality due to abnormal brain development (review in [122]).

3.3. Biological functions of mitochondrial dynamics

During mitochondrial life, the shape, length and number of mitochondria are regulated by functional connection existing between mitochondrial dynamics and mitochondrial turnover comprising mitochondrial biogenesis and the segregation of impaired mitochondria by mitophagy [135]. These events are related to mitochondrial quality control in order to limit mitochondrial damage and ensure the integrity of a healthy mitochondrial population within the cells but also the integrity of the cell itself [136] (Figure 12).

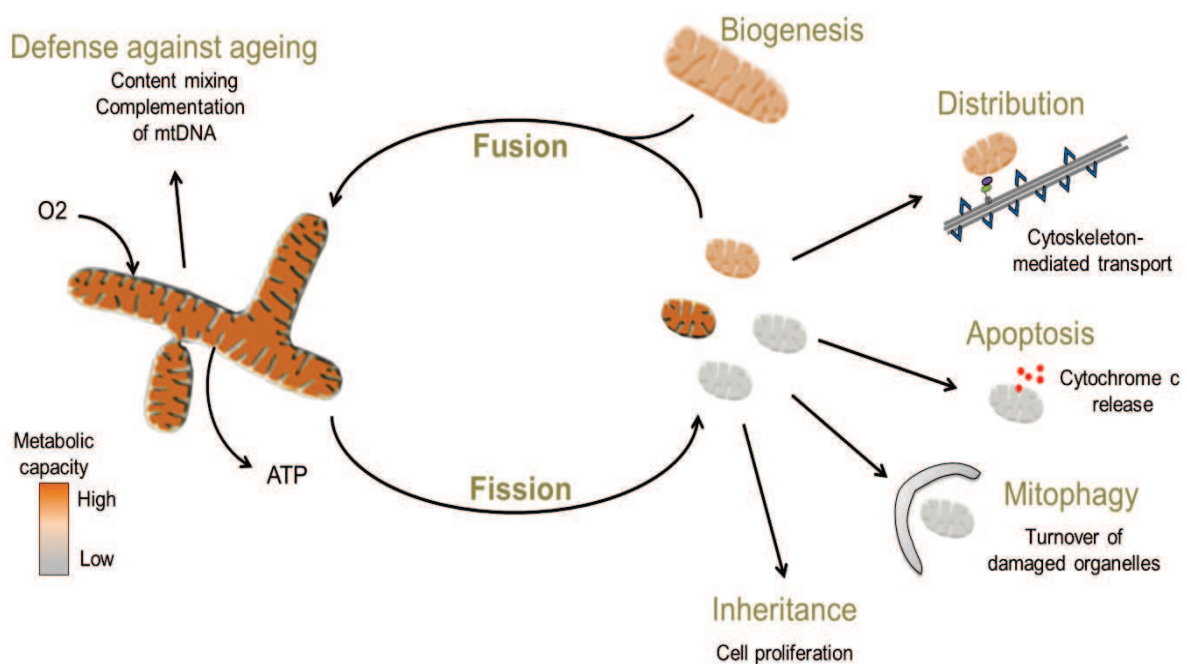


Figure 12: Biological functions of mitochondrial dynamics.

The mitochondrial life cycle begins with growth and division of pre-existing organelles (biogenesis) and ends with selective sequestration and subsequent degradation of the dysfunctional or surplus mitochondrion by mitophagy (adapted from [115, 118]).

When mitochondria fuse with each other under normal condition, the outer membranes, the inner membranes and the intramitochondrial contents including mtDNA and metabolic byproducts (e.g. ATP, NAD⁺) are exchanged to unify the mitochondrial compartment which allows the complementation of contents from healthy and dysfunctional mitochondria (e.g. containing mtDNA with ROS-induced mutations) (review in [137, 138]). However a complete fusion is not always necessary. Mitochondrial fusion assays using photoactivatable green fluorescent protein indicate that organelles can undergo exchange of contents necessary for proper functioning while maintaining a desired morphology [139]. This

type of fusion event has been termed “kiss-and run”. The high frequency of such content exchange events implies that they are functionally important.

In contrast to fusion, mitochondrial division frequently generates two uneven daughter organelles. While one maintains an intact mitochondrial membrane potential (high MMP) and is able to re-fuse with the mitochondrial network, the second might be depolarized with a low respiration activity, depleted of OPA1 as well as high accumulation of mtDNA ROS-induced mutations, thereby preventing further cycles of fusion and subsequently leading to mitophagy [140-142]. In addition to the control of mitochondrial shape, fusion and fission are also important for the bioenergetic function of mitochondria [143, 144]. Fibroblasts that lack both MFN1 and MFN2 have reduced respiratory capacity, and individual mitochondria show great heterogeneity in shape and membrane potential. Cells that lack OPA1 show similar defects, with an even greater reduction in respiratory capacity [145, 146].

The changes in the shape of mitochondrial network are also believed to affect the ability of cells to distribute their mitochondria to specific subcellular locations correlated to the specific bioenergetic requirements of the cell. This function is especially important in highly polarized cells, such as neurons (review in [147]). When DRP1 function is disrupted in neurons, it results in drastically reduced numbers of synaptic and dendritic mitochondria and, as a consequence, disruption of sustained neurotransmission and dendritic morphogenesis, respectively [148, 149].

Along with the important consequences for mitochondrial integrity, mitochondrial morphology transitions have been described to be involved in retrograde signaling pathways through the production and release of metabolic byproducts from mitochondria to the cytoplasm and nucleus [118]. Retrograde signaling including calcium ions, ROS, ATP/ADP/AMP and NAD⁺/NADH is believed, at least under certain physiological states, to trigger adaptive cellular responses orchestrated by activating nutrient or redox sensors to coordinate changes in gene expression [150, 151]. While mitochondrial morphology transitions, via their effect on intracellular signaling pathways, can significantly impact cellular function and survival, other byproducts are involved in the initiation of apoptosis (review in [152]). Cells undergoing extensive network fragmentation resulting from disruption of mitochondrial fission are more susceptible to apoptotic cell death through mechanisms possibly involving the mitochondrial permeability transition pore (mPTP) by regulating the release of intermembrane-space proteins (e.g. cytochrome c, calcium ions) into the cytosol [84, 132].

A growing body of evidence revealed an interesting functional connection between the machinery of mitochondrial dynamics and other organelles such as the endoplasmic

reticulum and peroxisomes in order to coordinate their activities in common such as steroid production and beta-oxidation of fatty acids, respectively [153, 154].

While mitochondrial dynamics are fundamental processes necessary for the health and the functional state of mitochondria, it becomes clear that the integration of mitochondrial shape changes into other cellular pathways is critically important for cellular function. Of note, a major unsolved issue is to understand how the bidirectional relationship between mitochondrial dynamics and the rest of cell is precisely coordinated in health. This point is particularly challenging in the explication of many pathological cases (e.g. Alzheimer's disease, Parkinson's disease) in order to establish clear cause-effect relationship.

4. Circadian clock regulation of mitochondrial functions

Because of the close-fitting relationship between circadian rhythms and metabolism, it has been suggested that numerous mitochondrial functions may be regulated remotely or closely by the circadian clock, and therefore possibly may serve as the pivotal constituent in the interplay between the clock and cellular energy metabolism [155].

With the emergence of the -omics technology (metabolomic, transcriptomic, genomic and proteomic), circadian databases provide evidences supporting circadian oscillations in mitochondrial functions in various tissues from mice including the SCN and the liver [156]. It has been reported that mRNA of several nuclear-encoded mitochondrial proteins involved in mitochondrial oxidative phosphorylation as well as key bioenergetic parameters (e.g.: mitochondrial membrane potential, cytochrome c oxidase activity and Ca^{2+} homeostasis) display circadian oscillations [17, 157, 158]. Together, these findings support the concept of temporal organization of mitochondrial metabolism and bioenergetics within important brain regions.

Accumulating evidence also supports circadian and/or diurnal oscillations in mitochondrial energy metabolism and associated oxidative pathways in peripheral tissues (review in [159]). Nevertheless, the underlying mechanism of the contributions of the molecular clock in mitochondrial functions remains mostly unclear. To better understand the molecular interplay, emerging data have been performed using tissues, cells and/ or isolated organelles from mice deficient in core clock components [160]. Outstandingly it is suggested that the mitochondrial metabolism seems rather to be controlled in a multilevel manner by the biological clock, including both transcriptional and post-transcriptional mechanisms. Furthermore, it has been reported that the clock transcription feedback loop produces cycles of NAD^+ biosynthesis which in turn influence mitochondrial oxidative function through

modulation of rhythmic mitochondrial protein acetylation [160]. This rhythmicity of acetylation event is related to the circadian activation of the mitochondrial NAD⁺-dependent deacetylase sirtuin 3 (SIRT3). In support of, several reports show a correlation between circadian alterations in liver metabolome and differentially acetylated mitochondrial proteins supporting the idea that the circadian clock regulates mitochondrial energy metabolism, in part, by a nontranscriptional mechanism (e.g.: acetylation) [161]. SIRT3 can also activate or repress transcription of genes regulated by peroxisome proliferator-activated receptor gamma coactivator 1 α (PGC-1 α), a master regulator of mitochondrial biogenesis suggesting a circadian control of the mitochondrial biogenesis (review in [159, 161]).

Although compelling evidence arises regularly that normal mitochondrial respiratory chain function and bioenergetics are dependent on the molecular clock to meet daily fluctuations in cellular energy demands, the implication of the clock remains unresolved in the cellular mitochondrial network (governed by mitochondrial fusion and fission) considering that alterations in mitochondrial dynamics also impact cellular bioenergetics. Thus, perturbations in the circadian clock may be a key initiating factor in diseases linked to mitochondrial impairment such Alzheimer's disease.

C. Mitochondrial dysfunction: Aging, Amyloid β , and tau – a deleterious trio

AD is the most common neurodegenerative disorder among elderly individuals. It accounts for up to 80% of all dementia cases and ranks as the fourth leading cause of death among those above 65 years of age [162]. With the increasing average life span of humans, it is highly probable that the number of AD cases will dangerously rise since aging is the primary risk factor for major human pathologies, including cancer, diabetes, cardiovascular disorders, and neurodegenerative diseases [163]. The pathology of AD characterized by abnormal formation of amyloid plaques (aggregates of amyloid- β [$A\beta$]) and neurofibrillary tangles (NFT; aggregates of tau) was shown to be accompanied by mitochondrial dysfunction. However, the mechanisms underlying this dysfunction are poorly understood. Within the past few years, several cell culture models as well as single, double and, more recently, triple transgenic mouse models have been developed that reproduce diverse aspects of AD. These models help in understanding the pathogenic mechanisms that lead to mitochondrial failure in AD, and in particular the interplay of AD-related cellular modifications within this process [107, 164].

1. Etiological factors and clinical symptoms

AD is a progressive, neurodegenerative disorder, characterized by an age-dependent loss of memory and an impairment of multiple cognitive functions [165]. From a histopathological point of view, AD encompasses reduced synaptic density, neuronal loss in selected brain areas, as well as A β -containing plaques and neurofibrillary tangles (NFTs) (Figure 13). Interestingly, positron emission tomography (PET) measurements demonstrate reduced energy metabolism in affected brain regions of AD patients and suggest that a cellular energy deficit may precede cognitive symptoms [166] (Figure 13). In addition, mood disorders and behavioral abnormalities such as circadian disruption are frequently associated with aging, depressive disorders and Alzheimer's disease (AD). Nevertheless, a complete diagnosis is achieved only during post-mortem examination where the presence of A β -containing plaques and NFTs is confirmed in the brain region involved in learning and memory.

From a genetic point of view, AD can be classified into two different forms: rare familial forms (FAD) where the disease onset is at an age below 60 years (< 1% of the total number of AD case) and the vast majority of sporadic AD cases where onset occurs at an age over 60 years [167]. Genetic studies in FAD patients have identified autosomal dominant mutations in three different genes, encoding the APP (over 20 pathogenic mutations identified) and the presenilins PS1 and PS2 (more than 130 mutations identified) [168]. These mutations are directly linked to the increased production of A β from its precursor protein APP, suggesting a direct and pathological role for A β accumulation in the development of AD.

Although NFTs are a major hallmark in AD, mutations in the microtubule-associated protein tau (MAPT), protein responsible of NFTs formation, have not been yet linked to AD. Nevertheless, genetic studies showed that patients with fronto-temporal dementia (FTD) with Parkinsonism carry mutations linked to chromosome 17 (FTDP-17) [168]. Overall the findings that, in the FAD and FTDP, the genes encoding the proteins that are deposited in plaques and NFTs (APP and MAPT, respectively) are mutated suggested a causal role for these proteins in disease and led to generation of transgenic animal models with the aim to better understand the underlying mechanisms in the initiation and progression of the pathology.

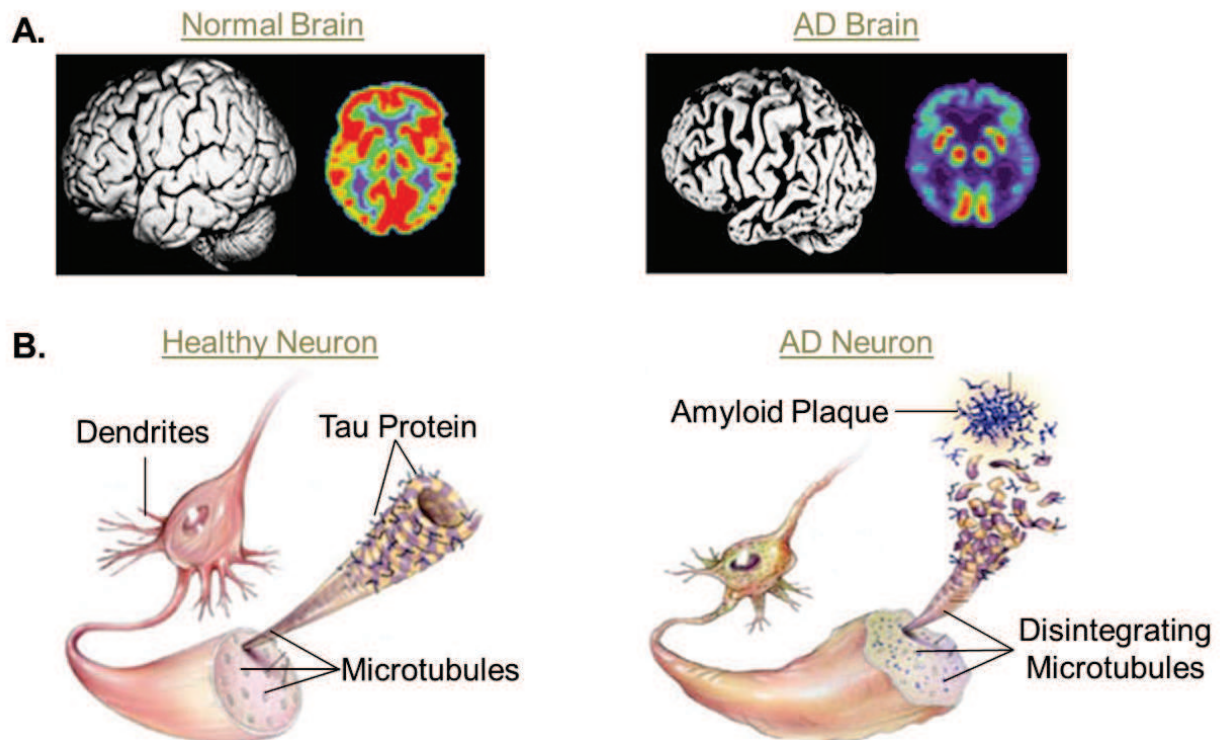


Figure 13: The pathology of Alzheimer's disease.

(A) In comparison to normal brain (left panel), AD results in shrinkage of brain regions involving in learning and memory combined with major reductions in cellular energy metabolism in living patients (right panel: AD brain picture and Positron Emission Tomography). (B) The pathology of AD is characterized by two histopathological hallmarks: abnormal formation of amyloid plaques (aggregates of amyloid- β [$A\beta$]) and neurofibrillary tangles (NFT; aggregates of hyperphosphorylated tau) resulting in dysfunctional neuron and thus neurodegeneration (adapted from [166]).

2. Histopathological Alzheimer's Disease related-features

Histopathologically, the brain of AD patients displays two hallmark lesions: extracellular $A\beta$ -containing plaques and intracellular neurofibrillary tangles made of abnormally hyperphosphorylated tau [169, 170].

2.1. Cleavage pathway of APP and $A\beta$ deposits

According to the first description of a “peculiar substance” by Alois Alzheimer, extensive evidence suggests that extracellular deposits composed of peptides of 39–43 amino acids called amyloid beta ($A\beta$) protein play a pivotal role in the pathogenesis of AD. $A\beta$ is derived from a larger precursor transmembrane protein called amyloid precursor protein (APP) (Figure 14.A.). Although still elusive, the role of APP has been suggested to be critical in neuron growth, survival, synaptic plasticity, cell adhesion and post-injury repair [171, 172]. APP is a type 1 integral 110–130 kDa glycoprotein, from 695 to 770 amino acids, with a large extracellular glycosylated amino-terminus, a shorter cytoplasmic carboxy-terminus and is partly inserted through its $A\beta$ fragment in the plasma membrane as well as in

several organelles, such as endoplasmic reticulum (ER), Golgi apparatus, and possibly mitochondria [173]. APP can be proteolytically processed by α -, β - and γ -secretases involved in two pathways: a nonamyloidogenic pathway and an amyloidogenic pathway.

The non-amyloidogenic pathway is initiated by three enzymes (ADAM 9, ADAM10 and ADAM17) belonging to ADAM family, a disintegrin- and metalloprotease- family enzyme with α -secretase activity. The cleavage occurs in the middle of the $A\beta$ sequence, and results in two fragments: sAPP α (secreted ectodomain of APP) and a C-terminal small membrane-anchored fragment (C83). The APPs α fragment is secreted and acts as a neurotrophic protein, whereas the CTF α is subsequently internalized and degraded by γ -secretase, a multimeric complex of the presenilin proteins PS1 and PS2, nicastrin, anterior pharynx defective 1, and presenilin enhancer 2, to form a short fragment termed p3 and $A\beta$ intracellular cytoplasmic domain (AICD) [168, 173]. Furthermore, α -secretase is involved in the nonamyloidogenic pathway by cleaving APP within the $A\beta$ domain, thus precluding $A\beta$ formation. The amyloidogenic pathway involves sequential cleavages by β -secretase (BACE-1) and γ -secretase (presenilins) and leads to release of neurotoxic $A\beta$ peptides and AICD. BACE-1 initially mediates the cleavage of APP at a position located 99 amino acids from the C-terminus, forming a 99 amino acid membrane-anchored fragment termed C99 and β APPs. While β APPs is released into the extracellular space, C99 is subsequently cleaved by γ -secretase producing $A\beta$ and AICD. Since the γ -secretase can cleave C99 between residues 38 and 43, $A\beta$ peptides released exist in varying length. In healthy individuals, the predominant full-length $A\beta$ peptide produced by brain cells throughout life is $A\beta$ 40 whereas the more amyloidogenic form $A\beta$ 42 is merely generated at a ratio of 10:1 [174, 175]. Interestingly, $A\beta$ 42 is more hydrophobic [176] and therefore is more readily to aggregate and form fibrils and induce neurotoxicity than the shorter form [177]. Nevertheless, in AD, both $A\beta$ variants may form oligomeric aggregates, protofibrils and fibrils which eventually deposit as plaques. Although $A\beta$ under the form of monomer does not appear toxic, the oligomer form has been described as the earliest pathological and toxic form by acting on oxidative stress, impairing the Ca^{2+} homeostasis and synaptic plasticity, driving to neuronal death [166, 178].

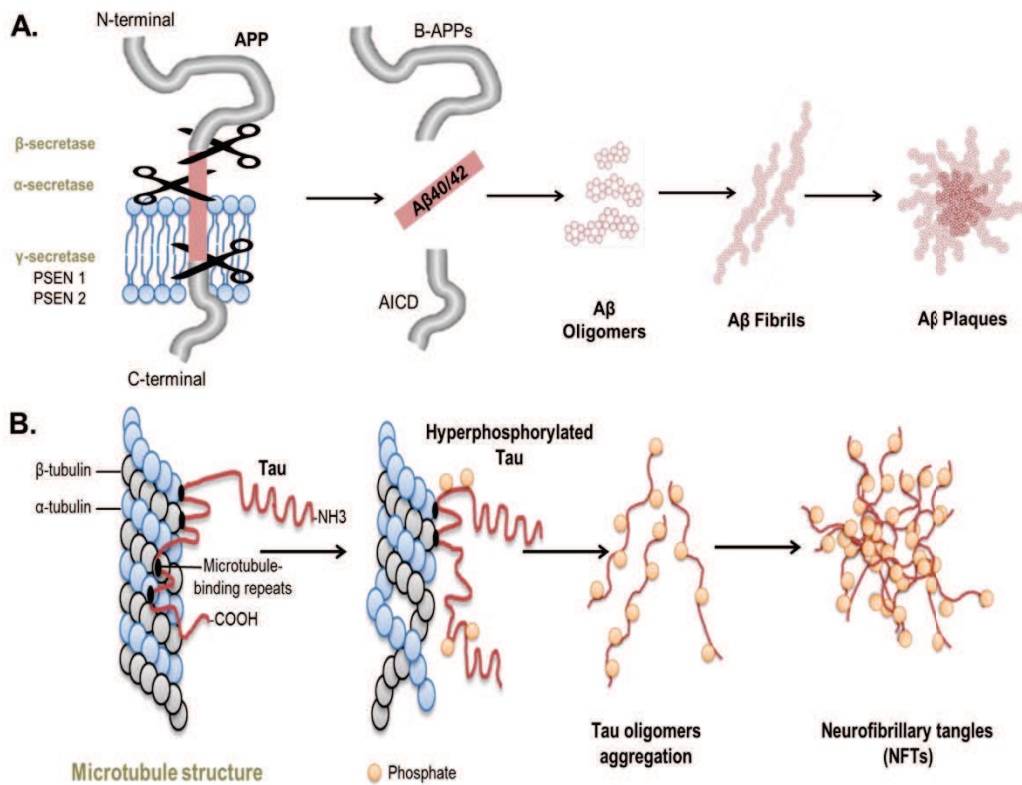


Figure 14: APP processing and tau phosphorylation.

(A) The amyloid- β ($A\beta$) peptide is derived by proteolytic cleavage from the amyloid precursor protein (APP). To liberate the $A\beta$ species, APP must undergo two sequential endoproteolytic steps that are mediated by distinct enzymatic activities known as β - and γ -secretase. The first cleavage releases an ectodomain (β APPs), and the last 99 amino acids of APP (C99) remains within the membrane. C99 is subsequently cleaved by γ -secretase complex, which generates $A\beta$ 40 and $A\beta$ 42 as well as AICD. (B) In AD, abnormally hyperphosphorylated tau contributes to a destabilized microtubule network, impaired axonal transport, and ultimately in neurofibrillary tangle (NFT) formation and neuronal death.

2.2. Phosphorylation of tau and development of neurofibrillary lesions

Alois Alzheimer observed in the brain of his original patient a second lesion which co-occurs with $A\beta$ plaques. But unlike $A\beta$ deposits, this protein aggregates were present intraneuronally. In the late 1980s, it was discovered that they are composed of abnormally hyperphosphorylated microtubule-associated protein tau [179, 180] (Figure 14.B.).

Human tau proteins belong to the family of microtubule-associated protein (MAP) that promote the assembly and the stabilization of the microtubular network, essential for normal axonal transport, cell polarity and shape as well as for normal crosstalk between mitochondria, cytoskeletal elements and plasma membrane [181]. Under physiological conditions, tau is predominantly localized to the axon for stabilization of microtubule, although partially present in soma but almost totally absent in dendrites.

Structurally, human tau proteins consist of a heterogeneous combination of six isoforms ranging from 50 to 70kDa and from 352 to 441 residues [182]. The isoforms are

derived by alternative mRNA splicing from a single gene (16 exons) located on chromosome 17. Tau is also a phosphoprotein owing to its high numbers of phosphorylation sites (almost 20% of the molecule, mostly due to high frequency of serine and threonine residues). Moreover its open structure affords easy access to many kinases including glycogen synthase kinase-3 β (GSK-3 β), cyclin-dependent kinase 5 (cdk5), extracellular signal-regulated kinase 2 (ERK2), protein kinase A and C, calcium-calmodulin dependent protein kinase II (CaMKII), and mitogen-associated protein affinity-regulating kinases (MARK) (review in [183]).

As consequence of a high rate of easy accessible phosphorylation sites near the regions of the microtubules binding domains, tauopathies including AD and FTDP-17 are commonly distinguished by the hyperphosphorylation of tau combined with conformational changes that results in the dissociation of tau from microtubules, causing them to depolymerize, while tau is deposited in aggregates such as neurofibrillary tangles (NFTs). Indeed, hyperphosphorylated tau has been shown to interfere with neuronal functions, such as mitochondrial respiration and axonal transport which eventually lead to neurodegeneration [170]). While no mutations in the gene encoding tau have been identified in patients with AD, the phosphorylation rate in AD brains was shown to be three- to four- fold higher compared to normal human brains.

3. Age-related A β and tau effects on mitochondria in AD.

Aging is an inevitable biological process that results in a progressive structural and functional decline, as well as biochemical alterations that altogether lead to reduced ability to adapt to environmental changes. Although aging is almost universally conserved among all organisms, the molecular mechanisms underlying this phenomenon still remain unclear. There are several theories of aging, in which free radical (oxidative stress), DNA, or protein modifications are suggested to play the major causative role [184, 185]. A growing body of evidence supports mitochondrial dysfunction as a prominent and early, chronic oxidative stress-associated event that contributes to synaptic abnormalities in aging and, ultimately, increased susceptibility to age-related disorders including Alzheimer's disease (AD) [186]. A growing body of evidence supports that, on the one hand, mitochondrial decline observed in brain aging is a determinant and early chronic oxidative stress-associated event in the onset of AD and, on the other hand, the close interrelationship of this organelle with A β and tau is crucial in the pathogenic process underlying AD contributing to synaptic abnormalities and, ultimately, selective neuronal degeneration in AD (Figure 15).

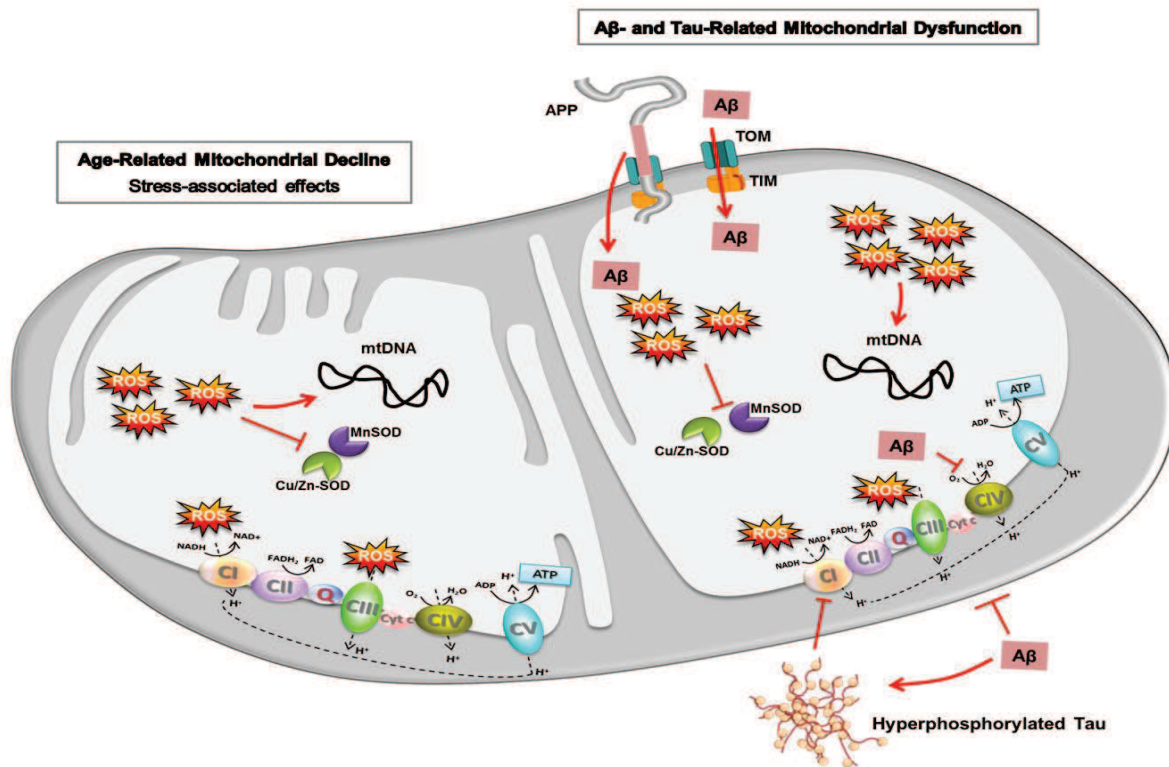


Figure 15: Aging, Amyloid-Beta and tau: toxic consequences on mitochondria.

The aging process may weaken the mitochondrial OxPhos (oxidative phosphorylation) system in a more general way by the accumulation of ROS-induced damage over many years thereby sowing the seeds for specific and destructive effects of Aβ and tau. ROS induce peroxidation of several mitochondrial macromolecules, such as mtDNA and mitochondrial lipids, contributing to mitochondrial impairment in the mitochondrial matrix. In AD, mitochondria were found to be a target of Aβ toxicity, which may act directly or indirectly on several proteins, leading to mitochondrial dysfunction. Indeed, Aβ was found in the OMM and IMM as well as in the matrix. The interaction of Aβ with the OMM might affect the transport of nuclear encoded mitochondrial proteins, such as subunits of the ETC CIV, into the organelle via the TOM import machinery. Aβ seems to be able to enter into the mitochondrial matrix through TOM and TIM or could be derived from mitochondria-associated APP metabolism. The interaction of Aβ with the IMM would bring it into contact with respiratory chain complexes with the potential for myriad effects on cellular metabolism. It may be that Aβ by these interactions affects the activity of several enzymes decreasing the ETC enzyme CIV, reducing the amount of hydrogen that is translocated from the matrix to the intermembrane space, thus impairing the MMP. The dysfunction of the ETC leads to a decreased CV activity and so to a lower ATP synthesis, in addition to an increased ROS production. Interestingly, deregulation of CI is mainly tau dependent, while deregulation of CIV is Aβ dependent, at both the protein and activity level. Aβ, amyloid-β; AD, Alzheimer's disease; APP, amyloid precursor protein; CI, complex I; CII, complex II; CIII, complex III; CIV, complex IV; CV, complex V, Cu/Zn-SOD, copper/zinc superoxide dismutase; cyt c, cytochrome c; ETC, electron transport chain; IMM, inner mitochondrial membrane; MMP, mitochondrial membrane potential; MnSOD, manganese superoxide dismutase; mtDNA, mitochondrial DNA; OMM, outer mitochondrial membrane; ROS, reactive oxygen species; TIM, translocase of the inner membrane; TOM, translocase of the outer membrane. (adapted from [107]).

3.1. *Mitochondrial aging—the beginning of the end in AD?*

As mentioned above, within the cell, metabolism is a highly dynamic process where mitochondrial network is a prominent actor in regulation of both energy metabolism and apoptotic pathways. Although commonly termed as ‘powerhouses of cells’, mitochondria are rather paradoxical organelles by being major sources of ROS and at the same time being susceptible targets of ROS toxicity (see section B.2. Mitochondria: paradoxical organelles). Therefore, it is believed that accumulation of ROS-induced damages within the cells may contribute significantly in aging [187-189]. Given that mtDNA is more susceptible to ROS-induced damages, especially in tissues with a high ATP demand like the brain and muscles [184, 190, 191], it has been described that accumulation of ROS-related mtDNA mutations can eventually result in the synthesis of mutant ETC proteins that, in turn, can lead to the leakage of more electrons and increased ROS production. This so-called “vicious cycle” is hypothesized to play a critical role in the aging process according to the mitochondrial theory of aging. However, age-associated change in mtDNA abundance seems to be tissue specific, as several studies have reported no change in mtDNA abundance with age in other than muscular tissues in both man and mouse [192, 193]. Many investigators have developed models for studying mitochondrial-related aging [194]. Among them senescence-accelerated mice (SAM) strains are especially useful models to understand the mechanisms of the age-related mitochondrial decline (review in [107]). In addition to behavioral studies showing deficits in learning and memory, several research groups highlighted an age-related impairment of mitochondrial functions including a decrease of COX activity, mitochondrial ATP content, as well as a dysbalance of the protective antioxidant machinery inside mitochondria at a relatively early age [195-200]. Besides the progressive mitochondrial decline and increased oxidative stress, an age-related increase in mRNA and protein levels of amyloid- β precursor protein (APP), followed by formation of amyloid plaques, as well as tau hyperphosphorylation were also observed at an early age in the brain of SAMP8 mice [201-203]. Altogether, these data indicate that mitochondrial dysfunction is a highly relevant event in the aging process, which is also known as the primary risk factor for AD and other prevalent neurodegenerative disorders.

3.2. *Separate modes of A β and tau toxicity on mitochondria*

Mitochondria were found to be a target for APP toxicity as both the full-length protein and A β accumulate in the mitochondrial import channels, and both lead to mitochondrial dysfunction [204-207]. Several evidences from cellular and animal AD models indicate that A β triggers mitochondrial dysfunction through a number of pathways such as impairment of OxPhos, elevation of ROS production, interaction with mitochondrial proteins, and alteration of mitochondrial dynamics followed by mitochondrial depletion from axons and dendrites and,

subsequently, synaptic loss [164, 173].

Using neuronal PC12 cells and neuroblastoma cells SH-SY5Y overexpressing APP, several studies demonstrated that the extensive expression of APP leads to an enhanced mitochondrial impairment counting impaired mitochondrial respiration followed by a decrease in ATP generation, impaired MMP and complex IV activity in correlation with an increase of ROS content (review in [164]). When intracellular A β production is prevented by a γ -secretase inhibitor, this restores nitric oxide and ATP levels, indicating a direct involvement of A β in these mechanisms. In addition, A β toxicity to native SH-SY5Y neuroblastoma was assessed by iTRAQ quantitative proteomics where numerous proteins, a quarter of which are involved in mitochondrial function and energy metabolism, were deregulated, indicating the key role of A β toxicity in the onset of mitochondrial dysfunction [208].

From the first APP mice model (called PDAPP) bearing the human “Indiana” mutation of the APP gene (V171F) established in 1995 [209] to the most aggressive models, double-transgenic APPS/L/PS1 (APPSwedish/London/PS1M141L) mice [210, 211], success in developing single and double transgenic mouse models that mimic the amyloid pathogenesis has greatly facilitated the understanding of physiopathological mechanisms underlying AD (review in [107, 164]). Interestingly, although each transgenic model is different in the mutation construction, they all displayed an age-related amyloid plaques formation combined with cognitive deficits as well as mitochondrial dysfunction including mitochondrial membrane potential, decreased complex IV activity, depletion of ATP content and antioxidant defense mechanisms as well as an escalation of oxidative stress.

Since mitochondrial function relies heavily on its morphology and distribution (see section A.3), alterations of which have been increasingly implicated in neurodegenerative diseases, such as AD. Indeed, abnormal mitochondrial dynamics have been identified in sporadic and familial AD cases [212, 213] as well as in AD mouse model [214]; a distortion probably mediated by altered expression of dynamin-like protein 1 (DRP1), regulator of mitochondrial fission and distribution, due to elevated oxidative and/or A β -induced stress. This modification can disturb the balance between fission and fusion of mitochondria in favor of mitochondrial fission followed by mitochondrial depletion from axons and dendrites and, subsequently, synaptic loss [213].

In its hyperphosphorylated form, tau, which forms the NFTs, the second hallmark lesion in AD, has been shown to block mitochondrial transport, which results in energy deprivation and oxidative stress at the synapse and, hence, neurodegeneration [215-217]. Based on the mutation in MAPT observed in FTD with Parkinsonism, a robust mouse model for tau pathology was created in 2001 [218]. The P301L tau-expressing pR5 mice (longest

four-repeat 4R2N) are characterized by an age-related occurrence of NFTs but also display several mitochondrial impairments. A mass spectrometric analysis of the brain proteins from these mice revealed mainly a deregulation of mitochondrial respiratory chain complex components (including complex V), antioxidant enzymes, and synaptic protein space [219]. The functional analysis demonstrated age-related mitochondrial dysfunction, together with reduced NADH ubiquinone oxidoreductase (complex I) activity as well as age-related impaired mitochondrial respiration together with depleted ATP content in pR5 mice model. Mitochondrial dysfunction was also associated with higher levels of ROS and the upregulation of antioxidant enzymes in response to oxidative stress in aged transgenic mice. Thus, this evidence demonstrated for the first time that not only A β but also tau pathology leads to metabolic impairment and oxidative stress by distinct mechanisms from that caused by A β in AD. Although A β impacts the mitochondrial dynamics in favor of mitochondrial fission, expression of human tau results in abnormal elongated mitochondrial architecture and distribution in cellular model as well as in both drosophila and mouse neurons [181, 220, 221]. Furthermore, mitochondrial shape imbalance was consistent with impairment of mitochondrial function including substantial complex I deficit accompanied by decreased ATP levels and increased susceptibility to oxidative stress [222].

Overall, these evidences highlighted new insights on the potential role of tau in disruption of mitochondrial dynamics and subsequently in mitochondrial metabolism observed in AD. Since not only A β but also tau pathology act on mitochondrial network integrity by distinct mechanisms in AD, both hallmarks should be investigated together in order to understand the likely interplay between them involved in the AD pathogenesis.

3.3. *Synergistic modes of A β and tau toxicity on mitochondria*

Although A β and tau pathologies are both known hallmarks of AD, the question whether these two molecules could synergistically affect mitochondrial integrity have remained unresolved until recently. Several studies suggest that A β aggregates and hyperphosphorylated tau may block the mitochondrial carriage to the synapse leading to energy deficiency and neurodegeneration [223]. Remarkably, intracerebral A β injections amplify preexisting tau pathology in several transgenic mouse models [224-226], whereas lack of tau abrogates A β toxicity [170, 216]. Consistent with the *in vivo* evidence, incubation of isolated mitochondria from pR5 mice with either oligomeric or fibrillar A β species caused an impairment of the mitochondrial membrane potential and respiration [227]. While both oligomeric and fibrillar A β species are toxic, they exert different degrees of toxicity on mitochondria – aged-related mitochondrial sensitivity to oligomeric species being more significant.

Additionally, in recent years triple transgenic mouse models have been established that combine $A\beta$ and tau pathologies. In these models the contribution of both AD-related proteins on the mitochondrial respiratory machinery and energy homeostasis has been investigated *in vivo* (review in [107]). In a novel triple transgenic mouse model (pR5/APP_{Sw}/PS2 N141I)—the ^{triple}AD mouse, mitochondrial dysfunction was investigated using proteomics followed by functional validation [228]. Particularly, deregulation of activity of complex I was found to be tau dependent, whereas deregulation of complex IV was $A\beta$ dependent, in 10-month-old ^{triple}AD mice. The convergent effects of $A\beta$ and tau led already at the age of 8 months to a depolarization of mitochondrial membrane potential in ^{triple}AD mice. Additionally, age-related oxidative stress also plays a significant part in the deleterious vicious cycle by exaggerating $A\beta$ - and tau-induced disturbances in the respiratory system and ATP synthesis, finally leading to synaptic failure.

These evidence complement those obtained in another triple transgenic mouse model 3xTg-AD (P301Ltau/APP_{Sw}/PS1 M146L) exhibiting mitochondrial dysfunction including age-related decrease in the activity of regulatory enzymes of OxPhos such as COX, or of the Krebs cycle such as pyruvate dehydrogenase [229, 230]. Importantly, mitochondrial bioenergetics deficits were found to precede the development of AD pathology in the 3xTg-AD mice. Extensive evidences support that AD-specific changes including cognitive impairments, $A\beta$ accumulation, $A\beta$ plaques, and mitochondrial dysfunction seem to occur at an earlier onset from single, double up to triple AD transgenic mice models. Together, the findings highlight the key role of mitochondria in AD pathogenesis and consolidate the notion that a synergistic effect of tau and $A\beta$ enhances the pathological weakening of mitochondria at an early stage of AD.

3.4. *The Alzheimer's disease mitochondrial cascade hypothesis*

Until recently, the leading AD molecular paradigm, the “amyloid- β cascade hypothesis”, was the main pathogenetic model of AD based on studies of rare autosomal dominant variants representing less than 1 % of the AD patients and its role in the majority of sporadic AD cases is unclear. In 2004, Swerdlow and Kahn proposed an alternative paradigm where mitochondria play a prominent role since morphological, biochemical and genetic abnormalities of the mitochondria that have been extensively reported in several AD tissues over the last decade [231, 232] (Figure 16). Accumulation of somatic mtDNA mutation over an individual's lifespan may cause mitochondrial decline leading to energy failure and increased oxidative stress. Eventually, once the age-related mitochondrial decline reaches a threshold, it may affect APP expression and processing as well as accumulation of $A\beta$, which in a vicious cycle may reinforce the mtDNA damage and the oxidative stress. $A\beta$ directly triggers mitochondrial dysfunction through interaction with different mitochondrial

targets including the outer mitochondrial membrane, inter-membrane space, inner mitochondrial membrane, and the matrix (review in [173, 233]). In parallel, A β can influence the rate of hyperphosphorylation of tau and NFTs formation that in turn disturb mitochondrial trafficking and function within the cell. Overall, several vicious cycles are interconnected within a larger vicious cycle where mitochondria play a key role in the cascade of events leading to AD. All of them, once set in motion, amplify their own processes, thus accelerating the development of AD. Finally, the critical role of mitochondria in the early pathogenesis of AD may make them attractive as a preferential target for treatment strategies.

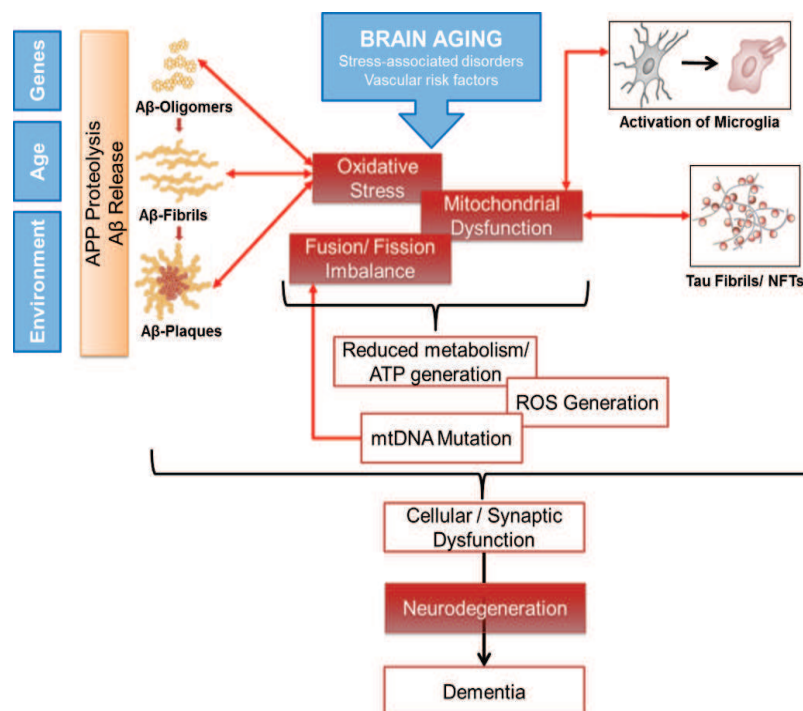


Figure 16: The AD mitochondrial cascade hypothesis.

As age-associated mitochondrial decline progresses, A β production increases and accumulation of A β reinforces in turn mitochondrial dysfunction, ROS production and neurofibrillary tangles (NFT) formation. All the intermediate vicious cycles are interconnected within a larger vicious cycle which amplify their own processes and eventually lead to synaptic failure and neurodegeneration.

4. Mitochondria: potential target of neurosteroids

In 1981, Baulieu and coworkers first demonstrated that steroid production also occurs within the nervous system itself, independently of peripheral glands [234]. In contrast to steroid hormones produced by endocrine glands, this category of molecules was named neurosteroids and defined as neuroactive molecules acting on the nervous system in an auto/paracrine manner. Neurosteroids exhibit several biological functions that are essential during the development as well as in adult brain [235]. Given their ability to easily cross

cellular membrane, neurosteroids can act on nuclear receptors and therefore induce gene transcription. They can also interact with membrane receptors such as GABA_A [236] and NMDA [237] receptors. The subsequent negative or positive allosteric modulation is specific to neurosteroids involved.

Taking place in mitochondria and endoplasmic reticulum (ER), neurosteroidogenesis encompasses several criss-cross biochemical pathways leading to generation of several neurosteroids derived from cholesterol and other blood-borne steroidal precursors. The first step, which is also the limiting step in the production of neurosteroids, is the transfer of molecules of cholesterol from the outer membrane to the inner mitochondrial membrane. The first enzyme, the cytochrome P450 cholesterol side chain cleavage enzyme (P450_{scc}), is located at the inner side of the mitochondrial membrane which permits the conversion of cholesterol to pregnenolone (PREG), precursor of all steroid hormones. PREG is then carried to the ER where the steroid is subsequently converted into neuroactive steroids. Additionally, recent findings demonstrated that mitochondrial fusion precedes and is required for steroid biosynthesis [154]. It has been suggested that mitochondrial fusion, through regulation of MFN2 expression, promotes the association of mitochondria with mitochondria-associated membranes (MAM). This association might then facilitate a non-vesicular traffic of PREG between the two compartments.

In the recent years, compelling evidence has shown that neurosteroids interact with mitochondria to counteract oxidative stress occurring in age-related diseases such as Alzheimer's disease (AD). In particular, estrogen treatment was shown to alleviate mitochondrial deficits including impairment of mitochondrial respiration and enhanced ROS level as well as excitotoxicity caused by imbalance in Ca²⁺ homeostasis, but also to enhance antioxidant defense in humans, animals and cellular models (review in [238]).

More recently, it has been reported that a mitochondrial enzyme named A β -binding alcohol dehydrogenase (ABAD), which is involved in the conversion of estradiol into estrone, is up-regulated in brains of AD mice [239] and AD patients [240]. It has been suggested that ABAD is directly modulated by A β peptide exacerbating mitochondrial dysfunction induced by A β (Figure 17). Moreover, to counteract the A β -ABAD interaction, new treatments with decoy peptide or ABAD-specific compound inhibitor (AG18051) were able to restore mitochondrial deficits (mitochondrial respiration, activity of mitochondrial respiratory complexes and ROS levels) in cellular and animal models [107, 241, 242] (for further details see Appendix D).

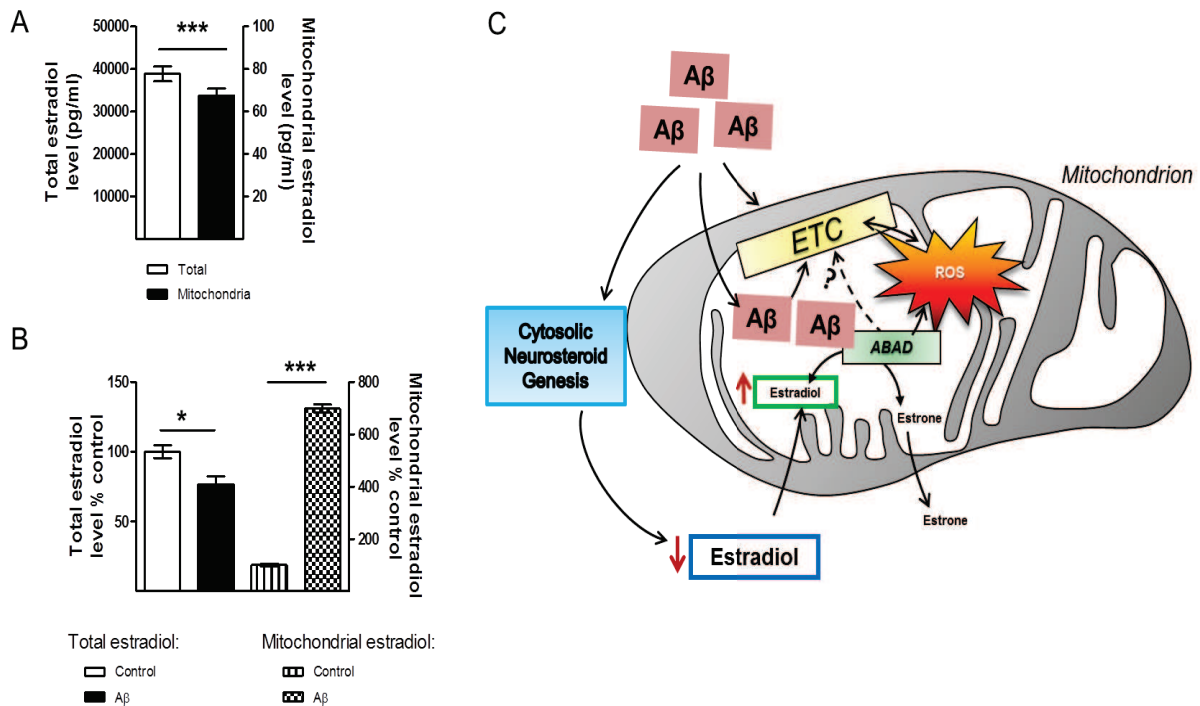


Figure 17: Aβ-ABAD interaction and estradiol level in mitochondria.

(A) Mitochondrial estradiol content is very low compared with total estradiol level in SH-SY5Y neuroblastoma cells. Unpaired t-test, $***p < 0.001$. (B) Estradiol level is differently influenced by Aβ peptide in the cytosol and in mitochondria. Paired t-test, $*p < 0.05$, $***p < 0.0001$. (C) Aβ₁₋₄₂ peptide is able to modulate ABAD function by binding directly to this mitochondrial enzyme. This results in the decrease of ABAD-induced conversion of estradiol into estrone with a concomitant increase of ROS levels and an impairment of the ETC in mitochondria. ABAD, Aβ-binding alcohol dehydrogenase (adapted from [107]) (for further details see Appendix A).

Although the neuroprotective effect of estrogen on mitochondria has been widely investigated, the potential role of other neurosteroids on mitochondria is rather poorly understood. The need to better understand the separate but as well the potential synergistic effects of different neurosteroids on mitochondrial function is considered as an emerging research field in the context of new drug development for AD management.

5. Circadian disruption in aging and AD

Aging is an inevitable biological process that results in a progressive loss of physiological integrity, as well as biochemical alterations that altogether lead to reduced ability to adapt to environmental changes and to increased vulnerability to death. Although aging is almost universally conserved among all organisms, the molecular mechanisms underlying this phenomenon still remain unclear. There are several theories of aging, in which free radical (oxidative stress), DNA, or protein modifications are suggested to play the

major causative role [163, 184, 185]. A growing body of evidence supports mitochondrial dysfunction as a prominent and early, chronic oxidative stress-associated event that contributes to synaptic abnormalities in aging and, ultimately, increased susceptibility to age-related disorders including Alzheimer's disease (AD) [186]. In situations of both physiological and pathological aging such as AD, several lines of evidence indicate an alteration of the circadian machinery, worsened in AD patients, leading to an increased number of nocturnal awakenings, a higher proportion of night-time wakefulness, reduced sleep efficiency and a reduction in rapid eye movement (REM) sleep [243-245]. Recent research suggests that hormonal changes during aging may influence negatively both homeostatic and circadian sleep regulatory [246, 247]. Although basic clock properties (e.g. period length, amplitude and phase) of peripheral cells did not change during aging, when in the presence of human serum from older donors, peripheral cells displayed shortened period length and advanced the phase of cellular circadian rhythms, indicating that a circulating factor might alter human chronotype [246]. Overall these evidences highlighted the bidirectional relationship between aging and daily "circadian" behavior in humans which in the case of disruption may contribute to pathological processes as AD.

In addition to circadian behavioral disruption, AD is associated with the deposition of aggregates named $A\beta$ plaques and neurofibrillary tangles in the brain (for details see section B). Interestingly, Holtzman and colleagues demonstrated that $A\beta$ dynamics is regulated by orexin and the sleep- wake cycle suggesting a key role of the sleep- wake cycle in the $A\beta$ aggregation process in AD [248]. While it is known that progression and worsening of cognitive impairment are paralleled by circadian disturbances in AD patients, the underlying mechanisms of when and how circadian rhythms influence the pathogenesis of AD, particularly the aggregation processes, remain mostly unresolved [249]. Of note, alterations of the circadian rhythms can already be observed in patients with mild AD, exhibiting an increased sleep propensity during daytime. Recent studies suggest that "sleep problems" already correlated with "subjective cognitive slowing" in Mild Cognitive Impairment (MCI) patients [250].

Degeneration of brain nuclei that contain sleep circuits and circadian clock-regulating circuits in the SCN [251], hypothalamus [252], basal forebrain [253] and brainstem [254] is one of the possible causes of sleep defects in patients with neurodegenerative diseases (review in [244]). Furthermore, it is believed that one of the main features of neurodegenerative disease is increased oxidative stress which leads to an increased accumulation of DNA oxidation product causing thus amplification of the processes and eventually synaptic failure and neurodegeneration (see section B. 2. Mitochondria: paradoxical organelles). As mentioned above in section A.3. Circadian rhythms and

metabolism, circadian clock and metabolism are closely linked. Indeed, disruption of the circadian clock leads to numerous defects in metabolism and to the development of metabolic syndromes, which are known to be associated with increased oxidative damage.

Taken together, this evidence of the correlation between neurodegeneration and circadian clock dysfunction raises important question. What comes first and when? The egg or the chicken? Given the AD mitochondrial cascade hypothesis, it is possible that circadian disturbance in both aging and AD belong to its own vicious cycle that amplify its own process along the vicious cycles involved in the AD mitochondrial cascade hypothesis. Of note, given that mitochondrial metabolism was connected, on the one hand, with circadian rhythms and, on the other hand with the pathogenesis of AD, it would be a thrilling challenge to highlight the impending interplay between mitochondrial network, circadian rhythm in both physiological and pathological conditions in order to expand our perspective on the cell biology common to neurodegenerative diseases.

REFERENCES

1. Vaze, K.M. and V.K. Sharma, *On the adaptive significance of circadian clocks for their owners*. Chronobiol Int, 2013. **30**(4): p. 413-33.
2. Albrecht, U., *Timing to perfection: the biology of central and peripheral circadian clocks*. Neuron, 2012. **74**(2): p. 246-60.
3. Albrecht, U., *Orchestration of gene expression and physiology by the circadian clock*. J Physiol Paris, 2006. **100**(5-6): p. 243-51.
4. Brown, S.A., E. Kowalska, and R. Dallmann, *(Re)inventing the circadian feedback loop*. Dev Cell, 2012. **22**(3): p. 477-87.
5. Dardente, H. and N. Cermakian, *Molecular circadian rhythms in central and peripheral clocks in mammals*. Chronobiol Int, 2007. **24**(2): p. 195-213.
6. Gachon, F., et al., *The mammalian circadian timing system: from gene expression to physiology*. Chromosoma, 2004. **113**(3): p. 103-12.
7. Mohawk, J.A., C.B. Green, and J.S. Takahashi, *Central and peripheral circadian clocks in mammals*. Annu Rev Neurosci, 2012. **35**: p. 445-62.
8. Ko, C.H. and J.S. Takahashi, *Molecular components of the mammalian circadian clock*. Hum Mol Genet, 2006. **15 Spec No 2**: p. R271-7.
9. Robinson, I. and A.B. Reddy, *Molecular mechanisms of the circadian clockwork in mammals*. FEBS Lett, 2014. **588**(15): p. 2477-83.
10. Sato, T.K., et al., *A functional genomics strategy reveals Rora as a component of the mammalian circadian clock*. Neuron, 2004. **43**(4): p. 527-37.
11. Akashi, M. and T. Takumi, *The orphan nuclear receptor RORalpha regulates circadian transcription of the mammalian core-clock Bmal1*. Nat Struct Mol Biol, 2005. **12**(5): p. 441-8.
12. Guillaumond, F., et al., *Differential control of Bmal1 circadian transcription by REV-ERB and ROR nuclear receptors*. J Biol Rhythms, 2005. **20**(5): p. 391-403.
13. Preitner, N., et al., *The orphan nuclear receptor REV-ERBalpha controls circadian transcription within the positive limb of the mammalian circadian oscillator*. Cell, 2002. **110**(2): p. 251-60.
14. Gallego, M. and D.M. Virshup, *Post-translational modifications regulate the ticking of the circadian clock*. Nat Rev Mol Cell Biol, 2007. **8**(2): p. 139-48.
15. Akashi, M., et al., *Control of intracellular dynamics of mammalian period proteins by casein kinase I epsilon (CKIepsilon) and CKIdelta in cultured cells*. Mol Cell Biol, 2002. **22**(6): p. 1693-703.
16. Jordan, S.D. and K.A. Lamia, *AMPK at the crossroads of circadian clocks and metabolism*. Mol Cell Endocrinol, 2013. **366**(2): p. 163-9.
17. Panda, S., et al., *Coordinated transcription of key pathways in the mouse by the circadian clock*. Cell, 2002. **109**(3): p. 307-20.
18. Hughes, M.E., et al., *Harmonics of circadian gene transcription in mammals*. PLoS Genet, 2009. **5**(4): p. e1000442.
19. O'Neill, J.S. and A.B. Reddy, *Circadian clocks in human red blood cells*. Nature, 2011. **469**(7331): p. 498-503.
20. O'Neill, J.S., et al., *Circadian rhythms persist without transcription in a eukaryote*. Nature, 2011. **469**(7331): p. 554-8.
21. Moore, R.Y. and V.B. Eichler, *Loss of a circadian adrenal corticosterone rhythm following suprachiasmatic lesions in the rat*. Brain Res, 1972. **42**(1): p. 201-6.
22. Stephan, F.K. and I. Zucker, *Circadian rhythms in drinking behavior and locomotor activity of rats are eliminated by hypothalamic lesions*. Proc Natl Acad Sci U S A, 1972. **69**(6): p. 1583-6.
23. Dibner, C., U. Schibler, and U. Albrecht, *The mammalian circadian timing system: organization and coordination of central and peripheral clocks*. Annu Rev Physiol, 2010. **72**: p. 517-49.
24. Ralph, M.R., et al., *Transplanted suprachiasmatic nucleus determines circadian period*. Science, 1990. **247**(4945): p. 975-8.

25. Ananthasubramaniam, B., E.D. Herzog, and H. Herzog, *Timing of neuropeptide coupling determines synchrony and entrainment in the mammalian circadian clock*. PLoS Comput Biol, 2014. **10**(4): p. e1003565.
26. Ko, C.H., et al., *Emergence of noise-induced oscillations in the central circadian pacemaker*. PLoS Biol, 2010. **8**(10): p. e1000513.
27. Welsh, D.K., et al., *Individual neurons dissociated from rat suprachiasmatic nucleus express independently phased circadian firing rhythms*. Neuron, 1995. **14**(4): p. 697-706.
28. Herzog, E.D., *Neurons and networks in daily rhythms*. Nat Rev Neurosci, 2007. **8**(10): p. 790-802.
29. Le Minh, N., et al., *Glucocorticoid hormones inhibit food-induced phase-shifting of peripheral circadian oscillators*. EMBO J, 2001. **20**(24): p. 7128-36.
30. Bollinger, T. and U. Schibler, *Circadian rhythms - from genes to physiology and disease*. Swiss Med Wkly, 2014. **144**: p. w13984.
31. Sun, Z.S., et al., *RIGUI, a putative mammalian ortholog of the Drosophila period gene*. Cell, 1997. **90**(6): p. 1003-11.
32. Zylka, M.J., et al., *Three period homologs in mammals: differential light responses in the suprachiasmatic circadian clock and oscillating transcripts outside of brain*. Neuron, 1998. **20**(6): p. 1103-10.
33. Plautz, J.D., et al., *Independent photoreceptive circadian clocks throughout Drosophila*. Science, 1997. **278**(5343): p. 1632-5.
34. Zanello, S.B., D.M. Jackson, and M.F. Holick, *Expression of the circadian clock genes clock and period1 in human skin*. J Invest Dermatol, 2000. **115**(4): p. 757-60.
35. Cuninkova, L. and S.A. Brown, *Peripheral circadian oscillators: interesting mechanisms and powerful tools*. Ann N Y Acad Sci, 2008. **1129**: p. 358-70.
36. Tosini, G. and M. Menaker, *Circadian rhythms in cultured mammalian retina*. Science, 1996. **272**(5260): p. 419-21.
37. Balsalobre, A., F. Damiola, and U. Schibler, *A serum shock induces circadian gene expression in mammalian tissue culture cells*. Cell, 1998. **93**(6): p. 929-37.
38. Yamamoto, T., et al., *Transcriptional oscillation of canonical clock genes in mouse peripheral tissues*. BMC Mol Biol, 2004. **5**: p. 18.
39. Gachon, F., et al., *The circadian PAR-domain basic leucine zipper transcription factors DBP, TEF, and HLF modulate basal and inducible xenobiotic detoxification*. Cell Metab, 2006. **4**(1): p. 25-36.
40. Gatfield, D. and U. Schibler, *Circadian glucose homeostasis requires compensatory interference between brain and liver clocks*. Proc Natl Acad Sci U S A, 2008. **105**(39): p. 14753-4.
41. Gachon, F., et al., *Proline- and acidic amino acid-rich basic leucine zipper proteins modulate peroxisome proliferator-activated receptor alpha (PPARalpha) activity*. Proc Natl Acad Sci U S A, 2011. **108**(12): p. 4794-9.
42. Damiola, F., et al., *Restricted feeding uncouples circadian oscillators in peripheral tissues from the central pacemaker in the suprachiasmatic nucleus*. Genes Dev, 2000. **14**(23): p. 2950-61.
43. Korencic, A., et al., *Timing of circadian genes in mammalian tissues*. Sci Rep, 2014. **4**: p. 5782.
44. Balsalobre, A., et al., *Resetting of circadian time in peripheral tissues by glucocorticoid signaling*. Science, 2000. **289**(5488): p. 2344-7.
45. Yagita, K., et al., *Molecular mechanisms of the biological clock in cultured fibroblasts*. Science, 2001. **292**(5515): p. 278-81.
46. Brown, S.A., et al., *Rhythms of mammalian body temperature can sustain peripheral circadian clocks*. Curr Biol, 2002. **12**(18): p. 1574-83.
47. Hirota, T., et al., *Glucose down-regulates Per1 and Per2 mRNA levels and induces circadian gene expression in cultured Rat-1 fibroblasts*. J Biol Chem, 2002. **277**(46): p. 44244-51.

48. Welsh, D.K., et al., *Bioluminescence imaging of individual fibroblasts reveals persistent, independently phased circadian rhythms of clock gene expression*. *Curr Biol*, 2004. **14**(24): p. 2289-95.
49. Brown, S.A., et al., *The period length of fibroblast circadian gene expression varies widely among human individuals*. *PLoS Biol*, 2005. **3**(10): p. e338.
50. Pando, M.P., et al., *Phenotypic rescue of a peripheral clock genetic defect via SCN hierarchical dominance*. *Cell*, 2002. **110**(1): p. 107-17.
51. Bergmann, O.J., S.C. Mogensen, and J. Ellegaard, *Herpes simplex virus and intraoral ulcers in immunocompromised patients with haematologic malignancies*. *Eur J Clin Microbiol Infect Dis*, 1990. **9**(3): p. 184-90.
52. Gamble, K.L., et al., *Circadian clock control of endocrine factors*. *Nat Rev Endocrinol*, 2014. **10**(8): p. 466-75.
53. Duffy, J.F. and D.J. Dijk, *Getting through to circadian oscillators: why use constant routines?* *J Biol Rhythms*, 2002. **17**(1): p. 4-13.
54. Verwey, M., B. Robinson, and S. Amir, *Recording and analysis of circadian rhythms in running-wheel activity in rodents*. *J Vis Exp*, 2013(71).
55. Yoo, S.H., et al., *PERIOD2::LUCIFERASE real-time reporting of circadian dynamics reveals persistent circadian oscillations in mouse peripheral tissues*. *Proc Natl Acad Sci U S A*, 2004. **101**(15): p. 5339-46.
56. Yamazaki, S., et al., *Resetting central and peripheral circadian oscillators in transgenic rats*. *Science*, 2000. **288**(5466): p. 682-5.
57. Nagoshi, E., et al., *Circadian gene expression in individual fibroblasts: cell-autonomous and self-sustained oscillators pass time to daughter cells*. *Cell*, 2004. **119**(5): p. 693-705.
58. Pagani, L., et al., *The physiological period length of the human circadian clock in vivo is directly proportional to period in human fibroblasts*. *PLoS One*, 2010. **5**(10): p. e13376.
59. Brown, S.A., et al., *Molecular insights into human daily behavior*. *Proc Natl Acad Sci U S A*, 2008. **105**(5): p. 1602-7.
60. Eckel-Mahan, K. and P. Sassone-Corsi, *Metabolism and the circadian clock converge*. *Physiol Rev*, 2013. **93**(1): p. 107-35.
61. Bass, J. and J.S. Takahashi, *Circadian integration of metabolism and energetics*. *Science*, 2010. **330**(6009): p. 1349-54.
62. O'Neill, J.S. and K.A. Feeney, *Circadian redox and metabolic oscillations in mammalian systems*. *Antioxid Redox Signal*, 2014. **20**(18): p. 2966-81.
63. Ouyang, Y., et al., *Resonating circadian clocks enhance fitness in cyanobacteria*. *Proc Natl Acad Sci U S A*, 1998. **95**(15): p. 8660-4.
64. Dodd, A.N., et al., *Plant circadian clocks increase photosynthesis, growth, survival, and competitive advantage*. *Science*, 2005. **309**(5734): p. 630-3.
65. Turek, F.W., et al., *Obesity and metabolic syndrome in circadian Clock mutant mice*. *Science*, 2005. **308**(5724): p. 1043-5.
66. Bass, J., *Circadian topology of metabolism*. *Nature*, 2012. **491**(7424): p. 348-56.
67. Rey, G. and A.B. Reddy, *Connecting cellular metabolism to circadian clocks*. *Trends Cell Biol*, 2013. **23**(5): p. 234-41.
68. Masri, S., et al., *The circadian clock transcriptional complex: metabolic feedback intersects with epigenetic control*. *Ann N Y Acad Sci*, 2012. **1264**: p. 103-9.
69. Nakahata, Y., et al., *The NAD⁺-dependent deacetylase SIRT1 modulates CLOCK-mediated chromatin remodeling and circadian control*. *Cell*, 2008. **134**(2): p. 329-40.
70. Asher, G., et al., *SIRT1 regulates circadian clock gene expression through PER2 deacetylation*. *Cell*, 2008. **134**(2): p. 317-28.
71. Hirayama, J., et al., *CLOCK-mediated acetylation of BMAL1 controls circadian function*. *Nature*, 2007. **450**(7172): p. 1086-90.
72. Rutter, J., et al., *Regulation of clock and NPAS2 DNA binding by the redox state of NAD cofactors*. *Science*, 2001. **293**(5529): p. 510-4.
73. Nakahata, Y., et al., *Circadian control of the NAD⁺ salvage pathway by CLOCK-SIRT1*. *Science*, 2009. **324**(5927): p. 654-7.

74. Ramsey, K.M., et al., *Circadian clock feedback cycle through NAMPT-mediated NAD⁺ biosynthesis*. *Science*, 2009. **324**(5927): p. 651-4.
75. Sahar, S., et al., *Altered behavioral and metabolic circadian rhythms in mice with disrupted NAD⁺ oscillation*. *Aging (Albany NY)*, 2011. **3**(8): p. 794-802.
76. Um, J.H., et al., *AMPK regulates circadian rhythms in a tissue- and isoform-specific manner*. *PLoS One*, 2011. **6**(3): p. e18450.
77. Lamia, K.A., et al., *AMPK regulates the circadian clock by cryptochrome phosphorylation and degradation*. *Science*, 2009. **326**(5951): p. 437-40.
78. Um, J.H., et al., *Activation of 5'-AMP-activated kinase with diabetes drug metformin induces casein kinase Iε (CKIε)-dependent degradation of clock protein mPer2*. *J Biol Chem*, 2007. **282**(29): p. 20794-8.
79. Oliva-Ramirez, J., et al., *Crosstalk between circadian rhythmicity, mitochondrial dynamics and macrophage bactericidal activity*. *Immunology*, 2014. **143**(3): p. 490-7.
80. Jacobi, D., et al., *Hepatic Bmal1 Regulates Rhythmic Mitochondrial Dynamics and Promotes Metabolic Fitness*. *Cell Metab*, 2015. **22**(4): p. 709-20.
81. Jacobson, J. and M.R. Duchon, *Interplay between mitochondria and cellular calcium signalling*. *Mol Cell Biochem*, 2004. **256-257**(1-2): p. 209-18.
82. Mattson, M.P., M. Gleichmann, and A. Cheng, *Mitochondria in neuroplasticity and neurological disorders*. *Neuron*, 2008. **60**(5): p. 748-66.
83. Scheffler, I.E., *A century of mitochondrial research: achievements and perspectives*. *Mitochondrion*, 2001. **1**(1): p. 3-31.
84. Scorrano, L., *Keeping mitochondria in shape: a matter of life and death*. *Eur J Clin Invest*, 2013. **43**(8): p. 886-93.
85. Zorov, D.B., M. Juhaszova, and S.J. Sollott, *Mitochondrial reactive oxygen species (ROS) and ROS-induced ROS release*. *Physiol Rev*, 2014. **94**(3): p. 909-50.
86. Gray, M.W., G. Burger, and B.F. Lang, *The origin and early evolution of mitochondria*, in *Genome Biol*. 2001. p. REVIEWS1018.
87. Friedman, J.R. and J. Nunnari, *Mitochondrial form and function*. *Nature*, 2014. **505**(7483): p. 335-43.
88. da Fonseca, R.R., et al., *The adaptive evolution of the mammalian mitochondrial genome*. *BMC Genomics*, 2008. **9**: p. 119.
89. Gellerich, F.N., et al., *Function of the mitochondrial outer membrane as a diffusion barrier in health and diseases*. *Biochem Soc Trans*, 2000. **28**(2): p. 164-9.
90. Kunji, E.R., *The role and structure of mitochondrial carriers*. *FEBS Lett*, 2004. **564**(3): p. 239-44.
91. Liu, X., et al., *Induction of apoptotic program in cell-free extracts: requirement for dATP and cytochrome c*. *Cell*, 1996. **86**(1): p. 147-57.
92. Susin, S.A., et al., *Molecular characterization of mitochondrial apoptosis-inducing factor*. *Nature*, 1999. **397**(6718): p. 441-6.
93. Smeitink, J., L. van den Heuvel, and S. DiMauro, *The genetics and pathology of oxidative phosphorylation*. *Nat Rev Genet*, 2001. **2**(5): p. 342-52.
94. van der Blik, A.M., Q. Shen, and S. Kawajiri, *Mechanisms of mitochondrial fission and fusion*. *Cold Spring Harb Perspect Biol*, 2013. **5**(6).
95. Palsson-McDermott, E.M. and L.A. O'Neill, *The Warburg effect then and now: from cancer to inflammatory diseases*. *Bioessays*, 2013. **35**(11): p. 965-73.
96. Bastin, J., *Regulation of mitochondrial fatty acid beta-oxidation in human: what can we learn from inborn fatty acid beta-oxidation deficiencies?* *Biochimie*, 2014. **96**: p. 113-20.
97. Schon, E.A., S. DiMauro, and M. Hirano, *Human mitochondrial DNA: roles of inherited and somatic mutations*. *Nat Rev Genet*, 2012. **13**(12): p. 878-90.
98. Huttemann, M., et al., *Regulation of mitochondrial oxidative phosphorylation through cell signaling*. *Biochim Biophys Acta*, 2007. **1773**(12): p. 1701-20.
99. Holt, I.J., et al., *Mammalian mitochondrial nucleoids: organizing an independently minded genome*. *Mitochondrion*, 2007. **7**(5): p. 311-21.
100. Alexeyev, M., et al., *The maintenance of mitochondrial DNA integrity--critical analysis and update*. *Cold Spring Harb Perspect Biol*, 2013. **5**(5): p. a012641.

101. Yakes, F.M. and B. Van Houten, *Mitochondrial DNA damage is more extensive and persists longer than nuclear DNA damage in human cells following oxidative stress*. Proc Natl Acad Sci U S A, 1997. **94**(2): p. 514-9.
102. Tuppen, H.A., et al., *Mitochondrial DNA mutations and human disease*. Biochim Biophys Acta, 2010. **1797**(2): p. 113-28.
103. Taylor, R.W. and D.M. Turnbull, *Mitochondrial DNA mutations in human disease*. Nat Rev Genet, 2005. **6**(5): p. 389-402.
104. Barrientos, A. and C. Ugalde, *I function, therefore I am: overcoming skepticism about mitochondrial supercomplexes*. Cell Metab, 2013. **18**(2): p. 147-9.
105. Benard, G., et al., *Physiological diversity of mitochondrial oxidative phosphorylation*. Am J Physiol Cell Physiol, 2006. **291**(6): p. C1172-82.
106. Osellame, L.D., T.S. Blacker, and M.R. Duchen, *Cellular and molecular mechanisms of mitochondrial function*. Best Pract Res Clin Endocrinol Metab, 2012. **26**(6): p. 711-23.
107. Schmitt, K., et al., *Insights into mitochondrial dysfunction: aging, amyloid-beta, and tau-A deleterious trio*. Antioxid Redox Signal, 2012. **16**(12): p. 1456-66.
108. Sena, L.A. and N.S. Chandel, *Physiological roles of mitochondrial reactive oxygen species*. Mol Cell, 2012. **48**(2): p. 158-67.
109. Murphy, M.P., *How mitochondria produce reactive oxygen species*. Biochem J, 2009. **417**(1): p. 1-13.
110. Finkel, T. and N.J. Holbrook, *Oxidants, oxidative stress and the biology of ageing*. Nature, 2000. **408**(6809): p. 239-47.
111. Mates, J.M. and F. Sanchez-Jimenez, *Antioxidant enzymes and their implications in pathophysiologic processes*. Front Biosci, 1999. **4**: p. D339-45.
112. Andrews, Z.B., S. Diano, and T.L. Horvath, *Mitochondrial uncoupling proteins in the CNS: in support of function and survival*. Nat Rev Neurosci, 2005. **6**(11): p. 829-40.
113. Cui, H., Y. Kong, and H. Zhang, *Oxidative stress, mitochondrial dysfunction, and aging*. J Signal Transduct, 2012. **2012**: p. 646354.
114. Wallace, D.C., *Mitochondrial diseases in man and mouse*. Science, 1999. **283**(5407): p. 1482-8.
115. Westermann, B., *Mitochondrial fusion and fission in cell life and death*. Nat Rev Mol Cell Biol, 2010. **11**(12): p. 872-84.
116. Chandel, N.S., *Mitochondria as signaling organelles*. BMC Biol, 2014. **12**: p. 34.
117. Detmer, S.A. and D.C. Chan, *Functions and dysfunctions of mitochondrial dynamics*. Nat Rev Mol Cell Biol, 2007. **8**(11): p. 870-9.
118. Picard, M., et al., *Mitochondrial morphology transitions and functions: implications for retrograde signaling?* Am J Physiol Regul Integr Comp Physiol, 2013. **304**(6): p. R393-406.
119. Benard, G. and R. Rossignol, *Ultrastructure of the mitochondrion and its bearing on function and bioenergetics*. Antioxid Redox Signal, 2008. **10**(8): p. 1313-42.
120. Santel, A. and S. Frank, *Shaping mitochondria: The complex posttranslational regulation of the mitochondrial fission protein DRP1*. IUBMB Life, 2008. **60**(7): p. 448-55.
121. Westermann, B., *Bioenergetic role of mitochondrial fusion and fission*. Biochim Biophys Acta, 2012. **1817**(10): p. 1833-8.
122. Chan, D.C., *Fusion and fission: interlinked processes critical for mitochondrial health*. Annu Rev Genet, 2012. **46**: p. 265-87.
123. Mishra, P. and D.C. Chan, *Mitochondrial dynamics and inheritance during cell division, development and disease*. Nat Rev Mol Cell Biol, 2014. **15**(10): p. 634-46.
124. Liesa, M., M. Palacin, and A. Zorzano, *Mitochondrial dynamics in mammalian health and disease*. Physiol Rev, 2009. **89**(3): p. 799-845.
125. de Brito, O.M. and L. Scorrano, *Mitofusin 2 tethers endoplasmic reticulum to mitochondria*. Nature, 2008. **456**(7222): p. 605-10.
126. Ishihara, N., et al., *Regulation of mitochondrial morphology through proteolytic cleavage of OPA1*. EMBO J, 2006. **25**(13): p. 2966-77.

127. Malka, F., et al., *Separate fusion of outer and inner mitochondrial membranes*. EMBO Rep, 2005. **6**(9): p. 853-9.
128. Koshiba, T., et al., *Structural basis of mitochondrial tethering by mitofusin complexes*. Science, 2004. **305**(5685): p. 858-62.
129. Griffin, E.E., S.A. Detmer, and D.C. Chan, *Molecular mechanism of mitochondrial membrane fusion*. Biochim Biophys Acta, 2006. **1763**(5-6): p. 482-9.
130. Smirnova, E., et al., *Dynamin-related protein Drp1 is required for mitochondrial division in mammalian cells*. Mol Biol Cell, 2001. **12**(8): p. 2245-56.
131. Cho, B., et al., *Physiological and pathological significance of dynamin-related protein 1 (drp1)-dependent mitochondrial fission in the nervous system*. Exp Neurol, 2013. **22**(3): p. 149-57.
132. Lee, Y.J., et al., *Roles of the mammalian mitochondrial fission and fusion mediators Fis1, Drp1, and Opa1 in apoptosis*. Mol Biol Cell, 2004. **15**(11): p. 5001-11.
133. Otera, H., et al., *Mff is an essential factor for mitochondrial recruitment of Drp1 during mitochondrial fission in mammalian cells*. J Cell Biol, 2010. **191**(6): p. 1141-58.
134. Chang, C.R. and C. Blackstone, *Dynamic regulation of mitochondrial fission through modification of the dynamin-related protein Drp1*. Ann N Y Acad Sci, 2010. **1201**: p. 34-9.
135. Ferree, A. and O. Shirihai, *Mitochondrial dynamics: the intersection of form and function*. Adv Exp Med Biol, 2012. **748**: p. 13-40.
136. Fischer, F., A. Hamann, and H.D. Osiewacz, *Mitochondrial quality control: an integrated network of pathways*. Trends Biochem Sci, 2012. **37**(7): p. 284-92.
137. Sheng, Z.H. and Q. Cai, *Mitochondrial transport in neurons: impact on synaptic homeostasis and neurodegeneration*. Nat Rev Neurosci, 2012. **13**(2): p. 77-93.
138. Chen, H., et al., *Mitochondrial fusion is required for mtDNA stability in skeletal muscle and tolerance of mtDNA mutations*. Cell, 2010. **141**(2): p. 280-9.
139. Liu, X., et al., *Mitochondrial 'kiss-and-run': interplay between mitochondrial motility and fusion-fission dynamics*. EMBO J, 2009. **28**(20): p. 3074-89.
140. Twig, G., et al., *Fission and selective fusion govern mitochondrial segregation and elimination by autophagy*. EMBO J, 2008. **27**(2): p. 433-46.
141. Mouli, P.K., G. Twig, and O.S. Shirihai, *Frequency and selectivity of mitochondrial fusion are key to its quality maintenance function*. Biophys J, 2009. **96**(9): p. 3509-18.
142. Otera, H., N. Ishihara, and K. Mihara, *New insights into the function and regulation of mitochondrial fission*. Biochim Biophys Acta, 2013. **1833**(5): p. 1256-68.
143. Chen, H. and D.C. Chan, *Physiological functions of mitochondrial fusion*. Ann N Y Acad Sci, 2010. **1201**: p. 21-5.
144. Chen, Y., Y. Liu, and G.W. Dorn, 2nd, *Mitochondrial fusion is essential for organelle function and cardiac homeostasis*. Circ Res, 2011. **109**(12): p. 1327-31.
145. Chen, H. and D.C. Chan, *Emerging functions of mammalian mitochondrial fusion and fission*. Hum Mol Genet, 2005. **14 Spec No. 2**: p. R283-9.
146. Chen, H., A. Chomyn, and D.C. Chan, *Disruption of fusion results in mitochondrial heterogeneity and dysfunction*. J Biol Chem, 2005. **280**(28): p. 26185-92.
147. Hoppins, S., L. Lackner, and J. Nunnari, *The machines that divide and fuse mitochondria*. Annu Rev Biochem, 2007. **76**: p. 751-80.
148. Verstreken, P., et al., *Synaptic mitochondria are critical for mobilization of reserve pool vesicles at Drosophila neuromuscular junctions*. Neuron, 2005. **47**(3): p. 365-78.
149. Li, Z., et al., *The importance of dendritic mitochondria in the morphogenesis and plasticity of spines and synapses*. Cell, 2004. **119**(6): p. 873-87.
150. Butow, R.A. and N.G. Avadhani, *Mitochondrial signaling: the retrograde response*. Mol Cell, 2004. **14**(1): p. 1-15.
151. Liu, Z. and R.A. Butow, *Mitochondrial retrograde signaling*. Annu Rev Genet, 2006. **40**: p. 159-85.
152. Edlich, F., et al., *Bcl-x(L) retrotranslocates Bax from the mitochondria into the cytosol*. Cell, 2011. **145**(1): p. 104-16.
153. Klecker, T., S. Bockler, and B. Westermann, *Making connections: interorganelle contacts orchestrate mitochondrial behavior*. Trends Cell Biol, 2014. **24**(9): p. 537-45.

154. Duarte, A., et al., *Mitochondrial fusion is essential for steroid biosynthesis*. PLoS One, 2012. **7**(9): p. e45829.
155. Langmesser, S. and U. Albrecht, *Life time-circadian clocks, mitochondria and metabolism*. Chronobiol Int, 2006. **23**(1-2): p. 151-7.
156. Patel, V.R., et al., *CircadiOmics: integrating circadian genomics, transcriptomics, proteomics and metabolomics*. Nat Methods, 2012. **9**(8): p. 772-3.
157. Isobe, Y., H. Hida, and H. Nishino, *Circadian rhythm of metabolic oscillation in suprachiasmatic nucleus depends on the mitochondrial oxidation state, reflected by cytochrome C oxidase and lactate dehydrogenase*. J Neurosci Res, 2011. **89**(6): p. 929-35.
158. Burkeen, J.F., et al., *Mitochondrial calcium signaling mediates rhythmic extracellular ATP accumulation in suprachiasmatic nucleus astrocytes*. J Neurosci, 2011. **31**(23): p. 8432-40.
159. Bailey, S.M., U.S. Udoh, and M.E. Young, *Circadian regulation of metabolism*. J Endocrinol, 2014. **222**(2): p. R75-96.
160. Peek, C.B., et al., *Circadian clock NAD⁺ cycle drives mitochondrial oxidative metabolism in mice*. Science, 2013. **342**(6158): p. 1243417.
161. Masri, S. and P. Sassone-Corsi, *Sirtuins and the circadian clock: bridging chromatin and metabolism*. Sci Signal, 2014. **7**(342): p. re6.
162. Nussbaum, R.L. and C.E. Ellis, *Alzheimer's disease and Parkinson's disease*. N Engl J Med, 2003. **348**(14): p. 1356-64.
163. Lopez-Otin, C., et al., *The hallmarks of aging*. Cell, 2013. **153**(6): p. 1194-217.
164. Eckert, A., K. Schmitt, and J. Gotz, *Mitochondrial dysfunction - the beginning of the end in Alzheimer's disease? Separate and synergistic modes of tau and amyloid-beta toxicity*. Alzheimers Res Ther, 2011. **3**(2): p. 15.
165. Shankar, G.M. and D.M. Walsh, *Alzheimer's disease: synaptic dysfunction and Abeta*. Mol Neurodegener, 2009. **4**: p. 48.
166. Mattson, M.P., *Pathways towards and away from Alzheimer's disease*. Nature, 2004. **430**(7000): p. 631-9.
167. Swerdlow, R.H., *Pathogenesis of Alzheimer's disease*. Clin Interv Aging, 2007. **2**(3): p. 347-59.
168. Gotz, J. and L.M. Ittner, *Animal models of Alzheimer's disease and frontotemporal dementia*. Nat Rev Neurosci, 2008. **9**(7): p. 532-44.
169. Leuner, K., et al., *Enhanced apoptosis, oxidative stress and mitochondrial dysfunction in lymphocytes as potential biomarkers for Alzheimer's disease*. J Neural Transm Suppl, 2007(72): p. 207-15.
170. Ittner, L.M. and J. Gotz, *Amyloid-beta and tau--a toxic pas de deux in Alzheimer's disease*. Nat Rev Neurosci, 2011. **12**(2): p. 65-72.
171. Turner, P.R., et al., *Roles of amyloid precursor protein and its fragments in regulating neural activity, plasticity and memory*. Prog Neurobiol, 2003. **70**(1): p. 1-32.
172. Priller, C., et al., *Synapse formation and function is modulated by the amyloid precursor protein*. J Neurosci, 2006. **26**(27): p. 7212-21.
173. Pagani, L. and A. Eckert, *Amyloid-Beta interaction with mitochondria*. Int J Alzheimers Dis, 2011. **2011**: p. 925050.
174. Glenner, G.G. and C.W. Wong, *Alzheimer's disease: initial report of the purification and characterization of a novel cerebrovascular amyloid protein*. Biochem Biophys Res Commun, 1984. **120**(3): p. 885-90.
175. Jan, A., et al., *The ratio of monomeric to aggregated forms of Abeta40 and Abeta42 is an important determinant of amyloid-beta aggregation, fibrillogenesis, and toxicity*. J Biol Chem, 2008. **283**(42): p. 28176-89.
176. Iwatsubo, T., et al., *Visualization of A beta 42(43) and A beta 40 in senile plaques with end-specific A beta monoclonals: evidence that an initially deposited species is A beta 42(43)*. Neuron, 1994. **13**(1): p. 45-53.
177. Jarrett, J.T., E.P. Berger, and P.T. Lansbury, Jr., *The carboxy terminus of the beta amyloid protein is critical for the seeding of amyloid formation: implications for the pathogenesis of Alzheimer's disease*. Biochemistry, 1993. **32**(18): p. 4693-7.

178. LaFerla, F.M., K.N. Green, and S. Oddo, *Intracellular amyloid-beta in Alzheimer's disease*. Nat Rev Neurosci, 2007. **8**(7): p. 499-509.
179. Grundke-Iqbal, I., et al., *Abnormal phosphorylation of the microtubule-associated protein tau (tau) in Alzheimer cytoskeletal pathology*. Proc Natl Acad Sci U S A, 1986. **83**(13): p. 4913-7.
180. Ihara, Y., et al., *Phosphorylated tau protein is integrated into paired helical filaments in Alzheimer's disease*. J Biochem, 1986. **99**(6): p. 1807-10.
181. Eckert, A., et al., *March separate, strike together--role of phosphorylated TAU in mitochondrial dysfunction in Alzheimer's disease*. Biochim Biophys Acta, 2014. **1842**(8): p. 1258-66.
182. Buee, L., et al., *Tau protein isoforms, phosphorylation and role in neurodegenerative disorders*. Brain Res Brain Res Rev, 2000. **33**(1): p. 95-130.
183. Ballatore, C., V.M. Lee, and J.Q. Trojanowski, *Tau-mediated neurodegeneration in Alzheimer's disease and related disorders*. Nat Rev Neurosci, 2007. **8**(9): p. 663-72.
184. Park, C.B. and N.G. Larsson, *Mitochondrial DNA mutations in disease and aging*. J Cell Biol, 2011. **193**(5): p. 809-18.
185. Swerdlow, R.H., *Brain aging, Alzheimer's disease, and mitochondria*. Biochim Biophys Acta, 2011. **1812**(12): p. 1630-9.
186. Reddy, P.H. and M.F. Beal, *Amyloid beta, mitochondrial dysfunction and synaptic damage: implications for cognitive decline in aging and Alzheimer's disease*. Trends Mol Med, 2008. **14**(2): p. 45-53.
187. Domek-Lopacinska, K.U. and J.B. Strosznajder, *Cyclic GMP and nitric oxide synthase in aging and Alzheimer's disease*. Mol Neurobiol, 2010. **41**(2-3): p. 129-37.
188. Jesko, H., M. Chalimoniuk, and J.B. Strosznajder, *Activation of constitutive nitric oxide synthase(s) and absence of inducible isoform in aged rat brain*. Neurochem Int, 2003. **42**(4): p. 315-22.
189. Strosznajder, J.B., et al., *Age-related alteration of activity and gene expression of endothelial nitric oxide synthase in different parts of the brain in rats*. Neurosci Lett, 2004. **370**(2-3): p. 175-9.
190. Barazzoni, R., K.R. Short, and K.S. Nair, *Effects of aging on mitochondrial DNA copy number and cytochrome c oxidase gene expression in rat skeletal muscle, liver, and heart*. J Biol Chem, 2000. **275**(5): p. 3343-7.
191. Short, K.R., et al., *Decline in skeletal muscle mitochondrial function with aging in humans*. Proc Natl Acad Sci U S A, 2005. **102**(15): p. 5618-23.
192. Masuyama, M., et al., *Quantitative change in mitochondrial DNA content in various mouse tissues during aging*. Biochim Biophys Acta, 2005. **1723**(1-3): p. 302-8.
193. Frahm, T., et al., *Lack of age-related increase of mitochondrial DNA amount in brain, skeletal muscle and human heart*. Mech Ageing Dev, 2005. **126**(11): p. 1192-200.
194. Kuro-o, M., *Disease model: human aging*. Trends Mol Med, 2001. **7**(4): p. 179-81.
195. Pallas, M., et al., *From aging to Alzheimer's disease: unveiling "the switch" with the senescence-accelerated mouse model (SAMP8)*. J Alzheimers Dis, 2008. **15**(4): p. 615-24.
196. Watanabe, K., et al., *Evidence for involvement of dysfunctional teeth in the senile process in the hippocampus of SAMP8 mice*. Exp Gerontol, 2001. **36**(2): p. 283-95.
197. Omata, N., et al., *Age-related changes in energy production in fresh senescence-accelerated mouse brain slices as revealed by positron autoradiography*. Dement Geriatr Cogn Disord, 2001. **12**(2): p. 78-84.
198. Kurokawa, T., et al., *Age-related changes in manganese superoxide dismutase activity in the cerebral cortex of senescence-accelerated prone and resistant mouse*. Neurosci Lett, 2001. **298**(2): p. 135-8.
199. Shi, C., et al., *Ginkgo biloba extract EGb761 protects against aging-associated mitochondrial dysfunction in platelets and hippocampi of SAMP8 mice*. Platelets, 2010. **21**(5): p. 373-9.
200. Xu, J., et al., *Mitochondrial dysfunction in platelets and hippocampi of senescence-accelerated mice*. J Bioenerg Biomembr, 2007. **39**(2): p. 195-202.

201. Alvarez-Garcia, O., et al., *Elevated oxidative stress in the brain of senescence-accelerated mice at 5 months of age*. Biogerontology, 2006. **7**(1): p. 43-52.
202. Sureda, F.X., et al., *Changes in oxidative stress parameters and neurodegeneration markers in the brain of the senescence-accelerated mice SAMP-8*. Exp Gerontol, 2006. **41**(4): p. 360-7.
203. Morley, J.E., et al., *Beta-amyloid precursor polypeptide in SAMP8 mice affects learning and memory*. Peptides, 2000. **21**(12): p. 1761-7.
204. Caspersen, C., et al., *Mitochondrial Abeta: a potential focal point for neuronal metabolic dysfunction in Alzheimer's disease*. FASEB J, 2005. **19**(14): p. 2040-1.
205. Manczak, M., et al., *Mitochondria are a direct site of A beta accumulation in Alzheimer's disease neurons: implications for free radical generation and oxidative damage in disease progression*. Hum Mol Genet, 2006. **15**(9): p. 1437-49.
206. Pavlov, P.F., et al., *Mitochondrial accumulation of APP and Abeta: significance for Alzheimer disease pathogenesis*. J Cell Mol Med, 2009. **13**(10): p. 4137-45.
207. Pavlov, P.F., et al., *Mitochondrial gamma-secretase participates in the metabolism of mitochondria-associated amyloid precursor protein*. FASEB J, 2011. **25**(1): p. 78-88.
208. Lim, Y.A., et al., *Abeta and human amylin share a common toxicity pathway via mitochondrial dysfunction*. Proteomics, 2010. **10**(8): p. 1621-33.
209. Games, D., et al., *Alzheimer-type neuropathology in transgenic mice overexpressing V717F beta-amyloid precursor protein*. Nature, 1995. **373**(6514): p. 523-7.
210. Blanchard, V., et al., *Time sequence of maturation of dystrophic neurites associated with Abeta deposits in APP/PS1 transgenic mice*. Exp Neurol, 2003. **184**(1): p. 247-63.
211. Eckert, A., et al., *Soluble beta-amyloid leads to mitochondrial defects in amyloid precursor protein and tau transgenic mice*. Neurodegener Dis, 2008. **5**(3-4): p. 157-9.
212. Manczak, M., M.J. Calkins, and P.H. Reddy, *Impaired mitochondrial dynamics and abnormal interaction of amyloid beta with mitochondrial protein Drp1 in neurons from patients with Alzheimer's disease: implications for neuronal damage*. Hum Mol Genet, 2011. **20**(13): p. 2495-509.
213. Wang, X., et al., *Dynamin-like protein 1 reduction underlies mitochondrial morphology and distribution abnormalities in fibroblasts from sporadic Alzheimer's disease patients*. Am J Pathol, 2008. **173**(2): p. 470-82.
214. Calkins, M.J., et al., *Impaired mitochondrial biogenesis, defective axonal transport of mitochondria, abnormal mitochondrial dynamics and synaptic degeneration in a mouse model of Alzheimer's disease*. Hum Mol Genet, 2011. **20**(23): p. 4515-29.
215. Gotz, J., et al., *Is tau aggregation toxic or protective: a sensible question in the absence of sensitive methods?* J Alzheimers Dis, 2008. **14**(4): p. 423-9.
216. Ittner, L.M., et al., *Dendritic function of tau mediates amyloid-beta toxicity in Alzheimer's disease mouse models*. Cell, 2010. **142**(3): p. 387-97.
217. Reddy, P.H., *Abnormal tau, mitochondrial dysfunction, impaired axonal transport of mitochondria, and synaptic deprivation in Alzheimer's disease*. Brain Res, 2011. **1415**: p. 136-48.
218. Gotz, J., et al., *Tau filament formation in transgenic mice expressing P301L tau*. J Biol Chem, 2001. **276**(1): p. 529-34.
219. David, D.C., et al., *Proteomic and functional analyses reveal a mitochondrial dysfunction in P301L tau transgenic mice*. J Biol Chem, 2005. **280**(25): p. 23802-14.
220. Schulz, K.L., et al., *A new link to mitochondrial impairment in tauopathies*. Mol Neurobiol, 2012. **46**(1): p. 205-16.
221. DuBoff, B., J. Gotz, and M.B. Feany, *Tau promotes neurodegeneration via DRP1 mislocalization in vivo*. Neuron, 2012. **75**(4): p. 618-32.
222. DuBoff, B., M. Feany, and J. Gotz, *Why size matters - balancing mitochondrial dynamics in Alzheimer's disease*. Trends Neurosci, 2013. **36**(6): p. 325-35.
223. Gotz, J., L.M. Ittner, and S. Kins, *Do axonal defects in tau and amyloid precursor protein transgenic animals model axonopathy in Alzheimer's disease?* J Neurochem, 2006. **98**(4): p. 993-1006.

224. Bolmont, T., et al., *Induction of tau pathology by intracerebral infusion of amyloid-beta-containing brain extract and by amyloid-beta deposition in APP x Tau transgenic mice*. Am J Pathol, 2007. **171**(6): p. 2012-20.
225. Gotz, J., et al., *Formation of neurofibrillary tangles in P301 tau transgenic mice induced by Abeta 42 fibrils*. Science, 2001. **293**(5534): p. 1491-5.
226. Gotz, J., et al., *Amyloid-induced neurofibrillary tangle formation in Alzheimer's disease: insight from transgenic mouse and tissue-culture models*. Int J Dev Neurosci, 2004. **22**(7): p. 453-65.
227. Eckert, A., et al., *Oligomeric and fibrillar species of beta-amyloid (A beta 42) both impair mitochondrial function in P301L tau transgenic mice*. J Mol Med (Berl), 2008. **86**(11): p. 1255-67.
228. Rhein, V., et al., *Amyloid-beta and tau synergistically impair the oxidative phosphorylation system in triple transgenic Alzheimer's disease mice*. Proc Natl Acad Sci U S A, 2009. **106**(47): p. 20057-62.
229. Oddo, S., et al., *Triple-transgenic model of Alzheimer's disease with plaques and tangles: intracellular Abeta and synaptic dysfunction*. Neuron, 2003. **39**(3): p. 409-21.
230. Yao, J., et al., *Mitochondrial bioenergetic deficit precedes Alzheimer's pathology in female mouse model of Alzheimer's disease*. Proc Natl Acad Sci U S A, 2009. **106**(34): p. 14670-5.
231. Swerdlow, R.H. and S.M. Khan, *A "mitochondrial cascade hypothesis" for sporadic Alzheimer's disease*. Med Hypotheses, 2004. **63**(1): p. 8-20.
232. Swerdlow, R.H., J.M. Burns, and S.M. Khan, *The Alzheimer's disease mitochondrial cascade hypothesis*. J Alzheimers Dis, 2010. **20 Suppl 2**: p. S265-79.
233. Swerdlow, R.H., J.M. Burns, and S.M. Khan, *The Alzheimer's disease mitochondrial cascade hypothesis: progress and perspectives*. Biochim Biophys Acta, 2014. **1842**(8): p. 1219-31.
234. Corpechot, C., et al., *Characterization and measurement of dehydroepiandrosterone sulfate in rat brain*. Proc Natl Acad Sci U S A, 1981. **78**(8): p. 4704-7.
235. Reddy, D.S., *Neurosteroids: endogenous role in the human brain and therapeutic potentials*. Prog Brain Res, 2010. **186**: p. 113-37.
236. Belelli, D. and J.J. Lambert, *Neurosteroids: endogenous regulators of the GABA(A) receptor*. Nat Rev Neurosci, 2005. **6**(7): p. 565-75.
237. Plassart-Schiess, E. and E.E. Baulieu, *Neurosteroids: recent findings*. Brain Res Brain Res Rev, 2001. **37**(1-3): p. 133-40.
238. Grimm, A., et al., *Alzheimer's disease, oestrogen and mitochondria: an ambiguous relationship*. Mol Neurobiol, 2012. **46**(1): p. 151-60.
239. Yan, S.D. and D.M. Stern, *Mitochondrial dysfunction and Alzheimer's disease: role of amyloid-beta peptide alcohol dehydrogenase (ABAD)*. Int J Exp Pathol, 2005. **86**(3): p. 161-71.
240. Kristofikova, Z., et al., *Enhanced levels of mitochondrial enzyme 17beta-hydroxysteroid dehydrogenase type 10 in patients with Alzheimer disease and multiple sclerosis*. Mol Biosyst, 2009. **5**(10): p. 1174-9.
241. Yao, J., et al., *Ovarian hormone loss induces bioenergetic deficits and mitochondrial beta-amyloid*. Neurobiol Aging, 2012. **33**(8): p. 1507-21.
242. Lim, Y.A., et al., *Inhibition of the mitochondrial enzyme ABAD restores the amyloid-beta-mediated deregulation of estradiol*. PLoS One, 2011. **6**(12): p. e28887.
243. Bonanni, E., et al., *Daytime sleepiness in mild and moderate Alzheimer's disease and its relationship with cognitive impairment*. J Sleep Res, 2005. **14**(3): p. 311-7.
244. Kondratova, A.A. and R.V. Kondratov, *The circadian clock and pathology of the ageing brain*. Nat Rev Neurosci, 2012. **13**(5): p. 325-35.
245. Wulff, K., et al., *Sleep and circadian rhythm disruption in psychiatric and neurodegenerative disease*. Nat Rev Neurosci, 2010. **11**(8): p. 589-99.
246. Pagani, L., et al., *Serum factors in older individuals change cellular clock properties*. Proc Natl Acad Sci U S A, 2011. **108**(17): p. 7218-23.
247. Brown, S.A., K. Schmitt, and A. Eckert, *Aging and circadian disruption: causes and effects*. Aging (Albany NY), 2011. **3**(8): p. 813-7.

248. Kang, J.E., et al., *Amyloid-beta dynamics are regulated by orexin and the sleep-wake cycle*. Science, 2009. **326**(5955): p. 1005-7.
249. Hastings, M.H. and M. Goedert, *Circadian clocks and neurodegenerative diseases: time to aggregate?* Curr Opin Neurobiol, 2013. **23**(5): p. 880-7.
250. Lobo, A., et al., *Non-cognitive psychopathological symptoms associated with incident mild cognitive impairment and dementia, Alzheimer's type*. Neurotox Res, 2008. **14**(2-3): p. 263-72.
251. Stopa, E.G., et al., *Pathologic evaluation of the human suprachiasmatic nucleus in severe dementia*. J Neuropathol Exp Neurol, 1999. **58**(1): p. 29-39.
252. Saper, C.B. and D.C. German, *Hypothalamic pathology in Alzheimer's disease*. Neurosci Lett, 1987. **74**(3): p. 364-70.
253. Teipel, S.J., et al., *The cholinergic system in mild cognitive impairment and Alzheimer's disease: an in vivo MRI and DTI study*. Hum Brain Mapp, 2011. **32**(9): p. 1349-62.
254. Brunnstrom, H., et al., *Differential degeneration of the locus coeruleus in dementia subtypes*. Clin Neuropathol, 2011. **30**(3): p. 104-10.

MANUSCRIPTS

Part I:

A. Circadian control of Drp1 activity regulates mitochondrial dynamics and bioenergetics

B. Improvement of neuronal bioenergetics by neurosteroids: Implications for age-related neurodegenerative disorders

Part II:

C. Amyloid- β -induced imbalance between mitochondrial network and bioenergetics

A. Circadian control of Drp1 activity regulates mitochondrial dynamics and bioenergetics

Authors: Karen Schmitt^{1,2,&}, Amandine Grimm^{1,2,&}, Robert Dallmann³, Bjoern Oettinghaus⁴, Lisa Michelle Restelli⁴, Undine E. Lang², Naotada Ishihara⁵, Katsuyoshi Mihara⁶, Jürgen A Ripperger⁷, Urs Albrecht⁷, Stephan Frank^{4#}, Steven A. Brown^{3*#}, Anne Eckert^{1,2*#}

Affiliations:

¹Neurobiology Lab for Brain Aging and Mental Health, Transfaculty Research Platform, Molecular & Cognitive Neuroscience, University of Basel, Basel, Switzerland

²Psychiatric University Clinics, University of Basel, Basel, Switzerland

³Institute of Pharmacology and Toxicology, University of Zurich, Zurich, Switzerland

⁴Division of Neuropathology, Institute of Pathology; University Hospital Basel, Basel, Switzerland

⁵Department of Protein Biochemistry, Institute of Life Science, Kurume University, Kurume 839-0864, Japan

⁶Department of Molecular Biology, Graduate School of Medical Science, Kyushu University, Fukuoka 812-8582, Japan

⁷Department of Biology, Unit of Biochemistry, University of Fribourg, Fribourg, Switzerland

Correspondence:

*To whom correspondence may be addressed: E-mail: steven.brown@pharma.uzh.ch or anne.eckert@upkbs.ch.

&These authors equally contributed to this work.

#These senior authors equally contributed to this work.

Summary

Circadian clocks are tightly connected to metabolic processes through reciprocal regulation from metabolites to transcription factors. Here, we demonstrate evidence of a novel coupling mechanism via mitochondrial morphology that is essential for circadian production of adenosine triphosphate (ATP). Within the cell, the mitochondrial network is a prominent actor in regulation of energy metabolism. Both *in vivo* and *in vitro*, mitochondrial fission-fusion dynamics are strongly clock-controlled, as well as all other aspects of mitochondrial bioenergetic homeostasis, including oxidative phosphorylation, generation of ATP and reactive oxygen species (ROS). We show that circadian control of the activity of the dynamin-related protein 1 (DRP1) is required for circadian oscillations of the mitochondrial network. Genetic or pharmacological abrogation of DRP1 activity abolished circadian mitochondrial network dynamics and mitochondrial respiratory activity, as well as eliminated circadian ATP production. Our findings provide new insights into a crosstalk governing the interplay between mitochondrial dynamics and circadian cycles.

Highlights:

- The circadian clock controls rhythmic mitochondrial dynamics and metabolic flux.
- The key protein regulating cell cycle-based mitochondrial morphology, DRP1, is phosphorylated in circadian fashion.
- Genetic or pharmacological suppression of DRP1 activity eliminates circadian ATP production.
- Blockade of DRP1 leads to an impaired core circadian clock.

eTOC Blurb/ In Brief:

The circadian clock globally regulates energy metabolism and mitochondrial morphology. Even in nondividing tissues, it co-opts cell cycle-based rhythmic control of DRP1 phosphorylation to direct circadian mitochondrial morphology. This control is essential for circadian production of ATP, and it furthermore feeds back to influence the core circadian clock.

Introduction

The circadian clock is a hierarchical network of oscillators that synchronize a wide variety of metabolic pathways to the optimal time of day, anticipating periodic changes of the external environment for all living organisms, from cyanobacteria and fungi (Brunner and Schafmeier, 2006) to insects (Rosato et al., 2006) and mammals (Gachon et al., 2004).

Over the years, a growing body of evidence suggested specifically that energy metabolism and cellular mechanisms defending against oxidative damage are coordinated by the circadian clock (Bailey et al., 2014, Kalsbeek et al., 2011, Langmesser and Albrecht, 2006). Conversely, disruption of the clock impairs metabolic homeostasis (Bugge et al., 2012, Cho et al., 2012, Marcheiva et al., 2010, Turek et al., 2005). This close relationship between circadian and metabolic cycles has been verified in studies demonstrating that the circadian clock exerts its control over metabolism by (i) controlling the expression of genes and enzymes involved in metabolic processes (Eckel-Mahan et al., 2012, Feng et al., 2011, Vollmers et al., 2009), (ii) intertwining nuclear receptors and nutrient sensors with the clock machinery, e.g. PER2/CLOCK and SIRT1 (Asher et al., 2008, Nakahata et al., 2008), PER2 and PPAR α /REV-ERB α (Schmutz et al., 2010), CRY1 and AMPK/GCR (Lamia et al., 2011, Lamia et al., 2009), REV-ERB α and HDAC3 (Zhang et al., 2015), and/or (iii) regulating metabolite levels (e.g. NAD⁺/NADH, ATP/ADP, cAMP) (Nakahata et al., 2009, O'Neill et al., 2008, Peek et al., 2013, Ramsey et al., 2009). In reverse, various hormones, nutrient sensors, redox sensors and metabolites not only act as clock output but can in turn also regulate the biological clock by acting as input signals (reviewed in (Bass, 2012, Eckel-Mahan and Sassone-Corsi, 2013)).

Within this network, the mechanistic relationship between the clock and the mitochondrial network remains mostly elusive. Mitochondria are highly dynamic cellular organelles playing a major role in cellular energy metabolism and homeostasis via generation of several metabolites including ATP (Scheffler, 2001). Several studies have shown diurnal oscillations in key mitochondrial bioenergetic parameters including expression of genes involved in mitochondrial respiration, membrane potential, and cytochrome c oxidase activity in the suprachiasmatic nuclei (Isobe et al., 2011, Panda et al., 2002). Moreover, one regulatory node for mitochondrial oxidative metabolism is the level of NAD⁺/NADH which regulates the activity of mitochondrial sirtuins and thereby mitochondrial protein acetylation (Nakahata et al., 2009, Peek et al., 2013). However, in the other systems global control of mitochondrial function is strongly coordinated with morphology. For example, in response to cues from the cell cycle, a tightly regulated equilibrium between opposing mitochondrial fusion and fission activities is required to meet changing demands for energy production and adjust mitochondrial function (Frank, 2006, Mishra and Chan, 2014,

Westermann, 2010). In this paper, we show that this cell cycle-mediated control is in effect co-opted by the circadian clock: even in nondividing cells and tissues, circadian regulation of dynamin-related protein 1 (DRP1) results in cycles of fission and fusion that are essential for circadian oscillations in ATP production. Our findings are consistent with the existence of a crosstalk between the clock and the mitochondrial network that maintains bioenergetic homeostasis in response to circadian metabolic changes.

Results

The circadian clock regulates cellular metabolic state.

Extensive circadian transcriptomic and metabolomic profiling has revealed the existence of a mutual and dynamic relation between the timing of the molecular clock and the network of metabolic pathways modulating energy charge and redox state. These *studies* were performed in different organs and matrices of both mice and men (Dallmann et al., 2012, Eckel-Mahan et al., 2012, Minami et al., 2009, Patel et al., 2012). To eliminate potential systemic and environmental influences upon metabolic measurements, we rigorously examined the influence of the circadian clock on metabolic flux in cultured cells *in vitro*. Global metabolomic profiles were obtained in cultured U2OS cells over the course of 24 hours after synchronizing circadian clocks with dexamethasone (Balsalobre et al., 2000), while the temporal pattern of selected metabolites including ATP, NAD⁺/NADH and reactive oxygen species (ROS) was determined in cultured human fibroblasts after synchronizing circadian clocks with serum shock (Balsalobre et al., 1998). Using gas and liquid chromatography with a mass spectrometer (GC/LC-MS) as previously (Dallmann et al., 2012), we identified a total of 228 metabolites in cell pellets from cultured U2OS cells (**Fig. 1**, **Table S1**). Consistent with but more dramatic than previous findings (Dallmann et al., 2012, Eckel-Mahan et al., 2012, Minami et al., 2009), periodic analysis of cellular data (Hughes et al., 2010) showed that ~29% of these metabolites (67 of 228) displayed circadian rhythmicity ($P < 0.05$) (**Fig. 1B-D**, **Table S1**). The majority of these identified metabolites are related to numerous metabolomic pathways involved in redox state and energy metabolism, including glycolysis and the TCA cycle, branched amino-acid metabolism and GSH/GSSG metabolism (**Fig. 1E-G**). In support of previous findings (Peek et al., 2013), we particularly observed robust circadian rhythmicity in total ATP content (**Fig. 2A**), in NAD⁺ and NADH levels (**Fig. S1A, C**), and in mitochondrial ROS content (**Fig. S2**). These circadian fluctuations occurred with a peak at 16 hours post-shock and a trough at 28 hours post-shock in cultured fibroblasts. Similarly, these metabolites displayed a circadian pattern in brain homogenates from wildtype mice, with maximal levels near the beginning of the resting period (circadian time CT4) and a trough occurring at CT16 (start of the activity period) (**Fig. 2B and Fig. S1B, D**). The role of core molecular clock transcription factors on ATP rhythmicity was further confirmed in mouse embryonic fibroblasts (MEFs) isolated from mice deficient in the clock transcriptional repressors (PER1 and PER2) that displayed completely abolished ATP rhythms compared to control MEFs, establishing a role for the circadian clock in cellular ATP oscillations (**Fig. 2C**).

Together, these metabolomics data show that circadian regulation of mitochondrial function likely extends across multiple steps within the oxidative phosphorylation process, and we therefore began to dissect the sources of this control.

Circadian clock synchronizes mitochondrial ATP oscillations via oxidative metabolism.

As ATP molecules are produced by two main pathways, cellular glycolysis and mitochondrial oxidative phosphorylation (OxPhos), we monitored ATP content in synchronized fibroblasts in the presence of an ATP synthase inhibitor (oligomycin, 2 μ M) or glycolysis inhibitor (2-deoxy-glucose, 4.5 g/L) in order to determine which pathway is causally involved in ATP oscillations (**Fig. 3A**). We observed that the circadian oscillations in ATP were significantly dampened in the presence of oligomycin. In contrast, only the amplitude was decreased in the presence of 2-deoxy-glucose. These findings reveal that the circadian rhythm of ATP is primarily generated from mitochondrial oxidative phosphorylation rather than through glycolytic contributions.

In order to confirm that the observed ATP oscillations are not associated with synchronous cell cycle (Marcussen and Larsen, 1996), we evaluated ATP content in synchronized fibroblasts treated with cytosine β -D-arabinofuranoside (AraC, 100 μ M) to eliminate cell division (**Fig 3B**). The AraC-induced inhibition of the cell cycle was confirmed at 24 hours post-shock using a BrdU Cell Proliferation Assay (**Fig. S3A**). Although pharmacological disruption of cell division with AraC led to a somewhat decreased level of rhythmic ATP content compared to untreated controls, no alteration in the amplitude of circadian ATP production was observed (**Fig. 3B**). To ensure that cell division could play no role in the oscillations we observed, and also demonstrate the significance of our findings *in vivo*, we further examined circadian ATP levels in adult brain, where dividing cells represent a tiny minority. Here, too, ATP levels were circadian (**Fig. 2B**). Together, these results demonstrate that circadian fluctuations in ATP levels mainly originated from mitochondrial oxidative metabolism, independent of the cell cycle.

To examine potential sources of circadian ATP levels, we further examined clock-related regulation of mitochondrial oxidative metabolism using a Seahorse Bioscience XF24 Flux Analyzer, measuring real-time oxygen consumption rate (OCR) in synchronized fibroblasts at 16 hours post-shock, corresponding to the total ATP peak, and at 28 hours post-shock, corresponding to the total ATP trough (**Fig. 3C**). OCR was assessed by sequential injection of (i) the ATP synthase inhibitor oligomycin (1 μ M) to determine the OCR devoted to ATP synthesis counterbalancing against ATP consumption (also called ATP turnover), (ii) an uncoupling agent, FCCP [carbonyl cyanide p (trifluoromethoxy)

phenylhydrazone] (0.7 μ M) to measure maximal respiration in the absence of a proton gradient, and (iii) inhibitors of activities of complexes I-III rotenone (2 μ M) and antimycin A (4 μ M), respectively, to evaluate the OCR of non-mitochondrial respiration (**Fig. 3C**). In parallel with the rhythmic oscillations in ATP content that we documented, we observed a lower OCR in the basal and maximal respiration (~19% and ~14%, respectively) as well as in ATP turnover (~24%) at 28 hours post-shock compared to the OCR measured at 16 hours post-shock (**Fig. 3D**). The spare respiratory capacity as a measure of the cellular ability to respond to an energetic demand as well as reflecting how closely to its theoretical maximum a cell is to respiring, was higher (~48%) at 28 hours post-shock compared to 16 hours post-shock (**Fig. S3B**). By contrast, the rates of oxygen consumption were not coupled to ATP production – i.e. those required to overcome the natural proton leak across the inner mitochondrial membrane (**Fig. S3C**), and those related to glycolysis indicated by the extracellular acidification rate (ECAR) (**Fig. S3D**) - were unchanged at different time points. Finally, we plotted the bioenergetic profile of synchronized human skin fibroblasts, representing OCR (basal respiration) versus ECAR (glycolysis) at 16 hours and 28 hours post-shock (**Fig. 3E**). Matching with the rhythmic oscillations in the ATP content, cells switched between a metabolically active state corresponding to 16 hours post-shock and a metabolic resting state corresponding to 28 hours post-shock, independently of glycolysis. Global circadian oscillations at every level of the mitochondrial function might be explained by a variety of mechanisms. It is formally possible that circadian control of expression of a key rate-limiting mitochondrial enzyme would be sufficient. We show in Fig. S4 circadian oscillations of gene expression in mitochondrial subunits of Complexes I (**Fig. S4A**), IV (**Fig. S4B**) and V (ATP synthase, **Fig. S4C**) in human fibroblasts. A second more persuasive idea is that circadian control of NAD⁺/NADH levels feeds back to control mitochondrial output (Asher and Schibler, 2011, Nakahata et al., 2009, Peek et al., 2013). Recently, it has been shown that changed NAD⁺/NADH levels can affect activity of the mitochondrial deacetylase SIRT3, thereby affecting global mitochondrial protein acetylation. Elegantly, such a mechanism could also account for non-circadian feeding driven oscillations in mitochondrial function (Peek et al., 2013). A third idea relates to mitochondrial morphology: in the case of the cell cycle, direct regulation of mitochondrial morphology itself regulates all aspects of oxidative respiration (Mishra and Chan, 2014, Westermann, 2010), and mitochondria from liver deficient in the clock gene *Bmal1*, or from worms deficient in the *Bmal1* homolog *aha-1*, are swollen and dysfunctional (Jacobi et al., 2015).

Variations in mitochondrial architecture are mediated by circadian clock.

As we discuss above, one way in which mitochondrial function is globally controlled is via morphological dynamics. Yet, only very recently evidence demonstrating circadian control

of this aspect has started surfacing, for example in peritoneal macrophages during infection (Oliva-Ramirez et al., 2014), and in comparing mitochondrial morphology and function between wildtype and *Bmal1* knockout mice (Jacobi et al., 2015). Since mitochondria are highly dynamic organelles (Detmer and Chan, 2007, Westermann, 2010), we investigated whether the circadian clock intervenes globally in control and maintenance of the mitochondrial network architecture (**Fig. 4**). Hence, we visualized mitochondrial morphology in Mitotracker CMXROS-treated synchronized human primary skin fibroblasts by confocal microscopy (**Fig. 4A**). We observed that mitochondrial network morphology displayed a circadian rhythmicity with three distinct states (tubular, intermediate or fragmented at 8, 16 or 24 hours post-shock, respectively). In parallel, we investigated the relationship between clock and mitochondrial architecture in brain and liver sections from wildtype mice at CT0 (onset of subjective day or rest period) and CT12 (onset of subjective night or activity period) by immunohistochemical labeling of VDAC (voltage-dependent anion channel), an outer mitochondrial membrane porin (**Fig. 4B**). Consistent with our *in vitro* observations, the mitochondrial network in both central and peripheral tissues exhibited a tubular morphology at CT0 (beginning of the rest period), while mitochondria appeared in a fragmented state at CT12 (beginning of the activity period).

Clock control of DRP1 activity modulates mitochondrial metabolism.

To understand how the circadian clock might control mitochondrial dynamics, we first analyzed circadian transcript levels of genes important for mitochondrial fusion (mitofusins 1 and 2, *MFN1* and 2; optic atrophy 1, *OPA1*) and fission (dynamamin-related protein1, *DRP1*; human fission protein 1, *hFIS1*) (Benard and Karbowski, 2009, Youle and van der Bliek, 2012). None of the genes displayed a circadian expression pattern in clock-synchronized fibroblasts (**Fig. 4C, S5**), suggesting that 24-hour oscillations observed in the mitochondrial network architecture *in vitro* and *in vivo* might be controlled by post-transcriptional modifications of mitochondrial shaping proteins.

In the case of the cell cycle, oscillations in mitochondrial fusion and fission are regulated via phosphorylation and activation / inactivation of DRP1 protein by cyclin-dependent kinases (Santel and Frank, 2008). Therefore, we next considered a potential contribution of the biological clock in the post-translational modification of DRP1 by phosphorylation at the key serine residue 637 (S637) using immunoblotting against DRP1 and phosphorylated DRP1 in lysates from synchronized confluent human primary skin fibroblasts (**Fig. 5A**). Again to demonstrate that the results were not cell-division-dependent, and to show their relevance *in vivo*, the same experiment was performed using extracts from brain of wild-type mice maintained in constant darkness (**Fig. 5B**). While total DRP1 protein

did not display circadian oscillation in both cell lysates and brain lysates, Ser637 phosphorylated DRP1 exhibited ~24hour rhythms with peaks occurring at 16 hours post-shock and at CT12 (onset of the subjective night), respectively. Taken together, these results suggest that the *in vitro* and *in vivo* mitochondrial network remodeling is controlled by the circadian clock, accompanied by the same post-translational modulation of DRP1 protein that directs such remodeling in other contexts. To determine whether circadian modulation of mitochondrial fission and fusion might directly regulate circadian mitochondrial output, we first took a pharmacological approach, treating clock-synchronized cells with the mitochondrial division inhibitor, mdivi-1 (50 μ M). Surprisingly, treatment with this drug completely abolished ATP oscillation compared to untreated human skin fibroblasts (**Fig. 6A**). To further confirm whether inhibition or absence of DRP1 is able to impact ATP oscillation, we evaluated ATP content in MEFs from *Drp1*^{-/-} mice as well as in hippocampi of adult *Drp1*^{-/-} mice kept in constant darkness (**Fig. 6B-C**) (Oettinghaus et al., 2015). MEFs lacking DRP1 did not display ATP oscillations compared to control MEFs (**Fig 6B**). In addition, ATP content was evaluated at CT4, near the beginning of the rest period and at CT16, the beginning of the activity period. Consistent with our *in vitro* observations, ATP measured in *Drp1*^{-/-} mouse hippocampi did not display a significant change between CT4 and CT16 compared to control hippocampi (**Fig. 6C**). Therefore, both *in vivo* and *in vitro*, circadian activation of DRP1 plays a central role in coupling circadian and mitochondrial metabolic cycles.

Feedback from mitochondrial morphology to the core clock.

A key aspect of previously documented modes of circadian regulation of oxidative respiration is their ability to feed back to the circadian clock: NAD⁺ is itself a cofactor of SIRT1, a nuclear deacetylase directly affecting circadian clock function (Asher et al., 2008, Nakahata et al., 2008); and purine nucleotide levels modulate AMPK activity to regulate phosphorylation of CRY clock proteins (Jordan and Lamia, 2013). If the morphology-driven circadian control mechanism that we have uncovered indeed affected circadian mitochondrial function and ATP levels, then it would be predicted that they should also signal back to influence circadian function. To address this question, first we characterized the circadian period length of dexamethasone-synchronized fibroblasts after disturbing either mitochondrial respiration or the mitochondrial network by infecting the cells with a circadian reporter construct (*Bmal1* promoter-driven expression of firefly luciferase)-harboring lentivirus (**Fig. 7A,B**). Rotenone, oligomycin or FCCP were used to inhibit mitochondrial respiration, leading to ATP depletion (**Fig. 3A, 7A**). Notably, cells had a significantly longer period length in the presence of mitochondrial respiration inhibitors compared to controls. Moreover,

disruption of mitochondrial division by mdivi-1 treatment significantly increased period length (**Fig. 7B**). These findings are consistent with the idea that DRP1-mediated mitochondrial ATP oscillations may also signal in retrograde fashion to the clock.

We further analyzed gene expression of the core clock activator *Bmal1* and repressors *Per1* and *Per2* in serum-shocked human skin fibroblasts treated with mdivi-1 (50 μ M) (**Fig. 7C-E**) and in serum-shocked DRP1-deficient MEFs (**Fig. 7F-H**). When the mitochondrial network was pharmacologically disrupted through inhibition of DRP1, we observed a suppression of circadian variation in the gene expression of clock activator *Bmal1* and repressors *Per1* and *Per2* (**Fig. 7C-E**), similar to results obtained in DRP1-deficient MEFs (**Fig. 7F-H**). These findings indicate that disruption of circadian mitochondrial dynamics leads to an impaired core circadian clock.

Discussion

A wide range of metabolic processes follows the rhythmicity of the circadian cycle to anticipate energetic requirements of diverse cellular functions in response to cellular and environmental constraints. Yet, only a few studies have characterized the mechanisms involved, demonstrating coupling via cyclic redox metabolite levels (e.g: NAD⁺), mitochondrial protein acetylation and chromatin modification (Asher and Schibler, 2011, Feng et al., 2011, Masri et al., 2013, Nakahata et al., 2009, Peek et al., 2013). Here, we identify and characterize a third, mitochondrial dynamics-based regulatory connection between the circadian clock and metabolism, and show that this connection is absolutely essential for circadian regulation of cellular ATP levels.

Mitochondrial morphology has previously been demonstrated to regulate nearly every aspect of mitochondrial function: mitochondrial fusion to form more extensive tubular networks results in global upregulation of oxidative respiration and all other functions, while fission of mitochondria into smaller fragments causes opposite effects (Westermann, 2010). Such regulation at the level of morphology has been extensively characterized within the context of the cell cycle, with different phases of the cell division process requiring specific energetic needs (Martinez-Diez et al., 2006, Mishra and Chan, 2014).

The first clues that similar global regulation of mitochondrial function might be operational can be gleaned from circadian “-omics” analyses and studies of individual metabolite levels. Metabolic flux analysis and supplementary analyses presented here (**Fig. 1, 2**) showed that many metabolites displayed circadian rhythmicity even in isolated cells, and the major circadian pathway signatures of the cellular metabolome that we have identified are consistent with those previously described in rodents (Eckel-Mahan et al.,

2012, Minami et al., 2009) and humans (Ang et al., 2012, Dallmann et al., 2012, Davies et al., 2014, Kasukawa et al., 2012). Fully half of rhythmic compounds identified were amino acids and associated metabolites known to be engaged in mitochondrial energetic homeostasis through branched-chain amino acid metabolism, glycolysis and TCA cycle to provide energetic substrates such as pyruvate for ATP generation through oxidative phosphorylation. Another large compound group was linked to glutathione metabolism (where, interestingly, molecular abundance varied more dramatically than redox state *per se*), processing of ROS, and redox homeostasis, or was metabolic byproducts of mitochondrial metabolism (i.e. ATP, the couple NAD^+/NADH). Interestingly, the group of mostly mitochondrial fuels showed peak expression levels about six hours earlier than the “byproduct” group.

Overall, mitochondrial oxygen consumption analyses showed time-of-day-dependent variation in each measurable step of the mitochondrial respiratory chain (**Fig. 3**, see also (Isobe et al., 2011, Peek et al., 2013)). When in resting state (low ATP), the cells exhibited a higher spare respiratory capacity. Remarkably, the bioenergetic profile showed that only mitochondrial respiration varied in a circadian manner over time, whereas glycolysis remained constant.

Taken together, the pervasive circadian regulation of metabolic flux, even in cultured cells, suggested global regulation of mitochondrial function. Remarkably, such global and dynamic regulation has also been observed in the cellular metabolic regulation by the cell cycle (Martinez-Diez et al., 2006, Mishra and Chan, 2014). Once perceived as solitary structures, mitochondria are now recognized as highly mobile (along cytoskeletal tracks), dynamic organelles that continually fuse and divide to upregulate and downregulate respiration in response to cellular energy requirements (Kasahara and Scorrano, 2014). Our findings demonstrate that the circadian mitochondrial bioenergetic is governed by circadian mitochondrial dynamics *in vivo* and *in vitro*. This coupling is completely independent of the cell cycle (in which it was initially characterized), both because it continues in the presence of cell cycle inhibitors *in vitro*, and because it equally occurs in mostly nondividing tissues like brain and liver. Moreover, it is functionally essential for circadian ATP production because its inhibition, either pharmacologically or genetically, abolishes circadian oscillations in ATP levels.

A well-defined set of proteins regulates mitochondrial fission and fusion, including mitofusins and dynamin-related proteins. Although another recent study has found circadian oscillation of these genes at a transcriptional level in liver (Jacobi et al., 2015), expression levels of these genes did not exhibit any circadian oscillations in cultured cells. Instead, we find that both phosphorylation of the protein DRP1 and its stability are regulated in a

circadian manner. An identical regulatory mechanism has been described for synchronizing mitochondrial function to the cell cycle: phosphorylation of DRP1 at serine 637 by cyclin B/CDK1 complexes is essential to cell cycle - coupled mitochondrial respiration (Cribbs and Strack, 2007, Kashatus et al., 2011, Santel and Frank, 2008). Our genetic and pharmacological inhibition experiments demonstrate that mitochondrial dynamics are also essential for circadian regulation in nondividing cells: analysis of regulation of DRP1 revealed that phosphorylation of serine 637 followed a circadian pattern, and pharmacological or genetic interference with DRP1 activity abolishes the circadian production of ATP. It has been suggested that DRP1 S637 phosphorylation is directed by protein kinase A (PKA), while DRP1 S637 dephosphorylation is mediated by calcineurin (Cereggetti et al., 2008, Cribbs and Strack, 2007). Moreover, it has been described that the activity of calcineurin, but not its protein expression, is under circadian regulation (Huang et al., 2012), suggesting that the oscillation of DRP1 phosphorylation may be dependent on calcineurin's phosphatase activity.

Importantly, the mitochondrial regulatory cascade that we uncover can feed back to modulate the circadian clock itself. When mitochondrial fission was pharmacologically inhibited, we observed not only dampening of mitochondrial ATP rhythm but also an increase of circadian period in human skin fibroblasts and a strong decrease in the circadian amplitude of clock gene transcription in fibroblasts. These results could be explained via two previously published feedback mechanisms from respiration to the circadian clock: on the one hand, ATP synthesis affects the balance of purine nucleotides in the cell, thereby modulating the activity of the nutrient-sensitive kinase AMPK in phosphorylation of the cryptochrome clock (Lamia et al., 2009, Um et al., 2011). On the other hand, circadian modulation of NAD⁺ and NADH levels affects the activity of the SIRT1 histone deacetylase, which can target both clock proteins and histones (Asher et al., 2008, Chang and Guarente, 2013, Nakahata et al., 2008, Nakahata et al., 2009). Consistent with either feedback loop, inhibition of mitochondrial flux in multiple different ways showed effects upon circadian clock properties and upon clock gene expression in fibroblasts. Therefore, the mitochondrial network acts as a central node in coupling circadian and metabolic cycles.

In summary, consistent with the growing body of evidence integrating cellular metabolism with circadian clocks (Rey and Reddy, 2013, Eckel-Mahan and Sassone-Corsi, 2013, Bass, 2012, Bass and Takahashi, 2010), our findings establish a molecular link between circadian control of the mitochondrial architecture and mitochondrial oxidative metabolism, suggesting a key role for global circadian regulation of mitochondrial function in controlling circadian metabolism. Our findings could have multiple implications in the context of metabolic homeostasis, both with respect to human health and disease, and with respect

to impairment in circadian clock and/ or mitochondrial function. Perturbations in the clock may be a key initiating factor for diseases linked to compromised mitochondrial function, including neurodegenerative disorders such as Alzheimer's disease.

Figures

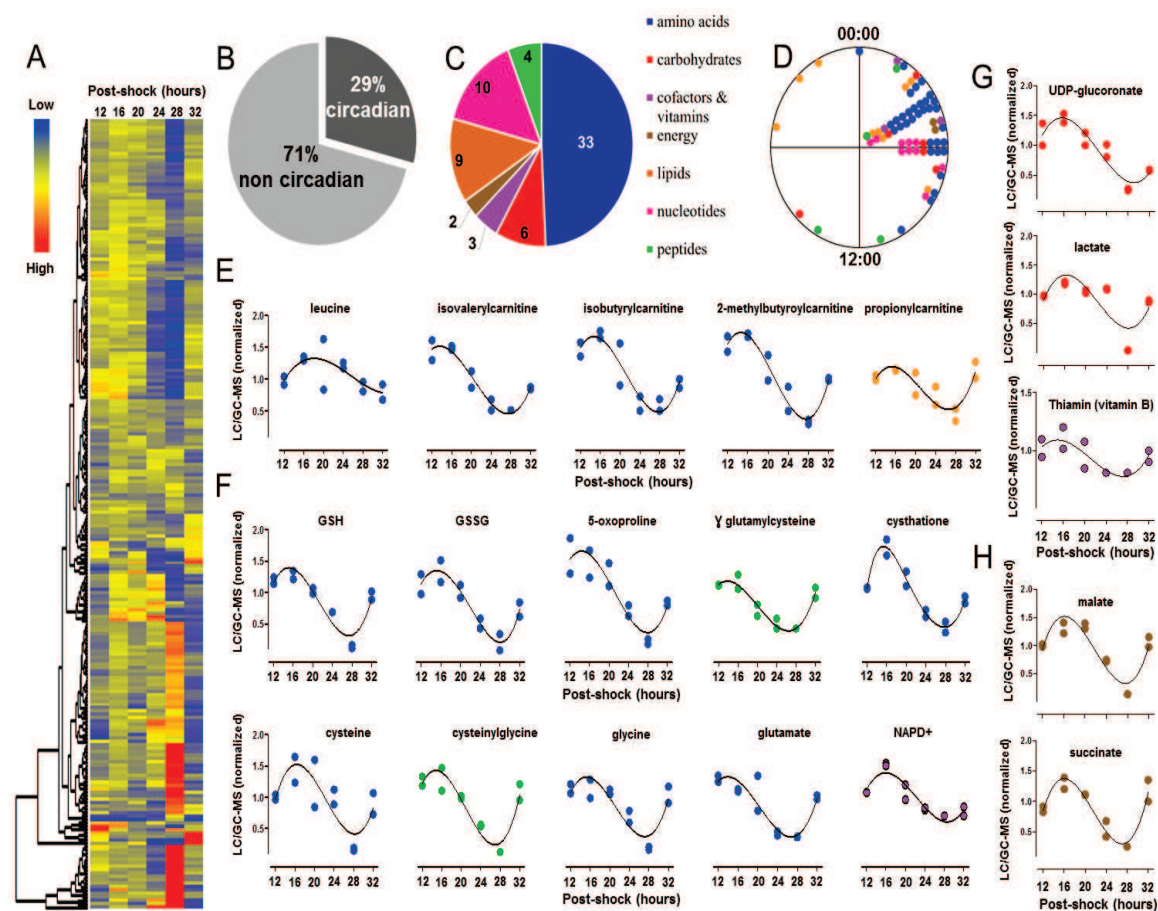


Figure 1: Circadian clock regulates globally the cellular metabolic flux.

(A) Heat plots for all identified metabolites in synchronized human U2OS cells. (B) Percentage of non-circadian and circadian metabolites based on JTK_CYCLE analysis (six time points, $n=2$ for each). Metabolites were considered circadian at a p -value cutoff of 0.05. Out of the 228 measured and identified, 67 metabolites exhibited circadian pattern. (C, D) Pathway analyses (C) and time-of-day distribution of peak phases (D) of rhythmic metabolites. (E-H) Accumulation profiles of oscillating metabolites involved in branched-chain amino acids metabolism (E), in GSH/GSSG metabolism (F), in glycolysis (G) and in TCA cycle (H), presented as mean \pm SEM. Pathways are color-coded as follows: amino acids, blue; carbohydrates, red; cofactors & vitamins, violet; energy, brown; lipids, orange; nucleotides, pink; peptides, green. See also Table 1.

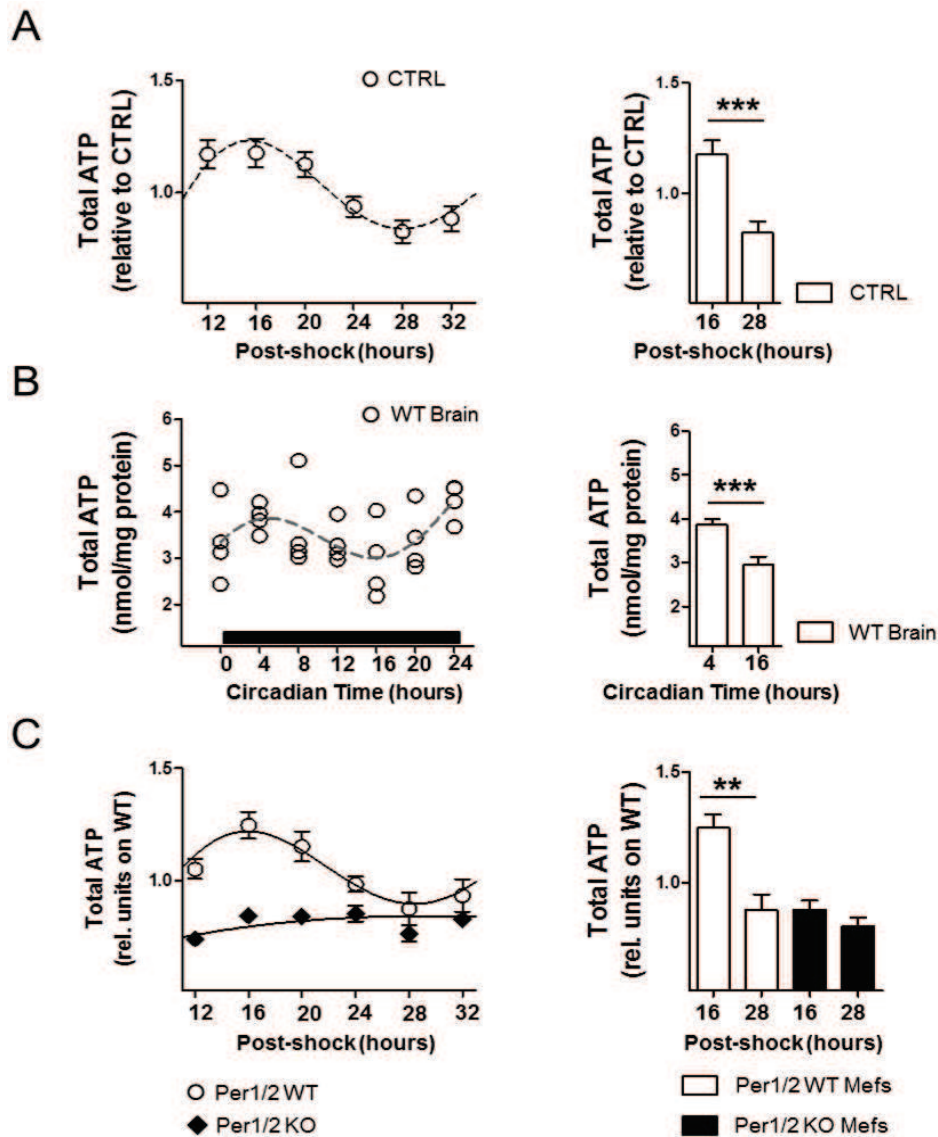


Figure 2: Cellular bioenergetic variations are driven by the circadian clock.

(A) Relative total ATP levels from serum-shocked human skin fibroblasts measured at the indicated time points (6 time points, $n=6$ for each, JTK_Cycle, $P<0.05$). Right panel displays relative total ATP level at 16 hours post-shock (peak of ATP content) and at 28 hours (trough of ATP content) in fibroblast cultures (One-way ANOVA, ATP variation pattern, $P<0.0001$; post hoc Tukey; 16 versus 28 hours, ***, $P < 0.001$). (B) Relative total ATP levels measured in brain of non-fasted wildtype mice kept in constant darkness (WT Brain) every 4 hours for 24 hours (7 time points, $n=4$ for each). Right panel displays relative total ATP level at circadian time 4 (CT4) (peak of ATP content) and at circadian time 16 (CT16) (trough of ATP content) in control and treated conditions (One-way ANOVA, ATP variation pattern, $P<0.0001$; post hoc Tukey; 16 versus 28 hours, ***, $P < 0.001$). (C) Relative total ATP level measured in serum-shocked *Per1/2*^{-/-} MEFs (KO P1P2) compared to WT MEFs (WT P1P2) (6 time points, $n=6$ for each, JTK_Cycle, $P_{WT P1P2}<0.05$). Right panel displays relative total ATP level measured in serum-shocked *Per1/2*^{-/-} MEFs (KO P1P2) compared to WT MEFs (WT P1P2) at 16 hours post-shock (peak of ATP content) and at 28 hours (trough of ATP content) (One-way ANOVA, ATP variation pattern in WT MEFs, $P<0.0001$; post hoc Tukey; 16 versus 28 hours, **, $P < 0.01$).

All data are represented as mean \pm SEM of at least three independent samples. See also [Figures S1, S2](#).

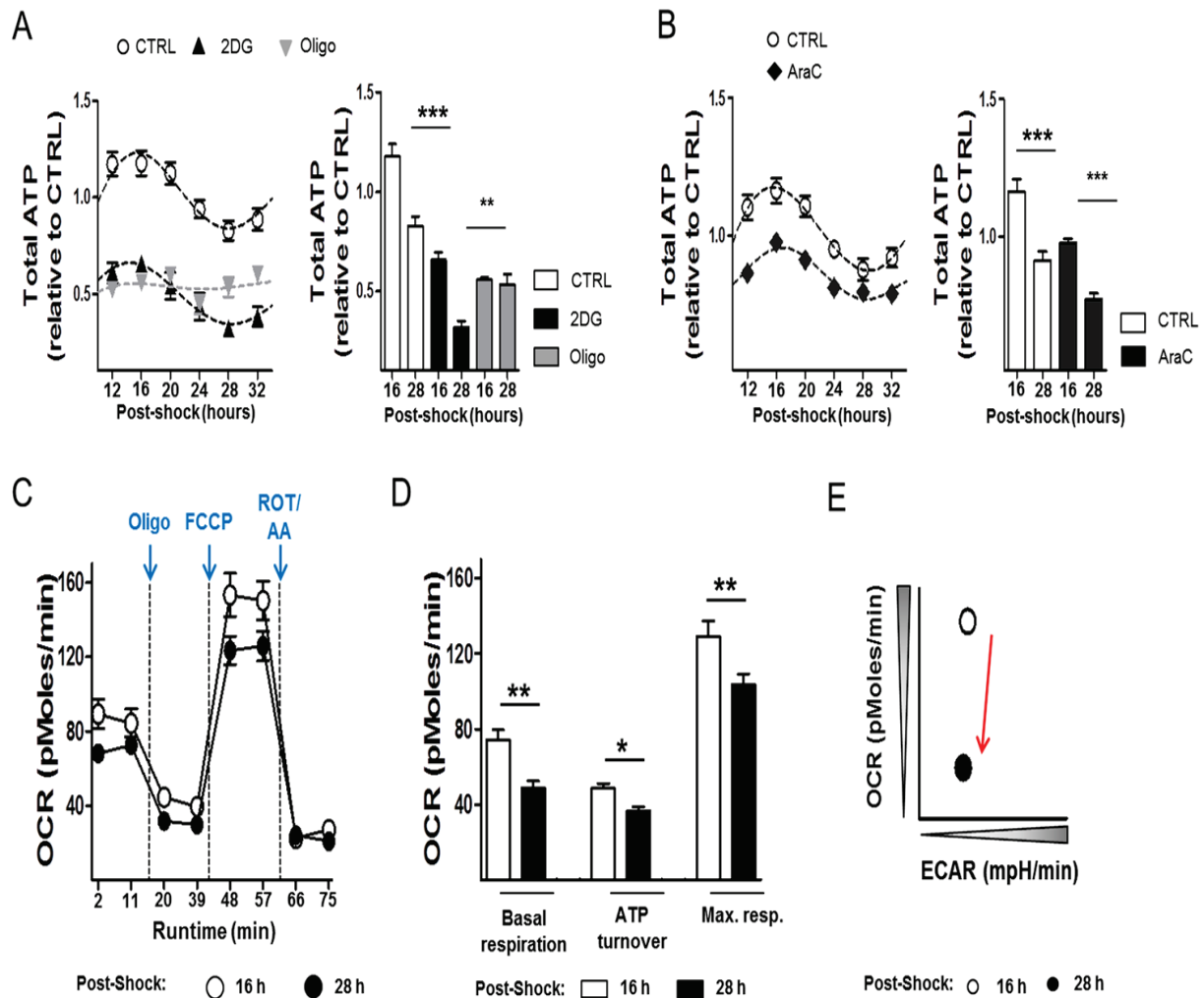


Figure 3: Circadian ATP oscillations result from mitochondrial respiratory activity.

(A) Relative total ATP levels from serum-shocked human skin fibroblasts treated with 2 - deoxy-D-glucose (2DG, 4.5g/L) or oligomycin (OLIGO, 2 μ M) compared to non-treated cells (CTRL) measured at the indicated time points (6 time points, n=6 for each, JTK_Cycle, $P_{CTRL}<0.05$, $P_{2DG}<0.05$). Right panel displays relative total ATP level at 16 hours post-shock (peak of ATP content) and at 28 hours (trough of ATP content) in control and treated conditions (One-way ANOVA, ATP variation pattern in control cells, $P<0.0001$; post hoc Tukey; 16 versus 28 hours, $***$, $P < 0.001$; ATP variation pattern in 2DG-treated cells, $P<0.0001$; post hoc Tukey; 16 versus 28 hours, $^{\circ}$, $P < 0.001$). (B) Relative total ATP contents from serum-shocked human skin fibroblasts treated with cytosine β -D-arabinofuranoside (AraC, 100 μ M) compared to non-treated cells (CTRL) measured at the indicated time points in cells (6 time points, n=6 for each, JTK_Cycle, $P_{CTRL}<0.05$, $P_{AraC}<0.05$). Right panel displays relative total ATP level at 16 hours post-shock (peak of ATP content) and at 28 hours (trough of ATP content) in control and treated conditions (One-way ANOVA, ATP variation pattern in control cells, $P<0.0001$; post hoc Tukey; 16 versus 28 hours, $***$, $P < 0.001$; ATP variation pattern in 2DG-treated cells, $P<0.0001$; post hoc Tukey; 16 versus 28 hours, $^{\circ}$, $P < 0.01$). All data are represented as mean \pm SEM of at least three independent samples. (C) Oxygen Consumption Rate (OCR) was evaluated in serum-shocked fibroblasts treated sequentially with oligomycin (Oligo, 2 μ M), FCCP (0.7 μ M), rotenone (ROT, 2 μ M) and antimycin A (AA, 4 μ M) at 16 and 28 hours post-shock, respectively. (D) Bioenergetic profile of synchronized fibroblasts at 16 and 28 hours post-shock, respectively. Basal respiration, ATP turnover and maximal respiration are determined after normalization to OCR allocated to non-mitochondrial respiration measured after antimycin A/rotenone injection (One-way ANOVA, OCR variation pattern $P<0.0001$; post hoc Tukey; 16 versus 28 hours, $**$, $P < 0.01$, $***$, $P < 0.001$). (E) Cellular bioenergetic profile (OCR versus ECAR) evaluated at 16 and 28 hours post-shock, respectively in human skin fibroblasts. The red arrow corresponds to the metabolic switch from a metabolic active (16 hours) to a resting state (28 hours). All data are represented as mean \pm SEM of three independent samples (2 time points, n= 11 replicates for each, three independent experiments).

See also [Figures S3, S4](#).

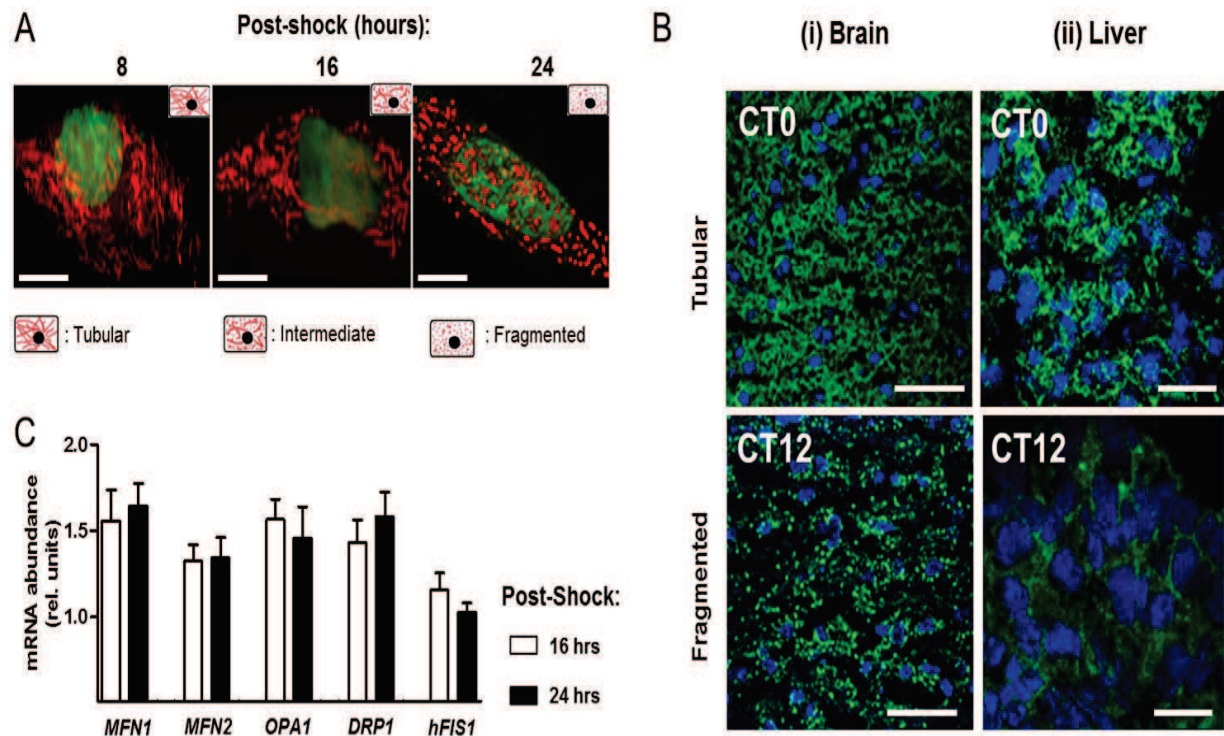


Figure 4: Dynamic mitochondrial architecture is controlled by the circadian clock.

(A) Mitochondrial network morphology assessed in serum-shocked human skin fibroblasts at 8, 16 and 24 hours. The three distinct states (tubular, intermediate and fragmented network) correspond to 8, 16 and 24 hours, respectively. Scale bars, 7.5 μm . (B) Mitochondrial network morphology assessed in (i) brain and (ii) liver from non-fasted wild-type mice kept in darkness condition at CT0 and CT12. The tubular and fragmented states correspond to CT0 and CT12, respectively. Scale bars, brain, 50 μm ; liver, 25 μm . (C) Relative mRNA expression of nuclearly-encoded genes related to mitochondrial fusion (*MFN1*, *MFN2* and *OPA1*) and fission (*DRP1* and *hFIS1*) measured at 16 hours and 24 hours in serum-shocked human skin fibroblasts (2 time points, n=6 for each). All data are represented as mean \pm SEM of at least three independent samples. See also [Figure S5](#).

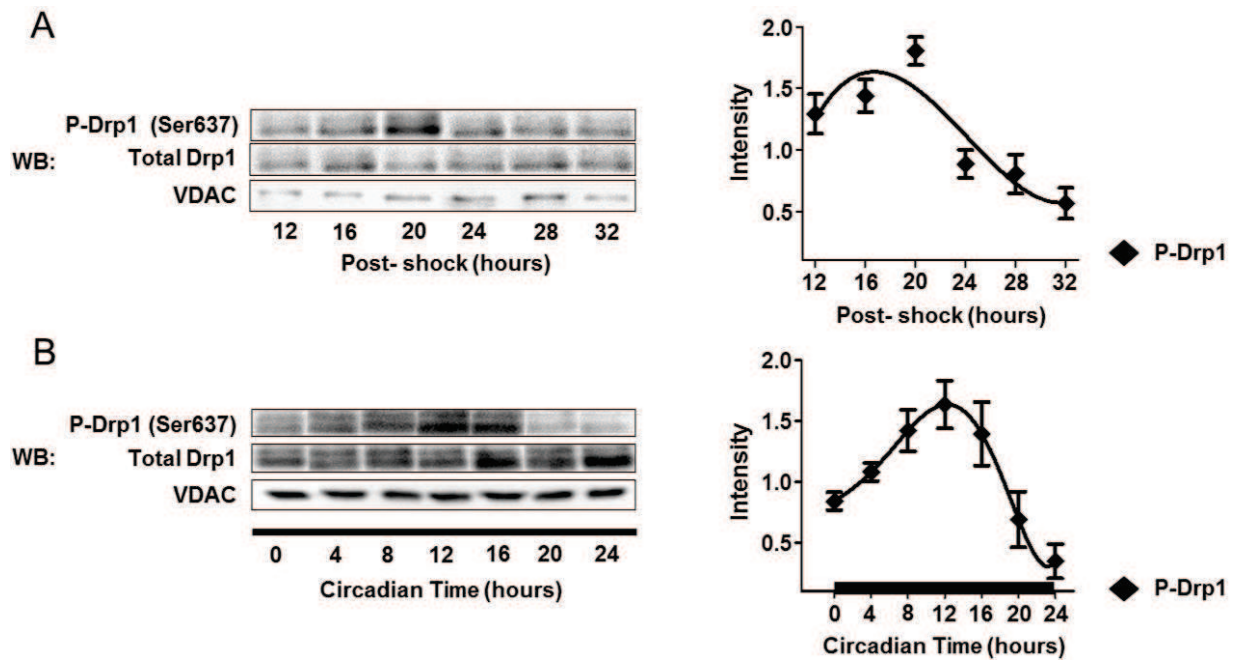


Figure 5: DRP1 mediates clock control of mitochondrial architecture.

(A, B) Phosphorylation of DRP1 on serine 637 (P-DRP1) and total DRP1 evaluated at the indicated time points in serum-shocked human skin fibroblasts (6 time points, n=6 for each, JTK_Cycle, P<0.05) (A) and in brain homogenate of non-fasted wildtype mice kept in constant darkness (7 time points, n=4 for each, JTK_Cycle, P<0.05) (B). Right panels display relative DRP1 phosphorylation measured in serum-shocked human skin fibroblasts (A) and in brain homogenate of non-fasted wildtype mice kept in constant darkness (B). All data are represented as mean \pm SEM of at least three independent samples.

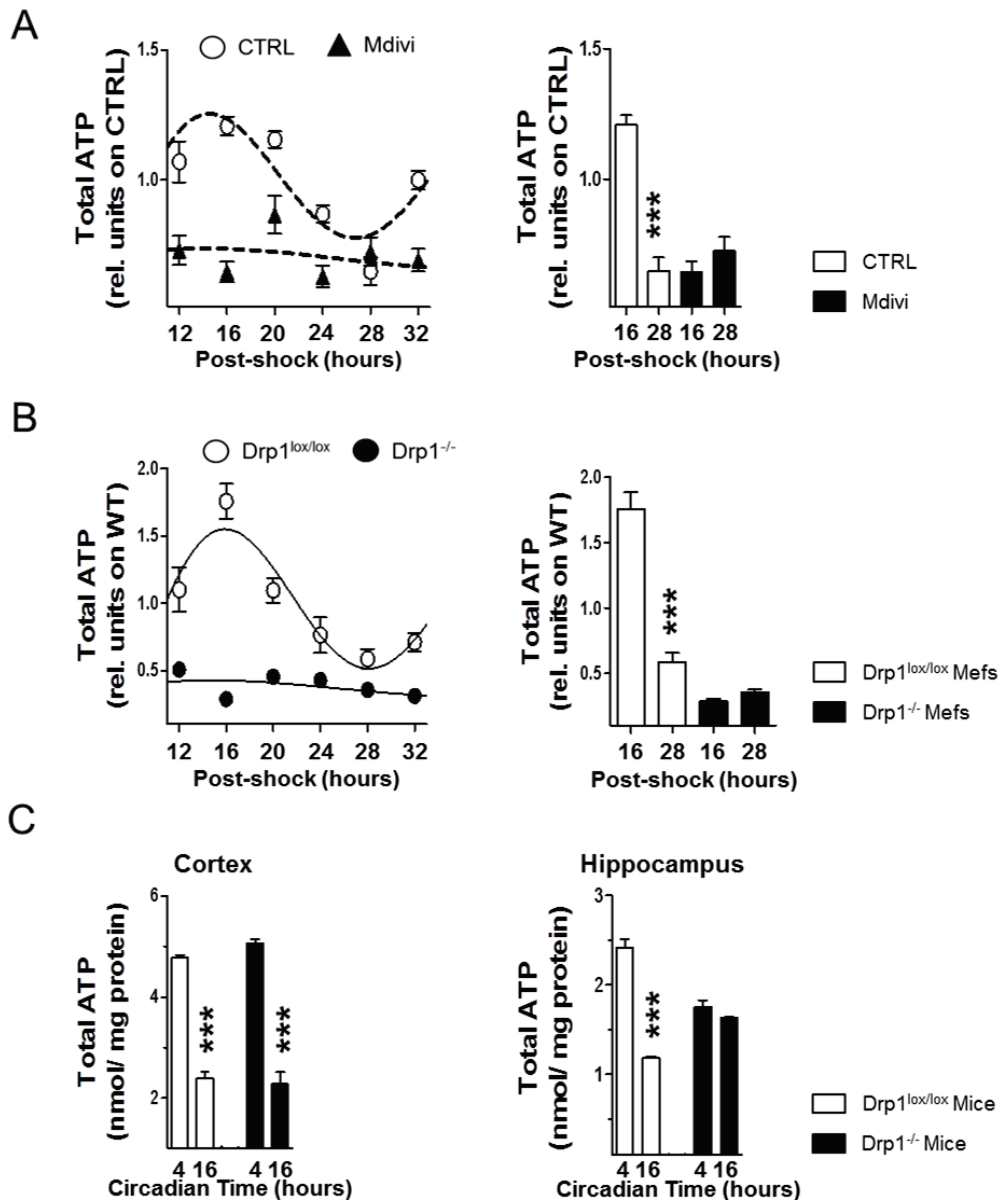


Figure 6: Mitochondrial metabolism is dependent to DRP1-related clock regulation.

(A) Relative total ATP level from serum-shocked human skin fibroblasts treated with mdivi-1 (50 μ M) compared to non-treated cells (CTRL) measured at the indicated time points (6 time points, $n=6$ for each, JTK_Cycle, $P_{CTRL}<0.05$). Right panel displays relative total ATP level at 16 hours post-shock (peak of ATP content) and at 28 hours (trough of ATP content) in control and treated conditions. (One-way ANOVA, ATP variation pattern in control cells, $P<0.0001$; post hoc Tukey; 16 versus 28 hours, $***, P < 0.001$). (B) Relative total ATP levels from *Drp1^{-/-}* MEFs compared to *Drp1^{lox/lox}* MEFs measured at the indicated time points (6 time points, $n=6$ for each, JTK_Cycle, $P_{Drp1lox/lox}<0.05$). Right panel displays relative total ATP level at 16 hours post-shock (peak of ATP content) and at 28 hours (trough of ATP content) in *Drp1^{lox/lox}* MEFs and *Drp1^{-/-}* MEFs (One-way ANOVA, ATP variation pattern, $P<0.0001$; post hoc Tukey; 16 versus 28 hours, $***, P < 0.001$). (C) Total ATP levels from cortex and hippocampus of non-fasted *Drp1^{-/-}* mice compared to *Drp1^{lox/lox}* mice kept in constant darkness measured at CT4 (peak of ATP content) and at CT16 (trough of ATP content) (2 time points, $n=4$ cortex for each). (One-way ANOVA, ATP variation pattern, $P<0.0001$; post hoc Tukey; CT4 versus CT12, $***, P < 0.001$). All data are represented as mean \pm SEM of at least three independent samples.

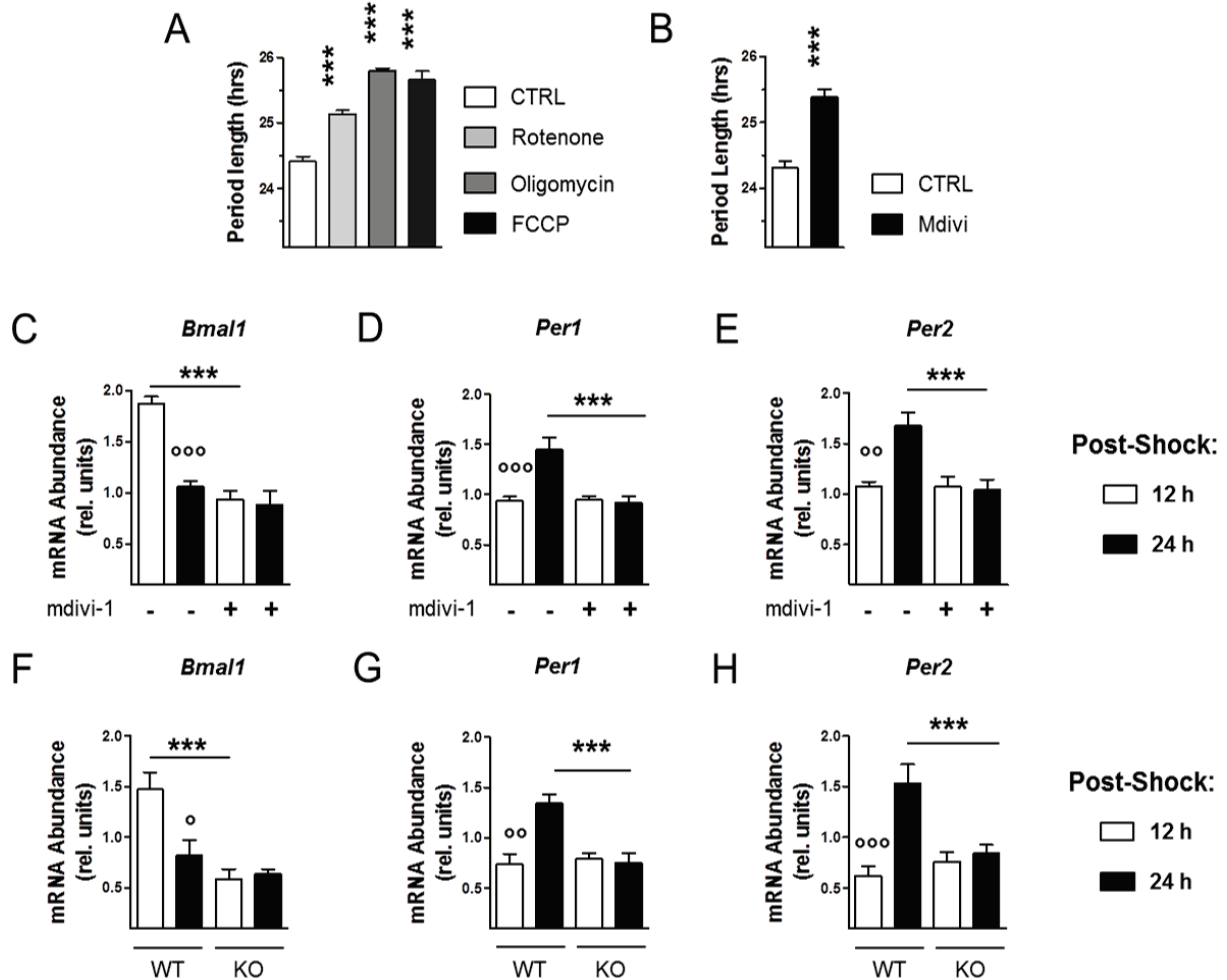


Figure 7: Mitochondrial network feeds back into the molecular core clock.

(A) Circadian period length determined in dexamethasone - synchronized human skin fibroblasts transfected with *Bmal1*::luciferase reporter in presence of rotenone (ROT, 1 µM), oligomycin (OLIGO, 2 µM) or FCCP (4 µM) compared to control (CTRL). (B) Circadian period length determined in dexamethasone - synchronized human skin fibroblasts transfected with *Bmal1*::luciferase reporter in presence of Mdiv-1 (50 µM) compared to control (CTRL). Bars represent the mean of three independent measurements ± SEM. *P < 0.05, **P < 0.01, ***P < 0.001 for Student's two-tailed t test comparing single time points. (C-E) Relative mRNA expression of *BMAL1* (C), *PER1* (D) and *PER2* (E) evaluated in serum-shocked human skin fibroblasts treated with mdivi-1 (50µM) compared to control cells (CTRL) at 12 hours and 24 hours (2 time points, n=6 for each) (One-way ANOVA, *Bmal1* mRNA variation pattern, P<0.0001, post hoc Tukey; 12 versus 24 hours, °°,P < 0.001; *Per1* mRNA variation pattern, P=0.0001, post hoc Tukey; 12 versus 24 hours, °°,P < 0.001 *Per2* mRNA variation pattern, P=0.0008, post hoc Tukey; 12 versus 24 hours, °°,P < 0.01; Two-way ANOVA, group effect: control versus mdivi-1, P_{*Bmal1*}<0.0001, post hoc Bonferroni, ***, P_{*Bmal1*}<0.001; group effect: control versus mdivi-1, P_{*Per1*}= 0.0011, post hoc Bonferroni, ***, P_{*Per1*}<0.001; group effect: control versus mdivi-1, P_{*Per2*}=0.0034, post hoc Bonferroni, ***, P_{*Per2*}<0.001). (F-H) Relative mRNA expression of *Bmal1* (F), *Per1* (G) and *Per2* (H) evaluated from in *Drp1*^{-/-} MEFs compared to *Drp1*^{lox/lox} MEFs at 12 hours and 24 hours (2 time points, n=6 for each) (One-way ANOVA, *Bmal1* mRNA variation pattern, P=0.0010, post hoc Tukey; 12 versus 24 hours, °,P < 0.001; *Per1* mRNA variation pattern, P=0.0008, post hoc Tukey; 12 versus 24 hours, °°,P < 0.01 *Per2* mRNA variation pattern, P=0.0010, post hoc Tukey; 12 versus 24 hours, °°,P < 0.01;Two-way ANOVA, group effect: WT versus KO, P_{*Bmal1*}=0.0002, post hoc Bonferroni, ***, P_{*Bmal1*}<0.001; group effect: WT versus KO, P_{*Per1*}= 0.0028, post hoc Bonferroni, ***, P_{*Per1*}<0.001; group effect: WT versus KO, P_{*Per2*}=0.0265, post hoc Bonferroni, ***, P_{*Per2*}<0.001).

All data are represented as mean ± SEM of at least three independent samples.

Supplemental Data

Table S1: Complete list of all identified metabolites in serum-shocked U2OS.

All values are normalized (mean±SEM). Rhythmic compounds are indicated in red color. Abbr.: RI: retention index, HMDB: identification numbers of biochemicals in Human Metabolome Database, PT-p: p-values computed with the permutation test as described in Methods, Per: Period, LAG: peak phases, Amp: amplitude of oscillation, defined as the maximum divided by the minimum level of a particular biochemical in the first 24hrs of the experiment. Phase: Phase of the peak for rhythmic biochemicals.

BIOCHEMICAL	PATHWAY	PLATFORM	RI	MASS	HMDB_ID	PT-p	PER	LAG	AMP	Post- Shock (hours)											
										12		16		20		24		28		32	
										mean	SEM	mean	SEM	mean	SEM	mean	SEM	mean	SEM	mean	SEM
10-heptadecenoate (17:1n7)	Lipid	LC/MS Neg	5558	267.3		1.0000	24	13	0.08	0.85	0.11	1.15	0.11	0.88	0.05	1.07	0.04	2.70	0.01	0.47	0.02
10-nonadecenoate (19:1n9)	Lipid	LC/MS Neg	5775	295.4		1.0000	24	13	0.06	0.84	0.10	1.16	0.14	0.92	0.06	1.03	0.02	1.91	0.13	0.53	0.04
1-arachidonoylglycerophosphoethanolamine*	Lipid	LC/MS Neg	5731	500.3	HMDB11517	1.0000	24	15	0.05	1.27	0.41	1.29	0.36	0.83	0.24	1.43	0.53	2.42	0.02	0.67	0.14
1-methylnicotinamide	Cofactors and vitamins	LC/MS Pos	688	137.1	HMDB00699	0.0009	24	2	0.34	1.38	0.07	1.24	0.03	0.97	0.11	0.75	0.06	0.46	0.06	1.04	0.11
1-myristoylglycerophosphocholine	Lipid	LC/MS Pos	5481	468.3	HMDB10379	0.5770	24	0	0.29	1.05	0.37	1.00	0.03	0.75	0.07	0.82	0.14	0.68	0.00	1.37	0.05
1-octadecanol	Lipid	GC/MS	1957.7	327.3	HMDB02350	1.0000	24	11	0.00	1.08	0.37	1.22	0.03	0.92	0.10	0.78	0.20	1.81	0.38	0.69	0.17
1-oleoylglycerol (1-monoolein)	Lipid	GC/MS	2181.2	397.4	HMDB11567	1.0000	24	11	0.22	0.68	0.00	1.31	0.12	1.05	0.17	0.71	0.42	3.69	1.35	0.39	0.24
1-oleoylglycerophosphocholine	Lipid	LC/MS Pos	5700	522.4		0.2485	24	0	0.09	1.52	0.40	0.95	0.12	0.87	0.07	0.51	0.05	3.47	0.30	1.00	0.00
1-oleoylglycerophosphoethanolamine	Lipid	LC/MS Neg	5928	478.3	HMDB11506	1.0000	24	17	0.32	1.54	0.86	1.28	0.68	0.61	0.03	1.66	0.34	2.74	0.09	0.48	0.17
1-palmitoylglycerol (1-monopalmitin)	Lipid	GC/MS	2119.5	371.3		1.0000	24	11	0.24	0.66	0.25	1.25	0.16	1.11	0.26	1.04	0.24	2.30	0.90	0.51	0.03
1-palmitoylglycerophosphocholine	Lipid	LC/MS Pos	5671	496.4		0.2485	24	0	0.19	1.69	0.55	1.12	0.18	0.85	0.02	0.61	0.15	3.98	0.01	1.00	0.00
1-palmitoylglycerophosphoethanolamine	Lipid	LC/MS Neg	5940	452.3	HMDB11503	1.0000	24	17	0.21	1.18	0.43	1.06	0.57	0.55	0.11	1.20	0.20	1.98	0.13	0.49	0.05
1-stearoylglycerol (1-monostearin)	Lipid	GC/MS	2186.6001	399.4		0.6640	24	13	0.41	0.65	0.41	1.26	0.45	0.84	0.10	1.30	0.00	2.28	0.51	0.64	0.07
1-stearoylglycerophosphocholine	Lipid	LC/MS Pos	5844	524.4		0.2485	24	0	0.33	3.31	2.29	1.32	0.33	0.77	0.07	0.56	0.00	2.21	0.14	1.15	0.30
1-stearoylglycerophosphoethanolamine	Lipid	LC/MS Neg	6200	480.4	HMDB11130	1.0000	24	11	0.19	1.50	1.00	1.18	0.58	0.53	0.12	1.61	0.26	1.55	0.14	0.35	0.02
1-stearoylglycerophosphoglycerol	Lipid	LC/MS Neg	5826	511.4		1.0000	24	17	0.09	0.62	0.20	0.83	0.21	1.24	0.21	0.35	0.00	2.56	0.02	0.77	0.23
1-stearoylglycerophosphoinositol	Lipid	LC/MS Neg	5800	599.4		1.0000	24	15	0.32	1.03	0.42	1.00	0.04	0.50	0.12	1.34	0.00	7.70	0.11	0.43	0.09
2-aminoadipate	Amino acid	GC/MS	1686.5	260.1	HMDB00510	0.0730	24	4	0.45	0.94	0.11	1.38	0.12	1.32	0.30	0.61	0.01	0.14	0.01	1.60	0.62
2-arachidonoylglycerophosphocholine*	Lipid	LC/MS Pos	5524	544.3		1.0000	24	13	0.07	0.95	0.10	0.82	0.06	1.09	0.14	0.93	0.17	3.26	0.44	0.76	0.01
2-arachidonoylglycerophosphoethanolamine*	Lipid	LC/MS Pos	5525	502.3		1.0000	24	11	0.01	1.20	0.18	0.99	0.05	1.05	0.08	0.71	0.13	3.68	0.63	0.85	0.05
2'-deoxyinosine	Nucleotide	LC/MS Neg	1700	251.1	HMDB00071	0.3533	24	7	0.08	0.93	0.04	1.23	0.22	1.07	0.16	1.21	0.22	0.87	0.00	1.01	0.14
2-docosahexaenoylglycerophosphocholine*	Lipid	LC/MS Pos	5507	568.3		1.0000	24	15	0.02	1.48	0.61	1.09	0.53	0.96	0.01	0.85	0.29	2.54	0.79	0.89	0.11
2-docosahexaenoylglycerophosphoethanolamine*	Lipid	LC/MS Pos	5512	526.2		1.0000	24	13	0.10	0.93	0.04	1.06	0.03	1.00	0.17	0.85	0.32	3.47	0.62	0.75	0.04
2-docosapentaenoylglycerophosphoethanolamine*	Lipid	LC/MS Pos	5548	528.2		1.0000	24	11	0.06	1.38	0.31	1.19	0.29	1.20	0.37	0.43	0.01	3.47	0.76	0.82	0.10
2-hydroxyglutarate	Lipid	GC/MS	1576	247	HMDB00606	0.1702	24	5	0.33	0.92	0.00	1.40	0.40	1.35	0.26	0.60	0.02	0.42	0.00	1.17	0.03
2-hydroxypalmitate	Lipid	LC/MS Neg	5508	271.3		0.0044	24	21	0.53	1.67	0.75	0.83	0.25	0.51	0.02	0.90	0.01	1.31	0.02	1.63	0.16
2-hydroxystearate	Lipid	LC/MS Neg	5705	299.4		0.0730	24	21	0.57	1.76	0.86	0.73	0.28	0.53	0.06	0.96	0.04	1.44	0.04	1.51	0.11
2-linoleoylglycerophosphocholine*	Lipid	LC/MS Pos	5544	520.4		0.0592	24	18	0.14	0.80	0.26	0.89	0.02	0.93	0.03	0.77	0.23	2.27	0.46	1.25	0.15

BIOCHEMICAL	PATHWAY	PLATFORM	RI	MASS	HMDB_ID	PT-p	PER	LAG	AMP	Post- Schock (hours)											
										12		16		20		24		28		32	
										mean	SEM	mean	SEM	mean	SEM	mean	SEM	mean	SEM	mean	SEM
2-linoleoylglycerophosphoethanolamine*	Lipid	LC/MS Neg	5650	476.4		1.0000	24	17	0.07	1.00	0.41	0.96	0.45	0.62	0.10	0.15	0.15	2.09	1.58	0.69	0.18
2-methylbutyrocarnitine	Amino acid	LC/MS Pos	2439	246.1	HMDB00378	0.00004	24	4	0.66	1.55	0.12	1.69	0.03	1.18	0.20	0.69	0.19	0.33	0.03	1.00	0.02
2-myristoylglycerol (2-monomyristin)	Lipid	GC/MS	2040	285.2		1.0000	24	15	0.79	0.45	0.00	0.45	0.00	0.58	0.13	0.45	0.00	1.44	0.15	0.45	0.00
2-myristoylglycerophosphocholine*	Lipid	LC/MS Pos	5450	468.3		0.8804	24	20	0.07	1.01	0.00	0.97	0.03	0.96	0.06	0.68	0.23	3.37	0.74	1.14	0.18
2-oleoylglycerol (2-monoolein)	Lipid	GC/MS	2170	410.1		1.0000	24	11	0.16	0.37	0.00	2.21	0.11	0.94	0.15	0.82	0.09	3.79	1.85	0.57	0.19
2-oleoylglycerophosphocholine*	Lipid	LC/MS Pos	5640	522.4		1.0000	24	13	0.04	1.20	0.15	0.94	0.06	1.00	0.07	0.50	0.10	3.51	0.51	0.99	0.01
2-oleoylglycerophosphoethanolamine*	Lipid	LC/MS Pos	5625	480.2		1.0000	24	13	0.03	1.35	0.19	0.98	0.03	0.96	0.09	0.70	0.27	3.98	0.47	0.95	0.04
2-oleoylglycerophosphoinositol*	Lipid	LC/MS Neg	5571	597.5		1.0000	24	17	0.18	0.70	0.57	0.96	0.17	0.36	0.22	1.07	0.20	2.13	0.12	0.16	0.02
2'-O-methylguanosine	Nucleotide	LC/MS Neg	1901	296.2		1.0000	24	9	0.14	0.82	0.00	0.92	0.08	0.82	0.00	1.50	0.27	0.82	0.00	0.82	0.00
2-palmitoleoylglycerophosphocholine*	Lipid	LC/MS Pos	5482	494.3		1.0000	24	13	0.09	1.05	0.14	1.00	0.11	0.93	0.10	0.62	0.16	3.93	0.47	1.02	0.05
2-palmitoleoylglycerophosphoethanolamine*	Lipid	LC/MS Pos	5487	452.1		0.8804	24	20	0.23	1.01	0.12	0.85	0.04	1.01	0.21	0.49	0.28	4.48	1.22	1.15	0.04
2-palmitoylglycerol (2-monopalmitin)	Lipid	GC/MS	2108	129		0.8804	24	13	0.20	0.76	0.04	1.33	0.22	1.13	0.20	1.00	0.06	2.36	0.43	0.78	0.13
2-palmitoylglycerophosphocholine*	Lipid	LC/MS Pos	5604	496.3		0.8804	24	9	0.00	1.08	0.08	0.91	0.09	0.96	0.05	0.50	0.01	3.76	0.49	1.05	0.06
2-palmitoylglycerophosphoethanolamine*	Lipid	LC/MS Pos	5598	454.2		0.5770	24	19	0.00	0.92	0.25	0.83	0.17	0.66	0.00	0.66	0.00	2.94	0.17	0.69	0.03
3-(4-hydroxyphenyl)lactate	Amino acid	LC/MS Neg	1395	181.1	HMDB00755	0.0931	24	7	0.19	0.90	0.10	1.18	0.20	1.26	0.22	0.93	0.15	0.78	0.00	0.84	0.06
3-dehydrocarnitine*	Lipid	LC/MS Pos	1020	160.2	HMDB12154	0.4899	24	3	0.26	1.00	0.04	1.05	0.27	1.07	0.20	0.69	0.05	0.64	0.00	1.46	0.22
3'-dephosphocoenzyme A	Cofactors and vitamins	LC/MS Neg	2010	686.2	HMDB01373	1.0000	24	13	0.10	1.79	0.69	1.10	0.43	0.53	0.00	0.86	0.14	3.15	1.41	0.59	0.07
4-hydroxybutyrate (GHB)	Lipid	GC/MS	1277	233.1	HMDB00710	0.0214	24	8	0.46	0.71	0.27	1.09	0.09	1.34	0.27	1.20	0.22	0.44	0.00	0.62	0.18
5-methyltetrahydrofolate (5MeTHF)	Cofactors and vitamins	LC/MS Neg	1838	458.2	HMDB01396	1.0000	24	5	0.08	0.83	0.08	1.06	0.10	0.99	0.10	0.97	0.12	0.75	0.00	1.17	0.13
5-methylthioadenosine (MTA)	Amino acid	LC/MS Pos	2427	298.1	HMDB01173	0.0001	24	4	0.24	1.10	0.03	1.26	0.09	1.09	0.09	0.40	0.02	0.30	0.07	0.96	0.04
5-oxoproline	Amino acid	LC/MS Neg	744	128.2	HMDB00267	0.0021	24	4	0.48	1.61	0.29	1.47	0.22	1.30	0.18	0.72	0.09	0.22	0.04	0.84	0.04
6-phosphogluconate	Carbohydrate	LC/MS Neg	588	275.1	HMDB01316	0.4216	24	14	0.19	0.85	0.00	1.05	0.34	1.61	0.64	1.12	0.12	1.94	0.90	0.78	0.08
7-alpha-hydroxycholesterol	Lipid	GC/MS	2300	456.2	HMDB01496	0.8804	24	17	0.21	0.93	0.24	1.20	0.29	0.77	0.03	1.07	0.25	1.88	0.31	1.00	0.01
7-beta-hydroxycholesterol	Lipid	GC/MS	2340	456.4	HMDB06119	0.2485	24	5	0.18	1.10	0.04	1.42	0.03	1.27	0.33	0.85	0.08	1.10	0.36	0.89	0.01
acetyl CoA	Cofactors and vitamins	LC/MS Neg	1900	808.1	HMDB01206	1.0000	24	15	0.03	0.73	0.07	0.98	0.12	0.88	0.01	1.38	0.12	0.65	0.00	1.71	0.06
acetylcarnitine	Lipid	LC/MS Pos	1203	204.2	HMDB00201	0.4899	24	2	0.36	1.01	0.01	1.11	0.11	0.97	0.17	0.51	0.03	0.25	0.08	1.52	0.02
acetylphosphate	Energy	GC/MS	1263	211	HMDB01494	1.0000	24	9	0.01	0.84	0.26	1.40	0.05	0.85	0.14	1.16	0.20	1.05	0.04	0.91	0.06
adenine	Nucleotide	GC/MS	1804.2	264	HMDB00034	0.0004	24	4	0.38	1.15	0.15	1.26	0.04	1.11	0.04	0.32	0.03	0.11	0.03	0.88	0.12
adenosine	Nucleotide	LC/MS Pos	1650	268.1	HMDB00050	1.0000	24	13	0.08	0.80	0.03	1.06	0.11	0.92	0.20	1.01	0.06	1.20	0.04	0.86	0.19
adenosine 3'-monophosphate (3'-AMP)	Nucleotide	LC/MS Neg	1268	346.1	HMDB03540	0.5770	24	16	0.17	0.90	0.10	0.90	0.07	0.86	0.05	1.59	0.25	3.00	1.01	0.81	0.00
adenosine 5'-diphosphate (ADP)	Nucleotide	LC/MS Neg	800	426.1	HMDB01341	1.0000	24	9	0.08	0.89	0.14	1.00	0.10	0.93	0.17	0.90	0.10	0.15	0.00	1.23	0.04
adenosine 5'diphosphoribose	Cofactors and vitamins	LC/MS Neg	964	558.1	HMDB01178	1.0000	24	17	0.65	0.77	0.00	0.77	0.00	0.77	0.00	0.77	0.00	1.00	0.23	0.77	0.00
adenosine 5'-monophosphate (AMP)	Nucleotide	LC/MS Pos	1210	348.1	HMDB00045	0.1702	24	3	0.17	1.09	0.05	1.08	0.07	0.86	0.13	0.79	0.06	0.54	0.09	1.17	0.04
adenylosuccinate	Nucleotide	LC/MS Pos	1870	464.1	HMDB00536	1.0000	24	7	0.08	0.28	0.02	0.87	0.44	1.13	0.13	0.26	0.00	0.41	0.15	1.26	0.03
adrenate (22:4n6)	Lipid	LC/MS Neg	5684	331.3	HMDB02226	1.0000	24	15	0.14	0.95	0.23	1.05	0.19	0.79	0.10	1.16	0.05	2.19	0.04	0.54	0.00
agmatine	Amino acid	GC/MS	1528	174	HMDB01432	0.6640	24	2	0.68	1.60	1.10	0.83	0.03	1.47	0.33	0.30	0.03	0.27	0.00	1.70	0.32
alanine	Amino acid	GC/MS	1147.6	115.9	HMDB00161	0.4899	24	7	0.11	1.05	0.11	1.07	0.15	1.17	0.23	1.13	0.07	0.46	0.07	0.96	0.12
alanylleucine	Peptide	LC/MS Pos	2150	203		0.6640	24	13	0.48	0.71	0.03	1.19	0.14	0.91	0.45	5.73	4.78	6.62	2.19	0.40	0.08
alanylthreonine	Peptide	LC/MS Neg	827	189		0.3009	24	16	1.28	0.11	0.00	0.11	0.00	0.13	0.02	0.56	0.44	1.16	0.12	0.11	0.00
allantoin	Nucleotide	GC/MS	1809.8	518.3	HMDB00462	0.8804	24	1	0.12	1.40	0.82	0.63	0.12	1.46	0.85	0.51	0.00	0.51	0.00	1.67	0.42
alpha-tocopherol	Cofactors and vitamins	GC/MS	2305.3999	502.5	HMDB01893	0.3009	24	2	0.25	1.30	0.24	1.28	0.12	0.92	0.00	0.49	0.08	0.98	0.57	0.68	0.26
arachidonate (20:4n6)	Lipid	LC/MS Neg	5525	303.4	HMDB01043	1.0000	24	15	0.00	1.00	0.00	1.03	0.00	0.84	0.03	1.05	0.14	2.30	0.07	0.51	0.03
arginine	Amino acid	LC/MS Neg	728	173.2	HMDB00517	0.0272	24	10	0.34	0.82	0.07	1.13	0.10	1.00	0.44	1.40	0.03	1.03	0.05	0.52	0.10

BIOCHEMICAL	PATHWAY	PLATFORM	RI	MASS	HMDB_ID	PT-p	PER	LAG	AMP	Post- Schock (hours)											
										12		16		20		24		28		32	
										mean	SEM	mean	SEM	mean	SEM	mean	SEM	mean	SEM	mean	SEM
asparagine	Amino acid	GC/MS	1651.2	231	HMDB00168	0.0272	24	4	0.30	1.21	0.04	1.20	0.32	1.10	0.02	0.40	0.12	0.04	0.00	1.21	0.29
aspartate	Amino acid	GC/MS	1529.7	232	HMDB00191	0.0272	24	4	0.15	1.09	0.06	1.15	0.10	1.00	0.06	0.54	0.03	0.07	0.01	1.13	0.17
aspartylphenylalanine	Peptide	LC/MS Pos	2538	281.1	HMDB00706	1.0000	24	9	0.10	0.90	0.12	1.21	0.05	1.49	0.85	0.86	0.13	1.54	0.43	0.54	0.16
beta-alanine	Amino acid	GC/MS	1451.8	174	HMDB00056	0.0454	24	4	0.25	1.53	0.65	1.82	0.57	0.82	0.18	0.71	0.19	0.07	0.00	1.18	0.11
betaine	Amino acid	LC/MS Pos	721	118.2	HMDB00043	0.0156	24	4	0.41	1.34	0.06	1.21	0.10	1.11	0.30	0.73	0.07	0.37	0.01	1.00	0.06
butyrylcarnitine	Lipid	LC/MS Pos	2007	232.2	HMDB02013	1.0000	24	7	0.12	0.90	0.07	1.15	0.13	2.01	0.85	0.50	0.08	0.87	0.06	2.75	0.00
caprate (10:0)	Lipid	LC/MS Neg	5092	171.2	HMDB00511	0.3533	24	13	0.19	0.79	0.03	1.05	0.01	0.87	0.08	1.14	0.06	3.29	0.14	0.81	0.10
caprylate (8:0)	Lipid	LC/MS Neg	4367	143.2	HMDB00482	1.0000	24	11	0.05	0.60	0.00	0.97	0.23	0.81	0.18	0.80	0.20	1.97	1.38	0.81	0.21
carnitine	Lipid	LC/MS Pos	702	162.2	HMDB00062	0.4899	24	4	0.14	1.00	0.02	1.10	0.01	0.96	0.17	0.76	0.12	0.40	0.02	1.27	0.02
C-glycosyltryptophan*	Amino acid	LC/MS Pos	1912	367.1		1.0000	24	7	0.06	0.96	0.03	1.17	0.17	0.90	0.11	1.02	0.29	0.55	0.00	1.15	0.10
cholesterol	Lipid	GC/MS	2316.8999	329.3	HMDB00067	1.0000	24	17	0.03	0.84	0.03	1.10	0.03	0.91	0.10	0.99	0.01	2.10	0.27	0.96	0.16
choline	Lipid	LC/MS Pos	674	104.2	HMDB00097	1.0000	24	7	0.09	1.19	0.01	1.14	0.14	0.99	0.09	0.80	0.05	1.16	0.17	0.82	0.03
choline phosphate	Lipid	LC/MS Pos	695	184.1	HMDB01565	0.0085	24	3	0.24	1.71	0.00	1.48	0.01	1.25	0.21	0.87	0.06	0.84	0.00	0.92	0.04
cis-vaccenate (18:1n7)	Lipid	GC/MS	1987	339.3		1.0000	24	13	0.10	0.73	0.19	1.13	0.12	0.84	0.18	1.09	0.11	2.19	0.42	0.47	0.06
citrate	Energy	GC/MS	1763.4	273.1	HMDB00094	1.0000	24	15	0.09	0.64	0.10	1.30	0.32	0.96	0.02	0.82	0.19	1.52	0.28	1.69	0.09
coenzyme A	Cofactors and vitamins	LC/MS Neg	1600	766.1	HMDB01423	0.4899	24	5	0.18	1.23	0.20	1.31	0.09	0.81	0.01	1.30	0.15	0.48	0.08	0.78	0.19
creatine	Amino acid	LC/MS Pos	758	132.1	HMDB00064	0.0021	24	3	0.27	1.23	0.06	1.16	0.05	1.00	0.07	0.62	0.02	0.60	0.05	0.99	0.07
cyclo(gly-phe)	Peptide	GC/MS	1830	257		0.0454	24	11	0.46	0.59	0.04	1.28	0.19	1.34	0.58	1.83	0.36	0.91	0.21	0.67	0.25
cystathionine	Amino acid	GC/MS	1979.6	218.1	HMDB00099	0.0004	24	5	0.44	1.07	0.01	1.73	0.13	1.22	0.12	0.67	0.05	0.45	0.08	0.89	0.05
cysteine	Amino acid	GC/MS	1560.1	218	HMDB00574	0.0454	24	6	0.25	1.00	0.04	1.44	0.21	1.22	0.38	1.00	0.12	0.17	0.02	0.90	0.17
cysteine sulfonic acid	Amino acid	GC/MS	1662	252	HMDB00996	0.0044	24	6	0.30	0.93	0.12	1.59	0.64	1.34	0.05	1.00	0.23	0.62	0.00	0.67	0.05
cysteinylglycine	Peptide	GC/MS	1763	257	HMDB00078	0.0021	24	4	0.36	1.26	0.07	1.29	0.18	1.00	0.02	0.55	0.01	0.11	0.01	1.08	0.13
cytidine	Nucleotide	LC/MS Pos	1065	244	HMDB00089	1.0000	24	13	0.67	0.55	0.05	1.68	0.94	0.85	0.40	2.14	0.29	6.98	0.17	0.36	0.09
cytidine 5'-diphosphocholine	Lipid	LC/MS Pos	777	489.1	HMDB01413	0.0001	24	4	0.32	1.17	0.02	1.26	0.08	1.00	0.06	0.69	0.01	0.68	0.00	0.77	0.09
cytidine 5'-monophosphate (5'-CMP)	Nucleotide	LC/MS Pos	887	324	HMDB00095	0.8804	24	3	0.11	1.08	0.00	1.27	0.29	0.85	0.17	0.98	0.17	0.76	0.16	0.92	0.12
cytidine-5'-diphosphoethanolamine	Lipid	LC/MS Pos	765	447	HMDB01564	0.2485	24	4	0.05	1.01	0.03	1.00	0.01	1.04	0.13	0.62	0.01	0.61	0.00	1.02	0.00
deoxycarnitine	Lipid	LC/MS Pos	759	146.1	HMDB01161	0.6640	24	7	0.12	1.00	0.09	1.12	0.04	0.91	0.06	0.81	0.22	0.56	0.08	1.47	0.10
dihomo-linoleate (20:2n6)	Lipid	LC/MS Neg	5722	307.3		1.0000	24	15	0.10	0.86	0.14	1.13	0.13	0.82	0.12	1.15	0.12	2.49	0.08	0.52	0.00
dimethylarginine (SDMA + ADMA)	Amino acid	LC/MS Pos	812	203.2	HMDB01539, HMDB03334	0.2485	24	11	0.36	0.76	0.02	1.00	0.01	1.03	0.50	1.29	0.00	1.32	0.07	0.56	0.11
docosadienoate (22:2n6)	Lipid	LC/MS Neg	6017	335.4		1.0000	24	13	0.08	0.88	0.14	1.13	0.21	0.91	0.14	1.08	0.10	1.88	0.02	0.55	0.01
docosahexaenoate (DHA; 22:6n3)	Lipid	LC/MS Neg	5518	327.3	HMDB02183	1.0000	24	11	0.04	0.96	0.00	1.16	0.04	1.02	0.02	0.98	0.02	2.13	0.09	0.72	0.00
docosapentaenoate (n3 DPA; 22:5n3)	Lipid	LC/MS Neg	5574	329.4	HMDB01976	1.0000	24	11	0.00	0.97	0.06	1.13	0.05	0.95	0.08	0.95	0.02	2.04	0.03	0.50	0.01
eicosapentaenoate (EPA; 20:5n3)	Lipid	LC/MS Neg	5442	301.3	HMDB01999	1.0000	24	15	0.02	0.96	0.08	1.11	0.02	0.88	0.09	1.02	0.17	3.19	0.12	0.61	0.04
eicosenoate (20:1n9 or 11)	Lipid	LC/MS Neg	5955	309.4	HMDB02231	1.0000	24	13	0.07	0.89	0.17	1.11	0.17	0.84	0.10	1.10	0.04	1.92	0.04	0.53	0.02
erythronate*	Carbohydrate	GC/MS	1546.9	292.1	HMDB00613	0.1417	24	2	0.48	1.08	0.08	0.89	0.32	0.85	0.17	0.23	0.11	0.19	0.06	1.24	0.18
ethanolamine	Lipid	GC/MS	1074	102	HMDB00149	0.0272	24	4	0.65	1.29	0.39	1.30	0.04	1.52	0.08	0.45	0.06	0.15	0.03	1.00	0.03
flavin adenine dinucleotide (FAD)	Cofactors and vitamins	LC/MS Neg	2413	784.1	HMDB01248	0.8804	24	14	0.06	0.82	0.10	1.07	0.06	0.94	0.10	1.02	0.03	1.45	0.06	0.90	0.05
fumarate	Energy	GC/MS	1382.1	245	HMDB00134	0.6640	24	6	0.04	0.88	0.07	1.12	0.25	1.27	0.16	0.92	0.20	0.40	0.08	1.15	0.09
gamma-aminobutyrate (GABA)	Amino acid	GC/MS	1539.7	304.1	HMDB00112	0.0454	24	3	0.51	1.32	0.48	1.97	0.33	0.61	0.04	0.53	0.21	0.33	0.00	1.42	0.26
gamma-glutamylcysteine	Peptide	LC/MS Pos	1274	251.1	HMDB01049	0.0021	24	2	0.37	1.13	0.01	1.19	0.12	0.73	0.09	0.51	0.08	0.43	0.00	1.01	0.08
gamma-glutamylglutamate	Peptide	LC/MS Pos	1036	277.1		0.0730	24	3	0.85	1.77	0.02	1.43	0.41	1.27	0.77	0.41	0.19	0.37	0.00	1.22	0.24
gamma-glutamylisoleucine*	Peptide	LC/MS Pos	2644	261.2	HMDB11170	0.3533	24	2	0.28	1.01	0.09	1.09	0.07	0.97	0.00	0.65	0.02	0.63	0.00	1.48	0.19

BIOCHEMICAL	PATHWAY	PLATFORM	RI	MASS	HMDB_ID	PT-p	PER	LAG	AMP	Post- Schock (hours)											
										12		16		20		24		28		32	
										mean	SEM	mean	SEM	mean	SEM	mean	SEM	mean	SEM	mean	SEM
gamma-glutamylleucine	Peptide	LC/MS Pos	2744	261.2	HMDB11171	1.0000	24	5	0.08	0.84	0.01	1.09	0.02	1.11	0.17	0.89	0.01	0.82	0.00	1.41	0.20
gamma-glutamylphenylalanine	Peptide	LC/MS Pos	2846	295.1	HMDB00594	1.0000	24	7	0.08	0.99	0.20	1.05	0.07	1.15	0.15	0.74	0.00	1.22	0.48	0.88	0.13
gamma-glutamylvaline	Peptide	LC/MS Pos	2040	247.2	HMDB11172	1.0000	24	7	0.01	0.84	0.06	1.09	0.18	1.00	0.09	0.99	0.11	0.77	0.00	1.76	0.06
glucose	Carbohydrate	GC/MS	1866.8	204.1	HMDB00122	0.0272	24	14	0.23	0.80	0.07	1.00	0.20	1.22	0.22	1.27	0.27	5.64	1.39	0.96	0.03
glucose 1-phosphate	Carbohydrate	GC/MS	1853	217.1	HMDB01586	0.4899	24	12	0.21	0.45	0.22	1.36	0.69	1.23	0.14	2.05	0.27	0.23	0.00	0.76	0.15
glutamate	Amino acid	LC/MS Pos	700	148.1	HMDB03339	0.0156	24	3	0.37	1.29	0.05	1.11	0.02	1.07	0.28	0.42	0.03	0.36	0.01	1.00	0.03
glutamate, gamma-methyl ester	Amino acid	LC/MS Pos	1062	162.1		0.4899	24	7	0.19	0.73	0.07	1.06	0.08	1.34	0.24	0.91	0.12	0.66	0.00	0.98	0.18
glutamine	Amino acid	GC/MS	1731.4	156	HMDB00641	0.0730	24	4	0.22	1.16	0.00	1.03	0.31	1.01	0.05	0.44	0.15	0.07	0.01	1.35	0.31
glutathione, oxidized (GSSG)	Amino acid	LC/MS Pos	1535	613.1	HMDB03337	0.00004	24	4	0.37	1.23	0.14	1.42	0.16	1.13	0.09	0.66	0.07	0.39	0.12	0.87	0.10
glutathione, reduced (GSH)	Amino acid	LC/MS Pos	1274	308.1	HMDB00125	0.00004	24	4	0.32	1.19	0.05	1.28	0.07	1.03	0.04	0.69	0.00	0.14	0.02	0.95	0.07
glycerol 3-phosphate (G3P)	Lipid	GC/MS	1719.7	357.1	HMDB00126	0.0156	24	22	0.28	1.88	0.04	0.96	0.09	0.93	0.28	0.80	0.05	0.91	0.04	3.83	1.27
glycerophosphoethanolamine	Lipid	GC/MS	1906	357.1	HMDB00114	0.2485	24	1	0.90	1.57	0.24	0.56	0.41	0.91	0.12	0.24	0.11	0.13	0.00	3.06	1.16
glycerophosphorylcholine (GPC)	Lipid	LC/MS Pos	694	258.1	HMDB00086	0.0454	24	19	0.54	1.30	0.11	0.63	0.19	0.54	0.07	0.56	0.09	2.33	0.07	1.50	0.29
glycine	Amino acid	GC/MS	1166	101.9	HMDB00123	0.0156	24	4	0.21	1.12	0.07	1.11	0.14	1.07	0.04	0.67	0.09	0.18	0.02	1.02	0.13
glycylglycine	Peptide	GC/MS	1757.9	174	HMDB11733	0.2485	24	7	0.59	0.97	0.33	1.61	0.23	1.09	0.58	1.61	0.15	0.44	0.03	0.57	0.13
glycylisoleucine	Peptide	LC/MS Pos	2080	189.1		0.2485	24	13	0.65	0.54	0.03	1.19	0.40	1.04	0.57	2.00	0.79	1.96	0.12	0.49	0.13
glycylleucine	Peptide	LC/MS Pos	2236	189.1	HMDB00759	0.2485	24	13	0.69	0.51	0.03	1.18	0.47	1.06	0.53	2.36	1.07	2.09	0.15	0.52	0.16
glycylphenylalanine	Peptide	LC/MS Neg	2193	221.2		0.2485	24	13	0.46	0.59	0.06	1.26	0.40	0.91	0.35	2.42	1.29	1.93	0.08	0.54	0.16
glycylproline	Peptide	LC/MS Pos	1115	173.1	HMDB00721	0.7722	24	8	0.51	0.62	0.09	1.36	0.06	1.10	0.55	1.12	0.21	1.02	0.55	0.73	0.27
glycylserine	Peptide	GC/MS	1854	174.1	HMDB00678	0.1702	24	10	0.66	0.97	0.19	1.88	0.16	1.66	1.12	2.65	0.31	0.69	0.14	0.63	0.11
glycyltyrosine	Peptide	LC/MS Pos	1728	239.1		0.0454	24	14	0.65	0.46	0.11	1.05	0.53	1.00	0.20	1.78	0.47	1.76	0.10	0.45	0.21
glycylvaline	Peptide	LC/MS Pos	1572	175.1		0.1132	24	13	0.62	0.25	0.00	0.89	0.37	0.83	0.35	1.54	0.54	1.31	0.05	0.39	0.09
guanine	Nucleotide	GC/MS	1942.3	352.1	HMDB00132	0.0454	24	6	0.50	1.43	0.18	1.56	0.73	1.23	0.67	1.26	0.09	0.21	0.01	0.66	0.11
guanosine	Nucleotide	LC/MS Pos	1676	284	HMDB00133	0.0272	24	7	0.52	0.90	0.09	1.51	0.17	1.17	0.17	1.30	0.16	0.39	0.16	0.43	0.02
guanosine 5'- monophosphate (GMP)	Nucleotide	LC/MS Pos	1300	364		1.0000	24	13	0.18	0.90	0.07	1.11	0.07	0.78	0.00	1.29	0.15	1.25	0.10	0.64	0.12
guanosine 5'-diphospho-fucose	Nucleotide	LC/MS Neg	797	588.1		0.0454	24	6	0.16	0.94	0.12	1.08	0.08	1.04	0.04	0.88	0.15	0.73	0.00	0.88	0.04
histidine	Amino acid	LC/MS Neg	757	154.1	HMDB00177	0.0454	24	6	0.21	1.03	0.11	1.28	0.12	1.26	0.41	1.19	0.12	0.29	0.05	0.81	0.08
hypotaurine	Amino acid	GC/MS	1598.5	188	HMDB00965	0.0085	24	4	0.22	1.78	0.63	1.68	0.51	0.97	0.03	0.76	0.18	0.14	0.03	1.21	0.21
hypoxanthine	Nucleotide	LC/MS Neg	1313	135.1	HMDB00157	0.0454	24	6	0.26	1.34	0.23	1.30	0.29	1.09	0.30	1.05	0.06	0.41	0.06	0.85	0.11
inosine	Nucleotide	LC/MS Neg	1630	267.2		0.0009	24	6	0.41	1.07	0.06	1.34	0.05	1.14	0.15	0.89	0.15	0.34	0.08	0.64	0.06
inosine 5'-monophosphate (IMP)	Nucleotide	LC/MS Pos	1310	349	HMDB00175	0.0009	24	8	0.64	0.75	0.08	1.87	0.04	1.61	0.49	1.00	0.05	0.37	0.00	0.44	0.07
inositol 1-phosphate (I1P)	Lipid	GC/MS	2057.8	318.1	HMDB00213	1.0000	24	17	0.01	0.76	0.21	1.20	0.18	1.02	0.22	0.95	0.03	1.97	0.18	0.88	0.26
Isobar: UDP-acetylglucosamine, UDP-acetylgalactosamine	Carbohydrate	LC/MS Neg	661	606.1		0.1132	24	4	0.48	1.99	0.43	1.46	0.06	1.06	0.18	0.89	0.17	0.76	0.17	0.64	0.11
isobutyrylcarnitine	Amino acid	LC/MS Pos	1941	232.2	HMDB00736	0.0003	24	4	0.60	1.47	0.11	1.70	0.06	1.23	0.33	0.62	0.11	0.60	0.09	0.93	0.07
isoleucine	Amino acid	LC/MS Pos	1614	132.1	HMDB00172	0.0730	24	7	0.21	0.96	0.05	1.30	0.02	1.25	0.37	1.10	0.05	0.57	0.08	0.89	0.10
isovalerylcarnitine	Amino acid	LC/MS Pos	2533	246.2	HMDB00688	0.0004	24	4	0.51	1.46	0.16	1.49	0.03	0.99	0.13	0.60	0.09	0.51	0.00	0.86	0.02
lactate	Carbohydrate	GC/MS	1102.8	116.9	HMDB00190	0.0085	24	6	0.12	0.97	0.01	1.19	0.02	1.05	0.03	1.09	0.01	0.04	0.01	0.88	0.02
lactose	Carbohydrate	GC/MS	2134	204	HMDB00186	0.0454	24	7	0.87	0.92	0.04	2.29	0.05	1.78	0.74	2.22	0.60	0.19	0.05	0.46	0.03
laurate (12:0)	Lipid	LC/MS Neg	5288	199.3	HMDB00638	0.4899	24	13	0.15	0.80	0.00	1.09	0.08	1.07	0.08	1.06	0.12	5.00	0.37	0.96	0.02
leucine	Amino acid	LC/MS Pos	1674	132.2	HMDB00687	0.0454	24	8	0.26	0.98	0.06	1.33	0.03	1.23	0.40	1.22	0.05	0.88	0.07	0.80	0.12
leucylleucine	Peptide	LC/MS Pos	3012	245.1		0.5770	24	13	0.56	0.32	0.05	1.08	0.23	0.44	0.17	1.65	0.49	1.77	0.43	0.46	0.18
linoleate (18:2n6)	Lipid	LC/MS Neg	5533	279.3	HMDB00673	0.4899	24	13	0.36	0.78	0.10	1.10	0.06	0.84	0.11	1.25	0.05	3.17	0.09	0.59	0.01
linolenate [alpha or gamma; (18:3n3 or 6)]	Lipid	LC/MS Neg	5450	277.3	HMDB01388	0.4899	24	13	0.25	0.71	0.02	1.06	0.01	0.83	0.12	1.08	0.00	2.75	0.16	0.55	0.00

BIOCHEMICAL	PATHWAY	PLATFORM	RI	MASS	HMDB_ID	PT-p	PER	LAG	AMP	Post- Schock (hours)											
										12		16		20		24		28		32	
										mean	SEM	mean	SEM	mean	SEM	mean	SEM	mean	SEM	mean	SEM
lysine	Amino acid	GC/MS	1836.7	317.2	HMDB00182	0.1702	24	6	0.38	0.92	0.30	1.58	0.27	1.06	0.47	1.65	0.17	0.23	0.00	0.66	0.12
malate	Energy	GC/MS	1502	233	HMDB00156	0.0085	24	5	0.38	1.00	0.02	1.31	0.09	1.34	0.05	0.73	0.02	0.14	0.00	1.06	0.09
margarate (17:0)	Lipid	GC/MS	1951.6	327.3	HMDB02259	1.0000	24	11	0.12	0.78	0.10	1.29	0.17	0.98	0.17	0.84	0.29	2.39	0.24	0.57	0.03
mead acid (20:3n9)	Lipid	LC/MS Neg	5642	305.4	HMDB10378	1.0000	24	15	0.18	0.94	0.19	1.00	0.13	0.68	0.06	1.25	0.10	2.02	0.09	0.71	0.02
methionine	Amino acid	LC/MS Pos	1252	150.1	HMDB00696	0.0454	24	8	0.27	0.98	0.06	1.27	0.07	1.25	0.43	1.15	0.02	0.69	0.06	0.82	0.14
methylphosphate	Nucleotide	GC/MS	1221	240.9		1.0000	24	13	0.01	0.66	0.00	1.14	0.19	1.14	0.00	0.88	0.01	1.07	0.26	1.13	0.09
myo-inositol	Lipid	GC/MS	1924.9	217	HMDB00211	0.1702	24	4	0.09	1.03	0.01	1.34	0.35	0.98	0.17	0.82	0.08	0.14	0.05	1.05	0.00
myristate (14:0)	Lipid	LC/MS Neg	5439	227.3	HMDB00806	0.4899	24	13	0.23	0.78	0.15	1.17	0.17	0.90	0.10	1.17	0.01	3.17	0.24	0.64	0.01
myristoleate (14:1n5)	Lipid	LC/MS Neg	5338	225.3	HMDB02000	1.0000	24	13	0.01	0.76	0.03	1.09	0.05	1.08	0.11	0.94	0.01	2.80	0.23	0.99	0.05
N1-methyladenosine	Nucleotide	LC/MS Pos	1356	282.1	HMDB03331	0.3009	24	7	0.20	0.81	0.05	1.14	0.10	0.93	0.29	1.12	0.12	0.64	0.00	0.70	0.06
N6-acetyllysine	Amino acid	LC/MS Pos	1134	189.1	HMDB00206	0.1702	24	8	0.26	0.93	0.08	1.30	0.14	1.24	0.60	1.19	0.19	0.91	0.12	0.58	0.09
N-acetylaniline	Amino acid	LC/MS Neg	882	130.1	HMDB00766	0.0272	24	6	0.24	1.05	0.13	1.22	0.18	1.03	0.18	0.92	0.08	0.67	0.00	0.83	0.16
N-acetylaspartate (NAA)	Amino acid	LC/MS Neg	620	174.1	HMDB00812	0.00001	24	4	0.36	1.14	0.09	1.31	0.04	1.04	0.01	0.72	0.02	0.31	0.00	0.86	0.11
N-acetyl-aspartyl-glutamate (NAAG)	Amino acid	LC/MS Pos	1563	305	HMDB01067	0.3533	24	5	0.01	0.96	0.01	1.13	0.03	1.00	0.03	0.93	0.11	0.31	0.05	1.09	0.07
N-acetylglutamate	Amino acid	GC/MS	1720.6	156	HMDB01138	0.1417	24	6	0.23	0.87	0.13	1.58	0.31	1.02	0.12	1.13	0.38	0.75	0.00	0.90	0.09
N-acetylmethionine	Amino acid	LC/MS Pos	2588	192.1	HMDB11745	0.1702	24	8	0.48	0.80	0.01	1.44	0.01	1.45	0.41	1.55	0.05	0.56	0.00	0.85	0.11
N-acetylserine	Amino acid	GC/MS	1526	218	HMDB02931	0.2485	24	7	0.15	0.83	0.16	1.11	0.11	1.17	0.12	0.99	0.09	0.26	0.07	0.98	0.19
N-acetylthreonine	Amino acid	LC/MS Neg	846	160.1		0.4899	24	2	0.04	1.19	0.18	0.98	0.00	1.04	0.08	1.02	0.23	0.79	0.00	1.05	0.08
n-Butyl Oleate	Lipid	GC/MS	2045	265.3		0.3009	24	16	0.25	0.65	0.06	0.99	0.40	0.93	0.31	0.96	0.11	2.21	0.20	0.81	0.19
N-formylmethionine	Amino acid	LC/MS Neg	1541	176.1	HMDB01015	0.0085	24	6	0.14	1.02	0.23	1.30	0.00	1.07	0.12	0.97	0.08	0.79	0.00	0.86	0.00
nicotinamide	Cofactors and vitamins	LC/MS Pos	1267	123.1	HMDB01406	0.1702	24	5	0.13	1.00	0.09	1.18	0.08	1.12	0.17	0.89	0.12	0.35	0.02	1.04	0.06
nicotinamide adenine dinucleotide (NAD+)	Cofactors and vitamins	LC/MS Pos	1370	664	HMDB00902	0.1132	24	4	0.07	1.03	0.04	1.29	0.28	0.98	0.05	0.65	0.18	0.07	0.00	1.24	0.03
nicotinamide adenine dinucleotide phosphate (NADP+)	Cofactors and vitamins	LC/MS Pos	1330	743.9	HMDB00217	0.0009	24	5	0.26	1.06	0.00	1.50	0.02	1.06	0.12	0.80	0.01	0.69	0.00	0.76	0.07
nicotinamide adenine dinucleotide reduced (NADH)	Cofactors and vitamins	LC/MS Neg	1554	664.1	HMDB01487	0.3533	24	3	0.29	0.94	0.13	1.26	0.33	0.90	0.20	0.66	0.05	0.61	0.00	1.34	0.03
oleate (18:1n9)	Lipid	GC/MS	1984.4	339.2	HMDB00207	1.0000	24	11	0.16	0.72	0.12	1.23	0.03	0.84	0.23	1.05	0.13	2.13	0.36	0.49	0.04
oleoylcarnitine	Lipid	LC/MS Pos	5202	426.4	HMDB05065	0.5770	24	1	0.43	1.00	0.16	1.02	0.27	1.72	0.72	0.22	0.04	0.45	0.27	7.25	2.04
ornithine	Amino acid	GC/MS	1763.8	141.9	HMDB03374	0.1702	24	6	0.08	0.82	0.17	1.52	0.23	1.02	0.01	1.77	0.07	0.51	0.25	0.91	0.01
palmitate (16:0)	Lipid	LC/MS Neg	5619	255.3	HMDB00220	0.8804	24	13	0.30	0.91	0.19	1.01	0.11	0.78	0.01	1.23	0.09	2.32	0.05	0.59	0.01
palmitoleate (16:1n7)	Lipid	LC/MS Neg	5477	253.3	HMDB03229	0.8804	24	13	0.19	0.76	0.07	1.14	0.08	0.84	0.10	1.10	0.01	2.97	0.15	0.45	0.01
palmitoyl sphingomyelin	Lipid	GC/MS	2524	311.3		1.0000	24	13	0.08	0.72	0.08	1.08	0.03	0.93	0.16	0.97	0.10	1.59	0.33	0.83	0.13
pantothenate	Cofactors and vitamins	LC/MS Pos	2218	220.1	HMDB00210	0.1702	24	8	0.32	0.61	0.02	1.18	0.18	2.14	0.27	0.66	0.00	0.44	0.00	1.19	0.14
pelargonate (9:0)	Lipid	LC/MS Neg	4847	157.2	HMDB00847	0.8804	24	13	0.06	0.77	0.03	1.06	0.05	0.93	0.10	0.98	0.08	3.16	0.16	0.86	0.12
pentadecanoate (15:0)	Lipid	GC/MS	1853.5	299.2	HMDB00826	1.0000	24	17	0.15	1.01	0.75	0.68	0.42	0.82	0.56	0.71	0.20	1.32	0.06	0.57	0.13
phenylacetyl glycine	Amino acid	LC/MS Neg	2377	192.1	HMDB00821	0.0730	24	4	0.44	1.07	0.20	1.15	0.13	1.26	0.32	0.57	0.02	0.55	0.00	1.02	0.04
phenylalanine	Amino acid	LC/MS Pos	2056	166.1	HMDB00159	0.1132	24	7	0.15	0.95	0.04	1.22	0.05	1.14	0.31	1.06	0.01	0.57	0.06	0.87	0.13
phosphate	Energy	LC/MS Neg	627	195	HMDB01429	0.8804	24	13	0.11	0.91	0.06	1.08	0.06	0.91	0.05	1.11	0.07	2.69	0.31	0.85	0.03
phosphoethanolamine	Lipid	GC/MS	1577.3	299.1	HMDB00224	0.1702	24	5	0.43	1.22	0.11	1.28	0.00	1.13	0.25	0.65	0.15	0.14	0.03	0.89	0.48
pro-hydroxy-pro	Peptide	LC/MS Pos	960	229.2	HMDB06695	1.0000	24	5	0.30	0.62	0.09	0.96	0.08	1.14	0.04	0.52	0.00	0.52	0.00	1.06	0.10
proline	Amino acid	LC/MS Pos	796	116.1	HMDB00162	0.0272	24	4	0.18	1.12	0.05	1.08	0.11	1.05	0.03	0.61	0.02	0.29	0.00	1.06	0.08
prolylleucine	Peptide	LC/MS Pos	2334	229.2		0.3533	24	11	0.24	0.82	0.07	1.43	0.44	1.29	0.69	2.15	1.14	1.18	0.16	0.56	0.21
propionylcarnitine	Lipid	LC/MS Pos	1589	218.2	HMDB00824	0.0454	24	4	0.16	1.02	0.04	1.15	0.01	0.93	0.18	0.74	0.14	0.44	0.10	1.14	0.13
pseudouridine	Nucleotide	LC/MS Neg	1104	243.1	HMDB00767	0.1132	24	6	0.55	0.81	0.01	1.49	0.04	1.00	0.16	1.83	0.22	0.34	0.00	0.36	0.02
putrescine	Amino acid	GC/MS	1705.8	174	HMDB01414	0.0009	24	2	0.34	2.67	1.37	2.14	0.87	0.88	0.02	0.84	0.01	0.08	0.03	1.15	0.05

BIOCHEMICAL	PATHWAY	PLATFORM	RI	MASS	HMDB_ID	PT-p	PER	LAG	AMP	Post- Schock (hours)											
										12		16		20		24		28		32	
										mean	SEM	mean	SEM	mean	SEM	mean	SEM	mean	SEM	mean	SEM
pyroglutamine*	Amino acid	LC/MS Pos	764	129.2		0.0363	24	0	0.61	1.35	0.35	1.15	0.19	0.70	0.15	0.43	0.12	0.86	0.55	1.63	0.19
pyrophosphate (PPi)	Energy	GC/MS	1642.3	451	HMDB00250	0.2485	24	13	0.21	0.46	0.19	1.10	0.23	0.87	0.28	1.44	0.31	1.10	0.09	0.91	0.07
pyruvate	Carbohydrate	GC/MS	1130.6	217	HMDB00243	1.0000	24	5	0.12	1.00	0.02	1.29	0.20	0.99	0.48	1.29	0.39	0.70	0.21	1.07	0.42
ribitol	Carbohydrate	GC/MS	1692.4	217	HMDB00508	0.0272	24	4	0.25	0.91	0.14	1.31	0.23	1.00	0.04	0.69	0.06	0.63	0.00	1.16	0.43
ribose	Carbohydrate	GC/MS	1639.2	204	HMDB00283	0.1417	24	6	0.44	1.43	0.43	1.51	0.12	1.65	0.90	0.74	0.09	0.95	0.36	0.61	0.01
ribulose	Carbohydrate	GC/MS	1662	306.1	HMDB00621, HMDB03371	0.0592	24	6	0.25	1.28	0.14	1.28	0.31	1.13	0.44	0.89	0.11	0.70	0.00	0.71	0.01
S-adenosylhomocysteine (SAH)	Amino acid	LC/MS Pos	1480	385.1	HMDB00939	0.0454	24	7	0.25	0.97	0.06	1.34	0.01	1.30	0.36	1.31	0.01	0.71	0.02	0.94	0.03
scyllo-inositol	Lipid	GC/MS	1893.8	318.2	HMDB06088	0.0021	24	3	0.70	1.83	0.02	1.59	0.07	1.00	0.02	0.54	0.01	0.10	0.05	1.19	0.27
serine	Amino acid	GC/MS	1389.1	204	HMDB03406	0.0730	24	6	0.20	1.03	0.07	1.36	0.18	1.29	0.47	1.06	0.15	0.22	0.02	0.84	0.20
sorbitol	Carbohydrate	GC/MS	1843	319.1	HMDB00247	0.0454	24	3	0.50	1.10	0.37	1.19	0.19	0.86	0.14	0.41	0.07	0.16	0.00	1.20	0.17
spermidine	Amino acid	LC/MS Pos	533	146.2	HMDB01257	0.0156	24	4	0.16	1.03	0.05	1.17	0.02	1.00	0.05	0.79	0.07	0.55	0.02	1.13	0.11
sphinganine	Lipid	LC/MS Pos	5175	302.3	HMDB00269	0.1702	24	19	0.26	1.00	0.01	0.83	0.22	0.84	0.14	0.58	0.29	2.38	0.08	1.53	0.32
sphingosine	Lipid	LC/MS Pos	5197	300.2	HMDB00252	0.0730	24	20	0.35	1.00	0.03	0.86	0.18	0.69	0.14	0.65	0.29	2.86	0.07	1.30	0.23
stearate (18:0)	Lipid	LC/MS Neg	5886	283.4	HMDB00827	1.0000	24	15	0.14	0.92	0.21	1.05	0.12	0.75	0.04	1.16	0.08	1.97	0.10	0.57	0.01
stearyl sphingomyelin	Lipid	GC/MS	2645	311.3	HMDB01348	0.2485	24	12	0.23	0.74	0.29	0.95	0.07	1.01	0.21	1.48	0.34	1.36	0.39	0.71	0.11
succinate	Energy	GC/MS	1348	247	HMDB00254	0.0454	24	5	0.29	0.87	0.04	1.30	0.09	1.11	0.01	0.55	0.13	0.26	0.00	1.18	0.18
succinyl CoA	Energy	LC/MS Neg	1800	866.1	HMDB01022	1.0000	24	11	0.00	0.70	0.00	1.09	0.40	0.70	0.00	0.92	0.23	0.70	0.00	0.77	0.08
thiamin (Vitamin B1)	Cofactors and vitamins	LC/MS Neg	1699	263.1	HMDB00235	0.0085	24	4	0.16	1.02	0.08	1.11	0.09	0.96	0.11	0.81	0.00	0.81	0.00	0.95	0.05
threonine	Amino acid	GC/MS	1412.3	218.1	HMDB00167	0.0454	24	4	0.15	1.03	0.08	1.22	0.21	1.31	0.31	0.77	0.14	0.19	0.01	1.16	0.17
thymidine 5'-monophosphate	Nucleotide	LC/MS Neg	924	321.1	HMDB01227	0.0156	24	6	0.16	1.00	0.12	1.30	0.11	1.00	0.02	0.97	0.15	0.82	0.00	0.85	0.04
trans-4-hydroxyproline	Amino acid	GC/MS	1537	140	HMDB00725	0.8804	24	2	0.51	1.04	0.04	1.13	0.22	1.18	0.27	0.41	0.14	0.16	0.00	2.29	0.26
tryptophan	Amino acid	LC/MS Pos	2445	205.1	HMDB00929	0.1132	24	5	0.09	0.95	0.07	1.24	0.14	1.24	0.39	1.00	0.02	0.39	0.04	0.91	0.11
tyrosine	Amino acid	LC/MS Pos	1516	182.1	HMDB00158	0.0454	24	6	0.19	1.00	0.08	1.30	0.11	1.27	0.39	1.10	0.04	0.50	0.04	0.84	0.10
UDP-glucuronate	Carbohydrate	LC/MS Neg	594	579.1	HMDB00935	0.0004	24	6	0.53	1.18	0.18	1.46	0.07	1.10	0.10	0.91	0.10	0.25	0.01	0.58	0.01
uracil	Nucleotide	GC/MS	1370.4	241	HMDB00300	0.0156	24	6	0.41	1.09	0.09	1.38	0.25	1.07	0.35	1.08	0.08	0.14	0.03	0.54	0.06
uridine	Nucleotide	LC/MS Neg	1467	243.1	HMDB00296	0.8804	24	10	0.17	0.65	0.06	1.24	0.20	1.02	0.06	0.97	0.19	1.56	0.25	0.41	0.02
uridine 5'-monophosphate (UMP)	Nucleotide	LC/MS Pos	1079	325	HMDB00288	0.0021	24	4	0.33	1.38	0.11	1.46	0.09	1.01	0.18	0.92	0.05	0.71	0.01	0.92	0.11
uridine 5'-triphosphate (UTP)	Nucleotide	LC/MS Neg	639	483	HMDB00285	1.0000	24	9	0.09	0.69	0.00	0.95	0.27	1.32	0.32	0.91	0.15	0.68	0.00	1.01	0.04
valine	Amino acid	LC/MS Pos	1040	118.1	HMDB00883	0.0730	24	7	0.31	1.00	0.01	1.33	0.08	1.22	0.38	1.15	0.13	0.65	0.03	0.80	0.10

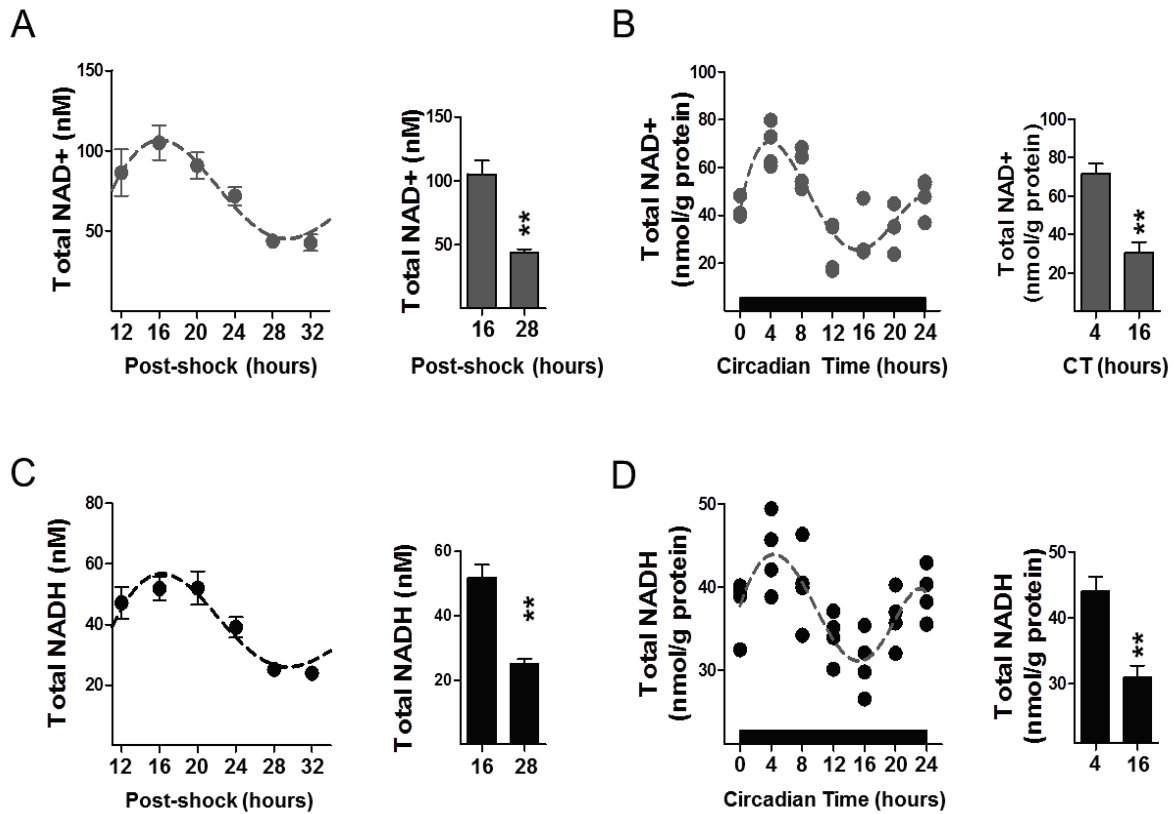


Figure S1, related to Figure 2: The couple NAD⁺/NADH is driven by the circadian clock

(A) Total NAD⁺ measured in serum-shocked human skin fibroblasts at the indicated time points (6 time points, n=6 for each, JTK_Cycle, P<0.05). Right panel displays relative total NAD⁺ level at 16 hours post-shock (peak) and at 28 hours (trough) (One-way ANOVA, NAD⁺ variation pattern, P<0.0001; post hoc Tukey; 16 versus 28 hours, **,P < 0.01). (B) Total NAD⁺ content assessed from brain of non-fasted wild-type mice kept in constant darkness every 4 hours for 24 hours (7 time points, n= 4 for each, JTK_Cycle, P<0.05). Right panel displays relative total NAD⁺ level at CT4 (peak) and at CT16 (trough) (One-way ANOVA, NAD⁺ variation pattern, P<0.0001; post hoc Tukey; 16 versus 28 hours, **,P < 0.01). (C) Total NADH measured in serum-shocked human skin fibroblasts at the indicated time points (6 time points, n=6 for each, JTK_Cycle, P<0.05). Right panel displays relative total NAD⁺ level at 16 hours post-shock (peak) and at 28 hours (trough) (One-way ANOVA, NADH variation pattern, P<0.0001; post hoc Tukey; 16 versus 28 hours, **,P < 0.01). (D) Total NADH content assessed from brain of non-fasted wild-type mice kept in constant darkness every 4 hours for 24 hours (7 time points, n= 4 for each, JTK_Cycle, P<0.05). Right panel displays relative total NAD⁺ level at CT4 (peak) and at CT16 (trough) (One-way ANOVA, NADH variation pattern, P<0.0001; post hoc Tukey; 16 versus 28 hours, **,P < 0.01). All data are represented as mean ± SEM of at least three independent samples.

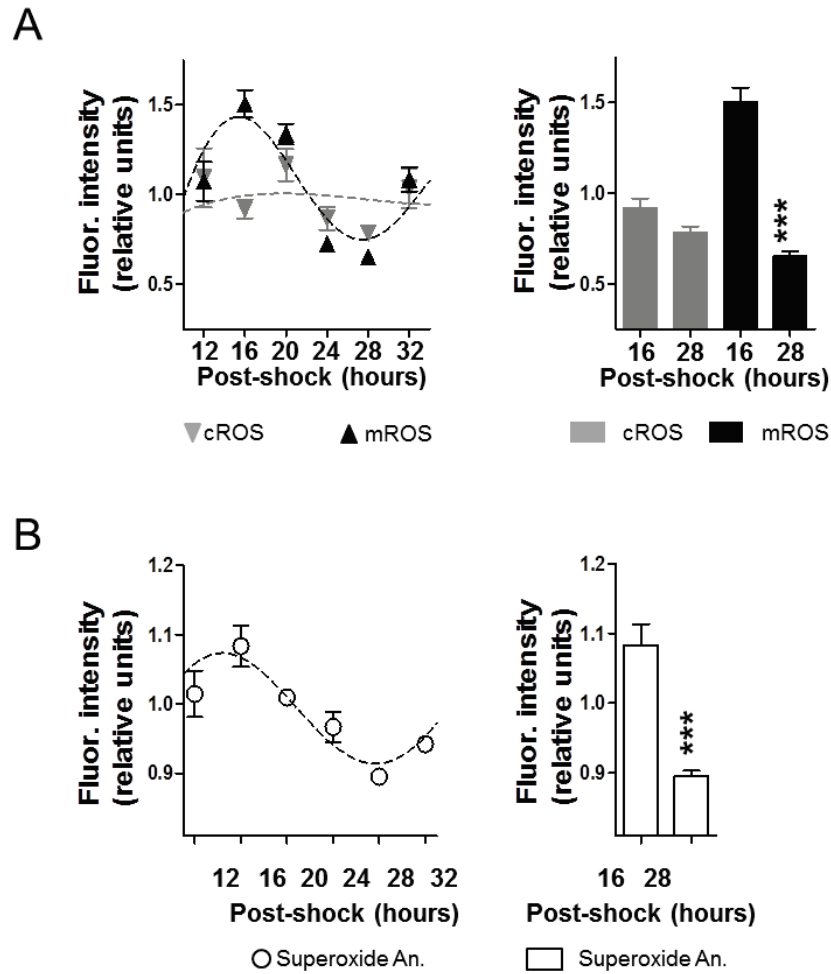


Figure S2, related to Figure 2: Circadian clock regulates mitochondrial reactive oxygen species

(A) Cytosolic (cROS) and mitochondrial (mROS) reactive oxygen species levels were evaluated in serum-shocked human skin fibroblasts (6 time points, $n=4$ for each, JTK_Cycle, $P_{mROS} < 0.05$). Right panel displays cROS and mROS levels at 16 hours post-shock (peak) and at 28 hours (trough) (One-way ANOVA, mROS variation pattern, $P < 0.0001$; post hoc Tukey; 16 versus 28 hours, $***, P < 0.001$). (B) Superoxide anions level were evaluated in serum-shocked human skin fibroblasts (6 time points, $n=4$ for each, JTK_Cycle, $P < 0.05$). Right panel displays superoxide anions level at 16 hours post-shock (peak) and at 28 hours (trough) (One-way ANOVA, superoxide anions variation pattern, $P < 0.0001$; post hoc Tukey; 16 versus 28 hours, $***, P < 0.001$).

All data are represented as mean \pm SEM of at least three independent samples.

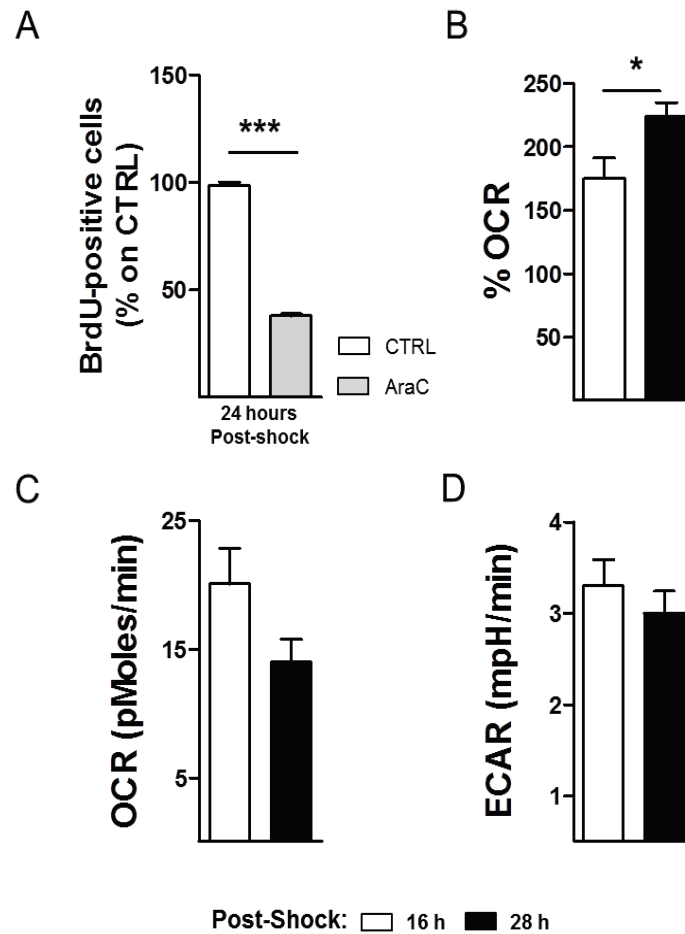


Figure S3, related to Figure 3: Circadian regulation of intrinsic mitochondrial function

(A) Percentage of BrdU- positive cells in absence and presence of AraC at 24 hours post-shock (student t-test, control versus AraC, ***, $P < 0.0001$). (B) Percentage of OCR linked to spare respiratory capacity (SRC) at 16 hours post-shock and 28 hours post-shock in human skin fibroblast (One-way ANOVA, OCR variation pattern, $P < 0.0001$; post hoc Tukey; 16 versus 28 hours, *, $P < 0.05$). (C) OCR related to the proton leak (independent to ATP production) at 16 hours post-shock and 28 hours post-shock in human skin fibroblast. (D) Extracellular Acidification Rate (ECAR) corresponding to glycolytic rate at 16 hours post-shock and 28 hours post-shock evaluated in human skin fibroblast.

All data are represented as mean \pm SEM of three independent samples (2 time points, $n = 11$ replicates for each, three independent experiments).

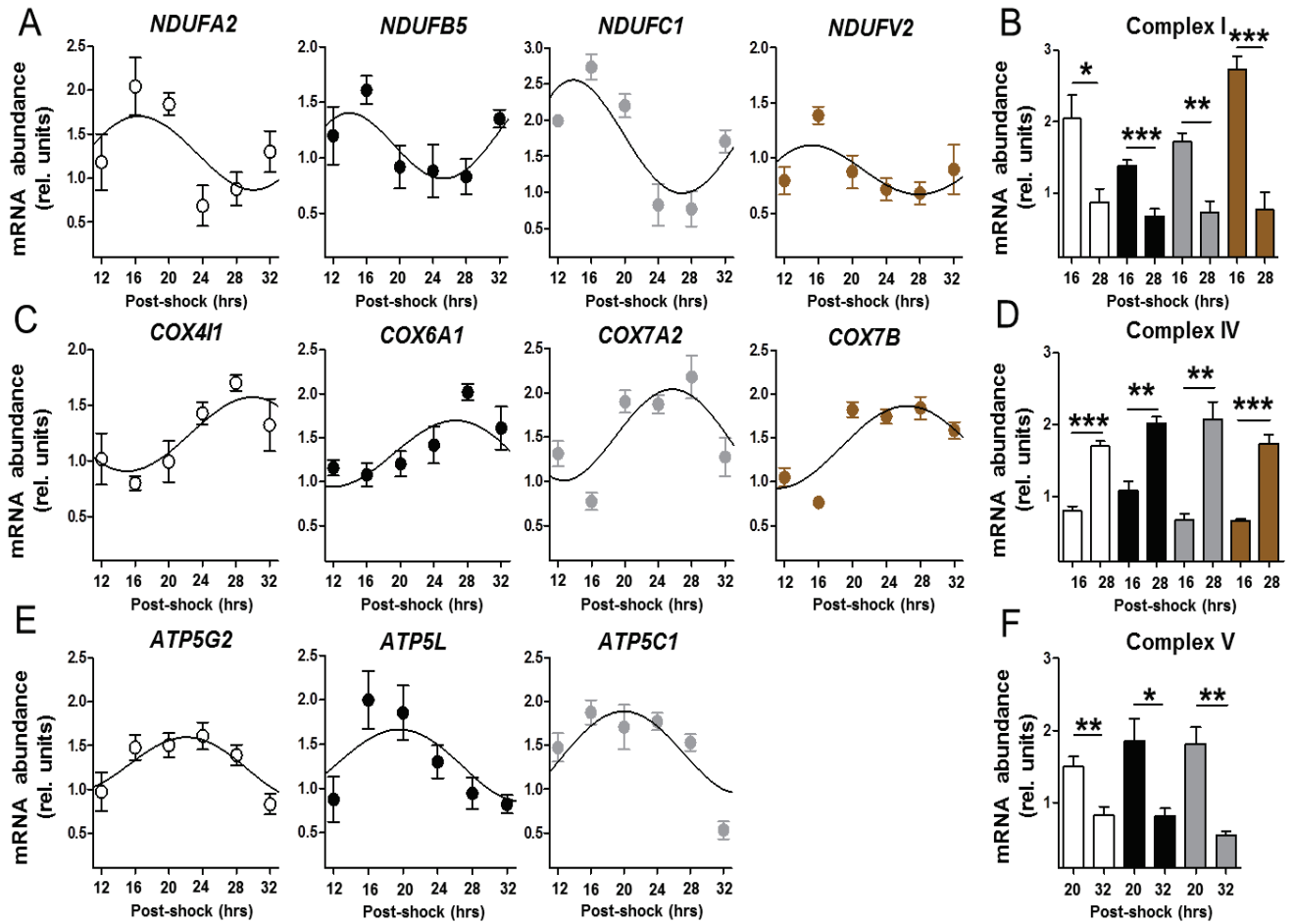


Figure S4, related to Figure 3: Circadian control of mitochondrial biogenesis

(A) Circadian profiles of relative mRNA expression of complex I subunits (*NDUFA2*, *NDUFB5*, *NDUFC1*, and *NDUFV2*) in serum-shocked human skin fibroblasts (6 time points, n= 4 for each, JTK_Cycle, P<0.05). (B) Relative mRNA expression of complex I subunits at 16 hours post-shock (corresponding to the peak in gene expression) and 28 hours post-shock (corresponding to the trough in gene expression) (One-way ANOVA, mRNA variation pattern, P<0.0001; post hoc Tukey; 16 versus 28 hours, *, P<0.05, **, P<0.01, ***, P < 0.001). (C) Circadian profiles of relative mRNA expression of complex IV subunits (*COX4I1*, *COX6A1*, *COX7A2* and *COX7B*) in serum-shocked human skin fibroblasts (6 time points, n= 4 for each, JTK_Cycle, P<0.05). (D) Relative mRNA expression of complex IV subunits at 16 hours post-shock (corresponding to the trough in gene expression) and 28 hours post-shock (corresponding to the peak in gene expression) (One-way ANOVA, mRNA variation pattern, P<0.0001; post hoc Tukey; 16 versus 28 hours, *, P<0.05, **, P<0.01, ***, P < 0.001). (E) Circadian profiles of relative mRNA expression of complex V subunits (*ATP5G2*, *ATP5L* and *ATP5C1*) in serum-shocked human skin fibroblasts (6 time points, n= 4 for each, JTK_Cycle, P<0.05). (F) Relative mRNA expression of complex V subunits at 20 hours post-shock and 32 hours post-shock (corresponding respectively to the peak and trough in gene expression) (One-way ANOVA, mRNA variation pattern, P<0.0001; post hoc Tukey; 20 versus 32 hours, *, P<0.05, **, P<0.01, ***, P < 0.001).

All data are represented as mean ± SEM of at least three independent samples.

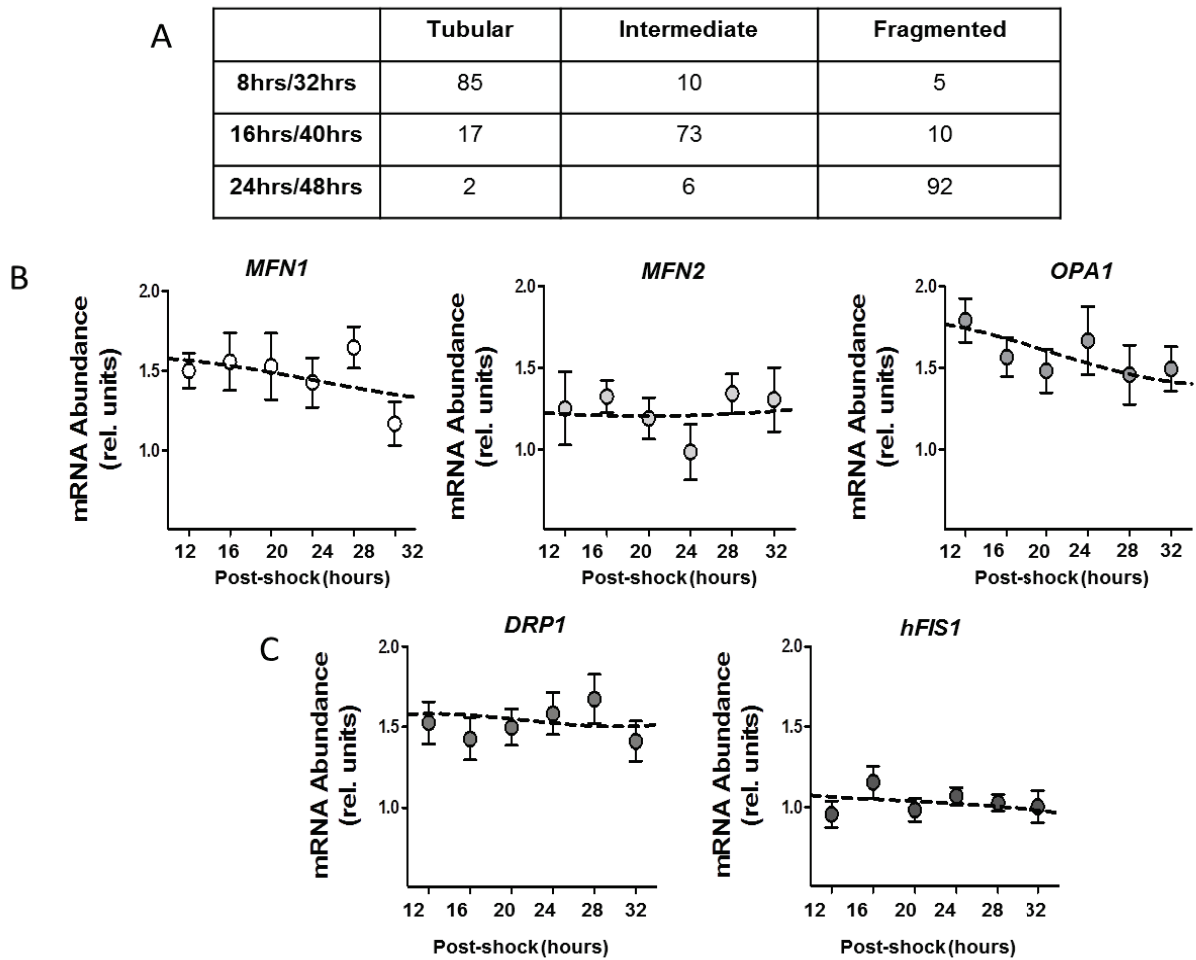


Figure S5, related to Figure 4: Circadian clock influences mitochondrial morphology

(A) Number of cells displaying one of the mitochondrial network states (tubular, intermediate and fragmented) determined in serum-shocked human skin fibroblasts from 8 hours post-shock every 8 hours over the course of 48 hours (mean of 3 independent experiments, 100 cells counted per conditions). (B) Profile of relative mRNA expression of nuclearly-encoded genes related to (B) mitochondrial fusion (*MFN1*, *MFN2* and *OPA1*) was evaluated in serum-shocked human skin fibroblasts (6 time points, n=6 for each). (C) Profile of relative mRNA expression of nuclearly-encoded genes related to fission (*DRP1* and *hFIS1*) was evaluated in serum-shocked human skin fibroblasts (6 time points, n=6 for each).

All data are represented as mean \pm SEM of at least three independent samples.

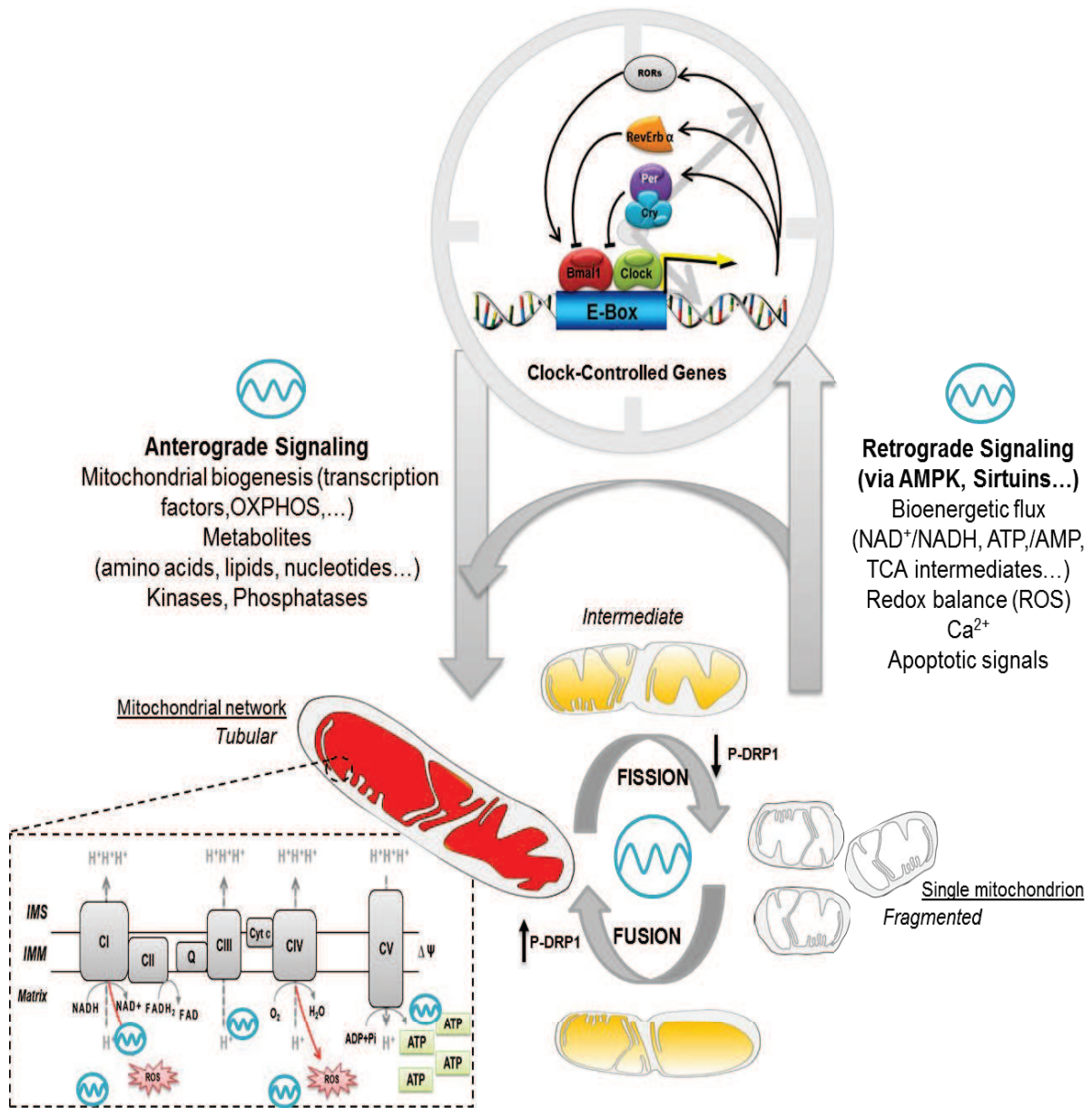


Figure S6: Schematic representation of the relationship between the core molecular clock and mitochondrial dynamics. CI, complex I; CII, complex II; CIII, complex III; CIV, complex IV; CV, complex V; ΔΨ, mitochondrial membrane potential; IMS, intermembrane space; IMM, inner mitochondrial membrane; Q, ubiquinone; Cyt C, cytochrome c; ROS, reactive oxygen species; Cry, cryptochrome; Per, Period; TCA, tricarboxylic acid cycle.

Experimental Procedures

Mice

Male C57BL/6, Male *Drp1*^{fix/fix} *CreERT2* (Ishihara et al., 2009) and *mPer1/mPer2* (Bae et al., 2001) double-mutant mice were housed for one week on a 12:12 light-dark cycle prior to placement in DD 5 days before the beginning of the experiment with free access to food and water. Circadian time 0 (CT0) is the start of subjective daytime and CT12 is the start of subjective night-time, under constant dark conditions, over 24 hours. All brain homogenate samples were normalized on 5 mg/ml of protein before ATP content measurement and on 1 mg/ml for NAD⁺/NADH content determination. See [Supplemental Experimental Procedures](#).

Cell culture

Human osteosarcoma U2OS cell and human skin fibroblasts infected with lentiviral circadian reporter mice *Bmal1::luciferase* were cultured in Dulbecco's modified Eagle's medium (DMEM) supplemented with 1% penicillin/streptomycin (Sigma), 1% Glutamax (Sigma) and 20% fetal bovine serum (FBS) (Sigma) as described previously (Brown et al., 2005, Pagani et al., 2010). Metabolic profiles also were obtained from dexamethasone-synchronized U2OS cells. Small-Molecule Determination Metabolon analyzed metabolites in dexamethasone-synchronized U2OS cells, as described previously (Dallmann et al., 2012, Lawton et al., 2008).

Drp1^{lox/lox} MEFs were prepared from E13.5 *Drp1*^{lox/lox} embryos and cultured as previously described (Ishihara et al., 2009). *Drp1*^{-/-} MEFs were subsequently generated by expression of Cre recombinase. The MEFs were maintained in (DMEM) supplemented with 1% penicillin/streptomycin (Sigma), 1% Glutamax (Sigma), 10% fetal bovine serum (FBS) and 1x non-essential amino acids.

MEFs lacking *mPer1* and *mPer2* isolated from double knockout mice were generated from E12 embryos as previously described (Nagoshi et al., 2004, Zheng et al., 2001) and cultured in DMEMc containing 10% FCS.

For measurements of nucleotide level, cell proliferation, ROS, oxygen consumption rate and mitochondrial morphology, cells were synchronized by serum shock treatment (50% horse serum supplemented DMEMc) for 2 hours at 37 °C. For period length determination, cells were synchronized by addition of 100 nM dexamethasone (Sigma) in DMEMc + 20% FBS.

See [Supplemental Experimental Procedures](#).

Nucleotide Measurements

Total ATP content from synchronized cell cultures and mice brain homogenates was determined using bioluminescence assay (ViaLighTM HT; Cambrex Bio Science) according to the instruction of the manufacturer. For measurement of NAD⁺ and NADH from synchronized fibroblasts and mice brain homogenates, NAD⁺ and NADH were separately extracted using an acid-base extraction (HCL 0.1 mol/l – NAOH 0.1 mol/l). For complete protocol, please refer to the [Supplemental Experimental Procedures](#).

ROS level

The formation of cytosolic (cROS), mitochondrial (mROS) reactive oxygen species and superoxide anions in synchronized fibroblasts were measured using, the fluorescent probe H₂DCF-DA (DCF) (10 μM, 15 min), the non-fluorescent dihydrorhodamine-123 (DHR) (10 μM, 15 min) and the Red Mitochondrial Superoxide Indicator (MitoSOX, 5 μM, 30 min), respectively. See [Supplemental Experimental Procedures](#).

Oxygen Consumption Rate (OCR) Measurements

OCR was measured in synchronized fibroblasts using a Seahorse Bioscience (North Billerica, MA, USA) XF24 Analyzer as previously described (Invernizzi et al., 2012). Experiments were performed at 16 hours post-shock and 28 hours post-shock. For complete protocol, please refer to the [Supplemental Experimental Procedures](#).

Quantitative Real-Time PCR

Total RNA was extracted from lysates of synchronized fibroblasts using RNeasy Mini KIT (Qiagen). cDNA was generated using Ready-to-Go You-Prime First-Strand Beads (GE Healthcare). For data analysis, human Cdk4 was used as an endogenous control. Data are expressed as relative expression for each individual gene normalized to their corresponding controls using the comparative CT method. The primers used were purchased from Applied Biosystems and Microsynth (Probe ID: see [Supplemental Experimental Procedures](#)). Data are expressed as relative expression for each individual gene normalized to their corresponding controls.

Mitochondrial Morphology

Mitochondrial staining was performed on serum-shocked fibroblasts with the mitochondrial membrane potential-sensitive dye Mitotracker[®] Red CMX ROS (75nM, 579/599, Life technologies). Sytox Green (167nM, 504/523, Invitrogen) was used as nuclei staining according to the manufacturer's recommendation.

For immunohistochemistry on brain and liver slices from C57BL/6 mice at CT0 (onset of subjective day or rest period) and CT12 (onset of subjective night or activity period), antibody against the outer mitochondrial membrane porin, Voltage-Dependent Anionic Channel (VDAC, 1:75, Cell Signaling) was used for determining mitochondrial morphology. A FITC-labeled anti-rabbit IgG (1:160, Sigma, 490/525) was used as secondary antibody. TO-PRO-3iodide (1 μ M, 642/661, Invitrogen) was used as nuclei staining according to the manufacturer's recommendation.

For complete protocol, please refer to the [Supplemental Experimental Procedures](#).

Protein Gel Electrophoresis and Immunoblotting

Lysates from serum-shocked fibroblast cultures and brain homogenate were prepared and protein expression levels were measured by standard western blot procedure. We used primary antibodies to DRP1 (1:500, Cell Signaling), ser637-phosphorylated DRP1 (1:500, Cell Signaling) and VDAC (1:500, Cell Signaling) and horseradish peroxidase-coupled IgG as secondary antibody (1:160, Sigma). Signals were detected by enhanced chemiluminescence using SuperSignal™ West Dura Chemiluminescent Substrate (Thermo Scientific). For complete protocol, please refer to the [Supplemental Experimental Procedures](#).

Circadian period length determination

In human skin fibroblast transfected with the lentiviral circadian reporter mice Bmal1::luciferase (Brown et al., 2005), light output was measured in homemade light-tight atmosphere-controlled boxes for at least 5 days. For complete protocol, please refer to the [Supplemental Experimental Procedures](#).

Statistical Analysis

Data were presented as mean \pm S.E.M. Statistical analyses were performed using the Graph Pad Prism software. For statistical comparisons, One-way ANOVA followed by Tukey's multiple comparison test or Two-way ANOVA followed by Bonferroni's multiple comparison test was used respectively. Rhythmicity of metabolites and genes expression was assessed using an algorithm previously described for rhythmic transcripts. The JTK-cycle algorithm was used as implemented in R by Kronauer as previously described (Dallmann et al., 2012, Hughes et al., 2010). A window of 24 h was used for the determination of circadian periodicity and a *P* value of <0.05 was considered as statistically significant. Metabolites profiles were crosschecked by visual inspection and false positive were excluded.

Supplemental Experimental Procedures

Mice

Drp1^{flx/flx} CreERT2 mice [20] were obtained by crossing *Drp1*^{flx/flx} mice with mice expressing an inducible Cre recombinase transgene under the control of the CamKII α promoter (Cre+), which is active in the hippocampus and the cortex of adult mice (from the European Mouse Mutant Archive EMMA strain 02125) (Ishihara et al., 2009). At 8 weeks of age mice were injected intraperitoneally with 1 mg tamoxifen (Sigma) twice daily for five consecutive days to induce recombination of the *Drp1* locus (Oettinghaus et al., 2015).

Brain Homogenate Preparation

Brains were dissected on ice and washed in ice-cold buffer (210 mM mannitol, 70 mM sucrose, 10 mM Hepes, 1 mM EDTA, 0.45% BSA, 0.5 mM DTT, and Complete Protease Inhibitor mixture tablets (RocheDiagnostics). After removing the cerebellum, tissue samples were homogenized in 2 ml of buffer with a glass homogenizer (10–15 strokes, 400 rpm). We used 10 μ l of the suspension for protein concentration determination

Human Skin Fibroblast

Fibroblasts were isolated from biopsies, infected with lentiviral circadian reporter mice *Bmal1::luciferase* and cultured in DMEM/1% penicillin/streptomycin (Sigma)/1% Glutamax (Sigma) (DMEMc)/20% FBS (Sigma) as described previously (Brown et al., 2005, Pagani et al., 2010). For measurements of nucleotide level, cell proliferation (BrdU assay), ROS, oxygen consumption rate and mitochondrial morphology in human skin fibroblasts, circadian rhythms were synchronized by serum shock treatment (50% horse serum supplemented DMEMc) for 2 hours at 37 °C. For period length determination, circadian rhythms were synchronized by 100 nM dexamethasone (Sigma) in DMEMc + 20% FBS. DMEMc without phenol red was supplemented with 0.1 mM luciferin (Molecular Probes) and 10% FBS to obtain the counting medium (CM).

U2OS Cells Metabolome

Small-Molecule Determination. Metabolon was used to analyze metabolites in dexamethasone-synchronized U2OS cells, as described previously (Dallmann et al., 2012, Lawton et al., 2008).

Oxygen Consumption Rate (OCR) Measurements

OCR was measured in synchronized fibroblasts as recommended as previously described (Invernizzi et al., 2012). Briefly, human skin fibroblasts were seeded at the density of 3×10^4 cells/100 μ l per well on Seahorse Biosciences 24-well culture plates one day prior to the beginning of assay. After serum shock synchronization, medium was exchanged to 500 μ l of assay medium (glucose-free RPMI-1640 medium containing 2% FBS, 2 mM sodium pyruvate, pH ~ 7.4). Prior to measurements the microplates were equilibrated in a CO₂ free incubator at 37 °C for 60 minutes. The drug injection ports of the XF Assay Cartridge were loaded with the assay reagents at 10X in assay medium. 55 μ l of oligomycin (10 μ M), 62 μ l of FCCP (7 μ M), 68 μ l of a mix of antimycin A (40 μ M) and rotenone (20 μ M) were added to ports A, B and C respectively. Experiments were performed at 16 hours post-shock and 28 hours post-shock.

Nucleotides Measurement

Total ATP content from synchronized human skin fibroblasts, *Drp1*^{lox/lox} and *Drp1*^{-/-} MEFs, *Per1/2*^{+/+} and *Per1/2*^{-/-} MEFs and mice brain homogenates was determined using bioluminescence assay (ViaLight™ HT; Cambrex Bio Science) according to the instruction of the manufacturer. The enzyme luciferase, which catalyzes the formation of light from ATP and luciferin was used. The emitted light is linearly related to the ATP concentration and is measured using a luminometer (VictorX5, Perkin Elmer). To define the origin of ATP oscillation, DMEMc without phenol red + 2% FBS supplemented with 2-Deoxy-D-glucose (4.5 g/l) a glycolysis inhibitor or oligomycin (2 μ M), an ATP synthase inhibitor was added on synchronized human skin fibroblasts. To test the possibility that rhythmic ATP is a byproduct of rhythmic cell division, pharmacological disruption of the cell cycle was accomplished with the inhibitor AraC, an anticancer drug that prevents cell division (100 μ M; Sigma). AraC was added to human skin fibroblasts cultures 3 hours after the seeding, directly after the medium exchange following the synchronization and then every 24 hours to assure continued

block of cell division. To verify if AraC treatment had an impact on cell cycle and blocked cell proliferation, the BrdU Cell Proliferation Assay (Calbiochem, Darmstadt, Germany) was used following the instructions of the manufacturer. To investigate the role of clock-regulated Drp1 in mitochondrial bioenergetics, mitochondrial fission was abolished by selective inhibition of mitochondrial division dynamin, Drp1, in presence of mdivi-1 (50 μ M, Sigma).

For measurement of NAD⁺ and NADH from synchronized fibroblasts and mice brain homogenates, NAD⁺ and NADH were separately extracted using an acid-base extraction (HCL 0.1 mol/l – NAOH 0.1 mol/l). The determination of both NAD⁺ and NADH was performed using an enzyme cycling assay based on passing the electron from ethanol through reduced pyridine nucleotides to MTT (3-(4,5-Dimethylthiazol-2-yl)-2,5-diphenyltetrazolium bromide) in a PES- (phenazine ethosulfate) coupled reaction resulting in a purple formazan product that can be quantitatively measured at a wavelength of 595 nm (VictorX5, Perkin Elmer). Experiments were performed starting from 12 hours post-synchronization time point and measured at 4 hours intervals for 6 time points.

Circadian period length determination

In fibroblast transfected with the lentiviral circadian reporter mice Bmal1::luciferase (Brown et al., 2005), light output was measured in homemade light-tight atmosphere-controlled boxes for at least 5 days. To measure the fibroblast basal circadian rhythms, CM was supplemented with 10% FBS; to determine the influence of ATP on circadian period length, CM was supplemented with mitochondrial respiration inhibitors: rotenone, a complex I inhibitor (1 μ M), oligomycin, ATP synthase inhibitor (2 μ M) or carbonyl-cyanide-p-trifluoromethoxyphenylhydrazone (FCCP), an uncoupler of proton gradient (4 μ M). To determine the role of Drp1-regulated mitochondrial bioenergetics, CM was supplemented with mdivi-1 (50 μ M, Sigma), a mitochondrial division inhibitor.

ROS Level

Synchronized fibroblasts were loaded for 15 min with 10 μ M DCF or 15 min with 10 μ M DHR at 37 °C. After washing twice with HBSS, the formation of the reduced fluorescent product dichlorofluorescein was detected using the VictorX5 multilabel reader (PerkinElmer Life Sciences) at 485 nm (excitation)/535 nm (emission). DHR,

which is oxidized to cationic rhodamine 123 which localizes in the mitochondria and exhibits green fluorescence, was detected using the VictorX5 multilabel reader at 490 nm (excitation)/590 nm (emission). The levels of superoxide anion radical were also assessed using the Red Mitochondrial Superoxide Indicator (MitoSOX, 5 μ M, 30 min). MitoSOX, which is specifically oxidized by mitochondrial superoxide, exhibits a red fluorescence detected at 535 nm (excitation)/595 nm (emission). The intensity of fluorescence was proportional to mROS levels or superoxide anion radicals in mitochondria. Experiments were performed starting from 12 hours post-synchronization time point and measured at 4 hours intervals.

Primer sequences

The primer sequences purchased from Applied Biosystems were: MFN1, Hs00250475_m1; MFN2, Hs00208382_m1; OPA1, Hs00323399_m1; DRP1, Hs00247147_m1; hFIS1; Hs00211420_m1; NDUFA2, Hs00159575_m1; NDUFB5, Hs00159582_m1; NDUFC1, Hs00159587_m1; NDUFV2, Hs00221478_m1; COX4I1, Hs00971639_m1; COX6A1, Hs01924685_g1; COX7A2, Hs01652418_m1; COX7B, Hs00371307_m1; ATP5G2, Hs01096582_m1; ATP5C1, Hs01101219_g1, ATP5L, Hs00758883_s1; Bmal1, Mm00500226_m1; Per1, Mm00501813_m1; Per2, Mm00478113_m1. The primer sequences purchased from Microsynth were: hBmal1 forward, 5'-GAAGACAACGAACCAGACAATGAG-3', hBmal1 reverse, 5'-ACATGAGAATGCAGTCGTCCAA-3', hBmal1 probe, 5'-Yakima Yellow-TGTAACCTCAGCTGCCTCGTCGCA-BHQ1-3'; hPer1 forward, 5'-CGCCTAACCCCGTATGTGA-3", hPer1 reverse, 5'-CGCGTAGTGAAAATCCTCTTGTC-3', hPer1 probe, 5'-Yakima Yellow-CGCATCCATTCGGGTTACGAAGCTC-BHQ1-3'; hPer2 forward, 5'-GGGCAGCCTTTCGACTATTCT-3', hPer2 reverse, 5'-GCTGGTGTCCAACGTGATGTACT-3', hPer2 probe, 5'-Yakima Yellow-CATTCGGTTTCGCGCCCGGG-BHQ1-3'.

Author Contributions

KS, AG, BO, LMR, RD performed experiments. JAR and UA provided *Per1/2*^{+/+} and *Per1/2*^{-/-} mice. SAB provided U2OS cells, *Per1/2*^{+/+} and *Per1/2*^{-/-} MEFs. NI and KM provided *Drp1*^{flx/flx} CreERT2 mice and *Drp1*^{lox/lox} and *Drp1*^{-/-} MEFs. UEL, SF, SAB and AE conceived the project, coordinated and supervised research. KS, SF, SAB and AE wrote the manuscript.

Acknowledgements

This work was supported by Swiss National Science Foundation (#31000_122572 to SAB, SF and AE and #31003A_149728 to AE), Novartis Foundation for Biomedical Research Basel, Synapsis Foundation and the Fonds der Freiwilligen Akademischen Gesellschaft Basel (all to AE). Further support of RD and SAB came from the Swiss National Science Foundation, the University Hospital of Zürich clinical priority program “Sleep and Health”, the Fyodor Lynen Foundation, and the Swiss Cancer Society. We thank Ginette Baysang and Fides Meier for technical assistance.

References

- ANG, J. E., REVELL, V., MANN, A., MANTELE, S., OTWAY, D. T., JOHNSTON, J. D., THUMSER, A. E., SKENE, D. J. & RAYNAUD, F. 2012. Identification of human plasma metabolites exhibiting time-of-day variation using an untargeted liquid chromatography-mass spectrometry metabolomic approach. *Chronobiol Int*, 29, 868-81.
- ASHER, G., GATFIELD, D., STRATMANN, M., REINKE, H., DIBNER, C., KREPEL, F., MOSTOSLAVSKY, R., ALT, F. W. & SCHIBLER, U. 2008. SIRT1 regulates circadian clock gene expression through PER2 deacetylation. *Cell*, 134, 317-28.
- ASHER, G. & SCHIBLER, U. 2011. Crosstalk between components of circadian and metabolic cycles in mammals. *Cell Metab*, 13, 125-37.
- BAE, K., JIN, X., MAYWOOD, E. S., HASTINGS, M. H., REPPERT, S. M. & WEAVER, D. R. 2001. Differential functions of mPer1, mPer2, and mPer3 in the SCN circadian clock. *Neuron*, 30, 525-36.
- BAILEY, S. M., UDOH, U. S. & YOUNG, M. E. 2014. Circadian regulation of metabolism. *J Endocrinol*, 222, R75-96.
- BALSALOBRE, A., BROWN, S. A., MARCACCI, L., TRONCHE, F., KELLENDONK, C., REICHARDT, H. M., SCHUTZ, G. & SCHIBLER, U. 2000. Resetting of circadian time in peripheral tissues by glucocorticoid signaling. *Science*, 289, 2344-7.
- BALSALOBRE, A., DAMIOLA, F. & SCHIBLER, U. 1998. A serum shock induces circadian gene expression in mammalian tissue culture cells. *Cell*, 93, 929-37.
- BASS, J. 2012. Circadian topology of metabolism. *Nature*, 491, 348-56.
- BASS, J. & TAKAHASHI, J. S. 2010. Circadian integration of metabolism and energetics. *Science*, 330, 1349-54.
- BENARD, G. & KARBOWSKI, M. 2009. Mitochondrial fusion and division: Regulation and role in cell viability. *Semin Cell Dev Biol*, 20, 365-74.
- BROWN, S. A., FLEURY-OLELA, F., NAGOSHI, E., HAUSER, C., JUGE, C., MEIER, C. A., CHICHEPORTICHE, R., DAYER, J. M., ALBRECHT, U. & SCHIBLER, U. 2005. The period length of fibroblast circadian gene expression varies widely among human individuals. *PLoS Biol*, 3, e338.
- BRUNNER, M. & SCHAFMEIER, T. 2006. Transcriptional and post-transcriptional regulation of the circadian clock of cyanobacteria and *Neurospora*. *Genes Dev*, 20, 1061-74.
- BUGGE, A., FENG, D., EVERETT, L. J., BRIGGS, E. R., MULLICAN, S. E., WANG, F., JAGER, J. & LAZAR, M. A. 2012. Rev-erbalpha and Rev-erbbeta coordinately protect the circadian clock and normal metabolic function. *Genes Dev*, 26, 657-67.
- CEREGHETTI, G. M., STANGHERLIN, A., MARTINS DE BRITO, O., CHANG, C. R., BLACKSTONE, C., BERNARDI, P. & SCORRANO, L. 2008. Dephosphorylation by calcineurin regulates translocation of Drp1 to mitochondria. *Proc Natl Acad Sci U S A*, 105, 15803-8.
- CHANG, H. C. & GUARENTE, L. 2013. SIRT1 mediates central circadian control in the SCN by a mechanism that decays with aging. *Cell*, 153, 1448-60.
- CHO, H., ZHAO, X., HATORI, M., YU, R. T., BARISH, G. D., LAM, M. T., CHONG, L. W., DITACCHIO, L., ATKINS, A. R., GLASS, C. K., LIDDLE, C., AUWERX, J., DOWNES, M., PANDA, S. & EVANS, R. M. 2012. Regulation of circadian behaviour and metabolism by REV-ERB-alpha and REV-ERB-beta. *Nature*, 485, 123-7.
- CRIBBS, J. T. & STRACK, S. 2007. Reversible phosphorylation of Drp1 by cyclic AMP-dependent protein kinase and calcineurin regulates mitochondrial fission and cell death. *EMBO Rep*, 8, 939-44.
- DALLMANN, R., VIOLA, A. U., TAROKH, L., CAJOCHEN, C. & BROWN, S. A. 2012. The human circadian metabolome. *Proc Natl Acad Sci U S A*, 109, 2625-9.
- DAVIES, S. K., ANG, J. E., REVELL, V. L., HOLMES, B., MANN, A., ROBERTSON, F. P., CUI, N., MIDDLETON, B., ACKERMANN, K., KAYSER, M., THUMSER, A. E.,

- RAYNAUD, F. I. & SKENE, D. J. 2014. Effect of sleep deprivation on the human metabolome. *Proc Natl Acad Sci U S A*, 111, 10761-6.
- DETMER, S. A. & CHAN, D. C. 2007. Functions and dysfunctions of mitochondrial dynamics. *Nat Rev Mol Cell Biol*, 8, 870-9.
- ECKEL-MAHAN, K. & SASSONE-CORSI, P. 2013. Metabolism and the circadian clock converge. *Physiol Rev*, 93, 107-35.
- ECKEL-MAHAN, K. L., PATEL, V. R., MOHNEY, R. P., VIGNOLA, K. S., BALDI, P. & SASSONE-CORSI, P. 2012. Coordination of the transcriptome and metabolome by the circadian clock. *Proc Natl Acad Sci U S A*, 109, 5541-6.
- FENG, D., LIU, T., SUN, Z., BUGGE, A., MULLICAN, S. E., ALENGHAT, T., LIU, X. S. & LAZAR, M. A. 2011. A circadian rhythm orchestrated by histone deacetylase 3 controls hepatic lipid metabolism. *Science*, 331, 1315-9.
- FRANK, S. 2006. Dysregulation of mitochondrial fusion and fission: an emerging concept in neurodegeneration. *Acta Neuropathol*, 111, 93-100.
- GACHON, F., NAGOSHI, E., BROWN, S. A., RIPPERGER, J. & SCHIBLER, U. 2004. The mammalian circadian timing system: from gene expression to physiology. *Chromosoma*, 113, 103-12.
- HUANG, C. C., KO, M. L., VERNIKOVSKAYA, D. I. & KO, G. Y. 2012. Calcineurin serves in the circadian output pathway to regulate the daily rhythm of L-type voltage-gated calcium channels in the retina. *J Cell Biochem*, 113, 911-22.
- HUGHES, M. E., HOGENESCH, J. B. & KORNACKER, K. 2010. JTK_CYCLE: an efficient nonparametric algorithm for detecting rhythmic components in genome-scale data sets. *J Biol Rhythms*, 25, 372-80.
- INVERNIZZI, F., D'AMATO, I., JENSEN, P. B., RAVAGLIA, S., ZEVIANI, M. & TIRANTI, V. 2012. Microscale oxygraphy reveals OXPHOS impairment in MRC mutant cells. *Mitochondrion*, 12, 328-35.
- ISHIHARA, N., NOMURA, M., JOFUKU, A., KATO, H., SUZUKI, S. O., MASUDA, K., OTERA, H., NAKANISHI, Y., NONAKA, I., GOTO, Y., TAGUCHI, N., MORINAGA, H., MAEDA, M., TAKAYANAGI, R., YOKOTA, S. & MIHARA, K. 2009. Mitochondrial fission factor Drp1 is essential for embryonic development and synapse formation in mice. *Nat Cell Biol*, 11, 958-66.
- ISOBE, Y., HIDA, H. & NISHINO, H. 2011. Circadian rhythm of metabolic oscillation in suprachiasmatic nucleus depends on the mitochondrial oxidation state, reflected by cytochrome C oxidase and lactate dehydrogenase. *J Neurosci Res*, 89, 929-35.
- JACOBI, D., LIU, S., BURKEWITZ, K., KORY, N., KNUDSEN, N. H., ALEXANDER, R. K., UNLUTURK, U., LI, X., KONG, X., HYDE, A. L., GANGL, M. R., MAIR, W. B. & LEE, C. H. 2015. Hepatic Bmal1 Regulates Rhythmic Mitochondrial Dynamics and Promotes Metabolic Fitness. *Cell Metab*, 22, 709-20.
- JORDAN, S. D. & LAMIA, K. A. 2013. AMPK at the crossroads of circadian clocks and metabolism. *Mol Cell Endocrinol*, 366, 163-9.
- KALSBECK, A., SCHEER, F. A., PERREAU-LENZ, S., LA FLEUR, S. E., YI, C. X., FLIERS, E. & BUIJS, R. M. 2011. Circadian disruption and SCN control of energy metabolism. *FEBS Lett*, 585, 1412-26.
- KASAHARA, A. & SCORRANO, L. 2014. Mitochondria: from cell death executioners to regulators of cell differentiation. *Trends Cell Biol*, 24, 761-70.
- KASHATUS, D. F., LIM, K. H., BRADY, D. C., PERSHING, N. L., COX, A. D. & COUNTER, C. M. 2011. RALA and RALBP1 regulate mitochondrial fission at mitosis. *Nat Cell Biol*, 13, 1108-15.
- KASUKAWA, T., SUGIMOTO, M., HIDA, A., MINAMI, Y., MORI, M., HONMA, S., HONMA, K., MISHIMA, K., SOGA, T. & UEDA, H. R. 2012. Human blood metabolite timetable indicates internal body time. *Proc Natl Acad Sci U S A*, 109, 15036-41.
- LAMIA, K. A., PAPP, S. J., YU, R. T., BARISH, G. D., UHLENHAUT, N. H., JONKER, J. W., DOWNES, M. & EVANS, R. M. 2011. Cryptochromes mediate rhythmic repression of the glucocorticoid receptor. *Nature*, 480, 552-6.
- LAMIA, K. A., SACHDEVA, U. M., DITACCHIO, L., WILLIAMS, E. C., ALVAREZ, J. G., EGAN, D. F., VASQUEZ, D. S., JUGUILON, H., PANDA, S., SHAW, R. J.,

- THOMPSON, C. B. & EVANS, R. M. 2009. AMPK regulates the circadian clock by cryptochrome phosphorylation and degradation. *Science*, 326, 437-40.
- LANGMESSER, S. & ALBRECHT, U. 2006. Life time-circadian clocks, mitochondria and metabolism. *Chronobiol Int*, 23, 151-7.
- LAWTON, K. A., BERGER, A., MITCHELL, M., MILGRAM, K. E., EVANS, A. M., GUO, L., HANSON, R. W., KALHAN, S. C., RYALS, J. A. & MILBURN, M. V. 2008. Analysis of the adult human plasma metabolome. *Pharmacogenomics*, 9, 383-97.
- MARCHEVA, B., RAMSEY, K. M., BUHR, E. D., KOBAYASHI, Y., SU, H., KO, C. H., IVANOVA, G., OMURA, C., MO, S., VITATERNA, M. H., LOPEZ, J. P., PHILIPSON, L. H., BRADFIELD, C. A., CROSBY, S. D., JEBAILLY, L., WANG, X., TAKAHASHI, J. S. & BASS, J. 2010. Disruption of the clock components CLOCK and BMAL1 leads to hypoinsulinaemia and diabetes. *Nature*, 466, 627-31.
- MARCUSSEN, M. & LARSEN, P. J. 1996. Cell cycle-dependent regulation of cellular ATP concentration, and depolymerization of the interphase microtubular network induced by elevated cellular ATP concentration in whole fibroblasts. *Cell Motil Cytoskeleton*, 35, 94-9.
- MARTINEZ-DIEZ, M., SANTAMARIA, G., ORTEGA, A. D. & CUEZVA, J. M. 2006. Biogenesis and dynamics of mitochondria during the cell cycle: significance of 3'UTRs. *PLoS One*, 1, e107.
- MASRI, S., PATEL, V. R., ECKEL-MAHAN, K. L., PELEG, S., FORNE, I., LADURNER, A. G., BALDI, P., IMHOF, A. & SASSONE-CORSI, P. 2013. Circadian acetylome reveals regulation of mitochondrial metabolic pathways. *Proc Natl Acad Sci U S A*, 110, 3339-44.
- MINAMI, Y., KASUKAWA, T., KAKAZU, Y., IIGO, M., SUGIMOTO, M., IKEDA, S., YASUI, A., VAN DER HORST, G. T., SOGA, T. & UEDA, H. R. 2009. Measurement of internal body time by blood metabolomics. *Proc Natl Acad Sci U S A*, 106, 9890-5.
- MISHRA, P. & CHAN, D. C. 2014. Mitochondrial dynamics and inheritance during cell division, development and disease. *Nat Rev Mol Cell Biol*, 15, 634-46.
- NAGOSHI, E., SAINI, C., BAUER, C., LAROCHE, T., NAEF, F. & SCHIBLER, U. 2004. Circadian gene expression in individual fibroblasts: cell-autonomous and self-sustained oscillators pass time to daughter cells. *Cell*, 119, 693-705.
- NAKAHATA, Y., KALUZOVA, M., GRIMALDI, B., SAHAR, S., HIRAYAMA, J., CHEN, D., GUARENTE, L. P. & SASSONE-CORSI, P. 2008. The NAD⁺-dependent deacetylase SIRT1 modulates CLOCK-mediated chromatin remodeling and circadian control. *Cell*, 134, 329-40.
- NAKAHATA, Y., SAHAR, S., ASTARITA, G., KALUZOVA, M. & SASSONE-CORSI, P. 2009. Circadian control of the NAD⁺ salvage pathway by CLOCK-SIRT1. *Science*, 324, 654-7.
- O'NEILL, J. S., MAYWOOD, E. S., CHESHAM, J. E., TAKAHASHI, J. S. & HASTINGS, M. H. 2008. cAMP-dependent signaling as a core component of the mammalian circadian pacemaker. *Science*, 320, 949-53.
- OETTINGHAUS, B., SCHULZ, J. M., RESTELLI, L. M., LICCI, M., SAVOIA, C., SCHMIDT, A., SCHMITT, K., GRIMM, A., MORE, L., HENCH, J., TOLNAY, M., ECKERT, A., D'ADAMO, P., FRANKEN, P., ISHIHARA, N., MIHARA, K., BISCHOFBERGER, J., SCORRANO, L. & FRANK, S. 2015. Synaptic dysfunction, memory deficits and hippocampal atrophy due to ablation of mitochondrial fission in adult forebrain neurons. *Cell Death Differ*.
- OLIVA-RAMIREZ, J., MORENO-ALTAMIRANO, M. M., PINEDA-OLVERA, B., CAUICH-SANCHEZ, P. & SANCHEZ-GARCIA, F. J. 2014. Crosstalk between circadian rhythmicity, mitochondrial dynamics and macrophage bactericidal activity. *Immunology*, 143, 490-7.
- PAGANI, L., SEMENOVA, E. A., MORIGGI, E., REVELL, V. L., HACK, L. M., LOCKLEY, S. W., ARENDT, J., SKENE, D. J., MEIER, F., IZAKOVIC, J., WIRZ-JUSTICE, A., CAJOCHEN, C., SERGEEVA, O. J., CHERESIZ, S. V., DANILENKO, K. V., ECKERT, A. & BROWN, S. A. 2010. The physiological period length of the human

- circadian clock in vivo is directly proportional to period in human fibroblasts. *PLoS One*, 5, e13376.
- PANDA, S., ANTOCH, M. P., MILLER, B. H., SU, A. I., SCHOOK, A. B., STRAUME, M., SCHULTZ, P. G., KAY, S. A., TAKAHASHI, J. S. & HOGENESCH, J. B. 2002. Coordinated transcription of key pathways in the mouse by the circadian clock. *Cell*, 109, 307-20.
- PATEL, V. R., ECKEL-MAHAN, K., SASSONE-CORSI, P. & BALDI, P. 2012. CircadiOmics: integrating circadian genomics, transcriptomics, proteomics and metabolomics. *Nat Methods*, 9, 772-3.
- PEEK, C. B., AFFINATI, A. H., RAMSEY, K. M., KUO, H. Y., YU, W., SENA, L. A., ILKAYEVA, O., MARCHEVA, B., KOBAYASHI, Y., OMURA, C., LEVINE, D. C., BACSIK, D. J., GIUS, D., NEWGARD, C. B., GOETZMAN, E., CHANDEL, N. S., DENU, J. M., MRKSICH, M. & BASS, J. 2013. Circadian clock NAD⁺ cycle drives mitochondrial oxidative metabolism in mice. *Science*, 342, 1243417.
- RAMSEY, K. M., YOSHINO, J., BRACE, C. S., ABRASSART, D., KOBAYASHI, Y., MARCHEVA, B., HONG, H. K., CHONG, J. L., BUHR, E. D., LEE, C., TAKAHASHI, J. S., IMAI, S. & BASS, J. 2009. Circadian clock feedback cycle through NAMPT-mediated NAD⁺ biosynthesis. *Science*, 324, 651-4.
- REY, G. & REDDY, A. B. 2013. Connecting cellular metabolism to circadian clocks. *Trends Cell Biol*, 23, 234-41.
- ROSATO, E., TAUBER, E. & KYRIACOU, C. P. 2006. Molecular genetics of the fruit-fly circadian clock. *Eur J Hum Genet*, 14, 729-38.
- SANTEL, A. & FRANK, S. 2008. Shaping mitochondria: The complex posttranslational regulation of the mitochondrial fission protein DRP1. *IUBMB Life*, 60, 448-55.
- SCHEFFLER, I. E. 2001. A century of mitochondrial research: achievements and perspectives. *Mitochondrion*, 1, 3-31.
- SCHMUTZ, I., RIPPERGER, J. A., BAERISWYL-AEBISCHER, S. & ALBRECHT, U. 2010. The mammalian clock component PERIOD2 coordinates circadian output by interaction with nuclear receptors. *Genes Dev*, 24, 345-57.
- TUREK, F. W., JOSHUA, C., KOHSAKA, A., LIN, E., IVANOVA, G., MCDEARMON, E., LAPOSKY, A., LOSEE-OLSON, S., EASTON, A., JENSEN, D. R., ECKEL, R. H., TAKAHASHI, J. S. & BASS, J. 2005. Obesity and metabolic syndrome in circadian Clock mutant mice. *Science*, 308, 1043-5.
- UM, J. H., PENDERGAST, J. S., SPRINGER, D. A., FORETZ, M., VIOLLET, B., BROWN, A., KIM, M. K., YAMAZAKI, S. & CHUNG, J. H. 2011. AMPK regulates circadian rhythms in a tissue- and isoform-specific manner. *PLoS One*, 6, e18450.
- VOLLMERS, C., GILL, S., DITACCHIO, L., PULIVARTHY, S. R., LE, H. D. & PANDA, S. 2009. Time of feeding and the intrinsic circadian clock drive rhythms in hepatic gene expression. *Proc Natl Acad Sci U S A*, 106, 21453-8.
- WESTERMANN, B. 2010. Mitochondrial fusion and fission in cell life and death. *Nat Rev Mol Cell Biol*, 11, 872-84.
- YOULE, R. J. & VAN DER BLIEK, A. M. 2012. Mitochondrial fission, fusion, and stress. *Science*, 337, 1062-5.
- ZHANG, Y., FANG, B., EMMETT, M. J., DAMLE, M., SUN, Z., FENG, D., ARMOUR, S. M., REMSBERG, J. R., JAGER, J., SOCCIO, R. E., STEGER, D. J. & LAZAR, M. A. 2015. GENE REGULATION. Discrete functions of nuclear receptor Rev-erbalpha couple metabolism to the clock. *Science*, 348, 1488-92.
- ZHENG, B., ALBRECHT, U., KAASIK, K., SAGE, M., LU, W., VAISHNAV, S., LI, Q., SUN, Z. S., EICHELE, G., BRADLEY, A. & LEE, C. C. 2001. Nonredundant roles of the mPer1 and mPer2 genes in the mammalian circadian clock. *Cell*, 105, 683-94.

Supplemental References

- BROWN, S. A., FLEURY-OLELA, F., NAGOSHI, E., HAUSER, C., JUGE, C., MEIER, C. A., CHICHEPORTICHE, R., DAYER, J. M., ALBRECHT, U. & SCHIBLER, U. 2005. The period length of fibroblast circadian gene expression varies widely among human individuals. *PLoS Biol*, 3, e338.
- DALLMANN, R., VIOLA, A. U., TAROKH, L., CAJOCHEN, C. & BROWN, S. A. 2012. The human circadian metabolome. *Proc Natl Acad Sci U S A*, 109, 2625-9.
- INVERNIZZI, F., D'AMATO, I., JENSEN, P. B., RAVAGLIA, S., ZEVIANI, M. & TIRANTI, V. 2012. Microscale oxygraphy reveals OXPHOS impairment in MRC mutant cells. *Mitochondrion*, 12, 328-35.
- ISHIHARA, N., NOMURA, M., JOFUKU, A., KATO, H., SUZUKI, S. O., MASUDA, K., OTERA, H., NAKANISHI, Y., NONAKA, I., GOTO, Y., TAGUCHI, N., MORINAGA, H., MAEDA, M., TAKAYANAGI, R., YOKOTA, S. & MIHARA, K. 2009. Mitochondrial fission factor Drp1 is essential for embryonic development and synapse formation in mice. *Nat Cell Biol*, 11, 958-66.
- LAWTON, K. A., BERGER, A., MITCHELL, M., MILGRAM, K. E., EVANS, A. M., GUO, L., HANSON, R. W., KALHAN, S. C., RYALS, J. A. & MILBURN, M. V. 2008. Analysis of the adult human plasma metabolome. *Pharmacogenomics*, 9, 383-97.
- OETTINGHAUS, B., SCHULZ, J. M., RESTELLI, L. M., LICCI, M., SAVOIA, C., SCHMIDT, A., SCHMITT, K., GRIMM, A., MORE, L., HENCH, J., TOLNAY, M., ECKERT, A., D'ADAMO, P., FRANKEN, P., ISHIHARA, N., MIHARA, K., BISCHOFBERGER, J., SCORRANO, L. & FRANK, S. 2015. Synaptic dysfunction, memory deficits and hippocampal atrophy due to ablation of mitochondrial fission in adult forebrain neurons. *Cell Death Differ*.
- PAGANI, L., SEMENOVA, E. A., MORIGGI, E., REVELL, V. L., HACK, L. M., LOCKLEY, S. W., ARENDT, J., SKENE, D. J., MEIER, F., IZAKOVIC, J., WIRZ-JUSTICE, A., CAJOCHEN, C., SERGEEVA, O. J., CHERESIZ, S. V., DANILENKO, K. V., ECKERT, A. & BROWN, S. A. 2010. The physiological period length of the human circadian clock in vivo is directly proportional to period in human fibroblasts. *PLoS One*, 5, e13376.

B. Improvement of neuronal bioenergetics by neurosteroids: Implications for age-related neurodegenerative disorders

Authors: Amandine Grimm^{a, b, c, &}, **Karen Schmitt**^{a, b, &}, Undine E. Lang^b, Ayikoe Guy Mensah-Nyagan^c, Anne Eckert^{a, b, *}

Affiliations:

^a Neurobiology Laboratory for Brain Aging and Mental Health, Transfaculty Research Platform, Molecular & Cognitive Neuroscience, University of Basel, Wilhelm Klein-Str. 27, CH-4012 Basel, Switzerland

^b Psychiatric University Clinics, University of Basel, Wilhelm Klein-Str. 27, CH-4012 Basel, Switzerland

^c Biopathologie de la Myéline, Neuroprotection et Stratégies Thérapeutiques, INSERM U1119, Fédération de Médecine Translationnelle de Strasbourg (FMTS), Université de Strasbourg, Bâtiment 3 de la Faculté de Médecine, 11 rue Humann, 67 000 Strasbourg, France

*Corresponding author at: Psychiatric University Clinics, University of Basel, Wilhelm Klein-Str. 27, CH-4012 Basel, Switzerland.

Tel.: +41 613255487; fax: +41 613255577.

E-mail address: anne.eckert@upkbs.ch (A. Eckert).

&These authors contributed equally to this work.

Biochimica et Biophysica Acta (BBA) - Molecular Basis of Disease, Volume 1842, Issue 12, Part A, December 2014, Pages 2427–2438, doi: 10.1016/j.bbadis.2014.09.013.

Received 2 July 2014, Revised 22 September 2014, Accepted 25 September 2014, Available online 2 October 2014

Abstract

The brain has high energy requirements to maintain neuronal activity. Consequently impaired mitochondrial function will lead to disease. Normal aging is associated with several alterations in neurosteroid production and secretion. Decreases in neurosteroid levels might contribute to brain aging and loss of important nervous functions, such as memory. Up to now, extensive studies only focused on estradiol as a promising neurosteroid compound that is able to ameliorate cellular bioenergetics, while the effects of other steroids on brain mitochondria are poorly understood or not investigated at all. Thus, we aimed to characterize the bioenergetic modulating profile of a panel of seven structurally diverse neurosteroids (progesterone, estradiol, estrone, testosterone, 3 α -androstenediol, DHEA and allopregnanolone), known to be involved in brain function regulation. Of note, most of the steroids tested were able to improve bioenergetic activity in neuronal cells by increasing ATP levels, mitochondrial membrane potential and basal mitochondrial respiration. In parallel, they modulated redox homeostasis by increasing antioxidant activity, probably as a compensatory mechanism to a slight enhancement of ROS which might result from the rise in oxygen consumption. Thereby, neurosteroids appeared to act via their corresponding receptors and exhibited specific bioenergetic profiles. Taken together, our results indicate that the ability to boost mitochondria is not unique to estradiol, but seems to be a rather common mechanism of different steroids in the brain. Thus, neurosteroids may act upon neuronal bioenergetics in a delicate balance and an age-related steroid disturbance might be involved in mitochondrial dysfunction underlying neurodegenerative disorders.

Keywords: Mitochondria, Neurosteroid, Bioenergetics, Amyloid- β peptide, tau protein.

Abbreviations:

3 α -A, 3 α -androstenediol; AD, Alzheimer's disease; APP, amyloid- β precursor protein; AP, allopregnanolone; D, DHEA (dihydroepiandrosterone); DHR, dihydrorhodamine 123; DMSO, dimethylsulfoxide; E1, estrone; E2, 17 β -estradiol; E3, estriol; ECAR, extracellular acidification rate; ETC, electron transport chain; MAS, mitochondrial assay solution; MPP, mitochondrial membrane potential; mtROS, mitochondrial reactive oxygen species; OCR, oxygen consumption rate; OXPHOS, Oxidative phosphorylation; P, progesterone; PD, Parkinson's disease; PMP, plasma membrane permeabilizer; RCR, respiratory control ratio; roGFP, redox sensitive green fluorescent protein; ROS, reactive oxygen species; SRA, steroid receptor antagonist; T, testosterone; TCA, tricyclic acid.

1. Introduction

The brain is a highly differentiated organ with high energy requirements, mainly in the form of adenosine triphosphate (ATP) molecules. Despite its small size, it accounts for about 20% of the body's total basal oxygen consumption (1). As a result, the brain is more sensitive to neuronal damage during hypometabolic states and impaired redox homeostasis, as observed in normal aging and in neurodegenerative diseases associated with a decline in energy production and changes in the redox status (2). In this context, mitochondria, small organelles that are present in almost all cell types playing a predominant role in cellular bioenergetics, are particularly important in the nervous system because of its high energy demand. Mitochondria are not only the “powerhouses of the cell”, providing the main source of cellular energy via ATP generation through oxidative phosphorylation, but they also contribute to plenty of cellular functions, including apoptosis, intracellular calcium homeostasis, alteration of the cellular reduction–oxidation (redox) state and synaptic plasticity (3; 4). Thus, it is more and more recognized that mitochondrial dysfunction is a significant and early event of neurodegeneration, and that the pathophysiological mechanisms of a range of neurodegenerative diseases, including Alzheimer's (AD) and Parkinson's disease (PD), are associated with a decline in bioenergetic activity and an increase in oxidative stress, particularly in mitochondria themselves (5-10).

Steroid hormones are molecules involved in the control of many physiological processes in the periphery, from reproductive behavior to the stress response. They are mainly produced by endocrine glands, such as the adrenal glands, gonads and placenta, but in 1981 Baulieu and co-workers were the first to demonstrate the production of steroids within the nervous system itself (11). This last category of molecules is now called “neurosteroids” and is defined as steroids that are synthesized within the nervous system independently of peripheral endocrine glands. Neurosteroid levels remain elevated even after adrenalectomy and castration (12; 13) and are involved in brain-specific functions. Since the ability to produce neurosteroids is conserved during vertebrate evolution, one can suggest that this family of molecules is important for living things and that the modulation of their biosynthesis plays an important role in the pathophysiology of neurodegenerative disorders.

Studies performed in humans, animals, and cellular models have shown alterations in the synthesis of neurosteroids that declined during brain aging paralleled by a loss of important nervous functions, such as memory, and were further associated with PD and AD (14-16). Thus, several neurosteroids have been quantified in various brain regions of aged AD patients and aged non-demented controls. This showed a general trend toward lower steroid levels in AD patients compared to controls, associated with a negative correlation between neurosteroid levels and amyloid- β (A β) and phospho-tau in some brain regions (17).

In accordance with these observations, previous data from our groups provided first evidence that, vice versa, A β and hyperphosphorylated tau differentially impacted neurosteroidogenesis (Fig. 1) (18-20). Indeed, a decrease of progesterone and 17-hydroxyprogesterone production was observed in amyloid precursor protein (APP)/A β -overexpressing cells, while 3 α -androstenediol and estradiol levels were increased (19). Moreover, *in vitro* treatment of human neuroblastoma cells with “non-toxic” A β concentrations (within the nanomolar range) revealed an increase in estradiol production, whereas toxic A β concentrations (within the micromolar range) showed the opposite effect (18). Overexpression of human wild type tau (hTau40) protein induced an increase in production of progesterone, 3 α -androstenediol, and 17-hydroxyprogesterone, in contrast to the abnormally hyperphosphorylated tau bearing the P301L mutation that led to decreased production of these neurosteroids (19).

Moreover, a growing body of evidence has highlighted neuroprotective effects of steroids, particularly estradiol, against AD-related injury (reviewed in (21)). Because the drop of estrogen in a post-menopausal woman is considered as a risk factor in AD (two-thirds of AD patients are women), the neuroprotective action of estrogen has been widely investigated (reviewed in (22)). One *in vivo* study showed that estradiol treatment of ovariectomized female rats up-regulated enzymes involved in glycolysis and oxidative phosphorylation, and increased ATP synthase expression which was translated into an increased mitochondrial respiration (23). These findings were additionally confirmed in an AD mouse model by Yao and coworkers (24).

However, there is little evidence that other steroids are also able to act on mitochondrial function, and to our knowledge, no study has aimed to compare the effects of neurosteroids besides estradiol on cellular bioenergetics and redox environment in neuronal cells. Thus, the objective of our study was to investigate the effects of different neurosteroids on bioenergetic activity *in vitro*. For this purpose, we selected seven neurosteroids - progesterone, estradiol and estrone, belonging to the estrogen family; testosterone and 3 α -androstenediol, belonging to androgen family; and DHEA and allopregnanolone - known to be involved in brain function regulation (12; 13; 25; 18; 19; 17). Neurosteroid effects on ATP production, mitochondrial membrane potential (MMP), mitochondrial respiration, glycolysis and the consequences on the modulation of the redox environment were investigated in neuronal cells.

2. Materials and methods

2.1. Chemicals and reagents

Dulbecco's-modified Eagle's medium (DMEM), RPMI-1640 medium, fetal calf serum (FCS), penicillin/streptomycin, progesterone, 17 β -estradiol, estrone, 3 α -androstenediol, DHR, TMRM, ADP, pyruvate, succinate and malate were from Sigma-Aldrich (St. Louis, MO USA). Glutamax, MitoSOX, DPBS, Neurobasal medium and B27 were from Gibco Invitrogen (Waltham, MA, USA). DHEA and allopregnanolone were from Calbiochem (Billerica, MA, USA). PMP and XF Cell Mitostress kit were from Seahorse Bioscience (North Billerica, MA, USA). Testosterone was from AppliChem (Darmstadt, Germany). Horse serum (HS) was from Amimed, Bioconcept (Allschwil, Switzerland). RU-486, ICI-187.780, and 2-hydroxy flutamide were from Cayman Chemical (Ann Arbor, MI, USA).

2.2. Cell culture

Human SH-SY5Y neuroblastoma cells were grown at 37 °C in a humidified incubator chamber under an atmosphere of 7.5% CO₂ in DMEM supplemented with 10% (v/v) heat-inactivated FCS, 5% (v/v) heat-inactivated HS, 2 mM Glutamax and 1% (v/v) penicillin/streptomycin. Cells were passaged 1-2 times per week, and plated for treatment when they reached 80–90% confluence.

2.3. Primary neuronal cultures

Mouse cortical neurons were prepared from E15 embryos according to the French guidelines, as previously described (26). Cells were plated in poly-L-lysine-coated plates at a density of 1.5×10^4 cells/well for ATP measurement (white 96-well plate) or 5×10^4 cells/well for measurement with the Seahorse XF24 Analyser (XF24 cell culture microplate). After 7 days at 37 °C, 50% of the medium was replaced with fresh medium every third day. ATP level, oxygen consumption rate (OCR) and extracellular acidification rate (ECAR) were investigated in this primary neuronal culture after a 24 h treatment with the different neurosteroids.

2.4. Treatment paradigm

Assessment of cell viability was performed on SH-SY5Y neuroblastoma cells to determine the potential toxic concentration range of neurosteroids (from 10 nM to 1000 nM, data not shown) and steroid receptor antagonists (SRA, from 1 nM to 1 μ M, data not shown) using a MTT reduction assay (Roche, Basel, Switzerland). On the basis of the MTT results, the concentrations 10 nM and 100 nM of steroids were then selected and used in all assays. SH-SY5Y cells were treated one day after plating either with DMEM (untreated control condition) or with a final concentration of 10 nM and 100 nM of progesterone, 17 β -estradiol,

estrone, testosterone, 3 α -androstenediol, DHEA or allopregnanolone made from a stock solution in DMSO for 24 h (final concentration of DMSO < 0.002%, no effect of the vehicle solution (DMSO) alone compared to the untreated condition). In the experiment using SRA, cells were pre-treated for 1 h. with 100 nM of RU-486 and ICI-187.780, and 1 μ M of 2-hydroxy flutamide (2OH-flutamide), and then treated for 24 h with the corresponding neurosteroids. To limit cell growth and to optimize mitochondrial respiration, treatment medium contained only a low amount of fetal calf serum (5% FCS) as well as glucose (1 g/l) and was supplemented with 4 mM pyruvate. Each assay was repeated at least 3 times.

2.5. *ATP levels*

Total ATP content of SH-SY5Y cells was determined using a bioluminescence assay (ViaLighTM HT, Cambrex Bio Science, Walkersville, MD, USA) according to the instruction of the manufacturer, as previously described (27). SH-SY5Y cells were plated in 5 replicates into a white 96-wells cell culture plate at a density of 1.5×10^4 cells/well. The bioluminescent method measures the formation of light from ATP and luciferin by luciferase. The emitted light was linearly related to the ATP concentration and was measured using the multilabel plate reader VictorX5 (Perkin Elmer).

2.6. *Cell proliferation assay*

To verify if our treatment had an impact on cell cycle and induced proliferation, the BrdU Cell Proliferation Assay (Calbiochem, Darmstadt, Germany) was used following the instructions of the manufacturer. Briefly, SH-SY5Y cells were plated in 6 replicates into a 96-wells cell culture plate at a density of 1×10^4 cells/well. During the final 12 h of neurosteroid treatment, BrdU was added to the wells and incorporated into the DNA of dividing cells. The detection of BrdU was performed using an anti-BrdU antibody recognized by a horseradish peroxidase-conjugated anti-mouse. After addition of the substrate (TMB), the color reaction was quantified using the multilabel plate reader VictorX5 at 450nm. Values are proportional to the number of dividing cells.

2.7. *Determination of mitochondrial membrane potential*

The MMP was measured using the fluorescent dye tetramethylrhodamine, methyl ester, and perchlorate (TMRM). SH-SY5Y cells were plated in 6 replicates into a black 96-well cell culture plate at a density of 1.5×10^4 cells/well. Cells were loaded with the dye at a concentration of 0.4 μ M for 15 min. After washing twice with HBSS, the fluorescence was detected using the multilabel plate reader VictorX5 (PerkinElmer) at 530 nm (excitation)/590 nm (emission). Transmembrane distribution of the dye was dependent on MMP.

2.8. *Oxygen consumption rate and extracellular acidification rate*

The Seahorse Bioscience XF24 Analyser was used to perform a simultaneous real-time measurement of oxygen consumption rate (OCR) and extracellular acidification rate (ECAR). XF24 cell culture microplates (Seahorse Bioscience) were coated with 0.1% gelatine and SH-SY5Y cells were plated at a density of 2.5×10^4 cells/well in 100 μ l of the treatment medium containing 5% FCS, 1 g/l glucose and 4 mM pyruvate. After neurosteroid treatment, cells were washed with PBS and incubated with 500 μ l of assay medium (DMEM, without NaHCO₃, without phenol red, with 1g/l glucose, 4 mM pyruvate, and 1% L-glutamine, pH 7.4) at 37 °C in a CO₂-free incubator for 1 h. The plate was placed in the XF24 Analyser and basal OCR and ECAR were recorded during 30 min. For primary neuronal culture, the same conditions were kept, except the medium; here DMEM was replaced by RPMI-1640 medium.

2.9. *Mitochondrial respiration*

The investigation of mitochondrial respiration was performed using the Seahorse Bioscience XF24 analyser. XF24 cell culture microplates were coated with 0.1% gelatine and cells were plated at a density of 2.5×10^4 cells/well in 100 μ l of treatment medium containing 5% FCS, 1 g/l glucose and 4 mM pyruvate. After neurosteroid treatment, cells were washed with 1 \times pre-warmed mitochondrial assay solution (MAS; 70 mM sucrose, 220 mM mannitol, 10 mM KH₂PO₄, 4.5 mM MgCl₂, 2 mM HEPES, 1 mM EGTA and 0.2% (w/v) fatty acid-free BSA, pH 7.2 at 37 °C) and 500 μ l of pre-warmed (37 °C) MAS containing 1 nM XF plasma membrane permeabilizer (PMP, Seahorse Bioscience), 10 mM pyruvate, 10 mM succinate and 2 mM malate was added to the wells. The PMP was used to permeabilize intact cells in culture, which circumvents the need for isolation of intact mitochondria and allows the investigation of the OCR under different respiratory states induced by the sequential injection of: i) ADP (4 mM) to induce state 3; ii) Oligomycin (0.5 μ M) to induce state 4_o; iii) FCCP (2 μ M) to induce state 3 uncoupled (3_u); and iv) Antimycin A/rotenone (0.5 μ M and 1 μ M respectively) to shut down mitochondrial respiration. Data were extracted from the Seahorse XF24 software and the respiratory control ratio (RCR: State 3/State 4_o), which reflects the mitochondrial respiratory capacity, was calculated.

2.10. *GABAA receptor expression*

Cells were lysed and total RNA was extracted using the RNeasy Mini Kit from Qiagen (Venlo, Netherlands), according to the instructions of the manufacturer to measure GABAA receptor (subunits α 1 and β 2) mRNA levels. The first cDNA strand was synthesized using all RNA extracted by reverse transcription in a final volume of 30 μ l using the Ready-to-Go You-Prime First-Strand Bead cDNA synthesis kit (GE Healthcare, Little Chalfont, UK) according to

the supplied protocol. After reverse transcription, the cDNA was diluted 1:3 and 3 μ l were amplified by real-time PCR (StepOne™ System) in 20 μ l using DyNAmy Flash Probe qPCR Kit (Thermo Scientific, Waltham, MA, USA) with conventional Applied Biosystems cycling parameters (40 cycles of 95°C, 5 s, and 60°C, 1 min). Primers for human and mouse GABAA receptor subunit α 1 and β 2 were obtained from Life Technologies (Waltham, MA, USA). References of the primers are: GABRA1: Hs00971228_m1; GABRB2: Hs00241451_m1; gabra1: Mm00439046_m1; and gabrb2: Mm00433467_m1. After amplification, the size of the quantitative real-time PCR products was verified by electrophoresis on 2% (wt/vol) ethidium bromide-stained agarose gel. CDK4 was used as control housekeeping gene to assess the validity of the cDNA mixture and the PCR reaction. The gene expression of CDK4 was clearly detected in SH-SY5Y (data not shown), but not that of GABAA receptor.

2.11. *Reactive oxygen species detection*

Total level of mitochondrial reactive oxygen species (mtROS) and specific level of mitochondrial superoxide anion radicals were assessed using the fluorescent dye dihydrorhodamine 123 (DHR) and the Red Mitochondrial Superoxide Indicator (MitoSOX), respectively. SH-SY5Y cells were plated in 6 replicates into a black 96-well cell culture plate at a density of 1.5×10^4 cells/well. After neurosteroid treatment, cells were loaded with 10 μ M of DHR for 15 min or 5 μ M of MitoSOX for 90 min at room temperature in the dark on an orbital shaker. After washing twice with HBSS (Sigma), DHR, which is oxidized to cationic rhodamine 123 localized within the mitochondria, exhibits a green fluorescence that was detected using the multilabel plate reader VictorX5 at 485 nm (excitation)/538 nm (emission). MitoSOX, which is specifically oxidized by mitochondrial superoxide, exhibits a red fluorescence detected at 535 nm (excitation)/595 nm (emission). The intensity of fluorescence was proportional to mtROS levels or superoxide anion radicals in mitochondria.

2.12. *MnSOD activity*

The DetectX Superoxide Dismutase (SOD) Activity Kit (Ann Arbor, MI, USA) was used to quantitatively measure manganese SOD (MnSOD) activity following the instructions of the manufacturer. Briefly, 1×10^6 SH-SY5Y cells were collected for protein extraction. After a short sonication in PBS, the cellular homogenate was centrifuged at $1.500 \times g$ for 10 min at 4 °C. The supernatant was then centrifuged at $10,000 \times g$ for 15 min and the obtained cell pellet was treated with 2 mM potassium cyanide, and assayed for MnSOD activity.

2.13. *Mitochondrial redox environment*

To investigate changes in mitochondrial redox environment, SH-SY5Y cells were transfected with a plasmid coding for a redox sensitive green fluorescent protein with a

mitochondrial targeting sequence (pRA305 in pEGFP-N1). In an oxidized environment the absorption increases at short wavelengths (390 nm) at the expense of absorption at longer wavelengths (485 nm). The fluorescence ratio indicates oxidation/reduction, i.e., the redox environment in the mitochondria (28). Cells were plated in 6 replicates into a black 96-well cell culture plate at a density of 1.5×10^4 cells/well. After neurosteroid treatment, cells were washed twice with PBS and placed in a HEPES buffer (130 mM NaCl, 5 mM KCl, 1 mM CaCl₂, 10 mM D-glucose, and 20 mM HEPES). The ratio 390 nm/485 nm was measured using the multilabel plate reader VictorX5 detecting fluorescence at 390 nm or 485 nm (excitation)/510 nm (emission). An increase of the ratio indicates a more oxidized environment.

2.14. Statistical Analysis

Data are given as the mean \pm SEM, normalized to the untreated control group (=100%). Statistical analyses were performed using the Graph Pad Prism software. For statistical comparisons of more than two groups, One-way ANOVA was used, followed by a Dunnett's multiple comparison test versus the control. For statistical comparisons of two groups, Student unpaired t-test was used. P values < 0.05 were considered statistically significant. Statistical correlations were determined using Pearson's correlation coefficients.

3. Results

3.1. Neurosteroids modulate mitochondrial bioenergetics

To investigate the effects of neurosteroids on cellular bioenergetic activity, we first studied the SH-SY5Y cell line, a commonly used neuronal culture *in vitro* model that expresses a variety of neuronal receptors, including steroid receptors (progesterone, estrogen and androgen receptors) (29; 30). Cells were treated with different neurosteroids: progesterone (P), estradiol (E2), estrone (E1), testosterone (T), 3 α -androstenediol (3 α -A), DHEA (D) or allopregnanolone (AP), at two physiologically relevant concentrations, 10 nM and 100 nM (31-35), and ATP level was measured after 24 h of treatment. All neurosteroids, except allopregnanolone, were able to significantly increase ATP level (Fig. 2A), ranging from a 10% increase after 3 α -A treatment (10 nM) up to a 22% increase induced by progesterone (100 nM) compared to the untreated control.

A pre-treatment for 1 h with different steroid receptor antagonists (SRA) including the progesterone receptor antagonist RU-486 (assay concentration 100 nM), the estrogen receptor antagonist ICI-182,780 (assay concentration 100 nM), and the androgen receptor antagonist 2OH-flutamide (assay concentration 1 μ M) completely abolished the action of P, E2 and E1, as well as T and 3 α -A, respectively (Fig. 2B). The SRAs alone were devoid of the effects of ATP production. These results indicate that the action of neurosteroids may be mediated by nuclear receptors via gene regulation, at least for those neurosteroids that act via these receptors (progesterone, estrogens, and androgens).

To exclude that this rise in ATP was due to enhanced cell proliferation, we investigated the effects of the different neurosteroids. Of note, only allopregnanolone at 100 nM induced a significant increase of cell division by about 6% compared to the control (Table 1). Thus, our results indicate that the neurosteroid-induced up-regulation of cellular energy levels was independent of cell proliferation demands.

To verify whether the increase of ATP levels was directly linked to mitochondrial activity, we investigated the effects of neurosteroids on MMP, an indicator of the proton motive force necessary for ATP synthesis by the mitochondrial ATP synthase (36). Our results show that, at least for one of the two concentrations tested, neurosteroids induced a significant increase in MMP (Fig. 2C). The low concentration of 10 nM was particularly effective, ranging from an 18% increase after estradiol treatment up to a 32% increase induced by DHEA. Again, allopregnanolone was not able to significantly modulate the MMP. Thus, the observed increase in ATP is consistent with the finding of a slight hyperpolarization of the MMP.

Because molecules of ATP are produced by two main pathways, the cellular glycolysis and oxidative phosphorylation (OXPHOS) in mitochondria, we determined whether and which of those neurosteroids were able to modulate one or both pathways. For this purpose, we simultaneously monitored in real-time the extracellular acidification rate (ECAR), an indicator of glycolysis, and the oxygen consumption rate (OCR), an indicator of basal respiration, using a Seahorse Bioscience XF24 Analyser (Fig. 3A-C). On the one hand, despite a slight general increase, only estradiol and DHEA were able to significantly modulate the ECAR after 24 h of treatment (about 16.4% and 19.4% respectively) (Fig. 3A). On the other hand, our findings demonstrate that estradiol, estrone, testosterone, 3 α -A and DHEA significantly increased the OCR, with the most pronounced effect detected after a testosterone treatment at 100 nM (+26.5% compared to the control) (Fig. 3B). To compare the action of neurosteroids on glycolysis and basal respiration, we characterized the bioenergetic profile of SH-SY5Y neuroblastoma cells, representing OCR versus ECAR under the different treatment conditions (Fig. 3C). Notably, after treatment with the neurosteroid panel cells were switched to a metabolically more active state, with a tendency to increase both, glycolytic activity (ECAR) and basal respiration (OCR).

A Pearson correlation was performed to study whether the ATP levels correlated with OCR, ECAR or MMP (Fig. 4). A positive linear correlation between ATP level and OCR (Fig. 4A), but not between ATP and ECAR (Fig. 4B) or MMP (Fig. 4C) was detected, suggesting that the improvement in ATP production was preferentially linked to an increase of mitochondrial respiration (oxygen consumption).

To investigate more deeply the effects of neurosteroids on mitochondrial OXPHOS, OCR was measured using permeabilized SH-SY5Y cells, which allows the evaluation of different respiratory states and the respiratory control ratio (RCR=state 3/state 4) (Fig. 5). Especially testosterone significantly up-regulated the mitochondrial respiratory capacity by increasing the respiratory state 3 (ADP-dependent), state 3 uncoupled (in the absence of proton gradient after injection of FCCP) and the RCR (Fig. 5A-C). The treatment with DHEA (10 nM) showed a similar effect on the RCR under these experimental conditions (Table 1), while the rest of the tested steroid compounds had no beneficial effect on RCR. Thus, our findings suggest that neurosteroids primarily act on basal respiration in neuroblastoma cells, and that testosterone and DHEA are additionally able to increase the capacity for substrate oxidation (high RCR), which is important when cells have specific or high energy demands.

Since SH-SY5Y cells and other cell lines are not as highly dependent on OXPHOS as primary cell cultures to produce ATP (37), we investigated the action of neurosteroids on primary cell cultures from mouse brain cortex. Data demonstrate that, except for the treatment with progesterone, the level of ATP was significantly increased with at least one of

the two concentrations tested, ranging from a 27% increase after treatment with estrone (100 nM) up to a 59% induced increase by DHEA (10 nM) (Fig 6A). Compared to the data obtained with SH-SY5Y neuroblastoma cells (Fig. 2A), the magnitude of the rise in ATP concentration was higher in the primary cortical cell culture (maximal increase of 22.6% in SH-SY5Y cells versus 59.2% in primary neurons). This result implies that primary cell cultures have a greater capacity to produce ATP than neuroblastoma cells. Moreover, both concentrations of allopregnanolone were able to increase ATP level in primary cells, which was not the case in SH-SY5Y cells. Allopregnanolone mainly acts as an allosteric positive modulator of GABAA receptor (GABAA-R). To verify the implication of this receptor, we first investigated whether it was expressed in both cell types. We found that SH-SY5Y cells do not express the GABAA-R subunits $\alpha 1$ and $\beta 2$ that are involved in the allopregnanolone binding site (38), in contrast to primary cortical neurons (Suppl. Fig. 1), indicating that GABAA-R may be involved in the modulation of bioenergetics by allopregnanolone in neurons.

To determine whether the increase in ATP level was due to an improvement of glycolytic activity or mitochondrial respiration in this cellular model, we again performed a simultaneous real-time monitoring of the ECAR and the OCR (Fig. 6B-D). We measured a significant effect on the OCR for most of the neurosteroids tested, starting with a 59% increase after treatment with testosterone (10 nM) up to a 128% increase induced by 3α -A (10 nM) (Fig. 6B). Again, the magnitude of change was higher compared to the neuroblastoma cell line (maximal increase of 26.5%). In parallel, we measured a slight, but not significant, decrease in the glycolytic activity, except for the treatment with progesterone at 100 nM which in contrast induced a huge increase in the ECAR (+51.% compared to the control condition) (Fig. 6C). The bioenergetic profile (OCR versus ECAR) revealed that after treatment with neurosteroids, the primary cortical neurons had the general tendency to switch to a more aerobic state (Fig. 6D) by increasing their oxygen consumption (OCR) and decreasing their glycolytic activity (ECAR), especially at the low concentration of 10 nM.

Taken together, these data indicate that in primary mouse neurons, most of the neurosteroids from the tested panel were able to increase ATP production via improvement of mitochondrial respiration.

3.2. Neurosteroids modulate the redox homeostasis

The increase of OXPHOS is often coupled with an increase in mitochondrial reactive oxygen species (mtROS) production (39; 40). Since neurosteroids were able to significantly increase mitochondrial respiration, we investigated whether ROS levels were also increased within mitochondria (mtROS) by measuring the oxidation of the fluorescent dye

dihydrorhodamine 123 (DHR). All neurosteroids induced a significant dose-dependent increase in mtROS levels, ranging from a 43% increase after DHEA treatment (10 nM) up to a 111.3% increase induced by testosterone (100 nM) (Fig. 7A). Moreover, the specific measure of mitochondrial superoxide anion radicals revealed that some of the ROS produced were indeed superoxide anions (Table 1). However, the extent of mtROS production, which in excess can lead to massive oxidative stress, and finally cell death, did not seem to be sufficient to trigger cell death under those experimental conditions (data not shown).

Therefore, we next tested the antioxidant defense system in mitochondria. We quantitatively measured the activity of the manganese superoxide dismutase activity (MnSOD), which is present within the mitochondrial matrix. Indeed, MnSOD activity was significantly increased (Fig. 7B) after treatment with the whole panel of neurosteroids, ranging from a 28.6% (progesterone, 100 nM) up to a 49.3% increase (testosterone, 100 nM). The increase in mtROS was paralleled by an increase of antioxidant activity. In addition, mtROS level and MnSOD activity correlated with one another (Fig. 7C), suggesting that the increase of MnSOD activity was substrate-dependent.

Finally, to verify whether the mitochondrial redox environment was impacted by this increase of ROS versus increase of antioxidant defenses, SH-SY5Y cells stably transfected with a reporter gene coding for a redox sensitive green fluorescent protein (AR305 roGFP) located within mitochondria were treated with our panel of neurosteroids (28). Figure 7D displays the oxidation/reduction state in mitochondria, and indicates that, despite a slight switch toward a more oxidized state, only testosterone (100 nM) and DHEA (100 nM) significantly modified the redox environment in mitochondria.

Taken together, our data indicate that neurosteroids increased mitochondrial activity, which was paralleled by an enhancement in mtROS levels. However, cell viability was still unchanged and the raise of mtROS appeared to be at least in part compensated by an increase in antioxidant activity, which in turn led to a slight switch to an oxidized state within mitochondria.

4. Discussion

The aim of our study was to investigate the effects of seven neurosteroids on cellular bioenergetics and redox homeostasis in neuronal cells. The key findings were that: i) the majority of these steroids increased energy metabolism, mainly via an up-regulation of the mitochondrial activity and at least in part via receptor activation, and ii) neurosteroids regulated redox homeostasis by increasing the antioxidant activity as a compensatory mechanism to the ROS level enhancement which might result from the acceleration in oxygen consumption accompanied by a greater electron leakage from the electron transport chain. Additionally, each neurosteroid seems to have a specific bioenergetic profile. The single profiles are delineated as pie charts for SH-SY5Y (Fig. 8A) and mouse primary cortical neurons (Fig. 8B).

Remarkably, each steroid doesn't seem to act in the same way on both cell types. For example, allopregnanolone, which had no effects on ATP level and basal respiration in SH-SY5Y cells, appeared to increase those two parameters in primary neuronal cells. On the contrary, progesterone was able to increase ATP production in SH-SY5Y cells, but showed a significant effect only on glycolysis in primary cells. One explanation could be that SH-SY5Y cells and primary neuronal culture may exhibit steroid receptor expression profiles that are slightly different. Steroid receptor expression, such as that of progesterone, estrogen and androgen receptors, has already been demonstrated in both SH-SY5Y cells (29; 30) and in mouse neurons (41-43), respectively. It is known that allopregnanolone doesn't bind to a conventional steroid receptor but mainly acts as a positive GABAA receptor (GABAA-R) allosteric modulator that strengthens the effects of GABA. We found that SH-SY5Y cells do not express GABAA-R unlike in primary neurons (Suppl. Fig. 1). This indicates that allopregnanolone may act via GABAA-R to increase ATP level especially in primary neurons and explains the lack of effect on ATP in SH-SY5Y cells. Furthermore, other signaling pathways and receptors may be involved in the effects of allopregnanolone upon bioenergetics in primary cortical neurons, such as the newly characterized pregnane xenobiotic receptor (44).

Moreover, it is known that proliferative cells and tumors have a net tendency to use the cellular glycolysis to produce ATP instead of the OXPHOS system. This phenomenon is called "Warburg effect" (37). On the contrary, primary neurons, which are differentiated cells, rely almost exclusively on the OXPHOS system to produce ATP and glycolysis is really low (raw data not shown). Indeed, in the latter model, ATP level appeared to be strictly coupled with the basal respiration. The bioenergetic profile of primary cortical cells revealed that neurosteroids preferentially increased mitochondrial respiration and not the glycolytic pathway, while both pathways were increased in SH-SY5Y cells (Fig. 3C, Fig. 6D).

In the recent years, neurosteroids have emerged as new potential therapeutic tools against neurodegeneration (45). Among the steroids, the family of sex steroid hormones is the most widely studied. They are in the focus of research on neurodegenerative diseases since cognitive decline and the risk to develop AD appear to be associated with an age-related loss of sex hormones (e.g. estradiol, testosterone but also progesterone) in both, women and men (46; 25), a hypothesis largely supported by epidemiological evidence (47). *In vitro* and *in vivo* studies demonstrated neuroprotective effects of sex hormones, particularly with mitochondria proposed as the primary site of action of estradiol (48; 32; 49; 24). Indeed, estrone (E1), estradiol (E2), and estriol (E3), are known to play a fundamental role in the regulation of the female metabolic system (50). It has been reported that estrogens can regulate mitochondrial metabolism by increasing the expression of glucose transporter subunits and by regulating some enzymes involved in the tricarboxylic acid cycle (TCA cycle) and glycolysis, which leads to an improvement in glucose utilization by cells (reviewed in (21)). Estrogens seem also able to up-regulate genes coding for some electron transport chain components such as subunits of mitochondrial complex I (CI), cytochrome c oxidase (complex IV), and the F1 subunit of ATP synthase. In line with these findings, our data demonstrated that both female sex hormones, estradiol (E2) and estrone (E1), were able to increase ATP levels, basal respiration, and MMP in neuroblastoma cells (Fig. 8A). Of note, the increase of ATP levels induced by E2 and E1 was abolished in the presence of ICI-182.780, an estrogen receptor (α and β) antagonist (Fig. 2B) suggesting that estrogens, such as E2 and E1, may act via these receptors to up-regulate genes involved in cellular bioenergetics, as mentioned above. Estradiol seemed to be more potent than estrone, because both concentrations (10 nM and 100 nM) were effective to increase ATP levels and mitochondrial respiration. In addition, estradiol was able to regulate glycolysis. This difference can be explained by the observation that, despite estrone's capability as an estrogenic compound, it is about 10 times less estrogenic than estradiol (21). The same finding was observed in primary neurons (Fig. 8B).

Regarding the predominantly male hormone testosterone, we witnessed an increase in ATP levels, basal respiration and mitochondrial membrane potential in neuroblastoma cells (Fig. 8A). Moreover, testosterone was also the only steroid besides DHEA inducing an acceleration of the respiratory control ratio (RCR), an indicator of the capacity for substrate oxidation (high RCR), which is important when cells have specific or high energy demands. The role of androgens on mitochondrial function, especially testosterone, has received little attention up to now, compared to the estrogens. Only one study demonstrated a similar effect of testosterone on MMP (51). Furthermore, it has been proposed that estradiol and testosterone can regulate energy production by inducing nuclear and mitochondrial OXPHOS genes, since the subunits of mitochondrial chain complexes are encoded by the nuclear and

the mitochondrial genome, respectively, and both contain hormone responsive elements (52). Again, those findings are in line with our results, since we have shown that the increase of ATP levels was blocked in the presence of estrogen and androgen receptor antagonists (Fig. 2B).

Progesterone is the second main female sex hormone but it is also a precursor for estrogens and androgens. Progesterone, and its 3 α -5 α -derivate allopregnanolone (or 3 α , 5 α -tetrahydroprogesterone) as well as 3 α -androstenediol, seem to play a role in mood modulation. Their therapeutic potential for the treatment of depression, anxiety (53-55) and more recently AD is currently under investigation (35). In the present study, we demonstrated that progesterone increased ATP levels and MMP without significant effects on basal respiration in neuroblastoma cells (Fig. 8A). An increase in glycolysis was also observed after treatment in the primary neurons (Fig. 8B). Again, the up-regulatory effect of progesterone on ATP levels was shut down in the presence of the progesterone receptor antagonist RU-486 (Fig. 2B), suggesting that progesterone also modulates cellular bioenergetics by regulating gene expression via a progesterone nuclear receptor. Studies performed on ovariectomized rats revealed that a 24 h treatment with progesterone (subcutaneous injection, 30 μ g/kg) increased OXPHOS capacity in isolated mitochondria, in part by enhancing cytochrome c oxidase activity and expression (32). Interestingly, the increase of OXPHOS capacity was suppressed by a co-treatment with estradiol and progesterone, suggesting a competitive mode of action between both steroids. Another study using wobbler ALS (amyotrophic lateral sclerosis) model mice showed that progesterone was able to normalize the deficits in mitochondrial complex I activity observed in motor neurons of the cervical spinal cord (56). Because progesterone seems to have different functional effects, one can speculate that its action on mitochondrial respiration may be distinct to specific nerve cell populations.

Allopregnanolone and 3 α -androstenediol have a distinct mode of action compared to sex hormones because they mainly act on membrane receptors (allosteric modulator of GABAA-R) and not nuclear receptors (57). Their effects on mitochondrial bioenergetics cannot be explained by a direct regulation of genes involved in the OXPHOS system as previously proposed for sex hormones. In our study, 3 α -androstenediol showed a similar effect compared to progesterone in the neuronal cell line, but was also able to significantly increase the basal respiration (at 100 nM) (Fig. 8A). Both concentrations were effective to increase ATP and respiration in primary cells (Fig. 8B). Allopregnanolone significantly regulated ATP levels and basal respiration only in primary neurons, whereas no effect was detected in the neuroblastoma cell line. Based on those observations, we can speculate that: i) GABAA-R is involved in the up-regulatory effect of allopregnanolone on ATP levels in

primary cells because no increase was observed in SH-SY5Y cells lacking of this receptor (Suppl. Fig. 1); and ii) 3 α -androstenediol could act via androgen receptor because its effect on ATP levels was abolished in the presence of an androgen receptor antagonist (Fig. 2B). However, further investigations will be required to understand the exact underlying mechanisms. Besides, due to the high complexity of the neurosteroid pathway synthesis, it is difficult to conclude that the effect which we observed on bioenergetics is due to the tested neurosteroid itself, or to one of its metabolites, because they all belong to crisscross pathways (Fig. 1). However, since blocking progesterone, estrogen and androgen receptors abolishes the effects of their respective agonists, we have good evidence that the neurosteroids themselves exhibit the mode of action. In the same way, we can exclude that progesterone is acting via its metabolite allopregnanolone because the latter has no effects on bioenergetics in SH-SY5Y cells. Nevertheless, it is also possible that 3 α -androstenediol doesn't act directly on androgen receptors but is converted in dihydrotestosterone, another testosterone metabolite which has high affinity for this receptor. In a similar way, DHEA can be converted in androgens and estrogens and may act via the corresponding steroid nuclear receptor.

DHEA (dehydroepiandrosterone) was the first neurosteroid identified in 1981 (11), and its physiological action involves both genomic and non-genomic mechanisms, in part via activation of androgen/estrogen receptors and allosteric modulation of NMDA receptors, respectively (58). Human studies showed an age-related decrease in DHEA levels in the brain and in the blood in relation to the age-associated cognitive decline (59; 17). *In vitro*, we showed that DHEA enhanced ATP levels and basal respiration in primary neurons (Fig. 8B). A similar effect was observed in the neuronal cell line with an additional increase in MMP, glycolysis and RCR (Fig. 8A, Table 1). In agreement with our findings, DHEA was able to improve mitochondrial respiration in the brain of old rats (18-24 months) which exhibited a decline in mitochondrial function when compared to young rats (8-10 weeks) (60). More specifically, DHEA stimulated the respiratory state 3 in old rats which consequently was similar to that of untreated young rats. Furthermore, DHEA increased cytochrome c content in young and old mouse brains and enhanced mitochondrial dehydrogenase activities.

Thus, the different bioenergetic profiles we observed after treatment with our panel of steroids could be explained by their distinct abilities to directly or indirectly regulate the transcription of genes involved in glycolysis and oxidative phosphorylation (probably, via steroid nuclear receptors), but also the content and activity of mitochondrial respiratory complexes. Further investigations are required to determine in more detail which genes are involved in these processes.

Mitochondria are known to be paradoxical organelles. They can be compared to a double-edged sword that, on one hand, produces the energy necessary for cell survival, and on the other hand, induces the formation of ROS that can be harmful for cells when produced in excess with mitochondria as the first target of toxicity (39; 40). In our study, the increase in ATP appeared to be coupled to an increase in MMP and improved basal respiration (Fig. 8A). In parallel, we detected higher mitochondrial ROS levels, supporting the hypothesis that increased mitochondrial activity generates more ROS. The only exception was observed after treatment with allopregnanolone where we detected more ROS but no increase in ATP level, MMP, or basal respiration. We can speculate that, in this model, allopregnanolone might be able to increase ROS-producing metabolic functions via other mechanisms. But with regard to the other neurosteroids, the increase of mitochondrial ROS was paralleled by an increase in MnSOD activity. The MnSOD is located in the mitochondrial matrix and represents one of the first antioxidant defenses against ROS produced by OXPHOS (61). Its improved activity could be in part explained by an up-regulation of gene expression and protein level of MnSOD. Indeed, in studies which focused on antioxidant effects of steroids in ovariectomized female rats, an increase of MnSOD protein level has been observed after treatment with estradiol or progesterone (32), whereas DHEA preferentially up-regulated the expression of Cu/ZnSOD (31). In orchietomized male rats, testosterone was also able to increase MnSOD protein level compared to the control (sham operated) (62). A similar observation was made in the wobbler ALS mouse model, where MnSOD expression was elevated after treatment with progesterone (56).

In our study, the correlation between mitochondrial ROS level and MnSOD activity implies that the increase of enzymatic SOD activity might be preferentially substrate-dependent, but can be explained, at least in part, by an up-regulation of gene expression.

Based on our observation, one can speculate that pre-treatment with neurosteroids may exert a protective action against oxidative stress, possibly through a preconditioning mechanism via their ability to increase antioxidant defenses (i.e. MnSOD activity). However, in an already oxidized environment, the presence of neurosteroids may be deleterious for cells because they also appear to further increase ROS production. This observation reinforces the “critical window hypothesis” of the therapeutic use of steroids as debated recently with regard to the hormone replacement therapy in post-menopausal women (63) and implies that this kind of therapy should begin at an age when the redox system is still balanced, thus favoring the reference postulating early onset administration.

It is known that some neurosteroid levels decline during aging and are further modified in neurodegenerative conditions (i.e. AD and PD). In addition, mitochondrial dysfunction has been well-documented in aging and age-related neurodegenerative diseases

(64). Steroids offer interesting therapeutic opportunities for promoting successful aging because of their pleiotropic effects in the nervous system. Our findings highlight, for the first time, up-regulatory effects of neurosteroids upon the neuronal bioenergetic activity via up-regulation of the mitochondrial oxygen consumption as a common mechanism underlying neurosteroid action. In addition, these steroids can modulate the redox homeostasis, by balancing the increase of ROS production via improved mitochondrial antioxidant activity (Fig. 9). Thus, our results provide new insights in re-defining the biological model of how neurosteroids control neuronal functions. Because each steroid appeared to have a specific profile in bioenergetic outcome and redox homeostasis, the underlying mechanisms have to be elucidated in more details in the future, as well as those in models of neurodegenerative diseases, such as AD.

Table 1: Effects of neurosteroids on cellular bioenergetics in neuroblastoma cells.

		Progesterone		Estradiol		Estrone		Testosterone		3 α -androstenediol		DHEA		Allo-pregnanolone	
		10 nM	100 nM	10 nM	100 nM	10 nM	100 nM	10 nM	100 nM	10 nM	100 nM	10 nM	100 nM	10 nM	100 nM
ATP level		113.9*	122.6*	113.4*	114.6*	116*	120.4*	110.7*	118*	110.1*	111.4*	107.6*	112.4*	95.8	100.3
Cell proliferation		98.7	100.9	98.2	100.3	97.2	99.2	97.9	102.1	100.1	103.8	97.6	103.7	101.7	106.2*
MMP		120*	108.2	118.5*	118.8*	120*	119.2*	128.1*	119.9*	123.2*	109.8	132.2*	119.9*	111.5	114.2
Glycolysis		115.4	102.7	119.4*	116.1*	113.8	111.1	108.1	105.5	105.7	106.6	106.2	116.4*	102.2	101.6
Mitochondrial respiration	Basal	111	105.9	118.3*	123.2*	110.9	118.1*	115.1*	126.5*	106.9	114.1*	110.8*	106.7	99.6	109.6
	RCR	97.9	98.7	93.7	89.6	100.6	102.8	132.7*	116.5*	95.3	104	120.3*	97.81	105.7	102.1
Mitochondrial ROS	Total	108.4	151.7*	122.9	160.8*	121.8	171.3*	145.2*	211.3*	148.4*	182.8*	143.9*	200.6*	151*	207.2*
	Superoxide	100.7	104*	103	106.2*	102.8	108*	103.6*	105.8*	103.8*	105.9*	105*	106.4*	103.6*	107.4*
MnSOD activity		110.6	128.6*	120.7	136.6*	128.7	141.9*	137.4*	149.3*	134.7*	127.6	135.3*	128.1*	128.7*	147.4*
Mitochondrial redox state		105.7	110.6	108.1	108.9	104.1	109.2	109.9	113.6*	109.8	109.1	104.2	113.3*	91.7	102.5

Values represent the mean normalized on 100% of the control group (untreated). * indicates when the percentage is significantly different from the control group. MMP; mitochondrial membrane potential, RCR; respiratory control ration, ROS; reactive oxygen species, MnSOD; manganese superoxide dismutase.

FIGURES

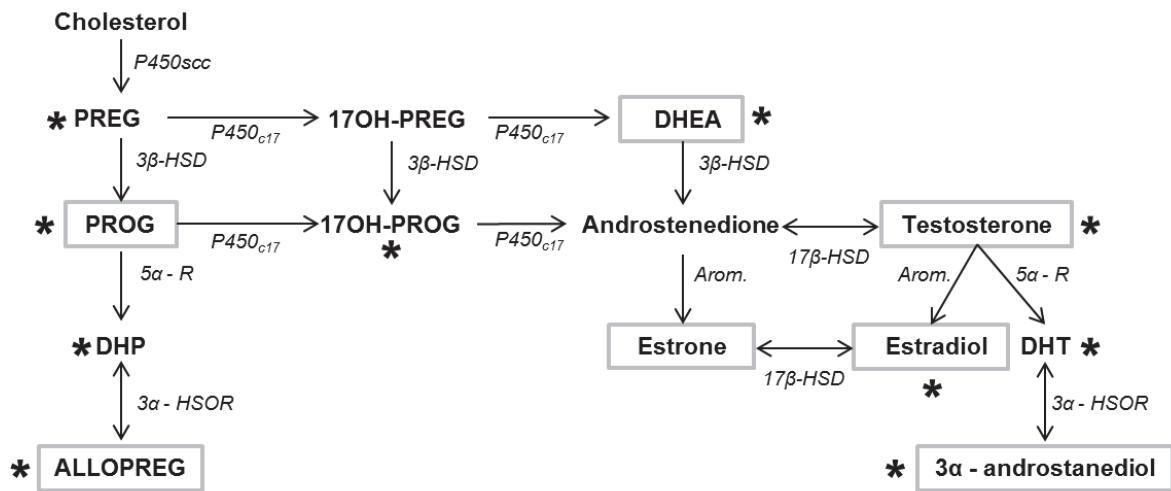


Fig. 1: Schematic representation of the main biochemical pathways for neurosteroidogenesis in the vertebrate brain. Boxes represent neurosteroids tested in our study. * indicates neurosteroids whose synthesis is impacted in AD. PREG; pregnenolone, PROG; progesterone, 17OH-PREG; 17-hydroxypregnenolone, 17OH-PROG; 17-hydroxyprogesterone, DHEA; dehydroepiandrosterone, DHP; dihydroprogesterone, ALLOPREG; allopregnanolone, DHT; dihydrotestosterone, P450_{scc}; cytochrome P450 cholesterol side chain cleavage, P450_{c17}; cytochrome P450c17, 3β-HSD; 3β-hydroxysteroid dehydrogenase, 5α-R; 5α-reductase, Arom.; aromatase, 21-OHase; 21-hydroxylase, 3α-HSOR; 3α-hydroxysteroid oxydoreductase, 17β-HSD; 17β- hydroxysteroid dehydrogenase

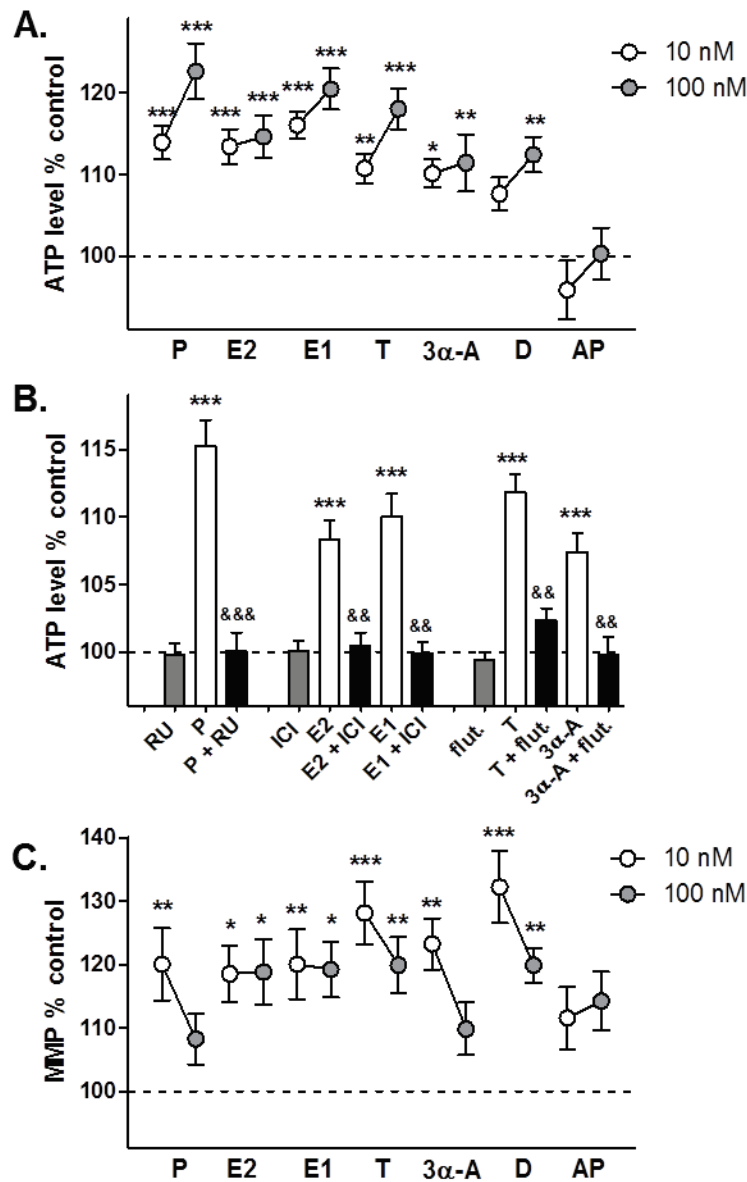


Fig. 2. Neurosteroids increase ATP level in SH-SY5Y neuroblastoma cells. (A) ATP level was significantly increased after neurosteroid treatment for 24 h at a concentration of 10 nM (white boxes) or 100 nM (gray boxes). (B) ATP level was measured after pre-treatment of cells for 1 h with either progesterone receptor antagonist RU-486 (100 nM), or estrogen receptor antagonist ICI-182.780 (100 nM), or androgen receptor antagonist 2OH-flutamide (1 μ M) and then treated for 24 h with the corresponding steroid agonist. (C) Mitochondrial membrane potential (MMP) was significantly increased after neurosteroid treatment for 24 h at a concentration of 10 nM (white boxes) or 100 nM (gray boxes). (A-C) Values represent the mean \pm SEM; n=12-18 replicates of three independent experiments. One-way ANOVA and post hoc Dunnetts' multiple comparison test versus control (untreated), *P<0.05; **P<0.01; ***P<0.001. Student unpaired t-test, && P<0.01; &&&P<0.001. P; progesterone, E2; estradiol, E1; estrone, T; testosterone, 3 α -A; 3 α -androstenediol, D; dihydroepiandrostanedione (DHEA), AP; allopregnanolone, RU; RU-486, ICI; ICI-182.780, flut.; 2OH-flutamide.

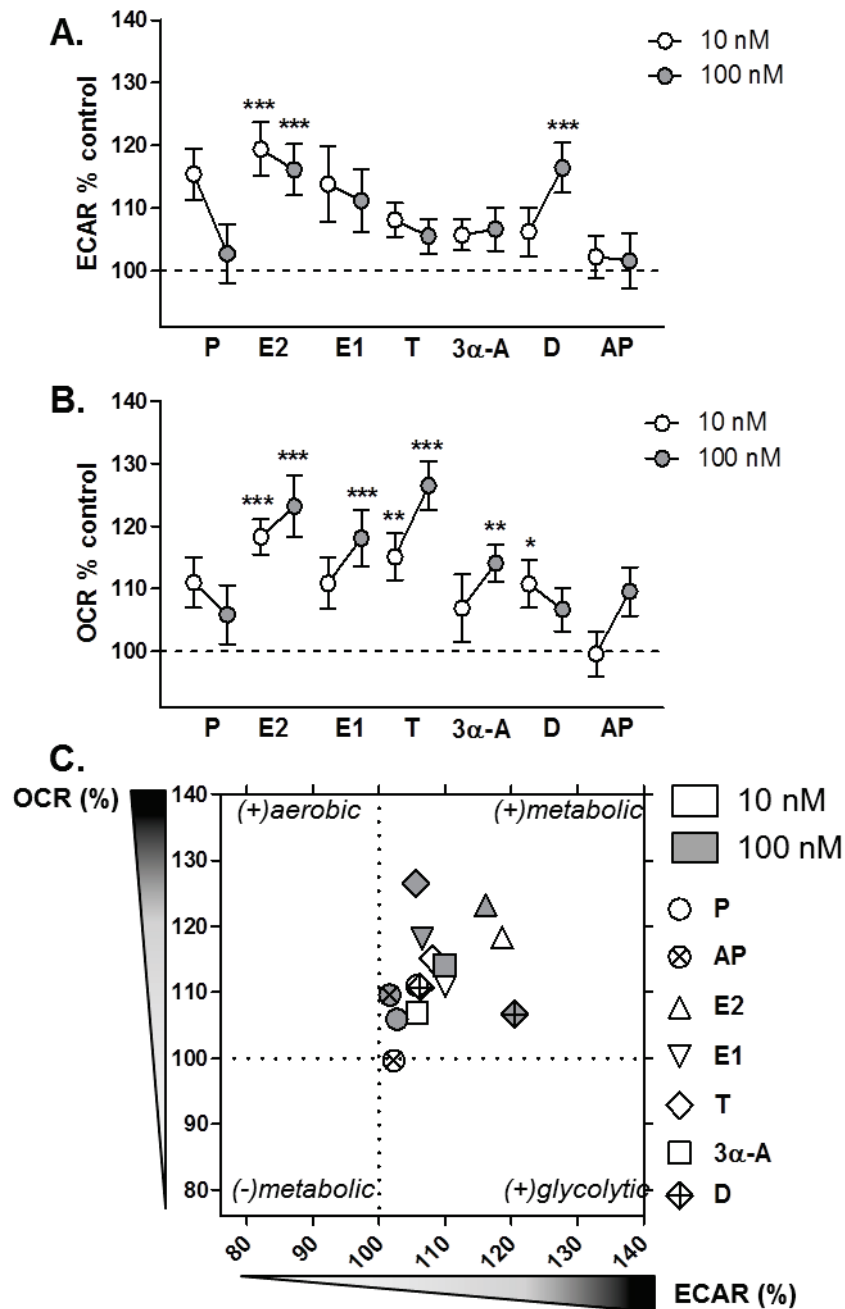


Fig. 3. Neurosteroids positively regulate bioenergetic activity in SH-SY5Y neuroblastoma cells.

(A) Extracellular acidification rate (ECAR) and (B) oxygen consumption rate (OCR) were measured simultaneously using a Seahorse Biosciences XF24 Analyser in the same experimental conditions. (C) Bioenergetic profiling of SH-SY5Y cells (OCR versus ECAR) revealed increased metabolic activity after treatment with neurosteroids. Values represent the mean of each group (mean of the ECAR in abscissa/mean of the OCR in ordinate) normalized to the untreated control group (=100%). (A-C) Values represent the mean \pm SEM; n=12-18 replicates of three independent experiments. One-way ANOVA and post hoc Dunnetts' multiple comparison test versus control (untreated), *P<0.05; **P<0.01; ***P<0.001; P; progesterone, E2; estradiol, E1; estrone, T; testosterone, 3 α -A; 3 α -androstenediol, D; dihydroepiandrostanedione (DHEA), AP; allopregnanolone.

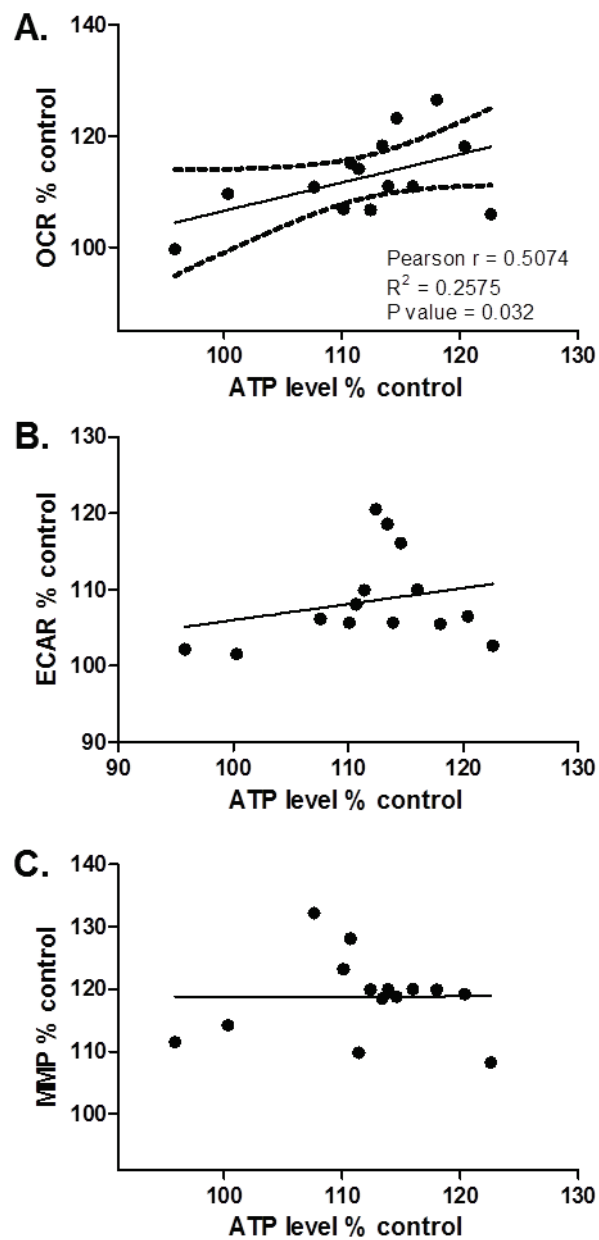


Fig. 4. ATP levels did correlate with basal mitochondrial respiration. Graph representing ATP levels in abscissa versus (A) OCR or (B) ECAR or (C) MMP in ordinate. Values represent the mean of each treatment group normalized to the control group (=100%). Pearson correlation $r=0.5074$, $R^2=0.2575$, $P=0.0032$. OCR; oxygen consumption rate, ECAR; extracellular acidification rate; MMP; mitochondrial membrane potential.

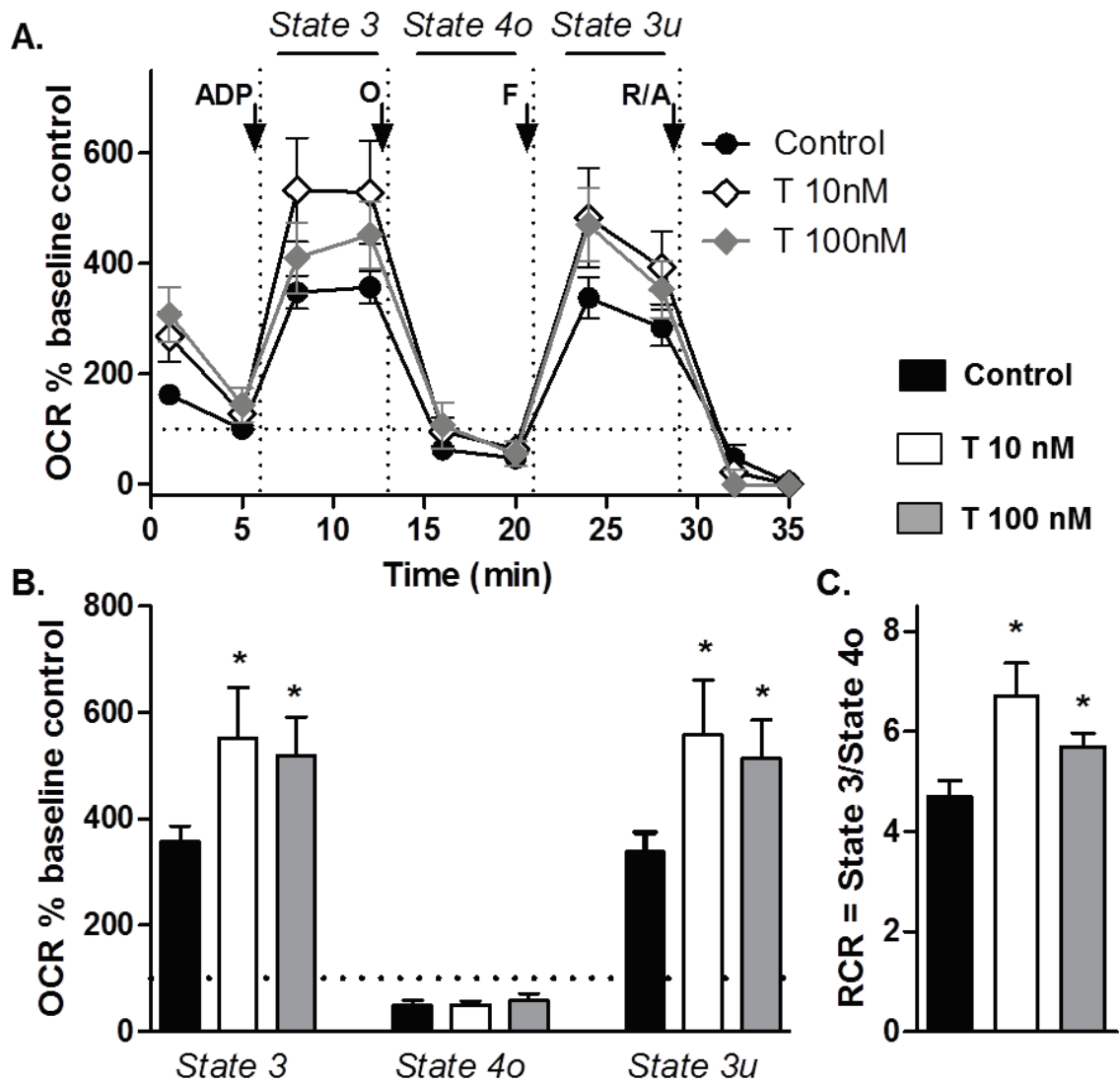


Fig. 5. Testosterone increased mitochondrial respiratory capacity. (A) Oxygen consumption rate (OCR), was measured on permeabilized SH-SY5Y cells after treatment with testosterone for 24 h, using a XF24 Analyser (Seahorse Bioscience). The sequential injection of mitochondrial inhibitors is indicated by arrows (see details in the Materials and Methods section). (B) Values corresponding to the different respiratory states are represented as mean \pm SEM (n= 15-18 replicate of three independent experiments/group) and were normalized to the basal respiration of the control group (=100%). (C) The respiratory control ratio (RCR= State 3/State 4o), which reflects the mitochondrial respiratory capacity, was increased by testosterone. Student unpaired t-test, *P<0.05. T 10 nM; testosterone at a concentration of 10 nM, T 100 nM; testosterone at a concentration of 100 nM, O; oligomycin, F; FCCP, R/A; rotenone/antimycin A.

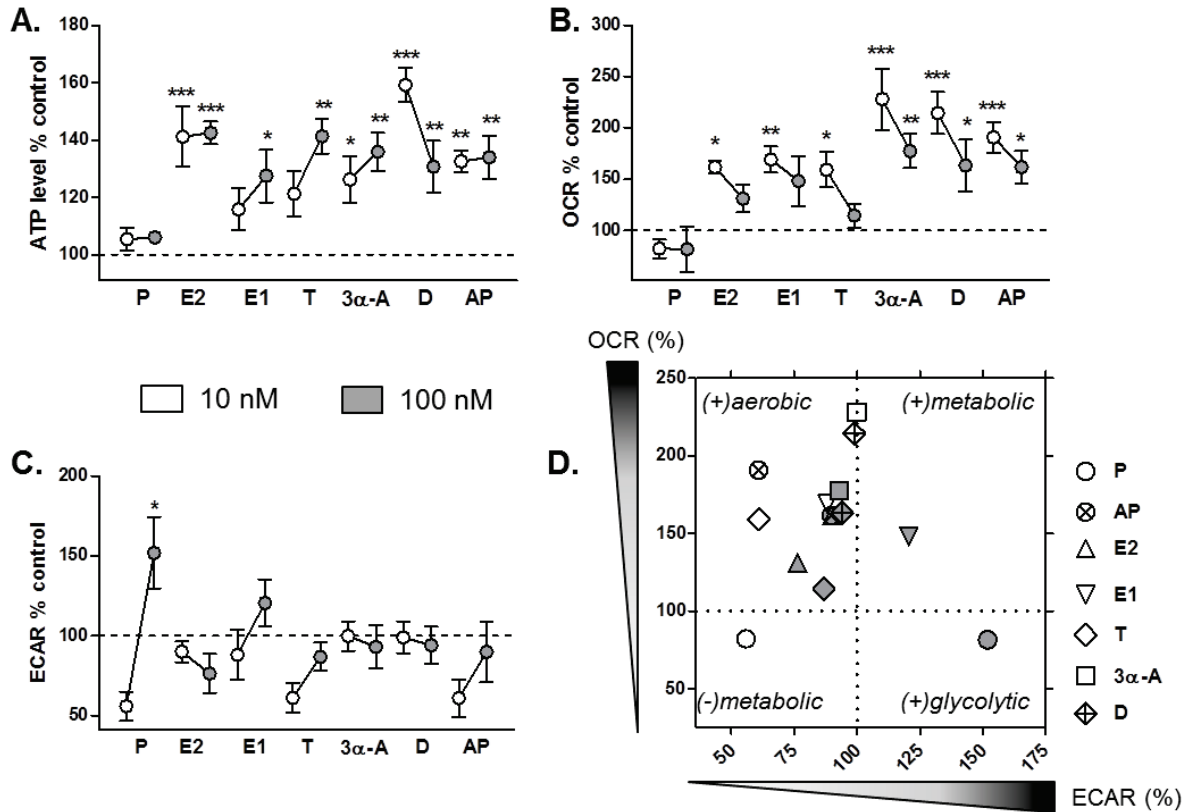


Fig. 6. Neurosteroids up-regulated the bioenergetic activity in primary cortical cells. (A) ATP level was significantly increased after neurosteroid treatment (24 h) at a concentration of 10nM (white boxes) and 100nM (gray boxes). (B) Oxygen consumption rate (OCR) and (C) extracellular acidification rate (ECAR) were measured simultaneously using a Seahorse Biosciences XF24 Analyser under the same experimental conditions. (D) Bioenergetic profile of primary cortical cells (OCR versus ECAR) revealed an increased aerobic activity (O₂ consumption) after treatment with neurosteroids. Values represent the mean of each group (mean of the ECAR in abscissa / mean of the OCR in ordinate) and were normalized to the control group (100%). (A-C) Values represent the mean ± SEM, n=4-6 replicates of three independent experiments / group, and were normalized to the control group (=100%). One-way ANOVA and post hoc Dunnetts' multiple comparison test versus control (untreated), *P<0.05; **P<0.01; ***P<0.001; P; progesterone, E2; estradiol, E1; estrone, T; testosterone, 3α-A; 3α-androstanediol, D; dihydroepiandrostanedione (DHEA), AP; allopregnanolone.

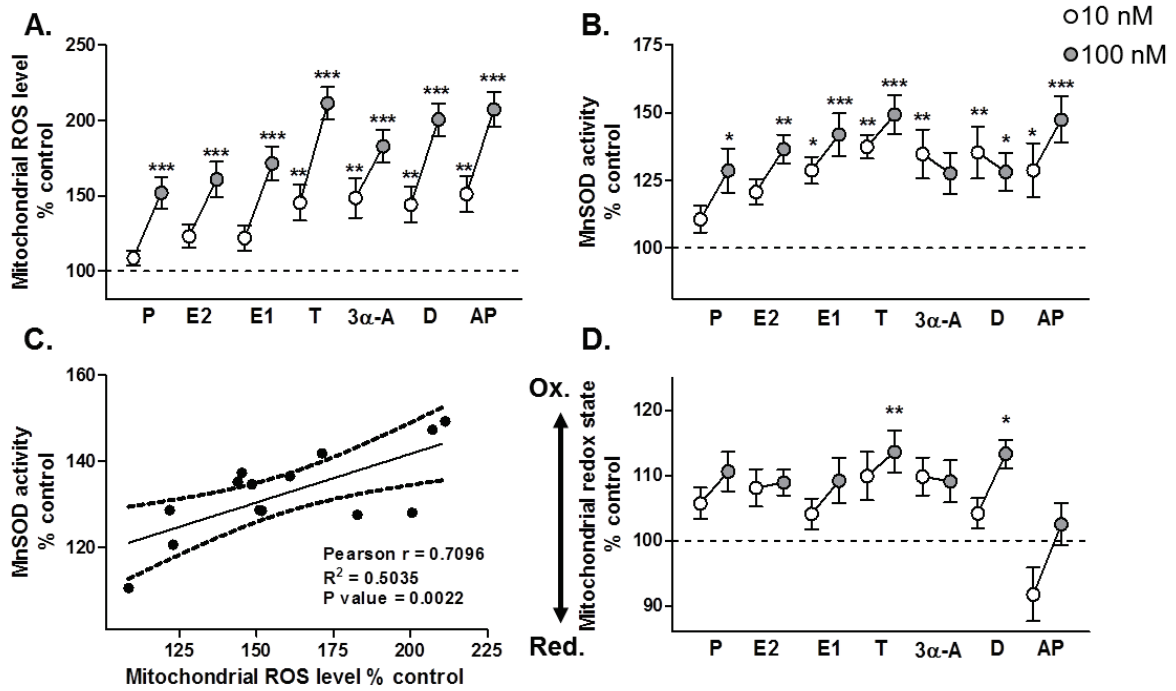


Fig. 7. Neurosteroids modulate the mitochondrial redox environment in SH-SY5Y neuroblastoma cells. (A) Mitochondrial reactive oxygen species (mtROS) levels were significantly increased after neurosteroid treatment (24 h) at a concentration of 10 nM (white boxes) and 100 nM (gray boxes). (B) This increase was accompanied by an up-regulation of manganese superoxide dismutase activity (MnSOD). (C) A positive correlation was observed between ROS levels and MnSOD activity. (D) Using a reporter gene coding for a redox sensitive green fluorescent protein (AR305 roGFP) located within mitochondria, the mitochondrial redox state underwent a switch to a more oxidized state after neurosteroid treatment compared to the untreated control. (A, B) Values represent the mean \pm SEM and were normalized to the corresponding untreated control group (=100%). (C) Values represent the mean of each group (mean of the mitochondrial ROS level in abscissa / mean of the MnSOD activity in ordinate) normalized to the untreated control group (=100%). Pearson correlation $r=0.7096$, $R^2=0.5035$, $P=0.0022$. (D) Values represent the mean \pm SEM of the ratio “oxidized state/reduced state”, $n=8-15$ replicates of three independent experiments/group. Values were normalized to the control group (=100%). One-way ANOVA and post hoc Dunnett’s multiple comparison test versus control (untreated), * $P<0.05$; ** $P<0.01$; *** $P<0.001$; P; progesterone, E2; estradiol, E1; estrone, T; testosterone, 3 α -A; 3 α -androstane diol, D; dihydroepiandrostanedione (DHEA), AP; allopregnanolone, Ox.; oxidized environment, Red.; reduced environment.

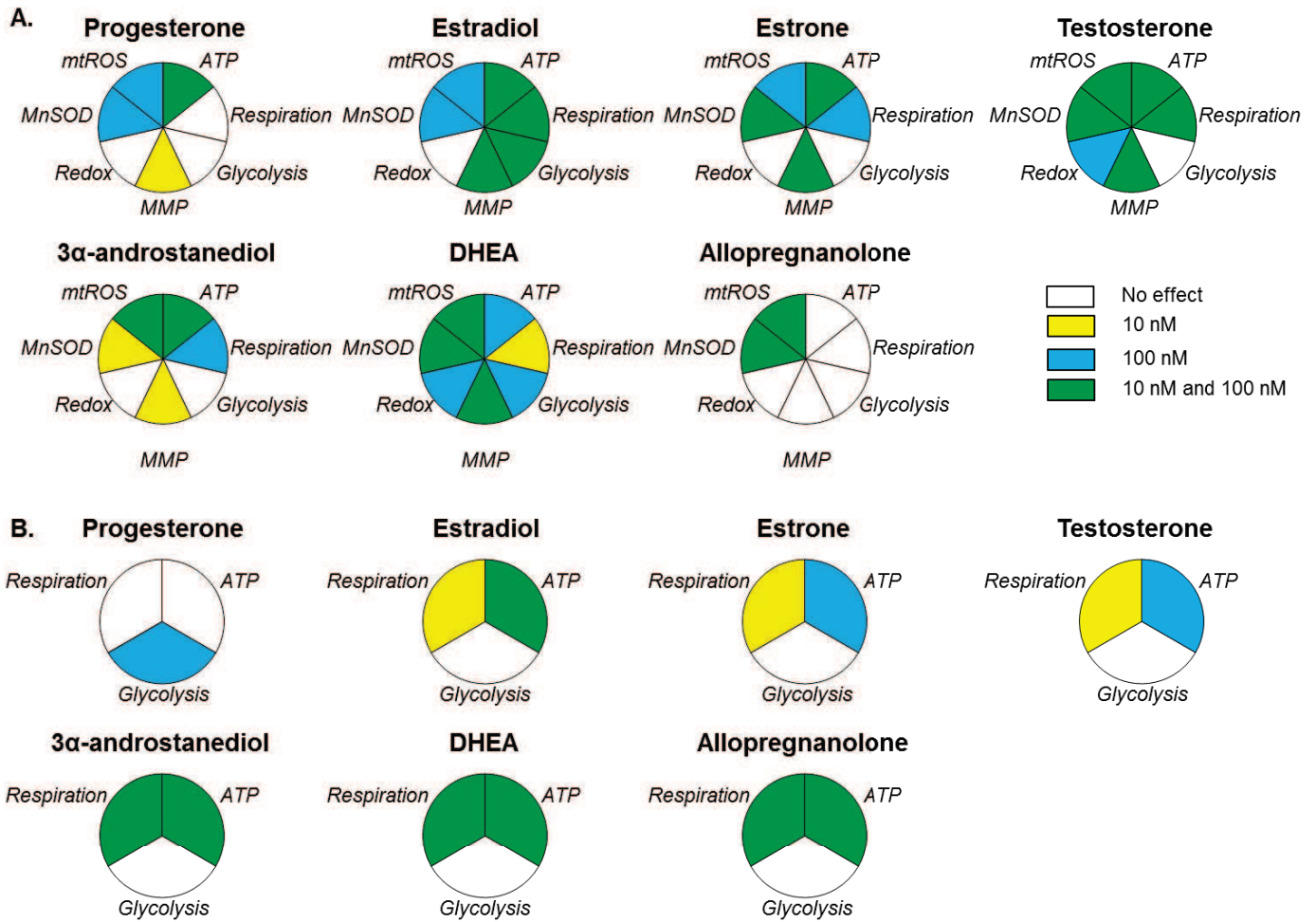


Fig. 8. Different action profile of neurosteroids on cellular bioenergetics. Representative diagrams of the effects of neurosteroids on the bioenergetic activity (ATP level, basal respiration, glycolysis, MMP) and the modulation of mitochondrial redox environment (mtROS levels, MnSOD activity, redox state) in SH-SH5Y neuroblastoma cells (**A**), and the bioenergetic activity in primary cortical cells (**B**). No effect is represented in white color. A significant increase of the respective parameter is marked either in yellow (significant only at 10 nM), blue (significant only at 100 nM), or green (significant at both concentrations). mtROS; mitochondrial reactive oxygen species, MMP; mitochondrial membrane potential, MnSOD; manganese superoxide dismutase activity.

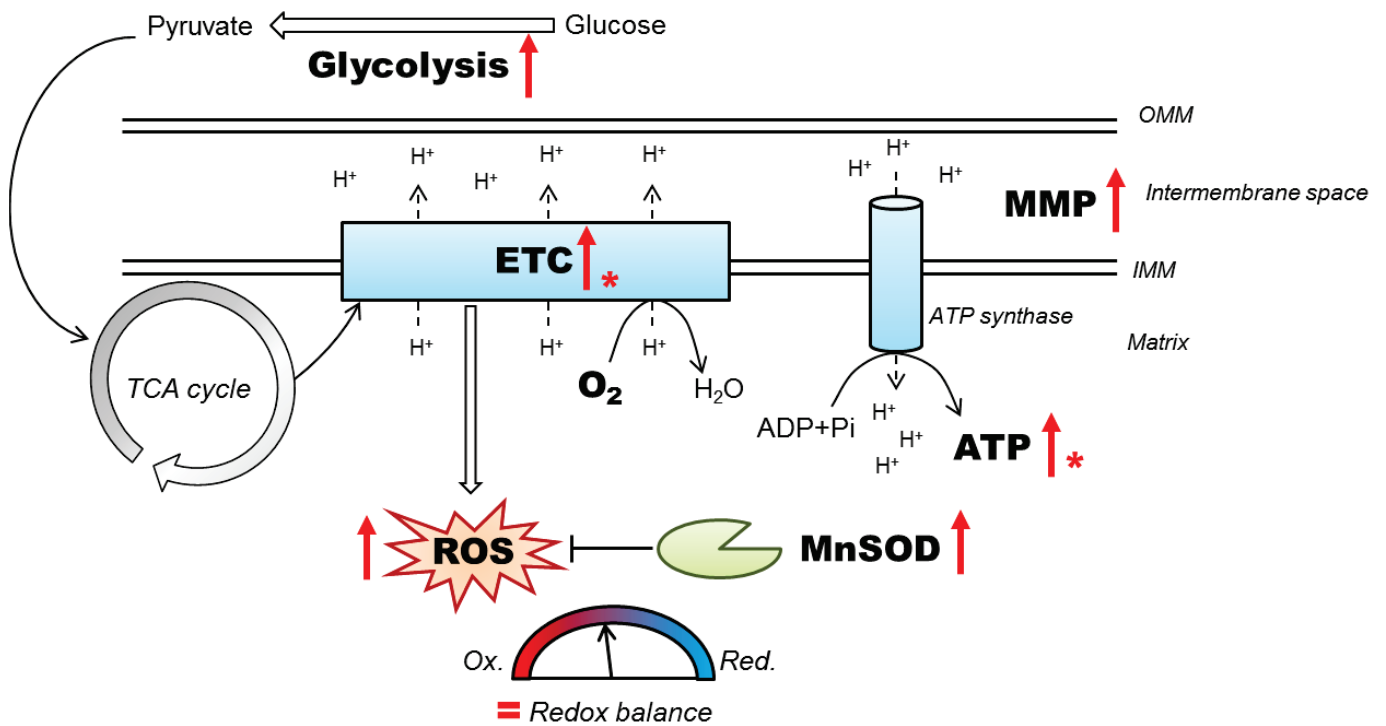
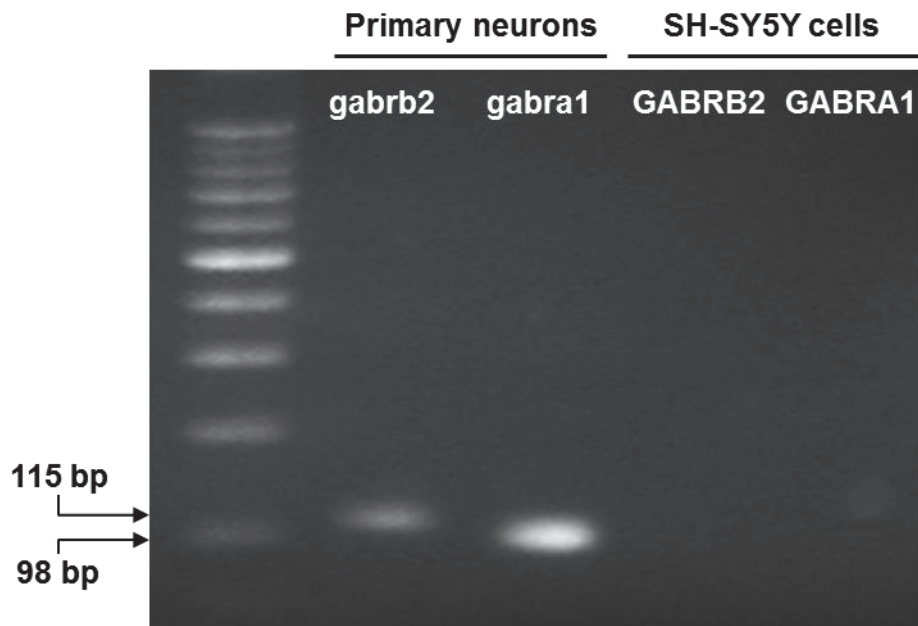


Fig. 9. Schematic representation of the effects of neurosteroids on mitochondrial bioenergetics and redox environment in SH-SH5Y neuroblastoma cells. * indicates that the effect was similar to that observed in primary cortical cells. ETC; electron transport chain, TCA; tricyclic acid, MnSOD; manganese superoxide dismutase, ROS; reactive oxygen species, MMP; mitochondrial membrane potential.



Suppl. Fig. 1. PCR analysis of GABAA receptor in SH-SY5Y human neuroblastoma cells and mouse primary cortical cells. Total RNA obtained from both cell types was amplified with the corresponding primers for human and mouse GABAA receptor subunits α 1 and β 2. GABRA1; human subunit α 1 (82 bp), GABRB2; human subunit β 2 (143 bp), gabra1; mouse subunit α 1 (98 bp), mouse; gabrb2; mouse subunit β 2 (115 bp).

Contributions

AG and KS performed experiments. UEL, AGMN and AE conceived the project, coordinated and supervised research. AG, AGMN and AE wrote the manuscript.

Acknowledgments

This study was co-supervised by AE and AGMN in the frame of a joint-PhD thesis (AG) between the University of Basel (Switzerland) and the University of Strasbourg (France). This work was supported by grants from Synapsis Foundation, Novartis Foundation for Biomedical Research Basel and the Swiss National Science Foundation (#31003A_149728) to AE.

References

- (1) Shulman R.G., Rothman D.L., Behar K.L. et al. (2004) Energetic basis of brain activity: implications for neuroimaging. *Trends in neurosciences* 27:489-495
- (2) Yin F., Boveris A., Cadenas E. (2014) Mitochondrial energy metabolism and redox signaling in brain aging and neurodegeneration. *Antioxid Redox Signal* 20:353-371
- (3) Mattson M.P., Gleichmann M., Cheng A. (2008) Mitochondria in neuroplasticity and neurological disorders. *Neuron* 60:748-766
- (4) Scheffler I.E. (2001) A century of mitochondrial research: achievements and perspectives. *Mitochondrion* 1:3-31
- (5) Knott A.B., Perkins G., Schwarzenbacher R. et al. (2008) Mitochondrial fragmentation in neurodegeneration. *Nat Rev Neurosci* 9:505-518
- (6) Leuner K., Muller W.E., Reichert A.S. (2012) From mitochondrial dysfunction to amyloid beta formation: novel insights into the pathogenesis of Alzheimer's disease. *Mol Neurobiol* 46:186-193
- (7) Muller W.E., Eckert A., Kurz C. et al. (2010) Mitochondrial dysfunction: common final pathway in brain aging and Alzheimer's disease--therapeutic aspects. *Mol Neurobiol* 41:159-171
- (8) Reddy P.H., Tripathi R., Troung Q. et al. (2012) Abnormal mitochondrial dynamics and synaptic degeneration as early events in Alzheimer's disease: implications to mitochondria-targeted antioxidant therapeutics. *Biochim Biophys Acta* 1822:639-649
- (9) Rhein V., Song X., Wiesner A. et al. (2009) Amyloid-beta and tau synergistically impair the oxidative phosphorylation system in triple transgenic Alzheimer's disease mice. *Proc Natl Acad Sci U S A* 106:20057-20062
- (10) Schmitt K., Grimm A., Kazmierczak A. et al. (2012) Insights into mitochondrial dysfunction: aging, amyloid-beta, and tau-A deleterious trio. *Antioxid Redox Signal* 16:1456-1466
- (11) Corpechot C., Robel P., Axelson M. et al. (1981) Characterization and measurement of dehydroepiandrosterone sulfate in rat brain. *Proc Natl Acad Sci U S A* 78:4704-4707
- (12) Mensah-Nyagan A.G., Do-Rego J.L., Beaujean D. et al. (1999) Neurosteroids: expression of steroidogenic enzymes and regulation of steroid biosynthesis in the central nervous system. *Pharmacological reviews* 51:63-81
- (13) Patte-Mensah C., Kibaly C., Boudard D. et al. (2006) Neurogenic pain and steroid synthesis in the spinal cord. *Journal of Molecular Neuroscience* 28:17-31
- (14) Brown R.C., Han Z., Cascio C. et al. (2003) Oxidative stress-mediated DHEA formation in Alzheimer's disease pathology. *Neurobiol Aging* 24:57-65
- (15) Caruso D., Barron A.M., Brown M.A. et al. (2013) Age-related changes in neuroactive steroid levels in 3xTg-AD mice. *Neurobiol Aging* 34:1080-1089

- (16) Smith C.D., Wekstein D.R., Markesbery W.R. et al. (2006) 3alpha,5alpha-THP: a potential plasma neurosteroid biomarker in Alzheimer's disease and perhaps non-Alzheimer's dementia. *Psychopharmacology (Berl)* 186:481-485
- (17) Schumacher M., Weill-Engerer S., Liere P. et al. (2003) Steroid hormones and neurosteroids in normal and pathological aging of the nervous system. *Prog Neurobiol* 71:3-29
- (18) Schaeffer V., Meyer L., Patte-Mensah C. et al. (2008) Dose-dependent and sequence-sensitive effects of amyloid-beta peptide on neurosteroidogenesis in human neuroblastoma cells. *Neurochem Int* 52:948-955
- (19) Schaeffer V., Patte-Mensah C., Eckert A. et al. (2006) Modulation of neurosteroid production in human neuroblastoma cells by Alzheimer's disease key proteins. *Journal of neurobiology* 66:868-881
- (20) Lim Y.A., Grimm A., Giese M. et al. (2011) Inhibition of the Mitochondrial Enzyme ABAD Restores the Amyloid-beta-Mediated Deregulation of Estradiol. *PLoS One* 6:e28887
- (21) Grimm A., Lim Y.A., Mensah-Nyagan A.G. et al. (2012) Alzheimer's Disease, Oestrogen and Mitochondria: an Ambiguous Relationship. *Mol Neurobiol*
- (22) Garcia-Segura L.M., Azcoitia I., DonCarlos L.L. (2001) Neuroprotection by estradiol. *Prog Neurobiol* 63:29-60
- (23) Nilsen J., Irwin R.W., Gallaher T.K. et al. (2007) Estradiol in vivo regulation of brain mitochondrial proteome. *J Neurosci* 27:14069-14077
- (24) Yao J., Irwin R., Chen S. et al. (2012) Ovarian hormone loss induces bioenergetic deficits and mitochondrial beta-amyloid. *Neurobiol Aging* 33:1507-1521
- (25) Rosario E.R., Chang L., Head E.H. et al. (2011) Brain levels of sex steroid hormones in men and women during normal aging and in Alzheimer's disease. *Neurobiol Aging* 32:604-613
- (26) Klein C., Patte-Mensah C., Taleb O. et al. (2013) The neuroprotector kynurenic acid increases neuronal cell survival through neprilysin induction. *Neuropharmacology* 70:254-260
- (27) Rhein V., Baysang G., Rao S. et al. (2009) Amyloid-beta leads to impaired cellular respiration, energy production and mitochondrial electron chain complex activities in human neuroblastoma cells. *Cell Mol Neurobiol* 29:1063-1071
- (28) Hanson G.T., Aggeler R., Oglesbee D. et al. (2004) Investigating mitochondrial redox potential with redox-sensitive green fluorescent protein indicators. *J Biol Chem* 279:13044-13053
- (29) Grassi D., Bellini M.J., Acaz-Fonseca E. et al. (2013) Estradiol and testosterone regulate arginine-vasopressin expression in SH-SY5Y human female neuroblastoma cells through estrogen receptors-alpha and -beta. *Endocrinology* 154:2092-2100

- (30) Takahashi K., Piao S., Yamatani H. et al. (2011) Estrogen induces neurite outgrowth via Rho family GTPases in neuroblastoma cells. *Molecular and cellular neurosciences* 48:217-224
- (31) Camporez J.P., Akamine E.H., Davel A.P. et al. (2011) Dehydroepiandrosterone protects against oxidative stress-induced endothelial dysfunction in ovariectomized rats. *The Journal of physiology* 589:2585-2596
- (32) Irwin R.W., Yao J., Hamilton R.T. et al. (2008) Progesterone and estrogen regulate oxidative metabolism in brain mitochondria. *Endocrinology* 149:3167-3175
- (33) Irwin R.W., Yao J., To J. et al. (2012) Selective oestrogen receptor modulators differentially potentiate brain mitochondrial function. *Journal of neuroendocrinology* 24:236-248
- (34) Meyer L., Patte-Mensah C., Taleb O. et al. (2013) Neurosteroid 3 α -androstenediol efficiently counteracts paclitaxel-induced peripheral neuropathy and painful symptoms. *PLoS One* 8:e80915
- (35) Singh C., Liu L., Wang J.M. et al. (2012) Allopregnanolone restores hippocampal-dependent learning and memory and neural progenitor survival in aging 3xTgAD and nonTg mice. *Neurobiol Aging* 33:1493-1506
- (36) Dimroth P., Kaim G., Matthey U. (2000) Crucial role of the membrane potential for ATP synthesis by F(1)F(o) ATP synthases. *The Journal of experimental biology* 203:51-59
- (37) Vander Heiden M.G., Cantley L.C., Thompson C.B. (2009) Understanding the Warburg effect: the metabolic requirements of cell proliferation. *Science* 324:1029-1033
- (38) Hosie A.M., Wilkins M.E., Smart T.G. (2007) Neurosteroid binding sites on GABA(A) receptors. *Pharmacology & therapeutics* 116:7-19
- (39) Korshunov S.S., Skulachev V.P., Starkov A.A. (1997) High protonic potential actuates a mechanism of production of reactive oxygen species in mitochondria. *FEBS Lett* 416:15-18
- (40) Turrens J.F. (2003) Mitochondrial formation of reactive oxygen species. *The Journal of physiology* 552:335-344
- (41) Lu S.F., McKenna S.E., Cologer-Clifford A. et al. (1998) Androgen receptor in mouse brain: sex differences and similarities in autoregulation. *Endocrinology* 139:1594-1601
- (42) Morissette M., Le Saux M., D'Astous M. et al. (2008) Contribution of estrogen receptors alpha and beta to the effects of estradiol in the brain. *J Steroid Biochem Mol Biol* 108:327-338
- (43) Wagner C.K., Pfau J.L., De Vries G.J. et al. (2001) Sex differences in progesterone receptor immunoreactivity in neonatal mouse brain depend on estrogen receptor alpha expression. *Journal of neurobiology* 47:176-182

- (44) Frye C.A., Koonce C.J., Walf A.A. (2014) Novel receptor targets for production and action of allopregnanolone in the central nervous system: a focus on pregnane xenobiotic receptor. *Frontiers in cellular neuroscience* 8:106
- (45) Panzica G.C., Balthazart J., Frye C.A. et al. (2012) Milestones on Steroids and the Nervous System: 10 years of basic and translational research. *Journal of neuroendocrinology* 24:1-15
- (46) Pike C.J., Carroll J.C., Rosario E.R. et al. (2009) Protective actions of sex steroid hormones in Alzheimer's disease. *Front Neuroendocrinol* 30:239-258
- (47) Brookmeyer R., Johnson E., Ziegler-Graham K. et al. (2007) Forecasting the global burden of Alzheimer's disease. *Alzheimer's & dementia : the journal of the Alzheimer's Association* 3:186-191
- (48) Borrás C., Gambini J., Lopez-Grueso R. et al. (2010) Direct antioxidant and protective effect of estradiol on isolated mitochondria. *Biochimica et Biophysica Acta* 1802:205-211
- (49) Psarra A.M., Solakidi S., Sekeris C.E. (2006) The mitochondrion as a primary site of action of steroid and thyroid hormones: presence and action of steroid and thyroid hormone receptors in mitochondria of animal cells. *Molecular and cellular endocrinology* 246:21-33
- (50) Rettberg J.R., Yao J., Brinton R.D. (2014) Estrogen: a master regulator of bioenergetic systems in the brain and body. *Front Neuroendocrinol* 35:8-30
- (51) Holmes S., Abbassi B., Su C. et al. (2013) Oxidative stress defines the neuroprotective or neurotoxic properties of androgens in immortalized female rat dopaminergic neuronal cells. *Endocrinology* 154:4281-4292
- (52) Vasconsuelo A., Milanesi L., Boland R. (2013) Actions of 17beta-estradiol and testosterone in the mitochondria and their implications in aging. *Ageing research reviews* 12:907-917
- (53) Frye C.A., Edinger K.L., Lephart E.D. et al. (2010) 3alpha-androstanediol, but not testosterone, attenuates age-related decrements in cognitive, anxiety, and depressive behavior of male rats. *Frontiers in aging neuroscience* 2:15
- (54) Frye C.A., Walf A.A. (2009) Progesterone reduces depression-like behavior in a murine model of Alzheimer's Disease. *Age* 31:143-153
- (55) Schule C., Nothdurfter C., Rupprecht R. (2014) The role of allopregnanolone in depression and anxiety. *Prog Neurobiol* 113:79-87
- (56) Deniselle M.C., Carreras M.C., Garay L. et al. (2012) Progesterone prevents mitochondrial dysfunction in the spinal cord of wobbler mice. *J Neurochem* 122:185-195
- (57) Carver C.M., Reddy D.S. (2013) Neurosteroid interactions with synaptic and extrasynaptic GABA(A) receptors: regulation of subunit plasticity, phasic and tonic inhibition, and neuronal network excitability. *Psychopharmacology (Berl)* 230:151-188

- (58) Webb S.J., Geoghegan T.E., Prough R.A. et al. (2006) The biological actions of dehydroepiandrosterone involves multiple receptors. *Drug metabolism reviews* 38:89-116
- (59) Chua C.K., Henderson V.W., Dennerstein L. et al. (2014) Dehydroepiandrosterone sulfate and cognition in midlife, post-menopausal women. *Neurobiol Aging* 35:1654-1655
- (60) Patel M.A., Katyare S.S. (2006) Treatment with dehydroepiandrosterone (DHEA) stimulates oxidative energy metabolism in the cerebral mitochondria. A comparative study of effects in old and young adult rats. *Neurosci Lett* 402:131-136
- (61) Wispe J.R., Clark J.C., Burhans M.S. et al. (1989) Synthesis and processing of the precursor for human mangano-superoxide dismutase. *Biochim Biophys Acta* 994:30-36
- (62) Razmara A., Duckles S.P., Krause D.N. et al. (2007) Estrogen suppresses brain mitochondrial oxidative stress in female and male rats. *Brain Res* 1176:71-81
- (63) Henderson V.W., Brinton R.D. (2010) Menopause and mitochondria: windows into estrogen effects on Alzheimer's disease risk and therapy. *Progress in brain research* 182:77-96
- (64) Reddy P.H. (2007) Mitochondrial dysfunction in aging and Alzheimer's disease: strategies to protect neurons. *Antioxid Redox Signal* 9:1647-1658

C. Amyloid- β -induced imbalance between mitochondrial network and bioenergetics

Authors: Karen Schmitt^{a,b}, Undine E. Lang^b, Jürgen Götz^c, Anne Eckert^{a,b,d*}

Affiliations:

^aNeurobiology Lab for Brain Aging and Mental Health, Transfaculty Research Platform, Molecular & Cognitive Neuroscience, University of Basel, Switzerland.

^bPsychiatric University Clinics, University of Basel, Wilhelm Klein-Str. 27 CH-4012 Basel, Switzerland.

^cClem Jones Centre for Ageing Dementia Research (CJCADR), Queensland Brain Institute (QBI), The University of Queensland, Brisbane, QLD 4072, Australia.

^dAssociated Research Group, Department Biomedicine, University of Basel, Switzerland.

***Corresponding author at:** Psychiatric University Clinics, University of Basel, Wilhelm Klein-Str. 27, CH-4012 Basel, Switzerland.

Tel.: +41 613255487; Fax: +41 613255577,

E-mail: anne.eckert@upkbs.ch (A. Eckert).

Abstract:

Mitochondria are the major bioenergetic provider of eukaryotic cells. They form a highly dynamic network that in response to metabolic, cellular and environmental changes adapts its architecture by fission and fusion processes to maintain the cellular bioenergetic homeostasis. Mitochondrial functions are impaired in aging and neurodegenerative diseases including Alzheimer's disease (AD) for which age is the highest risk factor. Deposition of amyloid- β ($A\beta$) represents one of the histopathological hallmarks of AD, and while $A\beta$ impairs mitochondrial function, it is not clearly understood how dysfunctions in mitochondrial dynamics and bioenergetics are coupled and contribute to the AD pathogenesis. Here we report that, under normal physiological conditions, the morphology of the mitochondrial network oscillates between three distinct states: tubular, intermediate and fragmented. Interestingly, during the transition from a tubular via an intermediate to a fragmented mitochondrial network, the ATP level displayed an inverted "U"-shape along with a higher oxygen consumption rate (OCR) in the basal respiration and maximal respiration at its peak. $A\beta$ abolished the oscillations in the mitochondrial network organization which were associated with a decline in mitochondrial metabolism including reduced ATP level and OCR. Our results indicate firstly that mitochondrial function is tightly coupled to mitochondrial morphology, and secondly that $A\beta$ -induced abnormal mitochondrial dynamics is likely to contribute to the decay of mitochondrial energy metabolism. Thus, an imbalance in the mitochondrial structure-function relationship may play a crucial role in the deleterious mitochondrial cascade of AD.

Keywords:

Alzheimer's disease, amyloid- β , bioenergetic balance, energetic state, mitochondria, mitochondrial dynamics.

Abbreviations: $A\beta$, amyloid- β ; AD, Alzheimer's disease; ATP, adenosine tri-phosphate; DRP1, dynamin-related protein 1; ECAR, extracellular acidification rate; hFIS1, human fission protein 1; MFN1/2, mitofusin 1/2; NAD^+ , nicotinamide adenine dinucleotide, oxidized form; NADH, nicotinamide adenine dinucleotide, reduced form; OCR, oxygen consumption rate; OxPhos, oxidative phosphorylation; OPA1, optic atrophy 1.

1. Introduction

Once thought to be solitary and rigidly structured, mitochondria are now recognized to constitute a population of highly dynamic organelles that participate in energy conversion, metabolism, intracellular signalling, cell migration and synaptic plasticity [1]. To achieve the integrity of a healthy mitochondrial population within cells but also the integrity of the cell itself, the mitochondrial network comes in varied morphologies and ultrastructures, ranged from fragmented to forming a tubular network, such as to meet the ever-changing requirements for energy production and additional mitochondrial functions [2]. This requires a tightly regulated equilibrium between opposing mitochondrial fusion and fission activities, with these activities collectively termed 'mitochondrial dynamics' [3, 4]. Since mitochondrial function relies heavily on the morphology and distribution of this organelle, alterations to the mitochondrial architecture will have severe consequences on neuronal activity and survival, which can, at least in part, contribute to the development of neurodegenerative disorders including Alzheimer's disease (AD).

AD is an age-related progressive neurodegenerative disorder. Over the last decade, extensive evidence from both cellular and animal models has led to the view that alterations in mitochondrial bioenergetics, including a reduced mitochondrial membrane potential, decreased complex activities, depletion of ATP content and antioxidant defence mechanisms as well as an escalation of oxidative stress, are associated with the pathogenesis of AD [5, 6]. Additionally, abnormal mitochondrial dynamics has been identified in sporadic and familial AD cases [7, 8] as well as in AD mouse models [9-12]. By assessing both protein and transcript levels, in general, levels of fission transcripts/proteins were found to be increased, and those of fusion transcripts/proteins decreased [7]. In one study, reduced levels of DRP1 and an increased mitochondrial length were found in AD fibroblasts [8]. Taken together, these findings indicate that a decline in both mitochondrial bioenergetics and dynamics is prominent and represents an early hallmark of Amyloid- β ($A\beta$)-induced neuronal degeneration in AD. Nevertheless, the underlying mechanism in how mitochondrial dynamics and bioenergetics are coupled in AD is not understood. Thus, we addressed the question of whether mitochondrial metabolism is directly connected to mitochondrial shape transitions in a physiological context and whether $A\beta$ -related alterations of mitochondrial dynamics are a direct cause of the bioenergetic decline observed in AD by impairing the integrity of the mitochondrial structure–function relationship. For this purpose, we investigated mitochondrial dynamics in parallel with the oxidative metabolism in cell cycle-synchronized human primary skin fibroblast, an already established model for studies of mitochondrial dynamics in AD [8], under both physiological and pathological conditions. Our findings are consistent with the concept that mitochondrial bioenergetics is coordinated by transitions in the mitochondrial

architecture and that $A\beta$ impairs this functional balance. This disruption of the synchronized transition of the mitochondrial architecture may have an important role in AD pathogenesis.

2. Materials and Methods

2.1. Chemicals and reagents

Dulbecco's-modified Eagle medium (DMEM), RPMI-1640 medium, foetal calf serum (FCS), penicillin/streptomycin, NAD^+ , NADH, MTT (3-(4,5-Dimethylthiazol-2-yl)-2,5-diphenyltetrazolium bromide) and PES (phenazine ethosulfate) were from Sigma-Aldrich (St. Louis, MO, USA). Glutamax and DPBS were from Life Technologies (Waltham, MA, USA). XF Cell Mitostress kit was from Seahorse Bioscience (North Billerica, MA, USA). Horse serum (HS) was from Amimed, Bioconcept (Allschwil, Switzerland).

2.2. Cell culture

Human fibroblasts were isolated from biopsies cultured in DMEM/1% penicillin-streptomycin (v/v)/1% Glutamax (v/v) (DMEM complete (DMEMc))/20% heat-inactivated FBS (v/v) as described previously [13]. Prior to the assessment of nucleotide levels, oxygen consumption rate (OCR) and mitochondrial morphology in human primary fibroblast culture, serum shock treatment (DMEMc supplemented with 50% heat-inactivated horse serum (v/v)) was performed for 2 hours at 37 °C to synchronize the cells [14, 15]. After serum shock treatment, the medium was exchanged to DMEM without phenol red/ 1% penicillin-streptomycin (v/v)/1% Glutamax (v/v)/2% FBS (v/v) for reduce cell growth.

2.3. Amyloid-beta peptide preparation and treatment

The amyloid- β ($\text{A}\beta$) peptide $\text{A}\beta_{1-42}$ (Bachem, Bubendorf, Switzerland) was rapidly dissolved in sterile PBS 1x, pH~7.4 (stock concentration 500 μM) and stored as aliquots at -80 °C until needed. One day before treatment with $\text{A}\beta$ peptide was initiated, a 50 μM working solution was prepared in PBS 1x, pH~7.4. After securing the cap with parafilm, the tube was incubated on a table-top thermomixer (Eppendorf, Hamburg, Germany) at 1000 rpm (~250 x g) at 37°C for 24 hours in order to induce aggregation of the $\text{A}\beta$ peptide into fibrils. Fibroblasts were then treated with 500 nM $\text{A}\beta$ in DMEM/1% penicillin-streptomycin (v/v)/1% Glutamax (v/v) (DMEMc)/20% FBS (v/v) for five days until analyzed.

2.4. Mitochondrial Morphology

To determine mitochondrial dynamics in synchronized fibroblasts, cells were seeded on collagen - coated coverslip (0.05 mg/ml, Corning, NY, USA) at a cell density sufficient to reach 50% confluency on the following day. After the serum shock treatment, the medium was exchanged to DMEMc without phenol red + 2% FBS (v/v) containing 75 nM Mitotracker® Red CMX ROS (579/599, Life Technologies, Waltham, MA, USA), a red-fluorescent dye that stains mitochondria in live cells and whose accumulation requires an intact membrane potential. From 8 hours post-synchronization and at 8 hour-intervals over the course of 24 hours, cells were fixed with 4% paraformaldehyde/PBS for 30 minutes at room temperature.

After extensive washes, the fixed cells were permeabilized with 0.15% Triton X-100 prior to staining the nuclei with Sytox Green (504/523, Life Technologies, Waltham, MA, USA) according to the manufacturer's recommendations. After mounting the coverslips, images were processed using a confocal microscope (60x oil objective, Leica).

2.5. Nucleotides Measurements

The total ATP content from synchronized human skin fibroblasts was determined using a bioluminescence assay (ViaLighTM HT; Cambrex Bio Science, Walkersville, MD USA) according to the instruction of the manufacturer. Cells were plated in 8 replicates into a 96-wells cell culture plate at a cell density sufficient to reach 40-50% of confluency on the following day. The enzyme luciferase, which catalyzes the formation of light from ATP and luciferin was used. The emitted light is linearly related to the ATP concentration and is measured using a multilabel plate reader VictorX5 (Perkin Elmer). The data were obtained at 8, 16 and 24 hours after cell synchronization.

To measure NAD⁺ and NADH, the two molecules were separately extracted using an acid-base extraction method (HCL 0.1 mol/l – NAOH 0.1 mol/l). To determinate both NAD⁺ and NADH, an enzyme cycling assay was used that is based on passing the electron from ethanol through reduced pyridine nucleotides to MTT (3-(4,5-Dimethylthiazol-2-yl)-2,5-diphenyltetrazolium bromide) in a PES (phenazine ethosulfate)-coupled reaction resulting in the formation of a purple precipitate (formazan) that, once dissolved, can be quantified at 595 nm (VictorX5, Perkin Elmer). The data were obtained at 8, 16 and 24 hours after cell synchronization.

2.6. Oxygen consumption rate (OCR) and extracellular acidification rate (ECAR)

The OCR and ECAR were evaluated in synchronized fibroblasts as previously described [16]. Briefly, human skin fibroblasts were seeded at the density of 3×10^4 cells/100 μ l per well on Seahorse Biosciences 24-well culture plates one day prior to the beginning of the assay. After serum shock synchronization, the medium was exchanged to 500 μ l of assay medium (glucose-free RPMI-1640 medium containing 2% FBS (v/v), 2 mM sodium pyruvate, pH~7.4). Prior to measurements, the microplates were equilibrated in a CO₂-free incubator at 37 °C for 60 minutes. The plate was placed in the Seahorse XF24 Analyzer and the OCR and ECAR were recorded in real-time over 75 min. The Mitostress Kit was used according to the instructions of the manufacturer to determine the OCR allocated to basal respiration, ATP turnover, proton leak, maximal respiration and non-mitochondrial respiration by sequential injection of oligomycin (1 μ M), FCCP [carbonyl cyanide p (trifluoromethoxy) phenylhydrazone] (0.7 μ M), a mix of antimycin A (4 μ M) and rotenone (2 μ M). Experiments were performed at 16 and 24 hours after synchronization.

2.7. Quantitative Real-Time PCR

Total RNA was extracted from lysates of synchronized fibroblasts using the RNeasy mini kit (Qiagen, Venlo, Netherlands). cDNA was generated using Ready-to-Go You-Prime First-Strand Beads (GE Healthcare, Little Chalfont, UK). For data analysis, human Cdk4 was used as an endogenous control. After reverse transcription, the cDNA was diluted 1:3 and amplified in the presence of the corresponding primers by real-time PCR using the DyNAmo Flash Probe qPCR kit (Thermo Scientific, Waltham, MA USA). Conventional Applied Biosystems cycling parameters (40 cycles of 95°C, 5 seconds, and 60°C, 30 seconds) were used. Data were expressed as relative expression for each individual gene normalized to their corresponding controls using the comparative CT method. The primers used were purchased from Applied Biosystems (Life Technologies, Waltham, MA, USA) (Probe ID: see Primer sequences section for details). Experiments were performed at 8, 16 and 24 hours after cell synchronization.

2.8. Primer sequences

	Primer	Probe ID (Applied Biosystems)
Fusion	<i>MFN1</i>	Hs00250475_m1
	<i>MFN2</i>	Hs00208382_m1
	<i>OPA1</i>	Hs00323399_m1
Fission	<i>DRP1</i>	Hs00247147_m1
	<i>FIS1</i>	Hs00211420_m1
OxPhos	<i>NDUFA2</i> (complex I)	Hs00159575_m1
	<i>NDUFB5</i> (complex I)	Hs00159582_m1
	<i>NDUFC1</i> (complex I)	Hs00159587_m1
	<i>NDUFV2</i> (complex I)	Hs00221478_m1
	<i>COX4I1</i> (complex IV)	Hs00971639_m1
	<i>COX6A1</i> (complex IV)	Hs01924685_g1
	<i>COX7A2</i> (complex IV)	Hs01652418_m1
	<i>COX7B</i> (complex IV)	Hs00371307_m1
	<i>ATP5G2</i> (ATP synthase)	Hs01096582_m1
	<i>ATP5C1</i> (ATP synthase)	Hs01101219_g1
<i>ATP5L</i> (ATP synthase)	Hs00758883_s1	

2.9. Statistical analysis

Data were presented as mean \pm S.E.M. Statistical analyses were performed using the Graph Pad Prism software. For statistical comparisons, unpaired Student's two-tailed *t*-test, One-way ANOVA followed by Tukey's multiple comparison test or Two-way ANOVA followed by Bonferroni's multiple comparison test was used respectively. P values less than 0.05 were considered statistically significant.

3. Results

3.1. $A\beta$ impairs the mitochondrial network organization

To analyze the impact of $A\beta$ on the mitochondrial network state, we first examined the mitochondrial morphology in $A\beta_{1-42}$ -treated human skin fibroblasts compared to untreated cells under cell division-synchronized conditions. Images were processed by confocal microscopy (**Fig. 1A**). We observed that under physiological conditions the mitochondrial network displayed three distinct states at the three time points chosen after cell synchronization (8, 16 and 24 hours) that were defined as tubular, intermediate and fragmented states, respectively. Of note, after 5 days of $A\beta_{1-42}$ -treatment, only the fragmented network was detected suggesting that $A\beta$ promotes mitochondrial fission events by interfering with the equilibrium of fusion and fission thereby affecting the network architecture of mitochondria.

As mitochondrial dynamics is tightly regulated, we next investigated whether $A\beta$ impacts the expression of the different fusion genes (mitofusins 1 and 2, MFN1 and 2; optic atrophy 1, OPA1) and fission genes (dynamamin-related protein1, DRP1; human fission protein 1, hFIS1) that are tightly regulated to maintain the integrity of the mitochondrial system (**Fig. 1B-F**). Relative quantification of mRNAs isolated from $A\beta_{1-42}$ -treated human skin fibroblasts showed that $A\beta$ -treatment significantly diminished the expression of the fusion gene OPA1 (*Two-way ANOVA, group effect: control versus $A\beta$, $P < 0.001$*) (**Fig. 1D**) and the fission gene DRP1 (*Two-way ANOVA, group effect: control versus $A\beta$, $P < 0.001$*) (**Fig. 1E**), while expression of the fission gene hFIS1 was significantly increased (*Two-way ANOVA, group effect: control versus $A\beta$, $P < 0.001$*) (**Fig. 1F**). No change was observed in the expression of the fusion genes MFN1 and 2 (**Fig. 1B, C**).

Consistent with previous observations in cultured neurons [17, 18], our findings indicate that $A\beta$ is capable of destabilizing the mitochondrial network by disturbing the equilibrium between fusion and fission, at least at the gene expression level, collectively promoting mitochondrial fragmentation.

3.2. $A\beta$ -related mitochondrial morphology alterations negatively impact mitochondrial homeostasis

As ATP is primarily generated via mitochondrial oxidative phosphorylation (OxPhos), we monitored whole cell ATP content as readout of OxPhos in $A\beta_{1-42}$ -treated compared with untreated human skin fibroblasts for the three time-points corresponding to tubular, intermediate and fragmented mitochondrial network states. Surprisingly, we found that total ATP levels displayed an inverted “U”-shape in control cells (*One-way ANOVA, variation of ATP level in control cells, $P < 0.0001$*) during the transition from a tubular via an intermediate

to a fragmented network (with the peak at 16 hours corresponding to the intermediate mitochondrial network), whereas ATP levels in the $A\beta$ -treated cells remained unaltered and were significantly reduced (*Two-way ANOVA, group effect: control versus $A\beta$, $P < 0.0001$*) (**Fig. 2A**). These findings suggest that large mitochondrial networks of fused mitochondria are a prerequisite for enabling a maximal energy supply for the cells, which is then transferred, with a short delay, from the mitochondrial pool of ATP to the cytosolic pool of ATP during the intermediate state [19].

To further investigate the $A\beta$ -induced imbalance in mitochondrial homeostasis, we next evaluated the $NAD^+/NADH$ ratio as an oxidative stress readout in $A\beta$ -treated human skin fibroblasts compared to untreated cells at the same three time-points (**Fig. 2B**). We observed that the $NAD^+/NADH$ ratio was significantly augmented by $A\beta_{1-42}$ treatment with the highest level at that time point (at 16 hours) (*One-way ANOVA, variation of $NAD^+/NADH$ ratio in $A\beta$ -treated cells, $P = 0.0136$*), when we had observed a maximum ATP peak but only in control cells. In contrast, the $NAD^+/NADH$ ratio was lower (*Two-way ANOVA, group effect: control versus $A\beta$, $P < 0.0001$*) and did not exhibit a variation pattern in control cells as detected for mitochondrial morphology and ATP. These findings indicate that, while the cellular defence systems are capable of perfectly stabilizing the oxidative stress generated by normally functioning mitochondria, $A\beta$ provokes a shift in the redox homeostasis toward a more oxidized state, with the peak at 16 hours. However, this increase in $NAD^+/NADH$ ratio does not seem to relate on the mitochondrial architecture oscillations, since they are abolished by $A\beta$, but may rather be dependent on the activation of cytosolic antioxidant defence enzymes.

Together, our findings suggest that $A\beta$ triggers a decline of mitochondrial bioenergetics including an abolishment of variations in ATP levels coupled to a shift in the redox homeostasis.

3.3. Alterations in $A\beta$ -related mitochondrial morphology lead to mitochondrial respiratory defects

Since mitochondria were found to be a target of $A\beta$ [20], leading to mitochondrial dysfunction including a decline in OxPhos, we further investigated the impact of $A\beta$ on mitochondrial oxidative metabolism and glycolysis. For this purpose, we monitored the real-time oxygen consumption rate (OCR), an indicator of mitochondrial respiration, and the extracellular acidification rate (ECAR), an indicator of the glycolytic state, in $A\beta$ -treated human skin fibroblasts compared to untreated cells at 16 hours corresponding to the ATP peak and at 24 hours related to the ATP trough using the Seahorse Bioscience XF24 Flux Analyzer (**Fig. 2A, 3**).

In untreated cells, the OCR was significantly decreased in general at the condition of an ATP trough and fragmented network (at 24 hours) compared to that of an ATP peak and intermediate network (at 16 hours) over the entire OCR measurement period (runtime 2 – 57 min; *Two-way ANOVA, group effect: 16 versus 24 hours, $P < 0.0001$*) (**Fig. 3A, left panel**). This is further indicated by a lower OCR for the basal respiration (~20%) as well as for ATP turnover (~25%) and maximal respiration (~15%) at 24 hours compared to the OCR measured at 16 hours after cell cycle synchronization (**Fig. 3B**). Moreover, the spare respiratory capacity was higher (~42%) at 24 hours compared to that at 16 hours suggesting that the mitochondrial network is metabolically more plastic to respond to an energy demand whilst in resting state (**Suppl. Fig. 1**). In contrast, $A\beta_{1-42}$ treatment completely abolished the OCR difference between ATP peak and trough conditions (**Fig. 3A right panel, 3B and Suppl. Fig. 1**). In addition, the bioenergetic readouts such as basal respiration, ATP turnover and maximal respiration were significantly reduced in $A\beta$ -treated compared to untreated cells at the two time points (*Two-way ANOVA, group effect: control versus $A\beta$, $P < 0.0001$*) (**Fig. 3B**) as well as the spare respiratory capacity at 24 hours after synchronization suggesting a mitochondrial inability to respond to an increasing metabolic demand in the presence of $A\beta$ (*Two-way ANOVA, group effect: control versus $A\beta$, $P = 0.0013$*) (**Suppl. Fig. 1**).

No variation pattern was observed in the OCR of control cells allocated to leakage of proton and to non-mitochondrial respiration confirming that the biphasic changes in ATP levels are primarily dependent on the activity of the electron transport chain and ATP synthase (complex V) (**Fig. 3B**), while a decreased proton leakage in the $A\beta$ -treated human skin fibroblasts at both time points (**Fig. 3B**) might indicate a damage in the coupling efficiency of mitochondria that has been associated with aging and age-related diseases as AD [21]. Moreover, OCR coupled to non-mitochondrial respiration was also significantly decreased in $A\beta$ -treated human skin fibroblasts (**Fig. 3B**) suggesting that $A\beta$, besides its effects on mitochondria, might also negatively impact on a subset of cellular enzymes that continue to consume oxygen after rotenone/ antimycin A addition.

In parallel to determining the OCR, ECAR as an indicator of the glycolytic state, was assessed. The glycolytic rate remained unchanged in untreated control cells between both time points (16 and 24 hours) and seems therefore to be independent of a change in the mitochondrial network (**Fig. 3C**). Moreover, treatment of human primary fibroblast cultures with $A\beta_{1-42}$ resulted in a higher ECAR than for untreated cells, suggesting an $A\beta$ -induced metabolic switch favoring glycolysis which can be interpreted as a cellular mechanism to compensate for the mitochondrial respiration decay and depletion in ATP production (**Fig. 3C**).

To compare the effects of $A\beta$ on glycolysis and mitochondrial respiration, we characterized the cellular bioenergetic profile of $A\beta$ -treated human skin fibroblasts compared to untreated cells, mapping OCR (basal respiration) versus ECAR (glycolysis) for the indicated time points (**Fig. 4A**). Remarkably, $A\beta$ -treated cells exhibited higher glycolytic states at the two time points corresponding to ATP peak and trough (16 and 24 hours), respectively, whereas untreated cells switched between a metabolically active state corresponding to the intermediate mitochondrial network (high ATP, 16 hours) and a metabolically resting state corresponding to the fragmented mitochondrial network (low ATP, 24 hours). Of note, this phenomenon could be confirmed for all other mitochondrial respiratory states exhibiting decreased oxygen consumption rates after treatment with $A\beta$ (**Suppl. Fig. 2**).

To determine whether the variations in ATP levels were due to the inverted “U”-shaped variation in OCR or the glycolytic rate, ATP levels for each group were plotted against the corresponding basal OCR or ECAR (**Fig. 4B and Suppl. Fig. 3**). The inverted “U”-shaped changes in ATP levels seem to be correlated with OCR but not ECAR in control cells. The $A\beta$ -induced increase in ECAR, which was regardless associated with lower ATP level in $A\beta$ -treated cells, suggests that glycolysis does not seem to be sufficient to counteract the depletion in ATP levels.

Together, these findings show that, after $A\beta_{1-42}$ treatment, mitochondria get stuck in a fragmented state coupled with a decrease in mitochondrial respiration, which consequently leads to a depletion in ATP levels. These findings further indicate that a balanced mitochondrial network might be a crucial precondition for the bioenergetic homeostasis as maintained under normal conditions.

To better understand the impact of the $A\beta$ -related deterioration of mitochondrial morphology and cellular bioenergetic activity, we further examined whether $A\beta$ impacts directly the integrity of the electron transport chain (ETC). For this purpose, we determined the gene expression of subunits involved in oxidative phosphorylation, particularly in the electron transport chain (complexes I and IV) and in ATP generation (ATP synthase or complex V) (**Fig. 5**). Relative quantification of mRNAs isolated from $A\beta$ -treated human skin fibroblasts showed that $A\beta$ negatively impacted gene expression by decreasing the expression of OxPhos genes involved in the function of complex I (NDUFA2, NDUFB5, NDUFC1 and NDUFV2) and ATP synthase (ATP5C1, ATPG2 and ATP5L) (**Fig. 5A, C**). Interestingly, subunits of complex IV (COX4I1 and COX6A1) exhibited a significantly higher gene expression in $A\beta$ -treated human skin fibroblasts compared to untreated cells suggesting that cells develop compensatory responses to alleviate the deleterious effect of

Aβ on mitochondrial function (**Fig. 5B**). The data show that *Aβ* induced aberrant and differential expression of nuclearly encoded ETC subunits which can potentially contribute to an impairment in the assembly of mitochondrial ETC complexes leading to a decline in mitochondrial respiration.

Taken together, these observations support the hypothesis that mitochondrial oxidative metabolism is dependent on the mitochondrial architecture and hence, that an *Aβ*-related imbalance of the mitochondrial network likely contributes to AD-related mitochondrial respiration deficiency, at least by disturbing the expression of ascertained OxPhos subunits.

4. Discussion

In our study, we aimed to investigate the changes in mitochondrial architecture at three time points (8, 16 and 24 hours) in synchronized fibroblasts under normal and $A\beta$ conditions. The two key findings of our study are that, (i) the mitochondrial oxidative metabolism as readout of normal mitochondrial activity displayed an inverted “U”-shaped pattern with a peak at 16 hours mirroring the pattern of the mitochondrial network under physiological conditions and, (ii) $A\beta$ provoked a shift in the mitochondrial architecture towards a fragmented network that negatively impacted several mitochondrial functions including bioenergetics along with an increase in oxidation.

Although in recent years our perception of mitochondria has changed from that of a static and singular to that of a dynamic organelle, only few studies provide support for the existence of a direct relationship between mitochondrial morphology and function [22]. Remarkably, in our study, the parallel examination of mitochondrial morphology and oxidative metabolism in human skin fibroblast revealed that both mitochondrial features are tightly linked. Surprisingly, shortly after the mitochondrial network displayed a tubular architecture, mitochondrial respiration and ATP level increased during the transition from tubular to fragmented network which corresponds to the intermediate state. Conversely, when the cells were in resting state (at 24 hours mirroring the fragmented network, low mitochondrial respiration along with low ATP), the mitochondrial morphology was shifted towards a fragmented network. Our findings confirm previous observations that, when the expression of mitochondrial fusion and fission proteins is genetically manipulated in different cellular models including human fibroblasts, the incurring abnormal mitochondrial morphology induces a dysfunction in mitochondrial respiration, and possibly coupling efficiency as well as a depletion in ATP content [22, 23]. Furthermore, this mitochondrial structure/function relationship was reflected by the transcriptional profiling, with the expression of several ETC subunits as well as in the ATP synthase appearing to be modulated by the mitochondrial morphology state in human skin fibroblasts. It is believed that mitochondrial fission is essential in the formation of the cristae and the proper assembly of mitochondrial electron transport chain complexes [24, 25]. Altogether, our data show for the first time that under physiological conditions, transitions in mitochondrial architecture directly influence mitochondrial functions including respiration and ATP generation.

Since both mitochondrial bioenergetics and dynamics are known as early and prominent features of AD-related neuronal toxicity induced by $A\beta$ [24, 26], we examined the potential impact of $A\beta$ on the integrity of the mitochondrial morphology/function relationship. We found, in contrast to the aforementioned observations, that $A\beta$ treatment of fibroblasts completely abolished the variation pattern in the mitochondrial architecture by causing an

imbalance in fusion and fission proteins which led to a network frozen in a fragmented state. This is consistent with *in vitro* observations made in APPwt (APP wild-typ) and APP^{sw}e (APP with Swedish mutation) - expressing M17 cells where DRP1 and OPA1 became reduced, whereas Fis1 became significantly increased [18]. However, while AD neurons exhibit increased fragmentation [8], fibroblasts from AD patients show elongated and highly interconnected mitochondrial network [8, 12, 27] suggesting that a tissue-related pattern in the expression and/or in post-translational modifications might also be involved in the A β -induced alterations in mitochondrial functions. Concomitantly, defects in mitochondrial dynamics induced a decline in mitochondrial metabolism including decreased mitochondrial respiration, depletion in ATP content and increased oxidative stress through drastic changes in the NAD⁺/NADH ratio. These findings are in agreement with previous observations from both animal models and AD patients that showed mitochondrial decline and elevated oxidative stress playing a crucial role in AD pathogenesis [25, 28, 29]. Additionally, an A β -induced mitochondrial bioenergetic defect can be partly explained by the down-regulation of several nuclearly-encoded OxPhos subunits which was also observed in MCI and AD brains at early stage [30, 31]. In contrast, up-regulation in the gene expression of complex IV subunits might be the result of a functional compensation by the cells to maintain the proton gradient needed for the ATP production [21]. It is known that the impairment of OxPhos efficiency can also be triggered and amplified by A β -related oxidative damage to mitochondrial membranes and proteins [32]. According to previous observations in 3xTg-AD neurons [26], the concurrent increase in glycolysis in A β -treated cells could be interpreted as a compensatory mechanism in which the cells switch to glycolysis to try to rescue the depletion in mitochondrial respiration-related ATP production. Nevertheless, this mechanism was not sufficient to recover the A β -induced decrease in ATP level in human primary fibroblast cultures.

In summary, we gained new insights, on the one hand, into the relevance of the coupling between mitochondrial morphology and function and, on the other hand, into the deleterious cascade of events involved in the abnormal coupling of mitochondrial structure-function mechanisms driven by A β . Our findings further emphasize the relevance of the mitochondrial cascade hypothesis of AD [33].

FIGURES

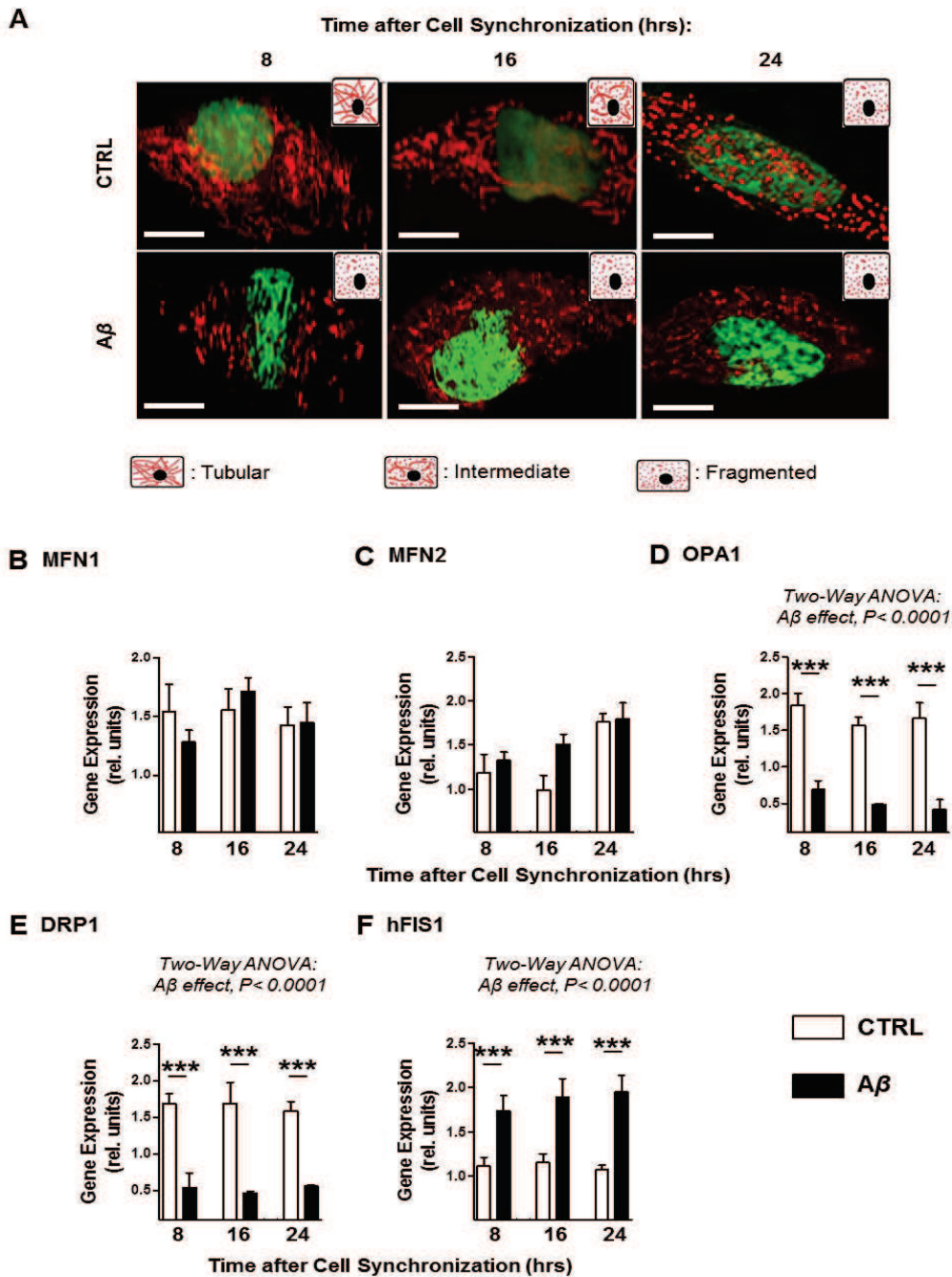


Fig. 1: Aβ-induced imbalance of mitochondrial fission/fusion proteins causes abnormal mitochondrial fragmentation in human primary fibroblasts. (A) Whereas mitochondrial morphology in untreated control cells oscillated between 3 distinct states (tubular, intermediate and fragmented network) corresponding to 8, 16 and 24 hours after cell synchronization, respectively. Only mitochondrial fragmentation was observed Aβ-treated cells at 8, 16 and 24 hours after cell synchronization. Scale bars, 7.5 μm. (B-F) Relative mRNA expression of nuclearly-encoded genes related to mitochondrial fusion: (B) *MFN1*, (C) *MFN2* and (D) *OPA1*, and fission: (E) *DRP1* and (F) *hFIS1* measured at 8, 16 and 24 hours in Aβ-treated human skin fibroblasts (black bars) compared to control cells (white bars). Aβ-induced expression of *OPA1* and *DRP1* was significantly decreased, while expression of *hFIS1* was significantly increased. (B-F) Values represent the mean ± SEM; n = 6-9 replicates of three independent experiments (Two-way ANOVA, group effect: control versus Aβ, post hoc Bonferroni, ***, $P < 0.001$).

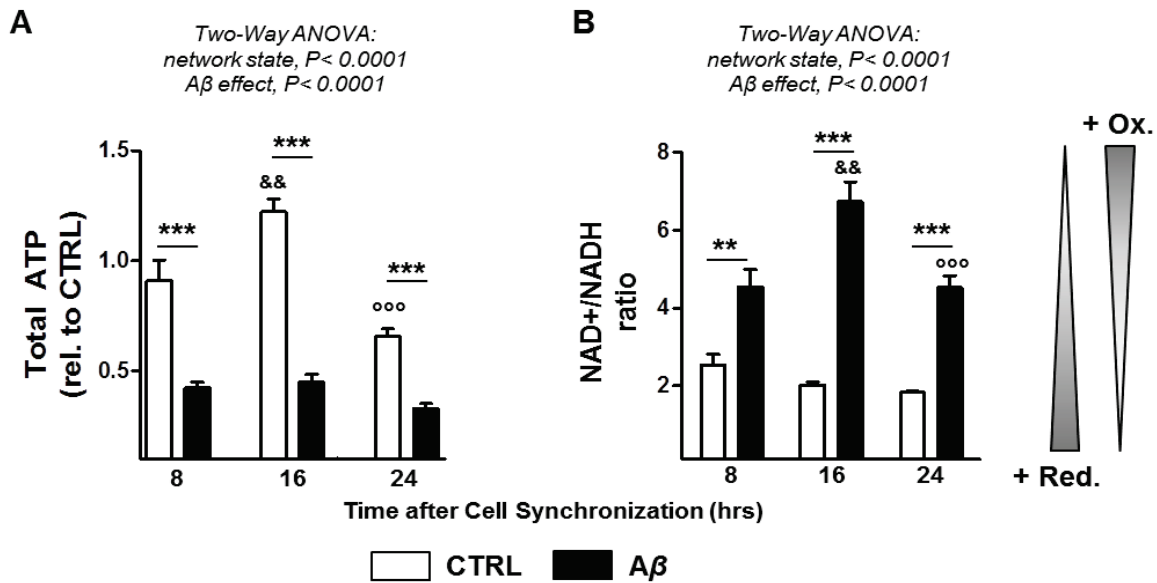


Figure 2: $A\beta$ -induced imbalance of mitochondrial dynamics is followed by a decline in bioenergetic homeostasis. (A) ATP levels were significantly reduced at 8, 16 and 24 hours after cell synchronization (Two-way ANOVA, group effect: control versus $A\beta$, $P < 0.0001$, post hoc Bonferroni, ***, $P < 0.0001$) without variation pattern in $A\beta$ -treated human skin fibroblasts (black bars) compared to untreated cells (white bars) which expressed a variation pattern with a biphasic regulation of ATP content that peaks at 16 hours (One-way ANOVA, ATP variation pattern in control cells, $P < 0.0001$; post hoc Tukey; 8 versus 16 hours, &&, $P < 0.01$; 16 versus 24 hours, ***, $P < 0.001$). (B) The NAD⁺/NADH ratio was significantly enhanced in $A\beta$ -treated human skin fibroblasts compared to untreated cells (Two-way ANOVA, group effect: control versus $A\beta$, $P < 0.0001$, post hoc Bonferroni, **, $P < 0.01$, *** $P < 0.001$) and expressed a variation pattern (One-way ANOVA, NAD⁺/NADH ratio variation pattern in $A\beta$ -treated cells, $P < 0.0001$; post hoc Tukey; 8 versus 16 hours, &&, $P < 0.01$; 16 versus 24 hours, ***, $P < 0.001$) that was absent in control cells. (A,B) Values represent the mean \pm SEM; n=9-12 replicates of three independent experiments.

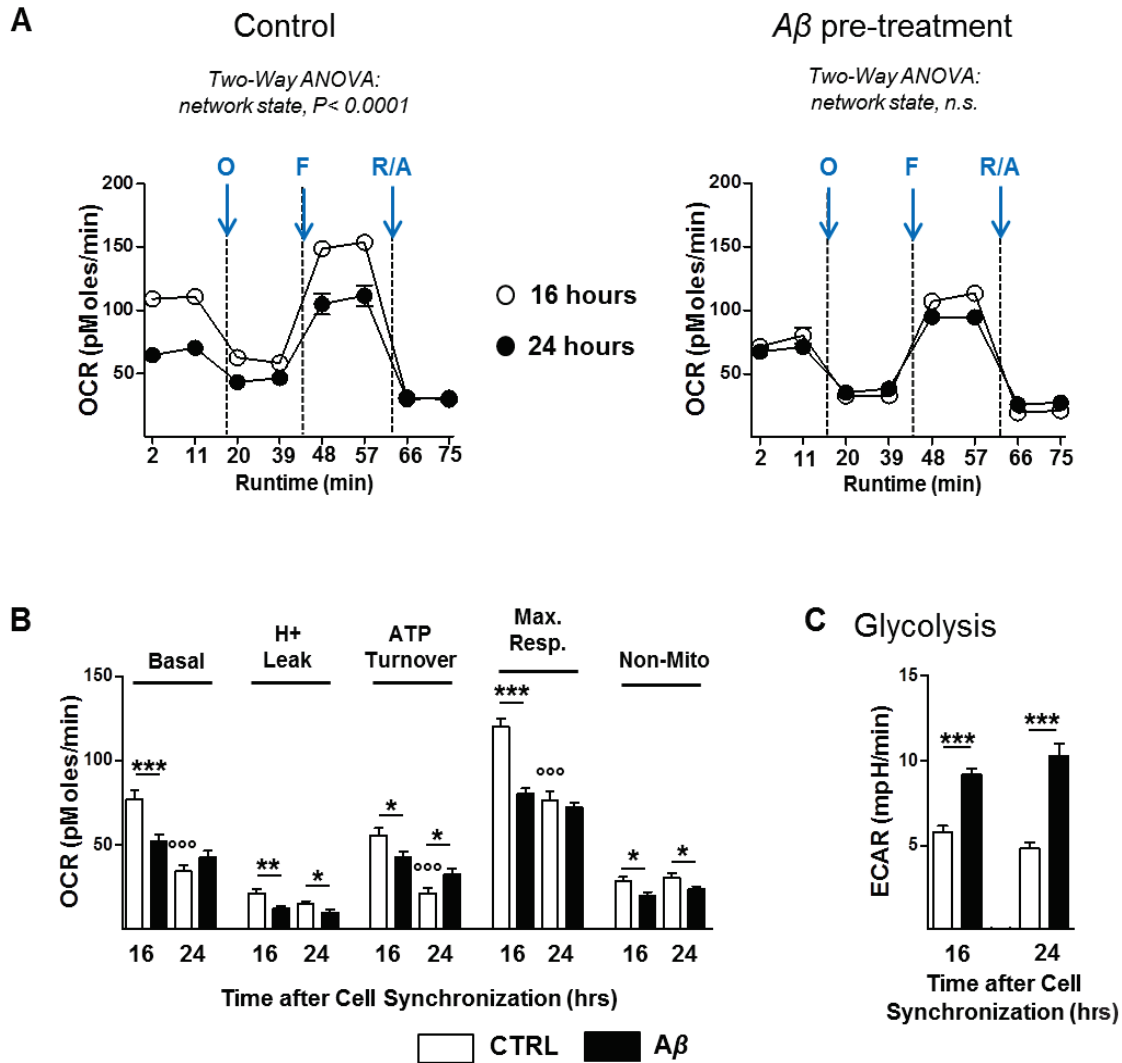


Figure 3: $A\beta$ -induced imbalance of mitochondrial dynamics leads to an impairment of mitochondrial respiration. (A) The oxygen consumption rate (OCR) was evaluated in $A\beta$ -treated human skin fibroblasts (right panel) compared to untreated control cells (left panel) at 16 hours, corresponding to the intermediate mitochondrial network as well as ATP peak and 24 hours, corresponding to the fragmented mitochondrial network as well as ATP trough. The sequential injection of mitochondrial inhibitors is indicated by blue arrows (for experimental details, see Materials and Methods) ($n = 11$ replicates /group, three independent experiments). (B) Basal respiration, proton (H^+) leak, ATP turnover and maximal respiration were determined after normalization to non-mitochondrial respiration. (C) Extracellular Acidification Rate (ECAR) corresponding to glycolytic rate was determined at the indicated time points in $A\beta$ -treated human skin fibroblasts compared to untreated cells. OCR and ECAR were measured simultaneously and in real time using a Seahorse XF24 analyzer under the same experimental conditions. (A-C) Values represent the mean \pm SEM ($n = 11$ of three independent experiments) (Two-way ANOVA, group effect: CTRL versus $A\beta$, post hoc Bonferroni, *, $P < 0.1$; **, $P < 0.01$; ***, $P < 0.001$; group effect: variation pattern 16 versus 24 hours, post hoc Bonferroni, $^{\circ}$, $P < 0.1$; $^{\circ\circ}$, $P < 0.01$; $^{\circ\circ\circ}$, $P < 0.001$). O, oligomycin; F, FCCP; R, rotenone; A, antimycin A; Basal, basal respiration; H+ leak, proton leak; Max. Resp., maximal respiration; Non-mito, non-mitochondrial respiration.

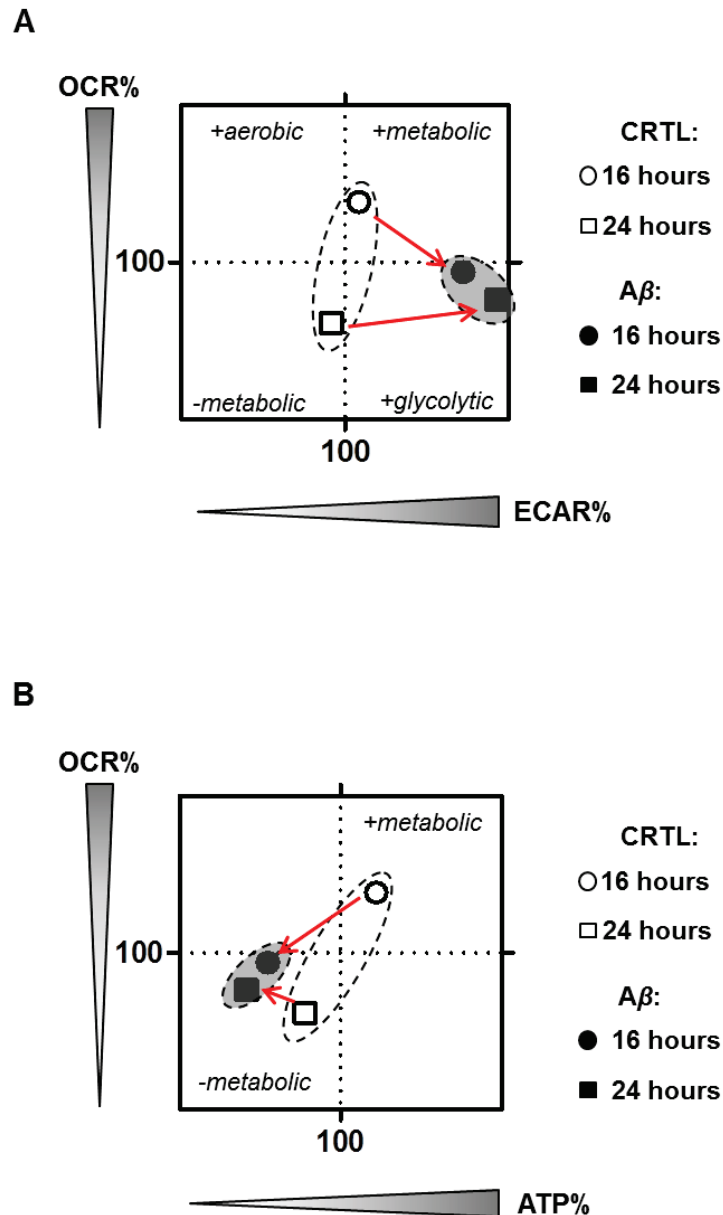


Figure 4: A β - treated fibroblasts exhibit decreased mitochondrial respiration and increased glycolysis. (A) OCR/ECAR: The basal oxygen consumption rates (OCR) corresponding to the intermediate (at 16 hours) and fragmented (at 24 hours) networks are plotted against the respective glycolytic rates (ECAR) under control (white symbols) and A β conditions (black symbols). Values represent the mean for each group (mean of the ECAR in abscissa/ mean of the OCR in ordinate); n= 11 replicates /group for three independent experiments. **(B) OCR/ATP:** The basal OCR corresponding to the intermediate (at 16 hours) and fragmented (at 24 hours) networks are plotted against the respective ATP content in control (white symbols) and A β conditions (black symbols). Values represent the mean of each group (mean of the ATP levels in abscissa/ mean of the OCR in ordinate); n= 11-12 replicates /group of three independent experiments. The red arrows highlight the A β -induced metabolic shift at 16 and 24 hours after cell synchronization.

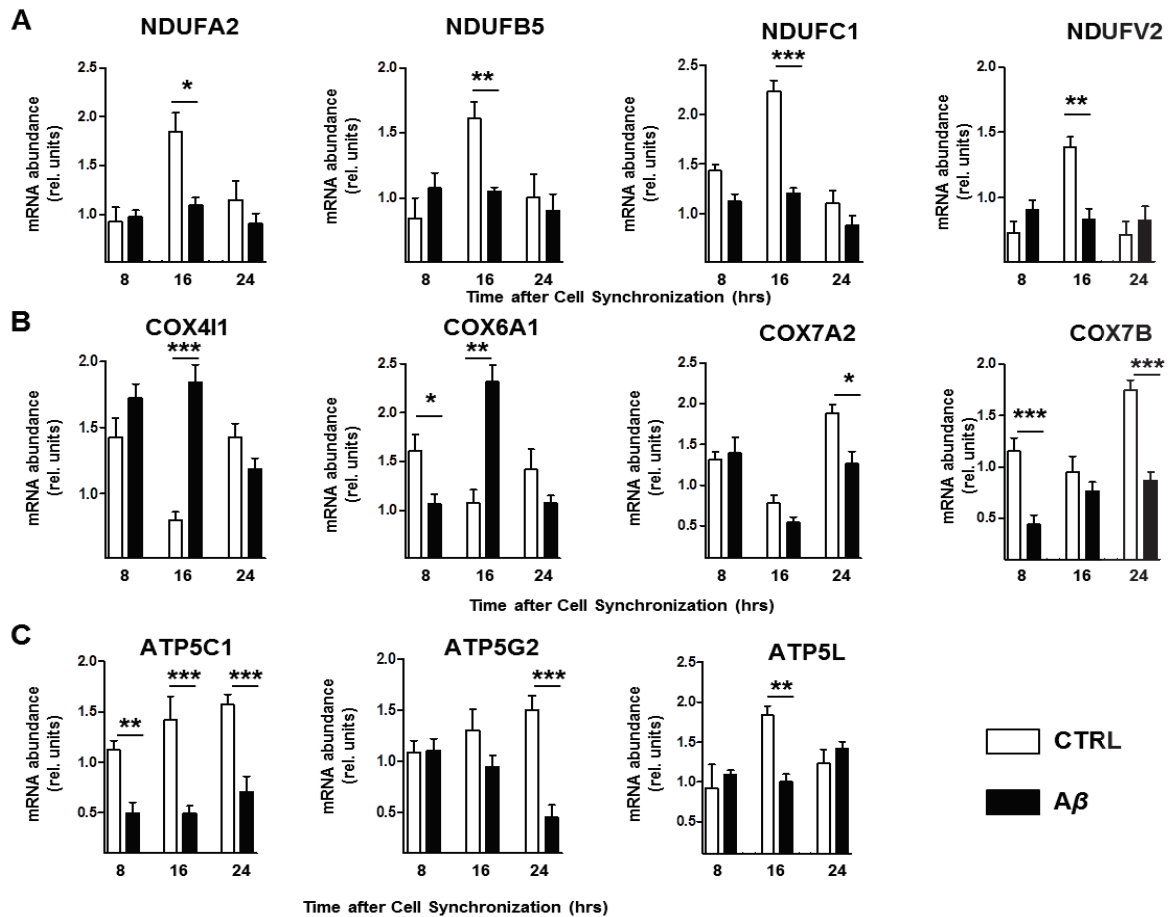
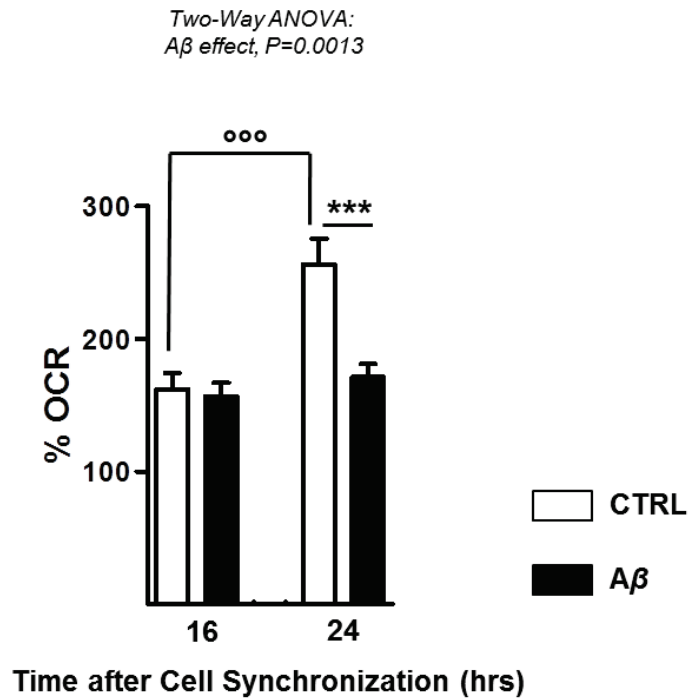
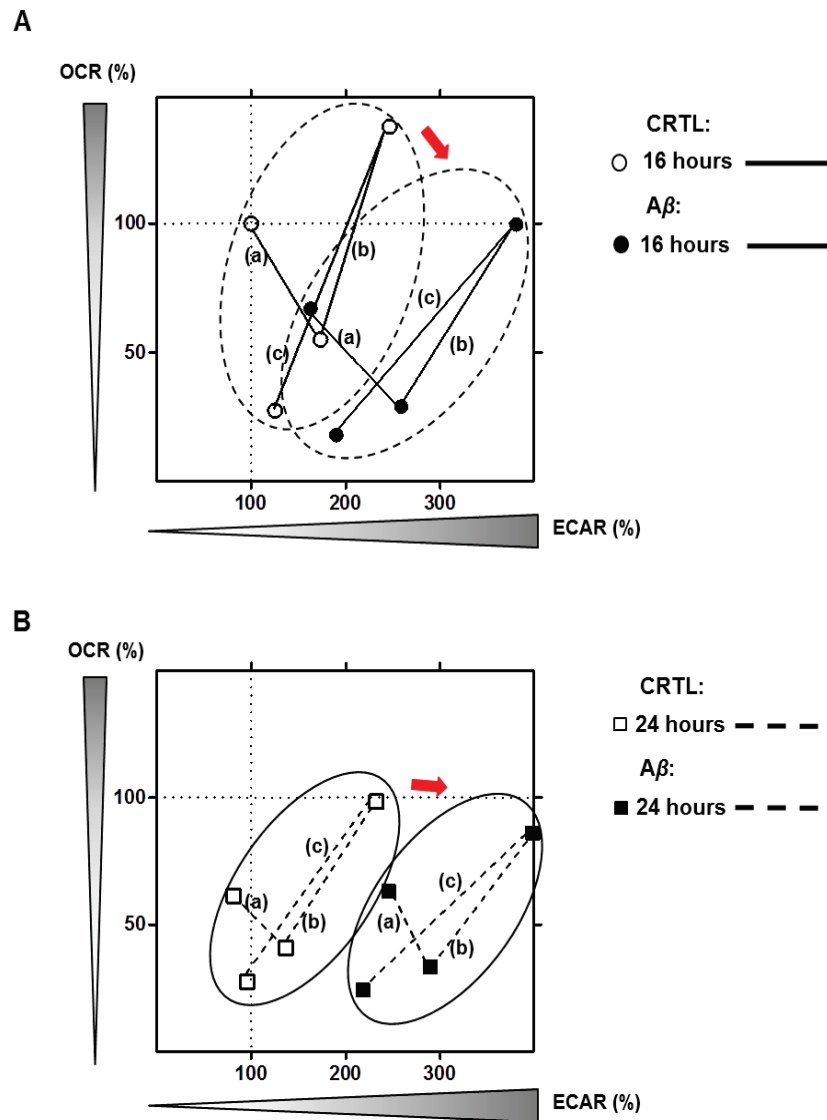


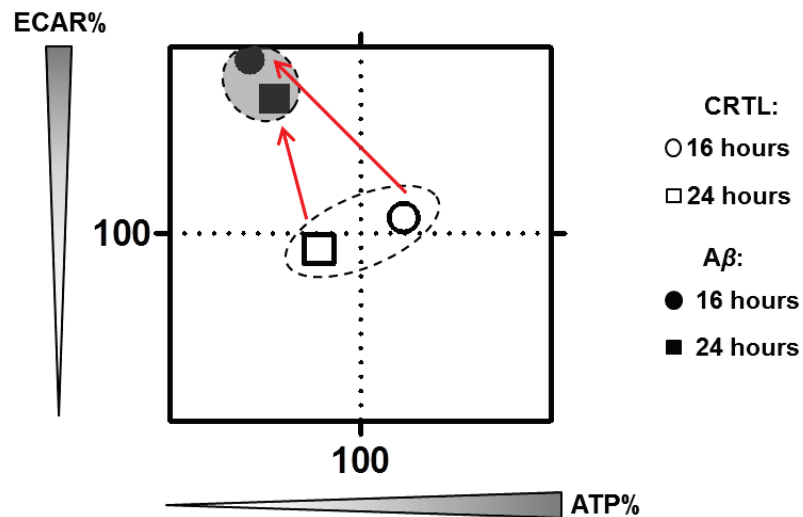
Figure 5: A β impairs the expression of genes with a role in mitochondrial oxidative metabolism. (A-C) Profiles of relative mRNA expression of nuclearly-encoded (A) complex I, (B) complex IV and (C) complex V-encoding subunits involved in the ETC and OxPhos in A β -treated human skin fibroblasts (black bars) compared to untreated cells (white bars) at 8, 16 and 24 hours after cell synchronization. Values represent the mean \pm SEM, n= 3. (A-C) Two-way ANOVA, group effect: control versus A β , $P < 0.0001$, post hoc Bonferroni, *, $P < 0.1$; **, $P < 0.01$; ***, $P < 0.001$.



Supplementary Figure 1: A β -treated fibroblasts exhibit a decreased ability to respond to an energetic demand. The spare respiratory capacity was determined based on the measurements taken in Fig. 3 (A). Values represent the mean \pm SEM (n= 11 of three independent experiments) (One-way ANOVA, spare respiratory capacity variation pattern in control cells, $P<0.0001$; post hoc Tukey, ^{ooo}, $P < 0.001$; Two-way ANOVA, group effect: control versus A β , $P=0.0013$. post hoc Bonferroni;***, $P < 0.001$).



Supplementary Figure 2: Bioenergetic profiling (OCR/ECAR) of human primary fibroblast cultures at (A) 16 hours and (B) 24 hours. OCR corresponding to the intermediate network is plotted versus the respective glycolytic rate (ECAR) in control (white symbol) and A β conditions (black symbol). The circle lines highlight the cloud data for untreated and A β -treated cells. The bioenergetic profile was calculated during basal respiration and after sequential exposure to mitochondrial inhibitors (a) oligomycin, (b) FCCP and (c) rotenone/antimycin A. Values represent mean of each group (mean of the ECAR in abscissa/ mean of the OCR in ordinate) normalized to the basal respiration at 16 hours under control condition (=100%/100%). The red arrows highlight the A β -induced metabolic shift towards an increased glycolytic rate.



Supplementary Figure 3: A β -induced depletion in ATP production is independent of metabolic switch toward a glycolytic state. ECAR/ATP: The glycolytic rates (ECAR) corresponding to the intermediate (at 16 hours) and fragmented (at 24 hours) networks are plotted against the respective ATP content under control (white symbols) and A β conditions (black symbols). Values represent the mean of each group (mean of the ATP levels in abscissa/ mean of the ECAR in ordinate); n= 11-12 replicates /group for three independent experiments. The red arrows highlight the A β -induced metabolic shift towards an increased glycolytic rate.

Contributions

KS performed experiments. UEL, JG and AE conceived the project, coordinated and supervised research. KS, JG and AE wrote the manuscript.

Acknowledgements

This work was supported by Swiss National Science Foundation (#31000_122572 and #31003A_149728) and Synapsis Foundation to AE.

References

- [1] H. Chen, D.C. Chan, Mitochondrial dynamics--fusion, fission, movement, and mitophagy--in neurodegenerative diseases, *Human molecular genetics*, 18 (2009) R169-176.
- [2] S. Hoppins, The regulation of mitochondrial dynamics, *Current opinion in cell biology*, 29 (2014) 46-52.
- [3] P. Mishra, D.C. Chan, Mitochondrial dynamics and inheritance during cell division, development and disease, *Nature reviews. Molecular cell biology*, 15 (2014) 634-646.
- [4] B. Westermann, Mitochondrial fusion and fission in cell life and death, *Nature reviews. Molecular cell biology*, 11 (2010) 872-884.
- [5] A. Eckert, K. Schmitt, J. Gotz, Mitochondrial dysfunction - the beginning of the end in Alzheimer's disease? Separate and synergistic modes of tau and amyloid-beta toxicity, *Alzheimer's research & therapy*, 3 (2011) 15.
- [6] L. Pagani, A. Eckert, Amyloid-Beta interaction with mitochondria, *International journal of Alzheimer's disease*, 2011 (2011) 925050.
- [7] M. Manczak, M.J. Calkins, P.H. Reddy, Impaired mitochondrial dynamics and abnormal interaction of amyloid beta with mitochondrial protein Drp1 in neurons from patients with Alzheimer's disease: implications for neuronal damage, *Human molecular genetics*, 20 (2011) 2495-2509.
- [8] X. Wang, B. Su, H. Fujioka, X. Zhu, Dynamin-like protein 1 reduction underlies mitochondrial morphology and distribution abnormalities in fibroblasts from sporadic Alzheimer's disease patients, *The American journal of pathology*, 173 (2008) 470-482.
- [9] M.J. Calkins, M. Manczak, P. Mao, U. Shirendeb, P.H. Reddy, Impaired mitochondrial biogenesis, defective axonal transport of mitochondria, abnormal mitochondrial dynamics and synaptic degeneration in a mouse model of Alzheimer's disease, *Human molecular genetics*, 20 (2011) 4515-4529.
- [10] B. DuBoff, J. Gotz, M.B. Feany, Tau promotes neurodegeneration via DRP1 mislocalization in vivo, *Neuron*, 75 (2012) 618-632.
- [11] B. DuBoff, M. Feany, J. Gotz, Why size matters - balancing mitochondrial dynamics in Alzheimer's disease, *Trends in neurosciences*, 36 (2013) 325-335.
- [12] X. Wang, B. Su, H.G. Lee, X. Li, G. Perry, M.A. Smith, X. Zhu, Impaired balance of mitochondrial fission and fusion in Alzheimer's disease, *The Journal of neuroscience : the official journal of the Society for Neuroscience*, 29 (2009) 9090-9103.
- [13] S.A. Brown, F. Fleury-Olela, E. Nagoshi, C. Hauser, C. Juge, C.A. Meier, R. Chicheportiche, J.M. Dayer, U. Albrecht, U. Schibler, The period length of fibroblast circadian gene expression varies widely among human individuals, *PLoS biology*, 3 (2005) e338.
- [14] S. Cooper, Rethinking synchronization of mammalian cells for cell cycle analysis, *Cellular and molecular life sciences : CMLS*, 60 (2003) 1099-1106.

- [15] M. Rosner, K. Schipany, M. Hengstschlager, Merging high-quality biochemical fractionation with a refined flow cytometry approach to monitor nucleocytoplasmic protein expression throughout the unperturbed mammalian cell cycle, *Nature protocols*, 8 (2013) 602-626.
- [16] F. Invernizzi, I. D'Amato, P.B. Jensen, S. Ravaglia, M. Zeviani, V. Tiranti, Microscale oxygraphy reveals OXPHOS impairment in MRC mutant cells, *Mitochondrion*, 12 (2012) 328-335.
- [17] M.J. Barsoum, H. Yuan, A.A. Gerencser, G. Liot, Y. Kushnareva, S. Graber, I. Kovacs, W.D. Lee, J. Waggoner, J. Cui, A.D. White, B. Bossy, J.C. Martinou, R.J. Youle, S.A. Lipton, M.H. Ellisman, G.A. Perkins, E. Bossy-Wetzel, Nitric oxide-induced mitochondrial fission is regulated by dynamin-related GTPases in neurons, *The EMBO journal*, 25 (2006) 3900-3911.
- [18] X. Wang, B. Su, S.L. Siedlak, P.I. Moreira, H. Fujioka, Y. Wang, G. Casadesus, X. Zhu, Amyloid-beta overproduction causes abnormal mitochondrial dynamics via differential modulation of mitochondrial fission/fusion proteins, *Proceedings of the National Academy of Sciences of the United States of America*, 105 (2008) 19318-19323.
- [19] M. Klingenberg, The ADP and ATP transport in mitochondria and its carrier, *Biochimica et biophysica acta*, 1778 (2008) 1978-2021.
- [20] K. Schmitt, A. Grimm, A. Kazmierczak, J.B. Strosznajder, J. Gotz, A. Eckert, Insights into mitochondrial dysfunction: aging, amyloid-beta, and tau-A deleterious trio, *Antioxidants & redox signaling*, 16 (2012) 1456-1466.
- [21] A.S. Divakaruni, M.D. Brand, The regulation and physiology of mitochondrial proton leak, *Physiology*, 26 (2011) 192-205.
- [22] M. Picard, O.S. Shirihai, B.J. Gentil, Y. Burelle, Mitochondrial morphology transitions and functions: implications for retrograde signaling?, *American journal of physiology. Regulatory, integrative and comparative physiology*, 304 (2013) R393-406.
- [23] G. Benard, R. Rossignol, Ultrastructure of the mitochondrion and its bearing on function and bioenergetics, *Antioxidants & redox signaling*, 10 (2008) 1313-1342.
- [24] V. Garcia-Escudero, P. Martin-Maestro, G. Perry, J. Avila, Deconstructing mitochondrial dysfunction in Alzheimer disease, *Oxidative medicine and cellular longevity*, 2013 (2013) 162152.
- [25] X. Zhu, G. Perry, M.A. Smith, X. Wang, Abnormal mitochondrial dynamics in the pathogenesis of Alzheimer's disease, *Journal of Alzheimer's disease : JAD*, 33 Suppl 1 (2013) S253-262.
- [26] J. Yao, R.W. Irwin, L. Zhao, J. Nilsen, R.T. Hamilton, R.D. Brinton, Mitochondrial bioenergetic deficit precedes Alzheimer's pathology in female mouse model of Alzheimer's

disease, *Proceedings of the National Academy of Sciences of the United States of America*, 106 (2009) 14670-14675.

[27] S. Wang, J. Song, M. Tan, K.M. Albers, J. Jia, Mitochondrial fission proteins in peripheral blood lymphocytes are potential biomarkers for Alzheimer's disease, *European journal of neurology : the official journal of the European Federation of Neurological Societies*, 19 (2012) 1015-1022.

[28] C. Cecchi, C. Fiorillo, S. Sorbi, S. Latorraca, B. Nacmias, S. Bagnoli, P. Nassi, G. Liguri, Oxidative stress and reduced antioxidant defenses in peripheral cells from familial Alzheimer's patients, *Free radical biology & medicine*, 33 (2002) 1372-1379.

[29] Q. Shi, G.E. Gibson, Oxidative stress and transcriptional regulation in Alzheimer disease, *Alzheimer disease and associated disorders*, 21 (2007) 276-291.

[30] M.Y. Aksenov, H.M. Tucker, P. Nair, M.V. Aksenova, D.A. Butterfield, S. Estus, W.R. Markesbery, The expression of several mitochondrial and nuclear genes encoding the subunits of electron transport chain enzyme complexes, cytochrome c oxidase, and NADH dehydrogenase, in different brain regions in Alzheimer's disease, *Neurochemical research*, 24 (1999) 767-774.

[31] M. Manczak, B.S. Park, Y. Jung, P.H. Reddy, Differential expression of oxidative phosphorylation genes in patients with Alzheimer's disease: implications for early mitochondrial dysfunction and oxidative damage, *Neuromolecular medicine*, 5 (2004) 147-162.

[32] P.H. Reddy, M.F. Beal, Amyloid beta, mitochondrial dysfunction and synaptic damage: implications for cognitive decline in aging and Alzheimer's disease, *Trends in molecular medicine*, 14 (2008) 45-53.

[33] R.H. Swerdlow, J.M. Burns, S.M. Khan, The Alzheimer's disease mitochondrial cascade hypothesis: progress and perspectives, *Biochimica et biophysica acta*, 1842 (2014) 1219-1231.

CONCLUSION

Mitochondria are highly dynamic and essential organelles in cell survival and death by regulation of both energy metabolism and apoptotic pathways. To fulfill their multiple tasks, the mitochondrial network comes in varied morphologies and ultrastructures to ensure the energy supply, stored in the form of adenosine triphosphate (ATP), by oxidative reactions from nutritional sources. A well-defined set of proteins regulates mitochondrial fission and fusion, including mitofusins and dynamin-related proteins. Because mitochondria are considered as the 'powerhouses' of the cell, a fine-tuning of both mitochondrial dynamics and metabolism is imperative to maintain the integrity of a healthy mitochondrial population within the cell but also the integrity of the cell itself. Even though the molecular mechanisms involved in mitochondrial fusion/fission and their roles in mitochondrial homeostasis are well established, the regulatory mechanisms behind the global control of mitochondrial functions are still mostly elusive. Additionally, a greater comprehension of the mechanisms involved in the physiological regulation of mitochondrial functions might be of great relevance for the understanding of the implication of mitochondrial deficiencies in the pathogenesis of neurodegenerative disorders, e.g. Alzheimer's disease (AD).

Thus, the aim of the present thesis was firstly to gain novel insights into the role of (i) the circadian clock and of (ii) neurosteroids on the modulation of mitochondrial homeostasis. In the second part (iii), we further investigated the consequence of $A\beta$ -induced abnormal mitochondrial morphology on mitochondrial bioenergetics to further underscore the mitochondrial cascade hypothesis of AD.

(i) A wide range of metabolic processes follows the rhythmicity of the circadian cycle to anticipate energetic requirements of diverse cellular functions in response to cellular and environmental constraints. Yet, only a few studies have characterized the mechanisms involved, demonstrating coupling via cyclic redox metabolite levels (e.g: NAD^+), mitochondrial protein acetylation and chromatin modification. Combining morphological and functional assays, we identified and characterized a novel mitochondrial dynamics-based regulatory connection between the circadian clock and metabolism, and showed that this connection is absolutely essential for the circadian regulation of cellular ATP levels. Specifically, the circadian transitions of mitochondrial bioenergetics were directly coupled to clock-controlled changes in mitochondrial ultrastructure. This coupling was completely independent of the cell cycle (in which it was initially characterized), both because it remains in the presence of cell cycle inhibitors *in vitro*, and because it equally occurs in mostly nondividing tissues like brain and liver. Moreover, analysis of regulation of DRP1 revealed that phosphorylation of serine 637 followed a circadian pattern and was functionally essential for circadian ATP production

because its inhibition, either pharmacologically or genetically, abolished circadian oscillations in ATP levels. Finally, inhibition of mitochondrial flux in multiple different ways showed effects upon circadian clock properties and upon clock gene expression *in vitro*.

Overall, consistent with the growing body of evidence stating the importance to integrate the cellular metabolism with circadian clocks [1], our findings established a new molecular link in which the mitochondrial network acts as a central node in coupling circadian and metabolic cycles. Our results further underline the importance of a well-coordinated metabolic system in human health as well as in disorders linked to impairments in circadian clock and/ or mitochondrial function. Although the effect of aging on the circadian system and mitochondrial homeostasis has been known for many years [2-5], disruption between the circadian system and the mitochondrial network may be a key initiating factor for age-related diseases such as AD.

(ii) A growing body of evidence supports that, on the one hand, some neurosteroid levels decline during aging and, on the other hand, mitochondrial dysfunction is a prominent and early age-associated event [6]. Both deteriorations are known to contribute in a separate manner to energy failure and increased oxidative stress which, once a threshold is reached, ultimately increased susceptibility to age-related disorders including AD. The enhanced neuronal vulnerability might, at least in part, result from the loss of neurosteroid-mediated neuroprotection [7, 8]. Nevertheless, only few studies, which especially concentrated on estradiol, showed that mitochondrial dysfunction can be partially recovered by neurosteroids [6]. Thus, our findings highlight for the first time that, besides estradiol, several neurosteroids are able to enhance mitochondrial metabolic activities at least in part via the activation of their particular receptors. Specifically, the up-regulation of the mitochondrial activity of each neurosteroid was subtly divergent suggesting a more complex regulatory system on mitochondrial activities. In addition, these steroids can modulate the redox homeostasis by balancing the increase of ROS production via improved mitochondrial antioxidant activity. Altogether, our findings re-define the crucial importance of neurosteroids in the development of therapeutic strategies to counterbalance the age-related mitochondrial decline which may result from a depletion in neurosteroid contents.

Since circadian clock and neurosteroids impact positively mitochondrial metabolism in a distinct manner, the next challenge would be to investigate the potential crosstalk between circadian clock and neurosteroids and its synergistic effect on the vital organelle homeostasis including mitochondrial dynamics and bioenergetics. It has been demonstrated that the circadian clock influences the concentrations of progesterone and its metabolite allopregnanolone in the female whole mouse brain [9]. Therefore, a better understanding of the interplay between mitochondrial function, neurosteroids and the circadian machinery in

health state would help to deepen our knowledge about the underlying mechanisms contributing to neurodegenerative disorders such as AD.

(iii) Based on the aforementioned findings, we investigated the impact of $A\beta$ on the balance between mitochondrial structures and function since both mitochondrial dynamics and bioenergetics are crucial hallmarks of $A\beta$ -induced neuronal toxicity in AD [4, 10]. In the line of evidence of previous findings [11, 12], we determined that $A\beta$ -treated cells undergo extensive network fragmentation. Concomitant with $A\beta$ -related alterations in mitochondrial dynamics, mitochondrial metabolism was drastically impaired including decreased mitochondrial respiration, depletion in ATP content and increased oxidative stress resulting from increased mitochondrial ROS levels and radical changes in $NAD^+/NADH$ ratio. Thus, our findings underline the AD mitochondrial cascade hypothesis which claims that bioenergetic defects ultimately trigger AD. Once the age-related mitochondrial decline reaches a critical threshold, it affects APP expression and processing as well as accumulation of $A\beta$, which can reinforce mtDNA damage and oxidative stress in a vicious cycle. Based on the complexity of the multifactorial nature of AD, the key role of mitochondrial dysfunction in the early pathogenic pathway by which $A\beta$ leads to neuronal dysfunction in AD is particularly challenging with respect to establishing disease-modifying treatments.

Taken together, our results provide the first evidence that the time-of-day-dependent oscillations in metabolic homeostatic parameters are consequent to a complex interplay between the circadian clock and the coupled mitochondrial structure-function relationship. Furthermore, neurosteroids, in term of gender-oriented neuroprotective candidates, are key factors in the fine-tuning of mitochondrial function, particularly the mitochondrial bioenergetic homeostasis. Finally, we gain novel insights into the cascade of the molecular and functional events initiating AD pathogenesis according to the AD mitochondrial cascade hypothesis [13]. However, further investigations are needed to *identify* the remaining gaps in the interplay between mitochondrial function, neurosteroids and the circadian machinery in health state as well as in aging with regard to the development of interventions that prevent the progression of the age-related mitochondrial decline (Figure 18).

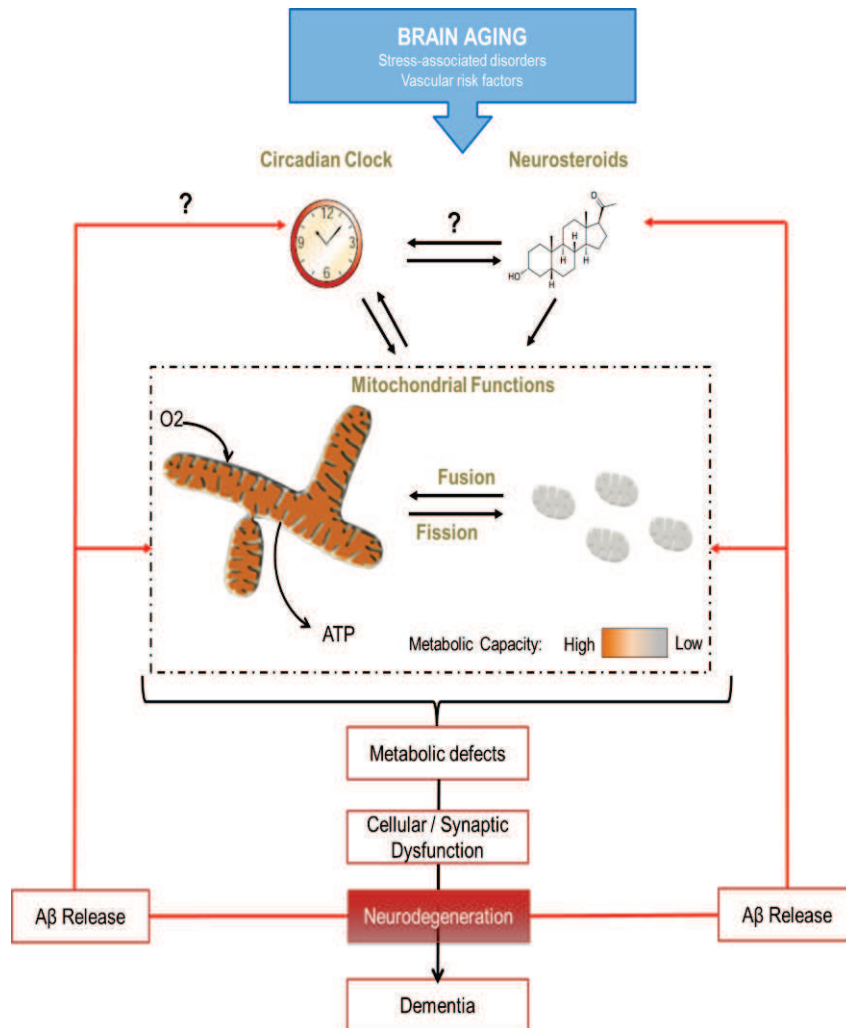


Figure 18 : A hypothetical sequence of the interplay between mitochondrial functions, the circadian clock and neurosteroids in health, aging and age-related diseases as AD.

References

1. Rey, G. and A.B. Reddy, *Connecting cellular metabolism to circadian clocks*. Trends Cell Biol, 2013. **23**(5): p. 234-41.
2. Hofman, M.A. and D.F. Swaab, *Living by the clock: the circadian pacemaker in older people*. Ageing Res Rev, 2006. **5**(1): p. 33-51.
3. Kondratova, A.A. and R.V. Kondratov, *The circadian clock and pathology of the ageing brain*. Nat Rev Neurosci, 2012. **13**(5): p. 325-35.
4. Schmitt, K., et al., *Insights into mitochondrial dysfunction: aging, amyloid-beta, and tau-A deleterious trio*. Antioxid Redox Signal, 2012. **16**(12): p. 1456-66.
5. Lee, H.C. and Y.H. Wei, *Mitochondria and aging*. Adv Exp Med Biol, 2012. **942**: p. 311-27.
6. Grimm, A., et al., *Alzheimer's disease, oestrogen and mitochondria: an ambiguous relationship*. Mol Neurobiol, 2012. **46**(1): p. 151-60.
7. Reddy, P.H. and M.F. Beal, *Amyloid beta, mitochondrial dysfunction and synaptic damage: implications for cognitive decline in aging and Alzheimer's disease*. Trends Mol Med, 2008. **14**(2): p. 45-53.
8. Schumacher, M., et al., *Steroid hormones and neurosteroids in normal and pathological aging of the nervous system*. Prog Neurobiol, 2003. **71**(1): p. 3-29.
9. Corpechot, C., et al., *Brain neurosteroids during the mouse oestrous cycle*. Brain Res, 1997. **766**(1-2): p. 276-80.
10. Eckert, A., K. Schmitt, and J. Gotz, *Mitochondrial dysfunction - the beginning of the end in Alzheimer's disease? Separate and synergistic modes of tau and amyloid-beta toxicity*. Alzheimers Res Ther, 2011. **3**(2): p. 15.
11. Zhu, X., et al., *Abnormal mitochondrial dynamics in the pathogenesis of Alzheimer's disease*. J Alzheimers Dis, 2013. **33 Suppl 1**: p. S253-62.
12. Trushina, E., et al., *Defects in mitochondrial dynamics and metabolomic signatures of evolving energetic stress in mouse models of familial Alzheimer's disease*. PLoS One, 2012. **7**(2): p. e32737.
13. Swerdlow, R.H., J.M. Burns, and S.M. Khan, *The Alzheimer's disease mitochondrial cascade hypothesis: progress and perspectives*. Biochim Biophys Acta, 2014. **1842**(8): p. 1219-31.

ABBREVIATIONS

2DG	2 deoxy-D-glucose
3 α -A	3 α -androstanediol
ABAD	A β binding protein alcohol dehydrogenase
AD	Alzheimer's disease
ADAM	A disintegrin and metalloproteinase
AICD	A β intracellular cytoplasmic domain
AIF	Apoptosis-inducing factor
AMPK	AMP-activated protein kinase
AP	allopregnanolone
APH1	Anterior pharynx-defective 1
APP	Amyloid precursor protein
ATP	Adenosine tri-phosphate
AVP	Arginine vasopressin
A β	Amyloid-beta peptide
Bmal1	Brain and muscle ARNT-like protein 1
C83	83-amino-acid Ct APP fragment
C99	99-amino-acid Ct APP fragment
CaMKII	Calcium-calmodulin dependent protein kinase II
cAMP	Cyclic adenosine monophosphate
CAT	Catalase
CCG	Clock-controlled gene
CLOCK	Circadian locomoter output cycles protein kaput
CO ₂	Carbon dioxide
COX	Cytochrome c oxidase
cROS	cytosolic reactive oxygen species
CRY	Cryptochrome
Ct	Carboxy-terminal
CT	Circadian time
Cu/Zn SOD	Copper/zinc superoxide dismutase
CYP	Cytochrome P 450
D	DHEA (dihydroepiandrosterone)
DD	Dark/dark
DHEA	Dehydroepiandrosterone
DHR	Dihydrorhodamine 123
DRP1	Dynamin-related protein 1
E1	Estrone
E2	17 β -estradiol
E3	Estriol
ECAR	Extracellular acidification rate
ER	Estrogen-receptor
ETC	Electron transport chain
FAD	Familial Alzheimer's disease form
FADH2	Flavin adenine dinucleotide
FTDP-17	Fronto-temporal dementia with Parkinsonism linked to chromosome 17
GABA	γ -aminobutyric acid
GPX	Glutathione peroxidase
GSH	Glutathione
GSK-3 β	Glycogen synthase kinase-3 β
H ₂ O ₂	Hydrogen peroxide
hFIS1	Human fission protein 1
IMM	Inner mitochondrial membrane
IMS	Intermembrane space
LD	Light/dark
MAOA	Monoamine oxidase A

ABBREVIATIONS

MAOB	Monoamine oxidase B
MARK	Mitogen-associated protein affinity-regulating kinases
MCI	Mild cognitive impairment
MDA	Malondialdehyde
MEF	Mouse embryonic fibroblast
MFN1/2	Mitofusin 1/ 2
MMP	Mitochondrial membrane permeabilization
MnSOD	Manganese superoxide dismutase
mRNA	Messenger ribonucleic acid
mROS	Mitochondrial reactive oxygen species
mtDNA	Mitochondrial DNA
NAD ⁺	Nicotinamide adenine dinucleotide, oxidized form
NADH	Nicotinamide adenine dinucleotide, reduced form
NAMPT	Nicotinamide phosphoribosyltransferase
nDNA	Nuclear DNA
NFTs	Neurofibrillary tangles
NMDA	N-methyl-D-aspartic acid
NO	Nitric oxide
NOS	Nitric oxide synthase
Npas2	Neuronal PAS domain-containing protein 2
NREM	Non rapid eye movement
Nt	Amino-terminal
O ₂ ⁻	Superoxide anion
OCR	Oxygen consumption rate
OH [·]	Hydroxyl radical
OMM	Outer mitochondrial membrane
ONOO ⁻	Peroxynitrite
OPA 1	Optic atrophy 1
OXPPOS	Oxidative phosphorylation;
P	Progesterone
PACAP	Pituitary adenylyl cyclase-activating polypeptide
PAS	PER-ARNT-SIM domain
PD	Parkinson's disease
Per	Clock gene Period
PET	Positron emission tomography
PKA	Protein kinase A
PKC	Protein kinase C
PLC	Phospholipase C
pR5	P301L mutant tau transgenic pR5 mice
PS1	Presenelin 1
PS2	Presenelin 2
REM	Rapid eye movement
RHT	Retina-hypothalamic tract
RNS	Reactive nitrogen species
ROR	Retinoic-related orphan nuclear receptor
RORE	Retinoic acid-related orphan receptor response element
ROS	Reactive oxygen species
SAD	Sporadic Alzheimer's disease form
SCN	Suprachiasmatic nucleus
Ser637	Residue serine 637
SIRT	Sirtuin
SRA	Steroid receptor antagonist;
T	Testosterone
TCA	Tricarboxylic acid cycle
TNF	Tumor necrosis factor
TOM	Translocator outer membrane

ABBREVIATIONS

UCPs	Uncoupling proteins
VDAC	Voltage-dependant anion channels
VDCC	Voltage-dependent Ca ²⁺ channel
VIP	Vasoactive intestinal peptide
ZT	Zeitgeber time

APPENDICES

A. Serum factors in older individuals change cellular clock properties

B. Aging and Circadian Disruption: Causes and Effects

C. Mitochondrial dysfunction - the beginning of the end in Alzheimer's disease? Separate and synergistic modes of tau and amyloid- β toxicity.

D. Insights into Mitochondrial Dysfunction: Aging, Amyloid- β , and Tau-A Deleterious Trio

E. Advanced mitochondrial respiration assay for evaluation of mitochondrial dysfunction in Alzheimer's disease

F. BDNF in sleep, insomnia, and sleep deprivation

A. Serum factors in older individuals change cellular clock properties

Authors: Pagani L^{a,b}, Schmitt K^a, Meier F^a, Izakovic J^c, Roemer K^d, Viola A^e, Cajochen C^e, Wirz-Justice A^e, Brown SA^{b,1,2}, and Eckert A^{a,1,2}

Affiliations:

^aNeurobiology Laboratory for Brain Aging and Mental Health,

^dForensic Psychiatry, and

^eCentre for Chronobiology, Psychiatric University Clinics, University of Basel, CH-4012 Basel, Switzerland;

^bChronobiology and Sleep Research Group, Institute of Pharmacology and Toxicology, University of Zurich, CH-8057 Zürich, Switzerland; and

^cAllergy Unit, Department of Dermatology, University Hospital Basel, CH-4031 Basel, Switzerland

¹S.A.B. and A.E. contributed equally to this work.

²To whom correspondence may be addressed:

E-mail: steven.brown@pharma.uzh.ch or anne.eckert@upkbs.ch.

Author contributions: L.P., C.C., A.W.-J., S.A.B., and A.E. designed research; L.P., K.S., F.M., J.I., and K.R. performed research; A.V. contributed new reagents/analytic tools; L.P., S.A.B., and A.E. analyzed data; and L.P., S.A.B., and A.E. wrote the paper.

Proc Natl Acad Sci U S A. 2011 Apr 26;108(17):7218-23. doi: 10.1073/pnas.1008882108.
Epub 2011 Apr 11.

Edited by Joseph S. Takahashi, Howard Hughes Medical Institute, University of Texas Southwestern Medical Center, Dallas, TX, and approved March 14, 2011 (received for review July 1, 2010)

Serum factors in older individuals change cellular clock properties

Lucia Pagani^{a,b}, Karen Schmitt^a, Fides Meier^a, Jan Izakovic^c, Konstanze Roemer^d, Antoine Viola^e, Christian Cajochen^e, Anna Wirz-Justice^e, Steven A. Brown^{b,1,2}, and Anne Eckert^{a,1,2}

^aNeurobiology Laboratory for Brain Aging and Mental Health, ^dForensic Psychiatry, and ^eCentre for Chronobiology, Psychiatric University Clinics, University of Basel, CH-4012 Basel, Switzerland; ^bChronobiology and Sleep Research Group, Institute of Pharmacology and Toxicology, University of Zurich, CH-8057 Zurich, Switzerland; and ^cAllergy Unit, Department of Dermatology, University Hospital Basel, CH-4031 Basel, Switzerland

Edited* by Joseph S. Takahashi, Howard Hughes Medical Institute, University of Texas Southwestern Medical Center, Dallas, TX, and approved March 14, 2011 (received for review July 1, 2010)

Human aging is accompanied by dramatic changes in daily sleep–wake behavior: Activity shifts to an earlier phase, and the consolidation of sleep and wake is disturbed. Although this daily circadian rhythm is brain-controlled, its mechanism is encoded by cell-autonomous circadian clocks functioning in nearly every cell of the body. In fact, human clock properties measured in peripheral cells such as fibroblasts closely mimic those measured physiologically and behaviorally in the same subjects. To understand better the molecular mechanisms by which human aging affects circadian clocks, we characterized the clock properties of fibroblasts cultivated from dermal biopsies of young and older subjects. Fibroblast period length, amplitude, and phase were identical in the two groups even though behavior was not, thereby suggesting that basic clock properties of peripheral cells do not change during aging. Interestingly, measurement of the same cells in the presence of human serum from older donors shortened period length and advanced the phase of cellular circadian rhythms compared with treatment with serum from young subjects, indicating that a circulating factor might alter human chronotype. Further experiments demonstrated that this effect is caused by a thermolabile factor present in serum of older individuals. Thus, even though the molecular machinery of peripheral circadian clocks does not change with age, some age-related circadian dysfunction observed in vivo might be of hormonal origin and therefore might be pharmacologically remediable.

chronobiology | peripheral oscillators | human behavior

Circadian clocks possess an endogenous periodicity of about 24 h and play a key role in physiological adaptation to the solar day for all living organisms, from cyanobacteria and fungi (1) to insects (2) and mammals (3). Circadian clocks influence nearly all aspects of physiology and behavior, including sleep–wake cycles, body temperature, and the function of many organs (3). During normal aging, clock function is attenuated, with consequences both for health and quality of life. Older individuals have an earlier phase of everyday activity compared with the young (4). Not only is the consolidation of sleep and wake dramatically reduced (5, 6), but overall circadian amplitude of hormones and body temperature are lower (7, 8), and many aging-associated sleep–wake pathologies have been reported (9–11). As a result, one in five healthy older individuals reports taking sleep medications regularly (9). In cases of pathological aging, chronobiological disturbance is even more acute: Huntington disease, Parkinson disease, and Alzheimer’s disease are all associated with profound alterations in sleeping patterns (10–12). These effects of aging on circadian rhythms—diminished circadian amplitude, earlier phase, shorter circadian period, and desynchronization of rhythms in peripheral organs—have been observed widely in several species of mammals (7, 13, 14). Paradoxically, however, even though the behavioral phase is earlier in aged humans, multiple studies conclude that the free-running period remains unchanged (15–18). Thus, changes in phase have been ascribed

to alterations in overall circadian amplitude and changed sleep architecture. However, the nature and mechanism of these changes remains entirely unknown.

Mammalian circadian clocks are organized in a hierarchical fashion: The suprachiasmatic nuclei (SCN) of the anterior hypothalamus serve as a master clock, receiving light signals from the external environment via the retina and retino-hypothalamic tract and elaborating these stimuli into signals that are sent all over the body to synchronize clocks in peripheral organs (3). Interestingly, the clock mechanism itself is cell-autonomous and involves interlocked feedback loops of transcription and translation. These loops are encoded by dedicated clock genes: For example, in one loop the heterodimer formed by the two transcription factors CLOCK and BMAL1 binds *cis*-acting E-box sequences present in *Per* and *Cry* gene promoters to activate their transcription. Subsequently, PER and CRY protein complexes inhibit the activity of CLOCK–BMAL1. As a consequence, *Cry* and *Per* mRNAs decrease in concentration, and a new cycle can start (19).

At a cellular level, the SCN and peripheral oscillators share the same molecular mechanism (20). Thus, cellular reporters composed of clock gene promoters driving expression of luciferase or GFP have proven to be very useful tools for the study of circadian rhythms in the SCN as well as in peripheral oscillators (21, 22). Using such reporters, we have shown previously that many differences in human circadian behavior also can be seen at a molecular level in peripheral cells. For example, the cellular clocks of early chronotypes (i.e., “larks”) have shorter circadian periods than those of later chronotypes (“owls”) (23), and circadian period length *in vitro* is proportional to physiological period *in vivo* (24). Under entrained conditions in which cellular clocks are constrained to 24 h via an entrainment protocol that mimics diurnal variations in mammalian body temperature (25), fibroblasts show the early or late circadian phases of their owners (23).

In principle, alterations in circadian behavior caused by aging could arise by a variety of mechanisms. Changing neural networks might perturb sleep–wake timing or alter the communication between the SCN clock and other brain regions. Hormonal signals critical for maintaining physiological homeostasis might be perturbed. On a cellular level, molecular changes associated with aging (e.g., oxidative damage, telomere attrition) might alter basic clock function. In this paper we have addressed the effects of

Author contributions: L.P., C.C., A.W.-J., S.A.B., and A.E. designed research; L.P., K.S., F.M., J.I., and K.R. performed research; A.V. contributed new reagents/analytic tools; L.P., S.A.B., and A.E. analyzed data; and L.P., S.A.B., and A.E. wrote the paper.

The authors declare no conflict of interest.

*This Direct Submission article had a prearranged editor.

¹S.A.B. and A.E. contributed equally to this work.

²To whom correspondence might be addressed. E-mail: steven.brown@pharma.uzh.ch or anne.eckert@upkbs.ch.

This article contains supporting information online at www.pnas.org/lookup/suppl/doi:10.1073/pnas.1008882108/-DCSupplemental.

aging on molecular circadian clock properties using a fibroblast-based assay. Our results are consistent with the hypothesis that the molecular machinery of circadian rhythms in peripheral oscillators is not altered by age but that molecules present in serum might be responsible for some of the circadian changes that occur in the elderly.

Results

Aging Changes Human Circadian Behavior in Vivo but Does Not Alter Fibroblast Circadian Clocks in Vitro. To try to understand the molecular changes that might underlie modifications in daily behavior in elderly individuals, we characterized the circadian rhythms of dermal skin fibroblasts obtained from young and older donors. Subjects were recruited based on age but also were asked to give information about daytime preference (their preferred waking time and bedtime both on workdays and during leisure) by completing the Munich Chronotype Questionnaire (MCTQ) (26). The 18 young and 18 older sex-matched subjects participating in our study are summarized in Table S1 and are described individually in Table S2.

From the completed MCTQ, older subjects in our study displayed a significantly earlier sleep phase compared with young subjects (Fig. 1A; unpaired *t* test; $P < 0.01$). This difference reflected well the epidemiological trend that is observed in the general population, e.g., as reported by Roenneberg and colleagues (27). To characterize possible cellular origins of these differences, two 2-mm dermal punch biopsies were taken from every subject. Primary fibroblast cultures were isolated from the biopsies and infected with a lentivirus that harbored a circadian reporter construct (the *Bmal1* promoter driving expression of the firefly luciferase gene (28)). Circadian clocks in infected fibroblast cultures were synchronized with dexamethasone (29), and circadian bioluminescence corresponding to *Bmal1* promoter activity was measured for at least 5 d under constant conditions in a cell-culture incubator. The circadian oscillations from fibroblasts from young and elderly subjects then were examined systematically for differences in period length, amplitude, and phase. It had been shown previously that chronotype correlates negatively with period length in vivo (30) and in vitro (23). Hence, if the origins of aging-related differences were cell intrinsic, we hoped to see correlations between clock properties in vitro and subject age.

The period length for each individual is shown in Fig. 1B. As we have reported for other subject populations (28), fibroblast period differed significantly among different individuals but not between

different biopsies from the same individual (Fig. S1A). No differences were observed between the groups (Fig. 1B *Inset*; unpaired *t* test; $P > 0.05$; and Table S1). Additionally, no correlation was seen between period length and MCTQ sleep phase in either older or younger subjects (Fig. S1B; linear regression: $P > 0.05$). [Previous studies showing correlations between questionnaire-based sleep-wake behavior and period length were based on comparisons of extreme early vs. late chronotypes (23, 30).]

In addition to period length, other clock properties include amplitude (the difference between peak and nadir expression values) and phase (the relative timing of each cycle relative to a periodic entraining stimulus). We also studied the circadian amplitude of the oscillations that we observed in vitro. No correlation with aging was observed, nor did amplitude correlate with fibroblast cell passage number (i.e., a longer or shorter time in cultivation) (Fig. S2A–C; unpaired *t* test; $P > 0.05$).

Theoretically and biologically, period and phase are tightly coupled: A longer period leads to a later phase. Under certain circumstances, amplitude and phase also are coupled, with lower amplitude leading to earlier phase (23). Nevertheless, phase differences also can be driven by rhythmic inputs from outside the circadian oscillator (e.g., by the timing of light to the retina in mammals). To measure circadian phase in fibroblasts in vitro, we entrained fibroblast clocks to a 24-h daily cycle using periodic oscillations of incubator temperature between 34 and 37 °C. After 6 d, fibroblast daily rhythms entrained well to these cycles in both young and old subjects regardless of their period lengths. On day 7, we measured the phase of reporter gene expression relative to the temperature cycle. An earlier phase was not observed in older vs. younger subjects (Fig. S2D; unpaired *t* test; $P > 0.05$), confirming the lack of effect of subject age on period and amplitude that we already had observed. In total, none of the physiological signs of human circadian aging could be detected or duplicated in cultured fibroblasts from elder subjects.

Human Sera Influence Fibroblast Circadian Period Length and Phase.

Even if the peripheral cells of elderly subjects do not differ from younger subjects in their chronobiological properties, it is well documented that the milieu in which these cells are found undergoes dramatic changes as individuals age (7, 31), and peripheral organs certainly show altered function with aging (7, 13, 14, 17, 32). If cellular circadian properties per se do not change with aging, we reasoned that age-related circadian alterations might be provoked by a circulating factor. To test this possibility,

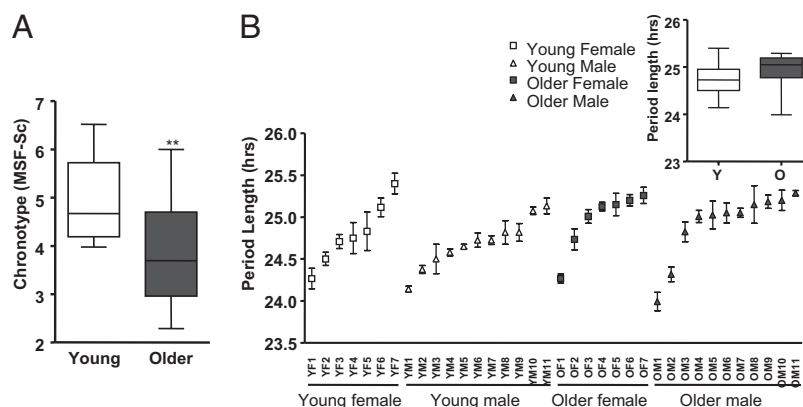


Fig. 1. Influence of age on period length and chronotype. (A) Chronotype of young and old subjects, as measured by the MCTQ. The y axis shows subject MSF-Sc. This statistic (the output of the MCTQ) is widely used as a reliable measure of human chronotype (27). Dataset variation is shown as a standard boxplot ($n = 18$; unpaired *t* test; $**P < 0.01$). (B) Period length of the primary fibroblasts of each subject participating in this study. For ease of display, data are sorted on the basis of the period length. Data are mean of six independent measurements of the period length for every subject \pm SEM. (*Inset*) Population average of period lengths of skin fibroblasts from young (Y) and older (O) subjects, shown as a standard boxplot. No statistical difference was observed ($n = 18$; unpaired *t* test; $P > 0.05$).

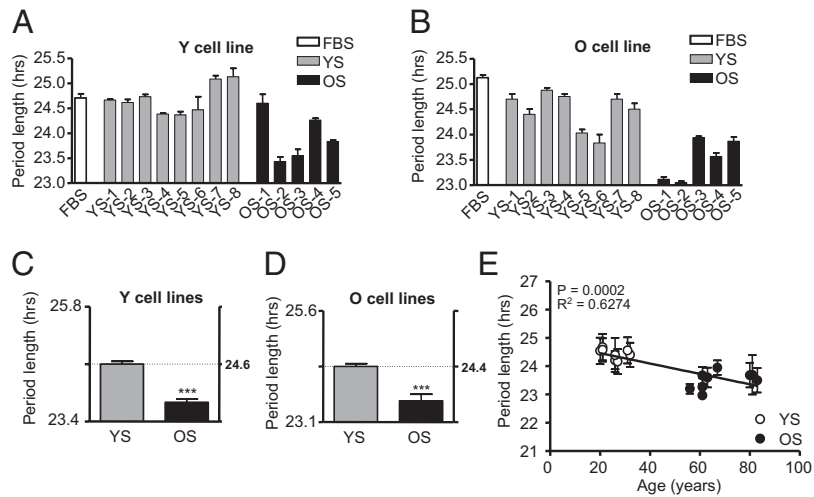


Fig. 2. Length of circadian period of skin fibroblasts treated with media containing human serum. (A) Lengths of circadian period in one representative cell line taken from a young subject (Y) measured in medium containing FBS (white) and media containing human serum from eight young (YS; gray) and five older (OS; black) donors. Bars represent the mean of three independent measurements \pm SEM. (B) Equivalent measurements from a representative cell line from an older subject (O). (C) Bar graph showing the average differences in period length in four Y cell lines treated with YS and OS. Results are expressed as average \pm SEM. (D) Equivalent measurements for two O cell lines. In both cases, treatment with YS gave a highly different period length (unpaired *t* test; $***P < 0.001$ compared with the treatment with OS in Y cell lines). (E) Average period length across experiments using human serum, as a function of the age of the serum donor (linear regression: $P < 0.0002$; $r^2 = 0.6274$).

we replaced the normal standardized FBS used in our cell cultures with human serum harvested from donors of different ages. The circadian rhythms of four young (Y) and two old (O) cell lines were measured in the presence of eight different media containing human serum from young (YS) male donors and five different media containing human serum from three older male donors and two postmenopausal female donors (OS). Data regarding these blood donors are listed in Table S3. Fig. 2A and B shows representative data from one Y and one O fibroblast cell line tested with all sera. (The complete data set is shown in Fig S3.) Fig. 2C and D shows averages from all cell lines and all sera collectively. Irrespective of whether the treated fibroblasts were from young or older subjects, cells measured in serum from older donors had a significantly shorter circadian period than cells in serum from young donors (Fig. 2C and D; unpaired *t* test; $P_Y < 0.001$; $P_O < 0.001$). In the presence of YS, cells from young and older subjects showed a period length of 24.61 ± 0.18 h and 24.35 ± 0.18 h, respectively, whereas in the presence of OS cells from young and older subjects showed a period length of 23.79 ± 0.16 h and 23.60 ± 0.33 h, respectively. Analyzed individually, period measurements with different sera showed a strong correlation between donor age and period length (Fig. 2E; $P < 0.0001$; $R^2 = 0.91$).

Because changes in period are coupled to changes in phase (as described above), to verify these results we wanted to ensure that the dramatic changes in circadian period that we observed were mirrored by corresponding changes in phase. Using the temperature entrainment paradigm described earlier to entrain clocks in all cells to rhythms of 24 h, we measured the circadian phase after temperature entrainment of two Y cell lines and two O cell lines in the presence of two YS and two OS. Serum from older subjects indeed phase-advanced the circadian rhythms of cells from both young (Fig. 3A) and older (Fig. 3B) subjects, compared with the same cells in YS (unpaired *t* test; $P < 0.05$), and there was a strong correlation between period length and phase shifting in individual sera (Fig. 3C; $P = 0.0265$; $R^2 = 0.66$). Therefore, the shortened period observed with sera from older individuals manifested as earlier phase under entrained conditions, at least in cells.

Influence of Human Serum on Period Length Is Caused by Heat-Sensitive Substances in Sera from Older Subjects. Our results suggested that one or more substances in human serum can recapitulate at a cellular level the differences in circadian phase seen between younger and older subjects. In principle, such effects could arise from substances either in YS or in OS. To investigate further the nature of the substance(s) responsible for the aging effects, we attempted to heat-inactivate four YS

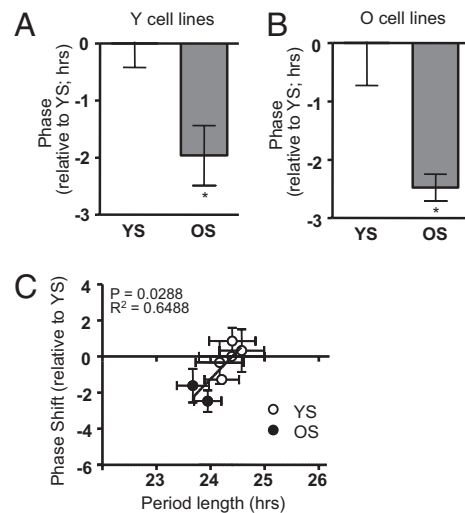


Fig. 3. Circadian phase of fibroblasts in the presence of serum from young and older subjects. (A) Phase of cell lines from young subjects (Y) was determined after temperature entrainment in the presence of serum from younger subjects (YS) or from older subjects (OS). Results are expressed as phase difference (in h) between the two treatments. Each bar results from the average of two different cell lines, each treated with two different sera, \pm SEM. (B) Equivalent data using cell lines from older subjects. In both cases, there was a significant advance in the phase of cells treated with OS compared with the same cell lines treated with YS (unpaired *t* test; $*P < 0.05$). (C) Correlation between phase-shift differences seen in this figure and differences in period length seen in Fig. 2. Phase shifts are plotted relative to the average phase for all sera from young subjects (linear regression: $P = 0.0265$; $r^2 = 0.6488$).

did not show differences in period length compared with untreated cells, we conclude that cortisol is not the factor responsible for our effects (Fig. S5D).

Discussion

In this study, we have shown that skin fibroblasts taken from young and older subjects do not differ in their circadian properties per se, but incubation of both cells in serum from older subjects results in a shortening of circadian period and a shift to earlier phase compared with incubation with serum from younger subjects. Moreover, the effects that we observe are caused by a thermolabile activity in serum from older subjects. Our results suggest that hormonal changes can alter cellular clocks, and these changes in turn might underlie the differences in circadian behavior caused by aging.

Various theories have been proposed to explain a shift toward earlier behavior in elderly individuals. According to one hypothesis, fragmentation of the sleep–wake cycle coupled with increased daytime napping results in less nighttime sleep and a shift to an earlier activity phase (6, 33). In this scenario, changes in sleep structure alter self-selected timing of light, and thereby circadian phase. Such changes in sleep structure might be caused by age-related reduction in the evening circadian signal that opposes homeostatic sleep pressure (15, 34). According to another theory, changes in eye physiology with age (e.g., lens yellowing and senile miosis or cataracts) and changes in behavior (less time in direct sunlight outdoors) are thought to reduce the entraining effects of solar light, exacerbating a circadian entrainment problem in elderly individuals (35). Recent studies corroborate these hypotheses and demonstrate clearly that the circadian system in the elderly is less sensitive to light (36, 37).

The results that we present provide an additional cellular explanation for the shift toward earlier chronotype based on changes in hormone balance in elderly individuals. The putative causal factor could be constantly present in serum and use asymmetry in phase-response curves to shift overall phase. In this case, we would expect that the magnitude of the factor would be different in older and younger individuals at all times of day. Alternatively, if the factor were rhythmically secreted, it could have the same amplitude but a different phase profile in older and younger individuals. In this case, the difference in abundance that we saw by sampling at a single time would reflect different circadian dynamics of the putative clock-modifying substance in older and younger individuals.

Nevertheless, there is one obvious problem with this idea: Excellent studies suggest that the physiological period of human beings does not change with age (15, 16, 38). If a circulating hormone were shortening period, then why does free-running physiological period remain unchanged? We propose that such a factor might act upon non-SCN regions of the human brain and periphery but not upon the SCN itself. This hypothesis would explain our data and also would explain nicely why the phase of sleep–wake timing is shifted earlier relative to the timing of the endogenous circadian clock even in “forced desynchrony” laboratory studies. In rodents, brain structures other than the SCN (e.g., hippocampus, thalamus, and cortex) actually show an entrainment reminiscent of peripheral cells: They have a clock phase 4 h later than the SCN, and they are entrained to feeding and temperature-entrainment signals, whereas the SCN is not (25, 39). Other types of decoupling of locomotor activity rhythms from SCN clock phase (e.g., by methamphetamine in rats or by darkness in certain mouse strains) also are accompanied by alterations in the phase of clock gene expression in non-SCN brain areas (40, 41).

Overall, compelling evidence exists for all three models, and it is likely that each could contribute to the dramatic changes in behavior seen in elderly individuals (a model is shown in Fig. 4D). Our findings open the possibility that circadian difficulties

associated with aging might be hormonally driven in part and therefore might be pharmacologically treatable without recourse to potentially addictive sleep aids. If so, this approach would represent a major benefit to health.

Materials and Methods

Subject Recruitment Criteria and Chronotype Determination. Eighteen healthy young (age 21–30 y) and 18 healthy older subjects (age 60–88 y) were chosen for participation based on age alone and were asked to fill out the MCTQ. MSF-Sc was calculated from this questionnaire and used as a measure of chronotype (26). Subject statistics are shown in Table S1. Prior ethical consent for the use of human skin tissues was given by the Ethical Committee of Basel, and informed written consent for participation in this study was obtained from all human subjects.

Tissue Isolation, Fibroblast Culture, and Viral Infection. Two cylindrical cutaneous biopsies (2 mm diameter) were taken from the buttocks of each recruited healthy subjects. Fibroblasts were isolated from biopsies by 4-h digestion of tissue in DMEM/1% penicillin streptomycin (Sigma)/1% Glutamax (Sigma) (DMEMc)/20% FBS (Sigma)/87.5 ng/mL Liberase (Roche), and cultured in DMEMc/20% FBS. Confluent cells were infected using Bmal1::luciferase lentivirus. Transfected cells were positively selected 3 d after infection (28).

Harvesting of Sera. At 2:00 PM, 45 mL of blood were collected from eight healthy young male (age 25.5 ± 4.6 y) and five healthy older (three male and two postmenopausal female; age 74.4 ± 9.8 y) subjects in clot-activator vacutainers (BD Vacutainer System). Whole blood was incubated 30 min at room temperature and then centrifuged 10 min at $2,000 \times g$. Serum was harvested and stored at -20°C . When specified, human serum was heat-inactivated by treatment for 30 min at 56°C .

Synchronization and Measurement of Circadian Period and Phase. Five days or more after human fibroblast infection, circadian rhythms were synchronized by 100 nM dexamethasone (Sigma) in DMEMc + 20% FBS (42). DMEMc without phenol red was supplemented with 0.1 mM luciferin (Molecular Probes) to obtain the counting medium (CM), and light output was measured in homemade light-tight atmosphere-controlled boxes for at least 5 d. To measure the fibroblast basal circadian rhythms, CM was supplemented with 10% FBS; to determine the influence of human serum on circadian period length, CM was supplemented with 10% human serum; to determine the influence of cortisol on period length, CM was supplemented with 10% FBS or 10% FBS and 25 ng/mL cortisol (Sigma) or 10% FBS and 75 ng/mL cortisol; to determine the influence of heat-inactivated human serum on period length, CM was supplemented with 10% heat-inactivated human serum. For phase determination experiments, cells in luciferin-supplemented medium were synchronized by incubation for 6 d in a temperature-controlled incubator under a 16 h/8 h $35^\circ\text{C}/37^\circ\text{C}$ daily temperature cycle. On day 7, cells were transferred to the Lumicycle device at 37°C , and bioluminescence was measured for an additional 16 h. Cellular phase was determined by measuring the time of the transcriptional maximum of reporter gene expression in the smoothed and normalized dataset during this interval (23).

Melatonin Determination in Sera. A direct double-antibody RIA was used for the melatonin assay, validated by gas chromatography-mass spectroscopy (Buehlmann Laboratories). The minimum detectable dose of melatonin (analytical sensitivity) was determined to be 0.2 pg/mL. The functional least-detectable dose using the <20% coefficient of interassay variation criterion was <0.65 pg/mL. Melatonin concentrations in the sera were expressed as pg/mL of serum.

Cortisol Determination in Sera. Quantification of cortisol in sera was performed using a Cortisol ELISA Kit (R&D) following the manufacturer's instruction. Cortisol concentration in the sera was expressed as ng/mL of serum, and the assays were performed in duplicate.

Statistical Methods. Details of statistical methods are given in *SI Materials and Methods*.

ACKNOWLEDGMENTS. We thank Robert Dallmann for critical reading of this manuscript. This project was supported by Grant E.U. #LSHM-CT-2006-018741 from EUCLOCK, Grants #310000-122572 and #31003-113874 from the Swiss National Science Foundation, and by grants from the Désirée et Niels Yde Foundation and from the Fonds der Freiwilligen Akademischen Gesellschaft Basel.

1. Brunner M, Schafmeier T (2006) Transcriptional and post-transcriptional regulation of the circadian clock of cyanobacteria and Neurospora. *Genes Dev* 20:1061–1074.
2. Rosato E, Tauber E, Kyriacou CP (2006) Molecular genetics of the fruit-fly circadian clock. *Eur J Hum Genet* 14:729–738.
3. Gachon F, Nagoshi E, Brown SA, Ripperger J, Schibler U (2004) The mammalian circadian timing system: From gene expression to physiology. *Chromosoma* 113:103–112.
4. Roenneberg T, et al. (2004) A marker for the end of adolescence. *Curr Biol* 14:R1038–R1039.
5. Renfrew JW, Pettigrew KD, Rapoport SI (1987) Motor activity and sleep duration as a function of age in healthy men. *Physiol Behav* 41:627–634.
6. Dijk DJ, Duffy JF, Czeisler CA (2001) Age-related increase in awakenings: Impaired consolidation of nonREM sleep at all circadian phases. *Sleep* 24:565–577.
7. Ferrari E, et al. (2001) Age-related changes of the hypothalamic-pituitary-adrenal axis: Pathophysiological correlates. *Eur J Endocrinol* 144:319–329.
8. Weinert D (2010) Circadian temperature variation and ageing. *Ageing Res Rev* 9(1):51–60.
9. Englert S, Linden M (1998) Differences in self-reported sleep complaints in elderly persons living in the community who do or do not take sleep medication. *J Clin Psychiatry* 59:137–144, quiz 145.
10. Morton AJ, et al. (2005) Disintegration of the sleep-wake cycle and circadian timing in Huntington's disease. *J Neurosci* 25:157–163.
11. Wu YH, Swaab DF (2007) Disturbance and strategies for reactivation of the circadian rhythm system in aging and Alzheimer's disease. *Sleep Med* 8:623–636.
12. Willis GL (2008) Parkinson's disease as a neuroendocrine disorder of circadian function: Dopamine-melatonin imbalance and the visual system in the genesis and progression of the degenerative process. *Rev Neurosci* 19:245–316.
13. Davidson AJ, Yamazaki S, Arble DM, Menaker M, Block GD (2008) Resetting of central and peripheral circadian oscillators in aged rats. *Neurobiol Aging* 29:471–477.
14. Yamazaki S, et al. (2002) Effects of aging on central and peripheral mammalian clocks. *Proc Natl Acad Sci USA* 99:10801–10806.
15. Dijk DJ, Duffy JF, Riel E, Shanahan TL, Czeisler CA (1999) Ageing and the circadian and homeostatic regulation of human sleep during forced desynchrony of rest, melatonin and temperature rhythms. *J Physiol* 516:611–627.
16. Duffy JF, Dijk DJ, Klerman EB, Czeisler CA (1998) Later endogenous circadian temperature nadir relative to an earlier wake time in older people. *Am J Physiol* 275:R1478–R1487.
17. Duffy JF, et al. (2002) Peak of circadian melatonin rhythm occurs later within the sleep of older subjects. *Am J Physiol Endocrinol Metab* 282:E297–E303.
18. Yoon IY, et al. (2003) Age-related changes of circadian rhythms and sleep-wake cycles. *J Am Geriatr Soc* 51:1085–1091.
19. Ripperger J, Brown SA (2009) *The Circadian Clock*, ed Albrecht U (Springer, New York), Vol 12, pp 37–78.
20. Yagita K, Tamanini F, van Der Horst GT, Okamura H (2001) Molecular mechanisms of the biological clock in cultured fibroblasts. *Science* 292:278–281.
21. Lowrey PL, et al. (2000) Positional syntenic cloning and functional characterization of the mammalian circadian mutation tau. *Science* 288:483–492.
22. Yoo SH, et al. (2004) PERIOD2:LUCIFERASE real-time reporting of circadian dynamics reveals persistent circadian oscillations in mouse peripheral tissues. *Proc Natl Acad Sci USA* 101:5339–5346.
23. Brown SA, et al. (2008) Molecular insights into human daily behavior. *Proc Natl Acad Sci USA* 105:1602–1607.
24. Pagani L, et al. (2010) The physiological period length of the human circadian clock in vivo is directly proportional to period in human fibroblasts. *PLoS ONE* 5:e13376.
25. Brown SA, Zumberg G, Fleury-Olela F, Preitner N, Schibler U (2002) Rhythms of mammalian body temperature can sustain peripheral circadian clocks. *Curr Biol* 12:1574–1583.
26. Roenneberg T, Wirz-Justice A, Mrosovsky M (2003) Life between clocks: Daily temporal patterns of human chronotypes. *J Biol Rhythms* 18:80–90.
27. Roenneberg T, et al. (2007) Epidemiology of the human circadian clock. *Sleep Med Rev* 11:429–438.
28. Brown SA, et al. (2005) The period length of fibroblast circadian gene expression varies widely among human individuals. *PLoS Biol* 3:e338.
29. Balsalobre A, Marcacci L, Schibler U (2000) Multiple signaling pathways elicit circadian gene expression in cultured Rat-1 fibroblasts. *Curr Biol* 10:1291–1294.
30. Duffy JF, Rimmer DW, Czeisler CA (2001) Association of intrinsic circadian period with morningness-eveningness, usual wake time, and circadian phase. *Behav Neurosci* 115:895–899.
31. Van Cauter E, Plat L, Leproult R, Copinschi G (1998) Alterations of circadian rhythmicity and sleep in aging: Endocrine consequences. *Horm Res* 49:147–152.
32. Dori D, et al. (1994) Chrono-neuroendocrinological aspects of physiological aging and senile dementia. *Chronobiologia* 21:121–126.
33. Dijk DJ, Duffy JF (1999) Circadian regulation of human sleep and age-related changes in its timing, consolidation and EEG characteristics. *Ann Med* 31:130–140.
34. Cajochen C, Münch M, Knoblauch V, Blatter K, Wirz-Justice A (2006) Age-related changes in the circadian and homeostatic regulation of human sleep. *Chronobiol Int* 23:461–474.
35. Charman WN (2003) Age, lens transmittance, and the possible effects of light on melatonin suppression. *Ophthalmic Physiol Opt* 23:181–187.
36. Duffy JF, Zeitzer JM, Czeisler CA (2007) Decreased sensitivity to phase-delaying effects of moderate intensity light in older subjects. *Neurobiol Aging* 28:799–807.
37. Sletten TL, Revell VL, Middleton B, Lederle KA, Skene DJ (2009) Age-related changes in acute and phase-advancing responses to monochromatic light. *J Biol Rhythms* 24:73–84.
38. Duffy JF, Czeisler CA (2002) Age-related change in the relationship between circadian period, circadian phase, and diurnal preference in humans. *Neurosci Lett* 318:117–120.
39. Damiola F, et al. (2000) Restricted feeding uncouples circadian oscillators in peripheral tissues from the central pacemaker in the suprachiasmatic nucleus. *Genes Dev* 14:2950–2961.
40. Abe H, Honma S, Namihira M, Masubuchi S, Honma K (2001) Behavioural rhythm splitting in the CS mouse is related to clock gene expression outside the suprachiasmatic nucleus. *Eur J Neurosci* 14:1121–1128.
41. Masubuchi S, et al. (2000) Clock genes outside the suprachiasmatic nucleus involved in manifestation of locomotor activity rhythm in rats. *Eur J Neurosci* 12:4206–4214.
42. Balsalobre A, et al. (2000) Resetting of circadian time in peripheral tissues by glucocorticoid signaling. *Science* 289:2344–2347.

Supporting Information

Pagani et al. 10.1073/pnas.1008882108

SI Materials and Methods

Statistical Methods: Period. For each luciferase measurement, the period of oscillation was calculated by least-mean-squares fitting of dampened sine wave functions to the actual data. The period of the sine wave with the best least-squares fit to the data was assumed to be the true period of oscillation. Because the period length of the first day after synchronization varied according to the conditions of synchronization, it was not included in these calculations; rather, period was determined by analyzing only days 2–5. For each period measurement, at least three separate ex-

perimental measurements were done for each biopsy, using two biopsies from each individual. Period values are presented as mean \pm SE.

Statistical Methods: Relative Amplitude. The amplitudes of the second and third cycles of circadian expression were obtained as the difference between the peak and nadir expression values of these cycles. These measurements then were normalized using the absolute raw-data magnitude of the first peak as an approximate measure of reporter virus infection efficiency in each culture.

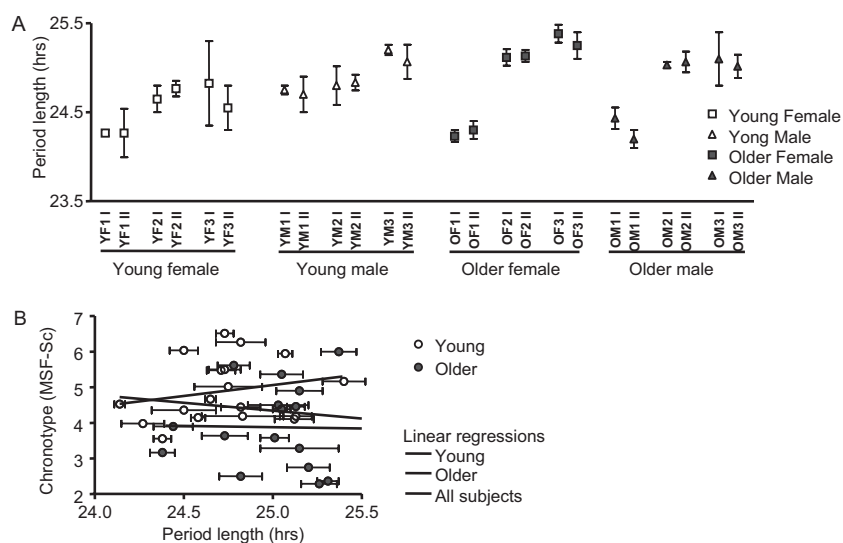


Fig. S1. (A) Period lengths obtained from two different biopsies taken from three young females (YF), three young males (YM), three older females (OF), and three older males (OM). Each bar represents the mean of three independent measurements per biopsy \pm SEM. (B) Comparison between chronotype and in vitro circadian period length for the two groups of subjects ($P_{all\ subjects} = 0.3707$; $P_Y = 0.3785$; $P_O = 0.9229$). The x axis shows period length in hours. Period length values are shown as the mean of six independent measurements \pm SEM. The y axis shows subject mean sleep phase corrected for sex and cumulative sleep debt (MSF-Sc). This statistic is the output of the Munich Chronotype Questionnaire and is widely used as a reliable measure of human chronotype.

Table S3. Blood donor characteristics

Blood donor	Sex	Age (y)	Medications
Y1	M	21	No
Y2	M	20	No
Y3	M	32	Citalopram-hormosan (120 mg/d)
Y4	M	21	No
Y5	M	26	No
Y6	M	27	No
Y7	M	31	No
Y8	M	26	No
O1	M	81	Daflon (500 mg/d)
O2	F	83	Aspirine Cardio (100 mg/d); metoprolol (50 mg/d); perindopril/indapamin (4 mg/d/1.25 mg/d)
O3	F	67	No
O4	M	80	Aspirine Cardio (100 mg/d); amlodipine maleate (2.5 mg/d); chlorthalidone (12,5 mg/d)
O5	M	61	Aspirine Cardio (100 mg/d); simvastatin (40 mg/d)
O6	F	61	No
O7	M	63	No
O8	F	56	No
O9	M	61	No

O, old; Y, young.

B. Aging and Circadian Disruption: Causes and Effects

Authors: Brown SA¹, Schmitt K², and Eckert A²

Affiliations:

¹ Department of Pharmacology and Toxicology, University of Zurich, Zurich, Switzerland

² Neurobiology Laboratory for Brain Aging and Mental Health, Psychiatric University Clinics Basel, Basel, Switzerland

Correspondence to Steven A. Brown, steven.brown@pharma.uzh.ch and Anne Eckert, anne.eckert@upkbs.ch.

AGING, August 2011 Vol. 3. No 8

Received: 7/09/11; Accepted: 7/27/11; Published: 8/22/11

Aging and Circadian Disruption: Causes and Effects

Steven A. Brown¹, Karen Schmitt², and Anne Eckert²

¹Department of Pharmacology and Toxicology, University of Zurich, Zurich, Switzerland

²Neurobiology Laboratory for Brain Aging and Mental Health, Psychiatric University Clinics Basel, Basel, Switzerland

Key words: circadian rhythms, aging, fibroblasts, peripheral cells, sleep

Received: 7/09/11; Accepted: 7/27/11; Published: 8/22/11

Correspondence to Steven A. Brown, steven.brown@pharma.uzh.ch and Anne Eckert, anne.eckert@upkbs.ch

Copyright: © Eckert et al. This is an open-access article distributed under the terms of the Creative Commons Attribution License, which permits unrestricted use, distribution, and reproduction in any medium, provided the original author and source are credited

Abstract: The relationship between aging and daily “circadian” behavior in humans is bidirectional: on the one hand, dysfunction of circadian clocks promotes age-related maladies; on the other, aging *per se* leads to changes and disruption in circadian behavior and physiology. For the latter case, recent research suggests that changes to both homeostatic and circadian sleep regulatory mechanisms may play a role. Could hormonal changes be in part responsible?

INTRODUCTION

Increasing evidence suggests that disruption of circadian clock function – either genetically or environmentally – can exacerbate a wide range of age-related pathologies, ranging from cataracts to cancer. An excellent review on this subject was published recently in this journal [1]. Equally relevant, however, and even more painfully obvious, is the impairment of circadian function that occurs as a natural process of aging. The German language has invented the term “*senile Bettflucht*” (literally, senile bed evacuation) to describe the difficulty that elderly individuals have in sleeping at night, and the early hour at which they rise. Indeed, one in four aged persons reports regular use of a prescribed sleep medication [2]. Since such medications treat only the symptoms and are also potentially addictive, the origins of this sleep disturbance are an important public health question.

Age-related sleeping difficulties are actually twofold. On the one hand, elderly individuals will rise and also go to bed an average of two hours earlier than young adults [3]. Secondly, their nighttime sleep is considerably more fragmented, and contains a much lower proportion of “deep” or slow-wave sleep (SWS)

[4]. Whether these two phenomena are linked or independent remains a subject of debate. Underlying causes are a matter of speculation.

Recently, by using primary human fibroblast cells as a model system, our laboratories reported that serum-borne factors (i.e. hormones) could play a role in age-related circadian disturbances [5]. Rather than being a comprehensive review, this Perspective is an attempt to set our findings more explicitly within the context of other data in the field than was possible in the context of the original research communication.

THE EXPERIMENT UNDER DISCUSSION

Exploiting the fact that human circadian clocks are conserved in most cell types, Pagani et al. examined the circadian properties of primary fibroblasts from older and younger individuals. Although the cells from both groups showed identical circadian properties (period, amplitude, entrained phase) when cultured identically, inclusion of serum from older individuals resulted in a shortening of circadian period and an earlier entrained phase in either cell type. This change was likely due to a substance in the serum of older individuals, because heat treatment gave older persons’ sera the circadian

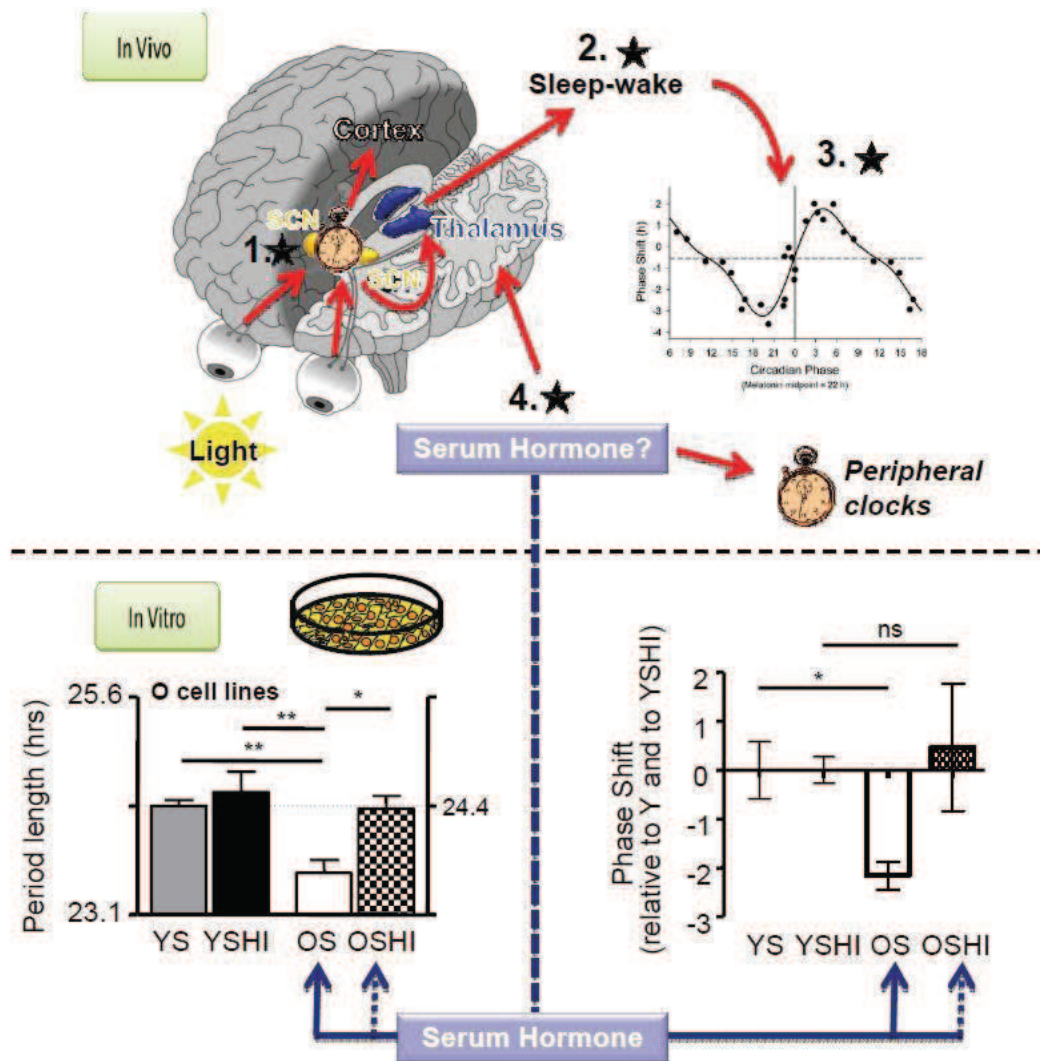


Figure 1: Top panel. *In vivo*, a central clock in the suprachiasmatic nucleus (SCN) determines the timing of daily behavior, and communicates this timing to peripheral clocks in other tissues and brain loci that control sleep. The timing of sleep influences clock phase by controlling when the eyes receive environmental light. *Inset graph*, This light phase-shifts the clock differently at different times of day (Data reproduced from [11]). *Black stars*, Feedback loops affecting sleep in the elderly. 1. A shorter period in the SCN would shift sleep earlier, but this has not been observed experimentally in humans. 2. Changes to sleep-wake structure, either by affecting homeostatic sleep or by affecting the circadian drive to sleep at night, 3. could feed back to affect light availability and therefore clock phase because of natural time-dependent differences in phase shifting. 4. Hormones could directly affect peripheral clocks at sleep-wake centers to affect sleep timing without altering the central clock in the SCN. **Bottom panel.** *In vitro*, treatment of primary human fibroblasts with serum from older subjects (OS) results in a shorter period and an earlier phase of cellular circadian rhythms than that obtained with serum from younger subjects (YS). Heat treatment (OSHI) abolished this effect. (Data reproduced from [5].)

properties of younger persons' sera, but did not change the properties of younger persons' sera (Figure 1, bottom) [5].

Background

In principle, sleep is regulated by two separable processes: a circadian one, which pushes diurnal species

such as humans to sleep preferentially at night; and a homeostatic one, by which sleep drive increases with increasing time spent awake [6].

The circadian process is driven by a biological "circadian" clock. In mammals, the central clock controlling diurnal behavior is located in the suprachiasmatic nucleus of the brain hypothalamus (the

SCN). Its mechanism is cell-autonomous, and is duplicated in “slave” clocks in nearly all the cells of the body. The molecular mechanism of this clock has been reviewed previously, including in this journal [1]. Numerous studies have demonstrated that its genetically encoded period length (the time taken for one complete cycle under constant conditions) directly affects the phase of human behavior and gene expression: individuals with longer periods have a later phase than those with shorter periods, looking either at human behavior or at gene expression [7-9].

In mammals, entrainment of the circadian clock to its environment is driven predominantly at the ocular level by environmental light. Hence, blind individuals with an endogenous clock period significantly different from 24 hours are unable to synchronize to the solar day [10]. The response of the clock to light is asymmetric, and light at different times of the day or night will shift the clock in different directions and by different amounts (Figure 1, bottom inset). As one might predict, evening light delays the clock, and morning light advances it [11].

The homeostatic process is much less well understood at the molecular level, but may be a fundamental property of neural assemblies [12]. It involves global synchronization of rhythmic thalamocortical firing patterns whose hallmark is a predominance of particular frequencies measured by EEG. Sleep is divided into different “stages” characterized by different frequency bands, and an individual will typically alternate among these stages in a defined pattern for several episodes during the night. The “intensity” of sleep is determined by time spent awake, by genetic factors, and by environmental disturbance, with more profound sleep characterized by a greater intensity of these EEG frequencies, indicative of more pervasive neuronal synchrony [13].

Theory

Purely theoretically, based upon the mechanisms outlined above, numerous hypotheses can be advanced to explain the disruption of sleep in the elderly. Let us consider the two features of this disruption separately. The earlier bedtime and waking time of elderly individuals could be a result of a shortening of endogenous circadian period. It could also arise from a change in the way the clock changes phase in response to light: anything that resulted in a net gain of morning light or loss of evening light would result in an earlier

phase. Finally, the early phase of elderly individuals could arise from homeostatic effects: an increased sleep need would advance bedtime or delay wake time, and a decreased sleep need would advance wake time or delay bedtime.

The second property of sleep in the elderly is its fragmentation. Lower circadian amplitude would result in greater difficulty in sleeping at night, and greater ease of napping. Alternatively, homeostatic processes could play a role: lower homeostatic sleep drive would also result in sleep fragmentation. Greater susceptibility to environmental disturbance would have the same effect.

By imagining age-related changes to both homeostatic and circadian mechanisms, it is possible to rationalize separately the earlier phase and the increased fragmentation of sleep that occur in elderly individuals [14]. However, explaining both effects with the same hypothesis is not simple. One idea is that dampened circadian amplitude results in sleep fragmentation at night and daytime napping [15]. These changed sleep patterns would be reinforced by changes in the timing of light, which shifts phase earlier [16]. A second hypothesis suggests that reduction in homeostatic sleep drive could accomplish the same effect, fragmenting sleep directly and shifting phase via altered light choice [17]. These models are shown schematically in Figure 1.

OBSERVATIONS

Although numerous behavioral studies have been conducted over the past decade to address these hypotheses, no clear picture has emerged. Evidence to support and contradict each of them exists:

Circadian period length: Although a shortened behavioral period length as a consequence of age has been observed in some animals [18], careful studies of older humans under conditions of “forced desynchrony” show no hint of such changes. In these experiments, subjects were kept under photoperiods so long (28h) that their endogenous circadian clocks could not adjust. Circadian period was determined under these “free-running” conditions by measuring rhythmic expression of the hormone melatonin, or diurnal variation in body temperature [14]. Pagani et al. showed shortening of period in human fibroblasts, but only in the presence of blood serum from older individuals [5].

Phase shifting: In humans, phase shifts in response to very bright light do not differ significantly between

older and younger subjects, at least for phase delays [19, 20]. Phase advances were attenuated in some studies [19, 21], but this data would not explain *earlier* phases in older individuals. Moreover, these studies used very bright light to obtain maximum phase-shifting. Whether these results can be generalized to dimmer light remains an open question, because considerable reduction in lens transmission occurs with age [22], and reduced phase delays in response to moderate light have been reported [23].

Circadian Amplitude: Changes in circadian amplitude are more difficult to measure. Certainly, melatonin production has been shown in multiple studies to diminish with age [24], but it is not clear that this reflects a change in circadian amplitude *per se*: size and calcification of the pineal gland that produces melatonin also diminish with age [25, 26]. Circadian rhythms of body temperature also decline with aging, but these are in part activity-determined [27].

Sleep fragmentation: Changes in sleep patterns in the elderly have been well-documented, but ascribing them specifically to circadian or homeostatic changes are more difficult. For example, a tendency toward shallow, fragmented sleep could be explained by a weakened circadian arousal signal at that time [15]. Surprisingly, recent studies suggest that older adults have *less* daytime sleep propensity than younger ones [4]. At the same time, total sleep duration is reduced, *and* sleep fragmentation increases. These results imply effects upon homeostatic control -- specifically, a reduction in sleep need has been documented in elderly individuals [28], accompanied by a reduction in sleep efficiency. Partly contradicting this, the response to low sleep pressure in laboratory conditions is similar in younger and older individuals, suggesting an interplay between circadian and homeostatic effects [29].

UNCERTAIN CONCLUSIONS

So far, little evidence exists to suggest that the period length of circadian behavior is changed in elderly individuals. Moreover, although studies suggest that homeostatic sleep is affected in fundamental ways in older individuals, these observations are likely insufficient to explain the marked circadian changes observed. In forced desynchrony studies that showed increased sleep fragmentation, investigators also observed an earlier sleep onset relative to the phase of the hormone melatonin [14]. Similarly, under constant routine studies under constant dim light, the phase of

gene expression in blood cells is still advanced [30]. Since the light cycle in these studies was *not* systematically affecting the circadian clock, these results imply that changes in circadian phase are unlikely to be explained via strictly homeostatic mechanisms affecting light choice. Of course, homeostatic sleep mechanisms might also have more direct effects upon the circadian oscillator [31, 32], but these mechanisms remain to be explored.

Against this context, Pagani *et al.* postulated that hormonal changes in elderly individuals could alter circadian period in peripheral cells. In an environment entrained by the solar day, such changes would easily translate into changes in phase. These observations do not, however, explain age-related changes in circadian amplitude or in homeostatic sleep. Moreover, such an explanation presumes that nuclei in the brain directing sleep timing are affected by this hormone, but that the master clock in the suprachiasmatic nuclei is not (since no corresponding changes in human behavioral period have been documented). Thus, it is at best a partial explanation. What makes it attractive is that hormonal changes offer the likely possibility of pharmacological remedy.

FUTURE DIRECTIONS

This Perspective has confined itself (mostly) to discussion of specific theories about the interplay among aging, sleep, and the circadian clock. Already, mutation and gene profiling studies have implicated specific clock genes in the ageing process [1, 33, 34]. In fact, however, the best evidence for any model comes in the form of detailed mechanisms, and here is undoubtedly where future research will be directed. For example, in rodent models, aging is correlated with losses of specific classes of neurons (orexin and CRH) that could affect sleep architecture [35]. Experiments to address whether these changes are necessary and sufficient to explain fragmented sleep -- and whether similar changes are observed in the aged human brain that correlate with sleep disturbance -- will reinforce homeostatic models. Similarly, it is well-known that human aging is accompanied by large alterations in hormone balance, both in the hypothalamic-pituitary-adrenal axis and elsewhere [36]. If Pagani *et al.* wish to suggest that a hormone is in part responsible for age-related circadian dysfunction, then the best evidence in their favor would be identification of the suspected factor and characterization of its effects.

REFERENCES

1. Yu EA and Weaver DR. Disrupting the circadian clock: Gene-specific effects on aging, cancer, and other phenotypes. *Aging (Albany NY)*. 2011; 3: 479-93.
2. Englert S and Linden M. Differences in self-reported sleep complaints in elderly persons living in the community who do or do not take sleep medication. *J Clin Psychiatry*. 1998; 59: 137-44; quiz 145.
3. Roenneberg T, Kuehne T, Juda M, Kantermann T, Allebrandt K, Gordijn M, and Meroow M. Epidemiology of the human circadian clock. *Sleep Med Rev*. 2007; 11: 429-38.
4. Dijk DJ, Groeger JA, Stanley N, and Deacon S. Age-related reduction in daytime sleep propensity and nocturnal slow wave sleep. *Sleep*. 2010; 33: 211-23.
5. Pagani L, Schmitt K, Meier F, Izakovic J, Roemer K, Viola A, Cajochen C, Wirz-Justice A, Brown SA, and Eckert A. Serum factors in older individuals change cellular clock properties. *Proc Natl Acad Sci U S A*. 2011; 108: 7218-23.
6. Borbely AA. A two process model of sleep regulation. *Hum Neurobiol*. 1982; 1: 195-204.
7. Archer SN, Viola AU, Kyriakopoulou V, von Schantz M, and Dijk DJ. Inter-individual differences in habitual sleep timing and entrained phase of endogenous circadian rhythms of BMAL1, PER2 and PER3 mRNA in human leukocytes. *Sleep*. 2008; 31: 608-17.
8. Brown SA, Kunz D, Dumas A, Westermark PO, Vanselow K, Tilmann-Wahnschaffe A, Herzel H, and Kramer A. Molecular insights into human daily behavior. *Proc Natl Acad Sci U S A*. 2008; 105: 1602-7.
9. Duffy JF, Dijk DJ, Klerman EB, and Czeisler CA. Later endogenous circadian temperature nadir relative to an earlier wake time in older people. *Am J Physiol*. 1998; 275: R1478-87.
10. Lockley SW, Arendt J, and Skene DJ. Visual impairment and circadian rhythm disorders. *Dialogues Clin Neurosci*. 2007; 9: 301-14.
11. Khalsa SB, Jewett ME, Cajochen C, and Czeisler CA. A phase response curve to single bright light pulses in human subjects. *J Physiol*. 2003; 549: 945-52.
12. Krueger JM, Rector DM, Roy S, Van Dongen HP, Belenky G, and Panksepp J. Sleep as a fundamental property of neuronal assemblies. *Nat Rev Neurosci*. 2008; 9: 910-9.
13. Dijk DJ. Regulation and functional correlates of slow wave sleep. *J Clin Sleep Med*. 2009; 5: S6-15.
14. Dijk DJ, Duffy JF, Riel E, Shanahan TL, and Czeisler CA. Ageing and the circadian and homeostatic regulation of human sleep during forced desynchrony of rest, melatonin and temperature rhythms. *J Physiol*. 1999; 516 (Pt 2): 611-27.
15. Cajochen C, Munch M, Knoblauch V, Blatter K, and Wirz-Justice A. Age-related changes in the circadian and homeostatic regulation of human sleep. *Chronobiol Int*. 2006; 23: 461-74.
16. Dijk DJ, Duffy JF, and Czeisler CA. Contribution of circadian physiology and sleep homeostasis to age-related changes in human sleep. *Chronobiol Int*. 2000; 17: 285-311.
17. Yoon IY, Kripke DF, Elliott JA, Youngstedt SD, Rex KM, and Hauger RL. Age-related changes of circadian rhythms and sleep-wake cycles. *J Am Geriatr Soc*. 2003; 51: 1085-91.
18. Aujard F, Cayetanot F, Bentivoglio M, and Perret M. Age-related effects on the biological clock and its behavioral output in a primate. *Chronobiol Int*. 2006; 23: 451-60.
19. Klerman EB, Duffy JF, Dijk DJ, and Czeisler CA. Circadian phase resetting in older people by ocular bright light exposure. *J Investig Med*. 2001; 49: 30-40.
20. Benloucif S, Green K, L'Hermite-Baleriaux M, Weintraub S, Wolfe LF, and Zee PC. Responsiveness of the aging circadian clock to light. *Neurobiol Aging*. 2006; 27: 1870-9.
21. Sletten TL, Revell VL, Middleton B, Lederle KA, and Skene DJ. Age-related changes in acute and phase-advancing responses to monochromatic light. *J Biol Rhythms*. 2009; 24: 73-84.
22. Said FS and Weale RA. The variation with age of the spectral transmissivity of the living human crystalline lens. *Gerontologia*. 1959; 3: 213-31.
23. Duffy JF, Zeitzer JM, and Czeisler CA. Decreased sensitivity to phase-delaying effects of moderate intensity light in older subjects. *Neurobiol Aging*. 2007; 28: 799-807.
24. Reiter RJ and Richardson BA. Some perturbations that disturb the circadian melatonin rhythm. *Chronobiol Int*. 1992; 9: 314-21.
25. Schmid HA, Requintina PJ, Oxenkrug GF, and Sturner W. Calcium, calcification, and melatonin biosynthesis in the human pineal gland: a postmortem study into age-related factors. *J Pineal Res*. 1994; 16: 178-83.
26. Kunz D, Schmitz S, Mahlberg R, Mohr A, Stoter C, Wolf KJ, and Herrmann WM. A new concept for melatonin deficit: on pineal calcification and melatonin excretion. *Neuropsychopharmacology*. 1999; 21: 765-72.
27. Weinert D and Waterhouse J. The circadian rhythm of core temperature: effects of physical activity and aging. *Physiol Behav*. 2007; 90: 246-56.
28. Duffy JF, Willson HJ, Wang W, and Czeisler CA. Healthy older adults better tolerate sleep deprivation than young adults. *J Am Geriatr Soc*. 2009; 57: 1245-51.
29. Munch M, Knoblauch V, Blatter K, Wirz-Justice A, and Cajochen C. Is homeostatic sleep regulation under low sleep pressure modified by age? *Sleep*. 2007; 30: 781-92.
30. Hida A, Kusanagi H, Satoh K, Kato T, Matsumoto Y, Echizenya M, Shimizu T, Higuchi S, and Mishima K. Expression profiles of PERIOD1, 2, and 3 in peripheral blood mononuclear cells from older subjects. *Life Sci*. 2009; 84: 33-7.
31. Mongrain V, Carrier J, and Dumont M. Circadian and homeostatic sleep regulation in morningness-eveningness. *J Sleep Res*. 2006; 15: 162-6.
32. Maret S, Dorsaz S, Gurcel L, Pradervand S, Petit B, Pfister C, Hagenbuchle O, O'Hara BF, Franken P, and Tafti M. Homer1a is a core brain molecular correlate of sleep loss. *Proc Natl Acad Sci U S A*. 2007; 104: 20090-5.
33. Bauer J, Antosh M, Chang C, Schorl C, Kolli S, Neretti N, and Helfand SL. Comparative transcriptional profiling identifies takeout as a gene that regulates life span. *Aging (Albany NY)*. 2010; 2: 298-310.
34. Galikova M and Flatt T. Dietary restriction and other lifespan extending pathways converge at the activation of the downstream effector takeout. *Aging (Albany NY)*. 2010; 2: 387-9.
35. Kessler BA, Stanley EM, Frederick-Duus D, and Fadel J. Age-related loss of orexin/hypocretin neurons. *Neuroscience*. 2011; 178: 82-8.
36. Van Cauter E, Plat L, Leproult R, and Copinschi G. Alterations of circadian rhythmicity and sleep in aging: endocrine consequences. *Horm Res*. 1998; 49: 147-52.

C. Mitochondrial dysfunction - the beginning of the end in Alzheimer's disease? Separate and synergistic modes of tau and amyloid- β toxicity.

Authors: Eckert A^{1,*}, Schmitt K¹, Götz J²

Affiliations:

¹Neurobiology Laboratory for Brain Aging and Mental Health, Psychiatric University Clinics, University of Basel, CH-4012, Basel, Switzerland

²Alzheimer's and Parkinson's Disease Laboratory, Brain and Mind Research Institute, University of Sydney, Camperdown, NSW 2050, Australia

*Corresponding author. E-mail: anne.eckert@upkbs.ch

Alzheimers Res Ther. 2011 May 5;3(2):15. Published online May 5, 2011.

doi: 10.1186/alzrt74

REVIEW

Mitochondrial dysfunction - the beginning of the end in Alzheimer's disease? Separate and synergistic modes of tau and amyloid- β toxicity

Anne Eckert*¹, Karen Schmitt¹ and Jürgen Götz²

Abstract

The pathology of Alzheimer's disease (AD) is characterized by amyloid plaques (aggregates of amyloid- β (A β)) and neurofibrillary tangles (aggregates of tau) and is accompanied by mitochondrial dysfunction, but the mechanisms underlying this dysfunction are poorly understood. In this review, we discuss the critical role of mitochondria and the close inter-relationship of this organelle with the two main pathological features in the pathogenic process underlying AD. Moreover, we summarize evidence from AD post-mortem brain as well as cellular and animal AD models showing that A β and tau protein trigger mitochondrial dysfunction through a number of pathways, such as impairment of oxidative phosphorylation, elevation of reactive oxygen species production, alteration of mitochondrial dynamics, and interaction with mitochondrial proteins. A vicious cycle as well as several vicious circles within the cycle, each accelerating the other, can be drawn, emphasizing the synergistic deterioration of mitochondria by tau and A β .

Introduction

With the increasing average lifespan of humans, Alzheimer's disease (AD) is the most common neurodegenerative disorder among elderly individuals. It accounts for up to 80% of all dementia cases and ranks as the fourth leading cause of death amongst those above 65 years of age [1]. Although the hallmark lesions of the disease were already described by Alois Alzheimer in 1906 - amyloid- β (A β)-containing plaques and microtubule-associated protein tau-containing neurofibrillary tangles (NFTs) - the

underlying molecular mechanisms that cause the formation of these end-stage lesions are not known [2]. Moreover, as only a small fraction of AD is caused by autosomal dominant mutations, this comes down to a question of what is causing the prevalent sporadic cases in the first place. A growing body of evidence supports mitochondrial dysfunction as a prominent and early, chronic oxidative stress-associated event that contributes to synaptic abnormalities and, ultimately, selective neuronal degeneration in AD [3-9]. Is oxidative stress accelerating the NFT and A β pathologies, are these lesions causing oxidative stress themselves, or are there other mechanisms involved? Within the past few years, several cell culture models as well as single, double and, more recently, triple transgenic mouse models have been developed that reproduce diverse aspects of AD. These models help in understanding the pathogenic mechanisms that lead to mitochondrial failure in AD, and in particular the interplay of AD-related cellular modifications within this process [10].

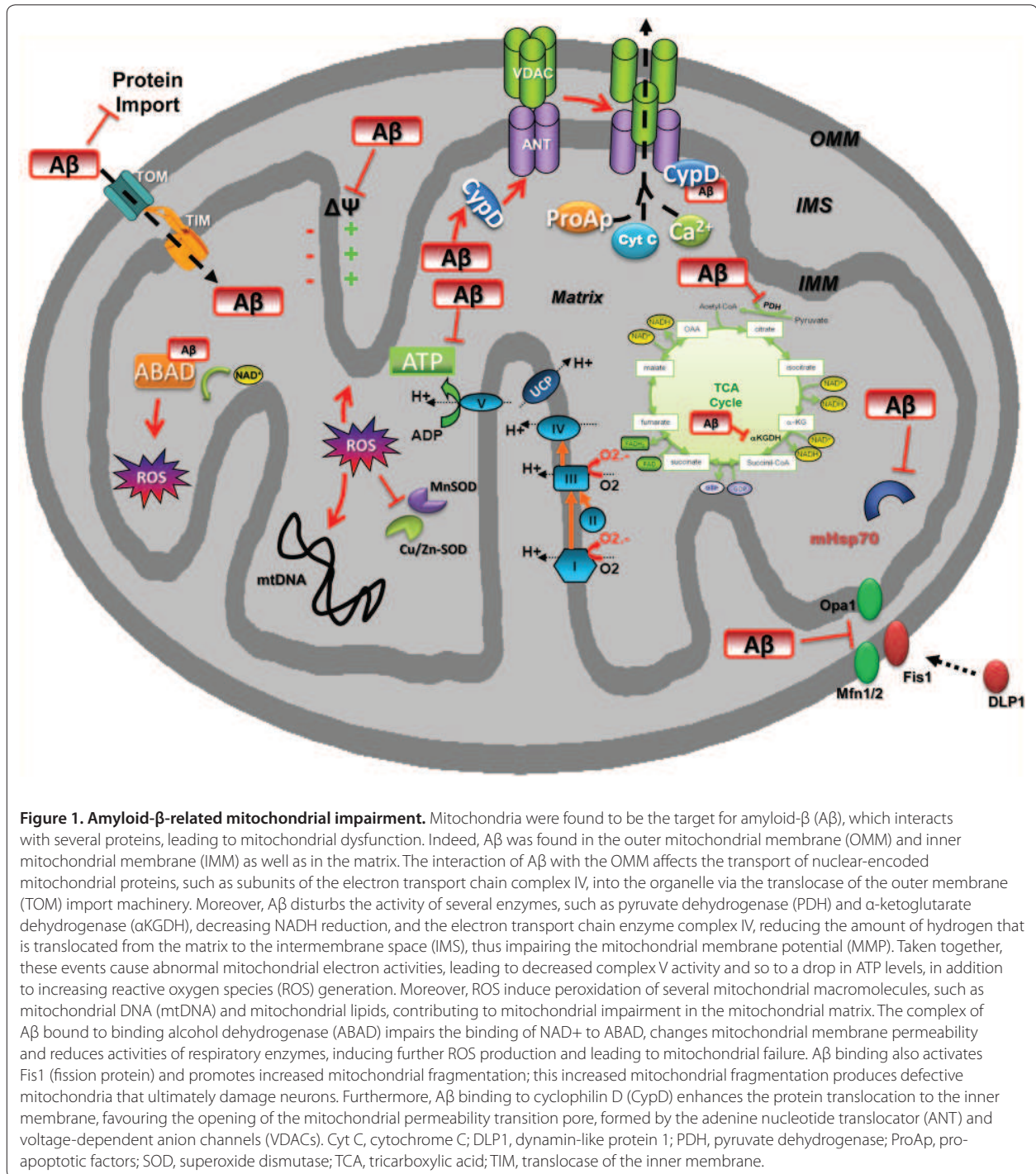
Mitochondria: paradoxical organelles

Mitochondria play a pivotal role in cell survival and death by regulating both energy metabolism and apoptotic pathways (Figure 1); they contribute to many cellular functions, including intracellular calcium homeostasis, the alteration of the cellular reduction-oxidation potential, cell cycle regulation and synaptic plasticity [11]. They are the 'powerhouses of cells', providing energy via ATP generation, which is accomplished through oxidative phosphorylation from nutritional sources [12]. Neurons have particularly high numbers of mitochondria, and they are especially enriched in synapses. Due to their limited glycolytic capacity, neurons are highly dependent on mitochondrial function for energy production [13]. However, when mitochondria fulfil their physiological function, it is as if Pandora's box has been opened, as this vital organelle contains potentially harmful proteins and biochemical reaction centres: mitochondria are the major producers of reactive oxygen species (ROS) and at the same time targets of ROS toxicity. These include

*Correspondence: anne.eckert@upkbs.ch

¹Neurobiology Laboratory for Brain Aging and Mental Health, Psychiatric University Clinics, University of Basel, CH-4012, Basel, Switzerland

Full list of author information is available at the end of the article



mitochondrial DNA, lipids of the mitochondrial membrane, and mitochondrial proteins. Dysregulation of mitochondrial function because of these insults leads to synaptic stress, disruption of synaptic transmission, apoptosis and, ultimately, neurodegeneration [14,15]. Thus, it is important to understand the mechanisms of mitochondrial stress related to the pathogenesis of AD

and to exploit this insight for developing therapeutic strategies for AD.

Evidence of mitochondrial dysfunction in post-mortem AD brain and peripheral cells

Mitochondrial dysfunction has been proposed as an underlying mechanism in the early stages of AD since


	Target	Impairment	References
A D P A T I E N T S		↓ glucose utilization (early region-specific)	Blass et al., 2001 [3]; Mosconi et al., 2008 [17]
		TCA: ↓ α-ketoglutarate, pyruvate dehydrogenase	Gibson et al., 1998 [18]; Blass et al., 2001[3]; Casley et al., 2002[23]
		ETC: ↓ Cytochrome c oxidase, ATP level ↑ ROS level	Kish et al., 1992 [26]; Mutisya et al., 1994 [27]; Cardoso et al., 2004 [25]
		Mitochondrial proteins: ↓ nuclear coded proteins	Liang et al., 2008 [29]
		Oxidative Stress: ↑ Protein oxidation / nitration, lipid peroxidation ↓ Antioxidants enzymes	Aksenov et al., 1998 [28]; Perry et al., 2000 [31]
		Mitochondrial dynamics ↑ Mitochondrial morpholgy/ distribution abnormalities	Wang et al., 2008 [32]; Cho et al., 2009 [33] Hirai et al., 2001 [22]

Figure 2. Mitochondrial impairment in the brain and peripheral cells of Alzheimer's disease patients. AD, Alzheimer's disease; ETC, electron transport chain; ROS, reactive oxygen species; TCA, tricarboxylic acid.

energy deficiency is a fundamental characteristic of the AD brain [16,17] as well as of peripheral cells derived from AD patients [18]. The similar findings in peripheral tissue highlight the potential of using surrogate tissue in the diagnosis of AD (Figure 2).

Brain imaging studies have demonstrated defects in glucose use in living AD patients, an abnormality that may occur well before the onset of clinical symptoms [17]. Furthermore, several lines of evidence suggest that mitochondria intervene in the mechanism by which Aβ, which is derived from amyloid precursor protein (APP), triggers synaptic failure and neurodegeneration. Crucial to this finding was the notion that both Aβ and the full length protein, APP, accumulate within mitochondria in the brains of AD patients [6,19-21].

Furthermore, morphometric analyses revealed that mitochondria display structural abnormalities, as illustrated by the accumulation of mitochondrial DNA and proteins in the cytoplasm and vacuoles; this accelerates mitochondrial degradation and thereby leads to a significant decrease in mitochondrial numbers in AD [22]. The mitochondrial accumulation of APP and Aβ in brain tissues causes both altered activities in key mitochondrial enzymes, including cytochrome c oxidase (COX, complex IV), pyruvate dehydrogenase (PDH) and α-ketoglutarate dehydrogenase complex (αKGDH), and import of nuclear-encoded proteins [3,18,21,23]. The activity of αKGDH, but not of PDH, has been found to be reduced in cultured skin fibroblasts from sporadic AD patients and in a subset of patients with presenilin-1 mutations. Sorbi and colleagues [24] observed a reduction

in PHD, ATP-citrate lyase and acetoacetyl-CoA thiolase in post-mortem brain tissues from AD-affected subjects and correlated the decrease of these enzymes to the decreased production of acetyl-coenzyme A and cholinergic defects that are observed in AD.

The impairment of mitochondrial oxidative phosphorylation in the AD brain was found to be proportional to clinical disability [3]. The most consistent defect in mitochondrial electron transport enzymes in AD is a deficiency in COX, a finding reported in AD post-mortem brain as well as in platelets and fibroblasts from AD patients [25,26]. Dysfunction of COX increases ROS production, reduces energy stores, and disturbs energy metabolism [27]. Altered levels of antioxidant enzymes, such as catalase, copper/zinc superoxide dismutase (Cu/Zn-SOD) and manganese superoxide dismutase (Mn-SOD) have been found in AD brain, supporting increased oxidative stress as a pathomechanism in AD [28].

Laser-capture microdissection has been applied to investigate distinct brain areas as some undergo neurodegeneration whereas others do not: the analysis of the expression of 80 metabolically relevant nuclear-encoded electron transport chain genes from non-NFT-bearing AD neurons revealed that 60 to 70% of these were significantly lower in metabolically affected areas such as the posterior cingulate cortex, the middle temporal gyrus, and the hippocampal CA1 region [29]. Post-mortem tissue also provides strong evidence for increased levels of cellular oxidative stress in vulnerable regions of AD brains compared to aged controls [30]. Increased protein oxidation, protein nitration, and lipid peroxidation were

detected in brain areas with overt NFTs and amyloid plaques [31].

More recently, abnormal mitochondrial dynamics has been identified in fibroblasts from sporadic and familial AD cases [32], a distortion probably mediated by altered expression of dynamin-like protein 1 (DLP1), a regulator of mitochondrial fission and distribution, due to elevated oxidative and/or A β -induced stress. Moreover, deregulated mitochondrial dynamics might be due to enhanced nitrosative stress generated by A β , such as S-nitrosylation of DLP1 in AD brain [33]. This modification can disturb the balance between fission and fusion of mitochondria in favour of mitochondrial fission followed by mitochondrial depletion from axons and dendrites and, subsequently, synaptic loss.

Altogether, these data indicate that mitochondrial dysfunction is a highly relevant event in AD pathophysiology. Post-mortem studies in AD brain allow the identification of long-term synergistic *in vivo* effects of tau and A β in human because, in the majority of AD cases, both pathologies persist in parallel for many years.

Mitochondrial dysfunction in cellular and transgenic mouse AD models

Understanding the molecular pathways by which the various pathological alterations including A β and tau compromise neuronal integrity and lead to clinical symptoms has been a long-standing goal of AD research. The successful development of cell and mouse models that mimic diverse aspects of the disease process have facilitated this effort and assisted in understanding of the interplay of A β and tau on bioenergetics processes *in vivo* [10] (Figure 3).

Mitochondria and A β

A β may exert its toxicity via a plethora of pathways and thereby induce synaptic and neuronal degeneration [2].

Using neuronal PC12 cells, we found that expression of one known APP gene mutation, the 'Swedish APP (APP^{Sw})' double mutation (KM670/671NL), leads to an enhanced vulnerability of these cells to oxidative stress and mitochondrial dysfunction, mediated by different caspases and the stress-activated protein kinase pathway [34-36] (Figure 3). Of note, we are able to study the effects of A β in a dose- dependent manner as cells transfected with APP^{Sw} had fivefold higher A β levels than wild-type APP (APP^{wt}) transfected cells, similar to the increase found in human carriers with the APP^{Sw} mutation compared to sporadic AD cases. The data suggest that the mitochondrial dysfunction induced by A β is probably mediated via enhanced nitric oxide production that reduces complex IV activity. This reduction leads to a depletion of intracellular ATP levels, finally initiating cell death [37]. When intracellular A β production is

prevented by a γ -secretase inhibitor, this restores nitric oxide and ATP levels, indicating a direct involvement of A β in these mechanisms.

Mitochondria were found to be a target for APP toxicity as both the full-length protein and A β accumulate in the mitochondrial import channels, and both lead to mitochondrial dysfunction. Recently, APP has been demonstrated as a substrate of the mitochondrial γ -secretase in cultured SH-SY5Y human neuroblastoma cells [38]. Pavlov and colleagues [38] proposed that APP processing in mitochondria may lead to local A β production, thereby contributing to mitochondrial dysfunction. Recently, our group investigated specific effects of A β on mitochondrial function under physiological conditions by analysing mitochondrial respiratory function and energy homeostasis in both control and APP^{wt}-expressing SH-SY5Y cells [8]. One possibility as to how chronic exposure to soluble A β may result in an impairment of energy homeostasis is through decreased respiratory capacity of the mitochondrial respiratory chain, mainly of complex IV, which, in turn, may accelerate neuronal demise.

Eventually, APP, through A β production, causes an imbalance of mitochondrial fission/fusion that results in mitochondrial fragmentation and abnormal distribution, which contributes to mitochondrial and neuronal dysfunction [39].

An interesting observation was made when the toxic effects of A β were compared with human amylin (HA), a protein aggregating in the pancreas of type 2 diabetic patients [40]. Both agents share amyloidogenic properties and are toxic to primary neuronal cultures, whereas the non-amyloidogenic rat amylin is not [41]. In a next step, HA and A β toxicity to SH-SY5Y neuroblastoma cells was assessed by iTRAQ quantitative proteomics [42]. This revealed the surprising observation that identical proteins are deregulated by HA and A β , but not rat amylin, and a quarter of these were mitochondrial, supporting the notion that mitochondrial dysfunction is a common target in these two amyloidoses. Functional validation revealed that A β and HA both exert a shared toxicity, at least in part, via deregulation of identical mitochondrial proteins and impairment of complex IV activity [42].

AD is believed to be a disease of the synapses, characterized by massive synaptic and, eventually, neuronal loss, and these features have been detected in AD transgenic mouse models (Figure 3). A decrease of the mitochondrially localized chaperone hsp70, which stabilizes proteins during their import into mitochondria, has been observed in synaptosomal fractions derived from the APP^{Sw} transgenic strain Tg2576, pointing to a mitochondrial stress response [43]. Significant differences were revealed in the protein subunit composition of respiratory chain complexes I and III. Moreover,

	Model	A β	Amylin	Target	Impairment	Target	Impairment	References
T A U I N D E P E N D E N T E F F E C T	PC12 (APP ^{Sw} & APP ^{Sw})	Synthetic			↑ Apoptosis		↓ ATP level, MMP, Complex IV activity ↑ ROS level (NO)	Eckert et al., 2001 [34] Leutz et al., 2002 [35] Keil et al., 2004 [37]
	SH-SY5Y (APP ^{Sw} & APP ^{Sw})	Synthetic	Synthetic		↑ Apoptosis		↓ ATP level, mitochondrial proteins, Complex IV activity, Mitochondrial respiration ↑ Mitochondrial APP, ROS level	Rhein et al., 2009 [8] Lim et al., 2010 [42] Pavlov et al., 2011 [38]
	M17 (APP ^{Sw} & APP ^{Sw})	Systemic			↓ Retinoic acid- induced differentiation		↓ ATP level, MMP ↑ ROS level, Mitochondrial dynamics (fusion/fission) and morphology/ distribution abnormalities	Wang et al., 2008 [39]
	APP ^{Sw} (KM595/596NL)	Systemic			↓ Synaptic transmission & LTP		↓ mitochondrial hsp70, subunits of complex I & IV	Crouch et al., 2005 [44] Gillardon et al., 2007 [43]
	APP ^{Sw} (KM595/596NL & V717I)	Systemic			↑ Apoptosis (Bcl-xL/Bax ratio)		↓ ATP level, MMP, mitochondrial respiration (complex IV activity), antioxidants enzymes ↑ ROS level, Lipid peroxidation	Keil et al., 2004 [37] Eckert et al., 2008 [8] Hauptmann et al., 2009 [5] Du et al., 2010 [46]
	APP ^{Sw} / PS1 (KM595/596NL; V717I & M141L)	Systemic			↑ Dystrophic neurites		↓ ATP level, MMP ↑ ROS level	Eckert et al., 2008 [4]
S Y N E R G I S T I C E F F E C T	APP ^{Sw} / PS2 (KM595/596NL & N141I)	Systemic			↓ LTP ↑ Inflammation (Amyloidosis)		↓ ATP level, MMP, Mitochondrial respiration, subunits of complex I & IV ↑ ROS level	Richards et al., 2003 [45] Rhein et al., 2009 [9]
	Tau pR5 (P301L)	Synthetic			↑ Apoptosis		↓ ATP level, MMP, Mitochondrial respiration (complex I activity), subunits of complex V ↑ ROS level	Götz et al., 2001 [56] David et al., 2005 & 2006 [57- 58] Eckert et al., 2008 [65]
	tau ^{AD} AD (P301L/APP ^{Sw} /PS2)	Systemic			↑ Inflammation (Amyloidosis), Apoptosis		↓ ATP level, MMP, subunits of complex I & IV, Mitochondrial respiration: Complex I (related to tau) & IV (related to A β) ↑ ROS level	Rhein et al., 2009 [9]
3xTgAD (P301Ltau/APP ^{Sw} /PS1)	Systemic				↓ LTP		↑ PDH1 α COX IV proteins, glycolysis, Oxidative Stress, Lipid peroxidation, Mitochondrial A β oligomers, ↓ Mitochondrial respiration, pyruvate dehydrogenase	Yao et al., 2009 [71] Hyun et al., 2010 [72]

Figure 3. Mitochondrial impairment in Alzheimer's disease cell culture and transgenic mice models. The successful development of Alzheimer's disease (AD) cell culture models as well as single, double and triple transgenic mice models that mimic diverse aspects of the disease have been helpful in understanding the pathogenic mechanisms on bioenergetic processes *in vivo*, particularly the interplay of AD-related amyloid- β (A β) and tau proteins, leading to the mitochondrial failures underlying AD. APP, amyloid precursor protein; LTP, long-term potentiation; MMP, mitochondrial membrane potential; NO, nitric oxide; PDH, pyruvate dehydrogenase; ROS, reactive oxygen species.

endogenous A β was found to be associated with brain mitochondria in these mice. Cu²⁺ ions have been shown to render A β more toxic, possibly in its dimeric conformation, as a potent inhibitor of COX, thereby contributing to neurodegeneration in AD [44]. In APP^{Sw} transgenic mice, reduced glucose metabolism was observed after [14C]-2-deoxyglucose infusion as well as impaired Cu/Zn SOD activity, both of which contribute to oxidative damage. In another transgenic mouse model, APPS/L, which combines the Swedish (K670M/N671L) with the London (V717I) mutation in the human APP gene, an early energy dysfunction was found as shown by a decreased mitochondrial membrane potential as well as decreased ATP levels at 3 months of age, when A β levels are elevated but plaques are not yet present [5,14,37]. A stronger reduction in mitochondrial membrane potential and in ATP levels was found in double transgenic APP/PS1 (APPS/L/PS1 M141L) mice, which generate higher levels of A β compared to their single transgenic littermates (APPS/L), and exhibit A β plaques already at an age of 3 months [4]. Together, this implies that an A β -dependent mitochondrial dysfunction starts at a very

young age and accelerates substantially with increasing age, as does the A β plaque load [4]. Consistent with this observation, APP/PS2 (APP^{Sw}/PS2 N141I) double transgenic mice display age-related cognitive deficits associated with discrete brain A β deposition and inflammation [45]. Furthermore, an A β insult in APPS/L mice caused early deficits in synaptic mitochondria, as shown by increased mitochondrial permeability transition, a decline in both respiratory function and activity of COX, and increased mitochondrial oxidative stress [46].

Of note, age-dependent impairment of oxygen consumption, such as a decrease of state 3 and of uncoupled respiration, was observed in several APP transgenic mouse models compared to aged-matched controls [5,14,43,47]. This indicates that mitochondrial deregulation is a common feature in A β -generating mice and independent of the mouse model used.

There is broad experimental proof that A β is indeed present in mitochondria. A β binds specifically to the mitochondrial A β -binding alcohol dehydrogenase (ABAD) [6], a mitochondrial matrix protein that is up-regulated in the temporal lobe of AD patients as well as in APP

transgenic mice [48]. The A β -ABAD interaction causes elevated ROS production, cell death, as well as spatial learning and memory deficits in 5-month-old APP/ABAD double transgenic mice [49]. The investigation of the crystal structure of ABAD-A β demonstrated that the formation of the complex prevents the binding of NAD⁺ to ABAD, thereby changing the mitochondrial membrane permeability and reducing the activities of respiratory enzymes, which then may lead to mitochondrial failure [6]. A β in mitochondria further interacts with cyclophilin D (CypD), an integral part of the mitochondrial permeability transition pore that potentiates free radical production, causes synaptic failure, and promotes opening of the pore leading to apoptosis [50]. It has been demonstrated previously that CypD is capable of forming complexes with A β within mitochondria of cortical neurons from APP mutant mice, increasing the translocation of CypD from the matrix to the inner membrane. Furthermore, in APP transgenic mice, the abrogation of CypD was capable of attenuating A β -mediated abnormal mitochondrial dysfunction, such as calcium-induced mitochondrial swelling, and it lowered mitochondrial calcium uptake capacity and impaired mitochondrial respiratory function. A β impaired calcium storage in mitochondria, altering neuronal function, as it is exported to the cytosol, together with other apoptotic factors (ProAp), such as cytochrome c (Figure 1). Finally, Anandatheerthavarada and Devi [51] showed that APP contains a mitochondrial targeting sequence and that an accumulation of APP in mitochondrial membranes leads to mitochondrial dysfunction in Tg2576 neurons. Taken together, these findings are in line with the recently proposed hypothesis of an intracellular A β toxicity cascade, which suggests that the toxic A β species that cause molecular and biochemical abnormalities are in fact intracellular oligomeric aggregates rather than the extracellular, insoluble plaques [6,20].

Mitochondria and tau protein

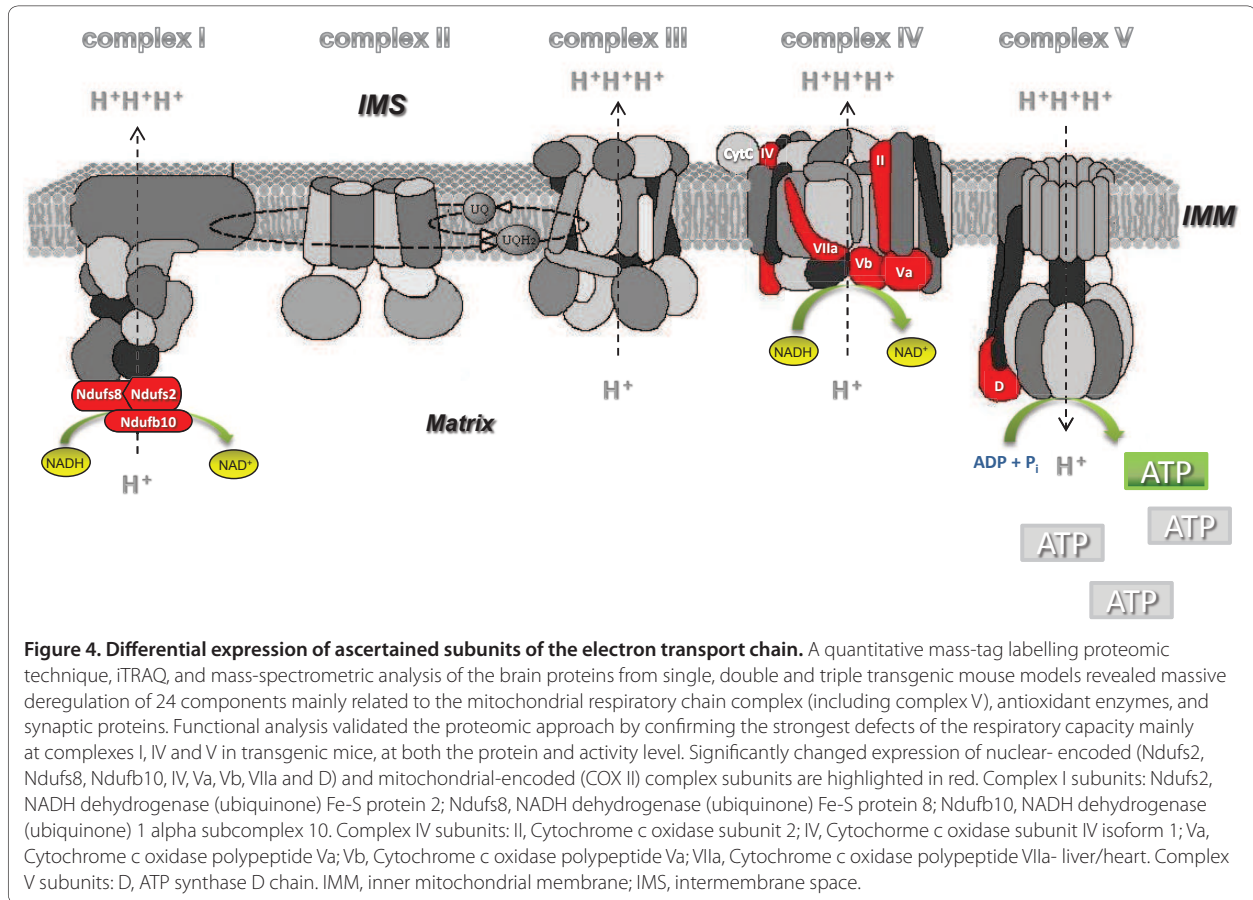
How does tau interfere with mitochondrial function? In its hyperphosphorylated form, tau, which forms the second hallmark lesion in AD, the NFTs, has been shown to block mitochondrial transport, which results in energy deprivation and oxidative stress at the synapse and, hence, neurodegeneration [52-55]. In transgenic pR5 mice that overexpress human P301L mutant tau [56], the biochemical consequences of tau pathology have been intensively investigated using proteomics followed by functional validation [57,58]. A mass-spectrometric analysis of the brain proteins from these mice revealed mainly a deregulation of mitochondrial respiratory chain complex components (including complex V), antioxidant enzymes, and synaptic proteins (Figure 4). The functional analysis demonstrated a mitochondrial dysfunction in

the mice, together with reduced NADH-ubiquinone oxidoreductase (complex I) activity and, with age, impaired mitochondrial respiration and ATP synthesis. Mitochondrial dysfunction was associated with higher levels of ROS in aged transgenic mice. Increased tau pathology as in aged homozygous pR5 mice revealed modified lipid peroxidation levels and the upregulation of antioxidant enzymes in response to oxidative stress [57]. Thus, this evidence demonstrated for the first time that not only A β but also tau pathology can lead to metabolic impairment and oxidative stress as in AD.

Consistent with observations of a cytosolic accumulation of the α -chain of ATP synthase observed at early stages of neurofibrillary degeneration in AD, one mechanism proposed is that tau accumulation could have direct consequences on mitochondrial activity through the cytosolic accumulation of the α -chain of ATP synthase. Reciprocally, hyperphosphorylation of tau may be directly attributable to mitochondrial oxidative stress in a mouse model lacking the mitochondrial detoxifying enzyme superoxide dismutase 2 (Sod2^{-/-}), consistent with a synergistic interaction of APP and mitochondrial oxidative stress in contributing to an AD-like neocortical pathology [59]. Furthermore, chronic respiratory chain dysfunction through inhibition of complex I led, besides a concentration-dependent decrease in ATP levels, to a redistribution of tau from the axon to the cell body, the retrograde transport of mitochondria and, finally, cell death [60]. Together, these findings support the notion that tau pathology involves a mitochondrial and oxidative stress disorder possibly distinct from that caused by A β .

Pathogenic convergence of A β and tau on mitochondria

Although A β and tau pathologies are both known hallmarks in AD, the underlying mechanisms of the interplay between plaques and NFTs (or A β and tau) have remained unresolved. However, a close relationship between mitochondrial impairment and A β on the one hand and tau on the other has been established. How do both features in AD relate to each other and might the two molecules synergistically affect mitochondrial integrity? Several studies suggest that A β aggregates and hyperphosphorylated tau may block mitochondrial carriage to the synapse, leading to energy defects and neurodegeneration [61]. Moreover, transport of APP into axons and dendrites may be inhibited by enhanced tau levels, causing impaired axonal transport, which suggests a link between tau and APP [52,55]. Remarkably, A β injections amplify a pre-existing tau pathology in several transgenic mouse models [56,62,63], whereas lack of tau abrogates A β toxicity [54,64]. Our findings indicate that mitochondria in tau transgenic pR5 mice display enhanced vulnerability towards A β insult *in vitro* [57,65], suggesting a synergistic action of tau and A β pathologies



on this organelle (Figure 3). The A β insult caused a greater reduction of mitochondrial membrane potential in cerebral cells from pR5 mice [57]. Furthermore, incubation of isolated mitochondria from pR5 mice with either oligomeric or fibrillar A β preparations resulted in impairment of the mitochondrial membrane potential and of respiration. Interestingly, aging particularly increased the sensitivity of mitochondria to oligomeric A β insult compared to that of fibrillar A β . This suggests that while both oligomeric and fibrillar A β are toxic, they exert different degrees of toxicity [65]. In a related study, Crouch and colleagues [66] demonstrated that increasing the bioavailability of intracellular copper can restore cognitive function by inhibiting the accumulation of neurotoxic A β trimers and phosphorylated tau in APP^{Sw}/PS1 transgenic mice. In yet another study, it was shown that exposure to A β induces tau hyperphosphorylation by promoting glycogen synthase kinase (GSK)3 β activity. This demonstrates an intimate relationship between A β accumulation and abnormal tau phosphorylation in causing the cognitive deficits that characterize AD, and highlights GSK3 β activity as an important intermediate [67]. In contrast, overexpression of the longest form of

human wild-type tau (tau441) in mouse neuroblastoma (N2A) showed an anti-apoptotic protective function of tau phosphorylation, which likely inhibited competitively phosphorylation of β -catenin by GSK-3 β , facilitating the function of β -catenin. Thus, overexpression of tau seems to attenuate A β -mediated cell death via suppression of the mitochondria-caspase-3 pathway [68,69]. Taken together, these studies illustrate a complex interplay between the two key proteins in AD.

In a step further, triple transgenic mouse models have recently been established that combine A β and tau pathologies, and the contributions of both AD-related proteins to the mitochondrial respiratory machinery and energy homeostasis have been investigated *in vivo* (Figure 3). Indeed, our group demonstrated a mitochondrial dysfunction in a novel triple transgenic mouse model (pR5/APP^{Sw}/PS2 N141I) - tripleAD mice - using proteomics followed by functional validation [9]. Notably, deregulation of complex I was found to be tau-dependent, while deregulation of complex IV was A β -dependent, at both the protein and activity level (Figure 5). Whereas down-regulation of several subunits of complex I was observed in tripleAD mice compared to both pR5 and

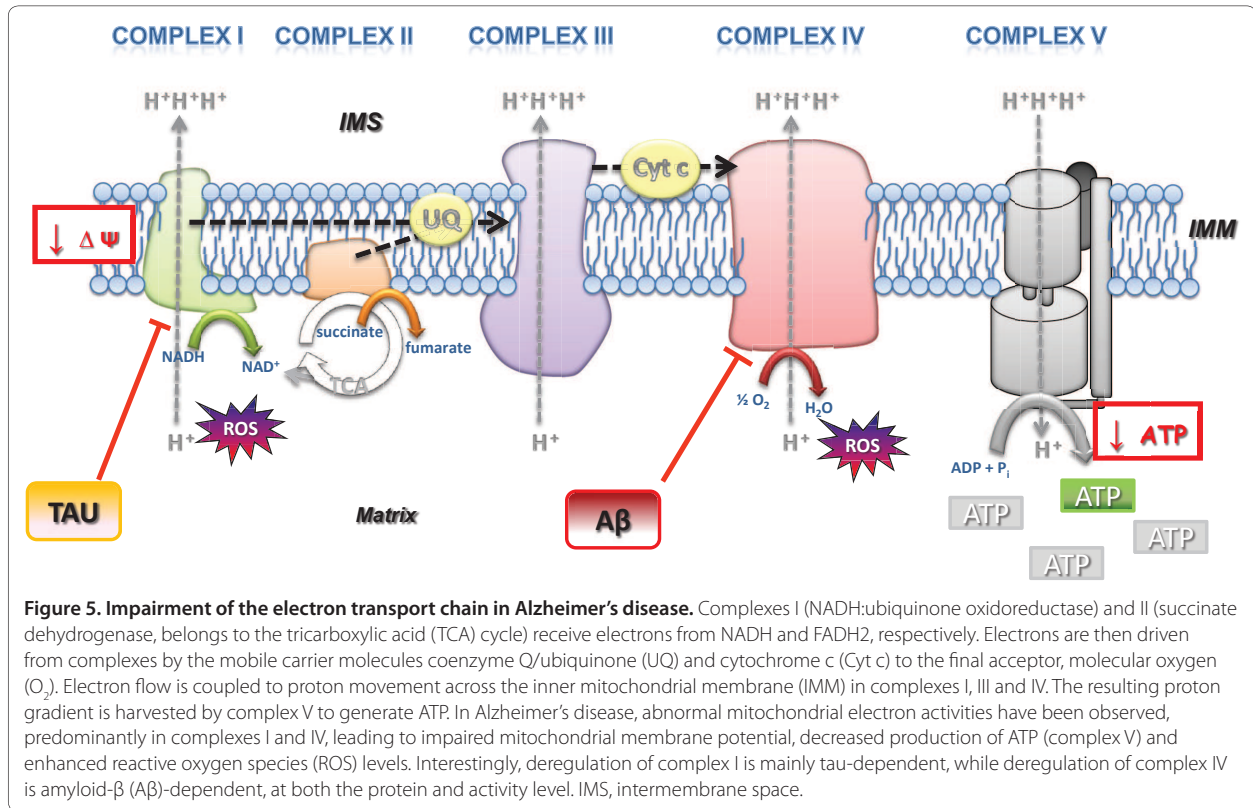


Figure 5. Impairment of the electron transport chain in Alzheimer's disease. Complexes I (NADH:ubiquinone oxidoreductase) and II (succinate dehydrogenase, belongs to the tricarboxylic acid (TCA) cycle) receive electrons from NADH and FADH₂, respectively. Electrons are then driven from complexes by the mobile carrier molecules coenzyme Q/ubiquinone (UQ) and cytochrome c (Cyt c) to the final acceptor, molecular oxygen (O₂). Electron flow is coupled to proton movement across the inner mitochondrial membrane (IMM) in complexes I, III and IV. The resulting proton gradient is harvested by complex V to generate ATP. In Alzheimer's disease, abnormal mitochondrial electron activities have been observed, predominantly in complexes I and IV, leading to impaired mitochondrial membrane potential, decreased production of ATP (complex V) and enhanced reactive oxygen species (ROS) levels. Interestingly, deregulation of complex I is mainly tau-dependent, while deregulation of complex IV is amyloid-β (Aβ)-dependent, at both the protein and activity level. IMS, intermembrane space.

APP^{Sw}/PS2 mice, deregulation of several subunits of complex V was seen in tripleAD mice compared to pR5 mice but not compared to APP^{Sw}/PS2 mice (Figure 4). The convergent effects of Aβ and tau led already at the age of 8 months to depolarized mitochondrial membrane potential in tripleAD mice. Additionally, we found that age-related oxidative stress at 12 months of age may exaggerate the disturbances in the respiratory system and synthesis of ATP and, in turn, take part in the vicious cycle that finally leads to cell death.

Together, our studies highlight the key role of mitochondria in AD pathogenesis, and the close interrelationship of this organelle and the two main pathological hallmarks of this disease. Our data complement those obtained in another triple transgenic mouse model, 3xTg-AD (P301Ltau/APP^{Sw}/PS1 M146L) [70]. Mitochondrial dysfunction was evidenced by age-related decreased activity of regulatory enzymes of the oxidative phosphorylation system, and of PDH and COX in 3xTg-AD mice aged from 3 to 12 months [71]. These mice also exhibited increased oxidative stress and lipid peroxidation. Most of the effects on mitochondria were seen at the age of 9 months, whereas mitochondrial respiration was significantly decreased at 12 months of age. Importantly, mitochondrial bioenergetics deficits were found to precede the development of AD pathology in the

3xTg-AD mice. More recently, Hyun and colleagues [72] demonstrated that the plasma membrane redox system (PMRS) is impaired in the 3xTg-AD mice and that the activities of PMRS enzymes may protect neurons against Aβ toxicity, suggesting enhancement of PMRS function as a novel approach for protecting neurons against oxidative damage in AD and related disorders. Collectively, these recent data consolidate the idea that a synergistic effect of tau and Aβ augments the pathological deterioration of mitochondria at an early stage of AD.

Conclusion

We discuss here the critical role of mitochondria and the close inter-relationship of this organelle with the two main pathological features in the pathogenic process underlying AD.

Mitochondrial impairment has been recognized as a prominent and early event in AD in terms of metabolic energy production associated with respiratory chain dysfunction and the regulation of levels of second messengers such as ROS or Ca²⁺. This is partially due to either accumulated damage to mitochondrial DNA or direct harmful effects of oxidative stress and/or Aβ on mitochondrial components. Also, mitochondrial trafficking as well as mitochondrial fusion/fission are known to be altered in AD, compromising normal neurophysiology

and a healthy cellular mitochondrial pool, which eventually leads to apoptosis. Specifically, the mitochondrial impairment integrates the close interplay of the two common hallmarks of AD, plaques and NFTs, or A β and tau, which act independently as well as synergistically on this vital organelle. With regards to the involvement of AD-related proteins in pathogenesis, a vicious cycle as well as several vicious circles within the cycle, each accelerating the other, can be drawn, emphasizing the potency of the synergistic destruction in mitochondria.

Finally, the key role of mitochondrial dysfunction in the early pathogenic pathways by which A β leads to neuronal dysfunction in AD is particularly challenging with respect to establishing therapeutic treatments. Besides the modulation and/or removal of both A β and tau pathology, strategies involving efforts to protect cells at the mitochondrial level by stabilizing or restoring mitochondrial function or by interfering with energy metabolism appear to be promising; these efforts also emphasize the importance of mitochondria in the pathogenesis of AD. Cellular models for AD as well as transgenic mice, and particularly triple transgenic models that combine both pathologies, are valuable tools in monitoring therapeutic interventions at the mitochondrial level. Eventually, this may lead to therapies that prevent the progression of A β deposits and tau hyperphosphorylation at an early stage of disease.

Abbreviations

A β , amyloid- β ; ABAD, A β -binding alcohol dehydrogenase; AD, Alzheimer's disease; APP, amyloid precursor protein; APP^{Sw}, Swedish amyloid precursor protein; APP^{wt}, wild-type amyloid precursor protein; α KGDH, α -ketoglutarate dehydrogenase complex; COX, cytochrome c oxidase; CypD, cyclophilin D; DLP1, dynamin-like protein 1; GSK, glycogen synthase kinase; HA, human amylin; NFT, neurofibrillary tangle; PDH, pyruvate dehydrogenase; PMRS, plasma membrane redox system; ROS, reactive oxygen species; SOD, superoxide dismutase.

Competing interests

The authors declare that they have no competing interests.

Author details

¹Neurobiology Laboratory for Brain Aging and Mental Health, Psychiatric University Clinics, University of Basel, CH-4012, Basel, Switzerland. ²Alzheimer's and Parkinson's Disease Laboratory, Brain and Mind Research Institute, University of Sydney, Camperdown, NSW 2050, Australia.

Published: 5 May 2011

References

1. Nussbaum RL, Ellis CE: Alzheimer's disease and Parkinson's disease. *N Engl J Med* 2003, **348**:1356-1364.
2. Gotz J, Ittner LM: Animal models of Alzheimer's disease and frontotemporal dementia. *Nat Rev Neurosci* 2008, **9**:532-544.
3. Blass JP: Cerebrometabolic abnormalities in Alzheimer's disease. *Neurol Res* 2003, **25**:556-566.
4. Eckert A, Hauptmann S, Scherping I, Rhein V, Muller-Spahn F, Gotz J, Muller WE: Soluble beta-amyloid leads to mitochondrial defects in amyloid precursor protein and tau transgenic mice. *Neurodegener Dis* 2008, **5**:157-159.
5. Hauptmann S, Scherping I, Drose S, Brandt U, Schulz KL, Jendrach M, Leuner K, Eckert A, Muller WE: Mitochondrial dysfunction: an early event in Alzheimer pathology accumulates with age in AD transgenic mice. *Neurobiol Aging* 2009, **30**:1574-1586.
6. Lustbader JW, Cirilli M, Lin C, Xu HW, Takuma K, Wang N, Caspersen C, Chen X, Pollak S, Chaney M, Trinchese F, Liu S, Gunn-Moore F, Lue LF, Walker DG, Kuppusamy P, Zewier ZL, Arancio O, Stern D, Yan SS, Wu H: ABAD directly links Abeta to mitochondrial toxicity in Alzheimer's disease. *Science* 2004, **304**:448-452.
7. Moreira PI, Santos MS, Oliveira CR: Alzheimer's disease: a lesson from mitochondrial dysfunction. *Antioxid Redox Signal* 2007, **9**:1621-1630.
8. Rhein V, Baysang G, Rao S, Meier F, Bonert A, Muller-Spahn F, Eckert A: Amyloid-beta leads to impaired cellular respiration, energy production and mitochondrial electron chain complex activities in human neuroblastoma cells. *Cell Mol Neurobiol* 2009, **29**:1063-1071.
9. Rhein V, Song X, Wiesner A, Ittner LM, Baysang G, Meier F, Ozmen L, Bluethmann H, Dröse S, Brandt U, Savaskan E, Czech C, Götz J, Eckert A: Amyloid-beta and tau synergistically impair the oxidative phosphorylation system in triple transgenic Alzheimer's disease mice. *Proc Natl Acad Sci U S A* 2009, **106**:20057-20062.
10. Eckert A, Schulz KL, Rhein V, Gotz J: Convergence of amyloid-beta and tau pathologies on mitochondria *in vivo*. *Mol Neurobiol* 2010, **41**:107-114.
11. Mattson MP, Gleichmann M, Cheng A: Mitochondria in neuroplasticity and neurological disorders. *Neuron* 2008, **60**:748-766.
12. Scheffler IE: A century of mitochondrial research: achievements and perspectives. *Mitochondrion* 2001, **1**:3-31.
13. Reddy PH: Mitochondrial dysfunction in aging and Alzheimer's disease: strategies to protect neurons. *Antioxid Redox Signal* 2007, **9**:1647-1658.
14. Caspersen C, Wang N, Yao J, Sosunov A, Chen X, Lustbader JW, Xu HW, Stern D, McKhann G, Yan SD: Mitochondrial Abeta: a potential focal point for neuronal metabolic dysfunction in Alzheimer's disease. *FASEB J* 2005, **19**:2040-2041.
15. Santos RX, Correia SC, Wang X, Perry G, Smith MA, Moreira PI, Zhu X: Alzheimer's disease: diverse aspects of mitochondrial malfunctioning. *Int J Clin Exp Pathol* 2010, **3**:570-581.
16. Manczak M, Park BS, Jung Y, Reddy PH: Differential expression of oxidative phosphorylation genes in patients with Alzheimer's disease: implications for early mitochondrial dysfunction and oxidative damage. *Neuromol Med* 2004, **5**:147-162.
17. Mosconi L, Pupi A, De Leon MJ: Brain glucose hypometabolism and oxidative stress in preclinical Alzheimer's disease. *Ann N Y Acad Sci* 2008, **1147**:180-195.
18. Gibson GE, Sheu KF, Blass JP: Abnormalities of mitochondrial enzymes in Alzheimer disease. *J Neural Transm* 1998, **105**:855-870.
19. Devi L, Prabhu BM, Galati DF, Avadhani NG, Anandatheerthavarada HK: Accumulation of amyloid precursor protein in the mitochondrial import channels of human Alzheimer's disease brain is associated with mitochondrial dysfunction. *J Neurosci* 2006, **26**:9057-9068.
20. Fernandez-Vizarra P, Fernandez AP, Castro-Blanco S, Serrano J, Bentura ML, Martinez-Murillo R, Martinez A, Rodrigo J: Intra- and extracellular Abeta and PHF in clinically evaluated cases of Alzheimer's disease. *Histol Histopathol* 2004, **19**:823-844.
21. Pavlov PF, Hansson Petersen C, Glaser E, Ankarcróna M: Mitochondrial accumulation of APP and Abeta: significance for Alzheimer disease pathogenesis. *J Cell Mol Med* 2009, **13**:4137-4145.
22. Hirai K, Aliev G, Nunomura A, Fujioka H, Russell RL, Atwood CS, Johnson AB, Kress Y, Vinters HV, Tabaton M, Shimohama S, Cash AD, Siedlak SL, Harris PL, Jones PK, Petersen RB, Perry G, Smith MA: Mitochondrial abnormalities in Alzheimer's disease. *J Neurosci* 2001, **21**:3017-3023.
23. Casley CS, Canevari L, Land JM, Clark JB, Sharpe MA: Beta-amyloid inhibits integrated mitochondrial respiration and key enzyme activities. *J Neurochem* 2002, **80**:91-100.
24. Sorbi S, Bird ED, Blass JP: Decreased pyruvate dehydrogenase complex activity in Huntington and Alzheimer brain. *Ann Neurol* 1983, **13**:72-78.
25. Cardoso SM, Proenca MT, Santos S, Santana I, Oliveira CR: Cytochrome c oxidase is decreased in Alzheimer's disease platelets. *Neurobiol Aging* 2004, **25**:105-110.
26. Kish SJ, Bergeron C, Rajput A, Dozic S, Mastrogiacomo F, Chang LJ, Wilson JM, DiStefano LM, Nobrega JN: Brain cytochrome oxidase in Alzheimer's disease. *J Neurochem* 1992, **59**:776-779.
27. Mutisya EM, Bowling AC, Beal MF: Cortical cytochrome oxidase activity is reduced in Alzheimer's disease. *J Neurochem* 1994, **63**:2179-2184.
28. Aksenov MY, Tucker HM, Nair P, Aksenova MV, Butterfield DA, Estus S, Markesbery WR: The expression of key oxidative stress-handling genes in

- different brain regions in Alzheimer's disease. *J Mol Neurosci* 1998, **11**:151-164.
29. Liang WS, Duncley T, Beach TG, Grover A, Mastroeni D, Ramsey K, Caselli RJ, Kukull WA, McKeel D, Morris JC, Hulette CM, Schmechel D, Reiman EM, Rogers J, Stephan DA: **Altered neuronal gene expression in brain regions differentially affected by Alzheimer's disease: a reference data set.** *Physiol Genomics* 2008, **33**:240-256.
 30. Moreira PI, Santos MS, Oliveira CR, Shenk JC, Nunomura A, Smith MA, Zhu X, Perry G: **Alzheimer disease and the role of free radicals in the pathogenesis of the disease.** *CNS Neurol Disord Drug Targets* 2008, **7**:3-10.
 31. Perry G, Nunomura A, Hirai K, Takeda A, Aliev G, Smith MA: **Oxidative damage in Alzheimer's disease: the metabolic dimension.** *Int J Dev Neurosci* 2000, **18**:417-421.
 32. Wang X, Su B, Fujioka H, Zhu X: **Dynammin-like protein 1 reduction underlies mitochondrial morphology and distribution abnormalities in fibroblasts from sporadic Alzheimer's disease patients.** *Am J Pathol* 2008, **173**:470-482.
 33. Cho DH, Nakamura T, Fang J, Cieplak P, Godzik A, Gu Z, Lipton SA: **S-nitrosylation of Drp1 mediates beta-amyloid-related mitochondrial fission and neuronal injury.** *Science* 2009, **324**:102-105.
 34. Eckert A, Steiner B, Marques C, Leutz S, Romig H, Haass C, Muller WE: **Elevated vulnerability to oxidative stress-induced cell death and activation of caspase-3 by the Swedish amyloid precursor protein mutation.** *J Neurosci Res* 2001, **64**:183-192.
 35. Leutz S, Steiner B, Marques CA, Haass C, Muller WE, Eckert A: **Reduction of trophic support enhances apoptosis in PC12 cells expressing Alzheimer's APP mutation and sensitizes cells to staurosporine-induced cell death.** *J Mol Neurosci* 2002, **18**:189-201.
 36. Marques CA, Keil U, Bonert A, Steiner B, Haass C, Muller WE, Eckert A: **Neurotoxic mechanisms caused by the Alzheimer's disease-linked Swedish amyloid precursor protein mutation: oxidative stress, caspases, and the JNK pathway.** *J Biol Chem* 2003, **278**:28294-28302.
 37. Keil U, Bonert A, Marques CA, Scherping I, Weyermann J, Strosznajder JB, Müller-Spahn F, Haass C, Czech C, Pradier L, Müller WE, Eckert A: **Amyloid beta-induced changes in nitric oxide production and mitochondrial activity lead to apoptosis.** *J Biol Chem* 2004, **279**:50310-50320.
 38. Pavlov PF, Wiehager B, Sakai J, Frykman S, Behbahani H, Winblad B, Ankarcrona M: **Mitochondrial gamma-secretase participates in the metabolism of mitochondria-associated amyloid precursor protein.** *FASEB J* 2011, **25**:78-88.
 39. Wang X, Su B, Siedlak SL, Moreira PI, Fujioka H, Wang Y, Casadesu G, Zhu X: **Amyloid-beta overproduction causes abnormal mitochondrial dynamics via differential modulation of mitochondrial fission/fusion proteins.** *Proc Natl Acad Sci U S A* 2008, **105**:19318-19323.
 40. Gotz J, Ittner LM, Lim YA: **Common features between diabetes mellitus and Alzheimer's disease.** *Cell Mol Life Sci* 2009, **66**:1321-1325.
 41. Lim YA, Ittner LM, Lim YL, Gotz J: **Human but not rat amylin shares neurotoxic properties with Abeta42 in long-term hippocampal and cortical cultures.** *FEBS Lett* 2008, **582**:2188-2194.
 42. Lim YA, Rhein V, Baysang G, Meier F, Poljak A, Raftery MJ, Guilhaus M, Ittner LM, Eckert A, Gotz J: **Abeta and human amylin share a common toxicity pathway via mitochondrial dysfunction.** *Proteomics* 2010, **10**:1621-1633.
 43. Gillardon F, Rist W, Kussmaul L, Vogel J, Berg M, Danzer K, Kraut N, Hengeler B: **Proteomic and functional alterations in brain mitochondria from Tg2576 mice occur before amyloid plaque deposition.** *Proteomics* 2007, **7**:605-616.
 44. Crouch PJ, Blake R, Duce JA, Ciccostoto GD, Li QX, Barnham KJ, Curtain CC, Cherny RA, Cappai R, Dyrks T, Masters CL, Trounce IA: **Copper-dependent inhibition of human cytochrome c oxidase by a dimeric conformer of amyloid-beta1-42.** *J Neurosci* 2005, **25**:672-679.
 45. Richards JG, Higgins GA, Ouagazzal AM, Ozmen L, Kew JN, Bohrmann B, Malherbe P, Brockhaus M, Loetscher H, Czech C, Huber G, Bluethmann H, Jacobsen H, Kemp JA: **PS2APP transgenic mice, coexpressing hPS2mut and hAPPsw, show age-related cognitive deficits associated with discrete brain amyloid deposition and inflammation.** *J Neurosci* 2003, **23**:8989-9003.
 46. Du H, Guo L, Yan S, Sosunov AA, McKhann GM, Yan SS: **Early deficits in synaptic mitochondria in an Alzheimer's disease mouse model.** *Proc Natl Acad Sci U S A* 2010, **107**:18670-18675.
 47. Muller WE, Eckert A, Kurz C, Eckert GP, Leuner K: **Mitochondrial dysfunction: common final pathway in brain aging and Alzheimer's disease - therapeutic aspects.** *Mol Neurobiol* 2010, **41**:159-171.
 48. Yan SD, Fu J, Soto C, Chen X, Zhu H, Al-Mohanna F, Collison K, Zhu A, Stern E, Saido T, Tohyama M, Ogawa S, Roher A, Stern D: **An intracellular protein that binds amyloid-beta peptide and mediates neurotoxicity in Alzheimer's disease.** *Nature* 1997, **389**:689-695.
 49. Yao J, Taylor M, Davey F, Ren Y, Aiton J, Coope P, Fang F, Chen JX, Yan SD, Gunn-Moore FJ: **Interaction of amyloid binding alcohol dehydrogenase/Abeta mediates up-regulation of peroxiredoxin II in the brains of Alzheimer's disease patients and a transgenic Alzheimer's disease mouse model.** *Mol Cell Neurosci* 2007, **35**:377-382.
 50. Du H, Yan SS: **Mitochondrial permeability transition pore in Alzheimer's disease: cyclophilin D and amyloid beta.** *Biochim Biophys Acta* 2010, **1802**:198-204.
 51. Anandatheerthavarada HK, Devi L: **Mitochondrial translocation of amyloid precursor protein and its cleaved products: relevance to mitochondrial dysfunction in Alzheimer's disease.** *Rev Neurosci* 2007, **18**:343-354.
 52. Ebneth A, Drewes G, Mandelkow EM, Mandelkow E: **Phosphorylation of MAP2c and MAP4 by MARK kinases leads to the destabilization of microtubules in cells.** *Cell Motil Cytoskeleton* 1999, **44**:209-224.
 53. Gotz J, Ittner LM, Fandrich M, Schonrock N: **Is tau aggregation toxic or protective: a sensible question in the absence of sensitive methods?** *J Alzheimers Dis* 2008, **14**:423-429.
 54. Ittner LM, Ke YD, Delerue F, Bi M, Gladbach A, van Eersel J, Wolfing H, Chieng BC, Christie MJ, Napier IA, Eckert A, Staufenbiel M, Hardeman E, Götz J: **Dendritic function of tau mediates amyloid-beta toxicity in Alzheimer's disease mouse models.** *Cell* 2010, **142**:387-397.
 55. Stamer K, Vogel R, Thies E, Mandelkow E, Mandelkow EM: **Tau blocks traffic of organelles, neurofilaments, and APP vesicles in neurons and enhances oxidative stress.** *J Cell Biol* 2002, **156**:1051-1063.
 56. Gotz J, Chen F, van Dorpe J, Nitsch RM: **Formation of neurofibrillary tangles in P301L tau transgenic mice induced by Abeta 42 fibrils.** *Science* 2001, **293**:1491-1495.
 57. David DC, Hauptmann S, Scherping I, Schuessel K, Keil U, Rizzo P, Ravid R, Dröse S, Brandt U, Müller WE, Eckert A, Götz J: **Proteomic and functional analyses reveal a mitochondrial dysfunction in P301L tau transgenic mice.** *J Biol Chem* 2005, **280**:23802-23814.
 58. David DC, Ittner LM, Gehrig P, Nergau D, Shepherd C, Halliday G, Gotz J: **Beta-amyloid treatment of two complementary P301L tau-expressing Alzheimer's disease models reveals similar deregulated cellular processes.** *Proteomics* 2006, **6**:6566-6577.
 59. Melov S, Adlard PA, Morten K, Johnson F, Golden TR, Hinerfeld D, Schilling B, Mavros C, Masters CL, Volitakis I, Li QX, Laughton K, Hubbard A, Cherny RA, Gibson B, Bush AI: **Mitochondrial oxidative stress causes hyperphosphorylation of tau.** *PLoS One* 2007, **2**:e536.
 60. Escobar-Khondiker M, Höllerhage M, Muriel MP, Champy P, Bach A, Depienne C, Respondek G, Yamada ES, Lannuzel A, Yagi T, Hirsch EC, Oertel WH, Jacob R, Michel PP, Ruberg M, Höglinger GU: **Annonacin, a natural mitochondrial complex I inhibitor, causes tau pathology in cultured neurons.** *J Neurosci* 2007, **27**:7827-7837.
 61. Gotz J, Ittner LM, Kins S: **Do axonal defects in tau and amyloid precursor protein transgenic animals model axonopathy in Alzheimer's disease?** *J Neurochem* 2006, **98**:993-1006.
 62. Bolmont T, Clavaguera F, Meyer-Luehmann M, Herzog MC, Radde R, Staufenbiel M, Lewis J, Hutton M, Tolnay M, Jucker M: **Induction of tau pathology by intracerebral infusion of amyloid-beta-containing brain extract and by amyloid-beta deposition in APP x Tau transgenic mice.** *Am J Pathol* 2007, **171**:2012-2020.
 63. Gotz J, Schild A, Hoernli F, Pennanen L: **Amyloid-induced neurofibrillary tangle formation in Alzheimer's disease: insight from transgenic mouse and tissue-culture models.** *Int J Dev Neurosci* 2004, **22**:453-465.
 64. Ittner LM, Gotz J: **Amyloid-beta and tau - a toxic pas de deux in Alzheimer's disease.** *Nat Rev Neurosci* 2011, **12**:65-72.
 65. Eckert A, Hauptmann S, Scherping I, Meinhardt J, Rhein V, Drose S, Brandt U, Fandrich M, Muller WE, Gotz J: **Oligomeric and fibrillar species of beta-amyloid (A beta 42) both impair mitochondrial function in P301L tau transgenic mice.** *J Mol Med* 2008, **86**:1255-1267.
 66. Crouch PJ, Hung LW, Adlard PA, Cortes M, Lal V, Filiz G, Perez KA, Nurjono M, Caragounis A, Du T, Laughton K, Volitakis I, Bush AI, Li QX, Masters CL, Cappai R, Cherny RA, Donnelly PS, White AR, Barnham KJ: **Increasing Cu bioavailability inhibits Abeta oligomers and tau phosphorylation.** *Proc Natl Acad Sci U S A* 2009, **106**:381-386.
 67. Hu M, Waring JF, Gopalakrishnan M, Li J: **Role of GSK-3beta activation and alpha7 nAChRs in Abeta(1-42)-induced tau phosphorylation in PC12 cells.** *J Neurochem* 2008, **106**:1371-1377.

68. Li HL, Wang HH, Liu SJ, Deng YQ, Zhang YJ, Tian Q, Wang XC, Chen XQ, Yang Y, Zhang JY, Wang Q, Xu H, Liao FF, Wang JZ: **Phosphorylation of tau antagonizes apoptosis by stabilizing beta-catenin, a mechanism involved in Alzheimer's neurodegeneration.** *Proc Natl Acad Sci U S A* 2007, **104**:3591-3596.
69. Wang ZF, Yin J, Zhang Y, Zhu LQ, Tian Q, Wang XC, Li HL, Wang JZ: **Overexpression of tau proteins antagonizes amyloid-beta-potentiated apoptosis through mitochondria-caspase-3 pathway in N2a cells.** *J Alzheimers Dis* 2010, **20**:145-157.
70. Oddo S, Caccamo A, Shepherd JD, Murphy MP, Golde TE, Kaye R, Metherate R, Mattson MP, Akbari Y, LaFerla FM: **Triple-transgenic model of Alzheimer's disease with plaques and tangles: intracellular Abeta and synaptic dysfunction.** *Neuron* 2003, **39**:409-421.
71. Yao J, Irwin RW, Zhao L, Nilsen J, Hamilton RT, Brinton RD: **Mitochondrial bioenergetic deficit precedes Alzheimer's pathology in female mouse model of Alzheimer's disease.** *Proc Natl Acad Sci U S A* 2009, **106**:14670-14675.
72. Hyun DH, Mughal MR, Yang H, Lee JH, Ko EJ, Hunt ND, de Cabo R, Mattson MP: **The plasma membrane redox system is impaired by amyloid beta-peptide and in the hippocampus and cerebral cortex of 3xTgAD mice.** *Exp Neurol* 2010, **225**:423-429.

doi:10.1186/alzrt74

Cite this article as: Eckert A, et al.: Mitochondrial dysfunction - the beginning of the end in Alzheimer's disease? Separate and synergistic modes of tau and amyloid- β toxicity. *Alzheimer's Research & Therapy* 2011, **3**:15.

**D. Insights into Mitochondrial Dysfunction: Aging, Amyloid- β ,
and Tau–A Deleterious Trio**

Authors: Schmitt K¹, Grimm A¹, Kazmierczak A^{1,2}, Strosznajder JB², Götz J³, and Eckert A¹

Affiliations:

¹Neurobiology Laboratory for Brain Aging and Mental Health, Psychiatric University Clinics, University of Basel, Basel, Switzerland

²Mossakowski Medical Research Center, Polish Academy of Sciences, Department of Cellular Signaling, Warsaw, Poland

³Alzheimer's and Parkinson's Disease Laboratory, Brain and Mind Research Institute, University of Sydney, Camperdown, New South Wales, Australia

Address correspondence to:

Dr. Anne Eckert

Neurobiology Laboratory for Brain Aging and Mental Health, Psychiatric University Clinics, University of Basel, CH-4012 Basel, Switzerland.

E-mail: anne.eckert@upkbs.ch

ANTIOXIDANTS & REDOX SIGNALING, Volume 16, Number 12, 2012, Mary Ann Liebert, Inc. DOI: 10.1089/ars.2011.4400

Date of first submission to ARS Central, November 10, 2011; date of acceptance, November 27, 2011

Insights into Mitochondrial Dysfunction: Aging, Amyloid- β , and Tau–A Deleterious Trio

Karen Schmitt,¹ Amandine Grimm,¹ Anna Kazmierczak,^{1,2} Joanna B. Strosznajder,²
Jürgen Götz,³ and Anne Eckert¹

Abstract

Significance: Alzheimer's disease (AD) is an age-related progressive neurodegenerative disorder mainly affecting elderly individuals. The pathology of AD is characterized by amyloid plaques (aggregates of amyloid- β [$A\beta$]) and neurofibrillary tangles (aggregates of tau), but the mechanisms underlying this dysfunction are still partially unclear. **Recent Advances:** A growing body of evidence supports mitochondrial dysfunction as a prominent and early, chronic oxidative stress-associated event that contributes to synaptic abnormalities and, ultimately, selective neuronal degeneration in AD. **Critical Issues:** In this review, we discuss on the one hand whether mitochondrial decline observed in brain aging is a determinant event in the onset of AD and on the other hand the close interrelationship of this organelle with $A\beta$ and tau in the pathogenic process underlying AD. Moreover, we summarize evidence from aging and Alzheimer models showing that the harmful trio "aging, $A\beta$, and tau protein" triggers mitochondrial dysfunction through a number of pathways, such as impairment of oxidative phosphorylation (OXPHOS), elevation of reactive oxygen species production, and interaction with mitochondrial proteins, contributing to the development and progression of the disease. **Future Directions:** The aging process may weaken the mitochondrial OXPHOS system in a more general way over many years providing a basis for the specific and destructive effects of $A\beta$ and tau. Establishing strategies involving efforts to protect cells at the mitochondrial level by stabilizing or restoring mitochondrial function and energy homeostasis appears to be challenging, but very promising route on the horizon. *Antioxid. Redox Signal.* 00, 000–000.

Introduction

AGING is an inevitable biological process that results in a progressive structural and functional decline, as well as biochemical alterations that altogether lead to reduced ability to adapt to environmental changes. Although aging is almost universally conserved among all organisms, the molecular mechanisms underlying this phenomenon still remain unclear. There are several theories of aging, in which free radical (oxidative stress), DNA, or protein modifications are suggested to play the major causative role (54, 72). A growing body of evidence supports mitochondrial dysfunction as a prominent and early, chronic oxidative stress-associated event that contributes to synaptic abnormalities in aging and, ultimately, increased susceptibility to age-related disorders including Alzheimer's disease (AD) (58). AD is the most common neurodegenerative disorder among elderly individuals. It accounts for up to 80% of all dementia cases and

ranks as the fourth leading cause of death among those above 65 years of age. With the increasing average life span of humans, it is highly probable that the number of AD cases will dangerously raise. The pathology of AD characterized by abnormal formation of amyloid plaques (aggregates of amyloid- β [$A\beta$]) and neurofibrillary tangles (NFT; aggregates of tau) was shown to be accompanied by mitochondrial dysfunction. However, the mechanisms underlying this dysfunction are poorly understood. There remain several open questions: Is age-related oxidative stress accelerating the NFT and $A\beta$ pathologies? Are these lesions causing oxidative stress themselves? Or are there other mechanisms involved? Within the past years, several mouse models have been developed that reproduce the aging process and diverse aspects of AD. These models help in understanding the age-related pathogenic mechanisms that lead to mitochondrial failure in AD, and in particular the interplay of AD-related cellular modifications within this process (17, 18).

¹Neurobiology Laboratory for Brain Aging and Mental Health, Psychiatric University Clinics, University of Basel, Basel, Switzerland.

²Mossakowski Medical Research Center, Polish Academy of Sciences, Department of Cellular Signaling, Warsaw, Poland.

³Alzheimer's and Parkinson's Disease Laboratory, Brain and Mind Research Institute, University of Sydney, Camperdown, New South Wales, Australia.

Mitochondrial Aging—the Beginning of the End in AD?

Mitochondria play a pivotal role in cell survival and death by regulating both energy metabolism and apoptotic pathways; they contribute to many cellular functions, including intracellular calcium homeostasis, the alteration of the cellular reduction-oxidation (redox) potential, cell cycle regulation, and synaptic plasticity (47). They are the “powerhouses of cells,” providing energy from nutritional sources *via* ATP generation, which is accomplished through oxidative phosphorylation (OXPHOS) (65). However, when mitochondria fulfill their physiological function, it is as if Pandora’s box has been opened, as this vital organelle contains potentially harmful proteins and biochemical reaction centers; mitochondria are the major producers of reactive oxygen species (ROS) at the same time being susceptible targets of ROS toxicity. Unstable ROS are capable of damaging many types of mitochondrial components; this includes oxidative deterioration of mitochondrial DNA (mtDNA), lipids of the mitochondrial membrane, and mitochondrial proteins, and it is thought that this damage that may accumulate over time from ROS generated from aerobic respiration may play a significant role in aging (Fig. 1). Moreover, it was previously demonstrated that nitrosative stress evoked by increased nitric oxide synthesis also leads to protein oxidation as well as mitochondrial and DNA damage, which are common mechanisms occurred in elderly (13, 34, 70).

Although most mitochondrial proteins are encoded by the nuclear genome, the mitochondrial genome encodes proteins required for 13 polypeptide complexes of the respiratory chain involved in ATP synthesis. Given that mtDNA exists in the inner matrix and this is in close proximity to the inner membrane where electrons can form unstable compounds, mtDNA, unlike nuclear DNA (nDNA), is not protected by histones (4) making it more vulnerable to oxidative stress and its mutation rate is about 10-fold higher than that of nDNA, especially in tissues with a high ATP demand like the brain (54). These mtDNA mutations occur in genes encoding electron transport chain (ETC) subunits including NADH dehydrogenase, cytochrome c oxidase (COX), and ATP synthase (83). Eventually, ROS-related mtDNA mutations can result in the synthesis of mutant ETC proteins that, in turn, can lead to the leakage of more electrons and increased ROS production. This so-called “vicious cycle” is hypothesized to play a critical role in the aging process according to the mitochondrial theory of aging. In addition to age-associated increase in mtDNA mutations, the amount of mtDNA also declines with age in various human and rodent tissues (2, 68). Furthermore, abundance of mtDNA correlates with the rate of mitochondrial ATP production (68), suggesting that age-related mitochondrial dysfunction in muscle is related to reduced mtDNA abundance. However, age-associated change in mtDNA abundance seems to be tissue specific, as several studies have reported no change in mtDNA abundance with age in other than muscular tissues in both man and mouse (20, 46).

How does the somatic mtDNA involved in aging phenotypes contribute to AD development? As only a small fraction of AD is caused by autosomal dominant mutations, this comes down to the question of what is causing the prevalent sporadic cases in the first place. Somatic mutations in mtDNA could cause energy deficiency, increased oxidative stress, and accumulation of A β , which act in a vicious cycle reinforcing

mtDNA damage and oxidative stress (45). Indeed, defects in mtDNA associated with decreased cytochrome oxidase activity have been found in AD patients (9). Although a similarly impaired mitochondrial function and subsequent compensatory response have been observed in both non-demented aged and AD subjects, no clear causative mutations in the mtDNA have been correlated to AD; although some variations have functional consequences, including changes in enzymatic activity (40). Perhaps the main differences are that, in AD brains, defects are more profound due to A β and tau accumulation, because of decreased compensatory response machinery (Fig. 1).

Many investigators have developed models for studying mitochondrial-related aging (36). Among them senescence-accelerated mice (SAM) strains are especially useful models to understand the mechanisms of the age-related mitochondrial decline. Behavioral studies showed that learning and memory deficits already started as early as 6 months and worsened with aging in SAMP8 mice (accelerated senescence-prone 8) (53, 77). Moreover, Omata and collaborators showed age-related changes in cerebral energy production in the 2-month-old SAMP8 followed by a decrease in mitochondrial function compared with SAMR1 mice (accelerated senescence-resistant 1) (51). Aging is not only connected with increased mitochondrial ROS production due to ETC impairment but also with a dysbalance of the protective antioxidant machinery inside mitochondria. For instance, age-related changes in levels of antioxidant enzymes, such as copper/zinc superoxide dismutase (Cu/Zn-SOD) and manganese SOD (Mn-SOD), have been found in liver and cortex of SAMP8 mice when compared with age-matched SAMR1 mice, supporting increased oxidative stress as a key mechanism involved in the aging process (37). More recently, Yew and collaborators have shown an impairment of mitochondrial functions including a decrease of COX activity, mitochondrial ATP content, and mitochondrial glutathione (GSH) level at a relatively early age in SAMP8 mice compared with SAMR1 mice (67, 78). Furthermore, the biochemical consequences of aging have been investigated using proteomic analysis in the brain of SAMP8 and SAMR1 mice at presymptomatic (5-month old) and symptomatic (15-month old) stages (84), revealing differentially expressed proteins with age in both mouse strains, such as Cu/Zn-SOD. Besides the progressive mitochondrial decline and increased oxidative stress, tau hyperphosphorylation was also observed at an early age in the brain of SAMP8 mice (1, 71). In addition, SAMP8 mice showed an age-related increase in mRNA and protein levels of amyloid- β precursor protein (APP). The cleavage product A β was significantly increased at 9 months in SAMP8 and amyloid plaques started to form at around 16 months of age (48, 73). Altogether, these data indicate that mitochondrial dysfunction is a highly relevant event in the aging process, which is also known as the primary risk factor for AD and other prevalent neurodegenerative disorders.

Age-Related A β and Tau Effects on Mitochondria in AD

AD is a progressive, neurodegenerative disorder, characterized by an age-dependent loss of memory and an impairment of multiple cognitive functions. From a genetic point of view, AD can be classified into two different forms: rare familial forms (FAD) where the disease onset is at an age below

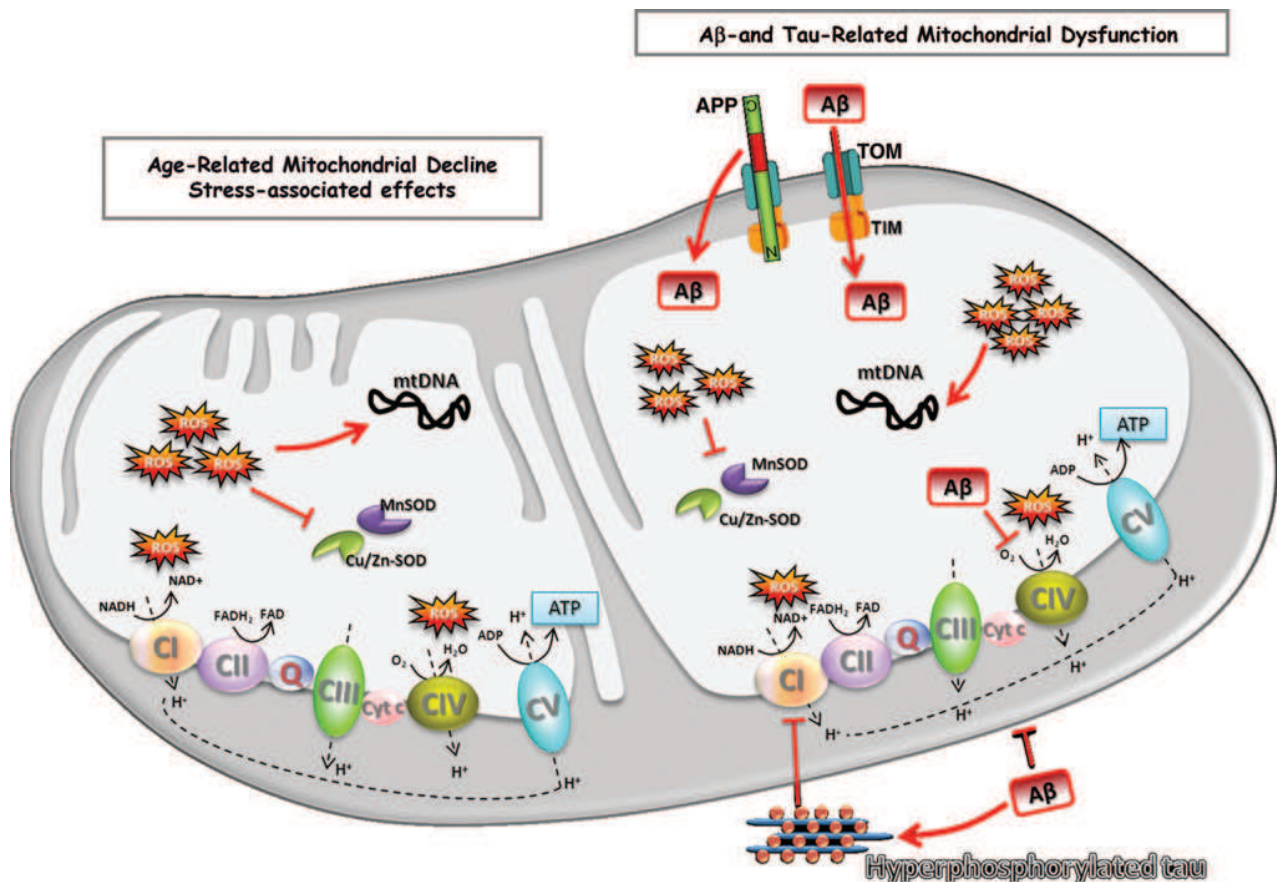


FIG. 1. Aging, A β , and tau: toxic consequence on mitochondria. The aging process may weaken the mitochondrial OXPHOS (oxidative phosphorylation) system in a more general way by the accumulation of ROS-induced damage over many years thereby sowing the seeds for specific and destructive effects of A β and tau. ROS induce peroxidation of several mitochondrial macromolecules, such as mtDNA and mitochondrial lipids, contributing to mitochondrial impairment in the mitochondrial matrix. In AD, mitochondria were found to be a target of A β toxicity, which may act directly or indirectly on several proteins, leading to mitochondrial dysfunction. Indeed, A β was found in the OMM and IMM as well as in the matrix. The interaction of A β with the OMM might affect the transport of nuclear-encoded mitochondrial proteins, such as subunits of the ETC CIV, into the organelle *via* the TOM import machinery. A β seems to be able to enter into the mitochondrial matrix through TOM and TIM or could be derived from mitochondria-associated APP metabolism. The interaction of A β with the IMM would bring it into contact with respiratory chain complexes with the potential for myriad effects on cellular metabolism. It may be that A β by these interactions affects the activity of several enzymes decreasing the ETC enzyme CIV, reducing the amount of hydrogen that is translocated from the matrix to the intermembrane space, thus impairing the MMP. The dysfunction of the ETC leads to a decreased CV activity and so to a lower ATP synthesis, in addition to an increased ROS production. Interestingly, deregulation of CI is mainly tau dependent, while deregulation of CIV is A β dependent, at both the protein and activity level. A β , amyloid- β ; AD, Alzheimer's disease; APP, amyloid precursor protein; CI, complex I; CII, complex II; CIII, complex III; CIV, complex IV; CV, complex V, Cu/Zn-SOD, copper/zinc superoxide dismutase; cyt c, cytochrome c; ETC, electron transport chain; IMM, inner mitochondrial membrane; MMP, mitochondrial membrane potential; MnSOD, manganese superoxide dismutase; mtDNA, mitochondrial DNA; OMM, outer mitochondrial membrane; ROS, reactive oxygen species; TIM, translocase of the inner membrane; TOM, translocase of the outer membrane. (To see this illustration in color the reader is referred to the Web version of this article at www.liebertonline.com/ars).

60 years (<1% of the total number of AD case) and the vast majority of sporadic AD cases where onset occurs at an age over 60 years. Genetic studies in FAD patients have identified autosomal dominant mutations in three different genes, encoding the APP (over 20 pathogenic mutations identified) and the presenilins PS1 and PS2 (more than 130 mutations identified) (26). These mutations are directly linked to the increased production of A β from its precursor protein APP, suggesting a direct and pathological role for A β accumulation in the development of AD.

Mitochondrial dysfunction has been proposed as an underlying mechanism in the early stages of AD, since energy deficiency is a fundamental characteristic feature of AD brains (44) as well as of peripheral cells derived from AD patients (22). Understanding the molecular pathways by which the various pathological alterations including A β and tau compromise neuronal integrity, leading to clinical symptoms, has been a long-standing goal of AD research. The successful development of mouse models that mimic diverse aspects of the AD process has facilitated this effort and assisted in

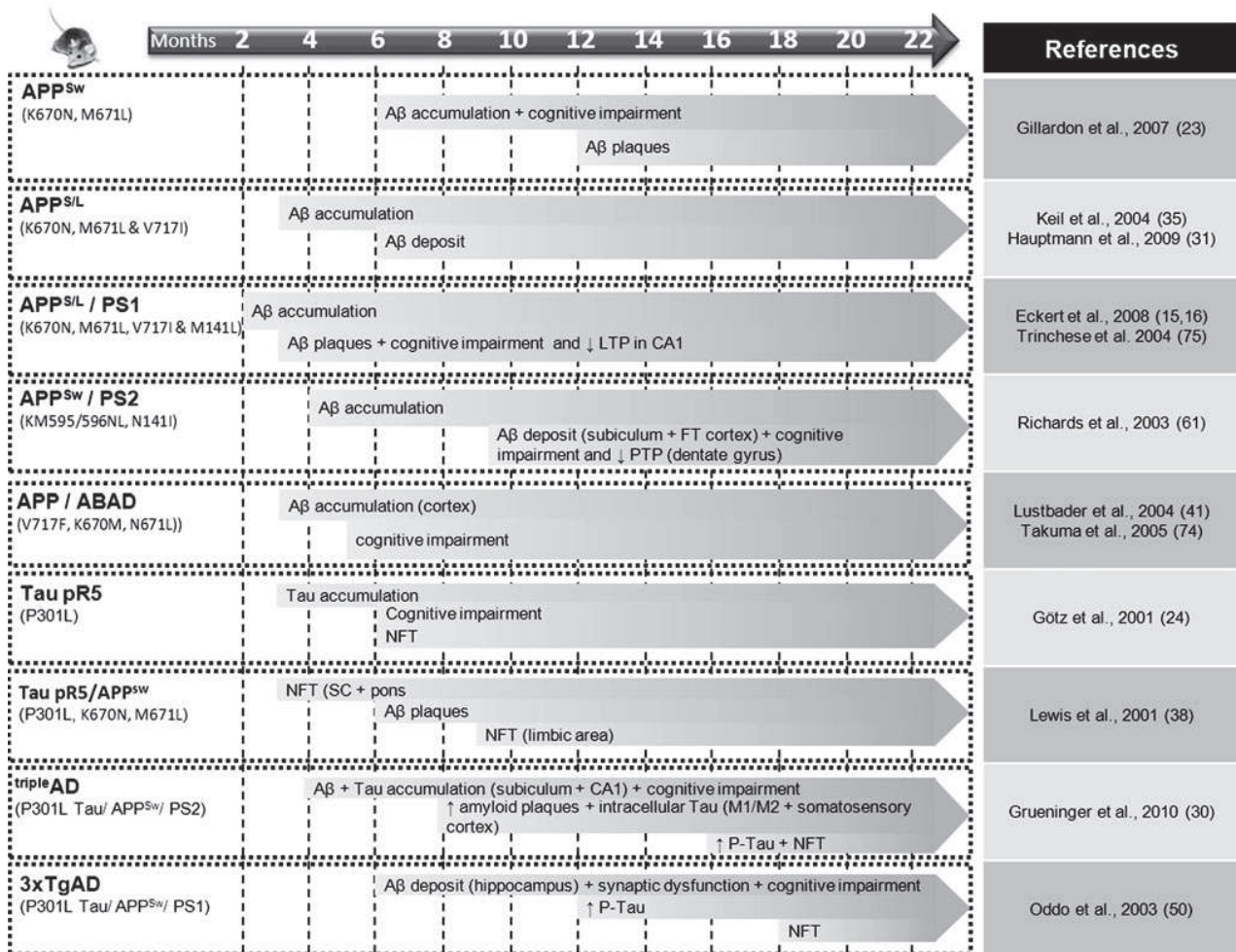


FIG. 2. Age-dependent appearance of histopathological hallmarks in transgenic AD mouse model.

understanding of the age-dependent interplay of $A\beta$ and tau on bioenergetics processes *in vivo* (Figs. 2 and 3).

Separate modes of $A\beta$ and tau toxicity on mitochondria

Mitochondria were found to be a target for APP toxicity as both the full-length protein and $A\beta$ accumulate in the mitochondrial import channels, and both lead to mitochondrial dysfunction (7, 42, 55, 56). Several evidences from cellular and animal AD models indicate that $A\beta$ triggers mitochondrial dysfunction through a number of pathways such as impairment of OXPHOS, elevation of ROS production, interaction with mitochondrial proteins, and alteration of mitochondrial dynamics (52). Indeed, abnormal mitochondrial dynamics have been identified in sporadic and familial AD cases (43, 76) as well as in AD mouse model (6); a distortion probably mediated by altered expression of dynamin-like protein 1 (DLP1), a regulator of mitochondrial fission and distribution, due to elevated oxidative and/or $A\beta$ -induced stress. This modification can disturb the balance between fission and fusion of mitochondria in favor of mitochondrial fission followed by mitochondrial depletion from axons and dendrites and, subsequently, synaptic loss.

Success in developing mouse models that mimic diverse facets of the disease process has greatly facilitated the understanding of physiopathological mechanisms underlying AD. Thus, in 1995, Games and collaborators established the first APP mice model (called PDAPP) bearing the human "Indiana" mutation of the APP gene (V171F). They observed the accumulation of $A\beta$ in the brain and subsequent amyloid plaque formation as well as astrogliosis and neuritic dystrophy (21). Interestingly, in this model cognitive deficits, such as spatial learning impairment, occur before the formation of $A\beta$ plaques and increase with age (8). This phenomenon was also observed in Tg2576 transgenic mice bearing the human Swedish mutation of the APP gene (K670N, M671L). In fact, in most of the APP mouse models, the cognitive impairment begins concomitantly with $A\beta$ oligomer formation in the brain (around 6 months of age), while neuritic amyloid deposits become visible only between 12 and 23 months and then the amount of deposits increases (23, 31, 35). Thus, memory deficits seem to directly correlate with the accumulation of intracellular $A\beta$ oligomers and not with amyloid plaque formation. Crossing APP transgenic mice with those bearing a mutation in presenilin 1 gene enabled an earlier onset of amyloid plaques compared with APP mice. In one of the most

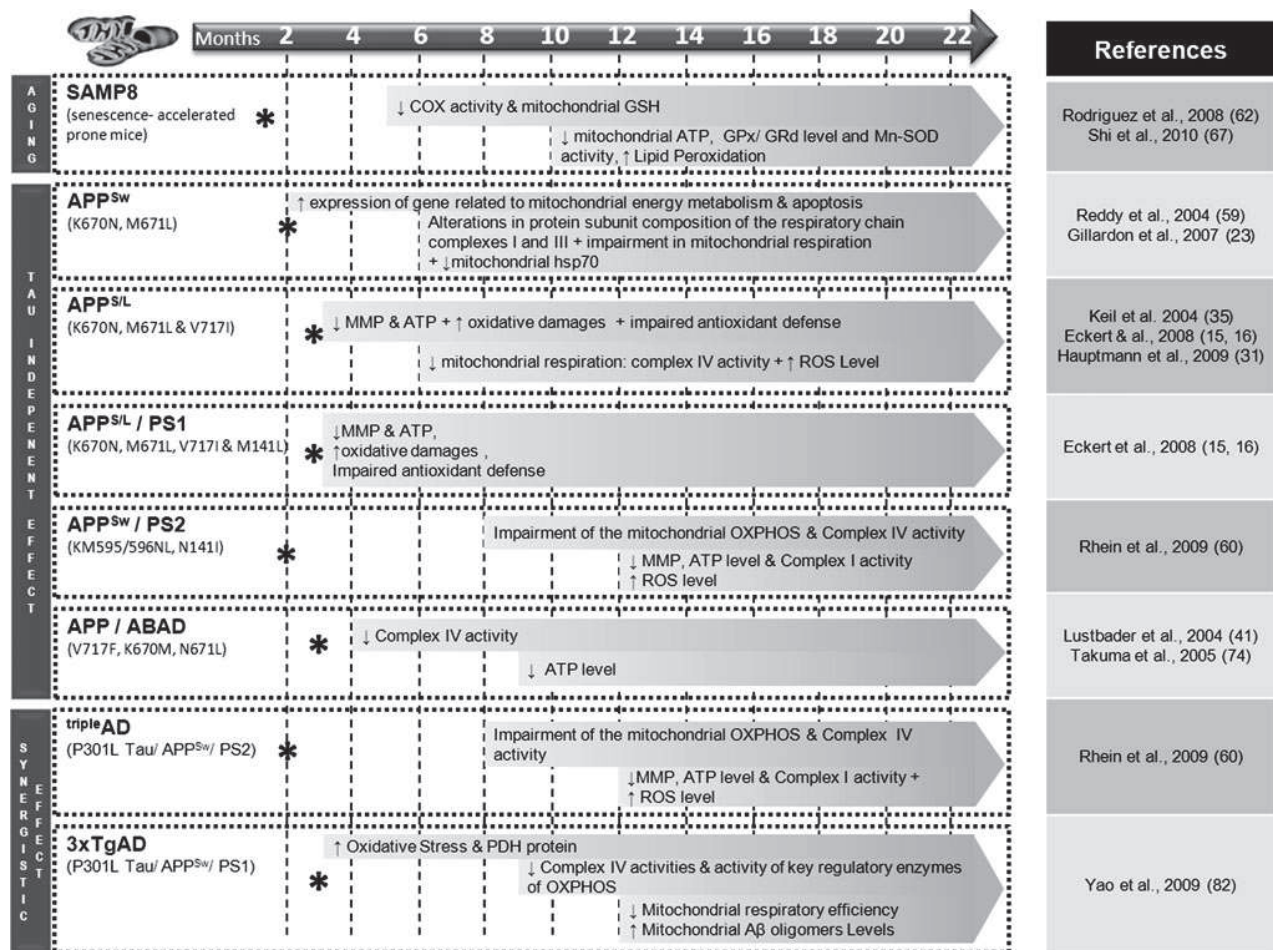


FIG. 3. Age-dependent mitochondrial dysfunction in senescence-accelerated and transgenic AD mouse models. (Star: start of the experiments).

aggressive models, double-transgenic APP^{S/L}/PS1 (APP^{Swedish/London}/PS1^{M141L}) mice, A β accumulation begins very soon at 1–2 months of age while cognitive deficits and amyloid plaque formation are already observed at 3 months (3, 16). A stronger decrease of mitochondrial membrane potential as well as ATP level was also found in these mice.

Mitochondrial dysfunctions also appear to a very early stage in these transgenic mouse models. For example, in the APP^{Sw} transgenic strain Tg2576, an upregulation of genes related to mitochondrial energy metabolism and apoptosis was observed already at 2 months of age. Alterations in composition of the mitochondrial respiratory chain complexes I and III protein subunit as well as impairment of mitochondrial respiration were detected around 6 months, when soluble A β accumulated in the brain without plaque formation (10, 23, 59). To test the hypothesis that oxidative stress can underlie the deleterious effects of PS mutations, Schuessel and collaborators analyzed lipid peroxidation products (4-hydroxynonenal [HNE] and malondialdehyde) and antioxidant defense mechanisms in brain tissue and ROS levels in splenic lymphocytes from transgenic mice bearing the human PS1 M146L mutation (PS1M146L) compared with those from mice transgenic for wild-type human PS1 (PS1wt) and non-

transgenic littermate control mice (66). In brain tissue, HNE levels were increased only in aged (19–22 months) PS1M146L transgenic animals compared with PS1wt mice and not in young (3–4 months) or middle-aged mice (13–15 months). Similarly, in splenic lymphocytes expressing the transgenic PS1 proteins, mitochondrial and cytosolic ROS levels were significantly elevated compared with controls only in cells from aged PS1M146L animals. Antioxidant defense mechanisms (activities of antioxidant enzymes including Cu/Zn-SOD, GSH peroxidase, and GSH reductase) as well as susceptibility to oxidative stress *in vitro* were unaltered. In summary, these results demonstrate that the PS1M146L mutation increases mitochondrial ROS formation and oxidative damage selectively in aged mice. Consistent with this observation, in Swedish amyloid precursor protein (APP^{Sw})/PS2 double-transgenic mice, mitochondrial impairment was first detected at 8 months of age, before amyloid plaque deposition, but after soluble A β accumulation (60, 61). Taken together, these findings are consistent with the recently proposed hypothesis of the age-related A β toxicity cascade that suggests that the most toxic A β species that cause majority of molecular and biochemical abnormalities are in fact intracellular soluble oligomeric

aggregates rather than the extracellular, insoluble plaques that may comprise the form of cellular defense against toxicity of oligomers (19). Interestingly, human amylin that aggregates in type 2 diabetic pancreas and shares with A β its amyloidogenic properties also causes an impaired complex IV activity, whereas nonamyloidogenic rat amylin did not (39).

How does tau interfere with mitochondrial function? In its hyperphosphorylated form, tau, which forms the NFTs, the second hallmark lesion in AD, has been shown to block mitochondrial transport, which results in energy deprivation and oxidative stress at the synapse and, hence, neurodegeneration (27, 33, 57). Till now, no mutations in microtubule-associated protein tau (MAPT) coding genes have been detected in relation to familial forms of AD. However, in familial frontotemporal dementia (FTD) with parkinsonism, mutations in the MAPT gene were identified on chromosome 17. This was the basis for creating a robust mouse model for tau pathology in 2001. These P301L tau-expressing pR5 mice (longest four-repeat 4R2N) show an accumulation of tau as soon as 3 months of age and develop NFTs around 6 months of age (24). A mass spectrometric analysis of the brain proteins from these mice revealed mainly a deregulation of mitochondrial respiratory chain complex components (including complex V), antioxidant enzymes, and synaptic protein space (11). The reduction in mitochondrial complex V levels in the P301L tau mice that was revealed using proteomics was also confirmed as decreased in human P301L FTDP-17 (FTD with parkinsonism linked to chromosome 17) brains. The functional analysis demonstrated age-related mitochondrial dysfunction, together with reduced NADH-ubiquinone oxidoreductase (complex I) activity as well as age-related impaired mitochondrial respiration and ATP synthesis in pR5 mice model. Mitochondrial dysfunction was also associated with higher levels of ROS in aged transgenic mice. Increased tau pathology resulted in modification of lipid peroxidation levels and the upregulation of antioxidant enzymes in response to oxidative stress (11). Thus, this evidence demonstrated for the first time that not only A β but also tau pathology leads to metabolic impairment and oxidative stress by distinct mechanisms from that caused by A β in AD.

Synergistic modes of A β and tau toxicity on mitochondria

Although A β and tau pathologies are both known hallmarks of AD, the mechanisms underlying the interplay between plaques and NFTs (or A β and tau, respectively) have remained unresolved. However, a close relationship between mitochondrial impairment and A β on the one hand and tau on the other hand has been already established. How do both AD features relate to each other? Is it possible that these two molecules synergistically affect mitochondrial integrity? Several studies suggest that A β aggregates and hyperphosphorylated tau may block the mitochondrial carriage to the synapse leading to energy deficiency and neurodegeneration (28). Moreover, the enhanced tau levels may inhibit the transport of APP into axons and dendrites, which suggests a direct link between tau and APP in axonal failure (14, 69). Remarkably, intracerebral A β injections amplify a preexisting tau pathology in several transgenic mouse models (5, 25, 29),

whereas lack of tau abrogates A β toxicity (32, 33). Our findings indicate that in tau transgenic pR5 mice, mitochondria display an enhanced vulnerability toward an A β insult *in vitro* (12, 15, 16), suggesting a synergistic action of tau and A β pathology on this organelle (Figs. 2 and 3). The A β caused a significant reduction of mitochondrial membrane potential in cerebral cells from pR5 mice (11). Furthermore, incubation of isolated mitochondria from pR5 mice with either oligomeric or fibrillar A β species resulted in an impairment of the mitochondrial membrane potential and respiration. Interestingly, aging particularly increased the sensitivity of mitochondria to oligomeric A β insult compared with that of fibrillar A β (15). This suggests that while both oligomeric and fibrillar A β species are toxic, they exert different degrees of toxicity. Crossing P301L mutant tau transgenic JNPL3 mice (shortest four-repeat [4R0N] tau together with the P301L mutation) with APP^{Sw} transgenic Tg2576 mice revealed the presence of NFT pathology in spinal cord and pons already at 3 months of age (38). A β plaques were detected at the age of 6 months and had the same morphology and distribution than in the 1-year-old Tg2576 mice. Taken together, these studies illustrate the existence of a complex interplay between the two key proteins in AD.

Additionally, in recent years triple-transgenic mouse models have been established that combine A β and tau pathologies (Figs. 2 and 3). In these models the contribution of both AD-related proteins on the mitochondrial respiratory machinery and energy homeostasis has been investigated *in vivo*. Indeed, our group demonstrated a mitochondrial dysfunction in a novel triple-transgenic mouse model (pR5/APP^{Sw}/PS2^{N141I})—tripleAD mice—using proteomics followed by functional validation (60). Particularly, deregulation of activity of complex I was found to be tau dependent, whereas deregulation of complex IV was A β dependent, in 10-month-old tripleAD mice. The convergent effects of A β and tau led already at the age of 8 months to a depolarization of mitochondrial membrane potential in tripleAD mice. Additionally, we found that age-related oxidative stress also plays a significant part in the deleterious vicious cycle by exaggerating A β - and tau-induced disturbances in the respiratory system and ATP synthesis, finally leading to synaptic failure.

Our data complement those obtained in another triple-transgenic mouse model 3xTg-AD (P301Ltau/APP^{Sw}/PS1 M146L) (50). In these studies, mitochondrial dysfunction was evidenced by an age-related decrease in the activity of regulatory enzymes of OXPHOS such as COX, or of the Krebs cycle such as pyruvate dehydrogenase, analyzing 3xTg-AD mice aged from 3 to 12 months (82). Besides, these mice also exhibited increased oxidative stress and lipid peroxidation. Most of the effects on mitochondria were seen at the age of 9 months, whereas mitochondrial respiration was significantly decreased at 12 months of age. Importantly, mitochondrial bioenergetics deficits were found to precede the development of AD pathology in the 3xTg-AD mice. Figure 4 nicely shows that AD-specific changes including cognitive impairments, A β accumulation, A β plaques, and mitochondrial dysfunction seem to occur at an earlier onset from single, double up to triple AD transgenic mice models. Together, our studies highlight the key role of mitochondria in AD pathogenesis and consolidate the notion that a synergistic effect of tau and A β enhances the pathological weakening of mitochondria at an early stage of AD.

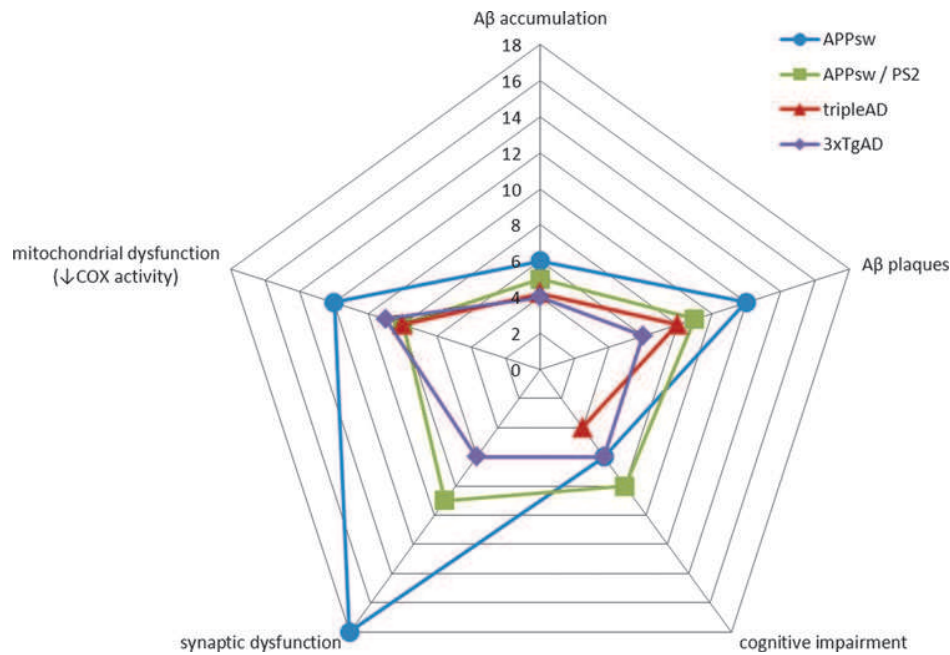


FIG. 4. Age-dependent onset of AD-associated pathological changes in different AD mouse models (age in months). In both triple Tg mouse models [^{Triple}AD, (60); 3xTgAD, (50–82)] an earlier onset in the appearance of AD-related changes in the brain can be detected when compared with double transgenic [APP^{Sw}/PS2 (60, 61)] and to mice bearing only APP mutations [APP^{Sw}, (24)], suggesting again a synergistic effect of A β and tau in the pathogenesis of AD. Age of the mice is given in months. APP^{Sw}, APP Swedish transgenic mice; APP^{Sw}/PS2, APP Swedish/presenilin 2 transgenic mice; tripleAD, APP Swedish/presenilin 2/P301L tau transgenic mice; 3xTgAD, APP Swedish/presenilin 1/P301L tau transgenic mice. (To see this illustration in color the reader is referred to the Web version of this article at www.liebertonline.com/ars).

A β -Binding Alcohol Dehydrogenase: A New Lead to Decode the Mechanisms of A β -Induced Mitochondrial Dysfunction

A few years ago, Yan and collaborators showed that the A β peptide can directly bind a mitochondrial enzyme called A β -binding alcohol dehydrogenase (ABAD) that is overexpressed in the brains of Alzheimer's patients and AD mouse models (79). The interaction of A β with this enzyme exacerbates mitochondrial dysfunction induced by A β (decrease of mitochondrial complex IV activity, diminution of O₂ consumption, and increase of ROS), as shown in double-transgenic mice overexpressing mutant APP and ABAD (81). Furthermore, these mice presented an earlier onset of cognitive impairment and histopathological changes when compared with APP mice, suggesting that the A β -ABAD interaction is an important mechanism underlying A β toxicity. The A β -ABAD complex could have a direct effect on the ETC because ABAD was found to be one of three proteins that comprise the fully functional mammalian mitochondrial RNase P (63), a function that may not require dehydrogenase activity and that links ABAD directly to the production of mitochondrial ETC proteins and ROS generation.

Recently, it has been shown that inhibition of A β -ABAD interaction by a decoy peptide can restore mitochondrial deficits and improve neuronal and cognitive function (81). Our findings, using SH-SY5Y neuroblastoma cells treated with A β ₁₋₄₂, a cellular model of AD, seem to confirm these observations (Lim *et al.*, unpublished observations). We employed a novel small ABAD-specific inhibitor to investigate

the role of this enzyme in A β toxicity. The inhibitor significantly improved metabolic functions impaired by A β , and specifically reduced A β -induced oxidative stress and cell death. Furthermore, we have shown previously that the production of estradiol, a well-known neuroprotective neurosteroid and ABAD substrate, is increased after 24 h in the presence of a "nontoxic" concentration of A β and is decreased when using a toxic concentration of this peptide (64), suggesting that A β is able to modulate (directly or indirectly) neurosteroid levels. Accordingly, new findings from our group demonstrate that the levels of estradiol in the cytosol and in mitochondria can differently be influenced by A β peptide (500 nM, 5 days of treatment) (Fig. 5A, B). We observed that cytosolic estradiol is reduced in the presence of A β , but at the same time mitochondrial estradiol load was significantly increased. We suggest that this increase is due to an A β -induced decrease of ABAD activity, thus limiting the conversion of estradiol in estrone within mitochondria (Fig. 5C). Inhibition of ABAD activity by A β peptide was already demonstrated by Yan and collaborators (80) using 17 β -estradiol as substrate of the enzyme. One mechanism that could explain this inhibition is the fact that A β -ABAD interaction changes the conformation of the enzyme, avoiding the binding of the cofactor NAD⁺, and this reduces the metabolic activity of ABAD (41). However, the total amount of estradiol is about 500-fold higher than in the mitochondrial fraction. Even if A β induced an increase in estradiol within mitochondria, the reduction of total estradiol level by other enzymes of the complex steroidogenic pathway may therefore be more relevant for cellular dysfunction. Besides,

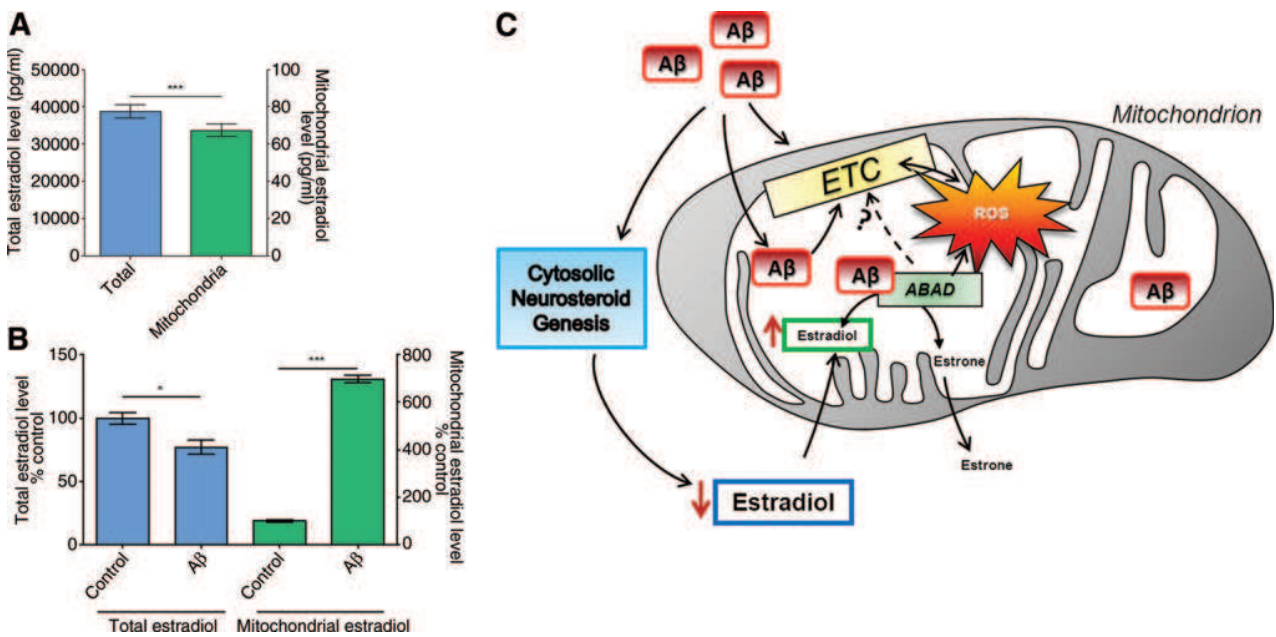


FIG. 5. A β -ABAD interaction and estradiol level in mitochondria. (A) Mitochondrial estradiol is very low compared with total estradiol level in SH-SY5Y neuroblastoma cells. Unpaired *t*-test, ****p* < 0.001. (B) Estradiol level is differently influenced by A β peptide in the cytosol and in mitochondria. Paired *t*-test, **p* < 0.05, ****p* < 0.0001. (C) A β peptide is able to modulate ABAD function by binding directly to this mitochondrial enzyme. This results in the decrease of ABAD-induced conversion of estradiol into estrone with a concomitant increase of ROS levels and an impairment of the ETC in mitochondria. ABAD, A β -binding alcohol dehydrogenase. (To see this illustration in color the reader is referred to the Web version of this article at www.liebertonline.com/ars).

it was also speculated that estradiol exhibits a “prooxidant effect” in the presence of ongoing oxidative stress (49). Thereby, estradiol is hydroxylated to catecholestrogens that can enter a redox cycle generating superoxide radicals, leading to a continuous formation of ROS that amplifies oxidative stress.

Thus, inhibition of the A β -ABAD interaction seems to be an interesting therapeutic target to block or prevent A β -induced mitochondrial toxicity because it could normalize the imbalance between ROS and estradiol levels in mitochondria and thereby help in improving mitochondrial and neuronal function.

Conclusion

We discuss here the recent findings regarding the possible shared mechanisms involving mitochondrial decline driven by brain aging and the close interrelationship of this organelle with the two main pathological features in the pathogenic process underlying AD.

According to the mitochondrial aging theory, ROS-induced damage and mtDNA mutations accumulate over time inducing ETC impairment and weaken mitochondria function in a rather unspecific way; thus, laying the ground for the two common hallmarks of AD, plaques and NFTs, or A β and tau, respectively, which destruct independently as well as synergistically this vital organelle *via* specific mode of actions on complexes I and IV.

Given the complexities of AD, the key role of mitochondrial dysfunction in the early pathogenic pathways by which A β

leads to neuronal dysfunction in AD is particularly challenging with respect to establishing therapeutic treatments. Besides the modulation and/or removal of both A β and tau pathology, strategies involving efforts to protect cells at the mitochondrial level by stabilizing or restoring mitochondrial function or by interfering with energy metabolism appear to be promising. Transgenic AD mice, and particularly triple-transgenic models that combine both pathologies in an age-dependent manner (Fig. 4), are valuable tools in monitoring therapeutic interventions at the mitochondrial level. Eventually, this may lead to therapies that prevent the progression of the age-related mitochondrial decline thereby reducing the vulnerability to A β and/or tau at an early stage of the disease.

Acknowledgments

This work has been supported by grants from the Swiss National Science Foundation (#31000_122572), Sciex_NMS^{CH} and Synapsis Foundation.

References

- Alvarez-Garcia O, Vega-Naredo I, Sierra V, Caballero B, Tomas-Zapico C, Camins A, Garcia JJ, Pallas M, and Coto-Montes A. Elevated oxidative stress in the brain of senescence-accelerated mice at 5 months of age. *Biogerontology* 7: 43–52, 2006.
- Barazzoni R, Short KR, and Nair KS. Effects of aging on mitochondrial DNA copy number and cytochrome c oxidase gene expression in rat skeletal muscle, liver, and heart. *J Biol Chem* 275: 3343–3347, 2000.

3. Blanchard V, Moussaoui S, Czech C, Touchet N, Bonici B, Planche M, Canton T, Jedidi I, Gohin M, Wirths O, Bayer TA, Langui D, Duyckaerts C, Tremp G, and Pradier L. Time sequence of maturation of dystrophic neurites associated with Abeta deposits in APP/PS1 transgenic mice. *Exp Neurol* 184: 247–263, 2003.
4. Bohr VA. Repair of oxidative DNA damage in nuclear and mitochondrial DNA, and some changes with aging in mammalian cells. *Free Radic Biol Med* 32: 804–812, 2002.
5. Bolmont T, Clavaguera F, Meyer-Luehmann M, Herzog MC, Radde R, Staufenbiel M, Lewis J, Hutton M, Tolnay M, and Jucker M. Induction of tau pathology by intracerebral infusion of amyloid-beta -containing brain extract and by amyloid-beta deposition in APP x Tau transgenic mice. *Am J Pathol* 171: 2012–2020, 2007.
6. Calkins MJ, Manczak M, Mao P, Shirendeb U, and Reddy PH. Impaired mitochondrial biogenesis, defective axonal transport of mitochondria, abnormal mitochondrial dynamics and synaptic degeneration in a mouse model of Alzheimer's disease. *Hum Mol Genet* 20: 4515–4529, 2011.
7. Caspersen C, Wang N, Yao J, Sosunov A, Chen X, Lustbader JW, Xu HW, Stern D, McKhann G, and Yan SD. Mitochondrial Abeta: a potential focal point for neuronal metabolic dysfunction in Alzheimer's disease. *FASEB J* 19: 2040–2041, 2005.
8. Chen G, Chen KS, Knox J, Inglis J, Bernard A, Martin SJ, Justice A, McConlogue L, Games D, Freedman SB, and Morris RG. A learning deficit related to age and beta-amyloid plaques in a mouse model of Alzheimer's disease. *Nature* 408: 975–979, 2000.
9. Coskun PE, Beal MF, and Wallace DC. Alzheimer's brains harbor somatic mtDNA control-region mutations that suppress mitochondrial transcription and replication. *Proc Natl Acad Sci U S A* 101: 10726–10731, 2004.
10. Crouch PJ, Blake R, Duce JA, Ciccotosto GD, Li QX, Barnham KJ, Curtain CC, Cherny RA, Cappai R, Dyrks T, Masters CL, and Troncone IA. Copper-dependent inhibition of human cytochrome c oxidase by a dimeric conformer of amyloid-beta1-42. *J Neurosci* 25: 672–679, 2005.
11. David DC, Hauptmann S, Scherping I, Schuessel K, Keil U, Rizzu P, Ravid R, Drose S, Brandt U, Muller WE, Eckert A, and Gotz J. Proteomic and functional analyses reveal a mitochondrial dysfunction in P301L tau transgenic mice. *J Biol Chem* 280: 23802–23814, 2005.
12. David DC, Ittner LM, Gehrig P, Nergensau D, Shepherd C, Halliday G, and Gotz J. Beta-amyloid treatment of two complementary P301L tau-expressing Alzheimer's disease models reveals similar deregulated cellular processes. *Proteomics* 6: 6566–6577, 2006.
13. Domek-Lopacinska KU and Strosznajder JB. Cyclic GMP and nitric oxide synthase in aging and Alzheimer's disease. *Mol Neurobiol* 41: 129–137, 2010.
14. Ebner A, Drewes G, Mandelkow EM, and Mandelkow E. Phosphorylation of MAP2c and MAP4 by MARK kinases leads to the destabilization of microtubules in cells. *Cell Motil Cytoskeleton* 44: 209–224, 1999.
15. Eckert A, Hauptmann S, Scherping I, Meinhardt J, Rhein V, Drose S, Brandt U, Fandrich M, Muller WE, and Gotz J. Oligomeric and fibrillar species of beta-amyloid (A beta 42) both impair mitochondrial function in P301L tau transgenic mice. *J Mol Med (Berl)* 86: 1255–1267, 2008.
16. Eckert A, Hauptmann S, Scherping I, Rhein V, Muller-Spahn F, Gotz J, and Muller WE. Soluble beta-amyloid leads to mitochondrial defects in amyloid precursor protein and tau transgenic mice. *Neurodegener Dis* 5: 157–159, 2008.
17. Eckert A, Schmitt K, and Gotz J. Mitochondrial dysfunction—the beginning of the end in Alzheimer's disease? Separate and synergistic modes of tau and amyloid-beta toxicity. *Alzheimers Res Ther* 3: 15, 2011.
18. Eckert A, Schulz KL, Rhein V, and Gotz J. Convergence of amyloid-beta and tau pathologies on mitochondria *in vivo*. *Mol Neurobiol* 41: 107–114, 2010.
19. Fernandez-Vizarra P, Fernandez AP, Castro-Blanco S, Serano J, Bentura ML, Martinez-Murillo R, Martinez A, and Rodrigo J. Intra- and extracellular Abeta and PHF in clinically evaluated cases of Alzheimer's disease. *Histol Histopathol* 19: 823–844, 2004.
20. Frahm T, Mohamed SA, Bruse P, Gemund C, Oehmichen M, and Meissner C. Lack of age-related increase of mitochondrial DNA amount in brain, skeletal muscle and human heart. *Mech Ageing Dev* 126: 1192–1200, 2005.
21. Games D, Adams D, Alessandrini R, Barbour R, Berthelette P, Blackwell C, Carr T, Clemens J, Donaldson T, Gillespie F, et al. Alzheimer-type neuropathology in transgenic mice overexpressing V717F beta-amyloid precursor protein. *Nature* 373: 523–527, 1995.
22. Gibson GE, Sheu KF, and Blass JP. Abnormalities of mitochondrial enzymes in Alzheimer disease. *J Neural Transm* 105: 855–870, 1998.
23. Gillardon F, Rist W, Kussmaul L, Vogel J, Berg M, Danzer K, Kraut N, and Hengerer B. Proteomic and functional alterations in brain mitochondria from Tg2576 mice occur before amyloid plaque deposition. *Proteomics* 7: 605–616, 2007.
24. Gotz J, Chen F, Barmettler R, and Nitsch RM. Tau filament formation in transgenic mice expressing P301L tau. *J Biol Chem* 276: 529–534, 2001.
25. Gotz J, Chen F, van Dorpe J, and Nitsch RM. Formation of neurofibrillary tangles in P301L tau transgenic mice induced by Abeta 42 fibrils. *Science* 293: 1491–1495, 2001.
26. Gotz J and Ittner LM. Animal models of Alzheimer's disease and frontotemporal dementia. *Nat Rev Neurosci* 9: 532–544, 2008.
27. Gotz J, Ittner LM, Fandrich M, and Schonrock N. Is tau aggregation toxic or protective: a sensible question in the absence of sensitive methods? *J Alzheimers Dis* 14: 423–429, 2008.
28. Gotz J, Ittner LM, and Kins S. Do axonal defects in tau and amyloid precursor protein transgenic animals model axonopathy in Alzheimer's disease? *J Neurochem* 98: 993–1006, 2006.
29. Gotz J, Schild A, Hoernli F, and Penanen L. Amyloid-induced neurofibrillary tangle formation in Alzheimer's disease: insight from transgenic mouse and tissue-culture models. *Int J Dev Neurosci* 22: 453–465, 2004.
30. Gruening F, Bohrmann B, Czech C, Ballard TM, Frey JR, Weidensteiner C, von Kienlin M, and Ozmen L. Phosphorylation of Tau at S422 is enhanced by Abeta in TauPS2APP triple transgenic mice. *Neurobiol Dis* 37: 294–306, 2010.
31. Hauptmann S, Scherping I, Drose S, Brandt U, Schulz KL, Jendrach M, Leuner K, Eckert A, and Muller WE. Mitochondrial dysfunction: an early event in Alzheimer pathology accumulates with age in AD transgenic mice. *Neurobiol Aging* 30: 1574–1586, 2009.
32. Ittner LM and Gotz J. Amyloid-beta and tau - a toxic pas de deux in Alzheimer's disease. *Nat Rev Neurosci* 12: 65–72, 2011.
33. Ittner LM, Ke YD, Delerue F, Bi M, Gladbach A, van Eersel J, Wolfing H, Chieng BC, Christie MJ, Napier IA, Eckert A, Staufenbiel M, Hardeman E, and Gotz J. Dendritic function of tau mediates amyloid-beta toxicity in Alzheimer's disease mouse models. *Cell* 142: 387–397, 2010.

34. Jesko H, Chalimoniuk M, and Strosznajder JB. Activation of constitutive nitric oxide synthase(s) and absence of inducible isoform in aged rat brain. *Neurochem Int* 42: 315–322, 2003.
35. Keil U, Bonert A, Marques CA, Scherping I, Weyermann J, Strosznajder JB, Muller-Spahn F, Haass C, Czech C, Pradier L, Muller WE, and Eckert A. Amyloid beta-induced changes in nitric oxide production and mitochondrial activity lead to apoptosis. *J Biol Chem* 279: 50310–50320, 2004.
36. Kuro-o M. Disease model: human aging. *Trends Mol Med* 7: 179–181, 2001.
37. Kurokawa T, Asada S, Nishitani S, and Hazeki O. Age-related changes in manganese superoxide dismutase activity in the cerebral cortex of senescence-accelerated prone and resistant mouse. *Neurosci Lett* 298: 135–138, 2001.
38. Lewis J, McGowan E, Rockwood J, Melrose H, Nacharaju P, Van Slegtenhorst M, Gwinn-Hardy K, Paul Murphy M, Baker M, Yu X, Duff K, Hardy J, Corral A, Lin WL, Yen SH, Dickson DW, Davies P, and Hutton M. Neurofibrillary tangles, amyotrophy and progressive motor disturbance in mice expressing mutant (P301L) tau protein. *Nat Genet* 25: 402–405, 2000.
39. Lim YA, Rhein V, Baysang G, Meier F, Poljak A, Raftery MJ, Guilhaus M, Ittner LM, Eckert A, and Gotz J. Abeta and human amylin share a common toxicity pathway via mitochondrial dysfunction. *Proteomics* 10: 1621–1633, 2010.
40. Lu J, Wang K, Rodova M, Esteves R, Berry D, Lezi E, Crafter A, Barrett M, Cardoso SM, Onyango I, Parker WD, Fontes J, Burns JM, and Swerdlow RH. Polymorphic variation in cytochrome oxidase subunit genes. *J Alzheimers Dis* 21: 141–154, 2010.
41. Lustbader JW, Cirilli M, Lin C, Xu HW, Takuma K, Wang N, Caspersen C, Chen X, Pollak S, Chaney M, Trinchese F, Liu S, Gunn-Moore F, Lue LF, Walker DG, Kuppusamy P, Zewier ZL, Arancio O, Stern D, Yan SS, and Wu H. ABAD directly links Abeta to mitochondrial toxicity in Alzheimer's disease. *Science* 304: 448–452, 2004.
42. Manczak M, Anekonda TS, Henson E, Park BS, Quinn J, and Reddy PH. Mitochondria are a direct site of A beta accumulation in Alzheimer's disease neurons: implications for free radical generation and oxidative damage in disease progression. *Hum Mol Genet* 15: 1437–1449, 2006.
43. Manczak M, Calkins MJ, and Reddy PH. Impaired mitochondrial dynamics and abnormal interaction of amyloid beta with mitochondrial protein Drp1 in neurons from patients with Alzheimer's disease: implications for neuronal damage. *Hum Mol Genet* 20: 2495–2509, 2011.
44. Manczak M, Park BS, Jung Y, and Reddy PH. Differential expression of oxidative phosphorylation genes in patients with Alzheimer's disease: implications for early mitochondrial dysfunction and oxidative damage. *Neuromolecular Med* 5: 147–162, 2004.
45. Mao P and Reddy PH. Aging and amyloid beta-induced oxidative DNA damage and mitochondrial dysfunction in Alzheimer's disease: Implications for early intervention and therapeutics. *Biochim Biophys Acta* 1812: 1359–1370, 2011.
46. Masuyama M, Iida R, Takatsuka H, Yasuda T, and Matsuki T. Quantitative change in mitochondrial DNA content in various mouse tissues during aging. *Biochim Biophys Acta* 1723: 302–308, 2005.
47. Mattson MP, Gleichmann M, and Cheng A. Mitochondria in neuroplasticity and neurological disorders. *Neuron* 60: 748–766, 2008.
48. Morley JE, Kumar VB, Bernardo AE, Farr SA, Uezu K, Tummala N, and Flood JF. Beta-amyloid precursor polypeptide in SAMP8 mice affects learning and memory. *Peptides* 21: 1761–1767, 2000.
49. Nilsen J. Estradiol and neurodegenerative oxidative stress. *Front Neuroendocrinol* 29: 463–475, 2008.
50. Oddo S, Caccamo A, Shepherd JD, Murphy MP, Golde TE, Kaye R, Metherate R, Mattson MP, Akbari Y, and LaFerla FM. Triple-transgenic model of Alzheimer's disease with plaques and tangles: intracellular Abeta and synaptic dysfunction. *Neuron* 39: 409–421, 2003.
51. Omata N, Murata T, Fujibayashi Y, Waki A, Sadato N, Yoshimoto M, Wada Y, and Yonekura Y. Age-related changes in energy production in fresh senescence-accelerated mouse brain slices as revealed by positron autoradiography. *Dement Geriatr Cogn Disord* 12: 78–84, 2001.
52. Pagani L and Eckert A. Amyloid-Beta interaction with mitochondria. *Int J Alzheimers Dis* 2011: 925050, 2011.
53. Pallas M, Camins A, Smith MA, Perry G, Lee HG, and Casadesus G. From aging to Alzheimer's disease: unveiling "the switch" with the senescence-accelerated mouse model (SAMP8). *J Alzheimers Dis* 15: 615–624, 2008.
54. Park CB and Larsson NG. Mitochondrial DNA mutations in disease and aging. *J Cell Biol* 193: 809–818, 2011.
55. Pavlov PF, Hansson Petersen C, Glaser E, and Ankarcona M. Mitochondrial accumulation of APP and Abeta: significance for Alzheimer disease pathogenesis. *J Cell Mol Med* 13: 4137–4145, 2009.
56. Pavlov PF, Wiehager B, Sakai J, Frykman S, Behbahani H, Winblad B, and Ankarcona M. Mitochondrial gamma-secretase participates in the metabolism of mitochondria-associated amyloid precursor protein. *FASEB J* 25: 78–88, 2011.
57. Reddy PH. Abnormal tau, mitochondrial dysfunction, impaired axonal transport of mitochondria, and synaptic deprivation in Alzheimer's disease. *Brain Res* 1415: 136–148, 2011.
58. Reddy PH and Beal MF. Amyloid beta, mitochondrial dysfunction and synaptic damage: implications for cognitive decline in aging and Alzheimer's disease. *Trends Mol Med* 14: 45–53, 2008.
59. Reddy PH, McWeeney S, Park BS, Manczak M, Gutala RV, Partovi D, Jung Y, Yau V, Searles R, Mori M, and Quinn J. Gene expression profiles of transcripts in amyloid precursor protein transgenic mice: up-regulation of mitochondrial metabolism and apoptotic genes is an early cellular change in Alzheimer's disease. *Hum Mol Genet* 13: 1225–1240, 2004.
60. Rhein V, Song X, Wiesner A, Ittner LM, Baysang G, Meier F, Ozmen L, Bluethmann H, Drose S, Brandt U, Savaskan E, Czech C, Gotz J, and Eckert A. Amyloid-beta and tau synergistically impair the oxidative phosphorylation system in triple transgenic Alzheimer's disease mice. *Proc Natl Acad Sci U S A* 106: 20057–20062, 2009.
61. Richards JG, Higgins GA, Ouagazzal AM, Ozmen L, Kew JN, Bohrmann B, Malherbe P, Brockhaus M, Loetscher H, Czech C, Huber G, Bluethmann H, Jacobsen H, and Kemp JA. PS2APP transgenic mice, coexpressing hPS2mut and hAPPswe, show age-related cognitive deficits associated with discrete brain amyloid deposition and inflammation. *J Neurosci* 23: 8989–9003, 2003.
62. Rodriguez MI, Escames G, Lopez LC, Lopez A, Garcia JA, Ortiz F, Sanchez V, Romeu M, and Acuna-Castroviejo D. Improved mitochondrial function and increased life span after chronic melatonin treatment in senescent prone mice. *Exp Gerontol* 43: 749–756, 2008.
63. Sapra AK, Anko ML, Grishina I, Lorenz M, Pabis M, Poser I, Rollins J, Weiland EM, and Neugebauer KM. SR protein family members display diverse activities in the formation of nascent and mature mRNPs *in vivo*. *Mol Cell* 34: 179–190, 2009.

64. Schaeffer V, Meyer L, Patte-Mensah C, Eckert A, and Mensah-Nyagan AG. Dose-dependent and sequence-sensitive effects of amyloid-beta peptide on neurosteroidogenesis in human neuroblastoma cells. *Neurochem Int* 52: 948–955, 2008.
65. Scheffler IE. A century of mitochondrial research: achievements and perspectives. *Mitochondrion* 1: 3–31, 2001.
66. Schuessel K, Frey C, Jourdan C, Keil U, Weber CC, Muller-Spahn F, Muller WE, and Eckert A. Aging sensitizes toward ROS formation and lipid peroxidation in PS1M146L transgenic mice. *Free Radic Biol Med* 40: 850–862, 2006.
67. Shi C, Xiao S, Liu J, Guo K, Wu F, Yew DT, and Xu J. Ginkgo biloba extract EGb761 protects against aging-associated mitochondrial dysfunction in platelets and hippocampi of SAMP8 mice. *Platelets* 21: 373–379, 2010.
68. Short KR, Bigelow ML, Kahl J, Singh R, Coenen-Schimke J, Raghavakaimal S, and Nair KS. Decline in skeletal muscle mitochondrial function with aging in humans. *Proc Natl Acad Sci U S A* 102: 5618–5623, 2005.
69. Stamer K, Vogel R, Thies E, Mandelkow E, and Mandelkow EM. Tau blocks traffic of organelles, neurofilaments, and APP vesicles in neurons and enhances oxidative stress. *J Cell Biol* 156: 1051–1063, 2002.
70. Strosznajder JB, Jesko H, Zambrzycka A, Eckert A, and Chalimoniuk M. Age-related alteration of activity and gene expression of endothelial nitric oxide synthase in different parts of the brain in rats. *Neurosci Lett* 370: 175–179, 2004.
71. Sureda FX, Gutierrez-Cuesta J, Romeu M, Mulero M, Canudas AM, Camins A, Mallol J, and Pallas M. Changes in oxidative stress parameters and neurodegeneration markers in the brain of the senescence-accelerated mice SAMP-8. *Exp Gerontol* 41: 360–367, 2006.
72. Swerdlow RH. Brain aging, Alzheimer's disease, and mitochondria. *Biochim Biophys Acta* 1812: 1630–1639, 2011.
73. Takemura M, Nakamura S, Akguchi I, Ueno M, Oka N, Ishikawa S, Shimada A, Kimura J, and Takeda T. Beta/A4 proteinlike immunoreactive granular structures in the brain of senescence-accelerated mouse. *Am J Pathol* 142: 1887–1897, 1993.
74. Takuma K, Yao J, Huang J, Xu H, Chen X, Luddy J, Trillat AC, Stern DM, Arancio O, and Yan SS. ABAD enhances Abeta-induced cell stress via mitochondrial dysfunction. *FASEB J* 19: 597–598, 2005.
75. Trinchese F, Liu S, Battaglia F, Walter S, Mathews PM, and Arancio O. Progressive age-related development of Alzheimer-like pathology in APP/PS1 mice. *Ann Neurol* 55: 801–814, 2004.
76. Wang X, Su B, Fujioka H, and Zhu X. Dynamin-like protein 1 reduction underlies mitochondrial morphology and distribution abnormalities in fibroblasts from sporadic Alzheimer's disease patients. *Am J Pathol* 173: 470–482, 2008.
77. Watanabe K, Tonosaki K, Kawase T, Karasawa N, Nagatsu I, Fujita M, and Onozuka M. Evidence for involvement of dysfunctional teeth in the senile process in the hippocampus of SAMP8 mice. *Exp Gerontol* 36: 283–295, 2001.
78. Xu J, Shi C, Li Q, Wu J, Forster EL, and Yew DT. Mitochondrial dysfunction in platelets and hippocampi of senescence-accelerated mice. *J Bioenerg Biomembr* 39: 195–202, 2007.
79. Yan SD, Fu J, Soto C, Chen X, Zhu H, Al-Mohanna F, Collison K, Zhu A, Stern E, Saido T, Tohyama M, Ogawa S, Roher A, and Stern D. An intracellular protein that binds amyloid-beta peptide and mediates neurotoxicity in Alzheimer's disease. *Nature* 389: 689–695, 1997.
80. Yan SD, Shi Y, Zhu A, Fu J, Zhu H, Zhu Y, Gibson L, Stern E, Collison K, Al-Mohanna F, Ogawa S, Roher A, Clarke SG, and Stern DM. Role of ERAB/L-3-hydroxyacyl-coenzyme A dehydrogenase type II activity in Abeta-induced cytotoxicity. *J Biol Chem* 274: 2145–2156, 1999.
81. Yao J, Du H, Yan S, Fang F, Wang C, Lue LF, Guo L, Chen D, Stern DM, Gunn Moore FJ, Xi Chen J, Arancio O, and Yan SS. Inhibition of amyloid-beta (Abeta) peptide-binding alcohol dehydrogenase-Abeta interaction reduces Abeta accumulation and improves mitochondrial function in a mouse model of Alzheimer's disease. *J Neurosci* 31: 2313–2320, 2011.
82. Yao J, Irwin RW, Zhao L, Nilsen J, Hamilton RT, and Brinton RD. Mitochondrial bioenergetic deficit precedes Alzheimer's pathology in female mouse model of Alzheimer's disease. *Proc Natl Acad Sci U S A* 106: 14670–14675, 2009.
83. Yen TC, Su JH, King KL, and Wei YH. Ageing-associated 5 kb deletion in human liver mitochondrial DNA. *Biochem Biophys Res Commun* 178: 124–131, 1991.
84. Zhu L, Yu J, Shi Q, Lu W, Liu B, Xu S, Wang L, Han J, and Wang X. Strain- and age-related alteration of proteins in the brain of SAMP8 and SAMR1 mice. *J Alzheimers Dis* 23: 641–654, 2011.

Address correspondence to:

Dr. Anne Eckert
Neurobiology Laboratory for Brain Aging and Mental Health
Psychiatric University Clinics
University of Basel
CH-4012 Basel
Switzerland

E-mail: anne.eckert@upkbs.ch

Date of first submission to ARS Central, November 10, 2011;
date of acceptance, November 27, 2011.

Abbreviations Used

$A\beta$	= amyloid- β
ABAD	= $A\beta$ -binding alcohol dehydrogenase
AD	= Alzheimer's disease
APP	= amyloid precursor protein
APP ^{Sw}	= Swedish amyloid precursor protein
APP ^{wt}	= wild-type amyloid precursor protein
COX	= cytochrome c oxidase
DLP1	= dynamin-like protein 1
ETC	= electron transport chain
FTD	= frontotemporal dementia
GSH	= glutathione
HA	= human amylin
HNE	= 4-hydroxynonenal
IMM	= inner mitochondrial membrane
MAPT	= microtubule-associated protein tau
MMP	= mitochondrial membrane potential
mtDNA	= mitochondrial DNA
nDNA	= nuclear DNA
NFT	= neurofibrillary tangle
NO	= nitric oxide
OMM	= outer mitochondrial membrane
OXPHOS	= oxidative phosphorylation
PDH	= pyruvate dehydrogenase
PS	= presenilin
ROS	= reactive oxygen species
SAM	= senescence-accelerated mice
SOD	= superoxide dismutase
TIM	= translocase of the inner membrane
TOM	= translocase of the outer membrane

**E. Advanced mitochondrial respiration assay for evaluation of
mitochondrial dysfunction in Alzheimer's disease**

Running head:

Mitochondrial dysfunction in Alzheimer's disease

Authors: Grimm A, **Schmitt K**, Eckert A*

Affiliations:

Neurobiology Laboratory for Brain Aging and Mental Health

Universitäre Psychiatrische Kliniken Basel

Wilhelm Klein-Str. 27

CH- 4012 Basel, Switzerland

*E-mail of the corresponding author: Anne.Eckert@upkbs.ch

*Phone number: +41(0)61 325 5487

Juan I. Castrillo and Stephen G. Oliver (eds.), Systems Biology of Alzheimer's Disease, Methods in Molecular Biology, vol. 1303, DOI 10.1007/978-1-4939-2627-5_9, © Springer Science+Business Media New York 2016

Advanced Mitochondrial Respiration Assay for Evaluation of Mitochondrial Dysfunction in Alzheimer's Disease

Amandine Grimm, Karen Schmitt, and Anne Eckert

Abstract

Alzheimer's disease (AD) is characterized by the presence of amyloid plaques (aggregates of amyloid- β [$A\beta$]) and neurofibrillary tangles (aggregates of tau) in the brain, but the underlying mechanisms of the disease are still partially unclear. A growing body of evidence supports mitochondrial dysfunction as a prominent and early, chronic oxidative stress-associated event that contributes to synaptic abnormalities, and, ultimately, selective neuronal degeneration in AD. Using a high-resolution respirometry system, we shed new light on the close interrelationship of this organelle with $A\beta$ and tau in the pathogenic process underlying AD by showing a synergistic effect of these two hallmark proteins on the oxidative phosphorylation capacity of mitochondria isolated from the brain of transgenic AD mice. In the present chapter, we first introduce the principle of the $A\beta$ and tau interaction on mitochondrial respiration, and secondly, we describe in detail the used respiratory protocol.

Key words Mitochondria, Alzheimer's disease, Amyloid- β , Tau, Oxygraph, High-resolution respirometry (HRR), Oxidative phosphorylation

1 Introduction

With the increasing average life span of humans, Alzheimer's disease (AD) is the most common neurodegenerative disorder among elderly individuals. It accounts for up to 80 % of all dementia cases and ranks as the fourth leading cause of death amongst those above 65 years of age [1]. Although the hallmark lesions of the disease were already described by Alois Alzheimer in 1906—amyloid- β ($A\beta$) containing plaques and microtubule-associated protein tau-containing neurofibrillary tangles (NFTs)—the underlying molecular mechanisms that cause the formation of these end-stage lesions are still poorly understood. However, a growing body of evidence supports mitochondrial dysfunction as a prominent and early chronic oxidative stress-associated event that contributes to synaptic abnormalities and, ultimately, selective neuronal degeneration in AD [2, 3]. Within the last few years, several cell culture models

as well as single, double, and more recently triple transgenic mouse models have been developed to reproduce diverse aspects of AD. These models help in understanding the pathogenic mechanisms that lead to mitochondrial failure in AD, and in particular the interplay of AD-related cellular modifications within this process [4]. In this chapter, we highlight the critical key role of mitochondria and the close inter-relationship of this organelle with the two main pathological features in the pathogenic process underlying AD. Particularly, we will emphasize on the recent insights showing independent as well as synergistic effects of A β peptide and hyperphosphorylated tau on mitochondrial function by using a high-resolution respirometry system (Oxygraph-2k).

1.1 A β and Tau Induce Mitochondrial Toxicity

Mitochondria play a pivotal role in cell survival and death by regulating both energy metabolism and apoptotic pathways. They are the “powerhouses of cells” providing energy via ATP generation which is accomplished through oxidative phosphorylation (OXPHOS) from nutritional sources [5] (Fig. 1). Neurons have particularly high numbers of mitochondria which are especially enriched in synapses. Due to the limited glycolytic capacity of neurons, those cells are

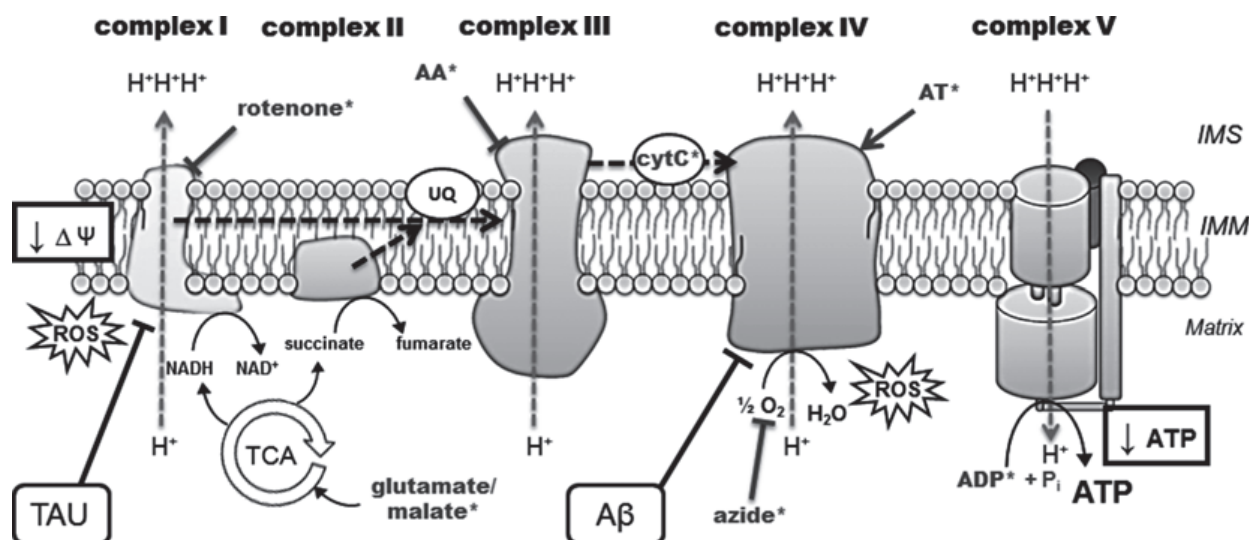


Fig. 1 The mitochondrial electron transport chain: impact of A β peptide, tau protein, and effects of mitochondrial substrates used during the measurement protocol with Oxygraph. Complexes I (NADH: ubiquinone oxidoreductase) and II (succinate dehydrogenase, belongs to the tricarboxylic acid (TCA) cycle) receive electrons from NADH and FADH₂, respectively. Electrons are then driven from complexes by the mobile carrier molecules coenzyme Q/ubiquinone (UQ) and cytochrome c (Cyt c) to the final acceptor, molecular oxygen (O₂). Electron flow is coupled to proton movement across the inner mitochondrial membrane (IMM) in complexes I, III and IV. The resulting proton gradient is harvested by complex V to generate ATP. In Alzheimer’s disease, abnormal mitochondrial electron activities have been observed, predominantly in complexes I and IV, leading to impaired mitochondrial membrane potential, decreased production of ATP (complex V), and increasing reactive oxygen species (ROS) levels. Interestingly, deregulation of complex I is mainly tau-dependent, while deregulation of complex IV is amyloid- β (A β)-dependent, at both the protein and activity levels. The targets of the different substrates used during the Oxygraph measurement are marked with an *asterisk* and their specific actions are summarized in Table 1. AA antimycin A, AT ascorbate/TMPD, IMS intermembrane space

highly dependent on mitochondrial function for energy production [6]. Thus, deregulation of mitochondrial function leads to synaptic stress, disruption of synaptic transmission, apoptosis and ultimately, systemic neurodegeneration [7, 8].

Evidences from cellular and animal AD models indicate that A β triggers mitochondrial dysfunction through a number of pathways such as impairment of OXPHOS, elevation of reactive oxygen species (ROS) production, interaction with mitochondrial proteins, and alteration of mitochondrial dynamics [9, 10]. Success in developing mouse models that mimic diverse facets of the disease process has greatly facilitated the understanding of pathophysiological mechanisms underlying AD. In 1995, Games and collaborators established the first amyloid precursor protein (APP) mouse model (called PDAPP) bearing the human "Indiana" mutation of the *APP* gene (V171F). They observed the accumulation of A β in the brain and subsequent amyloid plaque formation, as well as astrogliosis and neuritic dystrophy [4]. Interestingly, in most of the APP mouse models, the cognitive impairment begins concomitantly with A β oligomer formation in the brain (around 6 months of age), while neuritic amyloid deposits become visible only between 12 and 23 months and the amount of deposits increases in parallel [11]. Thus, memory deficits seem to correlate directly with the accumulation of intracellular A β oligomers and not with amyloid plaque formation. When those mice were crossed with those bearing a mutation in presenilin 1 gene (PS1), coding for a gene involved in APP processing, an earlier onset of amyloid plaques was observed, alongside a stronger decrease of mitochondrial membrane potential as well as ATP level [12].

Mitochondrial dysfunctions occur at a very early disease stage in AD transgenic mouse models. For example, in the APP^{sw} transgenic strain Tg2576 (Swedish mutation), an upregulation of genes related to mitochondrial energy metabolism and apoptosis was observed already at 2 months of age. Alterations in composition of the mitochondrial respiratory chain complexes I and III protein subunit as well as impairment of mitochondrial respiration were detected around 6 months, when soluble A β accumulated in the brain without plaque formation [13, 14].

Consistent with this observation, in APP^{sw}/presenilin 2 (PS2) double-transgenic mice, mitochondrial impairment was first detected at 8 months of age, before amyloid plaque deposition, but after soluble A β accumulation [15]. Taken together, these findings are consistent with the recently proposed hypothesis of an age-related A β toxicity cascade that suggests that the most toxic A β species that cause majority of molecular and biochemical abnormalities are in fact intracellular soluble oligomeric aggregates rather than the extracellular, insoluble plaques [16].

How does tau, the second hallmark lesion in AD, interfere with mitochondrial function? In its abnormally hyperphosphorylated form, which forms the neurofibrillary tangles (NFTs), tau has

been shown to block mitochondrial transport. This results in energy deprivation and oxidative stress at the synapse, and, consequently, neurodegeneration [17, 18]. Until now, no mutations in microtubule-associated protein tau (*MAPT*) coding genes have been detected in relation to familial forms of AD. However, in familial frontotemporal dementia (FTD) with parkinsonism, mutations in the microtubule-associated protein tau gene (*MAPT*) were identified on chromosome 17. This was the basis for creating a robust mouse model for tau pathology in 2001. These P301L tau-expressing pR5 mice show an accumulation of tau as soon as 3 months of age and develop NFTs around 6 months of age [19]. A mass spectrometric analysis of the brain proteins from these mice (aged from 8.5 to 10 months) revealed mainly a deregulation of mitochondrial respiratory chain complex components (including complex V), antioxidant enzymes, and synaptic protein space [20]. The reduction in mitochondrial complex V levels in the P301L tau mice was also confirmed in human P301L FTDP-17 (FTD with parkinsonism linked to chromosome 17) brains. The functional analysis demonstrated age-related mitochondrial dysfunction, together with reduced NADH ubiquinone oxidoreductase (complex I) activity as well as age-related impaired mitochondrial respiration and ATP synthesis in a pR5 mouse model. Mitochondrial dysfunction was also associated with higher levels of ROS in aged transgenic mice. Increased tau pathology resulted in modification of lipid peroxidation levels and the upregulation of antioxidant enzymes in response to oxidative stress [20]. Thus, this evidence demonstrated for the first time that not only A β but also tau pathology weakens gradually mitochondrial function in a rather specific way leading to metabolic impairment and oxidative stress in AD.

1.2 Synergistic Mode of Action of A β and Tau

Although A β and tau pathologies are both known hallmarks of AD, the mechanisms underlying the interplay between plaques and NFTs (or A β and tau, respectively) have remained unclear. However, a close relationship between mitochondrial impairment and A β on the one hand and tau on the other hand has been already established. How do both AD features relate to each other? Several studies suggest that A β aggregates and hyperphosphorylated tau may block the mitochondrial transport to the synapse leading to energy deficiency and neurodegeneration [21].

Remarkably, intracerebral A β injections amplify a pre-existing tau pathology in several transgenic mouse models [22, 23], whereas lack of tau abrogates A β toxicity [18, 24]. Our findings indicate that in tau transgenic pR5 mice, mitochondria display an enhanced vulnerability toward A β insult in vitro [2, 25], suggesting a synergistic action of tau and A β pathology on this organelle. Thus, these studies provide the first evidence for the existence of a complex interplay between A β and tau in AD whereby these two molecules damage mitochondria in multiple ways, but what about their specific effects on mitochondrial respiration?

1.3 High-Resolution Respirometry in Isolated Mitochondria to Evaluate OXPHOS Capacity

To address this question, we used a high-resolution respiratory system to evaluate the capacity of the entire oxidative phosphorylation system (OXPHOS) of cerebral mitochondria from mice bearing either an APP/PS2 mutation, P301L mutation (pR5 mice), or the triple mutation APP/PS2/P301L (^{triple}AD mice) compared to wild-type mice [26]. Measurement of oxygen (O₂) flux and consumption was performed at 37 °C using an Oroboros Oxygraph-2k system on freshly isolated mitochondria from cortical brains of age-matched wild-type, APP/PS2, pR5 and ^{triple}AD mice as follows. After detection of endogenous respiration, glutamate and malate were added to induce state 4 respiration (Figs. 1 and 2a), then ADP was added to stimulate state 3 respiration. After determining coupled respiration, a mitochondrial uncoupler (FCCP, *see* below) was added and the maximal respiratory capacity measured in the absence of a proton gradient. Cytochrome c (cyt c) injection was used to demonstrate mitochondrial membrane integrity. To inhibit activities of complexes I–III, rotenone (rot) and antimycin A (AA) were added. Complex IV activity was stimulated by ascorbate/TMPD (A/T) before terminating mitochondrial respiration by adding sodium azide (azide). Oxygen (O₂) consumption was normalized to the corresponding citrate synthase activity [3, 26].

We determined flux control ratios to obtain information on metabolic states of respiration. The respiratory control ratio (RCR_{3/4}) is an indicator of the state of coupling of mitochondria. State 3 is the rate of phosphorylating respiration in the presence of exogenous ADP, and state 4 is associated with proton leakage across the inner mitochondrial membrane in the absence of ADP. Our findings suggest a pronounced decrease of RCR_{3/4} in mitochondria from APP/PS2 and ^{triple}AD compared with age-matched wild-type mice already at 8 months of age. This decrease was also found in the oldest mice (12 months of age). When we examined the ETS/ROX (electron transport system/residual oxygen consumption) ratio, which yields an index of the maximum oxygen consumption capacity relative to the magnitude of residual oxygen consumption, we found that it was also decreased in APP/PS2 and ^{triple}AD compared with age-matched wild-type mice at 8 and 12 months of age. Interestingly, in a previous study, the decreased respiration of mitochondria from pR5 mice compared with wild-type controls was not detectable before the age of 24 months [20]. In contrast, APP/PS2 mitochondria showed a decrease in OXPHOS compared with wild-type already at the age of 8 months. At this age, OXPHOS of brain mitochondria from ^{triple}AD mice did not differ compared with that of age-matched APP/PS2 mitochondria, but it was significantly decreased in ^{triple}AD mice at the age of 12 months (Fig. 2b). Taken together, with increasing age, the global failure of the mitochondrial respiratory capacity deteriorated the strongest in mitochondria from ^{triple}AD mice, suggesting a synergistic destructive effect of tau and Aβ on mitochondria.

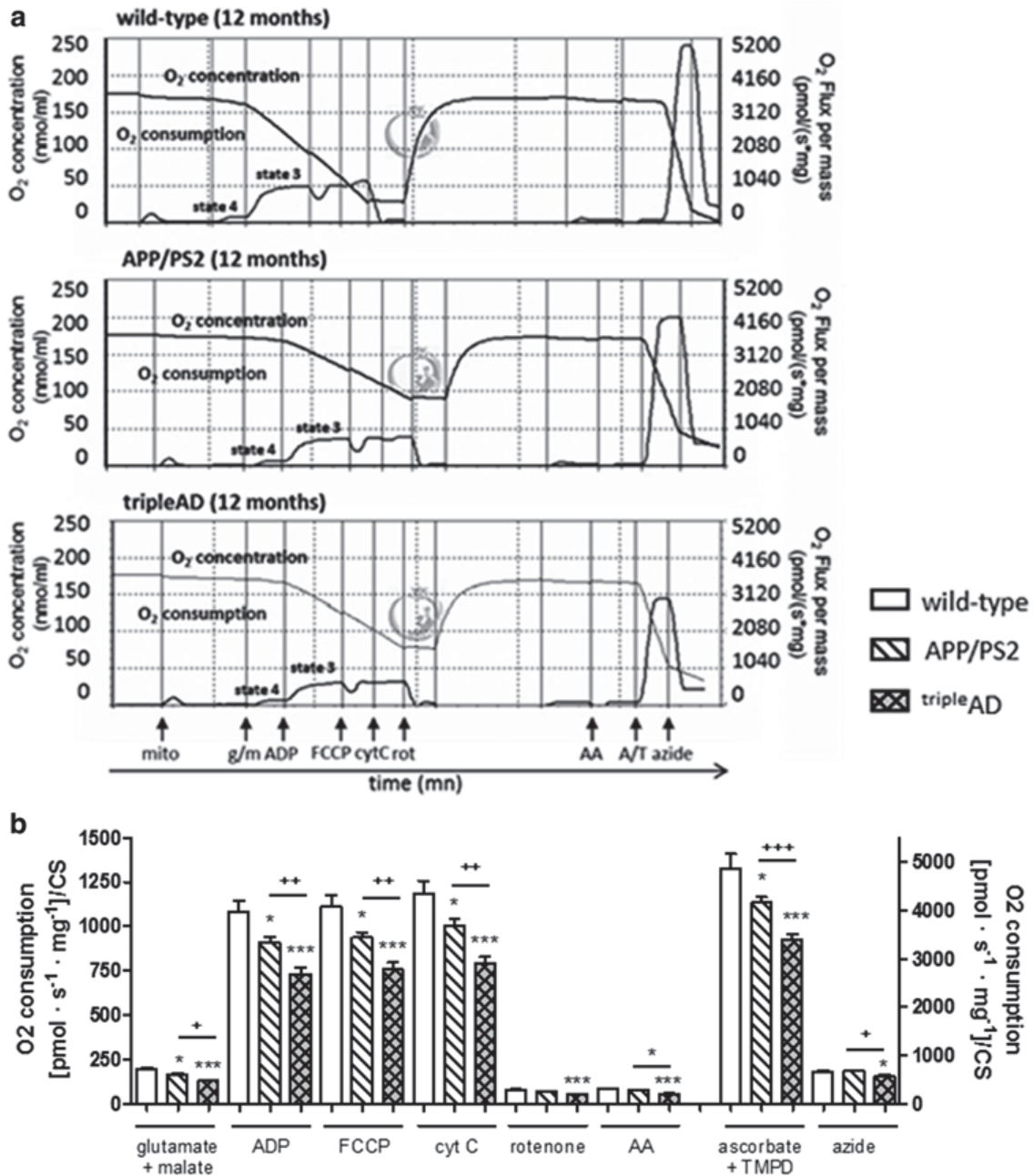


Fig. 2 Synergistic effects of A β and tau on mitochondrial respiration. (a) Representative diagrams of O₂ flux and consumption in mitochondria from 12-month-old wild-type, APP/PS2, and ^{triple}AD transgenic mice in response to titrated substrates and inhibitors of mitochondrial complexes. (b) Two-way ANOVA revealed a significant effect of on the respiratory rates of mitochondria between 12-month-old wild-type and APP/PS2 mice, and this impaired respiration was even more pronounced in ^{triple}AD mice. Two-way ANOVA post-hoc Bonferroni. **P*<0.05; ***P*<0.01; ****P*<0.001 vs. wild-type; +*P*<0.05; ++*P*<0.01; +++*P*<0.001 vs. APP/PS2 (*n*=7–12 animals/group). Modified from Rhein et al., PNAS (2009) [26] with permission

In conclusion, our studies highlight the key role of mitochondria in AD pathogenesis and the close interrelationship of this organelle and the two main pathological features of the disease. We showed that disturbances in the respiratory and energy system of ^{triple}AD mice seem to be due to a convergence of A β and tau on

mitochondria, accelerating defects in respiratory capacity, which consolidates the idea that a synergistic effect of tau and A β increase the pathological deterioration of mitochondria.

Now we will describe in detail the protocol which we followed previously [25]. After listing the material needed, we will describe the isolation of mitochondria from mouse brains and the steps required to measure the mitochondrial respiration. It is important to note that this protocol assumes that the Oroboros Oxygraph-2k system is routinely used in the laboratory and does not include technical details about oxygraph maintenance or calibration, but only experimental procedure regarding the assessment of mitochondrial respiration.

2 Materials

Prepare all solutions using ultrapure water (prepared by purifying deionized water to attain a sensitivity of 18 M Ω cm at 25 °C).

2.1 Solutions for Isolated Mitochondria Preparation

1. Medium 1: 138 mM NaCl, 5.4 mM KCl, 0.17 mM Na₂HPO₄, 0.22 mM KH₂PO₄, 5.5 mM glucose·H₂O, 58.4 mM sucrose, pH 7.35. To prepare 1 L of Medium 1, weigh 8 g of NaCl, 0.4 g of KCl, 0.024 g of Na₂HPO₄, 0.03 g of KH₂PO₄, 1.1 g of glucose·H₂O, 20 g of sucrose. Add water to a volume of 900 mL and mix with magnetic stir bar at room temperature until all powders are dissolved. Adjust pH and make up to 1 L with water. Store at 4 °C.
2. Isolated Mitochondria Buffer: 210 mM mannitol, 70 mM sucrose, 10 mM HEPES, 1 mM EDTA (tritriflex III), 0.45 % BSA, pH 7.4. To prepare 200 mL of buffer, weigh 7.65 g of mannitol, 4.79 g of sucrose, 477 mg of HEPES, 74.4 mg of EDTA (tritriflex III) and 0.9 g of BSA. Add water to a volume of 190 mL and mix with magnetic stir bar at room temperature until all powders are dissolved. Adjust pH and make up to 200 mL with water. Prepare aliquots of 10 mL and keep at -20 °C (*see Note 1*).
3. 1 M dithiothreitol (DTT) stock solution in water.

2.2 Solutions for Mitochondrial Respiration Assay

1. Mitochondrial Respiration Buffer: 65 mM sucrose, 10 mM KH₂PO₄, 10 mM Tris-HCl, 10 mM MgSO₄·7H₂O, 2 mM EDTA (tritriflex III)·2H₂O, pH 7. To prepare 200 mL, weigh 4.45 g of sucrose, 0.272 g of KH₂PO₄, 0.315 g of Tris-HCl, 0.493 g of MgSO₄·7H₂O, and 0.149 g of EDTA (tritriflex III)·2H₂O. Add water to a volume of ca. 190 mL and mix with magnetic stir bar at room temperature until all powders are dissolved. Adjust pH and make up to 200 mL with water. Prepare aliquots of 20 mL and keep them at -20 °C.

2. Mitochondrial Respiration Medium (MiR05): 0.5 mM EGTA, 3 mM MgCl₂·6H₂O, 60 mM K-lactobionate, 20 mM taurine, 10 mM KH₂PO₄, 20 mM HEPES, 110 mM sucrose, 1 g/L BSA, pH 7.1. First, prepare the 0.5 M K-lactobionate stock solution dissolving 35.83 g of lactobionic acid in 100 mL of H₂O, adjusting the pH to 7.0 with KOH and bringing the volume to 200 mL. To prepare 1 L of MiR05, weigh 0.190 g of EGTA, 0.610 g of MgCl₂·6H₂O, 2.502 g of taurine, 1.361 g of KH₂PO₄, 4.77 g of HEPES, 37.65 g of sucrose, and 1 g of BSA. Add ca. 750 mL of water and 120 mL of 0.5 M K-lactobionate stock solution. Mix with magnetic stir bar at room temperature, adjust the pH to 7.1 with 5 N KOH and make up to 1 L with water. Divide into 20 mL aliquots and store them frozen at -20 °C (*see Note 2*).
3. Substrates: The substrates (stock solutions) employed and details of preparation are summarized in Table 1 (*see Notes 3–13*).

2.3 Oxygraph System

Oroboros Oxygraph-2k system for high resolution respirometry (HRR) studies (<http://www.orooboros.at/?Oxygraph>).

3 Methods

Before experiment, perform an instrumental and chemical setup with the oxygraph.

3.1 Isolated Mitochondria Preparation

Prepare isolated mitochondria buffer (*see Note 1*) and keep on ice. Turn on the centrifuge (4 °C).

1. Kill the mice by decapitation and dissect one brain hemisphere on ice. Wash in 10 mL of ice-cold medium 1.
2. Put the preparation in the Potter-tube to homogenize in 1 mL of isolated mitochondria buffer. Pipette 10–15 times to homogenize the preparation (*see Note 14*).
3. Wash the Potter's plug three times with 150 µL of isolated mitochondria buffer and put the preparation in a 2 mL tube. Wash the Potter's tube three times with 150 µL of isolated mitochondria buffer and put the preparation in the same 2 mL tube. Vortex (*see Note 15*).
4. Centrifuge at 1,450 × *g* (4 °C) for 7 min and recover the supernatant in a new 2 mL tube. This step removes nuclei and tissue particles.
5. Centrifuge at 1,450 × *g* (4 °C) for 3 min and recover the supernatant again in a new 2 mL tube.
6. Centrifuge at 10,000 × *g* (4 °C) for 5 min. Throw away the supernatant and recover the pellet.

Table 1
Preparation and function of the substrates used to investigate the mitochondrial respiration using the Oroboros Oxygraph-2k system

		Name/formula	MW (g/mol)	Stock solution		Function	Note #
Mitochondrial substrates	Glutamate	Na-glutamate C ₅ H ₈ NO ₄ Na	169.1	2 M	3.382 g/10 mL H ₂ O	Induces state 4 respiration	4
	Malate	L-Malic acid C ₄ H ₆ O ₅	134.1	0.8 M	1.073 g/10 mL H ₂ O	Induces state 4 respiration	5
	ADP	K-adenosine 5' diphosphate dihydrate salt (C ₁₀ H ₁₅ N ₅ O ₁₀ P ₂ K·2H ₂ O)	501.32	0.5 M	0.501 g/2 mL H ₂ O	Induces state 3 respiration	6
	cytC	Cytochrome c	12,500	4 mM	50 mg/1 mL H ₂ O	Demonstrates mitochondrial membrane integrity	7
	Ascorbate	Ascorbate sodium salt C ₆ H ₇ O ₆ Na	198.1	0.8 M	1.584 g/10 mL H ₂ O	Stimulates complex IV activity	8
	TMPD	N,N,N',N'-Tetramethyl-p-phenylenediamine dihydrochloride C ₁₀ H ₁₆ N ₂ ·2HCl	237.2	0.2 M	47.4 mg/1 mL H ₂ O	Stimulates complex IV activity	9
Mitochondrial inhibitors	Rotenone	Rotenone C ₂₃ H ₂₂ O ₆	394.4	1 mM	3.94 mg/10 mL Ethanol	Inhibits complex I activity	10
	AA	Antimycin A	540	5 mM	11 mg/4 mL Ethanol	Inhibits complex III activity	11
	Azide	Sodium azide NaN ₃	65.01	1 M	65 mg/1 mL H ₂ O	Inhibits oxygen consumption	12
Mitochondrial uncouplers	FCCP	Carbonyl cyanide <i>p</i> -(trifluoromethoxy) phenylhydrazone C ₁₀ H ₅ F ₃ N ₄ O	254.2	0.32 mM	2.54 mg/10 mL ethanol results in a 1 mM solution. From here, dilute 1:3.125 in ethanol	Determines uncoupled respiration in absence of a proton gradient	13

7. Put the pellet (mitochondria) in 1 mL of isolated mitochondria buffer and mix 15 times using the pipette.
8. Repeat **steps 7 and 8** to obtain the mitochondrial fraction and put the pellet in 100 μL of isolated mitochondria buffer. Keep on ice until the measurement (*see Note 16*).

3.2 Mitochondrial Respiration Measurement: Preparations

Before experiment prepare the substrates (stock solutions) (Table 1) and the oxygraph (*see Note 17*).

1. Add 50 μL of isolated mitochondria preparation to each chamber and close the chamber (*see Note 18*). Mark it as (01-state 1).
2. Add 10 μL of 2 M glutamate/5 μL of 0.8 M malate (respirometry assay final concentrations will be 10 mM and 2 mM respectively). Mark it as (02-GM2).
3. Add 8 μL of 0.5 M ADP/chamber (final assay concentration, 2 mM). Mark it as (03-GM3).
4. Add 2.5 μL of 0.32 mM FCCP/chamber (assay concentration, 0.4 μM). Mark it as (04-GP3u).
5. Add 5 μL of 4 mM of Cytochrome c/chamber (assay concentration, 10 μM). Mark it as (05-GM3c).
6. Preparing from stock solution (Table 1), add 5 μL of 0.2 mM rotenone/chamber (assay concentration, 0.5 μM). Mark it as (06-rot).
7. Preparing from stock solution (Table 1), add 5 μL of 1 mM antimycin A/chamber (assay concentration, 2.5 μM). Mark it as (07-AA).
8. Add 5 μL of 0.8 M sodium ascorbate/chamber (assay concentration, 2 mM) and 5 μL of 0.2 M TMPD/chamber (assay concentration, 0.5 mM). Mark it as (08-AT).
9. Add 20 μL of 1 M sodium azide/chamber (assay concentration, 10 mM). Mark it as (09-azide).

3.3 Mitochondrial Respiration Measurement: High-Resolution Respirometry

Mitochondrial oxygen consumption is measured by high-resolution respirometry (HRR) at 37 °C using an Oroboros Oxygraph-2k system (<http://www.orooboros.at/?Oxygraph>) following the Gnaiger method [27].

3.4 Analysis

After the measurement, extract the raw data from the oxygraph software (DatLab) to an Excel file. Normalize the data on citrate synthase activity, which correlates with mitochondrial content (*see Note 19*). Perform the statistical analysis using GraphPad Prim software (or equivalent) and a two-way ANOVA followed by Bonferroni post hoc tests to compare the different groups. Consider statistically significant only P values < 0.05 . Represent data as means \pm SEM.

4 Notes

1. Just before starting the experiment, warm up the isolated mitochondria buffer. For two brain hemispheres, add one tablet of Complete^R Mini (protease inhibitor cocktail tablet) and 5 μ L of 1 M DTT to 10 mL of buffer (final concentration, 0.5 mM DTT). Prepare fresh, less than 3 h before use.
2. The MiR05 medium is stable for about 2–3 months. The K-lactobionate must be prepared fresh.
3. Manipulation of solutions at low temperature (4 °C). After rewarming, mix carefully since phase separation may occur and compounds may precipitate in cold mixtures. During the course of the experiment keep stock solutions on ice. Note: Solutions which contain ethanol may have a problem of evaporation and subsequent increase of concentration.
4. Glutamate solution (*see* Table 1). Adjust pH to 7.0 with 37 % HCl and divide into 0.5 mL aliquots. Store frozen at -20 °C.
5. Malate solution (*see* Table 1). Neutralize (adjust to pH 7.0) with 10 N KOH and divide into 0.5 mL aliquots. Store frozen at -20 °C.
6. ADP solution (*see* Table 1). Neutralize with 5 N KOH and divide into 100 μ L aliquots. Store at -80 °C.
7. Cytochrome c solution (*see* Table 1). Divide into 0.2 mL aliquots. Store frozen at -20 °C. Protect from light.
8. Ascorbate solution (*see* Table 1). To prevent autoxidation, prepare 0.8 M ascorbic acid solution (137.6 mg/mL, pH ca. 2). Adjust the pH of the sodium ascorbate solution to ca. 6 with ascorbic acid. Divide into 0.2 mL aliquots. Store frozen at -20 °C protected from light (light sensitive).
9. TMPD solution (*see* Table 1). To prevent autoxidation, neutralize with the ascorbate salt solution. Dilute 1:80 to result in a solution with 10 mM ascorbate final concentration. Divide into 0.2 mL aliquots. Store frozen at -20 °C.
10. Rotenone solution (*see* Table 1). Difficult to dissolve. Divide into 0.2 mL aliquots, store at -20 °C protected from light. Note: Light sensitive; very toxic. Handle with care.
11. Antimycin A (AA) solution (*see* Table 1). Divide into 0.2 mL aliquots, store frozen at -20 °C. Note: Very toxic. Handle with care.
12. Azide solution (*see* Table 1). Divide into 0.2 mL aliquots, store frozen at -20 °C. Note: Very toxic. Handle with care.
13. FCCP solution (*see* Table 1). Divide into 0.5 mL aliquots, store frozen at -20 °C.
14. Pipette gently up and down to avoid bubble formation and strong oxygenation of the sample.

15. If you have several mice, stop the process at this step, put the preparation on ice and use the next mouse to perform the centrifugation steps with all the samples at the same time. Since the Oxygraph contains two chambers, it is possible to investigate the mitochondrial respiration for only a few animals per day (6–8 mice/day).
16. A volume of 50 μL of the preparation will be used for the Oxygraph measurement. For protein determination, dilute 3 μL of isolated mitochondria in PBS (dilution 1:5) and perform the protein assay (e.g. Biorad DC™ Protein Assay and bovine serum albumin (BSA) for the standard curve).
17. The experiment requires an instrumental and chemical background following the protocol of the company (<http://www.orooboros.at/?Oxygraph>). Careful calibration will determine the “air saturation” (R1) and the “zero saturation” (R0) values.
18. When the oxygraph chambers are closed, check no air bubbles are left inside.
19. Citrate synthase activity is frequently used to normalize other mitochondrial enzymatic activities and mitochondrial respiration because it correlates to mitochondrial content. Citrate synthase activity can be measured following the reduction of 5,5'-dithiobis(2-nitrobenzoic acid) (DTNB) by citrate synthase at 412 nm (extinction coefficient of $13.6 \text{ mM}^{-1} \text{ cm}^{-1}$) in a coupled reaction with coenzyme A (CoA) and oxaloacetate [3, 26].

Acknowledgements

This work was supported by grants from the Swiss National Science Foundation (Grant SNF 310000–108223), Synapsis and Novartis Foundation for medical-biological research.

References

1. Gibson GE, Huang HM (2002) Oxidative processes in the brain and non-neuronal tissues as biomarkers of Alzheimer's disease. *Front Biosci* 7:d1007–d1015
2. Eckert A, Hauptmann S, Scherping I et al (2008) Soluble beta-amyloid leads to mitochondrial defects in amyloid precursor protein and tau transgenic mice. *Neurodegener Dis* 5:157–159
3. Rhein V, Baysang G, Rao S et al (2009) Amyloid-beta leads to impaired cellular respiration, energy production and mitochondrial electron chain complex activities in human neuroblastoma cells. *Cell Mol Neurobiol* 29: 1063–1071
4. Games D, Adams D, Alessandrini R et al (1995) Alzheimer-type neuropathology in transgenic mice overexpressing V717F beta-amyloid precursor protein. *Nature* 373:523–527
5. Scheffler IE (2001) A century of mitochondrial research: achievements and perspectives. *Mitochondrion* 1:3–31
6. Reddy PH (2007) Mitochondrial dysfunction in aging and Alzheimer's disease: strategies to protect neurons. *Antioxid Redox Signal* 9: 1647–1658

7. Caspersen C, Wang N, Yao J et al (2005) Mitochondrial Abeta: a potential focal point for neuronal metabolic dysfunction in Alzheimer's disease. *FASEB J* 19:2040–2041
8. Santos RX, Correia SC, Wang X et al (2010) Alzheimer's disease: diverse aspects of mitochondrial malfunctioning. *Int J Clin Exp Pathol* 3:570–581
9. Pagani L, Eckert A (2011) Amyloid-beta interaction with mitochondria. *Int J Alzheimers Dis* 2011:925050
10. Eckert A, Schmitt K, Gotz J (2011) Mitochondrial dysfunction—the beginning of the end in Alzheimer's disease? Separate and synergistic modes of tau and amyloid-beta toxicity. *Alzheimers Res Ther* 3:15
11. Schmitt K, Grimm A, Kazmierczak A et al (2012) Insights into mitochondrial dysfunction: aging, amyloid-beta, and tau-A deleterious trio. *Antioxid Redox Signal* 16:1456–1466
12. Blanchard V, Moussaoui S, Czech C et al (2003) Time sequence of maturation of dystrophic neurites associated with Abeta deposits in APP/PS1 transgenic mice. *Exp Neurol* 184:247–263
13. Gillardon F, Rist W, Kussmaul L et al (2007) Proteomic and functional alterations in brain mitochondria from Tg2576 mice occur before amyloid plaque deposition. *Proteomics* 7:605–616
14. Reddy PH, McWeeney S, Park BS et al (2004) Gene expression profiles of transcripts in amyloid precursor protein transgenic mice: up-regulation of mitochondrial metabolism and apoptotic genes is an early cellular change in Alzheimer's disease. *Hum Mol Genet* 13:1225–1240
15. Richards JG, Higgins GA, Ouagazzal AM et al (2003) PS2APP transgenic mice, coexpressing hPS2mut and hAPPswe, show age-related cognitive deficits associated with discrete brain amyloid deposition and inflammation. *J Neurosci* 23:8989–9003
16. Fernandez-Vizarra P, Fernandez AP, Castro-Blanco S et al (2004) Intra- and extracellular Abeta and PHF in clinically evaluated cases of Alzheimer's disease. *Histol Histopathol* 19:823–844
17. Gotz J, Ittner LM, Fandrich M, Schonrock N (2008) Is tau aggregation toxic or protective: a sensible question in the absence of sensitive methods? *J Alzheimers Dis* 14:423–429
18. Ittner LM, Ke YD, Delerue F et al (2010) Dendritic function of tau mediates amyloid-beta toxicity in Alzheimer's disease mouse models. *Cell* 142:387–397
19. Gotz J, Chen F, Barmettler R, Nitsch RM (2001) Tau filament formation in transgenic mice expressing P301L tau. *J Biol Chem* 276:529–534
20. David DC, Hauptmann S, Scherping I et al (2005) Proteomic and functional analyses reveal a mitochondrial dysfunction in P301L tau transgenic mice. *J Biol Chem* 280:23802–23814
21. Gotz J, Ittner LM, Kins S (2006) Do axonal defects in tau and amyloid precursor protein transgenic animals model axonopathy in Alzheimer's disease? *J Neurochem* 98:993–1006
22. Gotz J, Chen F, van Dorpe J, Nitsch RM (2001) Formation of neurofibrillary tangles in P301L tau transgenic mice induced by Abeta 42 fibrils. *Science* 293:1491–1495
23. Gotz J, Schild A, Hoerndli F, Pennanen L (2004) Amyloid-induced neurofibrillary tangle formation in Alzheimer's disease: insight from transgenic mouse and tissue-culture models. *Int J Dev Neurosci* 22:453–465
24. Ittner LM, Gotz J (2011) Amyloid-beta and tau—a toxic pas de deux in Alzheimer's disease. *Nat Rev Neurosci* 12:65–72
25. Eckert A, Hauptmann S, Scherping I et al (2008) Oligomeric and fibrillar species of beta-amyloid (A beta 42) both impair mitochondrial function in P301L tau transgenic mice. *J Mol Med* 86:1255–1267
26. Rhein V, Song X, Wiesner A et al (2009) Amyloid-beta and tau synergistically impair the oxidative phosphorylation system in triple transgenic Alzheimer's disease mice. *Proc Natl Acad Sci U S A* 106:20057–20062
27. Gnaiger E (2008) Polarographic oxygen sensors, the oxygraph, and high resolution respirometry to assess mitochondrial function. In: Dykens JA, Will Y (eds) *Drug-induced mitochondrial dysfunction*. Wiley, Hoboken, NJ, pp 327–348

F. BDNF in sleep, insomnia, and sleep deprivation

Running Title: BDNF in sleep, insomnia, and sleep deprivation

Authors: Schmitt K^{a,b}, Holsboer-Trachsler E^c, Eckert A^{a,b*}

^aNeurobiology Lab for Brain Aging and Mental Health, Transfaculty Research Platform, Molecular & Cognitive Neuroscience, University of Basel, Switzerland.

^bPsychiatric University Clinics, University of Basel, CH-4012 Basel, Switzerland.

^cCenter of Affective, Stress and Sleep Disorders, Psychiatric Hospital of the University of Basel, CH-4012 Basel, Switzerland

***Corresponding author at:** Psychiatric University Clinics, University of Basel, Wilhelm Klein-Str. 27, CH-4012 Basel, Switzerland.

Tel.: +41 613255487; Fax: +41 613255577,

E-mail: anne.eckert@upkbs.ch (A. Eckert).

ANNALS OF MEDICINE, 2015; Accepted 9 December 2015.

<http://dx.doi.org/10.3109/07853890.2015.1131327>

Abstract

The protein brain derived neurotrophic factor (BDNF) is a member of the neurotrophin family of growth factors involved in plasticity of neurons in several brain regions. There is numerous evidence that BDNF expression is decreased by experiencing psychological stress and that, accordingly, a lack of neurotrophic support causes major depression. Furthermore, disruption in sleep homeostatic processes results in higher stress vulnerability and is often associated with stress-related mental disorders. Recently, we reported, for the first time, a relationship between BDNF and insomnia and sleep deprivation (SD). Using a biphasic stress model as explanation approach, we discuss here the hypothesis that chronic stress might induce a deregulation of the hypothalamic- pituitary adrenal system. In the long-term it leads to sleep disturbance and depression as well as decreased BDNF levels, whereas acute stress like SD can be used as therapeutic intervention in some insomniac or depressed patients as compensatory process to normalize BDNF levels. Indeed, partial SD (PSD) induced a fast increase in BDNF serum levels within hours after PSD which is similar to effects seen after ketamine infusion, another fast-acting antidepressant intervention, while traditional antidepressants are characterized by a major delay until treatment response as well as delayed BDNF level increase.

Keywords

BDNF, major depression, rapid-acting antidepressants, sleep deprivation, therapy response.

Key Messages

- Brain-derived neurotrophic factor (BDNF) plays a key role in the pathophysiology of stress-related mood disorders.
- The interplay of stress and sleep impacts on BDNF level.
- Partial sleep deprivation (PSD) shows a fast action on BDNF level increase.

Introduction

In our modern industrialized environment, the brain is a primary mediator and target of stress resiliency and vulnerability processes because of its capacity to adapt the behavioural and physiological responses to the social and physical stresses (1, 2). Yet, depending on the individual genetic background and epigenetic factors, this ability is not infinite, which, once a threshold is reached, eventually increases the susceptibility to stress-related mental disorders like major depressive disorder (MDD).

Brain-derived neurotrophic factor (BDNF) belongs to the neurotrophin family and is produced by astrocytes, in addition to neurons, and the noradrenergic and serotonergic systems play a role in controlling BDNF synthesis (3-5). BDNF is abundant in various brain regions implicated in mood disorders, including the hippocampus, prefrontal cortex, and amygdala, and shows a remarkable activity-dependent regulation of expression and secretion. Thus, its neurotrophic functions are connected to various physiological functions in the brain particularly relevant in neuroplasticity, memory and sleep (6-9), suggesting its biological role over the entire life span.

Based on findings in brains from rodents (10, 11) and humans (12), the structure of the BDNF gene seems to be highly complex and contains numerous promoters each preceding one exon. This complexity leads through alternative splicing to the existence of distinct mRNA species that all contain exon IX, which encodes the BDNF protein (10). Although the differential regulation of these transcripts is essential and may dictate subcellular BDNF mRNA targeting and translational responses following neuronal stimulation, their potential implications in neuropsychiatric disorders remain mostly unclear. Notably, only one functional mature protein is generated, irrespective of the splice variant expressed. BDNF is synthesized as a larger precursor protein known as prepro-BDNF that is cleaved into pro-BDNF, which can then be further cleaved into mature BDNF (13). It has been suggested that pro-BDNF and mature BDNF activate different intracellular signaling pathways (reviewed in (14)). While pro-BDNF interacts with the low-affinity neurotrophin receptor p75, mature BDNF signals through its high-affinity tropomyosin-related kinase B (TrkB) receptor, which activates several downstream effectors. Moreover, a functional Val66Met polymorphism found in the human pro-BDNF gene induced an impairment

of the activity-dependent dendritic trafficking and secretion of mature BDNF protein in rat brain.

Given the complexity of BDNF system in terms of transcriptional, translational and post-translational regulatory mechanisms (10), pathological alteration of BDNF may lead to defects in neuronal survival and regeneration as well as structural brain abnormalities and reduced neuronal plasticity, which in turn may impair the individual's ability to adapt to crisis situation. Because of the role played by BDNF in regulating structural, synaptic, and morphological plasticity, BDNF has gained the most attention in the understanding of the mechanisms underlying stress-related mood disorders (**Figure 1**). Numerous evidence from preclinical and clinical studies demonstrated that the stress-related pathophysiology of MDD is accompanied by a down-regulation of BDNF and TrkB expression, which in turn contributes to atrophy and cell loss in various brain regions, including the hippocampus (15-17). It is known that major depression and inflammation are linked in many ways. Of particular interest in this context are findings showing that inflammatory events compromise neuroplasticity via reduction of BDNF and may lead in this way to the development of depression (reviewed in (18)). Accordingly, several studies demonstrated that inflammation induced a significant decrease in the expression of specific BDNF variants within the rat brain (19, 20).

Concomitantly, the "neurotrophin hypothesis of depression" postulates that stress-related mood disorders result from a stress-induced decrease in BDNF expression (7). The BDNF hypothesis predicts that agents that promote BDNF function might be clinically effective antidepressants. Over the years, numerous - but not the entirety of all - studies showed that antidepressant interventions were able to reverse depressive behaviours while concurrently increasing BDNF levels (15, 21). But increases in BDNF serum levels during antidepressant treatment appear to be confined to certain antidepressants, do not always parallel clinical characteristics like depression severity and may depend on therapy response (21, 22). Of note, lack of BDNF alone may not be sufficient to explain the pathology of stress-related mental disorders (23-25), but it certainly has a prominent role in the pathophysiology of these disorders. Given that BDNF plays an important role in the pathophysiology of the stress response and in the pathogenesis of stress-associated mood disorders, and that its restoration may represent a critical mechanism underlying antidepressant

therapeutic effect, many investigators have focused on serum BDNF as a “biomarker” predicting the therapy outcome in MDD, since the protein can cross the blood brain-barrier and circulating BDNF was correspondingly associated with cortical BDNF concentrations (16).

Sleep has a critical role in cognitive functioning including the consolidation of synaptic plasticity and long-term memory. Stress itself often disrupts sleep. Moreover, sleep disturbances such as insomnia following stressful events may further intensify the long-term changes in the brain occurring at the level of synaptic plasticity (26). Conversely, stress exposure after partial or total sleep loss impairs the hypothalamic- pituitary adrenal (HPA) response to an increase of cortisol (27, 28). Hence, sleep disturbances may result in higher stress vulnerability, reduced environmental adaptation and cognitive impairment. Interestingly, the introduction of SD therapy (SDT) in the 1970-80's was a major step forward in the sense of its rapid and fast (within 24 hours) recovery effect on depressive symptoms (29, 30). Particularly, it has been shown that REM- SD in MDD patients leads to a gradual improvement (30), suggesting that the antidepressant effects of both selective rapid eye movement (REM) SD and total SD are based on the suppression of slow wave activity (SWA) (31). Although fast-acting, SDT alone is not sufficient in most of the cases since the rate of relapse following the recovery night is rather high. However, the evidence for the rapid and robust efficacy of SDT in mood disorders is more sustainable for weeks to months when combined with antidepressant medication and/or chronotherapies (32-34). Transcriptomic studies in different species through the sleep-wake cycle and after SD revealed that genes encoding proteins involved in synaptic plasticity (e.g. BDNF), specifically long-term potentiation (LTP), were up-regulated during wakefulness and down-regulated during sleep (1, 35-37). Particularly, while short-term total SD appears to up-regulate the expression of BDNF in various regions of the brain (38-42), selective SD like REM or paradoxical SD in rats showed no alterations of BDNF expression (43). However, little is known regarding how the interactions between stress and sleep affect sleep-dependent plasticity and cognition, especially those explaining the rapid, even though temporary antidepressant effect of SD, since a relapse into depression occurs in most patients following the recovery night (44).

Challenges and progress towards understanding the role of BDNF in stress-related mental disorders regarding the interplay of stress and the sleep homeostasis may lead to new alternative treatment strategies, providing advantages over the currently available antidepressants that are characterized by significant limitations (i.e.: low response rates, treatment resistance, high incidence of relapse, and a time-lag of weeks to months for a response), highlighting a major unmet need for more efficacious and faster-acting antidepressants (45).

BDNF, sleep and insomnia

Sleep is an essential component of human cognitive performance and health. It is generally accepted that our modern society and its resulting stressors impact sleep in a negative way by altering both sleep quality and duration (46). Serotonin is a major neurotransmitter candidate playing a prominent role in the regulation of both sleep-wake circadian cycles as well as in the modulation of mood states in humans (47). In addition, it is known that BDNF production is stimulated by serotonin and conversely BDNF increases serotonergic signalling (4, 48). BDNF has been shown to induce SD and spontaneous wakefulness in animals (49). Moreover, a direct link with BDNF as prominent actor has been identified between the synaptic plasticity triggered by waking activities and the homeostatic sleep response (50). Particularly, the degree of BDNF expression during wakefulness is directly correlated to the extent of slow wave activity (SWA), a sensitive marker for sleep pressure and sleep need, in the subsequent period (8). Support for a role of BDNF in human sleep regulation comes also from a recent study reporting impaired intensity of SWA in non-rapid eye movement (NREM) sleep in Val66Met carriers relative to Val/Val homozygotes under basal conditions and immediately following a 40 hours period of waking (51). Although the exact mechanism by which BDNF induces an increase in sleep SWA remains uncertain, it has been proposed that the coupling of waking-associated synaptic potentiation among connected cells may directly contribute to SWA increase (8). Since the body's stress system plays a critical role in adapting to a continuously changing and challenging environment, it is a major question how stress-related disruption of sleep may impair BDNF contents and degrade sleep function. Stress has been associated with the activation of the hypothalamic- pituitary- adrenal (HPA) axis. The HPA axis is a stress-responsive system that has been implicated in both

mood regulation (particularly depression) and cognitive functioning. The system consists of forward-stimulating arms as well as feedback loops that together regulate the production of stress hormones including cortisol. The fact that the beginning and the end of sleep are both involved in the HPA axis activity provides a clue to estimate the effects of stress on sleep (52). Chronic stress can lead to a deregulation in this biological stress system (53-57), which was suggested to decrease BDNF levels in animal studies (58-61) as well as in stress-related mood disorders (16, 62, 63) (**Figure 1**). Sleep problems are common features in many stress-related disorders; problems that may lead to impairment of physical and mental health since sleep loss is often followed by higher stress vulnerability (64). Insomnia is considered as a state of 24-h hyperarousal rather than sleep loss and affects up to one third of the general population (65). Epidemiological and clinical studies showed that a higher number of insomnia subjects also suffer from a concomitant mood disorder, mainly depression or an anxiety disorder (66, 67). Stress-related insomnia is transient and persists for only few days. Of note, persistent insomnia increases the risk of relapse into a new major depressive disorder episode (68). Although a majority of studies have concentrated on specifying the role of BDNF in depression, the mechanism underlying the effect of the sleep on the interplay between stress and BDNF was unclear until recently. Our group investigated serum BDNF levels of adults with current symptoms of insomnia and non-sleep disturbed control subjects (69, 70). We demonstrated that subjects suffering from current symptoms of insomnia exhibited significantly decreased serum BDNF levels compared with sleep-healthy controls. In addition, serum BDNF levels were significantly correlated with severity of insomnia in all participants. Moreover, the significance of our data was further emphasized when we assessed an external control group that had recovered from occupational burnout. Again, serum BDNF levels were significantly lower in those subjects reporting symptoms of fatigue compared to sleep healthy subjects. Overall, these findings strongly support the hypothesis of increased stress vulnerability due to sleep loss, which may lead to decreased BDNF levels. A key follow-up analysis using a mediation model further suggests that sleep acts as a mediator in the interplay between stress experience and serum BDNF levels (**Figure 2, left panel**) (69), suggesting an important role of this relationship in the pathogenesis of stress-associated mental disorders. While we found reduced BDNF levels in association with insomnia, wakefulness given during SD, which can be considered as an “acute”

stressor for the brain, leads to an increase in BDNF content (71, 72). In line with a biphasic model of stress, chronic stress leads in the long-term to sleep disturbance and decrease of BDNF levels via HPA deregulation, while acute stress increases BDNF levels (**Figure 1**). Of note, the biphasic model of stress on BDNF level is in agreement with the biphasic model of stress on the glutamate system (73). The latter model argues that the acute stress-induced enhancement of glutamate transmission is dependent on activation of corticosterone receptors, while chronic stress induced opposite effects.

Major depression, sleep deprivation and circadian regulation of BDNF

Stress-related mood disorders like MDD are complex, multivariate and involve numerous neuronal substrates and brain regions. Multiple neurobiological mechanisms seem to mediate the therapeutic effects of antidepressant therapy. Some of these mechanisms, e.g. BDNF gene transcription inducing long-term potentiation, seem to play a role for neuroprotection and neurogenesis. The complexity could explain the slow onset of action in antidepressant treatments (74) (**Figure 2**). Furthermore, most currently available classical antidepressants primarily target the noradrenergic and serotonergic systems. The glutamate system has received much attention in recent years as an avenue for developing novel therapeutics since the glutamatergic system is also impaired in stress-related mood disorders (75, 76). The use at low doses of the noncompetitive N-methyl-D-aspartate (NMDA) receptor antagonist, ketamine, has been shown to have rapid antidepressant efficacy (75). In particular, patients with treatment-resistant depression benefit from sub-anaesthetic doses of ketamine with quick and persistent antidepressant effects (76, 77). It is suggested that the NMDA receptor blockade leads to an upregulation of the AMPA receptor expression and subsequent activation of the intracellular mammalian target of rapamycin (mTOR) cascade involved in ketamine's antidepressant action (78). In vitro studies also show that activation of AMPA receptors stimulates BDNF release via activation of L-type voltage-dependent calcium channels (VDCC) (79). This, in turn, is followed by an increase of synaptogenesis, which might be mirrored by the neuroplasticity marker BDNF (23, 80). In line, Haile and coworkers could demonstrate a rapid increase of plasma BDNF levels already 4 hours after intravenous infusion of ketamine (81). In addition to its

role as an NMDA antagonist, ketamine can also alter circadian rhythms by attenuating phase-shifting responses to light. Thereby it alters the diurnal rhythms of the widespread NMDA and AMPA receptors in the suprachiasmatic nucleus and increases the expression of the core clock genes *per1* and *per2* via its actions on the glutamate receptors (reviewed in (82)).

Some clinical studies have evaluated the changes of plasma or serum BDNF levels before and after antidepressant treatments among MDD patients and most studies report an increase of BDNF levels after antidepressant treatment (83, 84), although very recent data indicate that the normalization of BDNF during antidepressant treatment appears to be confined to some but not all antidepressants as well as to therapy response and does not correspond with amelioration of clinical symptoms (85). Nevertheless, different antidepressant strategies including antidepressant drugs and electroconvulsive therapy (ECT) were associated with an increase in BDNF levels (71). Besides ketamine, manipulations of the sleep-wake cycle such as *SD* (total or partial) or a phase advance of the *sleep* period are clinically well-documented, robust, and rapid-acting methods for the treatment of severely depressed patients (33). Other than *SD* for the whole night, partial *SD* (*PSD*) in the second half of the night has also shown comparable antidepressant effects in patients with major depression (33).

Moreover, a growing body of evidence also supports a role for BDNF and its tropomyosine-related kinase receptor B (*TrkB*) in the modulation and mediation of circadian rhythms that appear to be disturbed in mood disorders. Alterations in rhythmic behaviours such as sleep, mood, concentration, appetite and vigilance are typical symptoms linked to depression. With regard to the link between BDNF and the HPA axis alteration in MDD, about 60% of depressed patients present a circadian deregulation of the cortisol secretion with hypercortisolemia (86-88) or disturbances in the temporal pattern of secretion including a flattened circadian curve (89), a reduced duration of nocturnal quiescent period (90), and an earlier (91) or elevated nadir (92). Of note, the presence of a diurnal BDNF rhythm was also recently demonstrated in healthy humans where plasma BDNF displayed the highest concentrations in the morning, followed by a significant decrease throughout the day, and the lowest values at midnight (93, 94). However, diurnal variation of blood BDNF was neglected until now in studies investigating MDD patients. Therefore, our group

designed for the first time a study to investigate the potentially fast-acting effects of PSD on BDNF profiles in MDD patients and if a diurnal variation of serum BDNF plays a role for the therapy outcome (72). Thus, post-PSD BDNF levels were investigated within hours after PSD: up to 18 h by using a 6 h interval post-PSD, specifically at 8 am, 2pm, and 8 pm. This is in contrast to all other published studies where treatment-related BDNF changes were collected and analyzed no earlier than one to six weeks after antidepressive therapy with classic antidepressants.

We could confirm a similar pattern of diurnal variation of serum BDNF in patients identified as responders as it was previously reported in healthy subjects. After six hours post-PSD, we observed an increase in BDNF level, a fast effect comparable to that of ketamine on BDNF elevation in plasma, which was detectable already after 4 hours post-infusion and associated with therapeutic response. Importantly, early and rapid changes of BDNF levels after PSD and post-infusion of ketamine (81) imply a rapid adaptation mechanism at the synapses, e.g. remodelling of synapses following an increase and secretion of BDNF (reviewed in (6)). It can be speculated on the one hand that BDNF is secreted with a pulsatory circadian rhythm that is characterized by a progressive reduction in the amplitude of pulses throughout the day. On the other hand, it has been shown that brain BDNF is able to cross the blood brain barrier via a rapidly saturable transport system (95). While BDNF peaks around midnight in rat brains and thus may exert its modulating effect on neuroplasticity and long-term potentiation (96, 97), peripheral BDNF in the blood, namely both, of plasma and serum, peaks in the morning at 8 am and exhibits its lowest expression level at midnight, indicating that BDNF cycles in opposite phases in brain and blood. Thus, it seems legitimate to speculate that rapid changes to remodel neuronal networks involve the release of BDNF as a critical backbone, a phenomenon that might also occur in the periphery, since serum BDNF levels increase within hours (**Figure 2**).

Furthermore and unexpectedly, not only post-PSD BDNF but also pre-PSD serum BDNF levels exhibited a diurnal pattern that was only prominent in subjects who were identified as responders. For non-responders, serum BDNF remained flat throughout the day. Accordingly, Wolkowitz and colleagues (98) found that high baseline serum BDNF levels (at 10 am) before the treatment with a selective serotonin reuptake inhibitor, predicted therapy response in depressed patients.

Moreover, response after treatment with duloxetine – a serotonin-norepinephrine reuptake inhibitor - in patients with MDD was also associated with a higher baseline serum BDNF concentration (99). Recognition that circadian rhythm disruption might also play a key role in mood disorders has led to the development of the new antidepressant agomelatine. Recent data from various groups showed that agomelatine led to an increase in BDNF expression in treated animals, and that this effect follows a specific temporal profile (100). Overall, diurnal BDNF variation seems to precede, rather than follow a favorable treatment outcome in depressed patients, suggesting that diurnal BDNF change is a prerequisite for successful therapy response independent from the specific treatment strategy, e.g. antidepressant drugs or SD.

BDNF, acute and chronic stress

In summary, our findings are in line with the hypothesis of an increased stress vulnerability due to sleep loss which may lead to a decrease in BDNF. Such a decrease might be associated with a decrease in BDNF mRNA expression in peripheral blood mononuclear cells and/or might correspond to a BDNF decline in the brain. To what extent peripheral BDNF corresponds to brain BDNF level is still not known. Nevertheless, the use of serum BDNF as potential indicator of brain alteration was justified by substantial evidence, but a time delay to monitor brain tissue alterations in the periphery should be taken into account (101). While we report a reduction of BDNF levels linked to sleep disturbance reflecting chronic stress on the one side, we and others consistently showed that prolonged wakefulness caused by SD (partial or total), which can be considered as an acute stressor for the brain, leads to a rapid increase of BDNF (1, 36). However, little is known about the differential effects of chronic and acute stress on the molecular level. Nevertheless, previous studies provide valuable leads of a biphasic modulation of hippocampal plasticity by stress, demonstrating that the same chronic stress that elicited hippocampal dendritic atrophy also reduced levels of BDNF in the rodent hippocampus while acute stress triggered opposite effects on BDNF levels (**Figure 1**) (25, 59, 102). This suggests that BDNF could be a final point of convergence for the stress-induced effects in the hippocampus. BDNF-mediated signalling is involved in stress response, but the direction and nature of signalling seems to be region- specific (e.g. hippocampus

versus amygdala), stress- specific and influenced by epigenetic modifications along with post-translational modifications (102).

Using the biphasic model of stress on BDNF (**Figure 1**), we hypothesise that chronic stress might induce a deregulation of the HPA system leading in the long-term to sleep disturbance and decreased BDNF levels. In this scenario, sleep is a key mediator at the connection between stress and BDNF (**Figure 2, left panel**) and inadequate sleep, such as insomnia, can amplify the depletion in BDNF levels. In contrast, an acute stressor like SD, e.g. one night of SD, can be used as a fast-acting therapeutic intervention in some insomniac or depressed patients as a compensatory process to normalize BDNF levels.

Conclusion

We discuss here recent new insights regarding the association of sleep with BDNF, the stress-induced BDNF modifications that may be mediated by sleep and, the effect of PSD as fast-acting but transient antidepressant on serum BDNF levels (**Figures 1 and 2**).

Besides the biological link between BDNF and sleep, stress experience and subjective sleep perception interact with each other and directly affect BDNF levels, which eventually amplify the susceptibility to stress-associated mood disorders. Similar to ketamine, SD and PSD are able to induce a fast increase in serum BDNF levels within few hours. This is in contrast to the rather “delayed” effects of classical antidepressants (up to 6 weeks). Given the complexities of the pathogenesis of stress-related mood disorder, further studies including the monitoring of insomnia and sleep should be conducted. Especially the molecular mechanisms underlying the rapid response of ketamine and PSD on BDNF deserve further investigation as well as the downstream signalling pathways of BDNF and the relationship between BDNF and cortisol with regard to their role in the HPA axis deregulation.

Acknowledgements

This work was supported by the Swiss National Science Foundation (32003B_149317).

Disclosure of interest

The authors declare that the research was conducted in the absence of any commercial or financial relationships that could be construed as a potential conflict of interest.

References

1. Gronli J, Soule J, Bramham CR. Sleep and protein synthesis-dependent synaptic plasticity: impacts of sleep loss and stress. *Frontiers in behavioral neuroscience*. 2013;7:224.
2. McEwen BS, Gianaros PJ. Central role of the brain in stress and adaptation: links to socioeconomic status, health, and disease. *Annals of the New York Academy of Sciences*. 2010;1186:190-222.
3. Juric DM, Loncar D, Carman-Krzan M. Noradrenergic stimulation of BDNF synthesis in astrocytes: mediation via alpha1- and beta1/beta2-adrenergic receptors. *Neurochemistry international*. 2008;52(1-2):297-306.
4. Martinowich K, Lu B. Interaction between BDNF and serotonin: role in mood disorders. *Neuropsychopharmacology : official publication of the American College of Neuropsychopharmacology*. 2008;33(1):73-83.
5. Homberg JR, Molteni R, Calabrese F, Riva MA. The serotonin-BDNF duo: developmental implications for the vulnerability to psychopathology. *Neuroscience and biobehavioral reviews*. 2014;43:35-47.
6. Duman RS. Neurobiology of stress, depression, and rapid acting antidepressants: remodeling synaptic connections. *Depression and anxiety*. 2014;31(4):291-6.
7. Duman RS, Heninger GR, Nestler EJ. A molecular and cellular theory of depression. *Archives of general psychiatry*. 1997;54(7):597-606.
8. Faraguna U, Vyazovskiy VV, Nelson AB, Tononi G, Cirelli C. A causal role for brain-derived neurotrophic factor in the homeostatic regulation of sleep. *The Journal of neuroscience : the official journal of the Society for Neuroscience*. 2008;28(15):4088-95.
9. McAllister AK. Spatially restricted actions of BDNF. *Neuron*. 2002;36(4):549-50.
10. Aid T, Kazantseva A, Piirsoo M, Palm K, Timmusk T. Mouse and rat BDNF gene structure and expression revisited. *Journal of neuroscience research*. 2007;85(3):525-35.
11. Liu QR, Lu L, Zhu XG, Gong JP, Shaham Y, Uhl GR. Rodent BDNF genes, novel promoters, novel splice variants, and regulation by cocaine. *Brain research*. 2006;1067(1):1-12.
12. Liu QR, Walther D, Drgon T, Polesskaya O, Lesnick TG, Strain KJ, et al. Human brain derived neurotrophic factor (BDNF) genes, splicing patterns, and assessments of associations with substance abuse and Parkinson's Disease. *American journal of medical genetics Part B, Neuropsychiatric genetics : the official publication of the International Society of Psychiatric Genetics*. 2005;134B(1):93-103.
13. Lessmann V, Gottmann K, Malsangio M. Neurotrophin secretion: current facts and future prospects. *Progress in neurobiology*. 2003;69(5):341-74.
14. Autry AE, Monteggia LM. Brain-derived neurotrophic factor and neuropsychiatric disorders. *Pharmacological reviews*. 2012;64(2):238-58.
15. Duman RS, Monteggia LM. A neurotrophic model for stress-related mood disorders. *Biological psychiatry*. 2006;59(12):1116-27.
16. Karege F, Perret G, Bondolfi G, Schwald M, Bertschy G, Aubry JM. Decreased serum brain-derived neurotrophic factor levels in major depressed patients. *Psychiatry research*. 2002;109(2):143-8.
17. Warner-Schmidt JL, Duman RS. Hippocampal neurogenesis: opposing effects of stress and antidepressant treatment. *Hippocampus*. 2006;16(3):239-49.
18. Calabrese F, Rossetti AC, Racagni G, Gass P, Riva MA, Molteni R. Brain-derived neurotrophic factor: a bridge between inflammation and neuroplasticity. *Frontiers in cellular neuroscience*. 2014;8:430.
19. Chapman TR, Barrientos RM, Ahrendsen JT, Hoover JM, Maier SF, Patterson SL. Aging and infection reduce expression of specific brain-derived neurotrophic factor mRNAs in hippocampus. *Neurobiology of aging*. 2012;33(4):832 e1-14.
20. Thibault K, Lin WK, Rancillac A, Fan M, Snollaerts T, Sordoullet V, et al. BDNF-dependent plasticity induced by peripheral inflammation in the primary sensory and the cingulate cortex triggers cold allodynia and reveals a major role for endogenous BDNF as a

tuner of the affective aspect of pain. *The Journal of neuroscience : the official journal of the Society for Neuroscience*. 2014;34(44):14739-51.

21. Molendijk ML, Bus BA, Spinhoven P, Penninx BW, Kenis G, Prickaerts J, et al. Serum levels of brain-derived neurotrophic factor in major depressive disorder: state-trait issues, clinical features and pharmacological treatment. *Molecular psychiatry*. 2011;16(11):1088-95.
22. Tadic A, Wagner S, Schlicht KF, Peetz D, Borysenko L, Dreimuller N, et al. The early non-increase of serum BDNF predicts failure of antidepressant treatment in patients with major depression: a pilot study. *Progress in neuro-psychopharmacology & biological psychiatry*. 2011;35(2):415-20.
23. Autry AE, Adachi M, Nosyreva E, Na ES, Los MF, Cheng PF, et al. NMDA receptor blockade at rest triggers rapid behavioural antidepressant responses. *Nature*. 2011;475(7354):91-5.
24. Martinowich K, Manji H, Lu B. New insights into BDNF function in depression and anxiety. *Nature neuroscience*. 2007;10(9):1089-93.
25. Smith MA, Makino S, Kvetnansky R, Post RM. Stress and glucocorticoids affect the expression of brain-derived neurotrophic factor and neurotrophin-3 mRNAs in the hippocampus. *The Journal of neuroscience : the official journal of the Society for Neuroscience*. 1995;15(3 Pt 1):1768-77.
26. Ziegenhorn AA, Schulte-Herbruggen O, Danker-Hopfe H, Malbranc M, Hartung HD, Anders D, et al. Serum neurotrophins--a study on the time course and influencing factors in a large old age sample. *Neurobiology of aging*. 2007;28(9):1436-45.
27. Leproult R, Copinschi G, Buxton O, Van Cauter E. Sleep loss results in an elevation of cortisol levels the next evening. *Sleep*. 1997;20(10):865-70.
28. Meerlo P, Koehl M, van der Borght K, Turek FW. Sleep restriction alters the hypothalamic-pituitary-adrenal response to stress. *Journal of neuroendocrinology*. 2002;14(5):397-402.
29. Pflug B, Tolle R. Disturbance of the 24-hour rhythm in endogenous depression and the treatment of endogenous depression by sleep deprivation. *International pharmacopsychiatry*. 1971;6(3):187-96.
30. Vogel GW, Vogel F, McAbee RS, Thurmond AJ. Improvement of depression by REM sleep deprivation. New findings and a theory. *Archives of general psychiatry*. 1980;37(3):247-53.
31. Beersma DG, van den Hoofdakker RH. Can non-REM sleep be depressogenic? *Journal of affective disorders*. 1992;24(2):101-8.
32. Bunney BG, Bunney WE. Mechanisms of rapid antidepressant effects of sleep deprivation therapy: clock genes and circadian rhythms. *Biological psychiatry*. 2013;73(12):1164-71.
33. Giedke H, Schwarzler F. Therapeutic use of sleep deprivation in depression. *Sleep medicine reviews*. 2002;6(5):361-77.
34. Wu JC, Kelsoe JR, Schachat C, Bunney BG, DeModena A, Golshan S, et al. Rapid and sustained antidepressant response with sleep deprivation and chronotherapy in bipolar disorder. *Biological psychiatry*. 2009;66(3):298-301.
35. Tononi G, Cirelli C. Modulation of brain gene expression during sleep and wakefulness: a review of recent findings. *Neuropsychopharmacology : official publication of the American College of Neuropsychopharmacology*. 2001;25(5 Suppl):S28-35.
36. Elliott AS, Huber JD, O'Callaghan JP, Rosen CL, Miller DB. A review of sleep deprivation studies evaluating the brain transcriptome. *SpringerPlus*. 2014;3:728.
37. Porkka-Heiskanen T. Gene expression during sleep, wakefulness and sleep deprivation. *Frontiers in bioscience : a journal and virtual library*. 2003;8:s421-37.
38. Cirelli C, Tononi G. Gene expression in the brain across the sleep-waking cycle. *Brain research*. 2000;885(2):303-21.
39. Fujihara H, Sei H, Morita Y, Ueta Y, Morita K. Short-term sleep disturbance enhances brain-derived neurotrophic factor gene expression in rat hippocampus by acting as internal stressor. *Journal of molecular neuroscience : MN*. 2003;21(3):223-32.

40. Guzman-Marin R, Ying Z, Suntsova N, Methippara M, Bashir T, Szymusiak R, et al. Suppression of hippocampal plasticity-related gene expression by sleep deprivation in rats. *The Journal of physiology*. 2006;575(Pt 3):807-19.
41. Hairston IS, Peyron C, Denning DP, Ruby NF, Flores J, Sapolsky RM, et al. Sleep deprivation effects on growth factor expression in neonatal rats: a potential role for BDNF in the mediation of delta power. *Journal of neurophysiology*. 2004;91(4):1586-95.
42. Taishi P, Sanchez C, Wang Y, Fang J, Harding JW, Krueger JM. Conditions that affect sleep alter the expression of molecules associated with synaptic plasticity. *American journal of physiology Regulatory, integrative and comparative physiology*. 2001;281(3):R839-45.
43. Lee KS, Alvarenga TA, Guindalini C, Andersen ML, Castro RM, Tufik S. Validation of commonly used reference genes for sleep-related gene expression studies. *BMC molecular biology*. 2009;10:45.
44. Beck J, Hemmeter U, Brand S, Muheim F, Hatzinger M, Holsboer-Trachsler E. Modafinil reduces microsleep during partial sleep deprivation in depressed patients. *Journal of psychiatric research*. 2010;44(13):853-64.
45. Weizman S, Gonda X, Dome P, Faludi G. Pharmacogenetics of antidepressive drugs: a way towards personalized treatment of major depressive disorder. *Neuropsychopharmacologia Hungarica : a Magyar Pszichofarmakologiai Egyesulet lapja = official journal of the Hungarian Association of Psychopharmacology*. 2012;14(2):87-101.
46. Brunborg GS, Mentzoni RA, Molde H, Myrseth H, Skouveroe KJ, Bjorvatn B, et al. The relationship between media use in the bedroom, sleep habits and symptoms of insomnia. *Journal of sleep research*. 2011;20(4):569-75.
47. Dugovic C. Role of serotonin in sleep mechanisms. *Revue neurologique*. 2001;157(11 Pt 2):S16-9.
48. Mattson MP, Maudsley S, Martin B. BDNF and 5-HT: a dynamic duo in age-related neuronal plasticity and neurodegenerative disorders. *Trends in neurosciences*. 2004;27(10):589-94.
49. Cirelli C. Cellular consequences of sleep deprivation in the brain. *Sleep medicine reviews*. 2006;10(5):307-21.
50. Huber R, Esser SK, Ferrarelli F, Massimini M, Peterson MJ, Tononi G. TMS-induced cortical potentiation during wakefulness locally increases slow wave activity during sleep. *PloS one*. 2007;2(3):e276.
51. Bachmann V, Klein C, Bodenmann S, Schafer N, Berger W, Brugger P, et al. The BDNF Val66Met polymorphism modulates sleep intensity: EEG frequency- and state-specificity. *Sleep*. 2012;35(3):335-44.
52. Han KS, Kim L, Shim I. Stress and sleep disorder. *Experimental neurobiology*. 2012;21(4):141-50.
53. Holsboer F, Ising M. Stress hormone regulation: biological role and translation into therapy. *Annual review of psychology*. 2010;61:81-109, C1-11.
54. Miller GE, Chen E, Zhou ES. If it goes up, must it come down? Chronic stress and the hypothalamic-pituitary-adrenocortical axis in humans. *Psychological bulletin*. 2007;133(1):25-45.
55. Morsink MC, Steenbergen PJ, Vos JB, Karst H, Joels M, De Kloet ER, et al. Acute activation of hippocampal glucocorticoid receptors results in different waves of gene expression throughout time. *Journal of neuroendocrinology*. 2006;18(4):239-52.
56. Schulkin J, Gold PW, McEwen BS. Induction of corticotropin-releasing hormone gene expression by glucocorticoids: implication for understanding the states of fear and anxiety and allostatic load. *Psychoneuroendocrinology*. 1998;23(3):219-43.
57. Schulte-Herbruggen O, Chourbaji S, Ridder S, Brandwein C, Gass P, Hortnagl H, et al. Stress-resistant mice overexpressing glucocorticoid receptors display enhanced BDNF in the amygdala and hippocampus with unchanged NGF and serotonergic function. *Psychoneuroendocrinology*. 2006;31(10):1266-77.
58. Murakami S, Imbe H, Morikawa Y, Kubo C, Senba E. Chronic stress, as well as acute stress, reduces BDNF mRNA expression in the rat hippocampus but less robustly. *Neuroscience research*. 2005;53(2):129-39.

59. Nibuya M, Morinobu S, Duman RS. Regulation of BDNF and trkB mRNA in rat brain by chronic electroconvulsive seizure and antidepressant drug treatments. *The Journal of neuroscience : the official journal of the Society for Neuroscience*. 1995;15(11):7539-47.
60. Roceri M, Cirulli F, Pessina C, Peretto P, Racagni G, Riva MA. Postnatal repeated maternal deprivation produces age-dependent changes of brain-derived neurotrophic factor expression in selected rat brain regions. *Biological psychiatry*. 2004;55(7):708-14.
61. Ueyama T, Kawai Y, Nemoto K, Sekimoto M, Tone S, Senba E. Immobilization stress reduced the expression of neurotrophins and their receptors in the rat brain. *Neuroscience research*. 1997;28(2):103-10.
62. Diniz BS, Teixeira AL, Talib LL, Mendonca VA, Gattaz WF, Forlenza OV. Serum brain-derived neurotrophic factor level is reduced in antidepressant-free patients with late-life depression. *The world journal of biological psychiatry : the official journal of the World Federation of Societies of Biological Psychiatry*. 2010;11(3):550-5.
63. Shimizu E, Hashimoto K, Okamura N, Koike K, Komatsu N, Kumakiri C, et al. Alterations of serum levels of brain-derived neurotrophic factor (BDNF) in depressed patients with or without antidepressants. *Biological psychiatry*. 2003;54(1):70-5.
64. Morin CM, Rodrigue S, Ivers H. Role of stress, arousal, and coping skills in primary insomnia. *Psychosomatic medicine*. 2003;65(2):259-67.
65. Basta M, Chrousos GP, Vela-Bueno A, Vgontzas AN. Chronic Insomnia and Stress System. *Sleep medicine clinics*. 2007;2(2):279-91.
66. Staner L. Sleep and anxiety disorders. *Dialogues in clinical neuroscience*. 2003;5(3):249-58.
67. Ohayon MM, Roth T. Place of chronic insomnia in the course of depressive and anxiety disorders. *Journal of psychiatric research*. 2003;37(1):9-15.
68. Pigeon WR, Hegel M, Unutzer J, Fan MY, Sateia MJ, Lyness JM, et al. Is insomnia a perpetuating factor for late-life depression in the IMPACT cohort? *Sleep*. 2008;31(4):481-8.
69. Giese M, Unternaehrer E, Brand S, Calabrese P, Holsboer-Trachsler E, Eckert A. The interplay of stress and sleep impacts BDNF level. *PLoS one*. 2013;8(10):e76050.
70. Giese M, Unternaehrer E, Huttig H, Beck J, Brand S, Calabrese P, et al. BDNF: an indicator of insomnia? *Molecular psychiatry*. 2014;19(2):151-2.
71. Conti B, Maier R, Barr AM, Morale MC, Lu X, Sanna PP, et al. Region-specific transcriptional changes following the three antidepressant treatments electroconvulsive therapy, sleep deprivation and fluoxetine. *Molecular psychiatry*. 2007;12(2):167-89.
72. Giese M, Beck J, Brand S, Muheim F, Hemmeter U, Hatzinger M, et al. Fast BDNF serum level increase and diurnal BDNF oscillations are associated with therapeutic response after partial sleep deprivation. *Journal of psychiatric research*. 2014;59:1-7.
73. Musazzi L, Treccani G, Popoli M. Functional and structural remodeling of glutamate synapses in prefrontal and frontal cortex induced by behavioral stress. *Frontiers in psychiatry*. 2015;6:60.
74. Duman RS. Neural plasticity: consequences of stress and actions of antidepressant treatment. *Dialogues in clinical neuroscience*. 2004;6(2):157-69.
75. Berman RM, Cappiello A, Anand A, Oren DA, Heninger GR, Charney DS, et al. Antidepressant effects of ketamine in depressed patients. *Biological psychiatry*. 2000;47(4):351-4.
76. Zarate CA, Jr., Singh JB, Carlson PJ, Brutsche NE, Ameli R, Luckenbaugh DA, et al. A randomized trial of an N-methyl-D-aspartate antagonist in treatment-resistant major depression. *Archives of general psychiatry*. 2006;63(8):856-64.
77. Murrough JW, Iosifescu DV, Chang LC, Al Jurdi RK, Green CE, Perez AM, et al. Antidepressant efficacy of ketamine in treatment-resistant major depression: a two-site randomized controlled trial. *The American journal of psychiatry*. 2013;170(10):1134-42.
78. Li N, Lee B, Liu RJ, Banasr M, Dwyer JM, Iwata M, et al. mTOR-dependent synapse formation underlies the rapid antidepressant effects of NMDA antagonists. *Science*. 2010;329(5994):959-64.
79. Lepack AE, Fuchikami M, Dwyer JM, Banasr M, Duman RS. BDNF release is required for the behavioral actions of ketamine. *The international journal of*

neuropsychopharmacology / official scientific journal of the Collegium Internationale Neuropsychopharmacologicum. 2015;18(1).

80. Duman RS, Li N. A neurotrophic hypothesis of depression: role of synaptogenesis in the actions of NMDA receptor antagonists. *Philosophical transactions of the Royal Society of London Series B, Biological sciences*. 2012;367(1601):2475-84.

81. Haile CN, Murrugh JW, Iosifescu DV, Chang LC, Al Jurdi RK, Foulkes A, et al. Plasma brain derived neurotrophic factor (BDNF) and response to ketamine in treatment-resistant depression. *The international journal of neuropsychopharmacology / official scientific journal of the Collegium Internationale Neuropsychopharmacologicum*. 2014;17(2):331-6.

82. Bunney BG, Bunney WE. Rapid-acting antidepressant strategies: mechanisms of action. *The international journal of neuropsychopharmacology / official scientific journal of the Collegium Internationale Neuropsychopharmacologicum*. 2012;15(5):695-713.

83. Brunoni AR, Valiengo L, Baccaro A, Zanao TA, de Oliveira JF, Vieira GP, et al. Sertraline vs. Electrical Current Therapy for Treating Depression Clinical Trial--SELECT TDCS: design, rationale and objectives. *Contemporary clinical trials*. 2011;32(1):90-8.

84. Piccinni A, Marazziti D, Catena M, Domenici L, Del Debbio A, Bianchi C, et al. Plasma and serum brain-derived neurotrophic factor (BDNF) in depressed patients during 1 year of antidepressant treatments. *Journal of affective disorders*. 2008;105(1-3):279-83.

85. Molendijk ML, Bus BA, Spinhoven P, Penninx BW, Prickaerts J, Oude Voshaar RC, et al. Gender specific associations of serum levels of brain-derived neurotrophic factor in anxiety. *The world journal of biological psychiatry : the official journal of the World Federation of Societies of Biological Psychiatry*. 2012;13(7):535-43.

86. Gold PW, Loriaux DL, Roy A, Kling MA, Calabrese JR, Kellner CH, et al. Responses to corticotropin-releasing hormone in the hypercortisolism of depression and Cushing's disease. Pathophysiologic and diagnostic implications. *The New England journal of medicine*. 1986;314(21):1329-35.

87. Murphy BE. Treatment of major depression with steroid suppressive drugs. *The Journal of steroid biochemistry and molecular biology*. 1991;39(2):239-44.

88. Murphy BE. Steroids and depression. *The Journal of steroid biochemistry and molecular biology*. 1991;38(5):537-59.

89. Deuschle M, Schweiger U, Weber B, Gotthardt U, Korner A, Schmider J, et al. Diurnal activity and pulsatility of the hypothalamus-pituitary-adrenal system in male depressed patients and healthy controls. *The Journal of clinical endocrinology and metabolism*. 1997;82(1):234-8.

90. Halbreich U, Asnis GM, Shindilecker R, Zumoff B, Nathan RS. Cortisol secretion in endogenous depression. I. Basal plasma levels. *Archives of general psychiatry*. 1985;42(9):904-8.

91. Pfohl B, Sherman B, Schlechte J, Stone R. Pituitary-adrenal axis rhythm disturbances in psychiatric depression. *Archives of general psychiatry*. 1985;42(9):897-903.

92. Yehuda R, Teicher MH, Trestman RL, Levengood RA, Siever LJ. Cortisol regulation in posttraumatic stress disorder and major depression: a chronobiological analysis. *Biological psychiatry*. 1996;40(2):79-88.

93. Begliuomini S, Lenzi E, Ninni F, Casarosa E, Merlini S, Pluchino N, et al. Plasma brain-derived neurotrophic factor daily variations in men: correlation with cortisol circadian rhythm. *The Journal of endocrinology*. 2008;197(2):429-35.

94. Pluchino N, Cubeddu A, Begliuomini S, Merlini S, Giannini A, Bucci F, et al. Daily variation of brain-derived neurotrophic factor and cortisol in women with normal menstrual cycles, undergoing oral contraception and in postmenopause. *Human reproduction*. 2009;24(9):2303-9.

95. Pan W, Banks WA, Fasold MB, Bluth J, Kastin AJ. Transport of brain-derived neurotrophic factor across the blood-brain barrier. *Neuropharmacology*. 1998;37(12):1553-61.

96. Liang FQ, Sohrabji F, Miranda R, Earnest B, Earnest D. Expression of brain-derived neurotrophic factor and its cognate receptor, TrkB, in the rat suprachiasmatic nucleus. *Experimental neurology*. 1998;151(2):184-93.

97. Liang FQ, Walline R, Earnest DJ. Circadian rhythm of brain-derived neurotrophic factor in the rat suprachiasmatic nucleus. *Neuroscience letters*. 1998;242(2):89-92.
98. Wolkowitz OM, Wolf J, Shelly W, Rosser R, Burke HM, Lerner GK, et al. Serum BDNF levels before treatment predict SSRI response in depression. *Progress in neuro-psychopharmacology & biological psychiatry*. 2011;35(7):1623-30.
99. Mikoteit T, Beck J, Eckert A, Hemmeter U, Brand S, Bischof R, et al. High baseline BDNF serum levels and early psychopathological improvement are predictive of treatment outcome in major depression. *Psychopharmacology*. 2014;231(15):2955-65.
100. Soumier A, Banasr M, Lortet S, Masméjean F, Bernard N, Kerkerian-Le-Goff L, et al. Mechanisms contributing to the phase-dependent regulation of neurogenesis by the novel antidepressant, agomelatine, in the adult rat hippocampus. *Neuropsychopharmacology : official publication of the American College of Neuropsychopharmacology*. 2009;34(11):2390-403.
101. Sartorius A, Hellweg R, Litzke J, Vogt M, Dormann C, Vollmayr B, et al. Correlations and discrepancies between serum and brain tissue levels of neurotrophins after electroconvulsive treatment in rats. *Pharmacopsychiatry*. 2009;42(6):270-6.
102. Lakshminarasimhan H, Chattarji S. Stress leads to contrasting effects on the levels of brain derived neurotrophic factor in the hippocampus and amygdala. *PLoS one*. 2012;7(1):e30481.

Figures

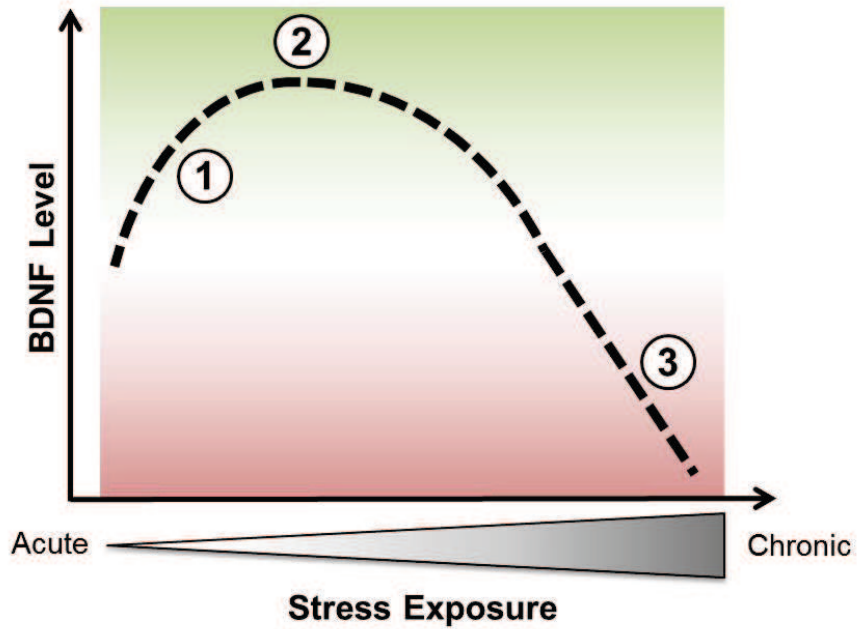


Figure 1: Conceptual representation of changes in BDNF level induced by stress: a biphasic process. Point 1 illustrates the increase of BDNF during acute stress while point 2 corresponds to a maximal benefit of short-term stress on BDNF level. Points 1 and 2 might be linked to an induced increase of synaptic transmission and plasticity. Point 3 illustrates the deleterious effects of chronic stress on BDNF content.

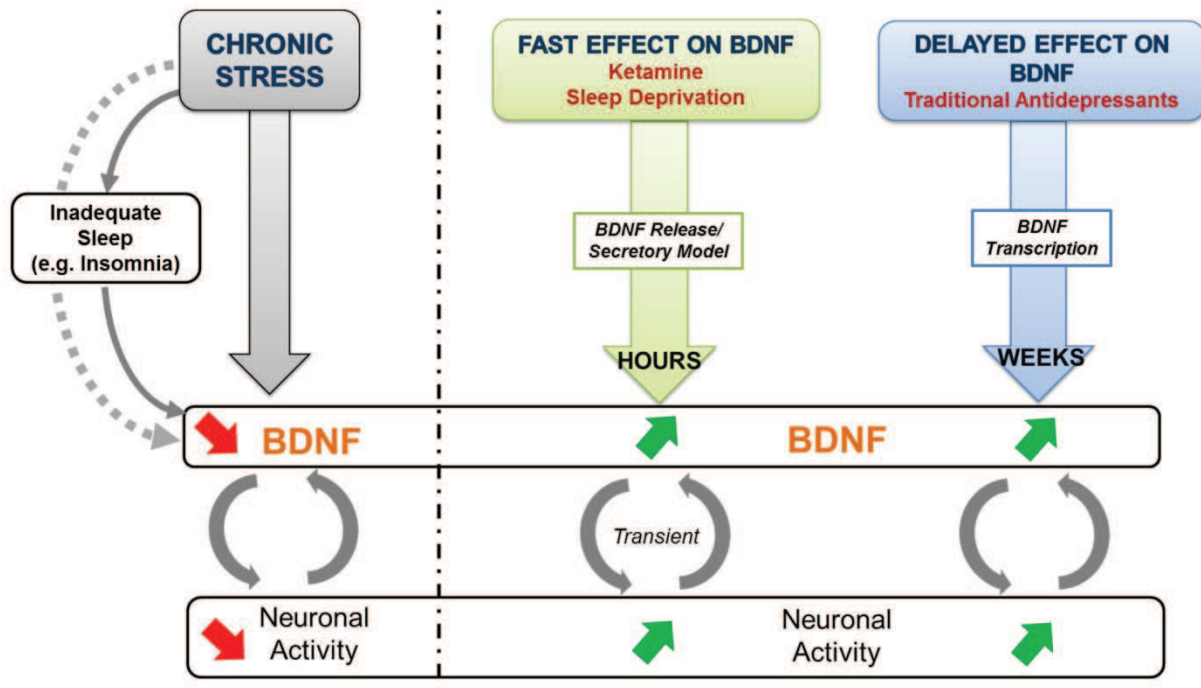


Figure 2: Left panel: Scheme representing the mediation model where sleep acts as key mediator in the association between stress and BDNF. Chronic stress and insomnia lead to a decrease in BDNF and synaptic activity. **Right panel:** Fast-acting effect of ketamine and sleep deprivation versus delayed long-term effects of classical antidepressants on BDNF levels.